CENPD-252-NP-A

BLOWDOWN ANALYSIS METHOD

POWER SYSTEMS
COMBUSTION ENGINEERING, INC.

7910050555

LEGAL NOTICE

THIS REPORT WAS PREPARED AS AN ACCOUNT OF WORK SPONSORED BY COMBUSTION ENGINEERING, INC. NEITHER COMBUSTION ENGINEERING NOR ANY PERSON ACTING ON ITS BEHALF:

A. MAKES ANY WARRANTY OR REPRESENTATION, EXPRESS OR IMPLIED INCLUDING THE WARRANTIES OF FITNESS FOR A PARTICULAR PURPOSE OR MERCHANTABILITY, WITH RESPECT TO THE ACCURACY, COMPLETENESS, OR USEFULNESS OF THE INFORMATION CONTAINED IN THIS REPORT, OR THAT THE USE OF ANY INFORMATION, APPARATUS, METHOD, OR PROCESS DISCLOSED IN THIS REPORT MAY NOT INFRINGE PRIVATELY OWNED RIGHTS; OR

B. ASSUMES ANY LIABILITIES WITH RESPECT TO THE USE OF, OR FOR DAMAGES RESULTING FROM THE USE OF, ANY INFORMATION, APPARATUS, METHOD OR PROCESS DISCLOSED IN THIS REPORT.

CENPD - 252 - NP - A

BLOWDOWN ANALYSIS METHOD

METHOD FOR THE ANALYSIS OF BLOWDOWN INDUCED FORCES IN A REACTOR VESSEL

BLOWDOWN LOADS GROUP

JULY, 1979

POWER SYSTEMS
COMBUSTION ENGINEERING, INC.

CRITERIA FOR PROPRIETARY INFORMATION

Code numbers 1-6 have been placed in the margin of the text to identify proprietary information. The following list explains the criteria associated with these code numbers.

Code	Criteria
1	The information reveals privileged cost or price information, commercial strategies, production capabilities, or budget levels of Combustion Engineering, Inc. its customers or suppliers.
2	The information reveals data or material concerning Combustion Engineering or customer funded research or development plans or programs of substantial present or potential competitive advantage to Combustion Engineering, Inc.
3	The use of the information by a competitor would substantially decrease his expenditures, in time or resources, in designing, producing or marketing a similar product.
4	The information consists of test data or other similar data concerning a process, method or component, the application of which results in a substantial competitive advantage to Combustion Engineering, Inc.
5	The information reveals special aspects of a process, method, component or the like, the exclusive use of which results in a substantial competitive advantage to Combustion Engineering, Inc.
6	The information contains ideas for which patent protection is likely to be sought.

UNITED STATES
NUCLEAR REGULATORY COMMISSION
WASHINGTON, D. C. 20555

FEB 2 8 1979

Mr. A. E. Scherer
Licensing Manager
Combustion Engineering, Inc.
1000 Prospect Hill Road
Windsor, Connecticut 06095

Dear Mr. Scherer:

SUBJECT: STAFF EVALUATION OF TOPICAL REPORT CENPD-252-P

Our letter to you dated February 12, 1979 transmitted our evaluation of topical report CENPD-252-P, "Blowdown Analysis Method - Method for Analysis of Blowdown Induced Forces in a Reactor Vessel." After receipt of the evaluation, representatives of Combustion Engineering (C-E) contacted us by telephone regarding the evaluation. They stated that it was their understanding that the CEFLASH-4B code discussed in CENPD-252-P was found acceptable for use during the early saturation portion of blowdown as well as the subcooled decompression; however, the evaluation of CENPD-252-P did not identify this as being acceptable.

We reviewed the evaluation and concluded that the summary and the cover letter are in error in this regard. Although we did not explicitly state it, we did find the use of CEFLASH-4B in the early saturation portion of blowdown as well as the subcooled decompression to be acceptable. In addition, we note that the "CEFLASH-4A" in Item 4 of the summary should be "CEFLASH-4B."

We request that you include this letter with the approved copy of CENPD-252-P. If you have any further questions on this topical report, please contact us.

Sincerely,

Robert L. Baer

Robert L. Baer, Chief
Light Water Reactors
Branch No. 2
Division of Project Management

596 006

UNITED STATES
NUCLEAR REGULATORY COMMISSION
WASHINGTON, D. C. 20555

FEB 12 1979

Mr. A. E. Scherer
Licensing Manager
Combustion Engineering
1000 Prospect Hill Road
Windsor, Connecticut 06095

Dear Mr. Scherer:

SUBJECT: STAFF EVALUATION OF TOPICAL REPORT CENPD-252-P

On December 15, 1977, Combustion Engineering submitted topical report CENPD-252-P, "Blowdown Analysis Method - Method for Analysis of Blowdown Induced Forces in a Reactor Vessel." The report was amended twice; Amendment 1-P was submitted on August 22, 1978 and Amendment 2-P was submitted on October 20, 1978. We have completed our review of CENPD-252-P and our evaluation appears as the Enclosure to this letter.

Subject to the limitations discussed in the Enclosure, we conclude that the CEFLASH-4B computer code is an acceptable code for evaluating the subcooled decompression response of a pressurized water reactor primary coolant system following a postulated loss-of-coolant accident. It is requested that CENPD-252-P be resubmitted as an approved report. The copies of the approved report should include this approval letter and the responses to our requests for information. However, the computer printouts provided in the responses need not be included in the approved report.

Should NRC criteria or regulations change such that our conclusions concerning CENPD-252-P are invalidated, you will be notified and given an opportunity to revise and resubmit your topical report should you so desire.

When CENPD-252-P is referenced in a license application, the non-proprietary version should also be referenced. We do not intend to repeat our review of this report when it appears as a reference in a particular license application.

Sincerely,

Robert L. Baer

Robert L. Baer, Chief
Light Water Reactors Branch No. 2
Division of Project Management

Enclosure:
Evaluation of CENPD-252-P

596 007

TOPICAL REPORT EVALUATION

CENPD-252-P: "Blowdown Analysis Method - Method for the Analysis of Blowdown Induced Forces in a Reactor Vessel."

A. Summary of Topical Report

This report describes the methods and procedures that are utilized by Combustion Engineering in calculating hydrodynamic loadings on a reactor coolant system undergoing a postulated loss-of-coolant accident (LOCA).

The hydrodynamics for both the subcooled and the saturated portions of the blowdown are calculated with the CEFLASH-4B digital computer program. A post-processing routine for the CEFLASH-4B program is used to calculate the hydraulic forces acting on the reactor vessel internals as a result of momentum changes in the coolant fluid.

At present, a rigid boundary assumption is made in the hydraulic analyses. The fluid boundaries are assumed to be constant and at rest during the CE-FLASH-4B analysis.

The CEFLASH-4B computer program (References 1, 2 and 3) solves the conservation equations for mass and energy, the one-dimensional continuity equation, and the equation of state for water. The CEFLASH-4B program permits the user to select the nodal representation that results in the best finite differencing of the fluid system to be analyzed. The program then solves the conservation equations for each node and the one-dimensional momentum equation for each flow path between nodes. CEFLASH-4B uses

explicit solution techniques. Various options as well as user input parameters enable the program to model the reactor core, reactor coolant pumps, steam generators, and connecting piping in any configuration and operating model desired.

The thermodynamic and transport fluid properties in CEFLASH-4B are obtained from functional fits to the properties based on the 1967 ASME Steam Tables.

CEFLASH-4B is used to compute the pressure response of a system during a decompression transient. The transient pressure response can then be used to evaluate the system's overall dynamic structure response. The asymmetric pressure field in the downcomer annulus of a PWR can be obtained. This pressure field can then be integrated over the core support barrel area to obtain the total dynamic load on the core support barrel.

The analysis is performed for the subcooled decompression and early saturation periods of the transient, where the hydraulic loads are greatest. These loads are used for the structural evaluation of the reactor pressure vessel system, in conjunction with other loads associated with a postulated LOCA and with a safe shutdown earthquake. The capability of the CEFLASH-4B analysis to account for the acoustic wave phenomena induced in subcooled water is demonstrated.

B. Regulatory Evaluation

CEFLASH-4B is a generalized computer program; however, the review of the CEFLASH-4B program was li ited to the representation of a PWR primary coolant system subjected to a postulated loss-of-coolant accident (LOCA), specifically during the subcooled and early saturation periods of the decompression transient.

The NRC evaluation of the CEFLASH-4B program covered three major areas of review:

1. Analytical Development
2. Application and System Modeling
3. Code Verification

The application of the one-dimensional CEFLASH-4B program to the calculation of the multi-dimensional downcomer pressure field represents the major portion of this review.

1.0 Conservation Equations

The basic assumption of equilibrium of the steam/water mixture is employed in the CEFLASH-4B program. The subcooled, transition, and early saturated regimes, for which the equilibrium fluid assumption is acceptable, can be evaluated. It is during this portion of the blowdown that the LOCA hydraulic loads are greatest.

The mass, momentum and energy conservation equations are developed for a one-dimensional system. Density and mass flow are assumed to be uniform over the space and solution time interval. Friction and buoyancy are included in the momentum equation. Included in the energy

equation is heat transfer associated with a reactor core and with a steam generator.

2.0 Equation of State and Sonic Velocity

The equation of state used in CEFLASH-4B is a set of functional fits to the data for liquid and steam properties for single and two-phase conditions. The properties values obtained from these fits were checked against the 1967 ASME Steam Tables and show good agreement over the range of interest.

The sonic velocity in water is not explicitly used in the CEFLASH-4B analysis. It can be derived, or implied, from the properties fits for an isentropic expansion process. The implied sound speed has been demonstrated to be in good agreement with the ASME values over the range of interest.

3.0 Method of Solution

The solution of the conservation equations, for the analyses of hydrodynamic loadings, is obtained by using the explicit numerical solution technique. The solution time step for stability is based on the system noding and the local acoustic wave speed. A time step study was performed for a typical LOCA loads model and the time step selected for licensing calculations is one-half that of the largest time step studied which showed a variation in the solution convergence.

The solution is assumed to be converged for the LOCA loads calculation when the time history results of the predicted pressures and momentum

flow parameters are all nearly identical to the respective values f[illegible]he preceeding smaller time step trial.

4.0 Discharge Flow Model and Non-Equilibrium Effects

The discharge flow model for the postulated break is the system forcing function. As such, the treatment of the subcooled critical flow and potential non-equilibrium effects must be properly accounted for in the development of the discharge flow model.

Combustion Engineering uses the CE critical flow model for computing the subcooled and saturated critical fluid discharge at the break. The CE correlation accounts for the non-equilibrium nature of the critical discharge during the subcooled portion of the transient. The CE critical flow model also yields higher, on the order of 10%, loads across the internal components than the equilibrium critical flow formulations. The Moody and the Homogeneous Equilibrium models were used for this comparison.

The break characteristics are modeled in CEFLASH-4B as a function of location in the coolant system, total area and time to develop the total area. The guillotine offset area is properly modeled as the two ends of the pipe separate to the full double-ended area or partial offset area.

The opening time history of a break in the NSS primary piping system is plant specific, and it depends on considerations such as the location of the break, the stiffness and mass of the piping system involved, and the type and location of pipe restraints/supports being used.

Combustion Engineering utilizes a mechanistic approach based on non-linear structural analysis techniques and the conservative assumption of instantaneous crack propagation to determine realistic break opening times. The break opening schedules, for the System 80 generic class of plants, are documented in Reference 4.

The hydrodynamic loads are directly proportional to the differential pressures applied to the structure. If, as a result of non-equilibrium the pressure at the break plane falls below the saturation pressure of the fluid, prior to the development of two-phase fluid conditions, an increased loading could result.

The effects of non-equilibrium could also increase the loading on the core support cylinder structure if this pressure "undershoot" could be transmitted to the downcomer annulus.

The reactor coolant system depressurization rate is, in part, a function of the break opening time and, in part, a function of the break area. Combustion Engineering has assessed the potential for non-equilibrium effects to occur in a PWR blowdown as well as assessing the resulting affects should non-equilibrium conditions be present. The behavior of experiments, with initial conditions and break characteristics

similar to the Combustion Engineering mechanistic break, were studied. For these conditions non-equilibrium effects were not observed. An assessment of the affects of a pressure "undershoot" on the impulse loading of the core support barrel was performed based on the analysis performed in reference 5. For this extreme case, the impulse loading increased less than one percent.

5.0 Multi-Dimensional Region Modeling

The downcomer region of a PWR can be considered at least 2-dimensional for analytical evaluations of subcooled decompression transients and, as such, should be properly modeled. Since CEFLASH-4B solves the 1-dimensional conservation equations, it was necessary to investigate the modeling procedures used to represent the multi-dimensional aspects of this region.

The modeling techniques used to represent a physical system can affect the results of the calculation. Not only must the mathematical equations be stable and the solution converged, but the nodal network representation should not exert undue influence (i.e., non-conservatism) on the calculation.

A set of experimental test geometries was selected to study the effects of the modeling techniques on the results of the calculations, by comparing the Combustion Engineering calculations to those performed by the NRC. The selected geometries contain two important features typical of PWRs: a downcomer annulus region and a core simulator region.

While the systems selected may not be properly scaled to a PWR system, in terms of the ratio of the downcomer length to circumferential

length, for the analysis of a subcooled decompression transient, the system behavior should be well defined for the postulated transients.

If the system is properly modeled, the analysis will predict the expected transient behavior. The selected tests were instrumented to obtain subcooled decompression data. The selected geometries were:

(1) LOFT Test L1-2.

This test was designed to represent a PWR during decompression. The break was designed to represent a large, inlet nozzle rupture.

(2) Containment Systems Experiment (CSE) Test B-75.

This test was run at an initial pressure of 1000 psig and the break was designed to represent a large, inlet nozzle rupture.

In addition to the experimental test geometries, three problems using simplified geometries were developed to evaluate the multi-dimensional nodal approa h. The results of these analyses were compared with multi-dimensional computer code calculations (Reference 6). The geometries represented typical PWR regions, such as the nozzle to downcomer interface region, flow obstructions, and the un-wrapped downcomer region. In addition to the multi-dimensional code calculations, similar calculations using RELAP4/MOD5 were performed for comparison with the CEFLASH-4B results (Reference 7).

The magnitude of the pressure wave penetrating into the downcomer annulus is the forcing function which determines the resulting hydraulic

loading on the vessel internals. The inertial factor used in the CEFLASH-4B computer code to represent the flow path between the inlet nozzle and the downcomer is calculated as the sum of the inertial factors within the nozzle and inertial factor within the downcomer. One of the above simple problems was developed to study the effects of modeling at this location.

Comparisons of the CEFLASH-4B analyses for the three sample problems to the analyses performed by the NRC demonstrate the capability of the CEFLASH-4B computer program to account for the acoustic wave transmission and reflection phenomenon induced in subcooled water. The CEFLASH-4B nodal representation for multi-dimensional regions is shown to be acceptable within the computer program limitations which restrict the amount of spacial detail available.

The methodology and nodal representations are further justified by the good agreement obtained for the CEFLASH-4B analyses of the selected test geometries.

6.0 Fluid-Structure Coupling

Fluid-structure interaction is not included in the CEFLASH-4B analysis of subcooled blowdown. Fluid boundaries are assumed to be rigid and at rest.

7.0 NRC Audit Calculations

The NRC has performed independent audit calculations for a System 80 PWR. In addition, calculations for the selected test geometries were performed.

The WHAM/MOD-007 computer code was used to perform the NPC audit calculations (Reference 8). The modeling techniques employed for these calculations were based on the evaluations of the three simple problems used to study the network modeling approach (Reference 9 and 10).

C. Regulatory Position

The CEFLASH-4B computer program is used by Combustiong Engineering to evaluate the hydrodynamic loadings on the reactor coolant system following a postulated loss-of-coolant accident (LOCA). Fluid-structure interaction is not included in the CEFLASH-4B analysis of subcooled blowdown. Fluid boundaries are assumed to be rigid and at rest. The downcomer region of the PWR is modeled to allow for the calculation of the induced hydrodynamic loads on the core support barrel. The methodology used results in a conservative calculation of the induced hydrodynamic loads on the reactor coolant system, reactor vessel supports, and reactor internals following a postulated LOCA.

1.0 Evaluation of Analytical Methods

The solution of the conservation equations and the equation of state in the CEFLASH-4B computer program can be shown to be nearly equivalent to the vector momentum equation governing nearly incompressible, low speed flow for a multi-dimensional analyses. Therefore, the use of the CEFLASH-4B code to evaluate subcooled decompression transients, for the multi-dimensional nodal models, is acceptable.

The potential effects of non-equilibrium have been addressed in an acceptable manner, and changes to account explicitly for this phenomenon are not required for licensing calculations.

The discharge flow model used for the analysis of subcooled decompression transients, the CE critical flow model, has been shown to yield conservative results for the calculation of the hydrodynamic loads.

CEFLASH-4B is a generalized computer program for the analysis of thermal-hydraulic systems, and the user has a number of options available for an analysis. During the course of this review a number of these options were explored and subsequently accepted for a licensing calculation. These options are listed in the Summary section to this report and are also identified in the audit analyses.

2.0 Break Characteristics

The break area models used in the CEFLASH-4B computer program are acceptable. The break opening time history of a break in the NSS primary piping system is plant specific, and it depends on conderations such as the location of the break, the stiffness and mass of the piping system involved, and the type and location of pipe restraints/supports being used. Combustion Engineering utilizes a mechanistic approach based on non-linear structural analysis techniques and the conservative assumption of instantaneous crack propagation to determine realistic break opening times.

3.0 System Modeling and Code Verification

The application of the CEFLASH-4B computer program for the analyses of multi-dimensional fluid transients can be shown to be equivalent to the vector momentum equation for nearly incompressible, low speed flow. This is demonstrated by comparisons of the simplied geometry problems to multi-dimensional computer code results. Further verification is obtained by comparing the CEFLASH-4B analyses to the selected experimental test geometry data. The evaluation of the modeling techniques employed by Combustion Engineering, for the representation of a PWR, is based on the results and observations made from the comparative analyses performed for the selected test geometries, and for the simplied geometry problem calculations.

There are four fundamental areas associated with this evaluation for the nodal hydraulic representation of the system:

1. The modeling of the primary coolant loops,

2. The modeling of the nozzle to downcomer interface,

3. The representation of the multi-dimensional downcomer region and,

4. The representation of the vessel internals; lower plenum, core, upper plenum.

The representation of the primary coolant loops as one-dimensional pipes is acceptable. The piping system can be represented, for practical purposes, as one-dimensional. When the proper engineering loss factors are accounted for, the one-dimensional flow equation is solved correctly.

The method for modeling the nozzle to downcomer region is acceptable. The inertial factor used in the CEFLASH-4B computer program is obtained by summing the inertial factors for the nozzle with the inertial factors for the downcomer to nozzle interface. This method properly accounts for the geometry of this region.

The procedures used by Combustion Engineering, to generate the nodal representation of a PWR for licensing calculations, result in a conservative hydraulic model. This is, in part, a result of the hydraulic nodal network employed to represent the downcomer annulus region. Independent audit calculations performed by the NRC show that the nodal network developed by Combustion Engineering for the LOCA analysis is conservative.

Computer limitations restrict the amount of detail that can be specified in the CEFLASH-4B model. This limits the user's ability to select a nodal representation, or finite differencing of the fluid system to be analyzed. Combustion Engineering performed a sensitivity study for the nodal representation of the downcomer annulus. Based on these studies, which included the evaluation of the hydraulic loads on the core support barrel, a design application model was selected. This model is acceptable for licensing calculations.

This model also includes the representations of the remainder of the primary system. The steam generator, pressurizer, coolant pumps and the vessel internals are described using the node and flow path modeling technique.

The multi-dimensional region modeling has been verified by comparing the CEFLASH-4B results to 2-dimensional computer code analyses of the three simplified geometry problem. These comparisons demonstrate the near equivalence of the CEFLASH-4B solutions for incompressible, low speed flow conditions. Further verifications were made by comparisons of the CEFLASH-4B results to the selected test geometry data. The analyses of the LOFT L1-2 and the Containment Systems Experiment test B-75 showed good agreement with the test data and the analytical results compared favorably with the NRC calculations. In general, the differential pressures obtained from the CEFLASH-4B analyses are larger than those reported in the test results and larger than those calculated with the NRC methodology. These differential pressures are similar to those which would be used to obtain the integrated hydraulic loads on the PWR core support barrel.

The methodology employed by Combustion Engineering to generate the nodal representation of the PWR system, specifically at the nozzle to downcomer interface, and for the development of the downcomer region itself, shall be incorporated into the final topical report documentation (see Appendix A). The development of a model using this methodology is acceptable for licensing calculations.

4.0 Audit Calculations

Combustion Engineering has performed an audit analysis with both a hot leg nozzle break and a partial double-ended guillotine rupture at the reactor inlet nozzle using the mechanistic break data. In addition, an analysis was performed for the inlet nozzle rupture using the design model but with a full double-ended guillotine break.

Comparisons of the Combustion Engineering analyses to the NRC independent analyses shows that the CEFLASH-4B methodology predicts higher hydraulic loads, for all cases evaluated.

The model developed by Combustion Engineering is based on the methodology reviewed for this evaluation. The CEFLASH-4B calculation of a postulated LOCA in a PWR for the purpose of determining the resultant hydrodynamic loads on the system, is acceptable for licensing calculations.

5.0 Fluid-Structure Coupling

Fluid-structure interaction is not included in the CEFLASH-4B analysis of subcooled blowdown. Fluid boundaries are assumed to be rigid and at rest.

Analytical evaluations of the effects of fluid-structure coupling, by a number of researchers (References 11, 12, and 13), have shown that for a coupled analysis the frequency and amplitude motions are lower than for an uncoupled analysis with the consequence of generally lower induced stresses.

The rigid boundary assumption used in the CEFLASH-4B analysis is acceptable for licensing calculations. However, the NRC will continue to monitor the on-going research in this area and will require, if necessary, a re-evaluation of the rigid boundary assumption. Part of this research will be performed in the German HDR subcooled blowdown experiments (Reference 14). Combustion Engineering has committed to perform a pre-test analysis of this experiment when test conditions have been established (Reference 15).

D. Summary

The Combustion Engineering CEFLASH-4B computer program is used to evaluate the subcooled decompression and early saturation response of a PWR primary coolant system following a postulated loss-of-coolant accident. This topical report describes the assumptions used and the methodology employed by Combustion Engineering to perform this evaluation.

Subject to the limitations of this review, the CEFLASH-4B computer program is an acceptable code for evaluating the subcooled decompression response of a PWR primary coolant system following a postulated loss-of-coolant accident. These limitations are:

(1) The CE critical flow model is to be used.

(2) The break opening schedules, including location, size and time based on the mechanistic break model employed by Combustion Engineering are to be referenced for licensing calculations.

(3) The Combustion Engineering design model for the annulus representation is to be used for licensing calculations.

(4) The evaluation of the blowdown induced forces following a postulated LOCA is acceptable provided a CEFLASH-4A licensing calculation is performed to obtain the hydraulic input data.

The responses to the NRC requests for additional information, as listed in Appendix A of this evaluation, are to be incorporated into the final version of the topical report to describe and develop the Combustion Engineering modeling methodology and to identify the assumptions and acceptable input parameters for a licensing calculation.

Combustion Engineering has committed to perform a pre-test analysis of the German HDR subcooled blowdown experiment when test conditions becomes available.

REFERENCES

1. CENPD-252-P,"Blowdown Analysis Method, Method for the Analysis of Blowdown Induced Forces in A Reactor Vessel," Combustion Engineering, Reactor Design, December, 1977.

2. CENPD-252-P, Amendment 1-P, Combustion Engineering, Blowdown Loads Group, August, 1978.

3. CENPD-252-P, Amendment 2-P, Combustion Engineering, Blowdown Loads Group, October, 1978.

4. CENPD-168-A, "Design Basis Pipe Breaks for the Combustion Engineering Two-Loop Reactor Coolant System," Combustion Engineering, June 1977.

5. Jackson, J.F., "Nuclear Reactor Safety Quarterly Progress Report: January 1 - March 31, 1977," LA-NUREG-6842-PR, June, 1977.

6. Cole, R.K., "Analysis of NRC Sample Problems Using the CSQ Computer Program," SANDIA, (to be published).

7. Cole, R.K., "Analysis of NRC Sample Problems Using the RELAP4/MOD5 Computer Program," SANDIA (to be published).

8. Throm, E.D., "Availability of the WHAM/MOD-007 Subcooled Blowdown Hydraulic Analysis Code," memo to Z.R. Rosztoczy, Chief, Analysis Branch, DSS, May 13, 1976.

9. Cole, R.K., "An Analysis of the Method of Streeter and Wylie for Multidimensional Wave Propagation," SAND77-0549, Sandia Laboratories, July, 1977.

10. Berman, M., Cole, R.K., et.al., "LOCA Analysis Quarterly Report April-June, 1977, SAND77-1530, Sandia Laboratories, December, 1977 (Section II).

11. Prelewicz, D.A., "Hydraulic Pressure Pulses with Structural Flexibility: Test and Analysis, "WAPD-TM-1227, Bettis Atomic Power Laboratory, April, 1976.

12. Takeuchi, K., "Hydraulic Force Calculation with Hydrostructural Interactions," Nuclear Technology, Vol. 39, July, 1978, pages 155-166.

13. Rivard, W.C., and M.D. Torrey, "Fluid-Structure Response of a Pressurized Water Reactor Core Barrel During Blowdown," NUREG/CR-0264, LA-7407, September, 1978.

14. Krieg, R., E.G. Schlechtendahl, K.- H. Scholl, "Design of the HDR Experimental Program on Blowdown Loading and Dynamic Response of PWR-Vessel Internals," Nuclear Engineering and Design, Vol. 43, 1977.

15. Letter from A.E. Scherer, Licensing Manager, Combustion Engineering, to K. Kniel, Chief, LWR-2, Division of Project Management, LD-77-032, April 7, 1977.

APPENDIX A

The responses to the following NRC requests for additional information (reference NRC letter from D.B. Vassallo, DPM, to A.E. Scherer, Licensing Manager, dated May 10,1978) are to be incorporated into the final version of the report to describe and develop the Combustion Engineering modeling methodology and to identify the assumptions and acceptable input parameters for a licensing calculation:

Questions	1.1	2.1	3.1
	1.2	2.2	3.2
	1.3	2.3	
	1.4	2.4 } without listings	
		2.5 }	
		2.6	

ABSTRACT

This report presents a description of the Combustion Engineering methodology for the prediction of the reactor pressure vessel pressure and flow distributions during the subcooled and early saturated portion of the blowdown period of a loss-of-coolant-accident. The analysis employs the CEFLASH-4B computer program. (CEFLASH-4B is the CEFLASH-4A code with several subroutines deleted to provide increased nodes and flowpaths. The CEFLASH-4A Computer Program has been approved by the NRC for use in Appendix K analyses.) The specific use of the CEFLASH-4B procedures for blowdown loads analysis is supported by analytical comparisons with results from the large scale LOFT L1-2 experimental blowdown and CEFLASH-4B model parametric studies.

Results for a typical application of this methodology to a loss-of-coolant-accident with mechanistically determined pipe breaks for the Combustion Engineering standard 3800 Mwt plants are presented.

TABLE OF CONTENTS

TABLE OF CONTENTS

TABLE OF CONTENTS

LIST OF APPENDICES

LIST OF SUPPLEMENTS

LIST OF TABLES

LIST OF FIGURES

LIST OF FIGURES (Cont'd.)

596 035

LIST OF FIGURES (Cont'd.)

1.0 INTRODUCTION

1.1 PURPOSE

The purpose of this document is to describe a Combustion Engineering methodology for performing the blowdown loads analysis of a reactor primary system with emphasis on the reactor vessel and its internals. The description includes a presentation of the CEFLASH-4B code, parametric studies performed to show the validity of the model, and a direct comparison of analytical predictions to experimental results in support of the methods.

1.2 Scope

Following the initiation of a postulated break in the primary piping, an imbalanced pressure distribution would develop throughout the initially subcooled fluid in the system. This pressure distribution would dissipate rapidly upon attainment of the local saturation pressures.

In order to predict the space - time distribution of subcooled and two-phase pressures and flow rates, a detailed representation of the primary system has been developed using the CEFLASH-4B computer program. The major portion of the available spacial representation in CEFLASH-4B has been used to represent the reactor vessel (nozzles, downcomer, annulus, lower plenum, core support barrel interior and upper plenum). Hence, the scope of the analyses performed by CEFLASH-4B is primarily focused on the blowdown loads in the region of the reactor vessel, its internals and fuel.

1.3 APPLICABILITY

The blowdown loads obtained with the methods described in this report are applicable to the analysis of the reactor coolant system and its supports with emphasis on the reactor vessel, internals and fuel.

1.4 HISTORICAL PERSPECTIVE

The analysis of the blowdown loads following a postulated pipe rupture has been a consistent part of the safety analysis for Combustion Engineering plants. However, the analytical procedures used to determine these loads have been refined from time to time. These refinements have reflected improvements in mathematical modeling of the physical processes as well as the growth of computer technology and the availability of blowdown test results against which the analytical methods can be compared.

The major contribution to the blowdown loads occurs during the early subcooled portion of the decompression. This is due to the low compressibility of the liquid and results in a large change in local pressures for a small change in density (where the density change results from fluid outflow through the broken pipe). Thus, in order to determine the blowdown loads in the reactor vessel Combustion Engineering initially relied on the WATER-HAMMER code (Reference 1-3) whose solution is limited to subcooled conditions by virtue of its mathematical and physical assumptions.

The analytical procedure for blowdown loads was extended, in 1972, in order to account for both the subcooled and the two-phase portions of the decompression. This procedure involved the use of two codes (WATERHAMMER and CEFLASH-4) and accounted for the considerable damping of the decompression following the occurrence of the local saturation pressures. The computer models for the above codes included an extensive representation of the various regions inside the reactor vessel. In particular, the fluid annulus between the vessel and the core support barrel was represented with a two dimensional (circumferential and axial) grid structure. Descriptions of the models applied to these codes, for PWR's, as well as experimental - analytical comparisons are given in Reference 1-1. NRC approval of these methods is documented in Reference 1-2.

1.5 THE CEFLASH-4B COMPUTER CODE

During the past few years much effort has been devoted to the analytical representation of the decompression process with emphasis on the Loss-of-Coolant Accident for emergency core cooling system considerations. This effort has resulted in the development of the CEFLASH-4A code (References 1-4, 1-5, and 1-6) at Combustion Engineering. For application to the analysis of blowdown loads, the CEFLASH-4A code has been modified to produce a version that is designated as CEFLASH-4B. The code modifications consisted of the removal of several features which do not influence the course of the early term decompression, and the expansion of the amount of spacial detail (volume nodes and flowpaths). The latter changes have increased the ability of the code to yield more detailed information for use in blowdown loads analysis. A description of the CEFLASH-4B code is presented in Section 2. That section also considers the validation of the CEFLASH-4B code version versus the approved CEFLASH-4A code. A comparison of results for the same problem run on both code versions demonstrated excellent agreement. Section 2 also reviews the adherence of the CEFLASH-4B formulation to the conservation laws of mass, energy and momentum for a representative PWR blowdown. It is shown that the numerical results associated with a blowdown loads analysis satisfy the above conservation laws with a high degree of accuracy.

The CEFLASH-4B code does not account for changes in local volumes and pressures which may be caused by structural displacements. The inclusion of such effects results in reduced blowdown loads, particularly on regions such as the core support barrel. Therefore, the exclusion of fluid-structure interaction effects are conservative for determination of blowdown loads.

1.6 EXPERIMENTAL VERIFICATION

The most direct verification of an analytical procedure consists of a comparison to a pertinent experiment. Such a comparison is presented in Section 3 for the LOFT blowdown test L1-2. The bases for selecting LOFT L1-2 for comparison are given in Appendix C and in Reference 1-7.

An extensive parametric study of the LOFT L1-2 test with the CEFLASH-4B code is presented in Appendix D.

1.7 ANALYTICAL STUDIES

In addition to the direct experimental comparison cited above, the CEFLASH-4B code has also been verified for mathematical solution convergence. The studies, which are reported in Section 4, consider the use of different computational time steps as well as various spacial representations for key regions of the reactor vessel model. These key regions are the reactor vessel nozzle adjacent to the postulated cold leg break and the vessel annulus.

As a result of these parametric studies the CEFLASH-4B model developed for a PWR is shown to give a converged solution for the blowdown loads resulting from a postulated pipe break. This conclusion is reinforced by the good experimental-analytical agreement shown in Section 3.

1.8 PWR MODEL

The full CEFLASH-4B model of a PWR is described in Section 5. Analytical results are shown for a System 80 type plant. Separate cases were analyzed for postulated breaks at the ends of the hot and the cold leg nozzles.

1.9 HYDRAULIC FORCES

Section 6 described the generation of the transient hydraulic forces during blowdown from the calculated fluid pressures and flowrates. These forces are subsequently used to drive the structural models of the reactor vessel and its internals in order to determine the response of the system.

1.10 APPENDICIES

The Appendicies to this report include the following supporting material:

A - A description of the input requirements of the CEFLASH-4B code.

B - A discussion of decompression thermodynamics. The emphasis is on the subject of nonequilibrium decompression (rapid pressure drop below the saturation value).

C - A documentation of the bases for selecting the LOFT L1-2 test results for comparison with the CEFLASH-4B predictions. Also, a CEFLASH-4B steady state output for LOFT test L1-2. This output demonstrates that a steady state was satisfied with the code prior to the initiation of the transient.

D - An extensive parametric study of LOFT L1-2 with CEFLASH-4B. These studies were proposed to the NRC in Reference 1-7.

1.11 REFERENCES FOR SECTION 1.0

1-1 Combustion Engineering, Inc., Section 3 ("Loss of Coolant Accident Loads") of "Topical Report on Dynamic Analysis of Reactor Vessel Internals Under Loss-of-Coolant Accident Conditions With Application of Analysis to C-E 800 MWe Class Reactors", CENPD-42, August, 1972 (proprietary).

1-2 Goller, K. R., Chief, Pressurized Water Reactors Branch No. 3, Directorate of Licensing, (AEC) letter to F. M. Stern, Director, NSSS projects, (C-E), December 5, 1973.

1-3 S. Fabic, "Early Blowdown (WATERHAMMER) Analysis for Loss of Fluid Test Facility", Kaiser Engineers, Report No. 65-38-RA, June 1965 (revised April 1967).

1-4 Combustion Engineering, Inc., "CEFLASH-4A: A FORTRAN IV Digital Computer Program for Reactor Blowdown Analysis", CENPD-133P, August 1974 (proprietary).

1-5 Combustion Engineering, Inc., "CEFLASH-4A: A FORTRAN-IV Digital Computer Program for Reactor Blowdown Analysis (Modifications)", CENPD-133P, Supplement 2, February, 1975 (proprietary).

1-6 Scherer, A. E., Manager of Licensing (C-E), letter to D. F. Ross, Assistant Director of Reactor Safety, Division of Systems Safety, LD-76-026, March 1976 (proprietary).

1-7 Scherer, A. E., Licensing Manager (C-E), letter to K. Kneil, Chief Light Water Reactors Branch No. 2, Attachment 1 to LD-77-03, April 7, 1977 (proprietary).

2.0 DESCRIPTION OF THE CEFLASH-4B COMPUTER PROGRAM

The CEFLASH-4B computer program is a modified version of the CEFLASH-4A code (see References 2-1, 2-2, and 2-3) currently approved by the NRC for use by C-E in performing Loss-of-Coolant-Accident (LOCA) analyses (References 2-4 and 2-5). In order to allow more nodal detail for the C-E PWR blowdown loads calculations, CEFLASH-4B has been provided with additional nodes and flowpaths (see Section 2.1.2 below). To accomplish this, several CEFLASH-4A subroutines and options not influencing the early portion of the blowdown have been eliminated. A list of these deleted options is presented in Table 2-1. The items removed from CEFLASH-4A play a negligible role during the subcooled and early saturated decompression. Therefore, the blowdown solutions generated by CEFLASH-4A and CEFLASH-4B are identical (see Section 2.2.1) during the early term.

The purpose of this section is to present the key features of the CEFLASH-4B computer code as they apply to blowdown loads determination. In this process, some information presented in References 2-1, 2-2, and 2-3 is repeated. This adds to the overall clarity and aids the reader in understanding the material that is to be presented in the following sections. In addition, results of a CEFLASH-4B code validation effort are also discussed.

2.1. FEATURES OF THE CEFLASH-4B COMPUTER PROGRAM

This section presents a summary of the important features of the CEFLASH-4B computer program. For additional details the reader is referred to the CEFLASH-4A reference manual and supplementary documents (See above references). A CEFLASH-4B input description may be found in Appendix A of this report.

2.1.1 CEFLASH-4B Equations and Their Solution

The CEFLASH-4B (or 4A) computer program is based on the node-flowpath concept, in which control volumes, denoted as nodes, are connected to other control volumes, in any desired manner via a flow area, denoted as a flow path. The code is formulated to conserve properties of mass, momentum and energy. In the node-flowpath method the equations of conservation of mass and energy are solved in the nodes, and the one-dimensional momentum equation is solved in the flowpaths.

The numerical solution is obtained with the CEFLASH-4B(or 4A) program by numerically integrating the one-dimensional equations for conservation of mass, energy and momentum using a node-flowpath network to model the reactor system. The hydraulic transient of the reactor is coupled to the thermal response of the core by analytically solving the one dimensional radial heat conduction equation in each core node. The system pressure and enthalpy are obtained by performing a property search, using functional fits to steam table data.

2.1.2 Node-Flowpath Detail

The CEFLASH-4B computer program has been developed from CEFLASH-4A, to allow additional nodes and flowpaths. A comparison of the available nodes and flowpaths in CEFLASH-4A and 4B is presented in Table 2-2.

TABLE 2-2

COMPARISON OF AVAILABLE NODES AND FLOWPATHS BETWEEN CEFLASH-4A AND CEFLASH-4B

Code	No. of Nodes	No. of Flowpaths
CEFLASH-4A	70	88
CEFLASH-4B	[	] [5]

The additional flexibility afforded with CEFLASH-4B resulted in the selection of this code for blowdown loads evaluation. Results in Section 4. indicate that lesser nodal detail is satisfactory for most circumstances.

2.1.3 Critical Flow Model

The C-E blowdown loads model uses the C-E[ ]critical [3,5] flow correlation for computing the subcooled and saturated critical fluid discharge through the break. This model has been chosen for several reasons. First, the C-E[ ]correlation, accounts for the non- [3,5] equilibrium nature of the critical discharge during the subcooled period of the vessel decompression. Thus, CEFLASH-4B using the C-E[[3,5]]critical discharge correlation, produces higher (~10%) loads across internal components than equilibrium critical flow formulations (see Section 4.4 for details). Second, as shown in Section 3, use of the C-E [ ]critical flow correlation results in predicted [3,5] blowdown pressures in good agreement with LOFT measurements.

2.1.4 Single Phase Liquid Equation of State

During the subcooled blowdown, fluid pressures, densities and enthalpies are related to one another, at each instant, through property fits checked against the ASME steam table data. All thermodynamic properties are assumed to exist in a state of thermodynamic equilibrium. This assumption is discussed in Appendix B.

2.1.5 Two Phase Phenomena

The C-E blowdown loads model considers voids, once generated, to be dispersed homogeneously throughout the nodal volume. During the blowdown period the bubble rise velocity is of negligible importance to the evaluation of dynamic loads.

Two phase densities, enthalpies and pressures are evaluated assuming the vapor and liquid phases always exist in a state of thermodynamic equilibrium.

Vapor properties are evaluated using numerical fits to saturation line steam data. Correspondingly fluid properties in a two phase node are evaluated from properties found along the liquid saturation curve. [

[3

] (For an additional discussion of this matter the reader is referred to Appendix B.)

2.1.6 Self-Initialization

CEFLASH-4B uses a subroutine recently added to CEFLASH-4A (Reference 2-3) for establishing pre-blowdown steady state conditions. The subroutine allows the CEFLASH-4B node-flowpath network to generate a steady state ("Self-Initialization") through direct use of designer supplied quantities (pressure drops, average reactor power, reactor core boundary conditions and steam generator boundary conditions). Use of raw data to set up a steady state, instead of the previously required system "K" factors, ensures a correctly balanced primary system. This option has been selected for use in blowdown loads analyses. Sample steady state absolute and differential pressure traces may be found in Section 5. Details of the Self-Initialization options can be found in Reference 2-3.

2.2 CODE VALIDATION

2.2.1 Comparsion of a Standard PWR Blowdown With CEFLASH-4A and CEFLASH-4B

A comparisor of predicted blowdown hydrodynamics obtained with CEFLASH-4A and CEFLASH-4B was made using the PWR model presented in Figure 4-1. Typical results of this comparisons are presented in Figures 2-1 and 2-2. The excellent agreement between the two code predictions confirms the similarity of CEFLASH-4A and CEFLASH-4B for blowdown loads analyses.

2.2.2 Adherence to Conservation Laws

Conservation of mass, energy and momentum was investigated by applying the respective conservation principles to the CEFLASH-4B computer output of a typical C-E PWR blowdown case. Conservation laws were evaluated at 20 msec intervals for the duration of a 400 msec blowdown.

2.2.2.1 Conservation of Mass

Mass conservation requires that the instantaneous mass, M(t), of the primary coolant system and containment equal the initial mass, Mo. The total mass was obtained by summing the mass in each node, at discrete times. The resultant instantaneous mass was compared with the initial mass. The results of this comparison, expressed in terms of a relative deviation, (Mo-M(t))/Mo, are presented in Figure 2-3(a). [

[3,5]

]

2.2.2.2 Conservation of Energy

Conservation of energy requires that for a control volume consisting of the primary coolant system and containment, the sum of all the total energy (kinetic energy plus potential energy plus internal energy) within the system be equal to the initial system energy plus any net heat input. The C-E PWR model contains a heat source (core) and two heat sinks (steam generators). CEFLASH-4B keeps track of the integrated energy input and removal from the respective heat sources and sinks. Using available CEFLASH-4B information, a computed total initial energy, E(t) was established by summing total nodal energies and subtracting the net integrated heat input.

If the conservation law is identically satisfied, this sum should be the total initial system energy, Eo. [

]

2.2.2.3 Conservation of Momentum

CEFLASH-4B conserves momentum in the flowpaths. Therefore, momentum conservation was checked dynamically by summing the total pressure drop (including the pump pressure rise) around an arbitrary closed primary coolant flow loop ($\Sigma\Delta P_{LOOP}$). The loop selected is identified in Figure 2-4 with a heavy line. For a conservative system the summation should be identically zero. In this manner the adherence to the momentum conservation law, as programmed in CEFLASH-4B, can be evaluated. The absolute deviations in pressures were converted into relative deviations by normalizing the net loop pressure drop to the instantaneous local pump head, ΔP_H. The results of this analysis are presented in Figure 2-3(c). [

]

2.3 REFERENCES FOR SECTION 2.0

2-1 Combustion Engineering, Inc., "CEFLASH-4A: A Fortran-IV Digital Computer Program for Reactor Blowdown Analysis", CENPD-133P, August 1974, (proprietary).

2-2 Combustion Engineering, Inc. "CEFLASH-4A: A FORTRAN-IV Digital Computer Program for Reactor Blowdown Analysis (Modifications)",CENPD-133P, Supplement 2, February, 1975 (proprietary).

2-3 Scherer, A.E., Licensing Manager, (C-E), Letter to D.F. Ross, Assistant Director of Reactor Safety Division of Systems Safety, LD-76-026, March, 1976 (proprietary).

2-4 Parr, O.D., Chief Light Water Reactor Project Branch 1-3, Division of Reactor Liscensing (NRC), Letter to F.M. Stern, Vice President of Projects (C-E), June,1975.

2-5 Kneil, K., Chief Light Water Reactors Branch No. 2, Letter to A.E. Scherer, Licensing Manager (C-E), August,1976, (Staff Evaluation of CENPD-213).

TABLE 2-1

MODIFICATION OF CEFLASH-4A

TO

CREATE CEFLASH-4B

Removed From CEFLASH-4A	Added To CEFLASH-4A
1. Vessel Wall Heat Conduction Model	1. Additional Volume Nodes
2. Two-Phase Bubble Rise Model	2. Additional Flowpaths
3. Safety Injection Tank Model	
4. Safety Injection Pump Model	
5. Clad Rupture Model	
6. Reactor Kinetics Model	
7. Check Valve Flowpath Model	
8. Restart Option	
9. Output Card Punch Option	

Figure 2-1
IDENTICAL TRANSIENT ABSOLUTE PRESSURE CALCULATED BY CEFLASH-4A AND CEFLASH-4B (DOWNCOMER ANNULUS: UPPER FLANGE REGION)

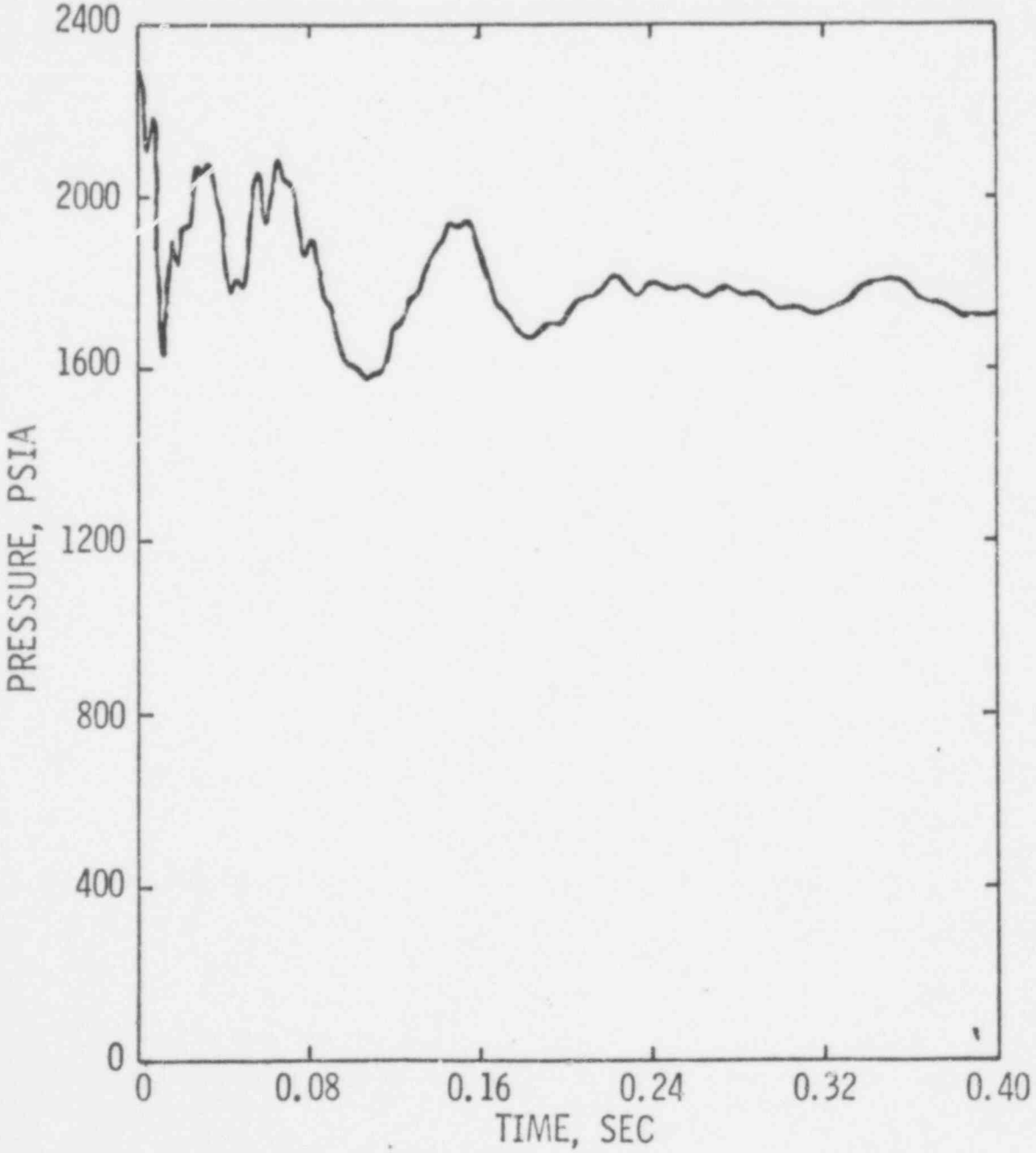

Figure 2-2
IDENTICAL TRANSIENT PRESSURE DROP CALCULATED BY CEFLASH-4A AND CEFLASH-4B (CORE SUPPORT BARREL RADIAL PRESSURE DROP: UPPER FLANGE ELEVATION)

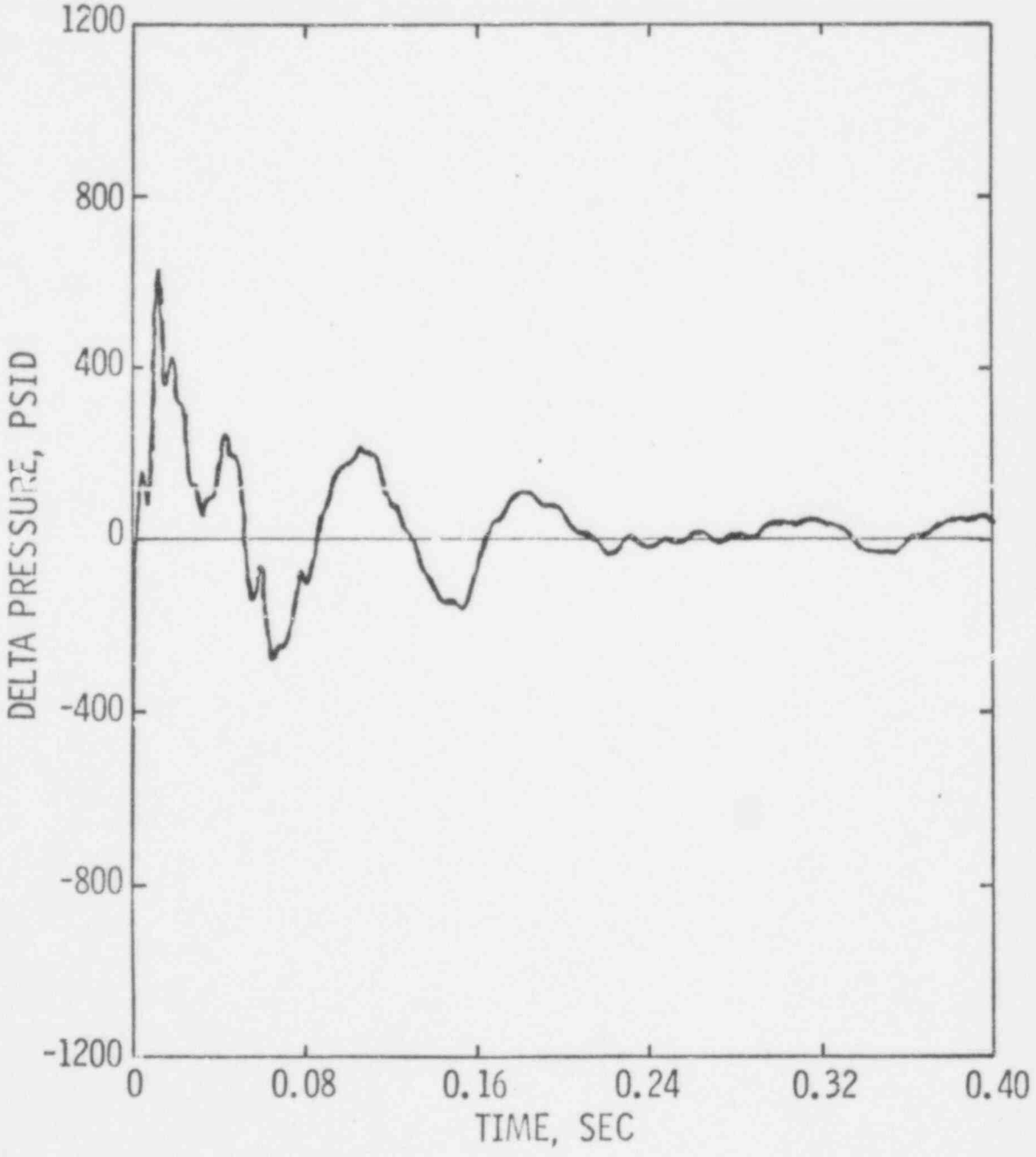

Figure 2-3
ADHERENCE OF CEFLASH-4B
TO CONSERVATION LAWS

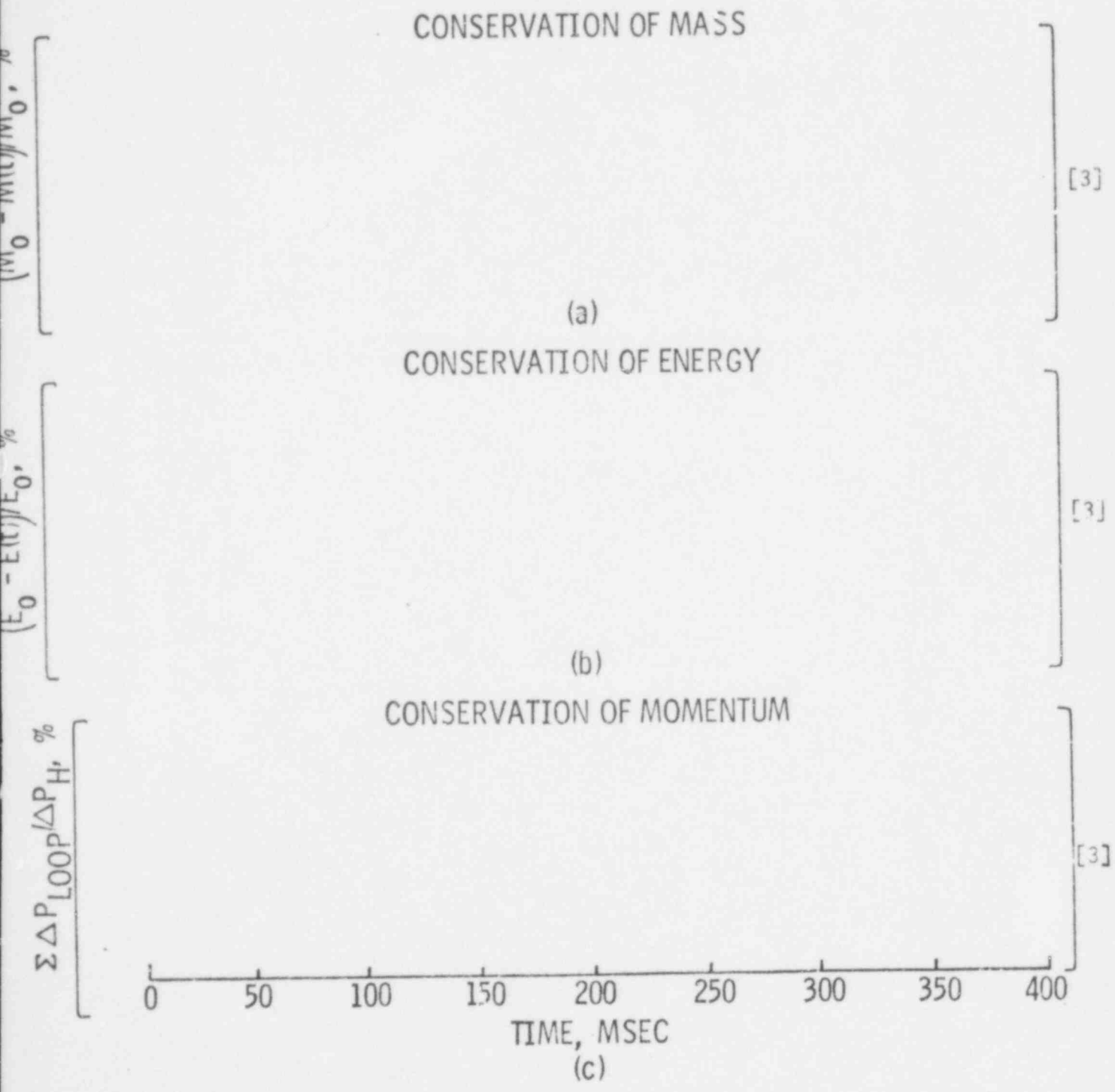

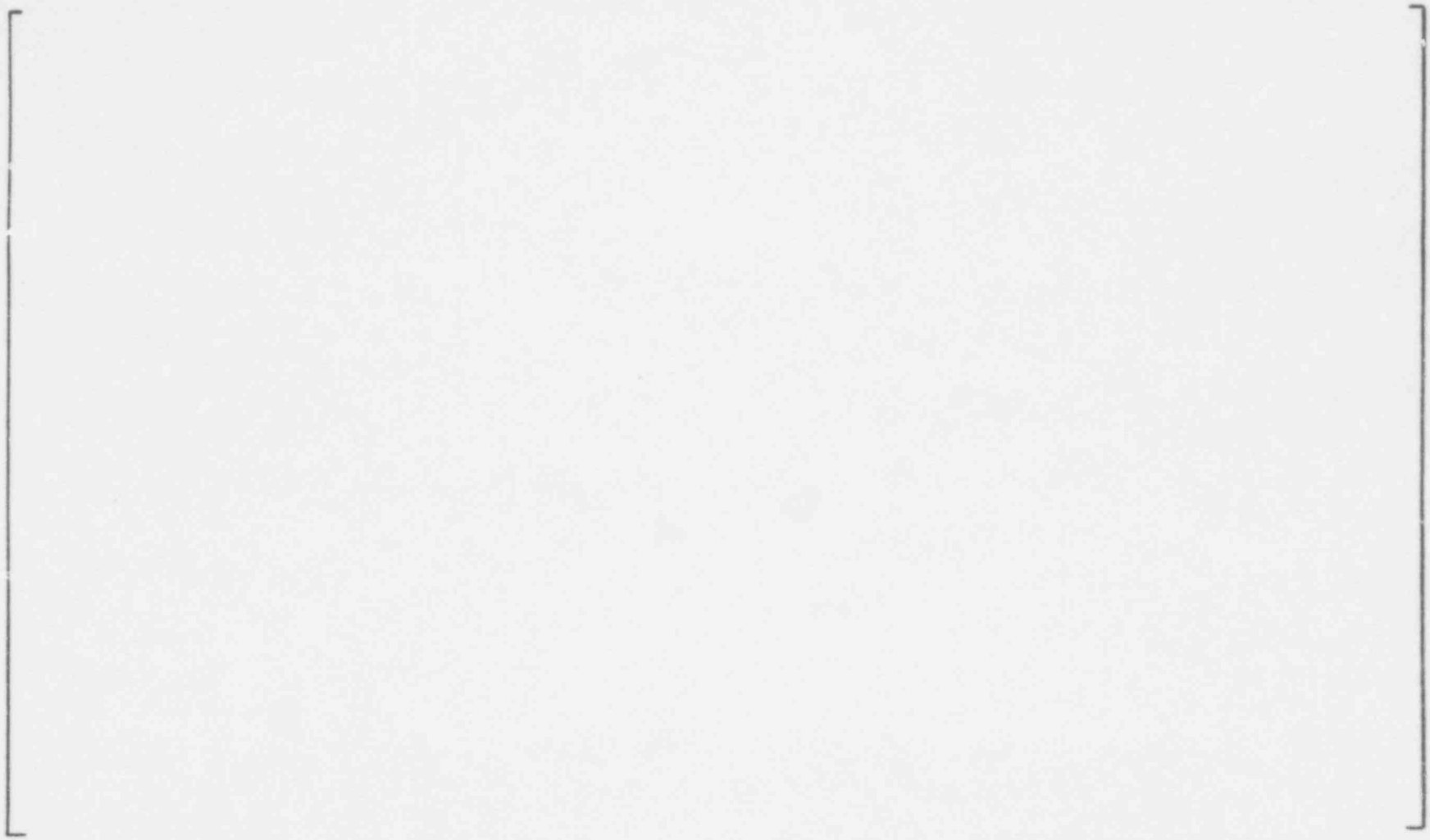

[3,5]

Figure 2-4 CEFLASH-4B MODEL AND PRIMARY CIRCUIT USED IN MOMENTUM CONSERVATION CHECK

3.0 EXPERIMENTAL-ANALYTICAL COMPARISON

This section presents the results of a comparison of CEFLASH-4B predicted pressures with data from the Loss of Fluid Test (LOFT) L1-2. These comparisons verify the capability of the CEFLASH-4B computer code to calculate blowdown pressures.

A series of parametric blowdown analyses for LOFT L1-2 is presented in Appendix D. Additional information regarding C-E's basis for selection of the LOFT experiment and a zero time edit may be found in Appendix C.

3.1 LOFT FACILITY DESCRIPTION

The LOFT system is designed to simulate the major components of a PWR during a LOCA. The system consists of five parts, namely; the reactor vessel, the operating loop, the blowdown loop, the suppression system, and the emergency core cooling system (ECCS). A detailed description of this system is presented in Reference 3-1.

The LOFT reactor vessel (see Figure 3-1) simulates the reactor vessel of a PWR. It has an annular downcomer which connects with the cold legs of both the operating loop and the blowdown system, a lower plenum, lower core support plates, a core simulator which contains orifices which simulate the resistance of the nuclear core and an upper plenum, which connects with the hot legs of both the operating loop and the blowdown system. The operating loop simulates the three intact loops of a 4 loop PWR. The loop contains two primary coolant pumps, a steam generator and a pressurizer.

The blowdown loop can be assembled to simulate the two broken loop during either a cold leg or hot leg guillotine break. Figure 3-2 shows the LOFT major components arranged to simulate a cold leg break. In their configuration the hot leg line of the blowdown system contains a steam generator simulator and a pump simulator.

The blowdown is initiated by the motion of an internal "piston-like" structure housed within the hot and cold leg Quick Opening Blowdown Valves (QOBV). Each valve is designed to linearly expose a 0.56 ft^2 area, with an adjustable break opening time between 10 and 50 milliseconds. The nominal opening time for the LOFT non-nuclear test series is 17.5 milliseconds (see Reference 3-2). Actual opening times varied from test to test. The restricting blowdown break area is defined by orifices at the break plane upstream of the QOBV. For test L1-2 the orifice area at the break plane is .09 ft^2.

The suppression system simulates the containment back pressure of a PWR. It consists of the suppression tank header which is connected to the suppression tank through four parallel vents, and a spray system which controls suppression tank pressure.

During the initial blowdown period, all ECCS systems (not shown) with the exception of parts of the reflood assist bypass are valved off from the main piping.

3.2 LOFT NON-NUCLEAR TEST L1-2

LOFT Test L1-2 was the second in the series of non-nuclear blowdown experiments to be conducted on the LOFT facility. Test L1-2 has been designed to simulate a 200% (double ended full offset shear) guillotine break at the cold leg reactor vessel nozzle. The test was initiated from representative PWR operating conditions. The actual test conditions (from Reference 3-3) are presented in Table 3-1.

TABLE 3-1

LOFT L1-2 PRE-BLOWDOWN

SYSTEM PARAMETERS

System Pressure	:	2270 psia
Fluid Temperature	:	540°F (Isothermal)
Reactor Pressure Vessel Mass Flow Rate	:	2.12×10^6 Lbm/hr

3.3 CEFLASH-4B COMPUTER SIMULATION OF LOFT TEST L1-2

Figure 3-3 shows the CEFLASH-4B network model, developed at Combustion Engineering, for LOFT Test L1-2. The CEFLASH-4B model consists of 65 control volumes and 100 flowpaths. A description of the nodal network is presented in Table 3-2. Flowpaths are identified in Table 3-3.

Nodes 63 and 64 are used to represent the volume of the piping downstream of the break plane orifice, up to and including each QOBV. The pipe rupture was mathematically simulated as a simultaneous linear opening of both QOBV's. A QOBV opening time of 28 milliseconds was selected based on LOFT L1-2 data presented in Reference 3-3.

With the exception of the pressurizer (node 22) and the suppression tank (node 65) all fluid paths and volumes were considered isothermal. The LOFT model has been constructed[ ](see Section 5.0). In particular, the annulus node-flowpath network permits both axial and circumferential transport of pressure waves. [[3]

[3]

] Furthermore, the loop noding arrangement has the same degree of detail as that used for describing a PWR.

The critical flow break model used in this analysis was the [[3]
] presented in Reference 3-4 in conjunction with a [ ] discharge coefficient. Prior to transient analysis a steady state [3]

case was run to ensure a balanced and drift-free pre-rupture condition (A zero time edit for the LOFT analysis can be found in Appendix C). Computations were performed with a [ ] second calculational time step. [ ] [3] The acceptability of this time interval for use in LOFT was justified through time step convergence studies (see Appendix D).

3.4 DISCUSSION OF RESULTS

3.4.1 Comparison of CEFLASH-4B with LOFT Data

Figures 3-4, 3-5 and 3-6 show comparisons of pressure vessel fluid pressure data from LOFT test L1-2 with CEFLASH-4B predictions. CEFLASH-4B pressures agree favorably with LOFT measurements. The zero time, for comparison purposes was taken as the initiation of motion of the QOBV piston. This is approximately ten (10) milliseconds earlier than the experimental "zero" time. (This procedure was also followed by the NRC staff in their LOFT WHAM comparison, Reference 3-5).

It can be seen that during the early phase of blowdown CEFLASH-4B predicts pressures to decay more rapidly than the measured decompressions. This is a consequence of the simplified CEFLASH-4B LOFT break treatment. To visualize this it is helpful to consider the actual LOFT break opening process. After valve actuation, but prior to "piston" unseating, the QOBV piston motion propagates a weak rarefaction wave into the LOFT loop. This "piston-like" behavior continues until the piston unseats and the high pressure loop fluid is vented to the suppression tank. Once the piston unseats, its subsequent motion has been programmed to linearly expose the QOBV pipe area. CEFLASH-4B simulates this process by a linear break area function using experimental opening time measurements for this phase of the process. The earlier decompression resulting from the motion of the piston prior to exposing the break is ignored. As a result, in the CEFLASH-4 model, fluid of initially higher pressure (~150 to 200 psi higher) is vented to the simulated suppression tank. Consequently, a faster initial decompression rate is predicted.

3.4.2 Discussion of Modeling Assumptions

In the preceeding comparisons the entire loop (with the exception of pressurizer and containment nodes) was isothermal. To investigate the

importance of this assumption a best estimate loop temperature distribution was constructed based on experimental data reported in Reference 3-3. Typical results of the study are shown for the LOFT core simulator in Figure 3-7. Predictions of the isothermal and non-isothermal loop transients are substantially the same, with the only minor differences being noted when saturation is achieved.

To substantiate the use of a 28 millisecond break opening time, results were compared with a similar transient in which both QOBV's opened in the average hot and cold leg opening time (22.5 milliseconds). Results of this study are shown in Figure 3-8. Predictions from both models are seen to be in close agreement.

3.5 REFERENCES FOR SECTION 3.0

3-1 Robinson, H. C., "LOFT Systems and Test Description (Loss-of-Coolant Experiments using a Core Simulator"), Tree-Nureg-1019, November 1976.

3-2 McPherson, G. D., "Results of the First Three Non-Nuclear Tests in the LOFT Facility", Nuclear Safety, Vol. 18, No. 3, May-June 1977.

3-3 Robinson, H. C., "Experiment Data Report for LOFT Non-Nuclear Test L1-2", Tree-Nureg-1026, January 1977.

3-4 Combustion Engineering, Inc., "Calculative Methods for the C-E Large Break LOCA Evaluation Model", CENPD-132P, August 1974,(Proprietary).

3-5 NRC Staff, "NRC Multiflex Review" (Presentation made by the NRC Staff to ACRS), May 25, 1977, Los Angeles.

3-6 Berta, V. T., et.al., "Experiment Prediction of LOFT Non-Nuclear Experiment L1-2", EP-L1-2, December, 1975.

TABLE 3-2

CEFLASH-4B LOFT L1-2 NODAL DESCRIPTION*

NODE NO.	DESCRIPTION
[	]

596 062

TABLE 3-2 (Cont'd.)

CEFLASH-4B LOFT L1-2 NODAL DESCRIPTION*

NODE NO.	DESCRIPTION
[	]

[3]

TABLE 3-2 (Cont'd.)

CEFLASH-4B LOFT L1-2 NODAL DESCRIPTION*

NODE NO.	DESCRIPTION
[	]

[3]

* Piping section numbers refer to the identification in Tables VI and XIV of Reference 3-1

TABLE 3-3

CEFLASH-4B LOFT L1-2 FLOWPATH DESCRIPTION

FLOWPATH NUMBER	DESCRIPTION
[	]

[3]

TABLE 3-3 (Cont'd)

CEFLASH-4B LOFT L1-2 FLOWPATH DESCRIPTION

FLOWPATH NUMBER	DESCRIPTION

TABLE 3-3 (Cont'd.)

CEFLASH-4B LOFT L1-2 FLOWPATH DESCRIPTION

FLOWPATH NUMBER	DESCRIPTION
[	] [3]

TABLE 3-3 (Cont'd.)

CEFLASH-4B LOFT L1-2 FLOWPATH DESCRIPTION

FLOWPATH NUMBER	DESCRIPTION
[	] [3]

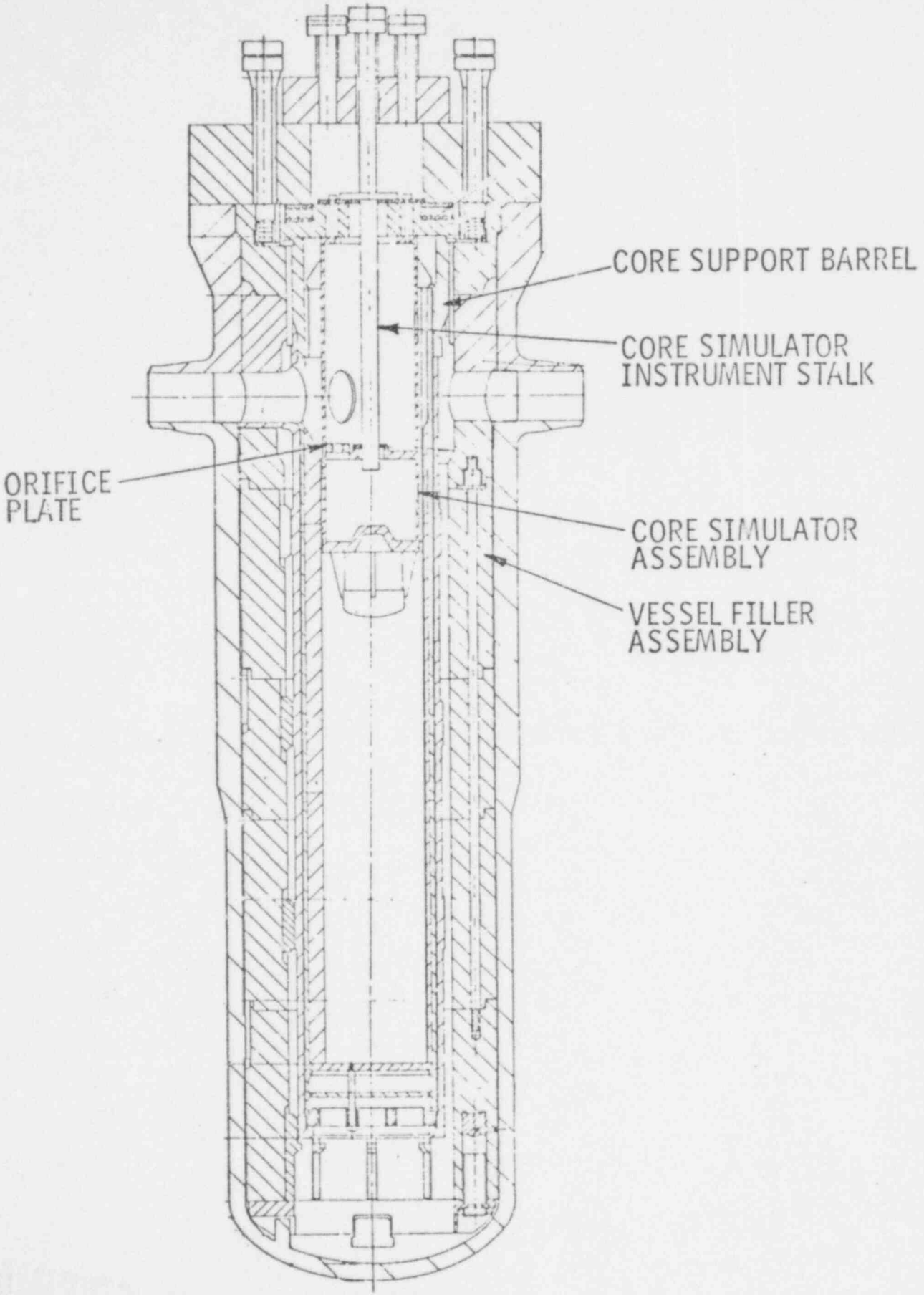

Figure 3-1
LOFT REACTOR PRESSURE VESSEL

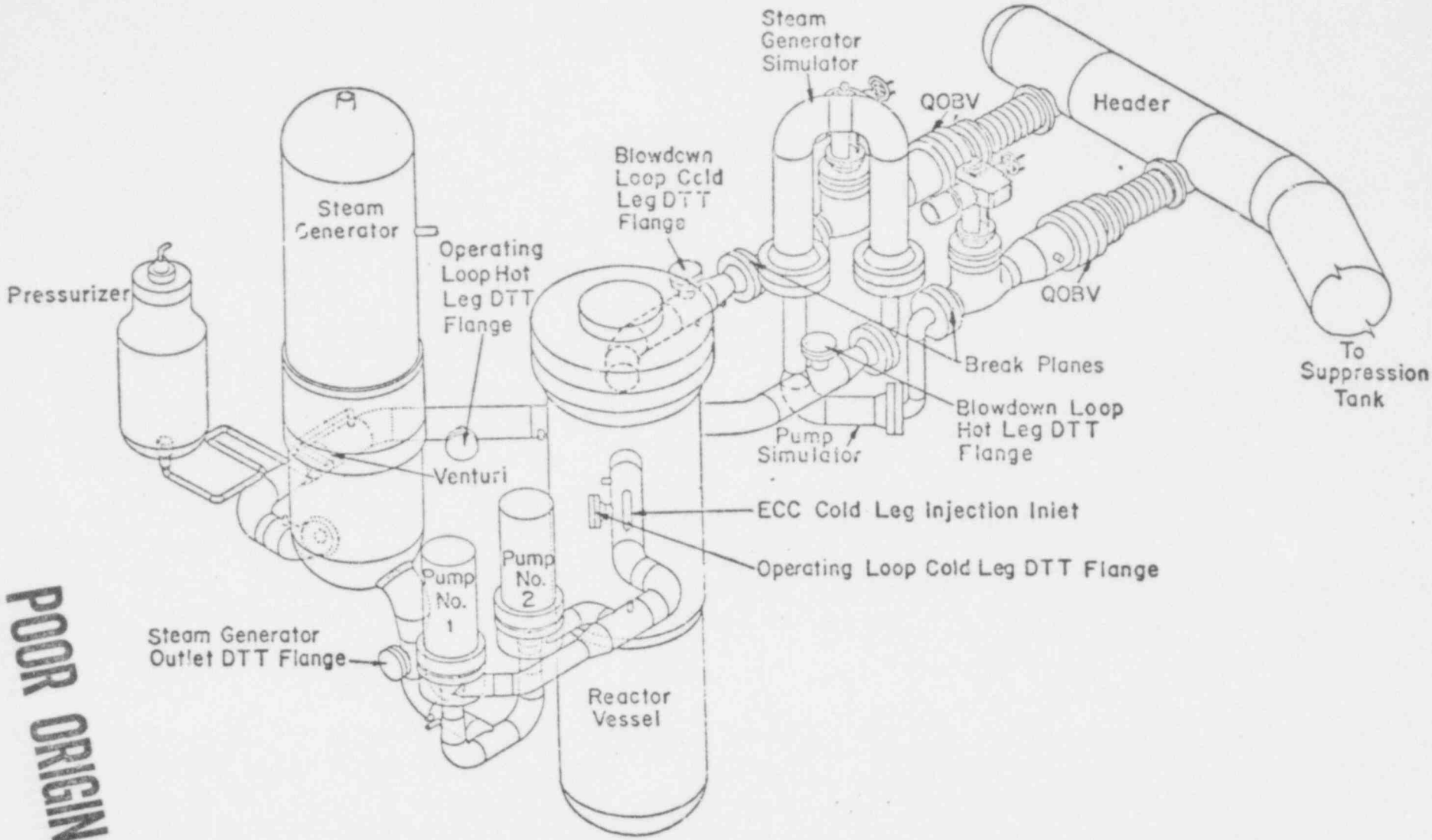

Figure 3-2
LOFT MAJOR COMPONENTS

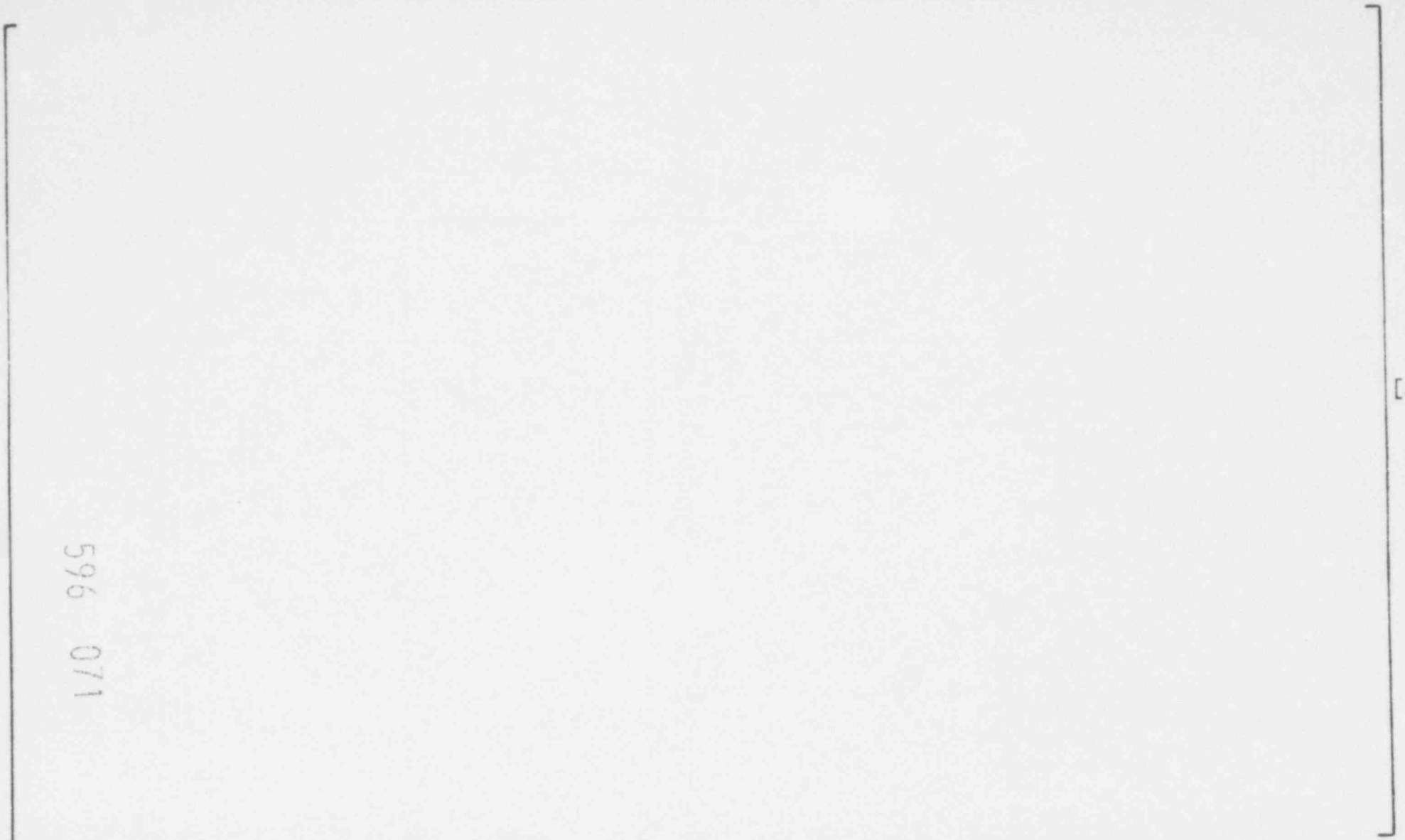

[3,5]

596 071

Figure 3-3
CEFLASH-4B MODEL OF LOFT L1-2

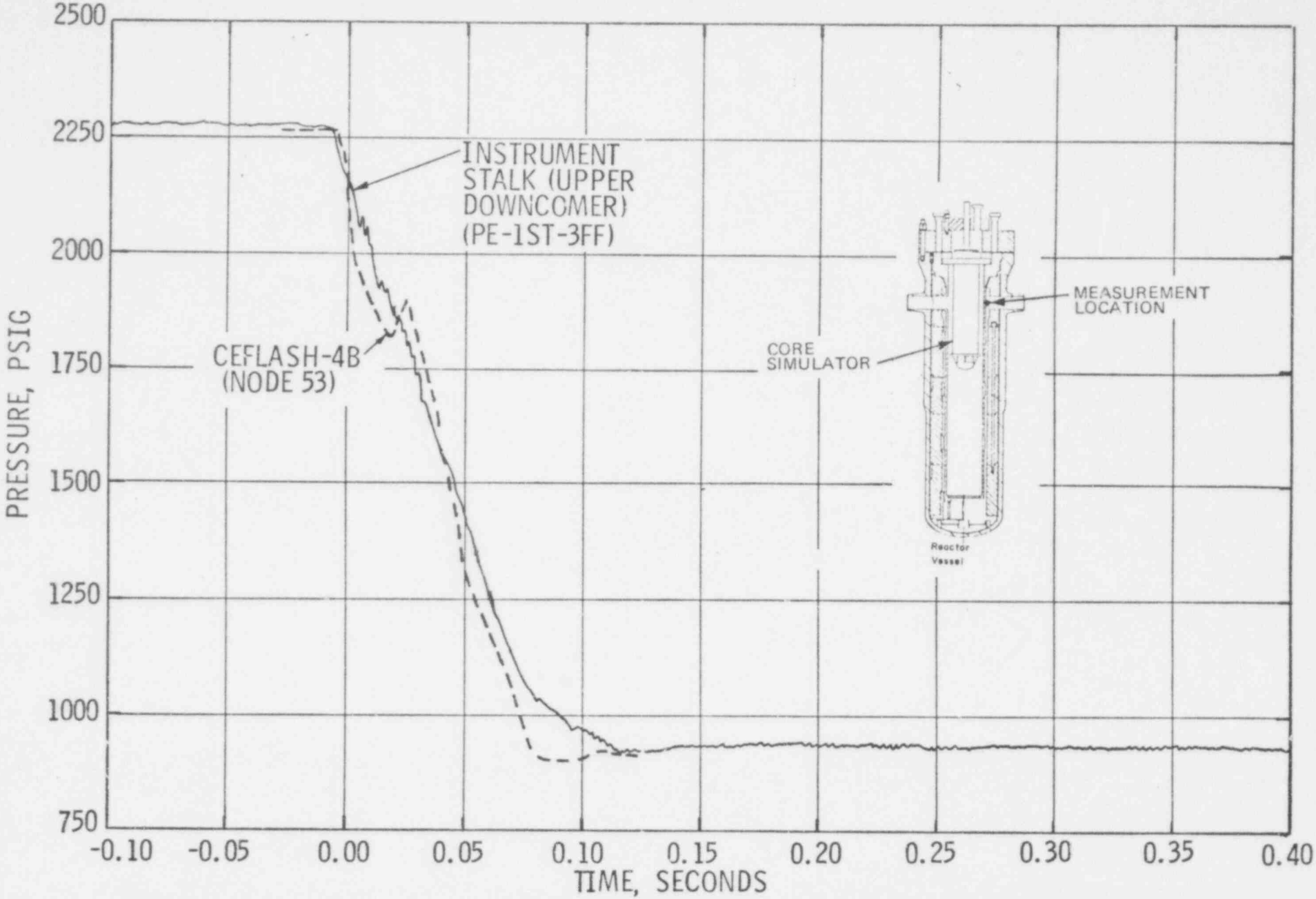
2500
2250
2000
1750
1500
1250
1000
750
PRESSURE, PSIG
-0.10
-0.05
0.00
0.05
0.10
0.15
0.20
0.25
0.30
0.35
0.40
TIME, SECONDS
INSTRUMENT STALK (UPPER DOWNCOMER) (PE-1ST-3FF)
CEFLASH-4B (NODE 53)
CORE SIMULATOR
MEASUREMENT LOCATION
Reactor Vessel

Figure 3-4

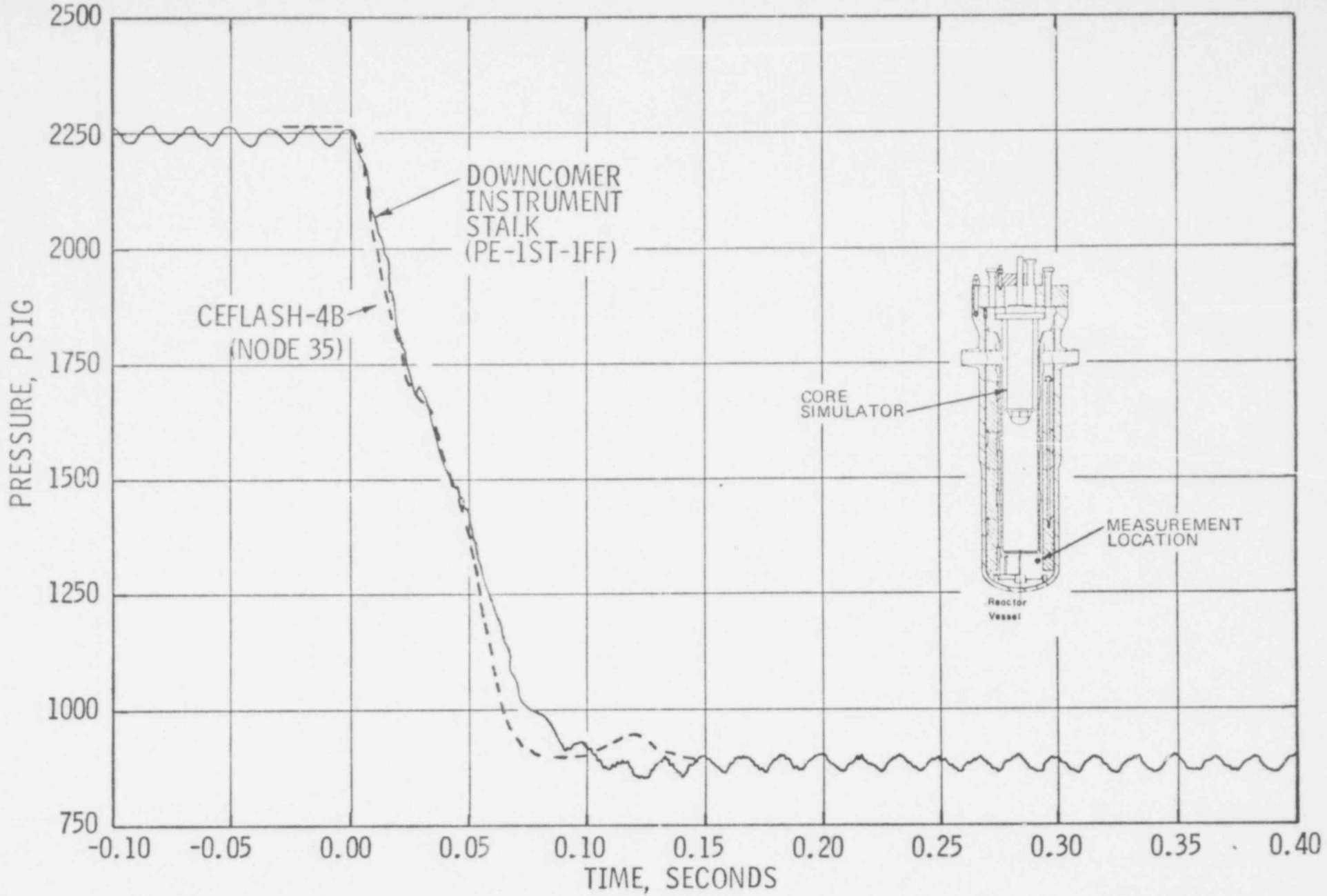

Figure 3-5

COMPARISON OF LOFT L1-2 DATA WITH CEFLASH-4B PREDICTIONS

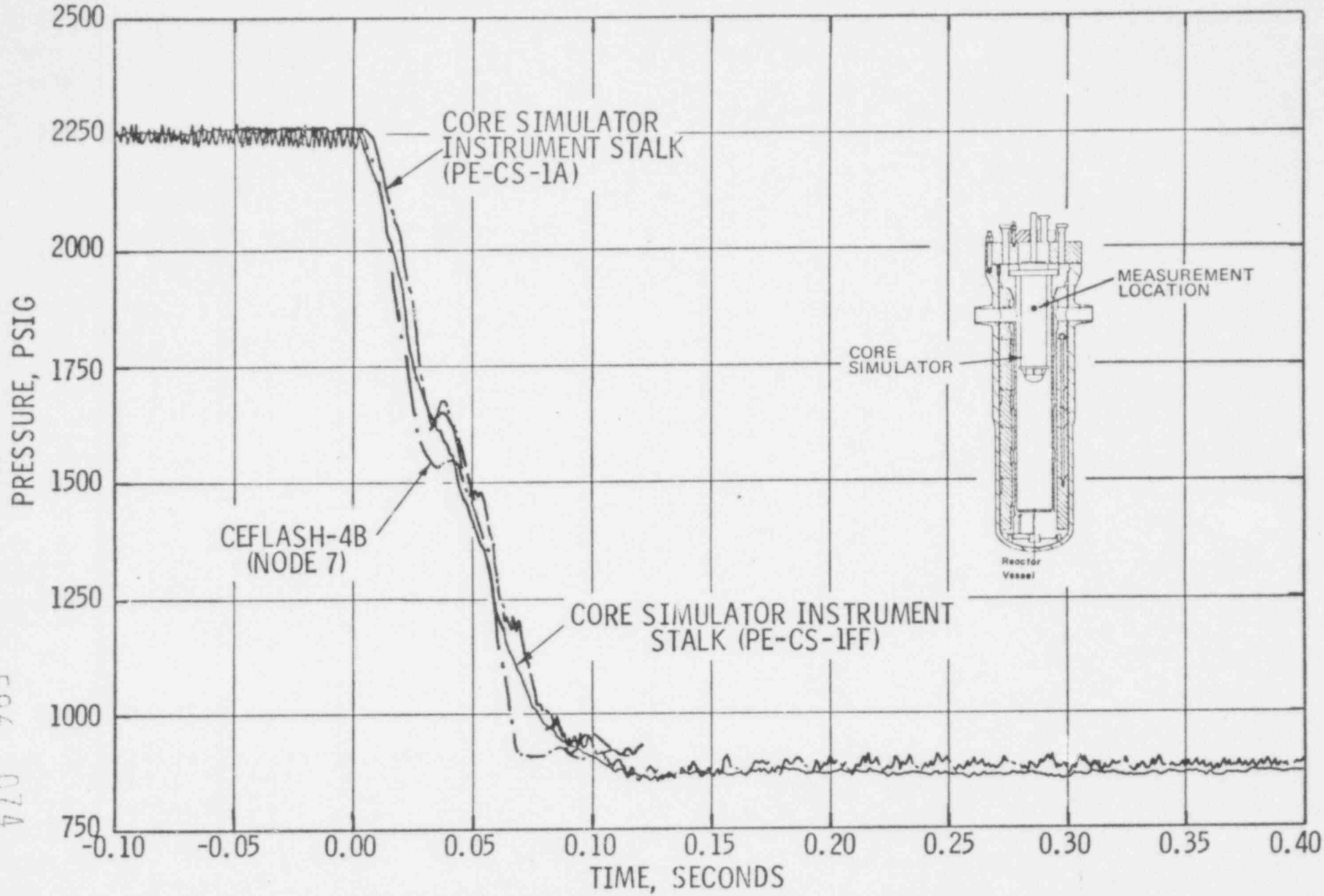

Figure 3-6

COMPARISON OF LOFT L1-2 DATA WITH CEFLASH-4B PREDICTIONS

Figure 3-7

EFFECT OF ISOTHERMAL LOOP
ASSUMPTION ON CEFLASH-4B PREDICTED PRESSURES
(CORE SIMULATOR: NODE 7)

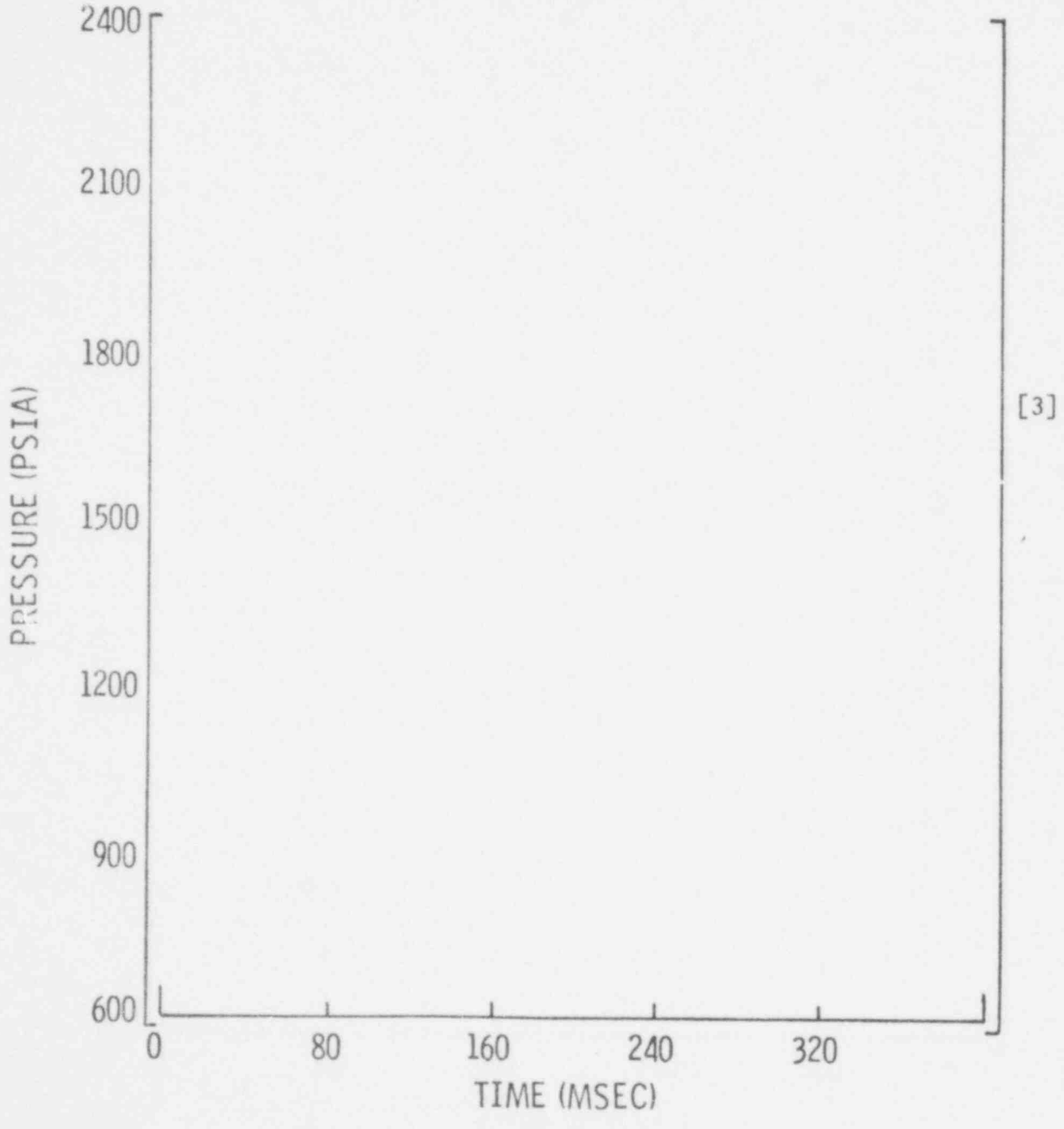

Figure 3-8

SENSITIVITY OF CEFLASH-4B
PREDICTED PRESSURES TO ASSUMED QOBV
OPENING TIME
(CORE SIMULATOR NODE 7)

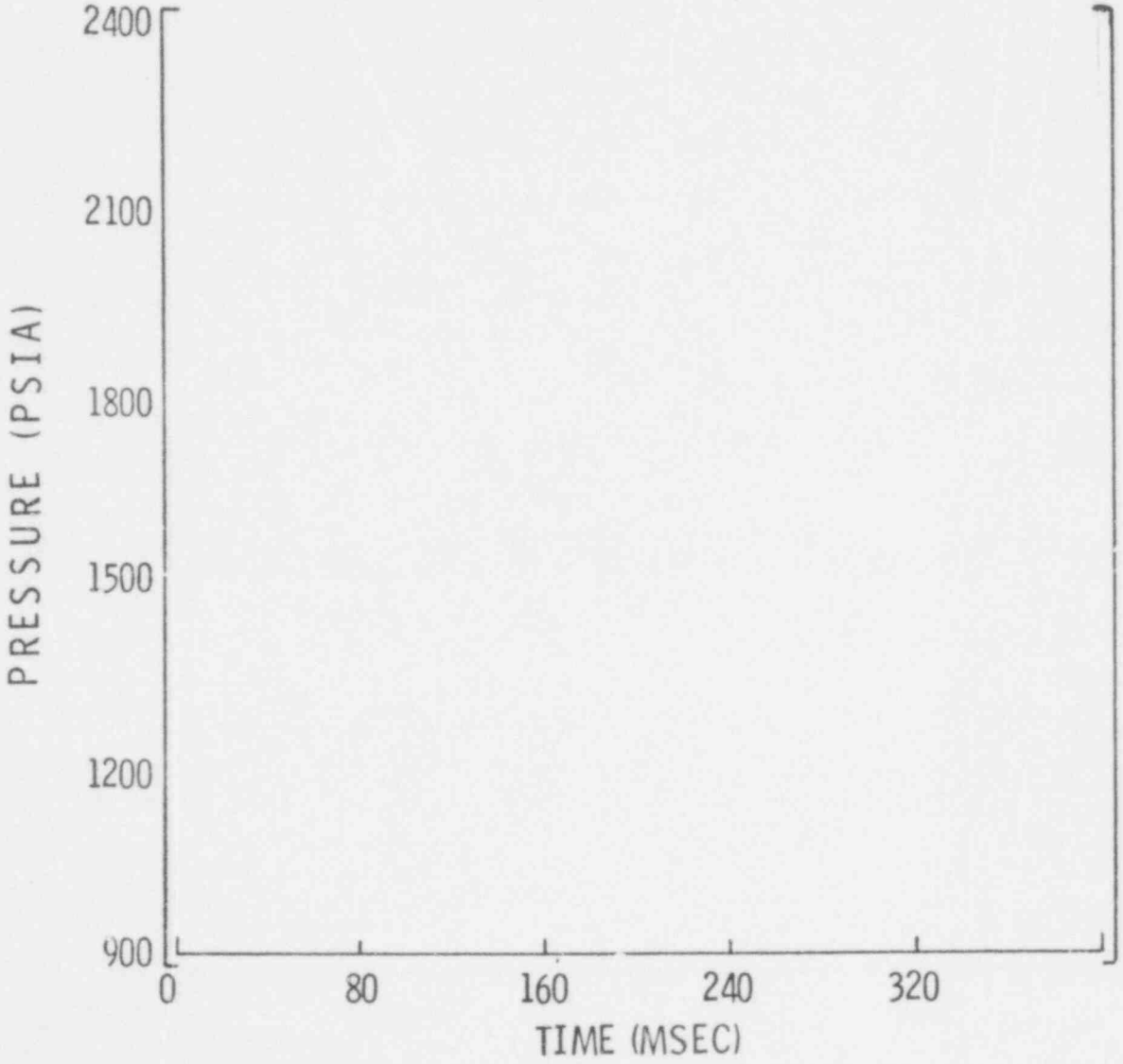

[3]

4.0 CEFLASH-4B PARAMETER STUDIES

This section presents the results of an extensive parametric investigation of several key elements in the blowdown loads analysis procedures. These studies have been used to establish and/or confirm modeling procedures and to understand their consequences.

Unless otherwise specified, the base computer model used for these studies was the CEFLASH-4A* computer simulation of a System 80 350 in^2 mechanistic break at the reactor cold leg nozzle. The node-flowpath network for this model is presented in Figure 4-1. The model consists of [ ] nodes and [ ] [3] flowpaths. Tables 4-1 and 4-2 provide the corresponding node and flowpath descriptions. The break parameters for the base case are as follows:

TABLE 4-3
CEFLASH-4A BASE MODEL
BREAK PARAMETERS

Total Break Area:	2.43 ft^2 (350 in^2) (See Reference 4-1)
Break Opening Time:	5.0 milliseconds
Break Opening Function:	[ ] [3]
Critical Flow Correlation:	
Nozzle Discharge Coefficient:	

Studies reported in this section investigate the sensitivity of the base model to variations in the size of the calculational time step, type of critical flow correlation, flowpath modeling and amount of spacial detail.

4.1 TIME STEP CONVERGENCE STUDY

The CEFLASH-4 (A or B) computer code requires that a computational time step (DELTN) be prescribed as input by the user (see Appendix A). The

* Results of these studies are considered applicable to CEFLASH-4B analyses (See Section 2.2.1).

596 077

value of this time step is important to the predictions in order to assure a convergent numerical solution.

Based on past experience with CEFLASH-4A analyses, the time step investigation was restricted to three calculation time intervals, [ ] second. Identical blowdown transients were run with each of the above values of DELTN. Typical results of this study are presented in Figures 4-2 through 4-4. Predicted pressures and momentum flow parameters obtained for the two smaller calculational time intervals are in excellent agreement, thus indicating the solutions to be convergent. Results of the model run with the largest [ ] time step display a small departure from the others, particularly at solution extrema. [3]

As a consequence of the above study a [ ] second computational time step was selected for use in blowdown loads design analyses. [3]

4.2 SENSITIVITY OF DYNAMIC LOADS TO THE CRITICAL FLOW CORRELATION

The Combustion Engineering Inc. blowdown loads procedure uses the C-E [ ] critical flow correlation (see Reference 4-2) to predict the subcooled and saturated nozzle critical discharge flowrates. The C-E [ ] formulation is a nonequilibrium correlation well suited to predict the subcooled phase of blowdown. The use of this correlation was shown to result in good agreement with LOFT L1-2 experimental data (see Section 3). The impact of this selection was investigated by comparing predicted absolute pressures and pressure differences from typical C-E PWR analyses with those obtained using the Moody and Homogeneous Equilibrium critical flow models. [3] [3]

Typical comparisons of the C-E base model predictions with those of the Moody and Homogeneous Equilibrium Model (HEM) are presented in Figures 4-5 through 4-8. With all other input parameters made equal the Combustion Engineering, Inc. model provides for a more rapid decompression and concomitent higher pressure loads than either of the other critical flow models.

596 078

This is a consequence of the nonequilibrium nature of the C-E[ ]model, which allows critical flowrates in excess of that predicted by either of the two equilibrium based critical flow models, with which it was compared. [3]

4.3 SENSITIVITY OF DYNAMIC LOADS TO FLOWPATH MODELING

In modeling typical C-E PWR's with CEFLASH-4B, some internal vessel components, specifically, the fuel alignment plate, upper guide structure plate and lower core support structure assembly are not treated discretely. Therefore, loads across these structures must be evaluated from CEFLASH-4B predicted fluid dynamic variables through use of the momentum control volume concept. Use of such a procedure has several advantages. Through careful definition of the control surfaces resultant plate loads can be accurately established. This is true, even for those models employing limited node detail in the vicinity of the structure. [

] [3]

This section presents an investigation of the sensitivity of CEFLASH-4B predicted nodal pressure drops and associated plate dynamic loads (obtained by control volume type analyses) to the plate flowpath definition. [

[3]

]

Two flowpath modeling procedures were compared. These were:

(1) [

[3]

]

(2)[

[3]

]

Diagrams describing these two methods are presented in Figures 4-9(a) and 4-9(b) respectively.

Figure 4-10 presents results of nodal differential pressure predictions between nodes across a representative internal plate (fuel alignment plate). Directly using the pressure drops obtained from the standard modeling procedure results in a higher plate load (5 -10 psid) than that obtained with the plate flowpath model. The lower pressure difference is representative of the actual plate load. [

[3]

] Depending on the model nodal scheme this can be substantially greater than the plate pressure drop.

Using the base model one can calculate the pressure drop across the plate. This is done in an approximate fashion for illustration only. For the subcooled blowdown the CEFLASH-4 (A or B) momentum equation can be used to derive the following approximate relationship between the plate pressure drop and the node center to node center pressure drop:

[

] (4-1) [3]

596 080

where:

[ ] [3,5]

Equation 4-1 is used as a vehicle to show the equivalence of the two CEFLASH-4B formulations, regarding plate loads. This procedure is not otherwise used in the Combustion Engineering blowdown loads methodology. In the derivation of the above equation the contribution of all non-inertial components to the upstream and downstream flowpath pressure drops of the plate have been assumed small compared to their inertial components.

Figure 4-11 superimposes the $\Delta P_{plate}(t)$ calculated from the equation 4-1, using information available from the base model, on the plate pressure drop computed with the CEFLASH-4A plate model (Method 2). Agreement between the two predicted plate pressure drops is excellent. Similar agreement was found for other C-E reactor plates.

596 081

During the subcooled blowdown phase of a LOCA plate loads can be treated, in the CEFLASH-4B computer code,[ ] [3]

] For both situations resultant pressure drops are converted into plate forces using a control volume analysis technique consistent with the CEFLASH-4B nodal representation (see Section 6.3). Thus, the model invariance of predicted plate blowdown forces is ensured.

4.4 SPACIAL CONVERGENCE STUDIES

The CEFLASH-4(A or B) computer code(s) represent a region of space via an assemblage of volume nodes and flowpaths. These codes have been employed with different volume node and flowpath models in order to assess the convergence of the transient pressure solutions following a postulated rupture of a RPV cold leg nozzle. The following spacial convergence studies indicate the adequacy of the node and flowpath models selected to represent a PWR for blowdown loads purposes.

4.4.1 Spacial Representation Of The Downcomer Annulus

This section presents the results of two annulus nodalization studies to determine the influence of the vessel annulus spacial representation on the downcomer space-time pressure response during decompression. These studies confirm the adequacy of a[ ] [3]]CEFLASH-4B downcomer annulus representation, for use in the prediction of blowdown pressures.

The first study investigated the asymmetric pressure response to a cold leg break for an idealized annular structure of dimensions similar to a C-E PWR. This study considered a restricted region of the reactor which consisted of the vessel annulus, portions of each of the four cold legs at appropriate angular locations about the vessel circumference, and a lower plenum region at the vessel bottom. The annulus region was modeled with

arrangements of{

[3]

} The distribution of the annulus volume and the flowpath descriptions for these three models is given in Tables 4-4 and 4-5 respectively. These annular nodal arrangements are presented schematically in Figure 4-15.

The vessel annulus representation, being limited in size, permitted different spacial models to be studied in more detail than would a full PWR model. The results of the annulus study provides a more rigorous test of convergence than does a full PWR model. This is because the initial liquid volume in the annulus region is considerably less than that in an entire PWR. Therefore, during an assumed pipe rupture the transient pressures in the annulus model fall more rapidly than do the pressures in the annulus region of a full PWR model for the same size breaks. Second, as a consequence of its reduced size, the annulus model experiences more frequent and stronger pressure reflections than are possible in a real PWR.

For these cases the base conditions are presented in Table 4-6.

TABLE 4-6

Base Conditions For Annulus Model Parametric Studies

region modeled	annulus, cold legs and lower plenum
volumetric distribution	see table 4-4
initial pressure	~2300 psia
initial temperature	565°F
break location	end of cold leg nozzle
break size	350 in^2
break opening time	5 millisecond{ } [3]

The portion of the annulus that experiences the most severe decompression is adjacent to the broken nozzle. The transient pressure response for this region for all three cases is shown in Figure 4-16. It is seen from this figure that there is little difference between the results for the three different annulus models. Good agreement is also obtained at locations in the annulus that are further away from the break. This can be seen in Figures 4-17 and 4-18 which compare these pressures at locations which are at the nozzle elevation and bottom of the annulus, and 180° around the annulus from the break.

Figure 4-19(a) presents a comparison of the transient pressure difference around the core barrel at the nozzle elevation for the three cases. This function is the difference between the pressure in the annulus node adjacent to the broken nozzle (Figure 4-16) and the node 180° around the annulus from the broken nozzle (Figure 4-17). As can be seen from Figure 4-19(a) there is excellent agreement among the three predictions for the first pulse (which has the greatest magnitude). For the subsequent pulses predictions of the[ ]models remain virtually identical, while some [3
differences are noted with the[ ]model. These differences are generally [3
observable only at the pressure pulse peaks, with the[ ]model giving the [3
highest magnitude pulses. Towards the lower portion of the downcomer these differences diminish and all three models demonstrate excellent agreement (see Figure 19 (b)). The larger liquid mass in a full PWR primary loop model will attenuate the rate of decompression relative to the annulus models. This should result in even better agreement for the annulus pressures.

The second study of the annulus models consisted of a full representation of a PWR (System 80) primary circuit. Two different models of this system were investigated. The principal difference between these models was in the treatment of the vessel annulus. PWR models with both[ ](see Figure 4-1) [3
and[ ]annulus nodal arrangements were studied. The[ ]node, PWR [3
network is presented and discussed in Chapter 5. Since the node and flowpath requirements of the later model would exceed the CEFLASH-4A, computer code capability, both studies were performed using its expanded, CEFLASH-4B, version.

The cold leg break conditions were studied for both a mechanistic (2.43 ft^2) and a full offset shear (9.817ft^2) double ended cold leg guillotine breaks. The latter break employed a representative break opening time of 18.5 milliseconds.

Comparisons of the transient pressure differences across the core support barrel for these two PWR models are shown in Figure 4-20 for a mechanistic break LOCA. As seen from this figure there is excellent agreement between the results obtained with the[ ]and[ ]annulus representations. Comparisons of predicted absolute pressures and pressure differences between the two models for the above full offset shear double ended guillotine simulation, similarly demonstrates good agreement (see Figure 4-21). [3]

Based on the above studies the[ ]node annulus representation has selected for design applications. [3,5]

[[3,5]

]

4.4.2 Spacial Representation of the Reactor Pressure Vessel Nozzle in the Broken Loop

This section describes the investigation into the influence of the spacial representation of the ruptured reactor pressure vessel nozzle on the prediction of blowdown pressures. The motivation for studying the spacial detail at this location, is to assure proper representation of the initial rarefaction wave entering the reactor pressure vessel downcomer.

Results of a spacial detail study indicates that treating the broken nozzle as a single node gives an adequate prediction of blowdown hydraulics.

To accomodate the added detail in the reactor pressure vessel nozzle model it was necessary to use the CEFLASH-4B computer code because of its greater node and flowpath capacity.

Three methods of modeling the broken nozzle region were analyzed. These were:

(1) [3]

This section describes the broken nozzle spacial representation models used in the analysis.

(2)

(3)

A sketch of these three models is presented in Figure 4-22. The basic nodal structure is similar to Figure 4-1.

Comparison of the absolute and differential pressures obtained from the three models are in excellent agreement. Typical comparisons of absolute pressure are presented in Figures 4-23, 4-24 and 4-25. Node numbers refer to control volume locations presented in Figure 4-1.

Comparisons of the radial pressure differential across the core barrel (inside-outside) are presented in Figures 4-26 and 4-27. The three break node models reveal no significant differences. The worst agreement was at the annulus node adjacent to nozzle where the break occurred (see Figure 4-26).

A study of the applied impulses* (see Table 4-7) shows the three cases produced virtually the same applied pressure load over the initial blowdown period. The impulse applied to [ ] the core barrel at the nozzle elevation over the first 31 msec (duration of the first impluse) showed that the [ ] nozzle case gave 0.11% higher impulse and the [ ] nozzle case gave 0.56% lower impulse than the base case with one node in the nozzle. [3]

TABLE 4-7

Integrated Impulse at the Nozzle Centerline Elevation

(Impulse Integrated from 0 to 31 msec)

($P_{NODE\ 34} - P_{NODE\ 12}$)

NODES IN RPV INLET NOZZLE	Integrated Impulse[1] ($\times 10^4$ lbf - sec)	Relative Difference To BASE CASE (%)
[ ] (BASE CASE)	[ ]	-
		0.11
		-0.56

[3]

(1) Impulse applies to Core Barrel projected Area segment of [ ] ft^2 [3]

The delta pressure across the core axially is virtually the same for all three break node models (Figure 4-28). This indicates that any pressure fluctuation between the models has died out by the time the decompression wave has reached the reactor vessel internals.

*The impluse over time t was calculated as $\int_0^t \Delta P.A.dt$, where ΔP is the pressure difference across the structure and A is the projected area of the structure on which the ΔP acts; t is time (see Reference 4-3).

These comparisons show that increased nodal detail, over modeling the RPV nozzle as a [ ] does not result in significant changes in predicted absolute pressures or hydraulic loads. Therefore, the [ ] has been selected for use in design analyses.

4.5 REFERENCES FOR SECTION 4.0

4-1 Combustion Engineering, Inc., "Design Basis Pipe Breaks", CENDP-168-A, June 1977

4-2 Combustion Engineering, Inc., "Calculative Methods for the C-E Large Break LOCA Evaluation Model", CENPD-123P, August 1974, (proprietary)

4-3 Fox, E.A., Mechanics, Harper & Row, New York, 1973,

TABLE 4-1

PARAMETER STUDY BASE MODEL NODAL DESCRIPTION

NODE NO.	DESCRIPTION
[3]	

596 089

TABLE 4-1 (Cont'd.)

PARAMETER STUDY BASE MODEL NODAL DESCRIPTION

NODE NO.	DESCRIPTION
[	] [3]

596 090

TABLE 4-2

PARAMETER STUDY BASE MODEL FLOWPATH DESCRIPTION

FLOWPATH NUMBER	DESCRIPTION
[3]	

TABLE 4-2 (Cont'd.)

PARAMETER STUDY BASE MODEL FLOWPATH DESCRIPTION

FLOWPATH NUMBER	DESCRIPTION
[	] [3]

596 092

TABLE 4-2 (Cont'd.)

PARAMETER STUDY BASE MODEL FLOWPATH DESCRIPTION

FLOWPATH NUMBER	DESCRIPTION
[3]	

TABLE 4-4

NODE DESCRIPTION FOR ANNULUS SPECIAL REPRESENTATION STUDY

NODE (s) NO. (s)	NODE DESCRIPTION
1, 3, 4, 6	[3,5]
2, 5	
7, 9, 10, 12	
8, 11	
13, 15, 16, 18	
14, 17	
19, 21, 22, 24	
20, 23	
25	

NODE DESCRIPTION FOR ANNULUS SPACIAL REPRESENTATION STUDY

NODE (s) NO. (s)	NODE DESCRIPTION
26	[3,5]
27	
28	
29	
30	
31	
32	
33	
34	
35	

TABLE 4-4 (Cont'd.)

NODE DESCRIPTION FOR ANNULUS SPACIAL REPRESENTATION STUDY

NODE (s) NO. (s)	NODE DESCRIPTION
36	[3,5]
37	
38	
39	
40	
41	
42	

TABLE 4-4 (Cont'd.)

NODE DESCRIPTION FOR ANNULUS SPACIAL REPRESENTATION STUDY

NODE (s) NO. (s)	NODE DESCRIPTION
43	[3,5]
44	
45	
46	

(1) Downcomer height is defined in this context as the distance between the top of the FAP and the bottom of the flow skirt.

TABLE 4-5

FLOWPATH DESCRIPTIONS FOR ANNULUS SPACIAL REPRESENTATION STUDY

FLOWPATH (s) NO. (s)	FLOWPATH DESCRIPTION
1, 4	
2, 5	
3, 6	
7, 8, 9, 10, 11, 12	
13, 16	
15, 18	
14, 17	
19, 20, 21, 22, 23, 24	
25, 28	

[3,5]

TABLE 4-5 (Cont'd.)

FLOWPATH DESCRIPTIONS FOR ANNULUS SPACIAL REPRESENTATION STUDY

FLOWPATH (s) NO. (s)	FLOWPATH DESCRIPTION
26, 29	[3,5]
27, 30	
31, 32, 33 34, 35, 36	
37, 40	
38, 41	
39, 42	
43, 44, 45, 46, 47, 48	
49	

TABLE 4-5 (cont'd.)

FLOWPATH DESCRIPTIONS FOR ANNULUS SPACIAL REPRESENTATION STUDY

FLOWPATH (s) NO. (s)	FLOWPATH DESCRIPTION
50, 51, 52	[3,5]
53	
54	
55	
56	
57	
58	
59, 60	
61, 62	

TABLE 4-5 (Cont'd.)

FLOWPATH DESCRIPTIONS FOR ANNULUS SPACIAL REPRESENTATION STUDY

FLOWPATH (s) NO. (s)	
63, 64	[3,5]
65, 66	
67, 68	
69, 70	
71, 72	
73	
74, 75, 76	
77	
78	
79	
80	
81	

[3,5]

Figure 4-1
PARAMETER STUDY BASE MODEL

Figure 4-2
TIME STEP STUDY
NODAL PRESSURE
(NODE 12)

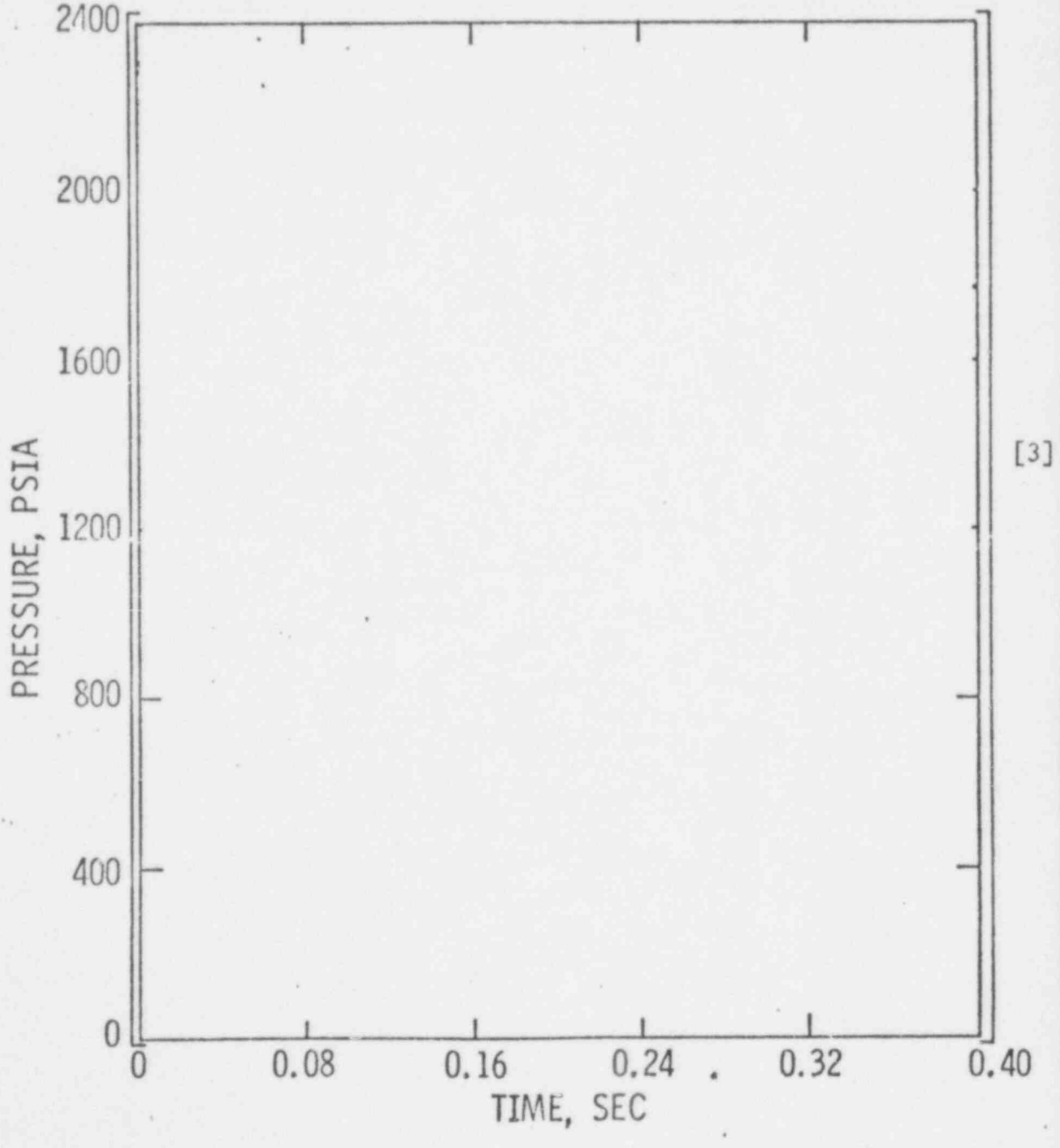

[3]

Figure 4-3
TIME STEP STUDY
CORE SUPPORT BARREL RADIAL PRESSURE DROP
(P_{34} - P_{12})

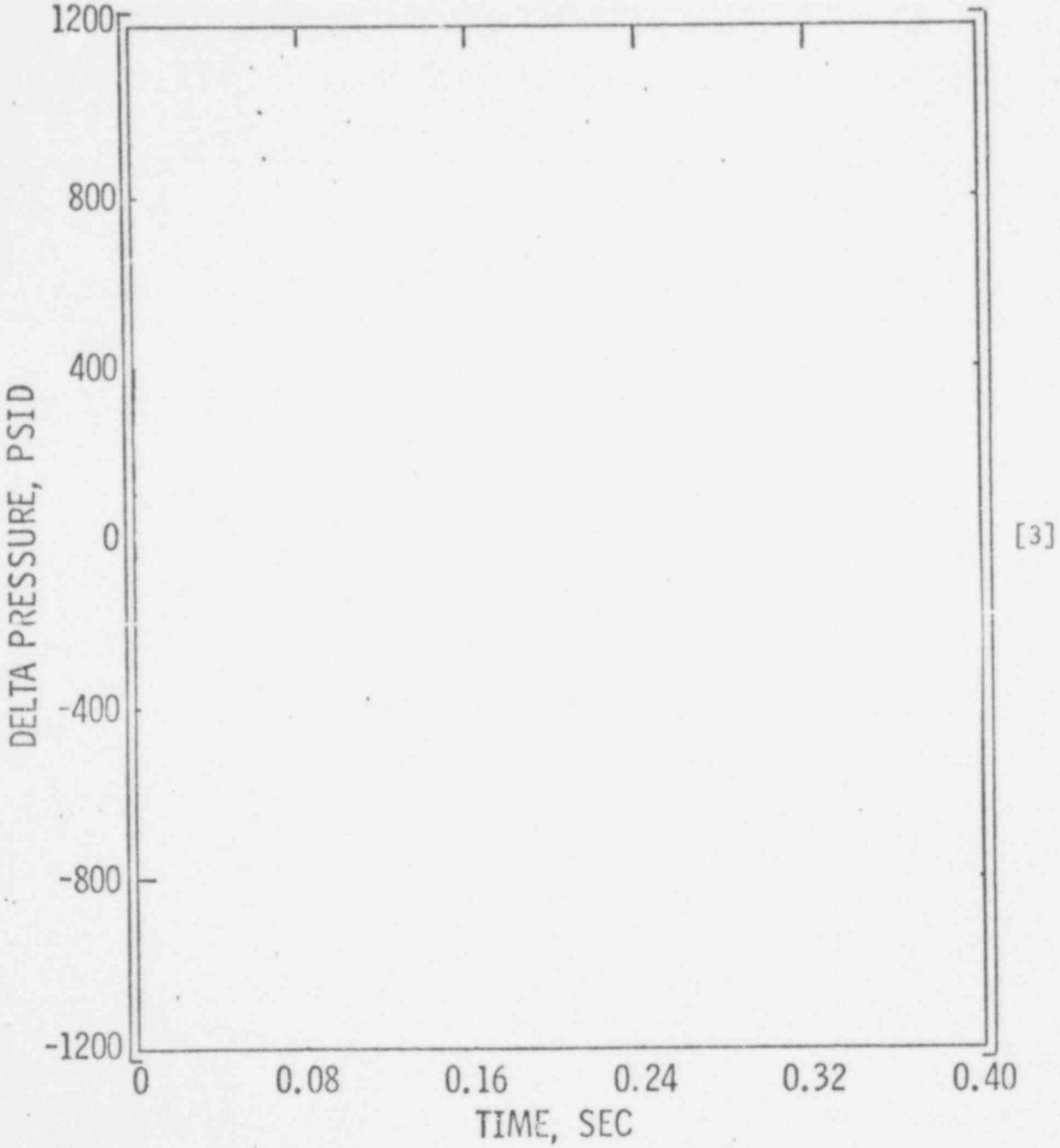

[3]

Figure 4-4
TIME STEP STUDY
MOMENTUM FLOW PARAMETER FOR FLOWPATH 3
(WEIGHT FLOW RATE SQUARED * SPECIFIC VOLUME)

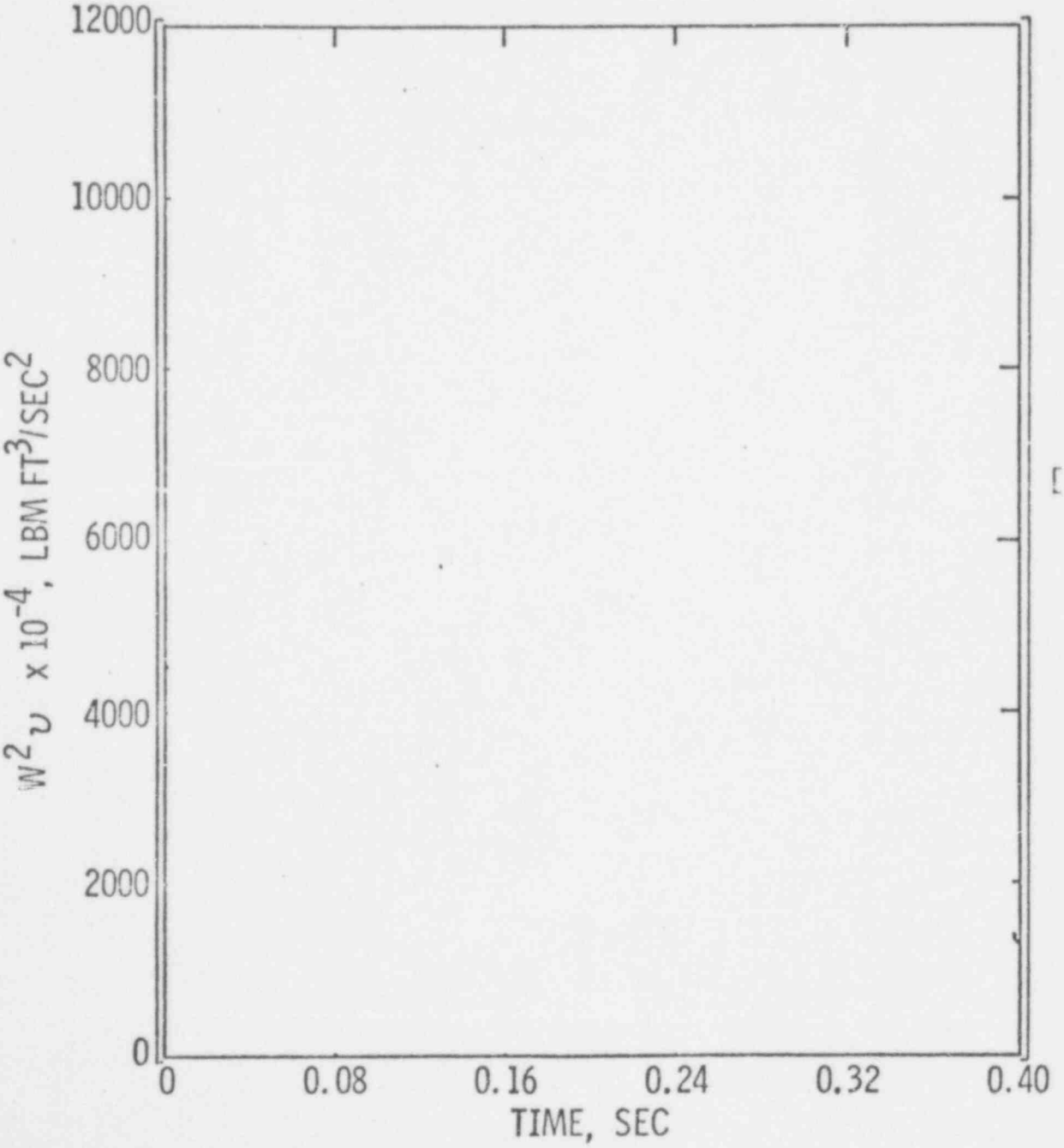

[3]

Figure 4-5
EFFECT OF CRITICAL FLOW FORMULATION
ON PRESSURE DECAY
(TOP INACTIVE CORE REGION: NODE 32)

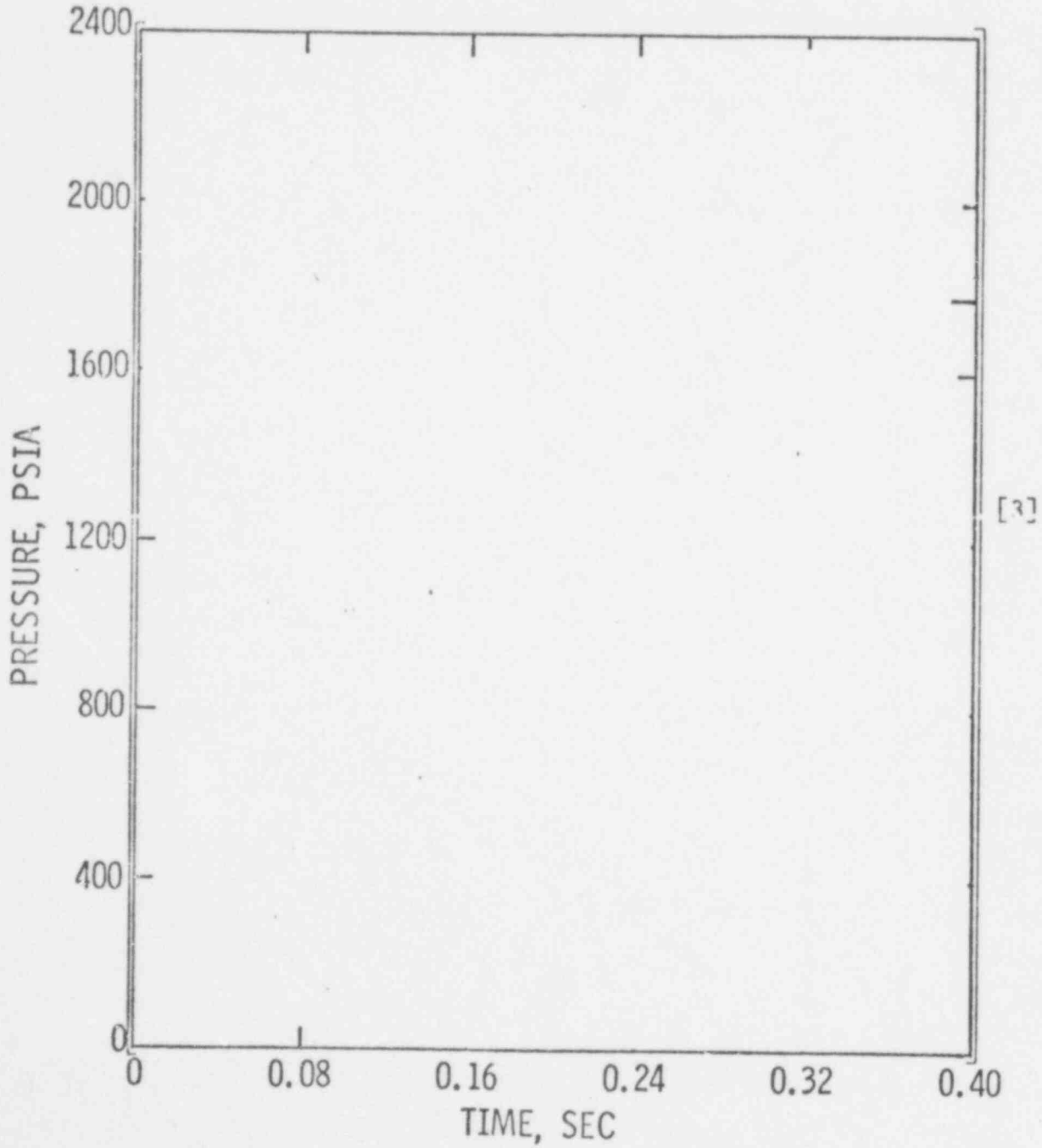

Figure 4-6
EFFECT OF CRITICAL FLOW FORMULATION
ON PREDICTED PRESSURE DECAY
(DOWNCOMER REGION NEAR BROKEN COLD LEG:
NODE 12)

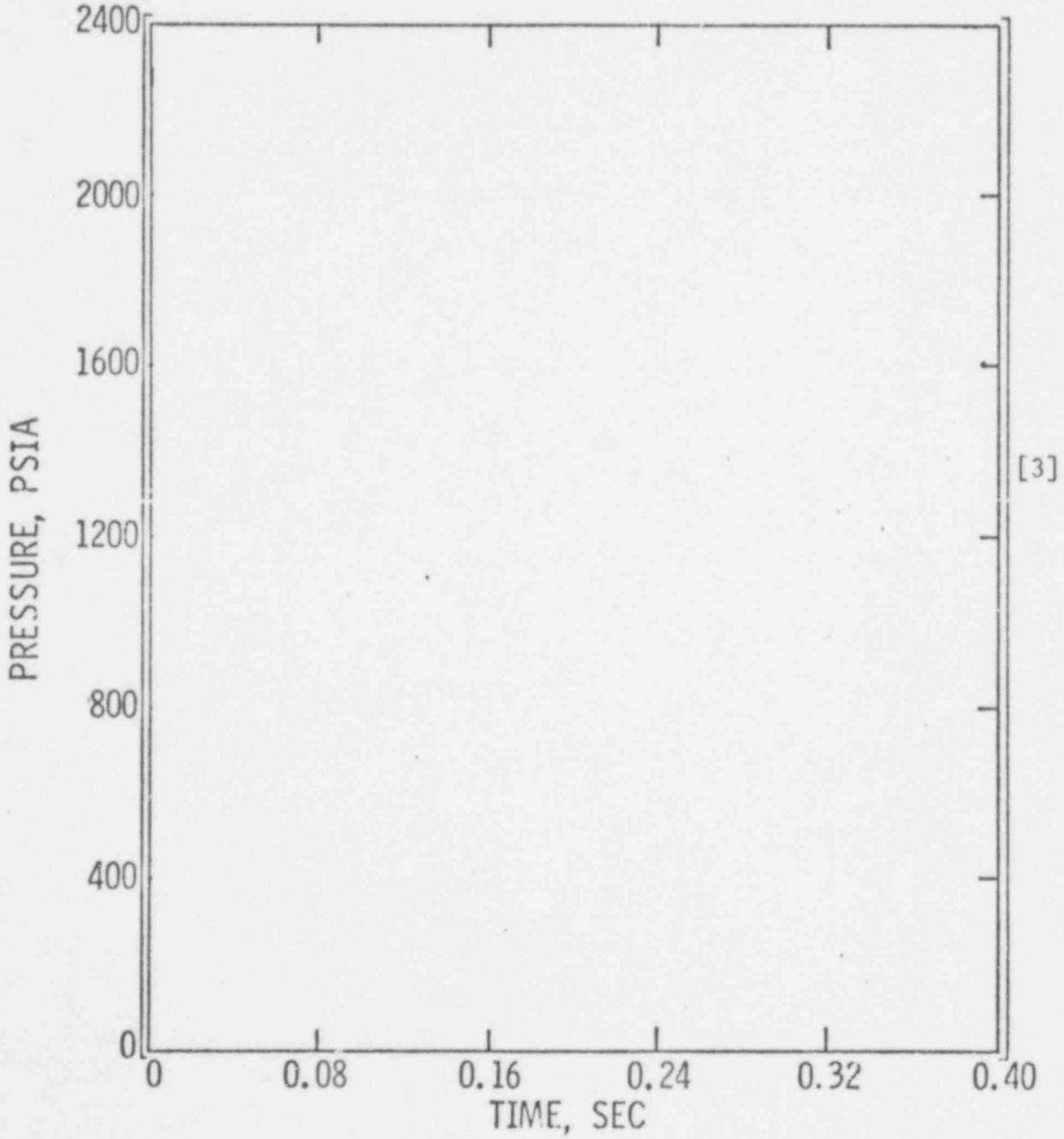

Figure 4-7
EFFECT OF CRITICAL FLOW FORMULATION
ON THE CORE SUPPORT BARREL RADIAL
PRESSURE DROP
$(P_{34} - P_{12})$

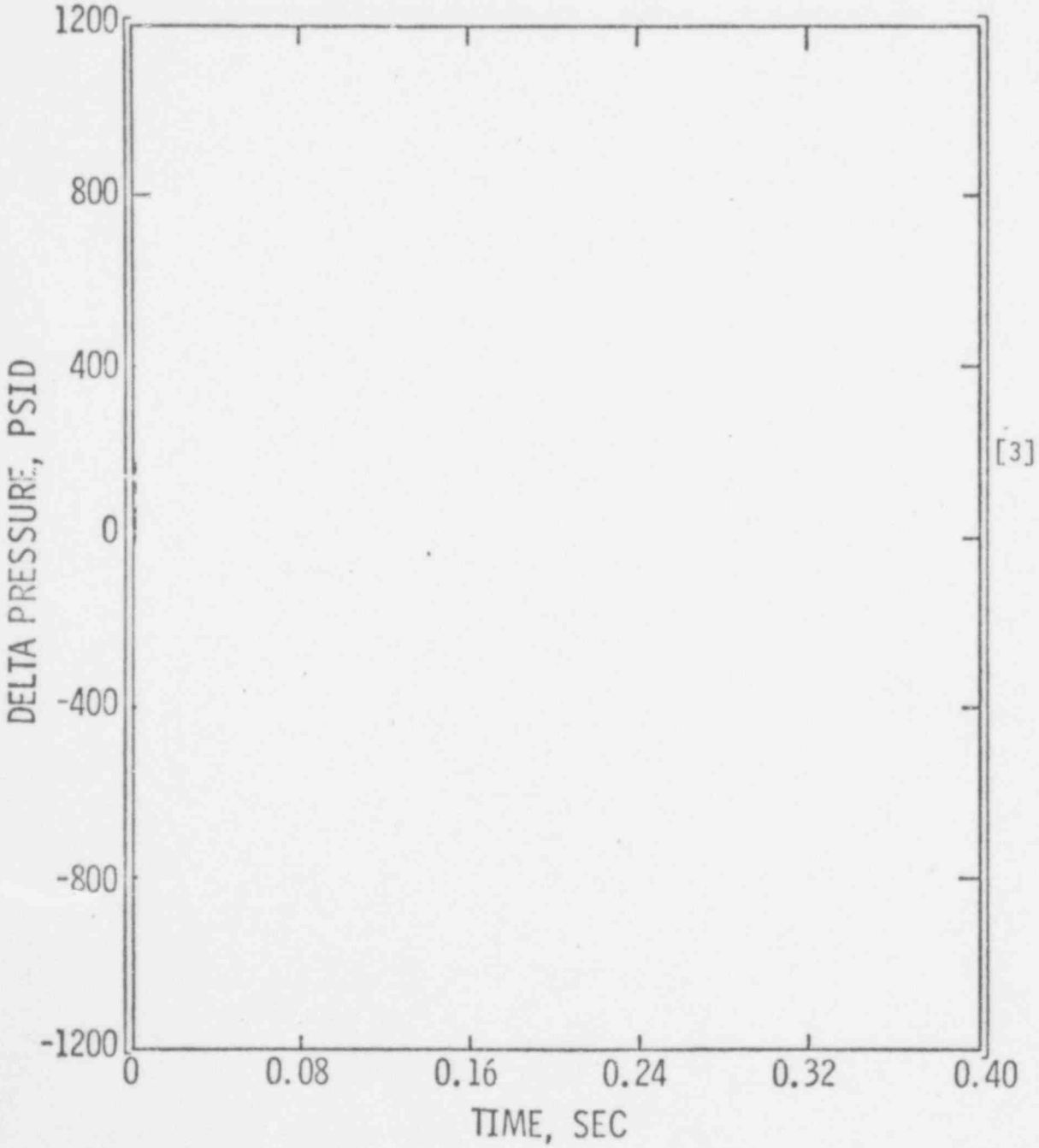

[3]

Figure 4-8
EFFECT OF CRITICAL FLOW FORMULATION
ON THE CORE AXIAL PRESSURE DROP
$(P_{28} - P_{32})$

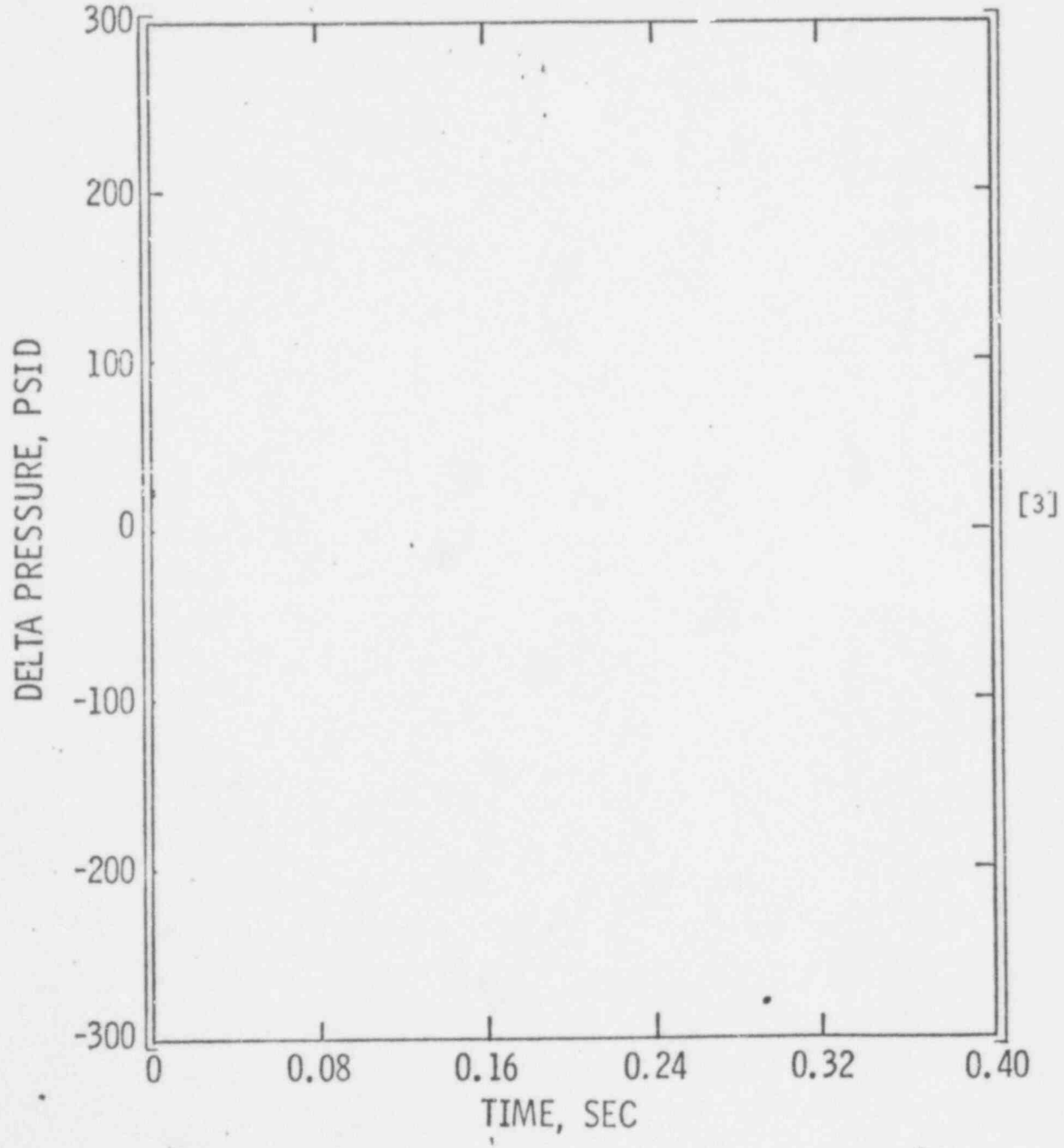

[3]

Figure 4-9

COMPARISON OF NODE/FLOWPATH PLATE
MODELING TECHNIQUES

[3,5]

Figure 4-10
PRESSURE DIFFERENCE ACROSS FUEL ALIGNMENT PLATE
350 IN^2 INLET BREAK

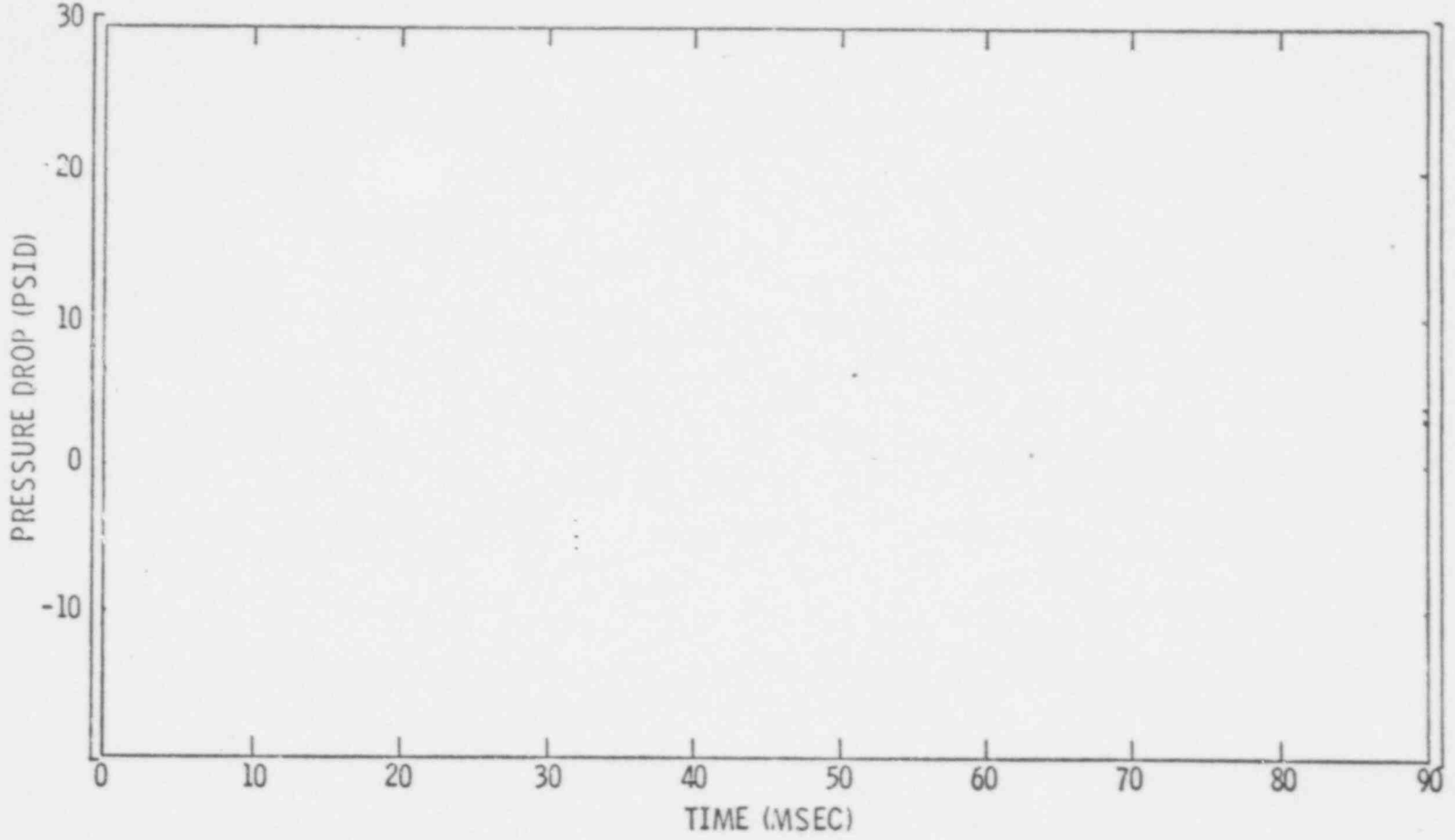

Figure 4-11

PRESSURE DIFFERENCE ACROSS FUEL ALIGNMENT PLATE

350 IN^2 INLET BREAK

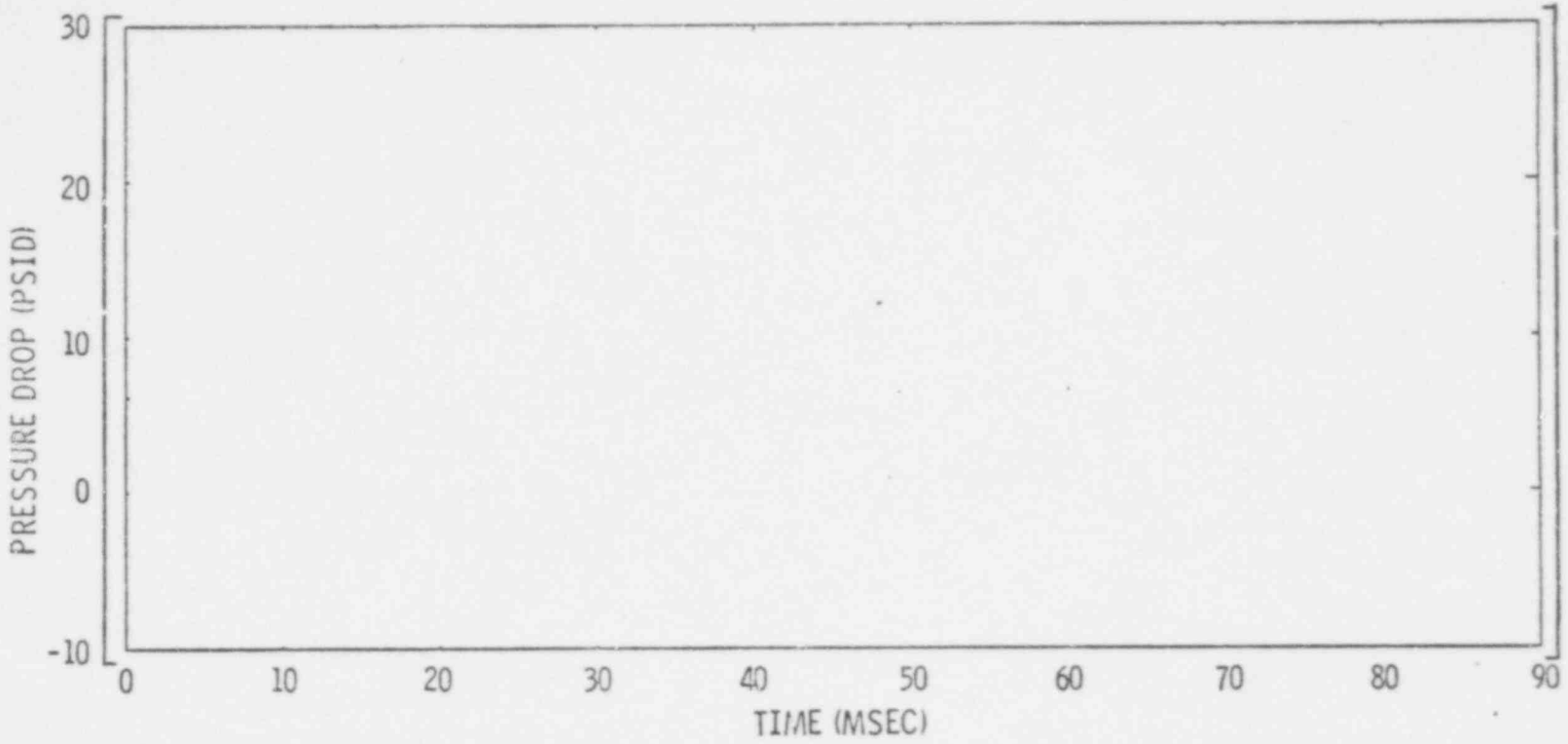

[3,5]

FIGURE 4-17

DOWNCOMER ANNULUS MODEL

Figure 4-13

DOWNCOMER ANNULUS MODEL

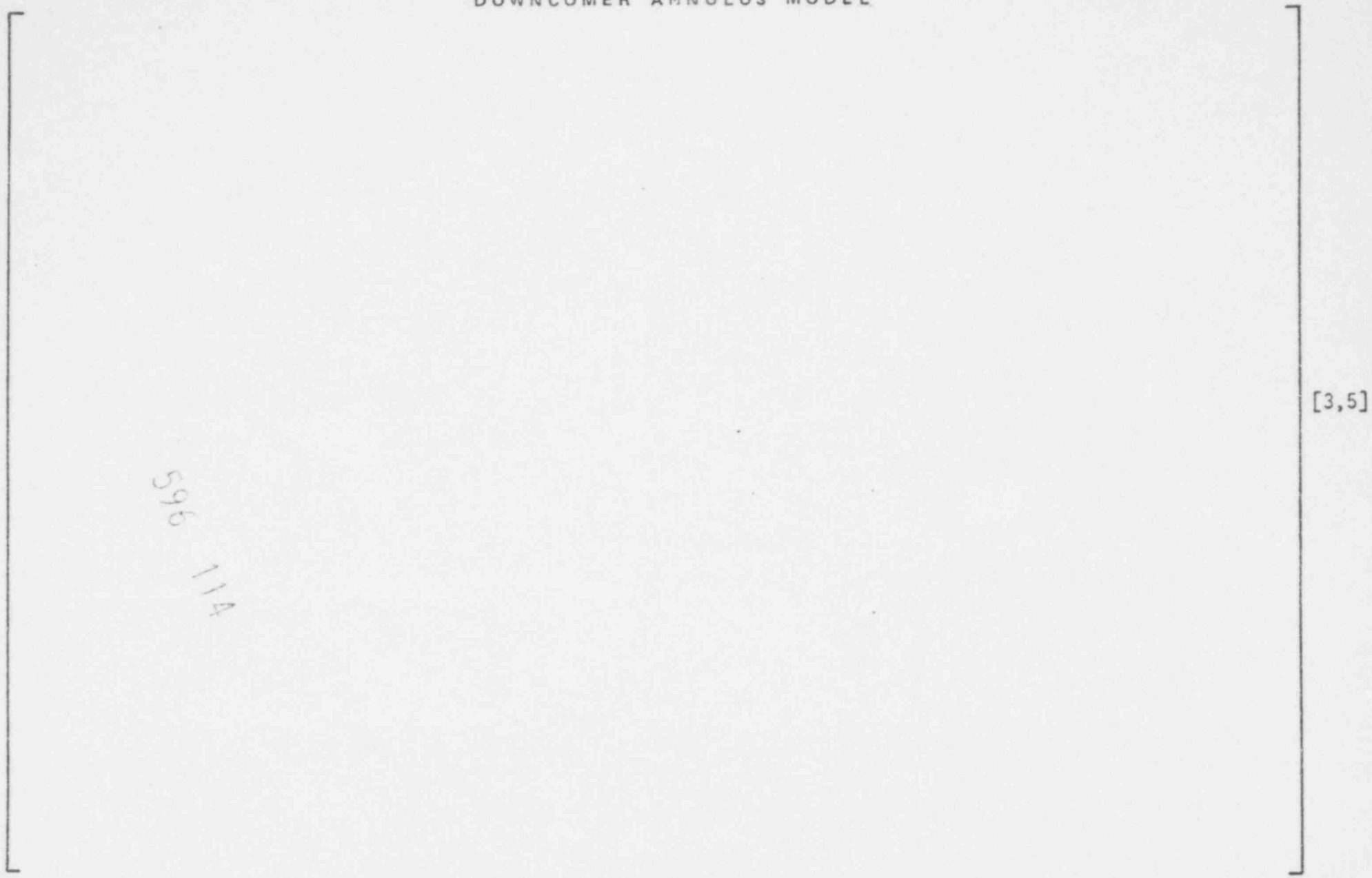

[3,5]

FIGURE 4-14

DOWNCOMER ANNULUS MODEL

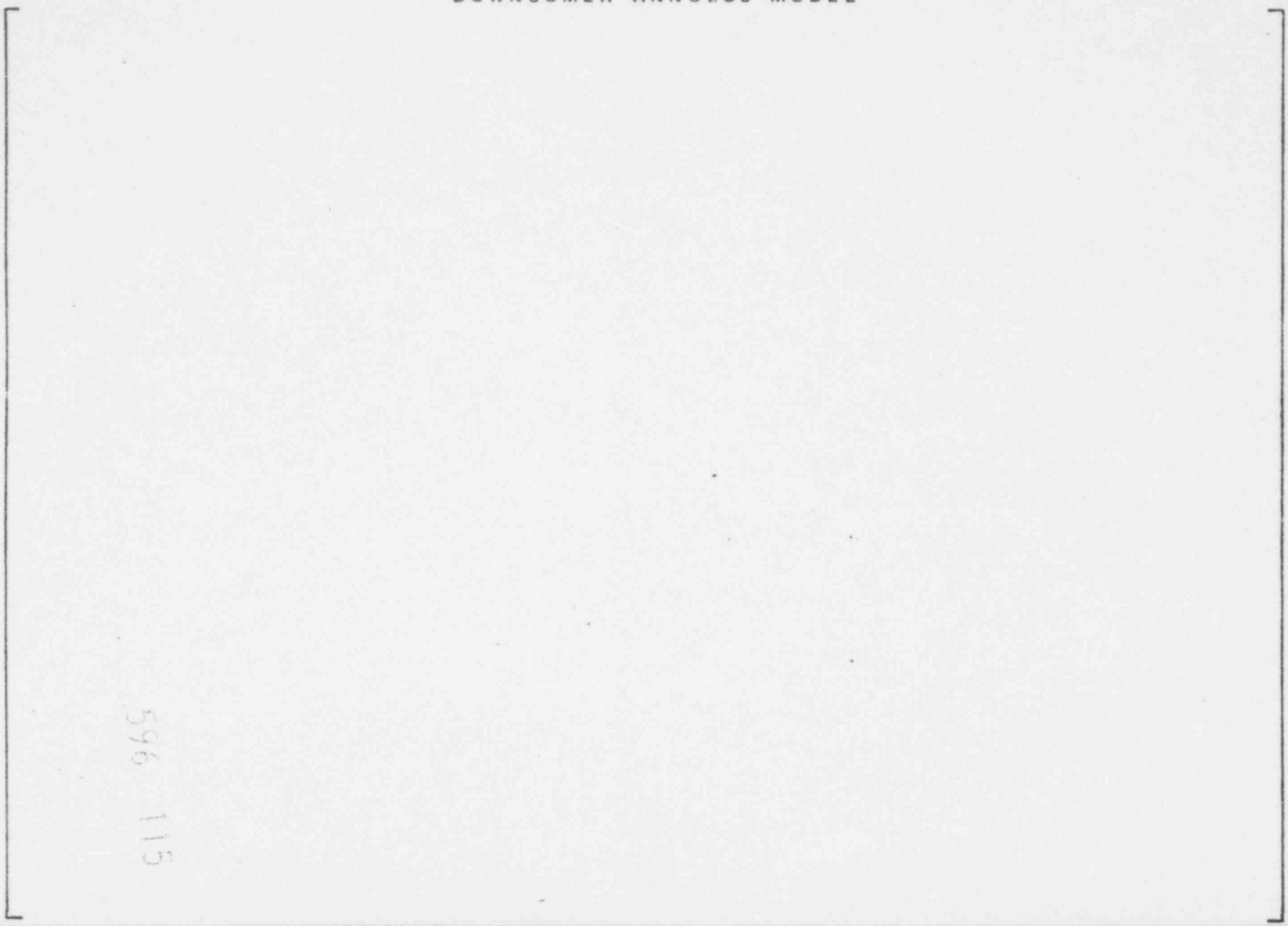

[3,5]

[3,5]

596 116

Figure 4-15
SPACIAL REPRESENTATION OF THE DOWNCOMER ANNULUS

Figure 4-16
ANNULUS REPRESENTATION STUDY
PRESSURE AT BROKEN NOZZLE LOCATION

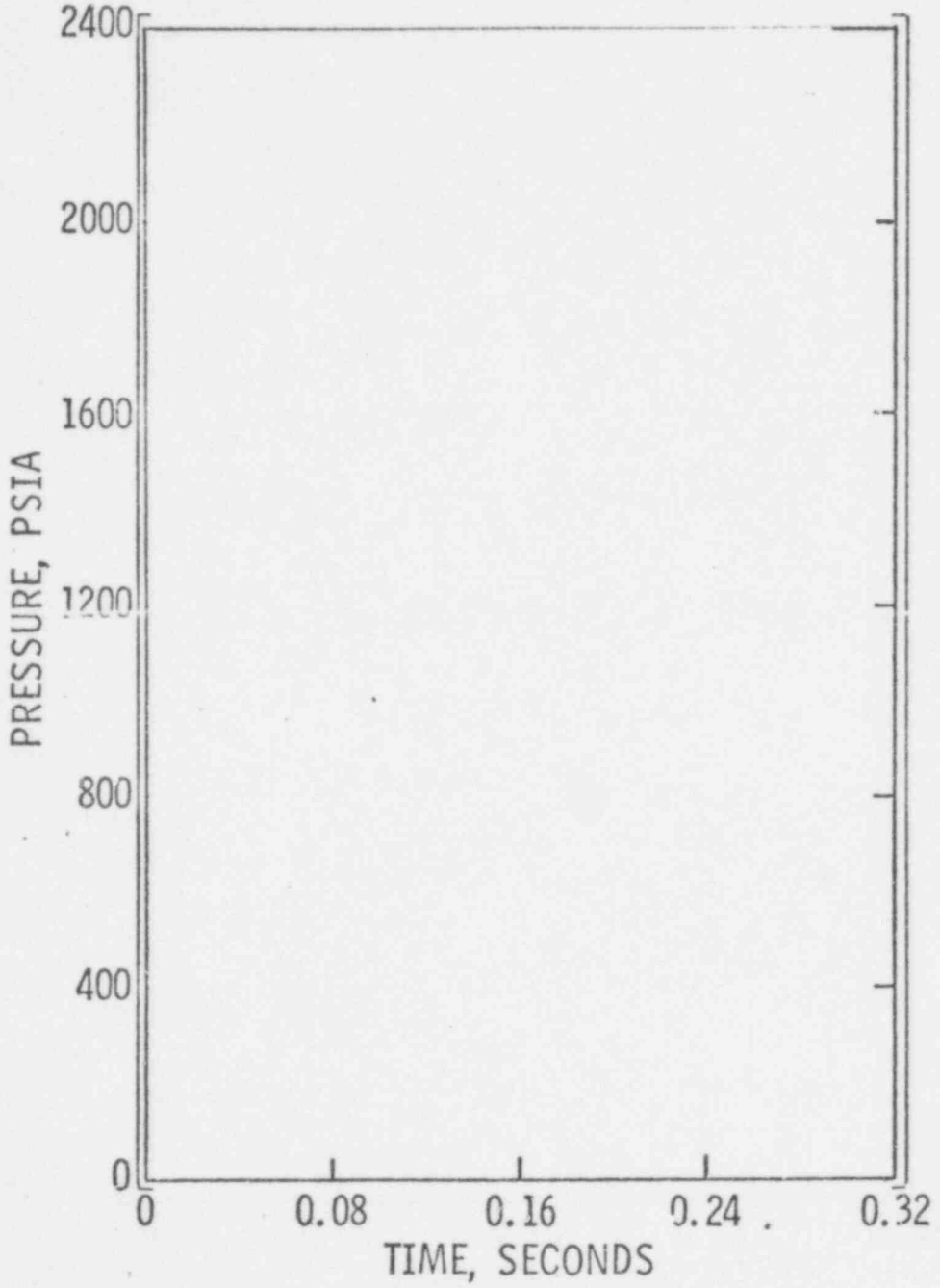

[3,5]

Figure 4-17
ANNULUS REPRESENTATION STUDY
PRESSURE OPPOSITE BROKEN NOZZLE LOCATION

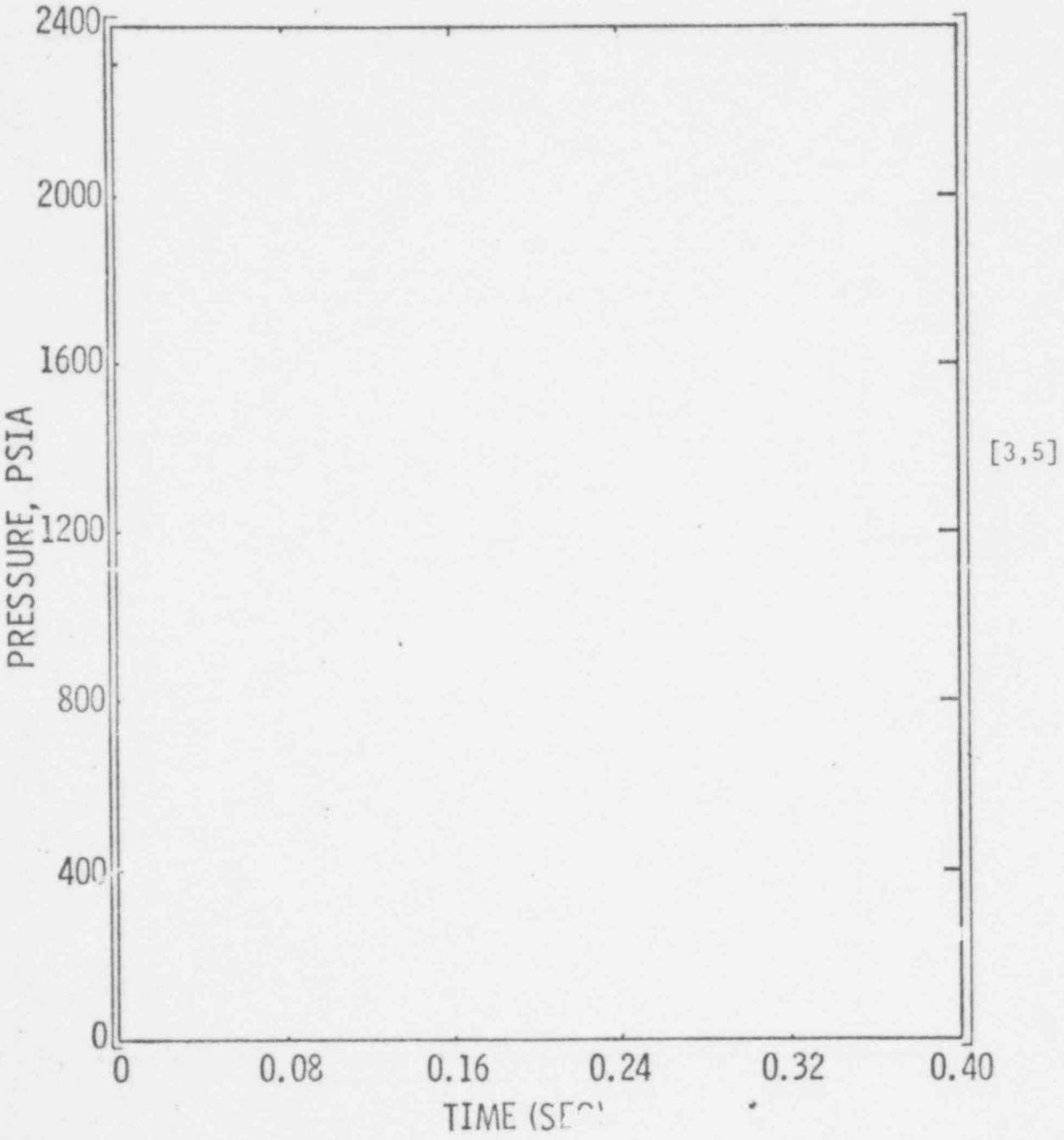

Figure 4-18
ANNULUS REPRESENTATION STUDY
PRESSURE OPPOSITE BREAK
(AXIAL ELEVATION
~10 FT ABOVE BOTTOM OF RPV)

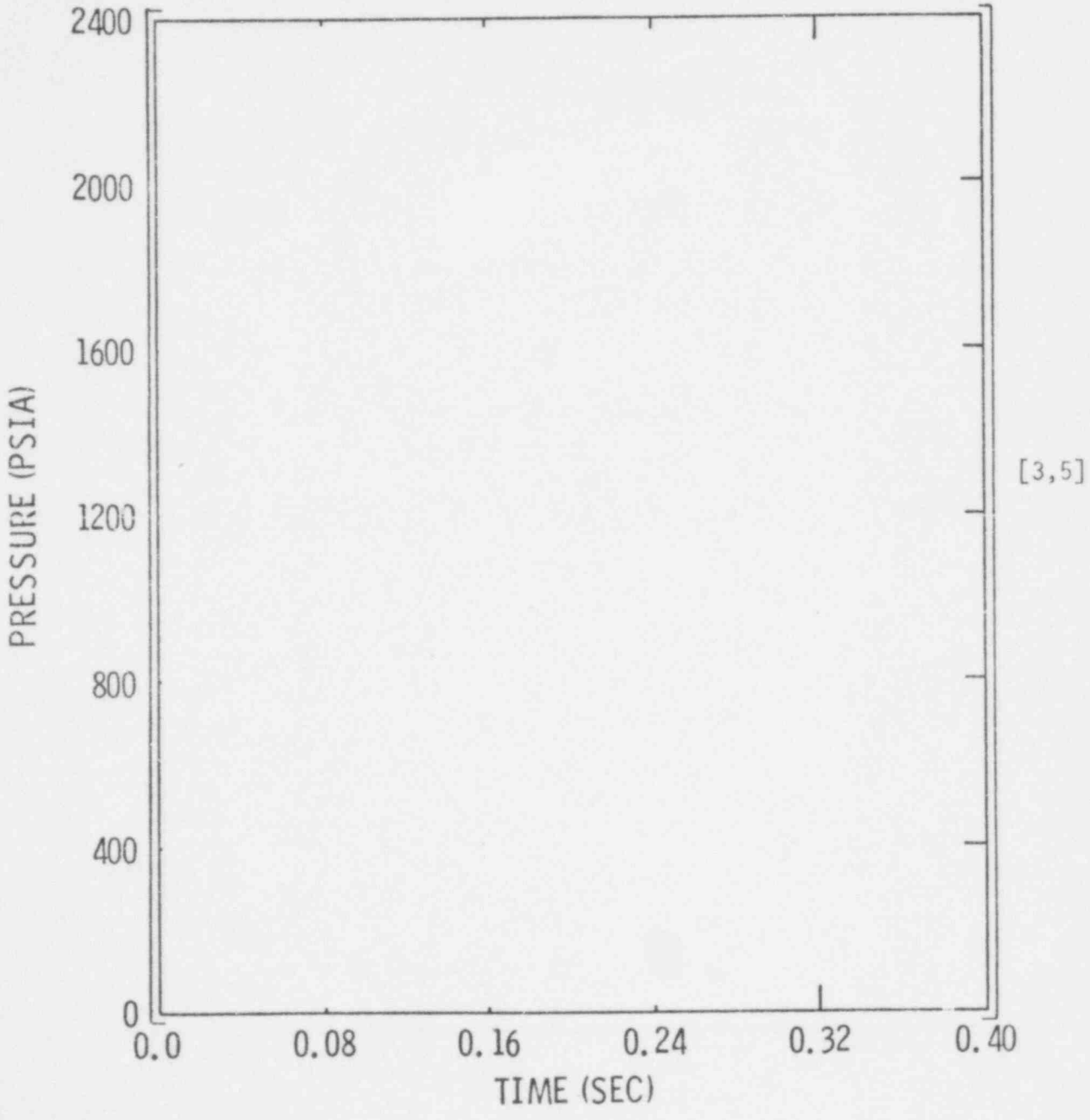

[3,5]

Figure 4-19
ANNULUS REPRESENTATION STUDY
PRESSURE DIFFERENCE ACROSS THE CORE BARREL
NOZZLE CENTERLINE ELEVATION

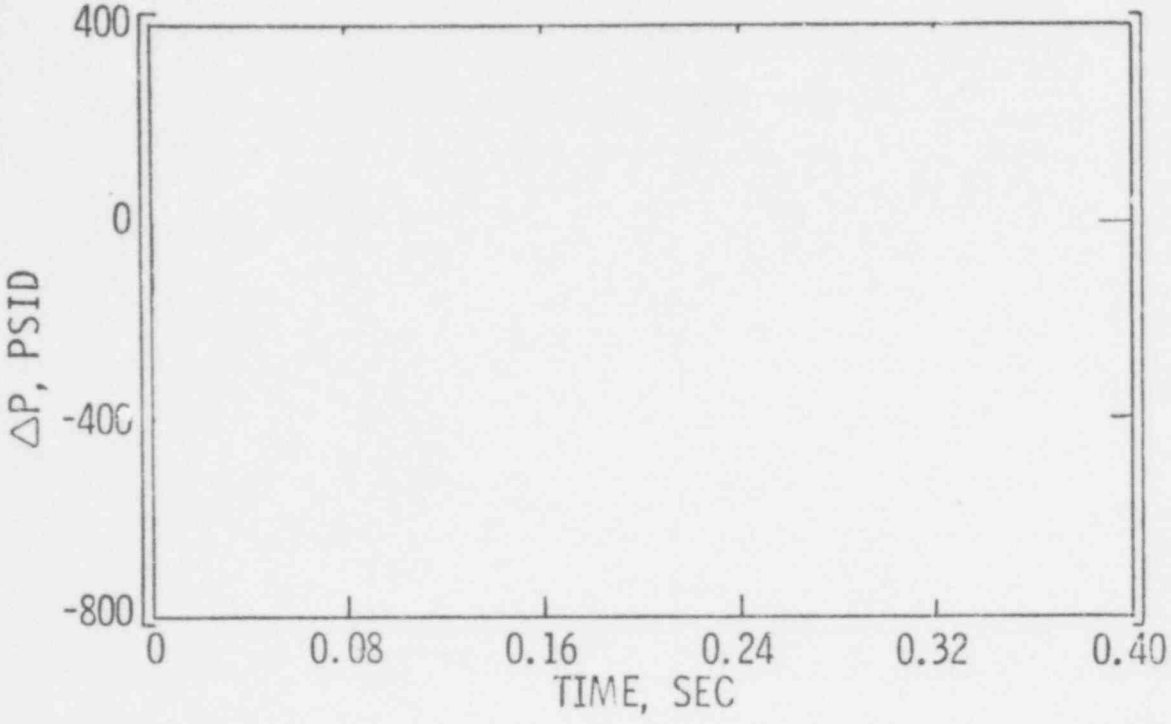

[3,5]

(a)

ELEVATION ~10 FEET ABOVE REACTOR PRESSURE VESSEL BOTTOM

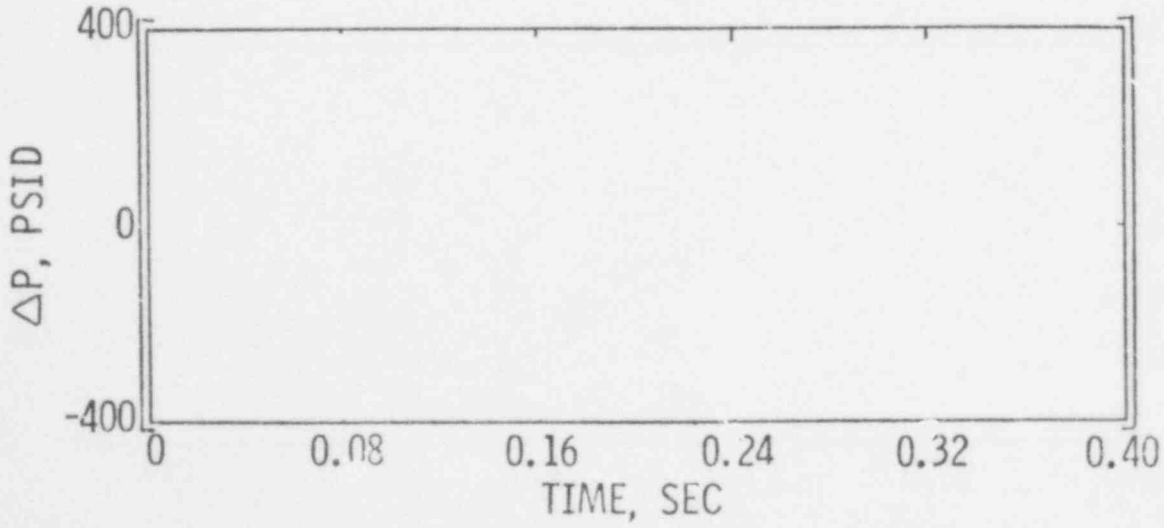

[3,5]

(b)

Figure 4-20
EFFECT OF PWR DOWNCOMER REPRESENTATION ON THE RADIAL CORE SUPPORT BARREL PRESSURE DIFFERENCE

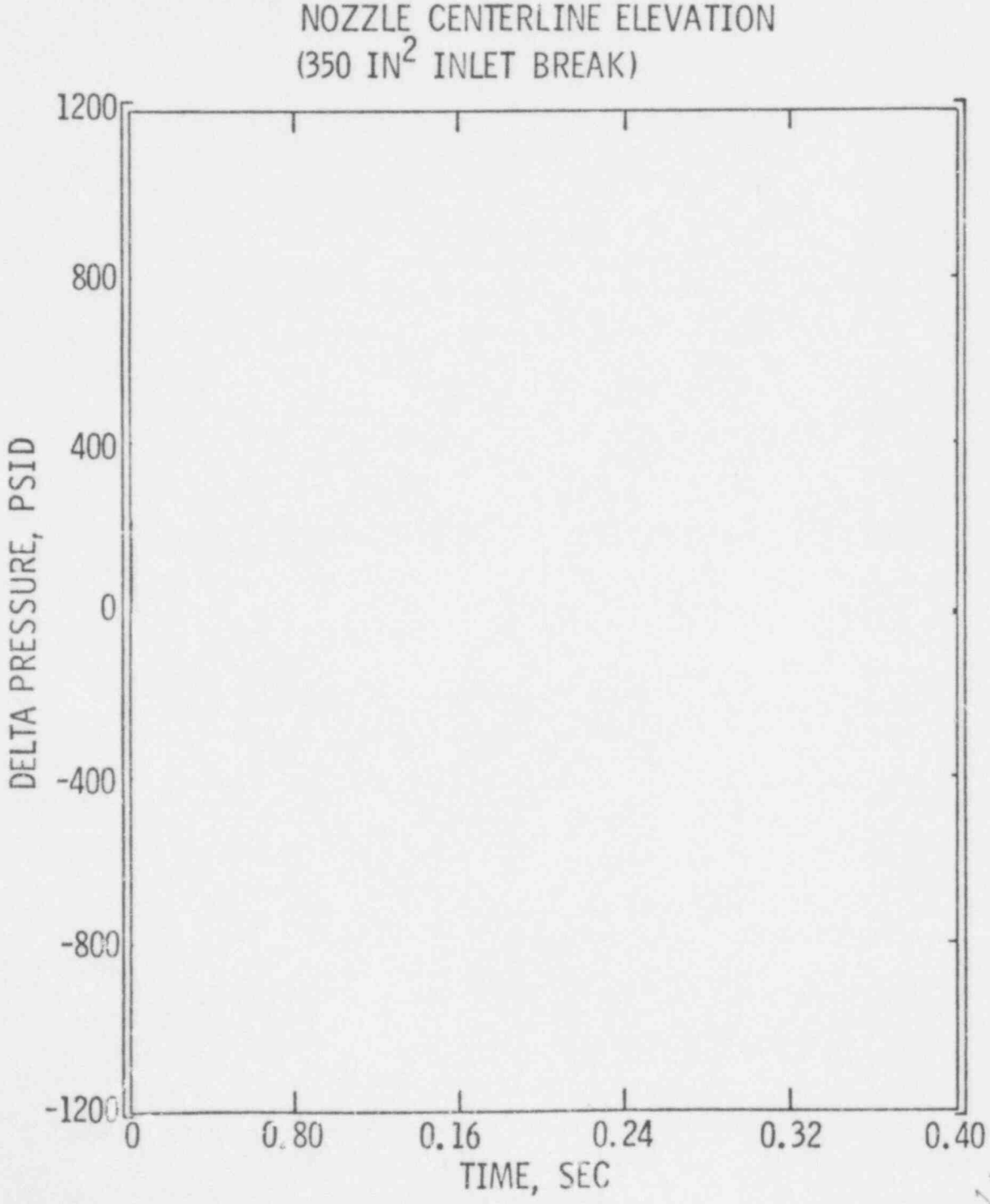

[3,5]

596 121

Figure 4-21
EFFECT OF PWR DOWNCOMER REPRESENTATION ON THE RADIAL CORE SUPPORT BARREL PRESSURE DIFFERENCE

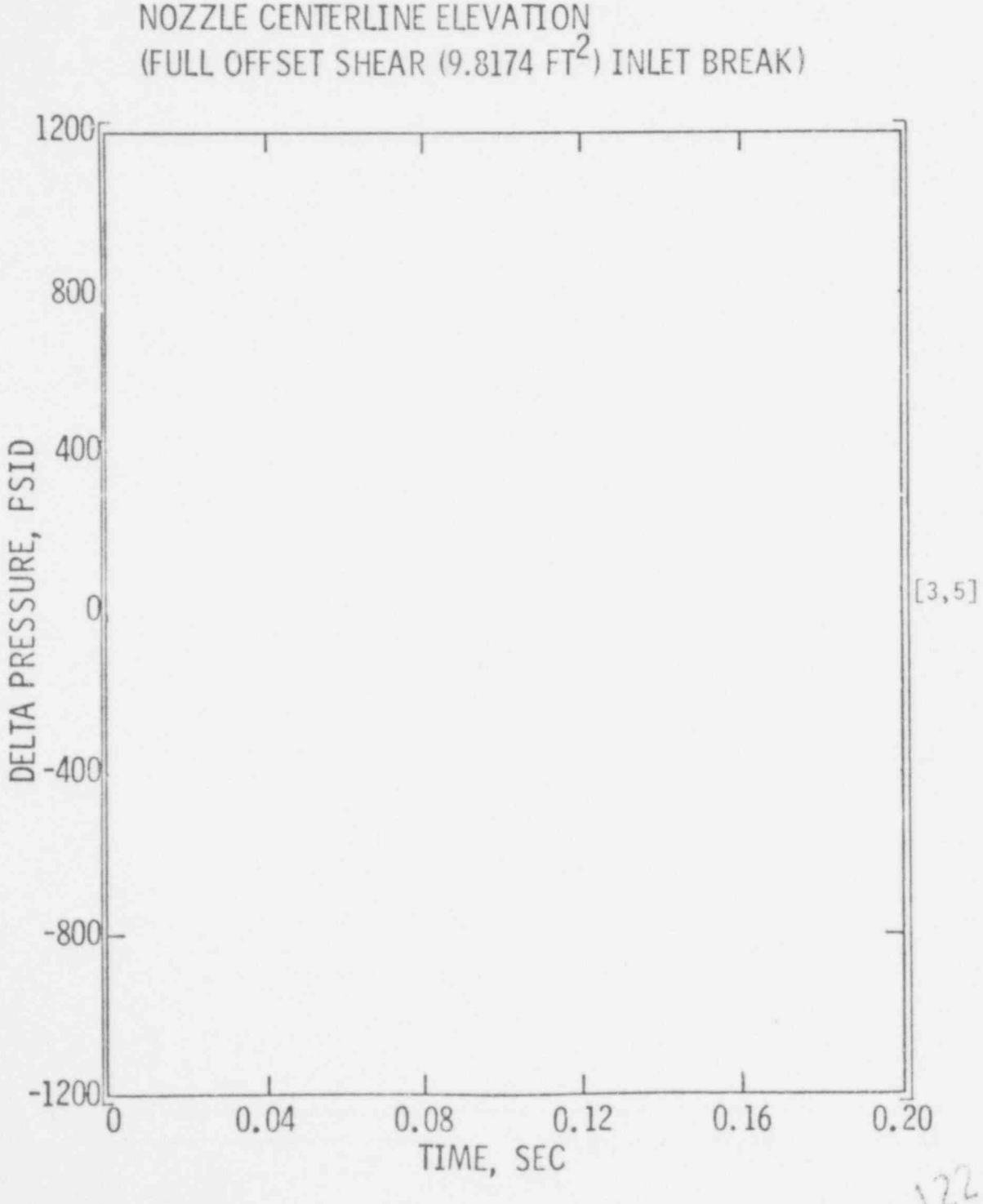

Figure 4-22
BREAK NODE MODEL REPRESENTATIONS

[3,5]

596 123

Figure 4-23
BREAK NODE REPRESENTATION STUDY
COMPARISON OF ABSOLUTE PRESSURES IN THE ANNULUS AT
UPPER GUIDE STRUCTURE FLANGE ELEVATION (NODE 6)

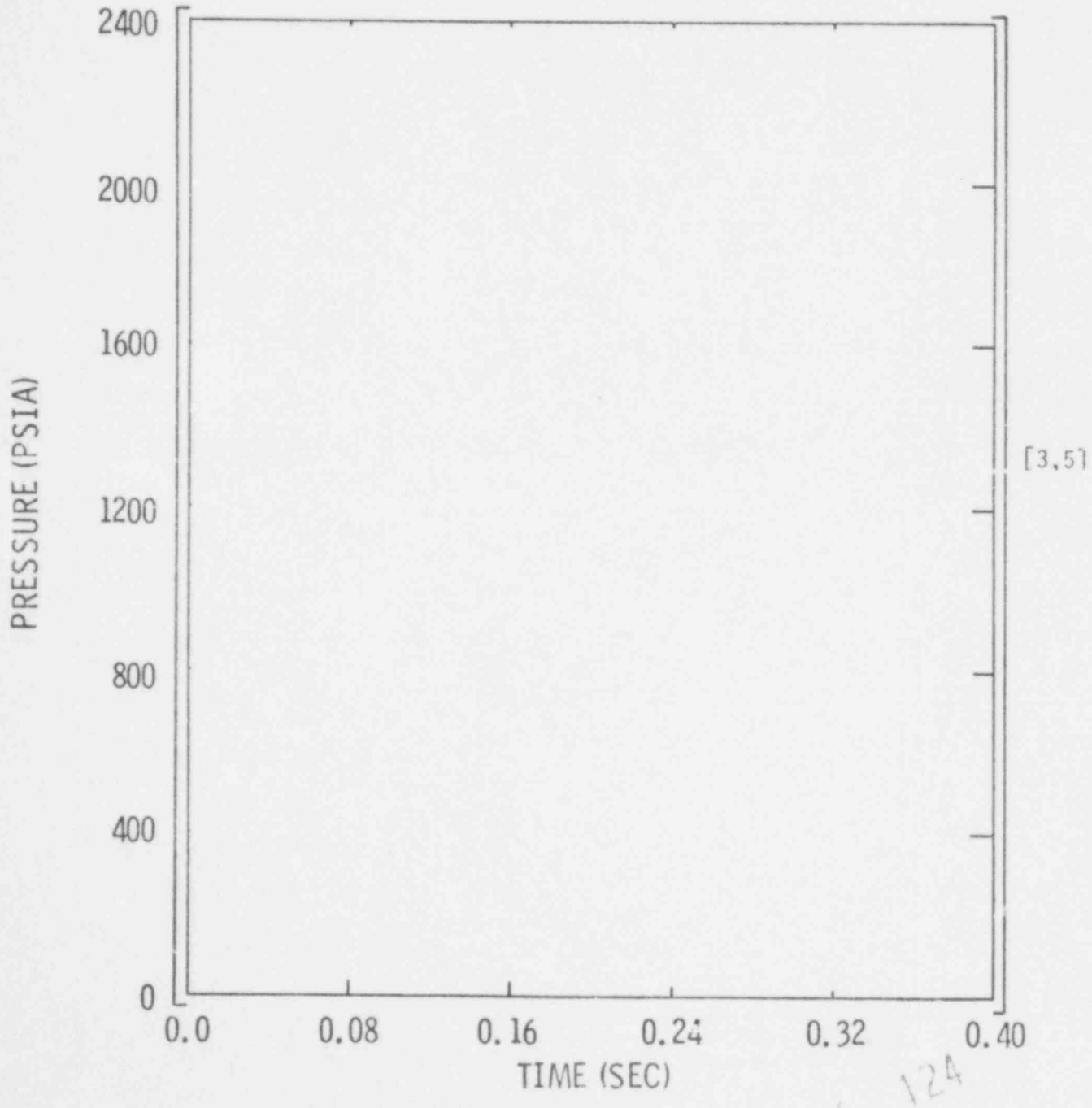

596 124

Figure 4-24
BREAK NODE REPRESENTATION STUDY
COMPARISON OF ABSOLUTE PRESSURES IN THE ANNULUS
AT NOZZLE CENTERLINE ELEVATION (NODE 12)

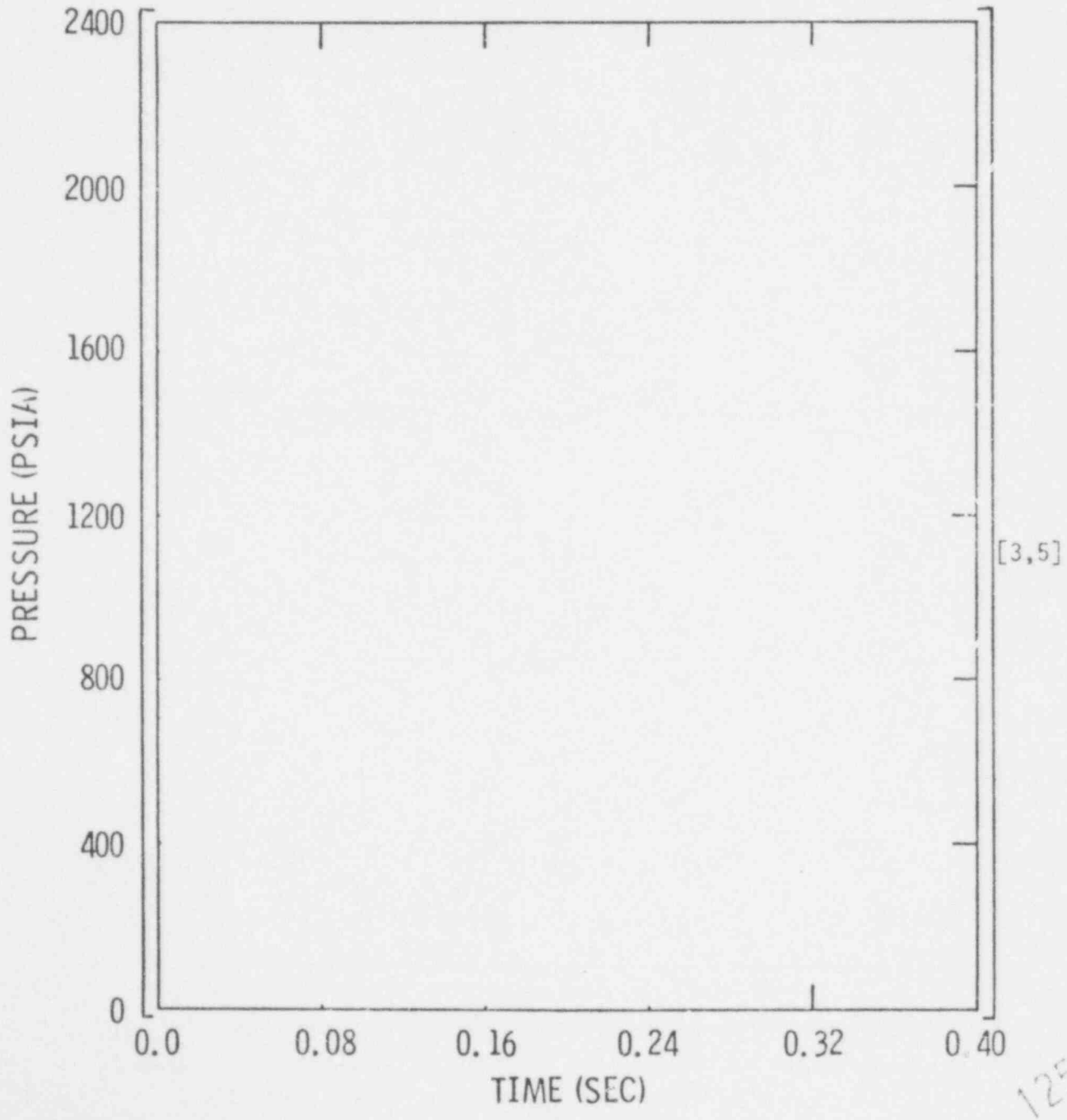

Figure 4-25
BREAK NODE REPRESENTATION STUDY
COMPARISON OF ABSOLUTE PRESSURES IN THE ANNULUS
AT LOWER CORE ELEVATION (NODE 24)

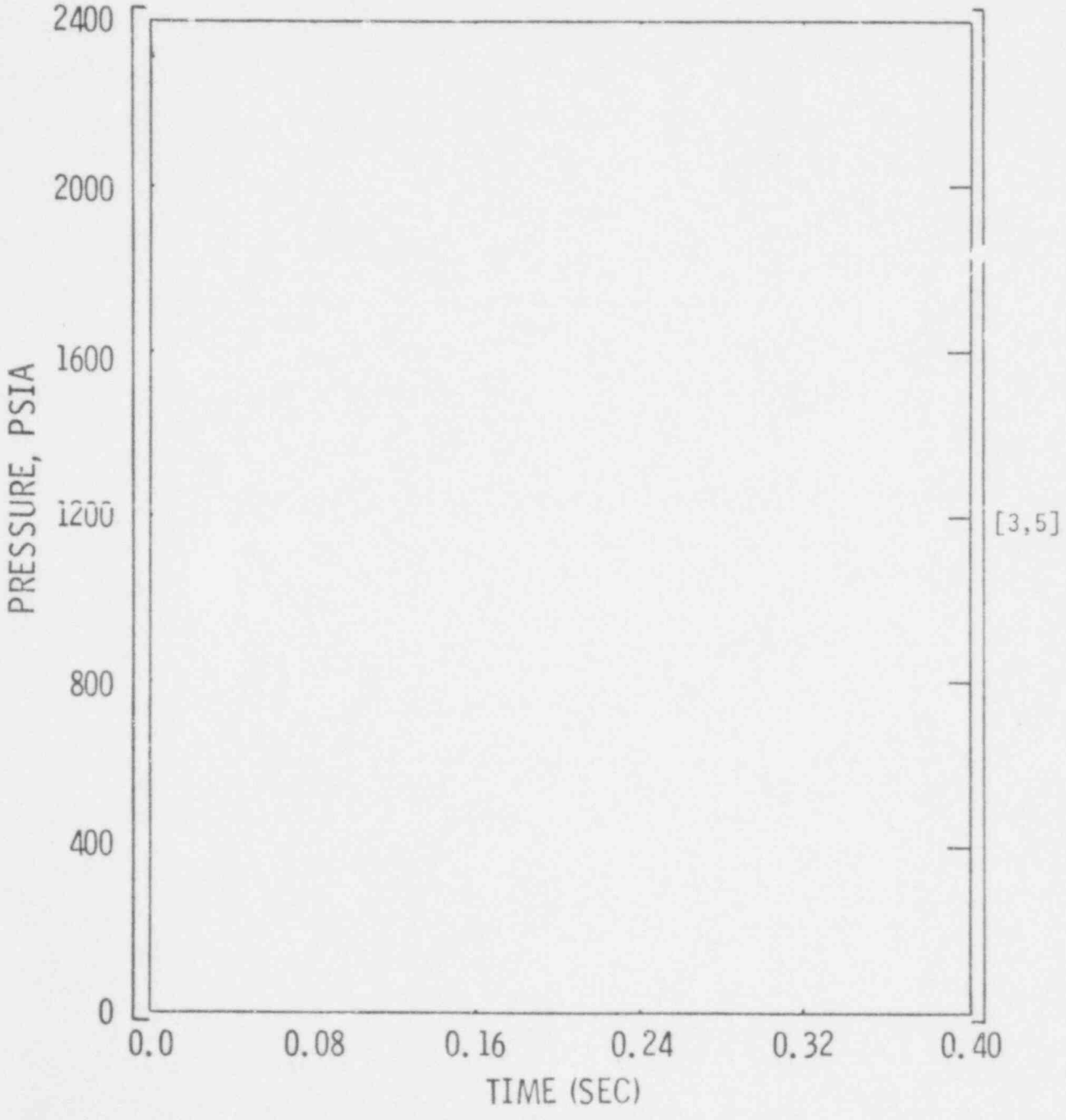

Figure 4-26
EFFECT OF SPACIAL REPRESENTATION OF THE RPV NOZZLE ON THE PRESSURE DIFFERENCE ACROSS THE CORE BARREL
(350 IN^2 INLET BREAK)

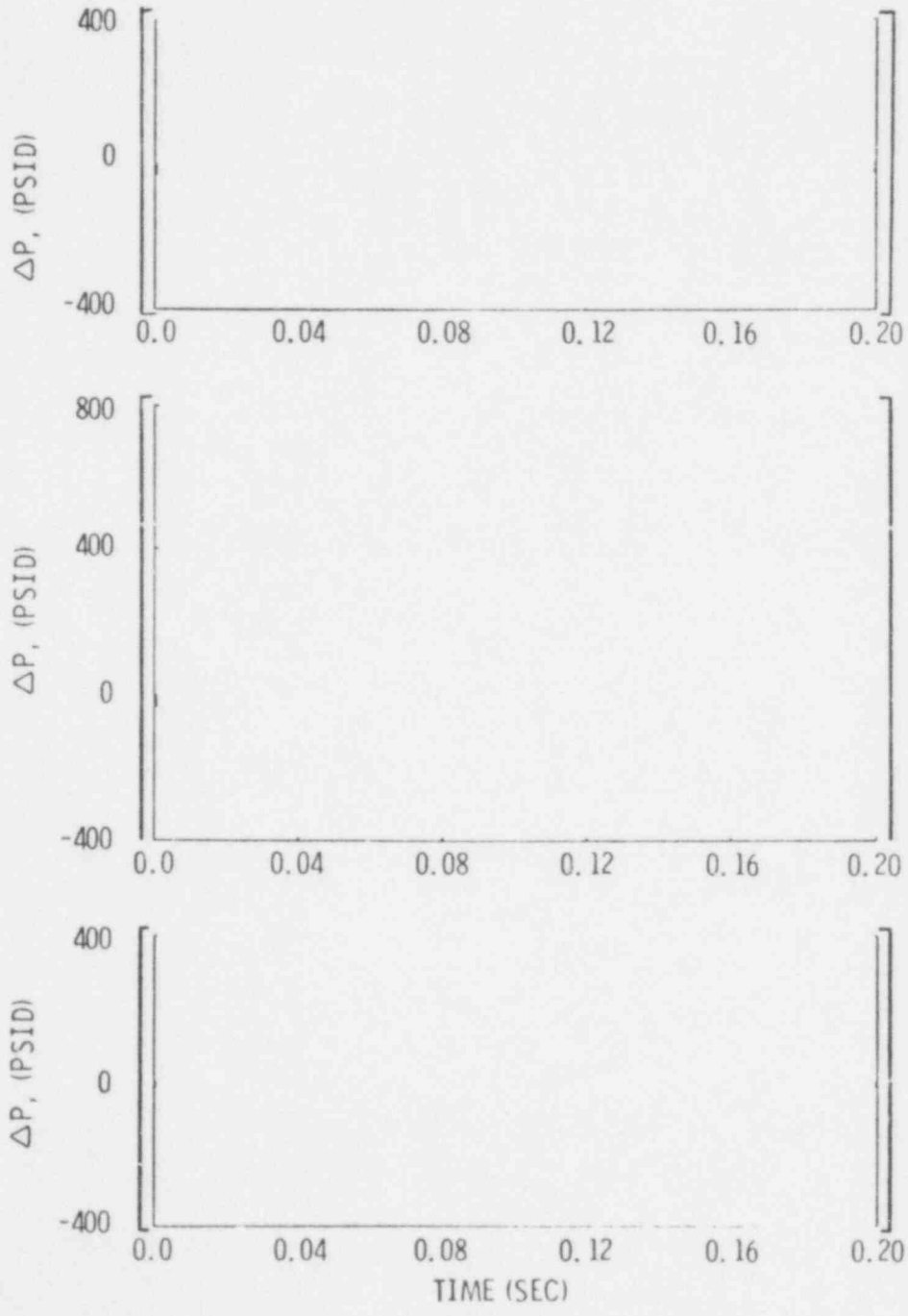

Figure 4-27

EFFECT OF SPACIAL REPRESENTATION OF THE RPV NOZZLE ON THE PRESSURE DIFFERENCE ACROSS THE CORE BARREL

NOZZLE CENTERLINE ELEVATION

(350 IN^2 INLET BREAK)

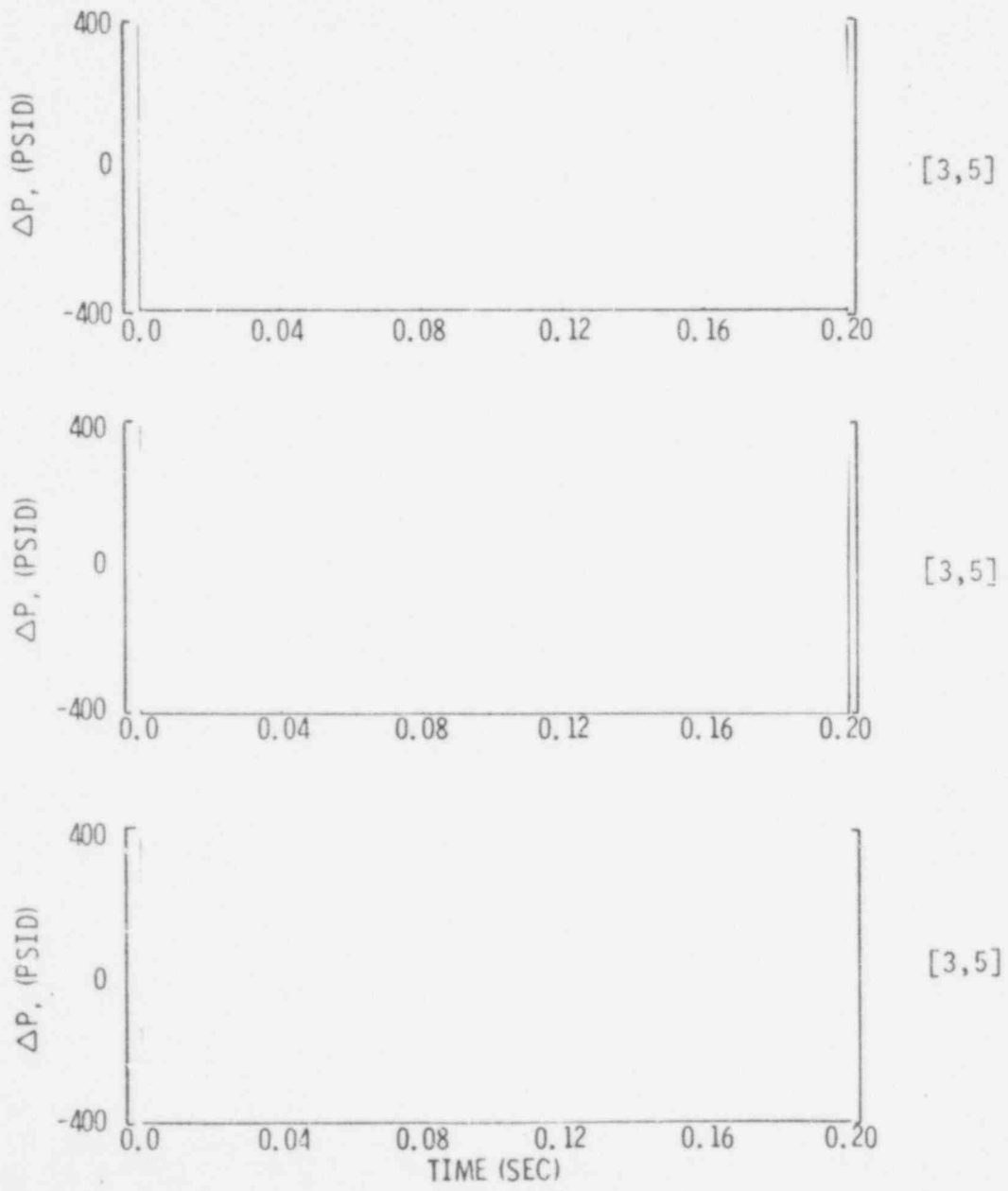

Figure 4-28

EFFECT OF NODALIZATION OF THE RPV NOZZLE ON THE CORE AXIAL PRESSURE DROP (P_{28} - P_{32}) (350 IN^2 INLET BREAK)

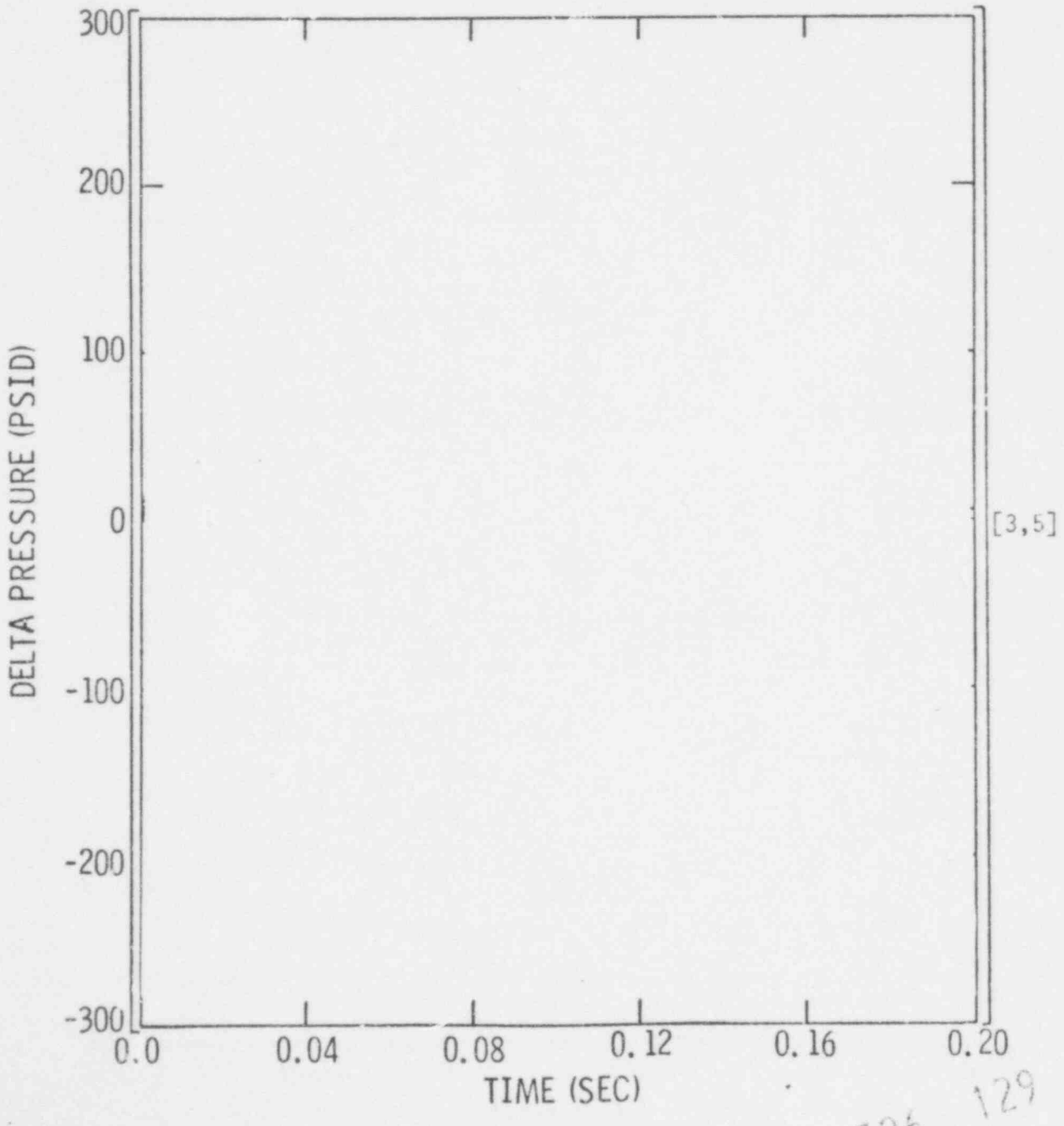

596 129

5.0 CEFLASH-4B ANALYSIS OF A PWR

This section presents the CEFLASH-4B computer model for the Combustion Engineering two loop pressurized water reactor. Results from computer analyses are presented to show the typical nature of the blowdown loads. The particular analytical results given are for the C-E System 80 (3800 Mwt) standard plant.

5.1 PRINCIPAL FEATURES OF A C-E PWR

The primary reactor coolant system (RCS) is presented in Figure 5-1 for a C-E two loop pressurized water reactor (PWR). Each RCS loop is characterized by a single hot leg which connects the outlet plenum of the reactor vessel (RV) to a vertical U-tube steam generator. There are two cold legs which connect each steam generator to the reactor vessel inlet nozzles. Each cold leg contains its own centrifugal pump. The reactor vessel inlet and outlet nozzles are spaced circumferentially around the reactor vessel at 60° intervals and the nozzle centerlines are located at the same elevation.

The major internal components of the reactor vessel are the core support barrel, fuel assemblies, upper guide structure, lower support structure assembly and core shroud. A typical layout of these components is shown in Figure 5-2 for the System 80 reactor vessel.

5.2 CEFLASH-4B MODEL OF A PWR

This section provides the features and key modeling assumptions in the CEFLASH-4B model of a PWR. Important parameters are presented and a description of the CEFLASH-4B break model is also given.

5.2.1 Characteristics of the CEFLASH-4B Model

Two models were developed for the analysis of a PWR, one for pipe breaks occurring in the cold leg and one for pipe breaks occurring in the hot leg.

Descriptions of the nodes and flowpaths for the CEFLASH-4B models are given in Tables 5-1 and 5-2. The network diagrams of the models are shown in Figure 5-3 and 5-4 for pipe breaks in the cold and hot legs, respectively. The cold leg model is comprised of[ ]nodes and[ ]flowpaths, whereas the hot leg model is comprised of[ ]nodes and[ ]flowpaths. [3,5]

The CEFLASH-4B model utilizes[ ]nodes to describe the downcomer annulus region. This is a result of the parameteric studies presented in Section 4.4.1. The model is arranged such that there are[[3,5] [3,5]

] Figure 5-5 depicts the angular orientation of the nodes in the annulus. The CEFLASH-4B model explicitly accounts for the respective reactor vessel nozzles for pipe breaks in the cold and hot legs.

The self-initialization option of the CEFLASH-4B computer code was used to compute the steady state pressure and energy balance. This requires the input to the code of reactor coolant system pressure drops, flow rates, core operating parameters and steam generator boundary conditions. The pressure loss in a flowpath due to friction is obtained assuming flow varying friction factors, dependent upon Reynolds number.

The calculational time step used in the PWR analyses was[ ] [3,5] This time step was shown to converge for the CEFLASH-4B model in Section 4.1.

5.2.2 CEFLASH-4B Break Model

CEFLASH-4B utilizes a[ ]with respect to time. [3,5] Figure 5-6 shows how a guillotine pipe break is described in CEFLASH-4B using a variable flow area flowpath.

Mechanistic pipe break sizes and locations for the System 80 reactor vessel blowdown analysis were determined from Reference 5-1. The pipe break sizes and break opening times are summarized in Table 5-3. These postulated breaks are assumed to occur at the respective reactor vessel inlet and outlet nozzles.

596 131

TABLE 5-3

BREAK PARAMETERS FOR SYSTEM 80 RV BLOWDOWN ANALYSIS

Break Type	Break Size (sq. in.)	Break Opening Time (sec)
Inlet Break: Guillotine	350	0.005
Outlet Break: Guillotine	100	0.003

Other parameters used in the CEFLASH-4B break model are given in Table 5-4.

TABLE 5-4

BREAK MODEL PARAMETERS

Break opening model:	[	] [3]
Critical flow model:		
Discharge coefficient:		

5.3 PREDICTED LOCA INDUCED HYDRODYNAMIC LOADS

The appropriate results from the blowdown loads analyses are used in the dynamic response analysis of the reactor vessel internals and supports. Transient time histories of node pressure, and flowpath flow squared times specific volume (W^2v) are stored on magnetic computer tape. The W^2v parameter is used in the evaluation of the drag force on the CEA shrouds. Chapter 6 explains how the blowdown loads data are applied to calculate the structural forcing functions due to a LOCA. The following sections give representative graphical output from several computer cases.

5.3.1 Steady State Loads

The self-initialization option of the CEFLASH-4B computer code permits the code to calculate the steady state pressure balance based on the specified input data. A steady state test case was run to show that the code has initialized properly with a stable solution. Figure 5-7 shows two steady state absolute pressure results. Node 5 is located inside the reactor vessel in the outlet plenum. Node 29 is in the downcomer annulus region at the nozzle centerline elevation, adjacent to the inlet nozzle used to model breaks occurring in the cold leg. Figure 5-8 shows the steady state pressure differential across the core support barrel (node inside CSB - node outside CSB) at the nozzle centerline elevation and the steady state pressure drop axially across the core. It is seen from these figures that a converged steady state pressure balance has been achieved.

5.3.2 350 Sq. Inch Mechanistic Inlet Break

The CEFLASH-4B model was used to analyze a postulated 350 sq. inch pipe break. The break was assumed to occur at the reactor vessel inlet nozzle corresponding to the 60° angular orientation (Figure 5-5). Figure 5-3 shows the CEFLASH-4B network diagram used in this calculation. Figure 5-9 gives the absolute pressure versus time histories during the decompression for selected nodes in the reactor vessel and the annulus. Figure 5-10 shows the pressure differential across the core barrel at various locations. Note that the magnitude of the pressure load decreases for locations further away from the break. Figure 5-11 presents the core axial delta pressure and Figure 5-12 provides the W^2v parameter for the two flowpaths in the outlet nozzles (See Section 6.1).

5.3.3 100 Sq. Inch Mechanistic Outlet Break

The 100 sq. inch pipe break is postulated to occur at the reactor vessel outlet nozzle corresponding to the 0° angular orientation. Figure 5-4 shows the CEFLASH-4B network diagram used in this calculation. Figure 5-13

presents selected absolute pressure results. In the case of a break occurring in the hot leg, the decompression in the annulus is symmetric early in the transient because the pressure wave must travel through the reactor vessel internals to reach the lower plenum from where the wave propagates up through the downcomer at the same sonic velocity. Figure 5-14 shows representative pressure differentials across the core barrel at several elevations in the reactor vessel. Figure 5-15 gives the core axial delta pressure and Figure 5-16 depicts the $W^2\nu$ parameter for the two flowpaths in the outlet plenum.

5.4 REFERENCES FOR SECTION 5.0

5-1 Combustion Engineering, Inc., "Design Basis Pipe Breaks for the Combustion Engineering Two Loop Reactor Coolant System," CENPD-168-A, June, 1977.

TABLE 5-1

CEFLASH-4B NODES FOR A PWR ANALYSIS

NODE NO.	DESCRIPTION
[	]

[3,5]

596 135

TABLE 5-1 (Cont'd)

CEFLASH-4B NODES FOR A PWR ANALYSIS

NODE NO.	DESCRIPTION
[	]

[3,5]

596 136

TABLE 5-1 (Cont'd)

CEFLASH-4B NODES FOR A PWR ANALYSIS

NODE NO.	DESCRIPTION
	OUTLET BREAK MODIFICATIONS
[	] [3,5]

* IB= inlet break model only.

**OB= outlet break model only

596 137

TABLE 5-2

CEFLASH-4B FLOWPATHS FOR A PWR ANALYSIS

FLOWPATH	DESCRIPTION
[	] [3,5]

TABLE 5-2 (Cont'd)

CEFLASH-4B FLOWPATHS FOR A PWR ANALYSIS

FLOWPATH	DESCRIPTION
[	]

[3

TABLE 5-2 (Cont'd)

CEFLASH-4B FLOWPATHS FOR A PWR ANALYSIS

FLOWPATH	DESCRIPTION

[3,5]

TABLE 5-2 (Cont'd)

CEFLASH-4B FLOWPATHS FOR PWR ANALYSIS

FLOWPATH	DESCRIPTION
[	]

[3,5

590 141

Figure 5-1
NUCLEAR STEAM SUPPLY SYSTEM ARRANGEMENT

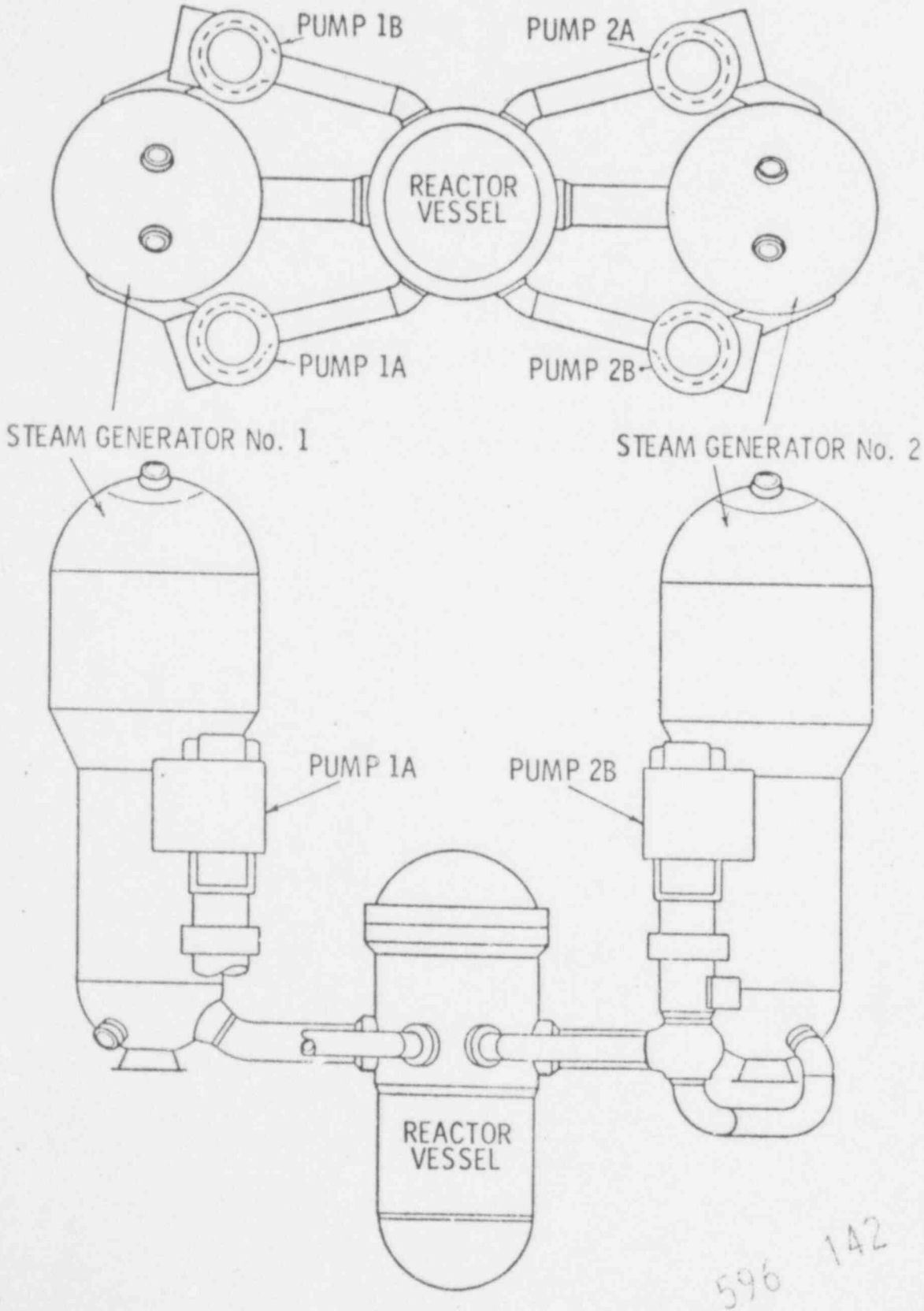

596 142

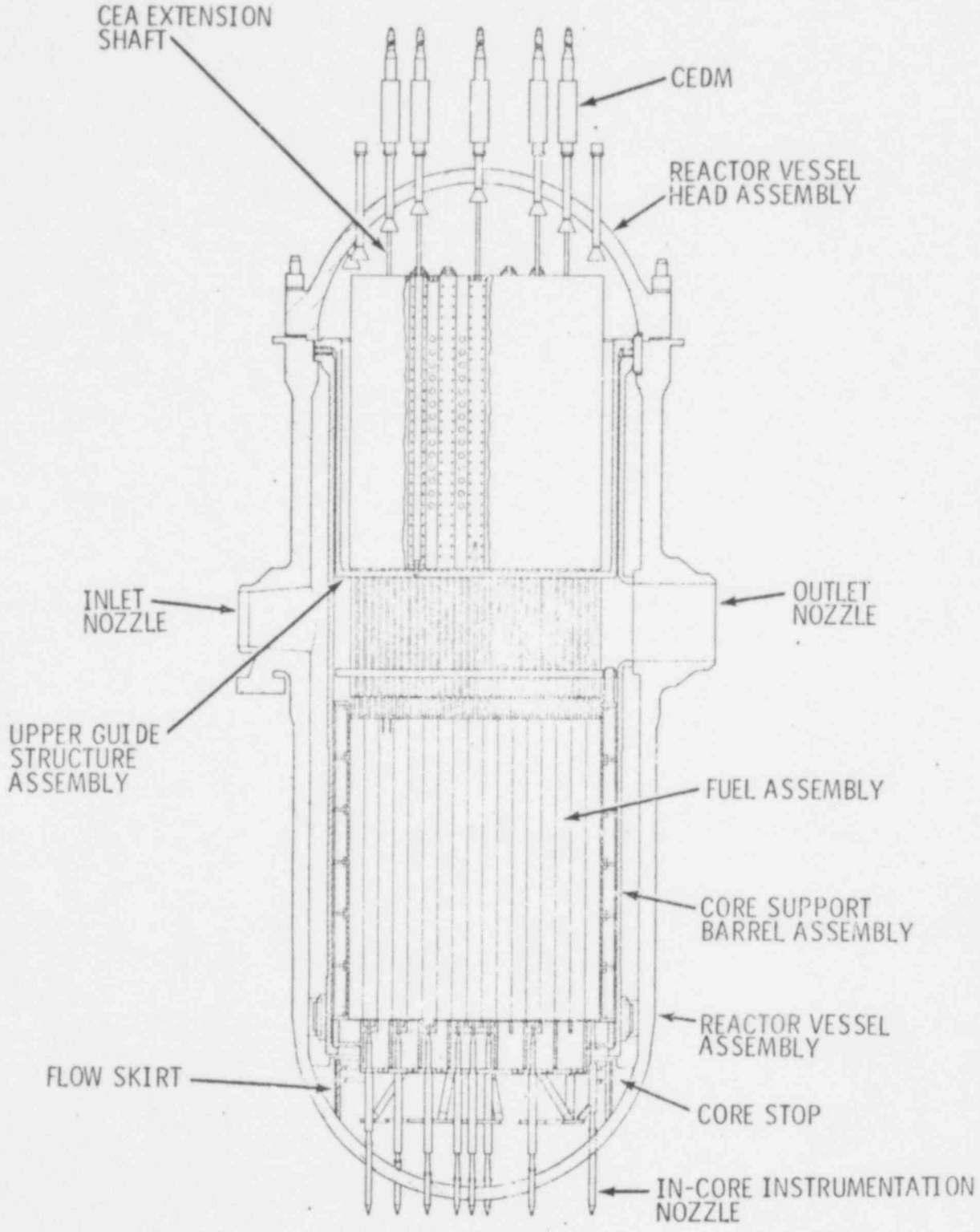

Figure 5-2
REACTOR VESSEL DETAIL

[3,5]

596 1AA

Figure 5-3 CEFLASH-4B BLOWDOWN LOADS MODEL FOR AN INLET BREAK

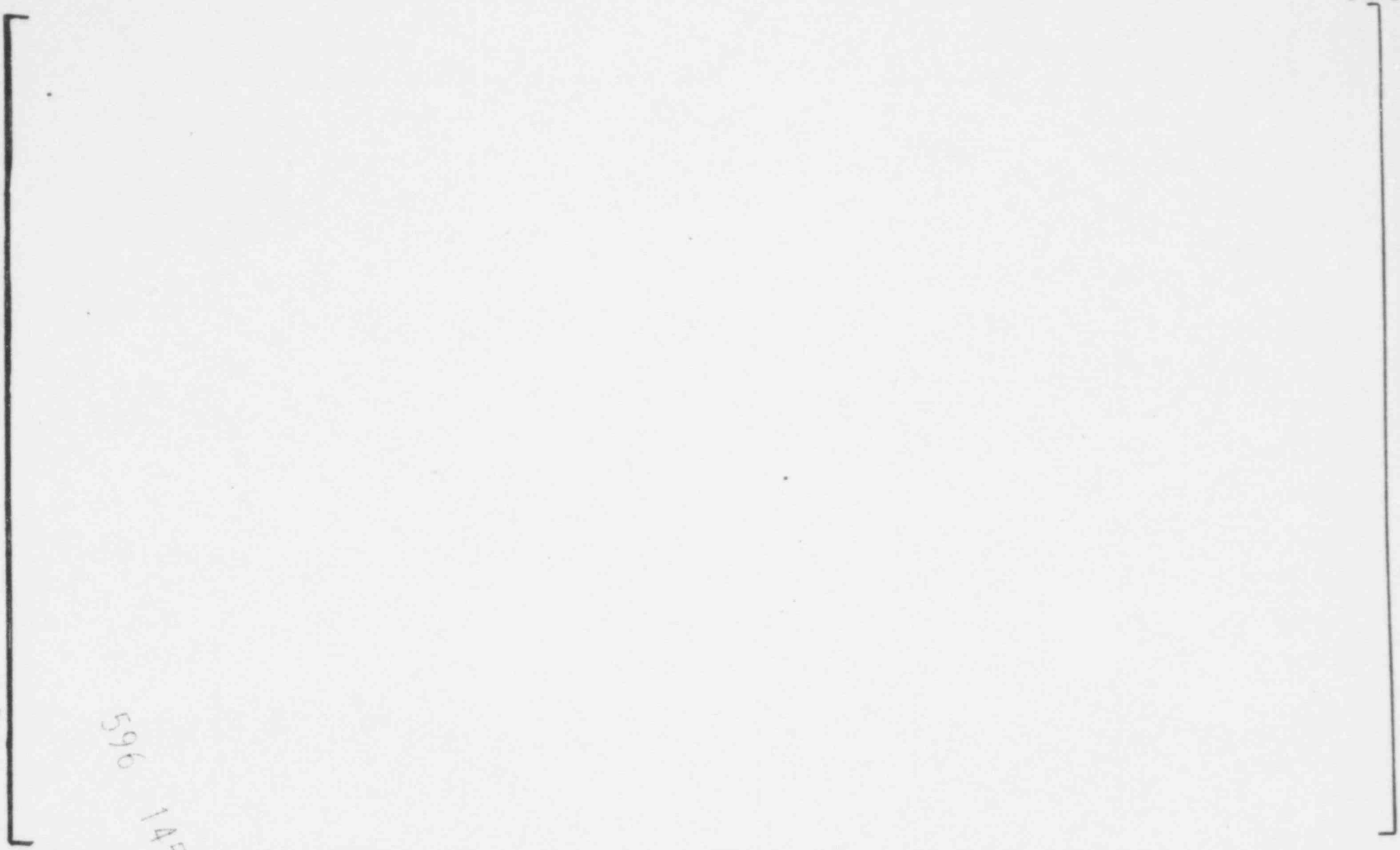

Figure 5-4 CEFLASH-4B BLOWDOWN LOADS MODEL FOR AN OUTLET BREAK

Figure 5-5

CROSS SECTION OF REACTOR VESSEL AT NOZZLE CENTERLINE ELEVATION
SHOWING ANNULUS NODE BOUNDARIES

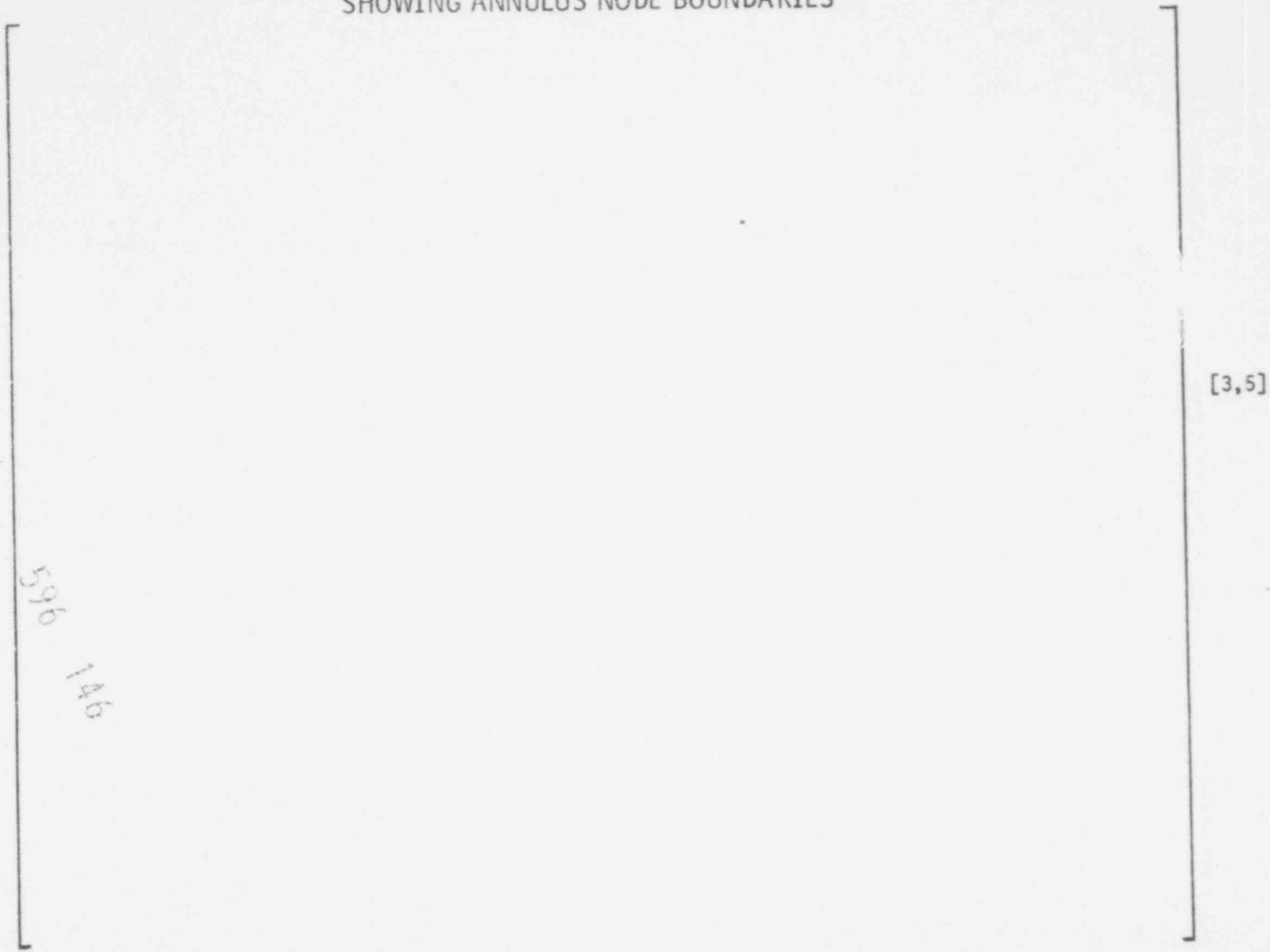

[3,5]

596 146

Figure 5-6
GUILLOTINE BREAK MODEL

[3,5

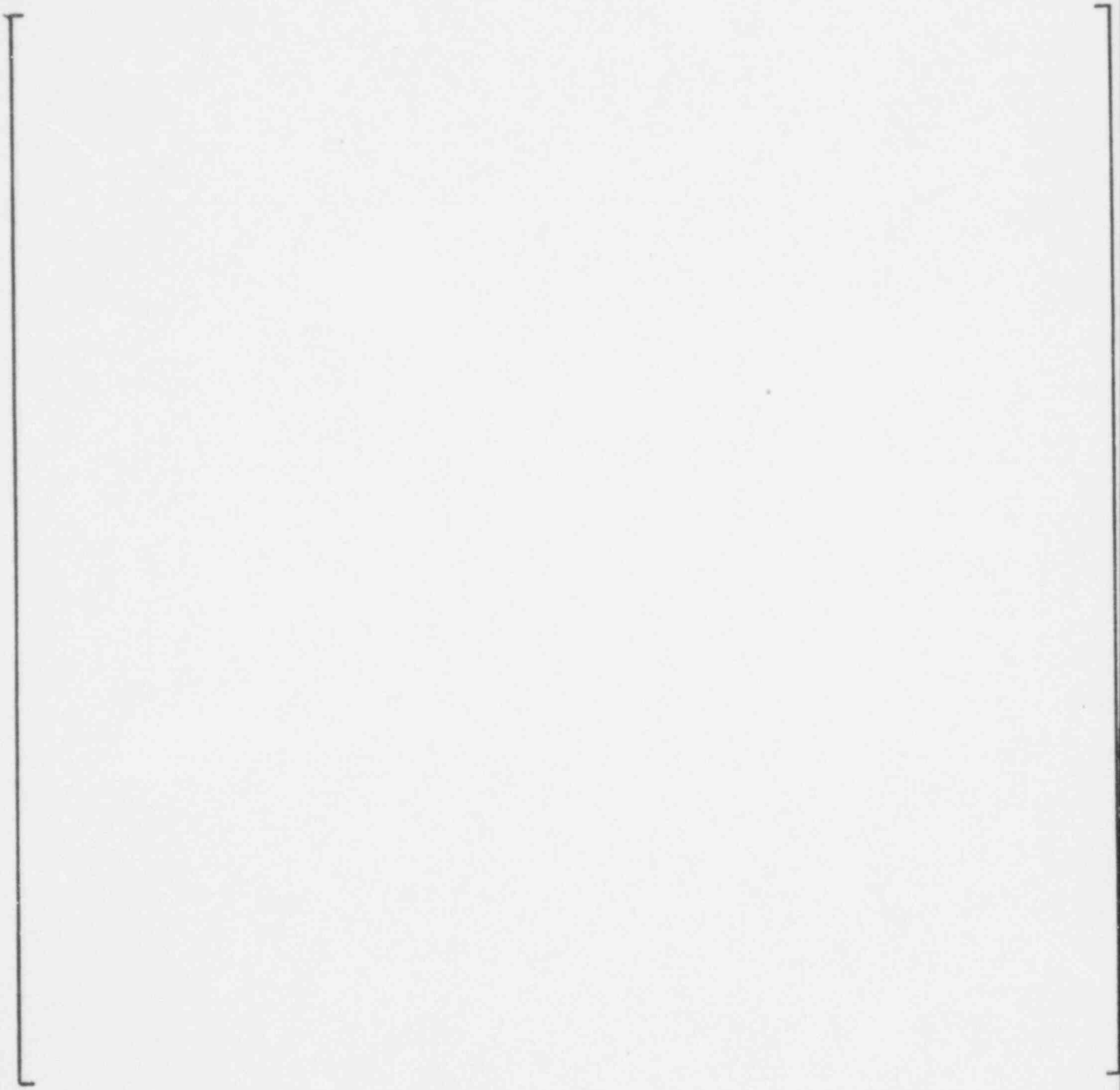

Figure 5-7
STEADY STATE ABSOLUTE PRESSURES FOR SYSTEM 80

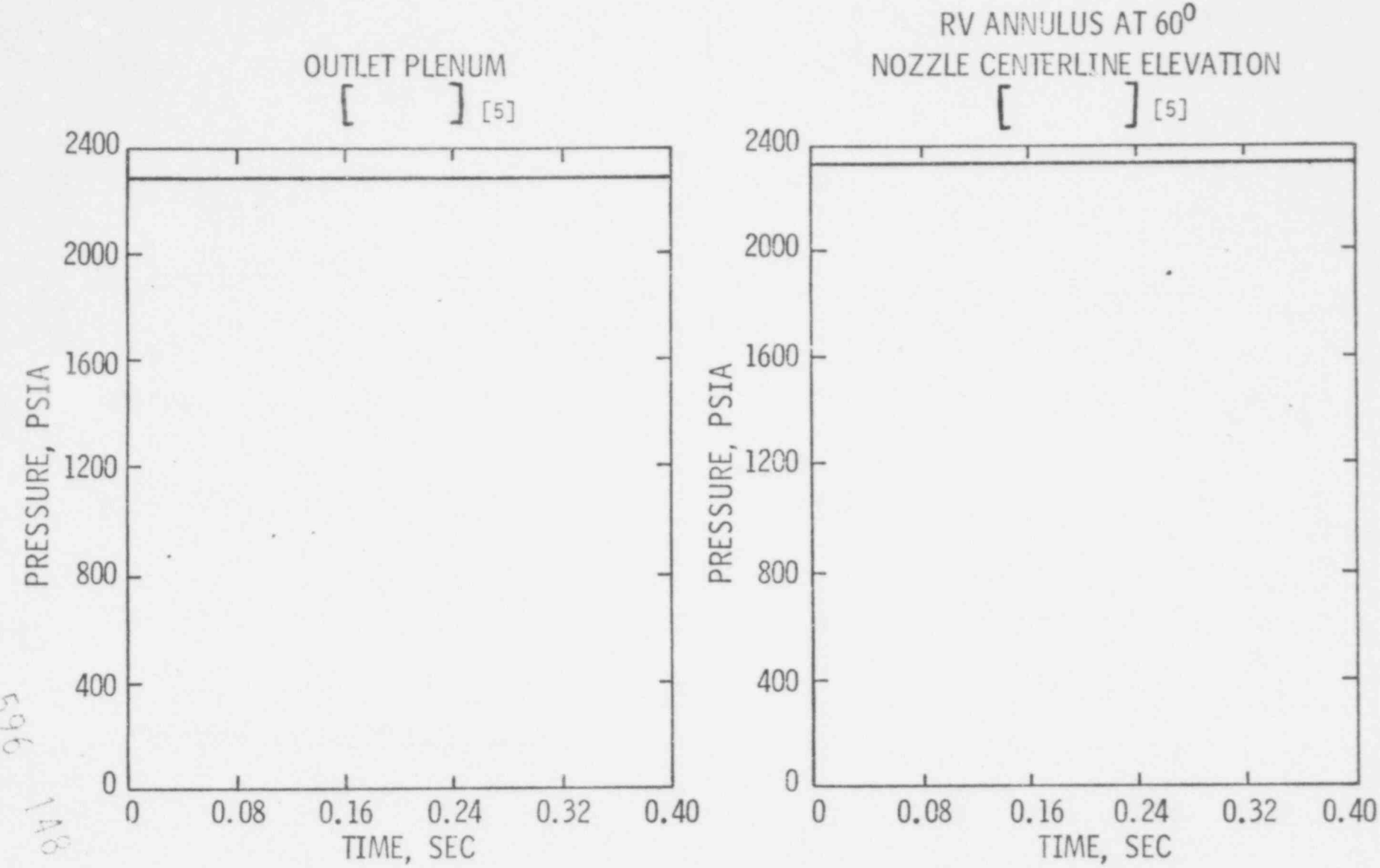

596 148

Figure 5-8

STEADY STATE PRESSURE DIFFERENTIALS FOR SYSTEM 80

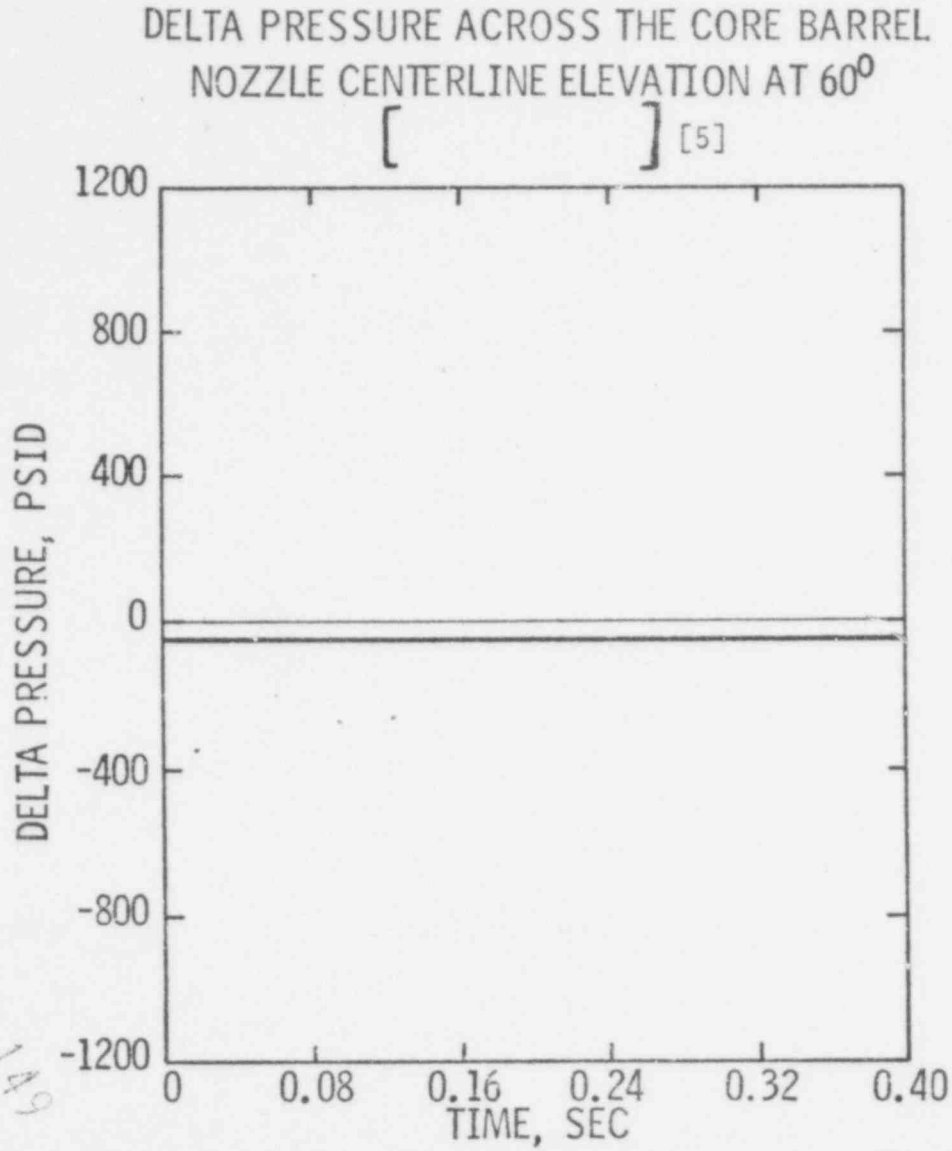

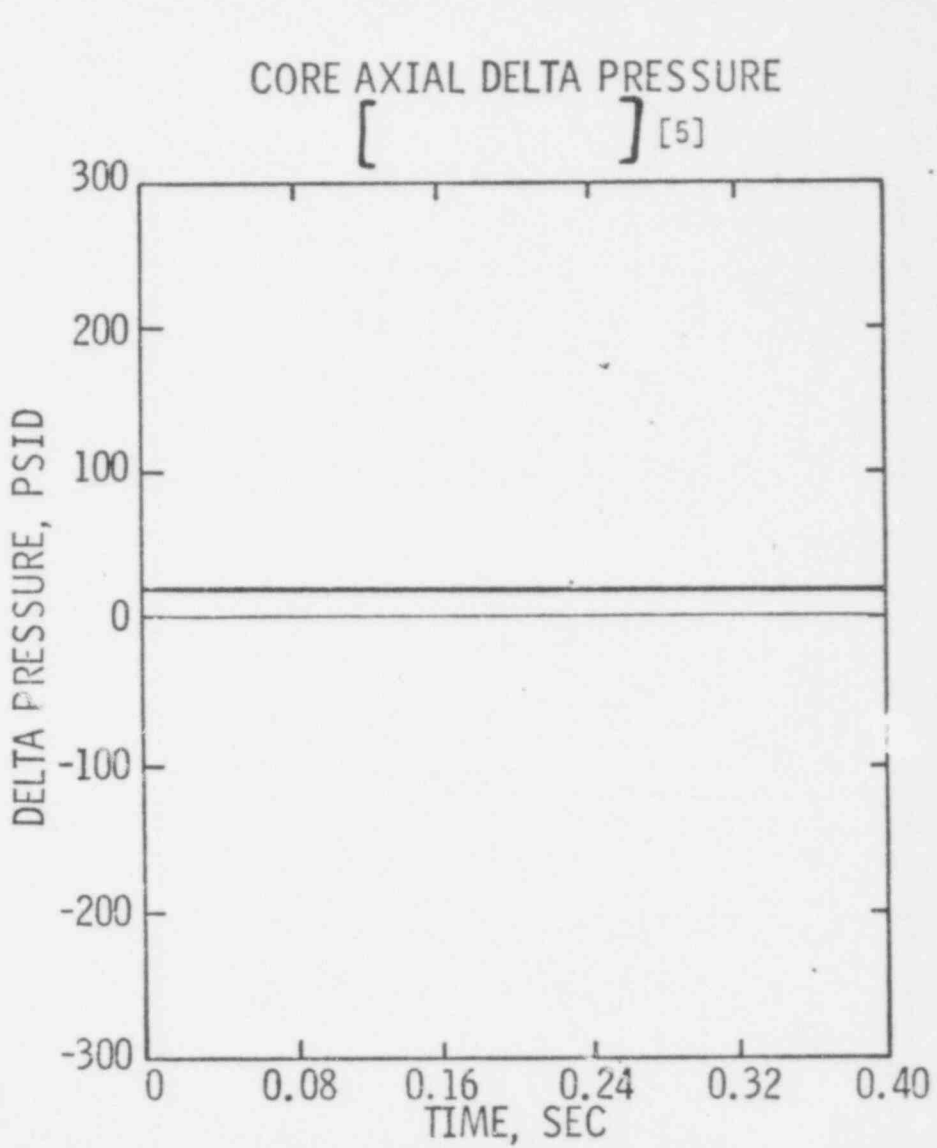

596 149

Figure 5-9

SYSTEM 80 350 SQ. INCH FULL POWER INLET BREAK
ABSOLUTE PRESSURE TIME HISTORIES

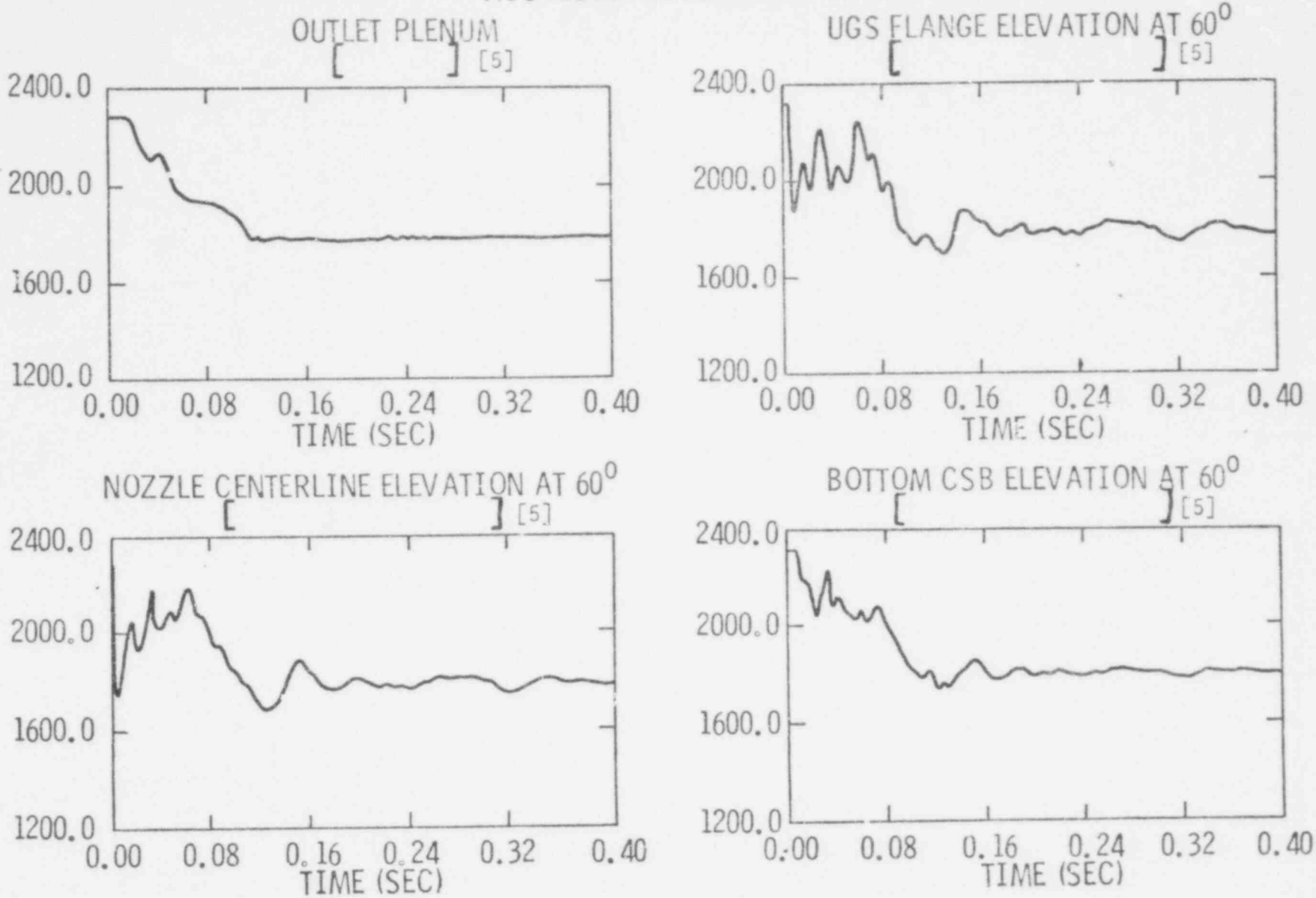

Figure 5-10

SYSTEM 80 350 SQ. INCH FULL POWER INLET BREAK

DELTA PRESSURE ACROSS THE CORE BARREL

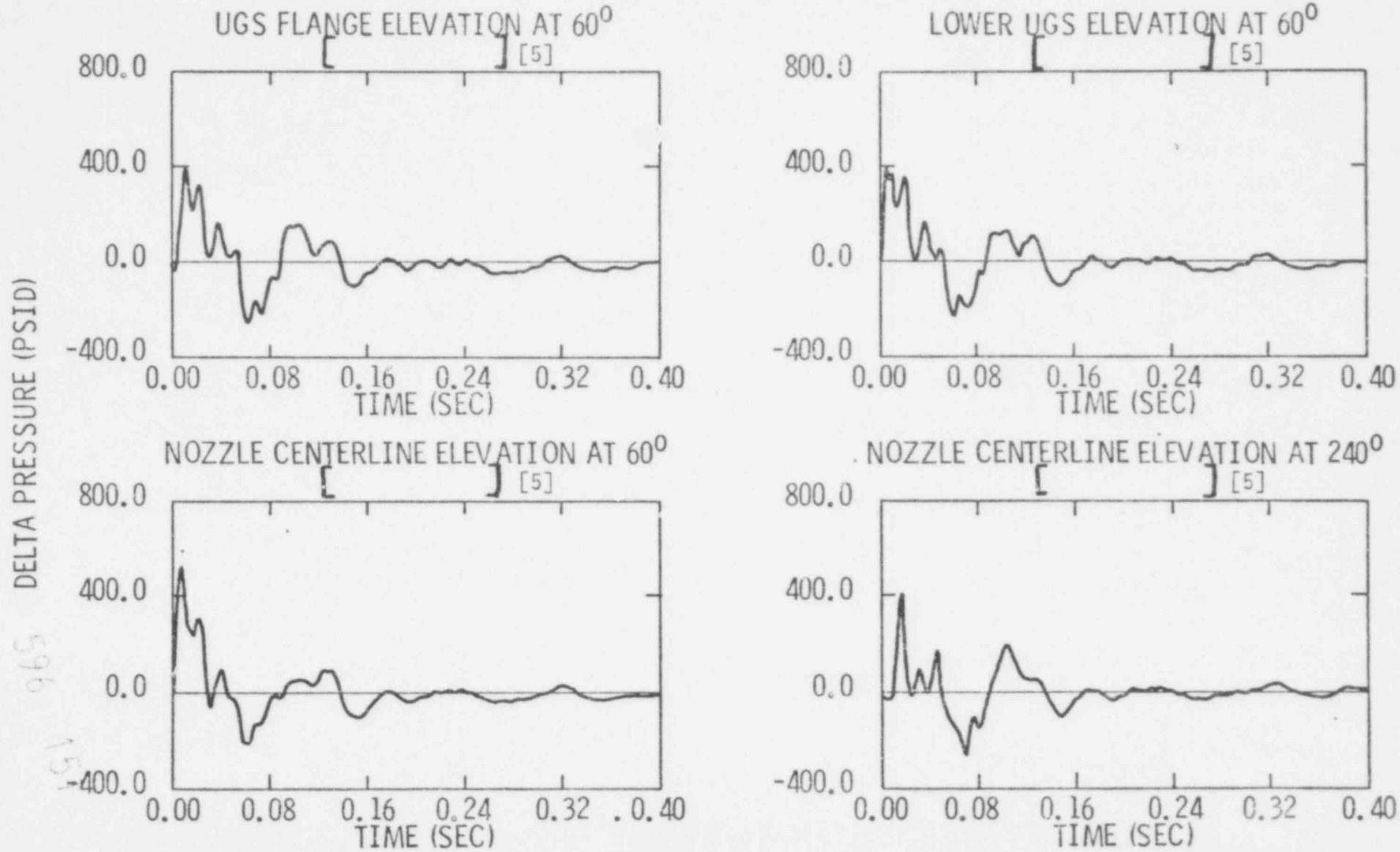

Figure 5-10 (Continued)
SYSTEM 80 350 SQ. INCH FULL POWER INLET BREAK
DELTA PRESSURE ACROSS THE CORE BARREL

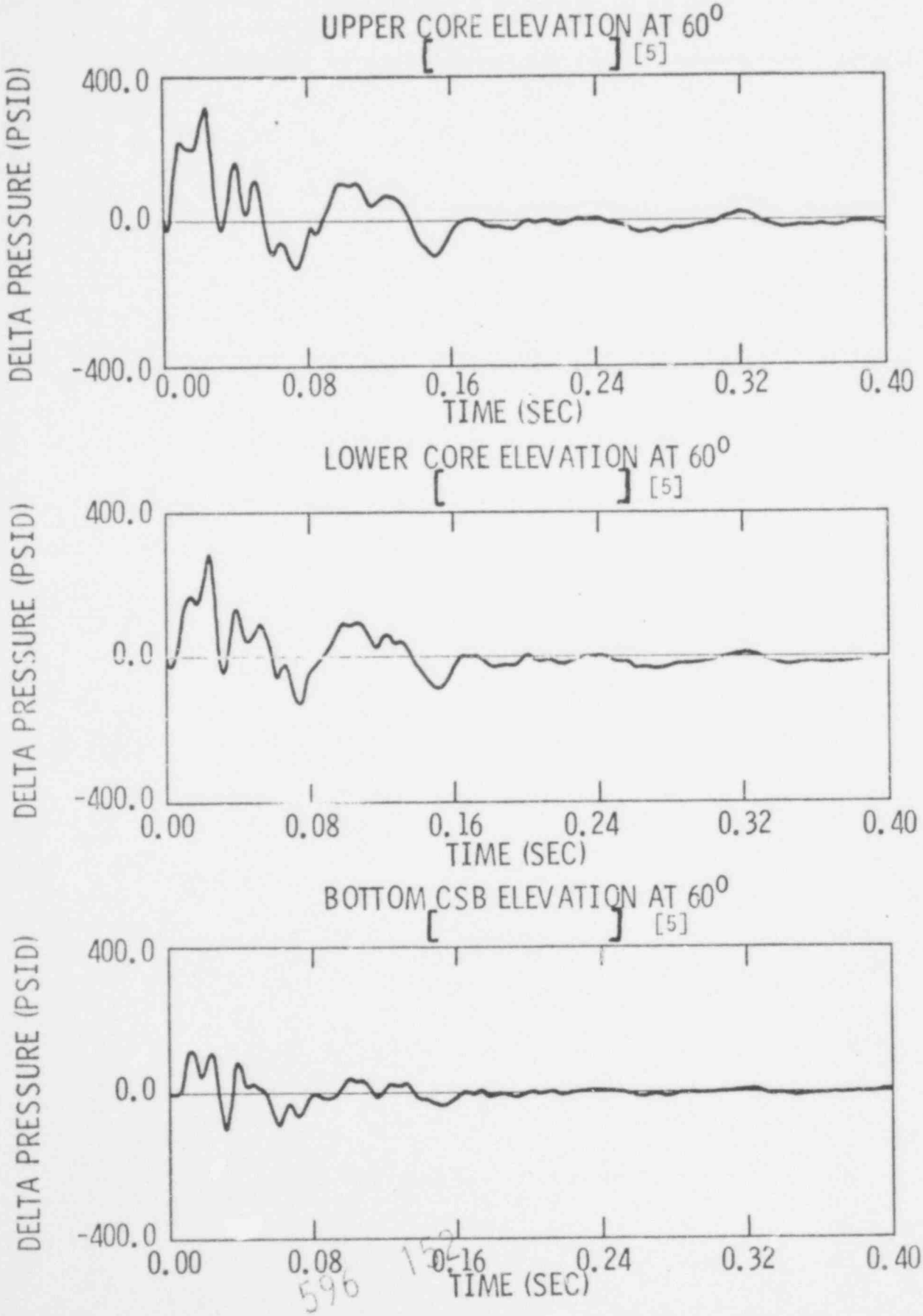

Figure 5-11

SYSTEM 80 350 SQ. INCH FULL POWER INLET BREAK
CORE AXIAL DELTA PRESSURE
[ ] [5]

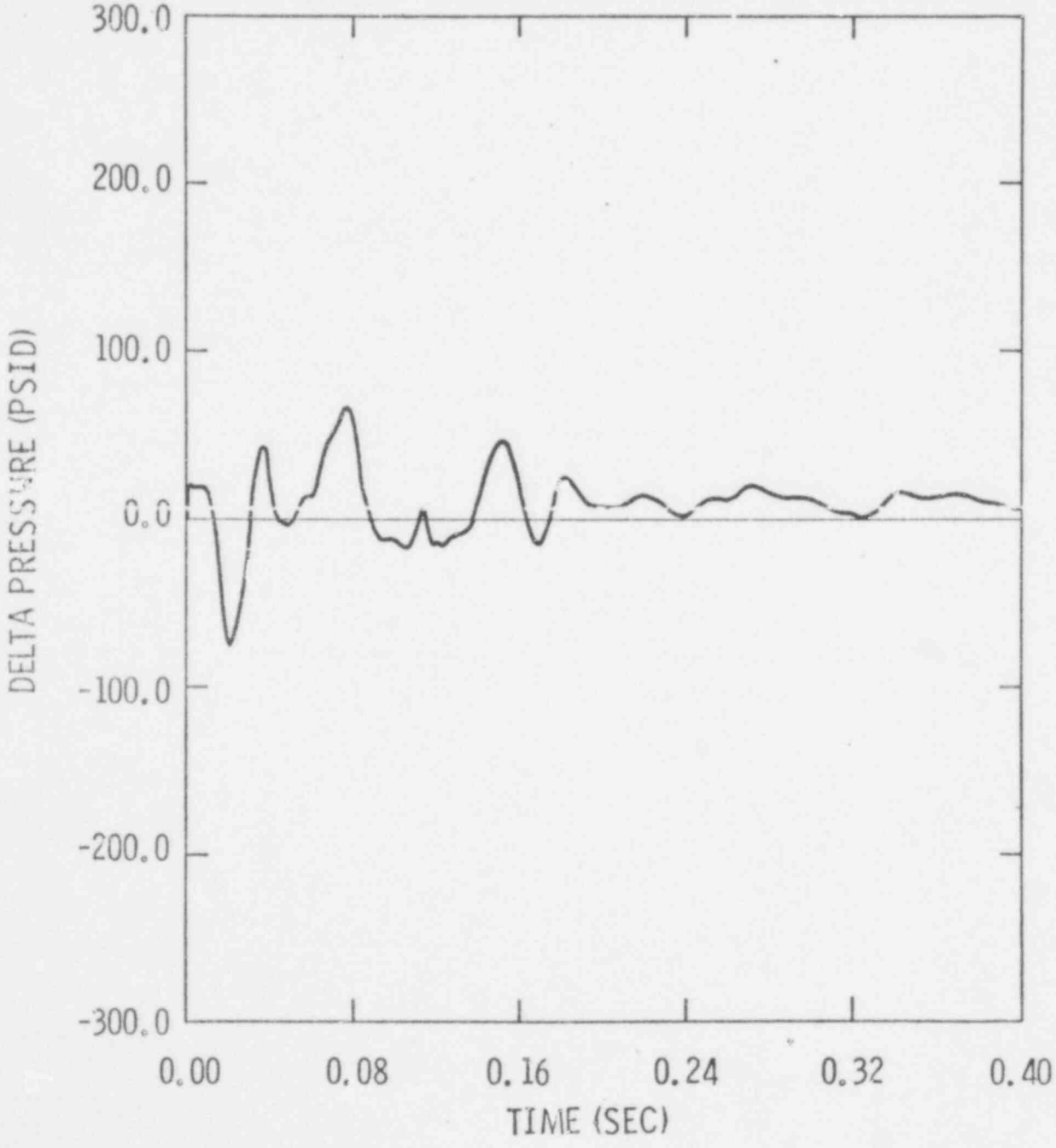

Figure 5-12

SYSTEM 80 350 SQ. INCH FULL POWER INLET BREAK
FLOW SQUARED TIMES SPECIFIC VOLUME ($W^2\nu$)

INTACT LOOP [ ] [5]

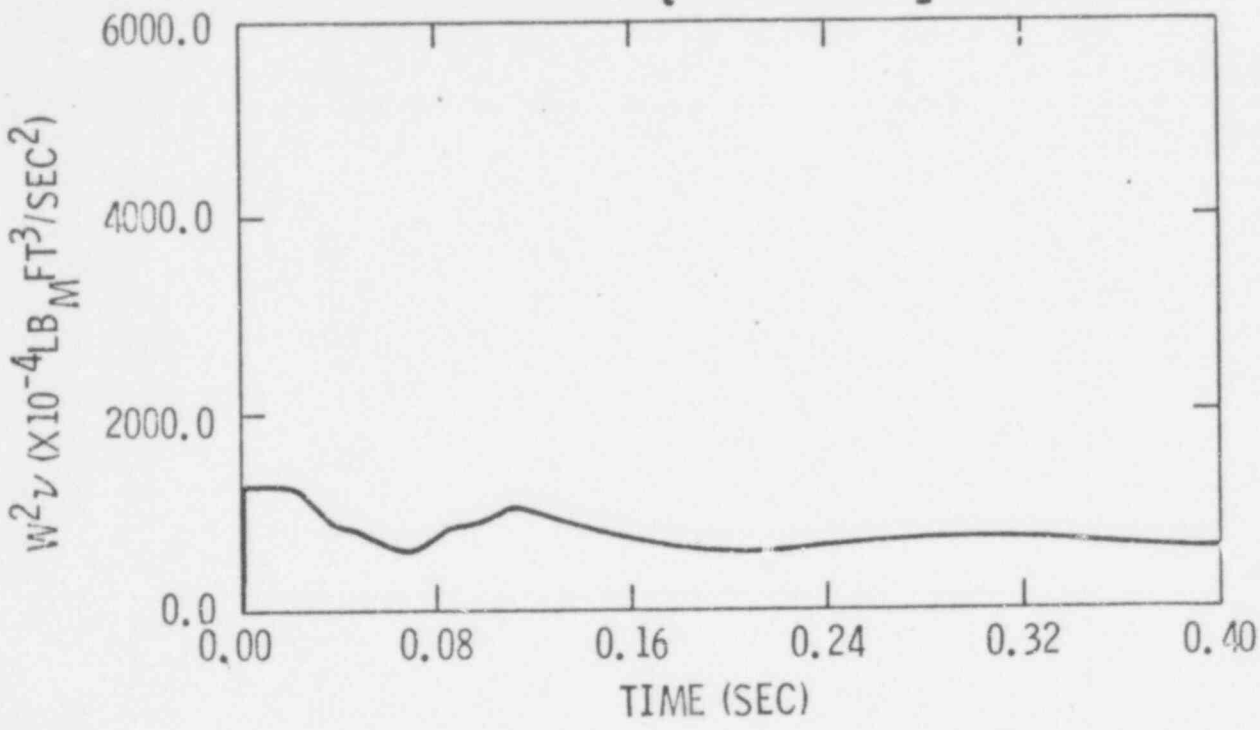

RUPTURED LOOP [ ] [5]

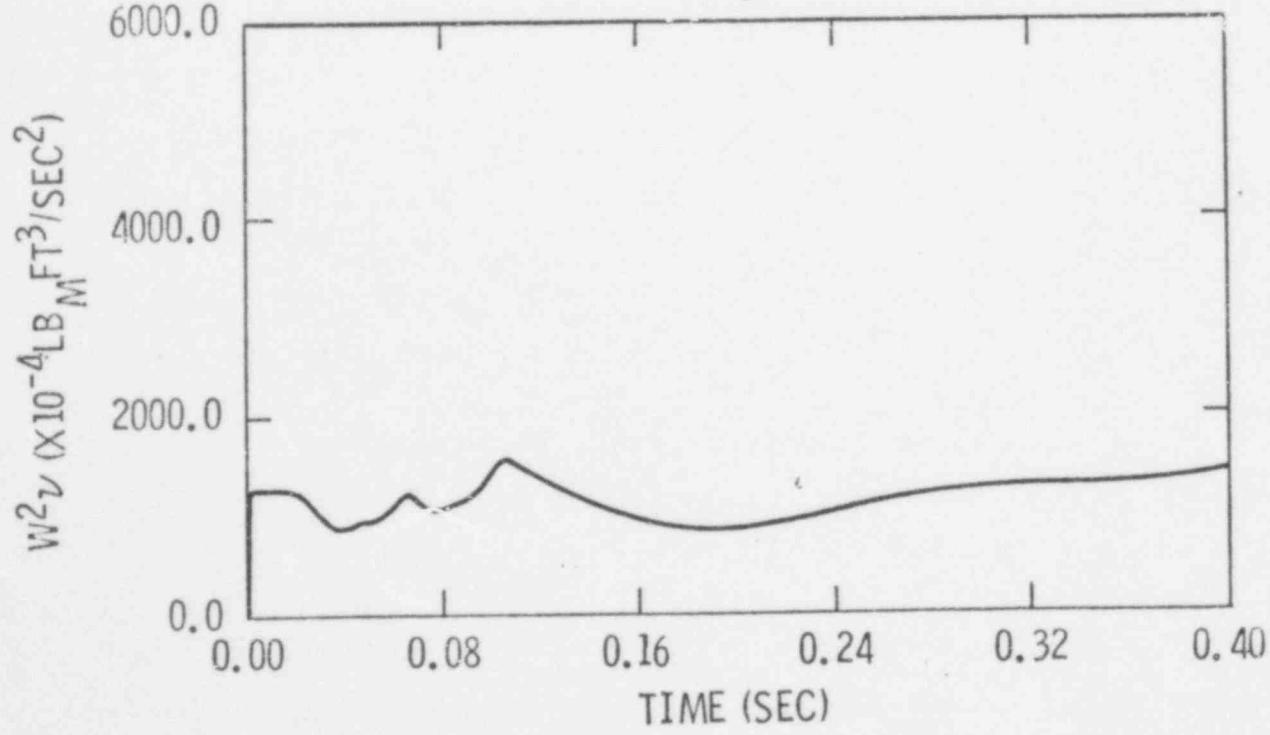

SYSTEM 80 100 SQ. INCH FULL POWER OUTLET BREAK
ABSOLUTE PRESSURE TIME HISTORIES

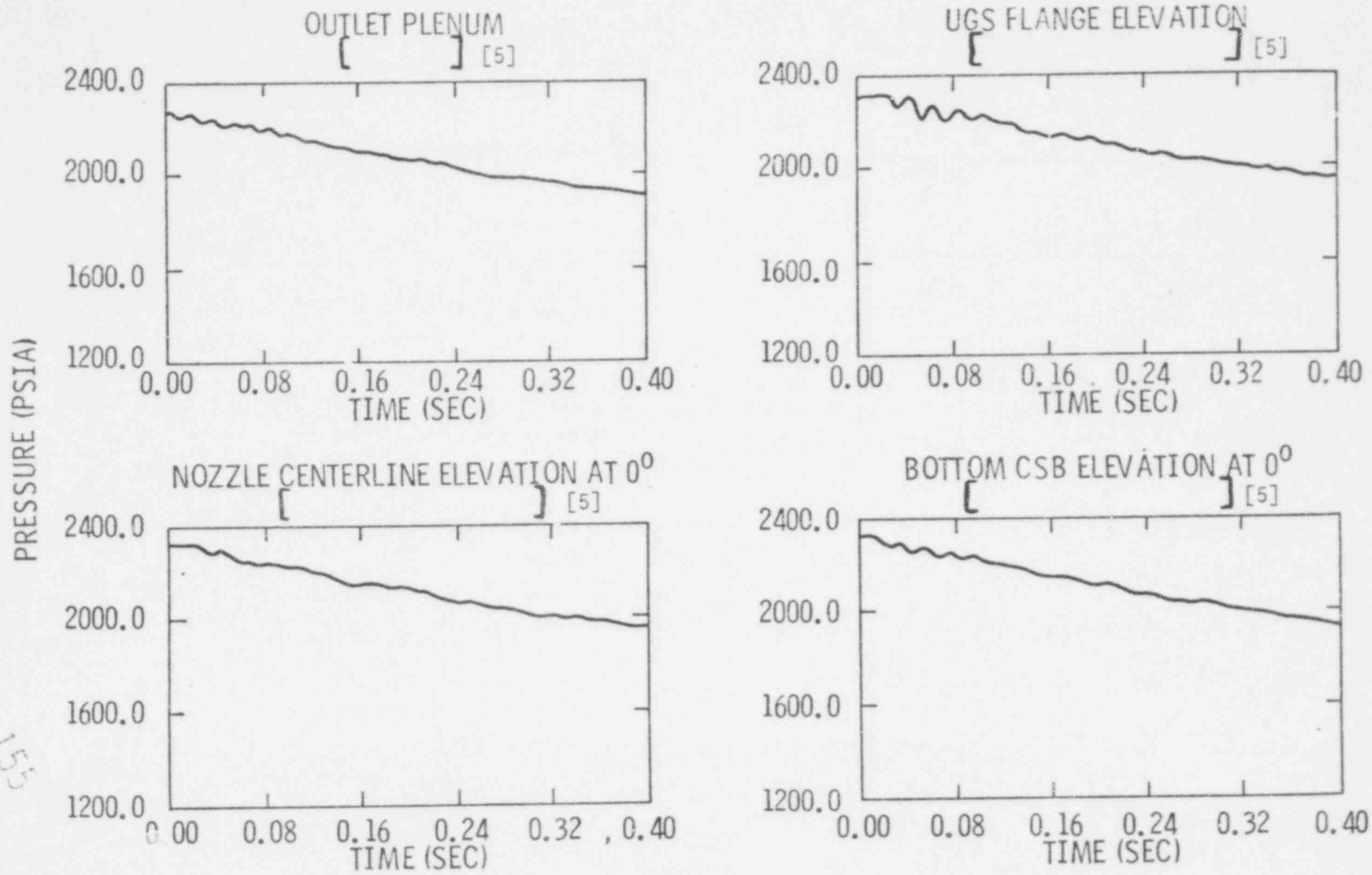

596
153

Figure 5-14

SYSTEM 80 100 SQ. INCH FULL POWER OUTLET BREAK
DELTA PRESSURE ACROSS THE CORE BARREL

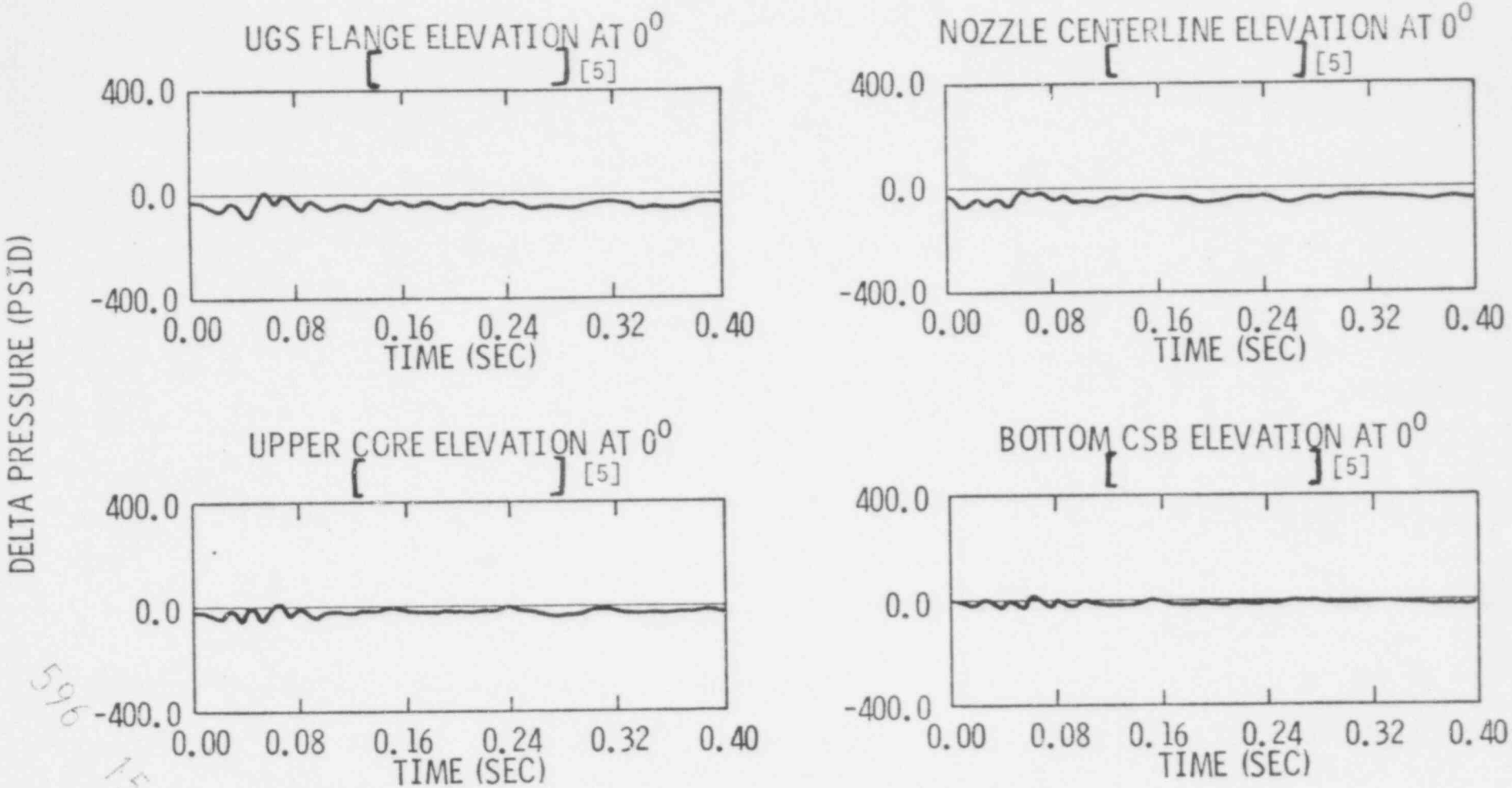

596
156

Figure 5-15

SYSTEM 80 100 SQ. INCH FULL POWER OUTLET BREAK
CORE AXIAL DELTA PRESSURE
[ ] [5]

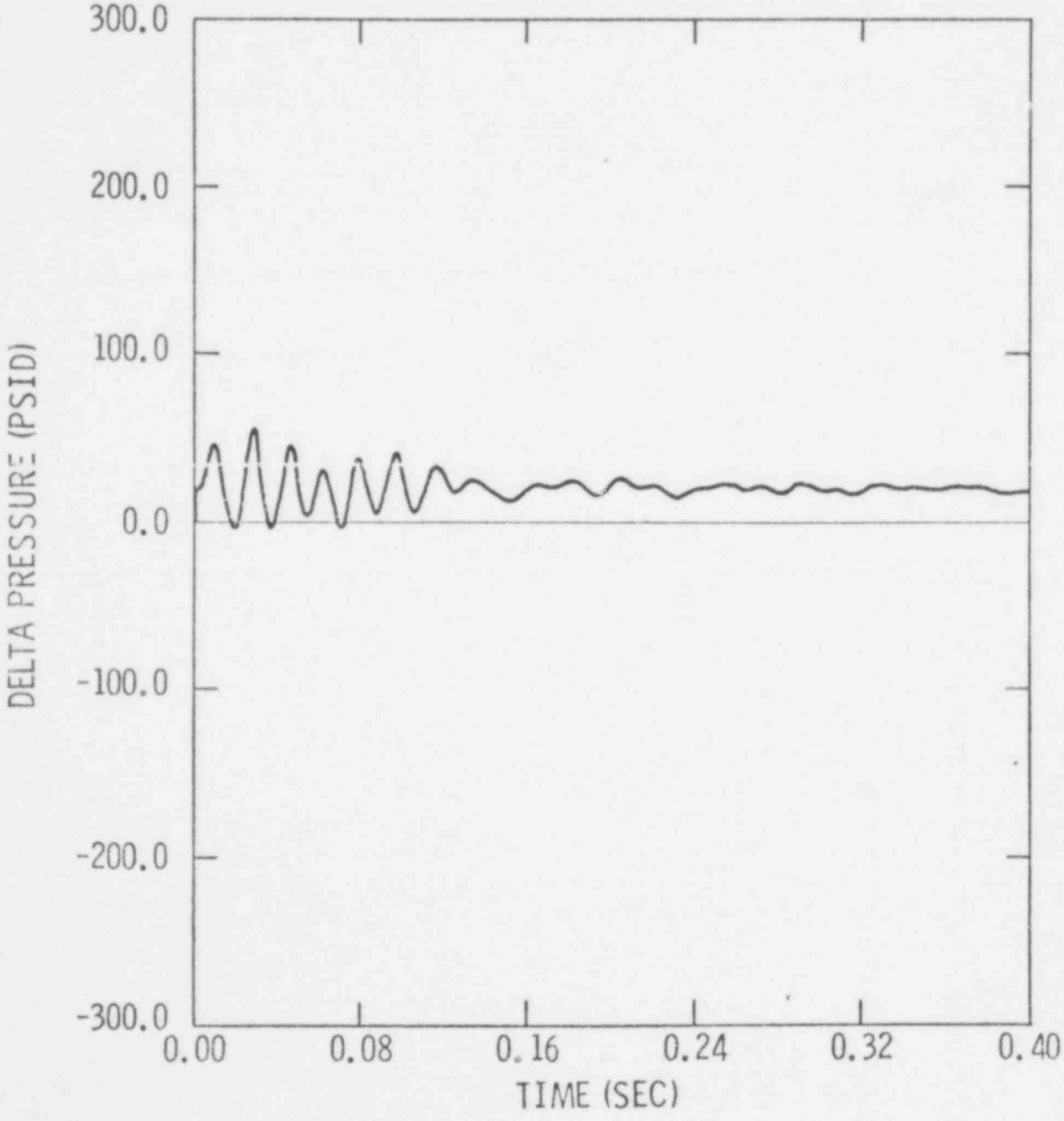

Figure 5-16

SYSTEM 80 100 SQ. INCH FULL POWER OUTLET BREAK
FLOW SQUARED TIMES SPECIFIC VOLUME ($W^2\nu$)

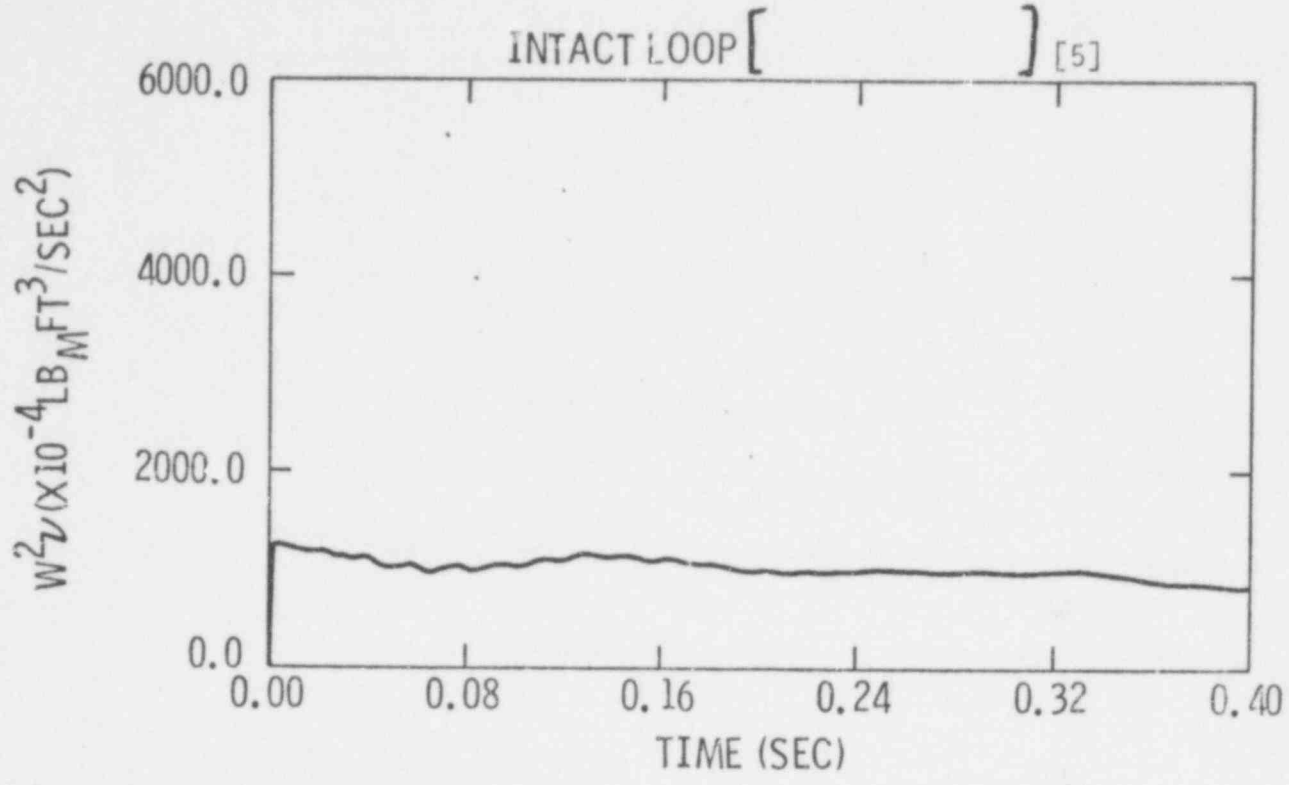

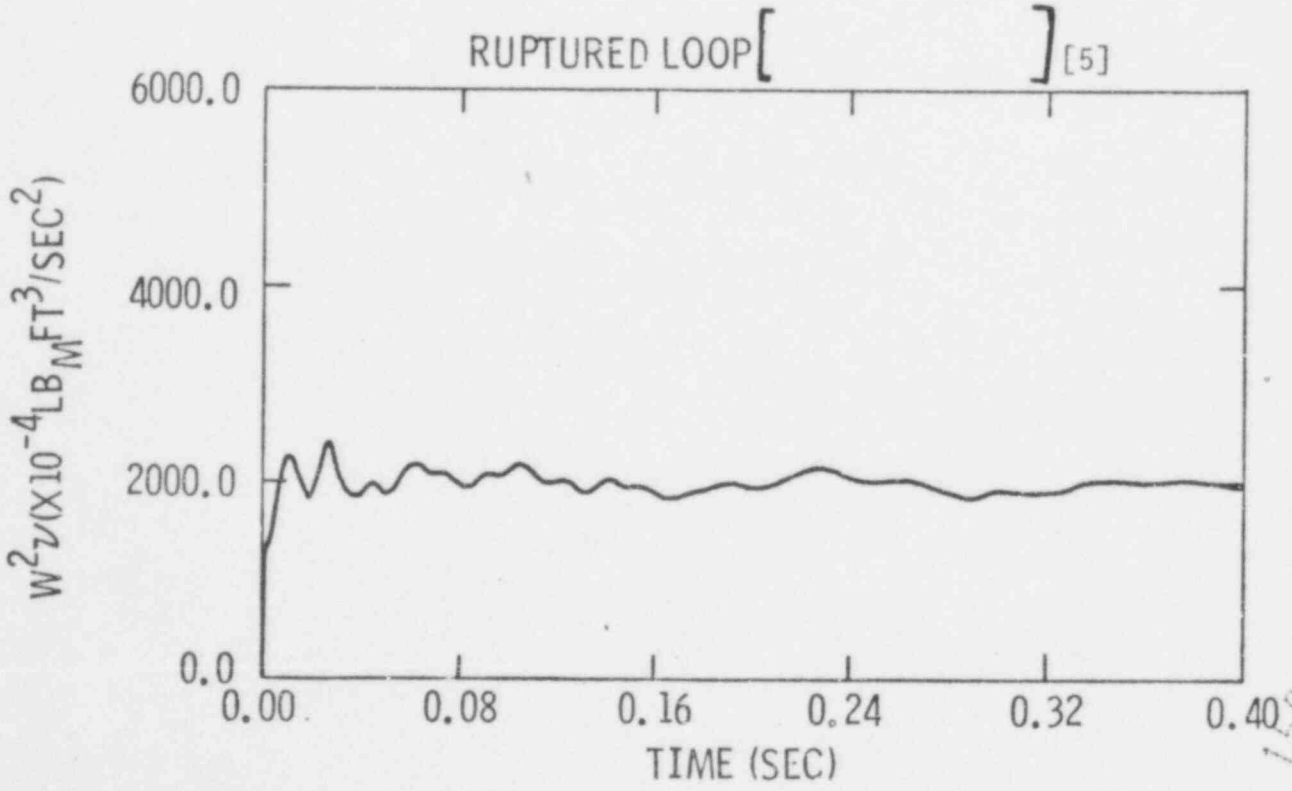

6.0 CALCULATION OF BLOWDOWN INDUCED HYDRAULIC FORCES

In the unlikely event of a primary pipe rupture, strong rarefaction pressure waves travel through the reactor primary system. Motion of these waves produces both large local pressure gradients across various reactor internal components and an acceleration (deceleration) of primary circuit fluid increasing (reducing) its associated component drag load, depending on the location of the pipe rupture. This section presents the methodology used for the evaluation of blowdown induced forces following a pipe rupture. Particular attention has been given to the evaluations of lateral blowdown loads on the Control Element Assembly (CEA) Upper Guide Structure (UGS).

6.1 EVALUATION OF LATERAL FORCES ON THE CONTROL ELEMENT ASSEMBLY UPPER GUIDE STRUCTURE

The Upper Guide Structure (UGS) assembly includes the upper guide structure support plate, control element assembly shrouds and the fuel alignment plate. A typical upper guide structure for a C-E System 80 reactor is shown in Figures 6.1 and 6.2. Among its many functions, the upper guide structure assembly maintains the CEA spacing and protects the CEA's from the adverse effects of coolant crossflow.

During steady state operation the coolant flows axially from the core up into the upper guide structure. Within the upper guide structure the coolant flow direction changes so that it exits radially via the hot leg nozzles. The transverse flow of the coolant across the CEA shrouds gives rise to loads which induce deflections in these shrouds. The magnitude of this transverse shroud flow, and the resulting deflections, are greatest following a double-ended break in a hot leg.

The drag forces have been determined from steady state, geometrically and dynamically similar, flow model experiments. Combustion Engineering, Inc., has conducted several such experiments in support of its CEA shroud tube

drag evaluation procedures. Prototype CEA loads were established by axially and azimuthally monitoring surface pressures on various scaled down CEA shrouds, through pressure taps mounted on their interior. These experimental pressures were then converted into equivalent shroud forces. (An example of the resultant model shroud forces is presented in Figure 6-3 for a typical scaled C-E System 80 CEA shroud simulation.) These measured shroud forces were then geometrically and dynamically scaled up to be representative of the prototype PWR upper guide structure.

[3

As a consequence of similarity conditions, the force at the same relative location on the same CEA shroud tube for the prototype PWR can be written as:

[3,5]

In applying the experimental forces to LOCA conditions it has been assumed that the ratio of the local model shroud drag force to its associated dynamic head is a constant.

Combining all known quantities in equation 6-3 into a proportionality factor k_j, the following relationship for the drag force on an individual CEA shroud tube results:

[ ] (6-4) [3,5]

The summation represents a vector sum over all (N) segments, where N is the number of independent axial shroud locations to be measured. In the computation of the CEA shroud drag force vectors are conservatively assumed to be directed along the centerline of hot leg flow.

[This section provides additional details on C-E's calculational methods for evaluating UGS CEA shroud forces.] [3,5]

[ ] [3,5]

The evaluation of the total force on the UGS is established by vectorally summing the individual CEA shroud tube forces (from equation 6-6) over all CEA shrouds in the upper guide structure.

6.2 CALCULATION OF LATERAL LOADS ON THE CORE SUPPORT BARREL

CEFLASH-4B pressures are supplied at [ ] approximately equally [3,5] spaced locations along the length and circumference of the core support barrel. [

[3,5]

] These pressures are differenced from the local interior barrel pressure at the same axial elevations to

obtain the local barrel radial pressure differentials. The procedure for evaluating lateral loads on the core support barrel from predicted surface pressure differentials is the same as that previously presented in Reference 6-1.

6.3 CALCULATION OF VERTICAL LOADS

Vertical loads on the individual structural components housed in the reactor pressure vessel are calculated using standard mass, momentum and energy control volume analysis techniques (see for example Reference 6-2). In these analyses, care is taken so that the control volumes are defined consistently with the CEFLASH-4B nodal network. An overview of this method is presented here for purposes of completeness.

Dependent on the structure, either one of two types of momentum control volumes are used to define the force acting on a component. Structures, such as plates, are typically defined by a control volume consisting of the structure and surrounding fluid. While other structures, for example the fuel rods, are handled more efficiently by defining the control volume to include the structure alone. In the latter case the load on the structures are determined by summing the forces resulting from all shearing and normal stresses acting on the control surface.

In the above analyses, fluid shear on the various structure control volumes are considered to be dependent on the local fluid Reynolds number. In the particular case of fuel rods, the wall shear forces and spacer grid losses are evaluated from Reynolds number dependent functions obtained from experimental data (see for example Reference 6-3).

6.4 REFERENCES FOR SECTION 6.0

6-1 Combustion Engineering, Inc., " "Dynamic Analysis of Reactor Vessel Internals Under Loss-of-Coolant-Accident Conditions With Application of Analysis to C-E 800 MWe Class Reactors" CENPD-42, August 1972 (proprietary)

6-2 Hansen, A.G., Fluid Mechanics, John Wiley and Sons, Inc., New York, 1967

6-3 Combustion Engineering, Inc., "SYSTEM 80 Preliminary Safety Analysis Report: Combustion Engineering Standard Systems Analysis Report" Docket No. STN-50-470, October, 1975

Figure 6-1
C-E SYSTEM 80 UPPER GUIDE STRUCTURE ASSEMBLY

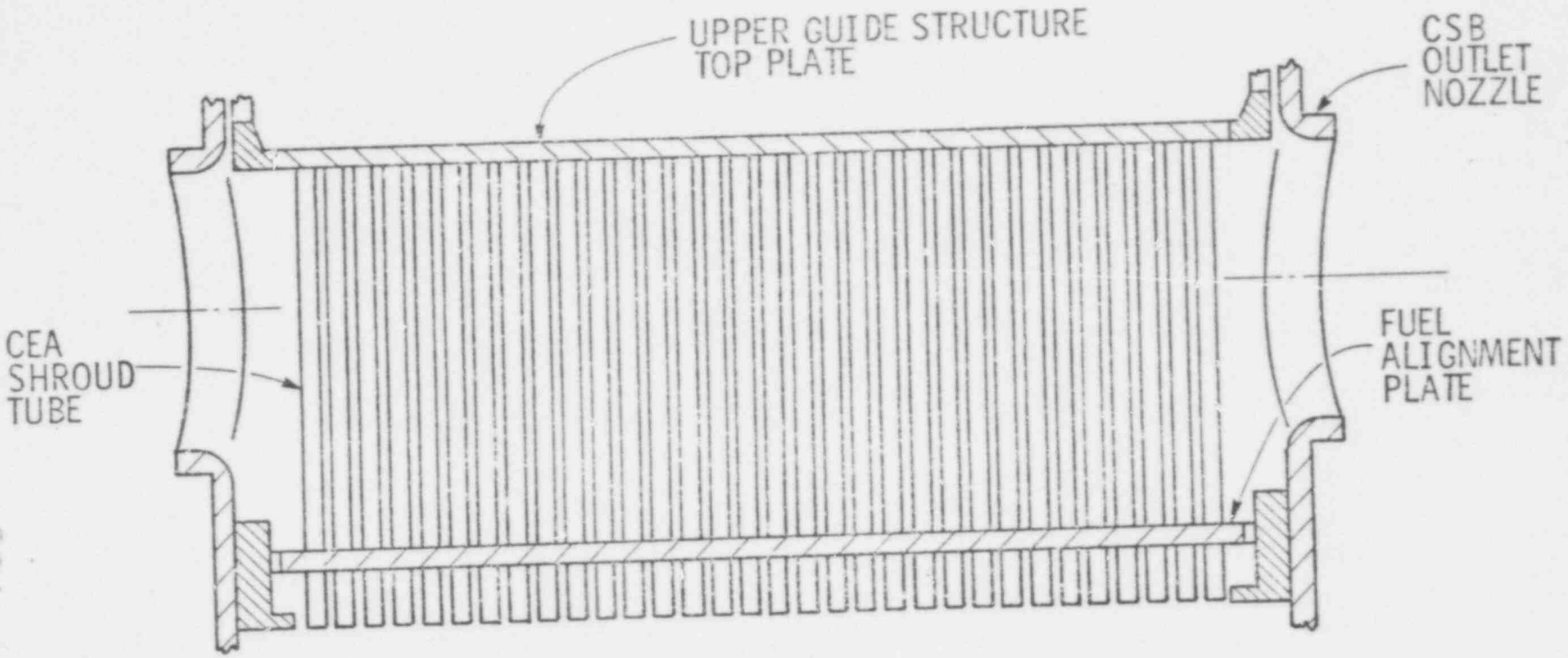

Figure 6-2

PLANAR VIEW OF
C-E SYSTEM 80 UPPER GUIDE STRUCTURE REGION

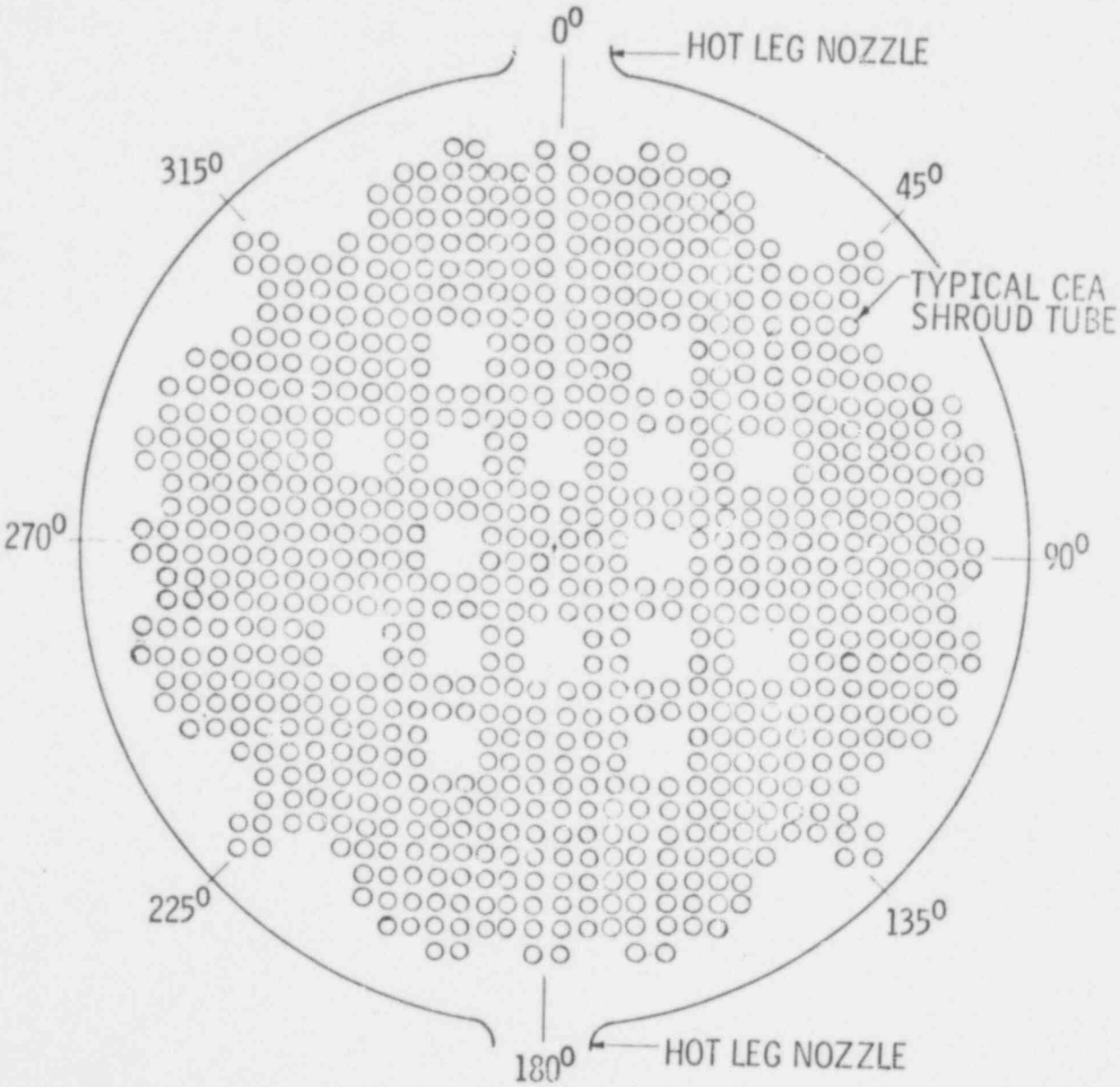

596 167

[4]

596 168

Figure 6-3
TYPICAL RESULTS OF CEA SHROUD FORCE SIMULATION

APPENDIX A

CEFLASH-4B INPUT DESCRIPTION

This section presents the CEFLASH-4B input description. Details of the CEFLASH-4B code are presented in Sections 1 and 2 of this report and are supplemented by CEFLASH-4A documentation of References A-1, A-2, and A-3.

A.1 CEFLASH-4B INPUT

CEFLASH-4B has the capability of merging four permanent files with punched card input to form an input deck to the code. The first card of punched card input is read as a comment card, then files are read in order of Tape 1, Tape 2, Tape 3, Tape 4. The reading of Tape 4 is followed by the reading of the remaining punched card input. The last card of any card series number is the one kept and used. No regular data cards may appear after the last card (· in column 9). CEFLASH-4B uses the Bettis Environmental[+] input package for the main input deck and specific FORTRAN formats for the first card and the plotting data.

Title Card

The title card appears at the top of the first page of each edit. The title card has an 8A10 format consisting of any alphameric character in columns 1 to 80.

Bettis Environmental input cards

Columns 1-8 should be blank. Punching must begin in Column 9. The cards are either Comment Cards or Data Cards.

Comment Cards

Column 9	*indicates a comment card
Columns 10-80	Any type of information (alphameric characters). This comment card will only appear in the listing of the input data.

[+] Pfeifer, C. J., "CDC 6600 FORTRAN Programming-Bettis Environmental Report", WAPD-TM-668, January, 1967.

Data Cards

The card number is punched beginning in column 9 followed by a comma and input data separated by commas. No comma follows the last piece of data on the card. In the description of the Card Series:

F indicates floating point numbers (e.g., 924.0, 9.24+2, .004). The letter E cannot be used.

I indicates integer numbers (e.g., 86, 5, 101).

DATA CARDS (Bettis Environmental Input)

Time and General Information

Card Series 1001-1010

1001, F1, F2, F3, F4, F5, I6, I7

F1	ENDT	Problem end time (sec)
F2	TRUP	Rupture time (sec)
F3	TPN	Leak opening time (sec)
F4	REFELV	Reference elevation for potential energy (ft)
F5	PSUDF	Multiplier on pseudo-pressure term (if equal to 0.0 term is not used)
I6	MAXSTP	Maximum number of steps (for terminating problem)
I7	MAXEDT	Maximum number of edits (for terminating problem)

General Option Information

Card Series 1011-1020

1011, I1, I2, I3, I4, I5

I1 IFMK — Option of using momentum flux term in momentum equation

- = 0 Do not use momentum flux term
- = 1 Use momentum flux term for flow paths selected on 42NN card series.

I2 IFTAX — Two phase correlation option

- = 1 Homogeneous model
- = 2 Martinelli-Nelson correlation
- = 3 Thom correlation (below 250 psia uses Martinelli-Nelson)

596 172

I3	IFKC	Isothermal friction factor option = 1 Constant friction factor = 2 Flow varying friction factor
I4	IFCF	Critical flow check option = 0 Critical flow check on surge line (Type 5) and break flow path (type 7) = 1 Critical flow check on flow paths selected on 42NN cards in addition to Types 5, 7.
I5	IFBL	= 1 Reactor system is initially balanced by the code

ime Step Information

ard Series 2001 - 2500

2001, $F1_1$, $F2_1$, $I3_1$, . . ., $F1_n$, $F2_n$, $I3_n$ ($1 \leq n \leq 20$)

F1	DELTN	Time step (sec)
F2	EOI	End of interval (sec)
I3	NIPPO	Number of steps per printout for this interval

596 173

Control Volumes (nodes - maximum of [ ]) [3]

Card Series 3001 - 3200

3001, $F1_1$, $F2_1$, $F3_1$, $F4_1$, $F5_1$, $F6_1$,.....,
$F1_n$, $F2_n$, $F3_n$, $F4_n$, $F5_n$, $F6_n$,($1 \leq n \leq$ [ ]) [3]

F1	A	Area (ft^2)
F2	ZTOT	Height of volume (ft)
F3	ELEX	Exit elevation (ft)
F4	ELIN	Inlet elevation (ft)
F5	ELBOT	Bottom elevation (ft)
F6	AGEE	Flow area for kinetic energy calculation (ft^2)

One array of six parameters for each control volume. All core nodes must be listed first.

Card Series 3201-3400 (necessary for certain nodes)*

3201, $I1_1$, $F2_1$, $F3_1$, $F4_1$, ..., $I1_n$, $F2_n$, $F3_n$, $F4_n$ ($1 \leq n \leq$ [ ]) [3]

I1	J	Node number
F2	P	Initial pressure (psia) must be less than 3000 psia
F3	WH	Initial enthalpy (BTU/lb) - if two-phase set = 0.0
F4	ZM	Initial level (ft) (reference to the bottom of the control volume) - if subcooled set = 0.0

*Non-zero values of pressure and enthalpy or two phase level must be input for certain nodes such as the containment node, secondary nodes, pressurizer node, and any 2ϕ node. For nodes with all inlet flow paths having zero initial flows one must input the enthalpy. A zero value of pressure may be input to signal the code to determine the pressure for this node.

Pressure Search Guide

Card Series 3601 - 3800

3601, $I1_1$, $I2_1$,.....$I1_n$, $I2_n$ ($1 \leq n \leq$ [ ]) [3]

I1	NFROM	Node whose pressure is input or has been already determined - upstream node
I2	NTO	Node connected to NFROM node but whose pressure is to be calculated - downstream node

The searching routine goes from NFROM to NTO, then continues by connecting flow paths until either a pump path, a node whose pressure is known, or a node specified by the next NFROM is encountered.

Containment Node

Card Series 3801

3801, I1

I1	NLAG	Node number for containment. The code will look for a maximum of 2 leak flow paths to this node.

596 175

Flow Paths

Card Series 4LNN.

LNN begins with 001 and has a maximum value of [ ] LNN must be in ascending (but not necessarily consecutive) order. The code will assign consecutive numbers to the flow paths.

L = 0,1 for types 2, 5, 8-10, 12
L = 2,3 for types 2, 5, 8-10, 12
} momentum-governed flow paths

L = 4 for type 7

All momentum governed paths must precede any and all leak flow paths.

Type Description

2	Pump path
5	Surge line
7	Leak path
8	Simple pipe
9	Flow area vs. pressure
10	Flow area vs. time
12	Lateral flow paths

All axial flow paths in the core matrix must be listed first. Flow paths 4001 to [and 4201 to [ ] must have the same consecutive numbering. Type 7 card must be numbered after the 40NN and 42NN cards.

596 176

Momentum-Governed Flow Paths

Types 2, 5, 8-10, 12 Flow Paths [3]

Card Series 4001-[ ]

40NN, I1, I2, I3, F4, F5, F6, F7, F8, F9

I1	NTYPE	Type (2, 5, 8, 9, 10, 12)
I2	NUP	From node
I3	NDOWN	To node
F4	W	Initial flow, W_o (lbs/sec)
F5	TLOA	Sum L/A (ft^{-1})
F6	TA	Area (ft^2)
F7	DIA	Hydraulic diameter (ft)
F8	AKUP	Momentum flux term upstream area (ft^2)
F9	AKDOWN	Momentum flux term downstream area (ft^2)

For every 40NN or 41NN there must be a 42NN or 43NN card.

596 177

Card Series 4201 [ ] [3]

41NN, F1, F2, F3, I4, I5, F6, F7

F1 TK — Friction K-factor (fℓ/D) (dimensionless) is input if initial flow = 0.0* Pressure drop (psi) is input if initial flow ≠ 0.0*

F2 XPOS — Geometric forward flow K-factor (dimensionless) is input if initial flow = 0.0* Pressure drop (psi) is input if initial flow ≠ 0.0*

F3 XNEG — Geometric reverse flow K-factor (dimensionless) is input if initial flow = 0.0* Pressure drop (psi) is input if initial flow ≠ 0.0*

---

*If flow rate is initially 0.0 one must input a non-zero value for the friction or the geometry K-factor. If friction is 0.0, L/D is set to 0.0 by the code and there will be no friction during the transient.

Frictional K-factor Calculation:

Once the flowpath up and downstream nodal pressures have been determined, the code will back calculate a frictional pressure drop using the momentum equation. This calculated frictional pressure drop will be compared to the input frictional drop and if they differ by more than 10^{-4} psi a message will be printed. The calculated frictional pressure drop will then be used in the K-factor calculation to insure that the steady state momentum equation is satisfied.

I4	IFMKFP	Option for using momentum flux term by flow path when IFMK on Card 1011 is 1 = 0 Do not use momentum flux term = 1 Use momentum flux term. Momentum entering and leaving (steady state) flow path is based on the nodal velocities. = 2 Use momentum flux term. Momentum leaving (steady state) flow path is based on the nodal velocity. = 3 Use momentum flux term. Momentum entering (steady state) flow path is based on the nodal velocity. = 4 Use momentum flux term. All contributing terms are based on the average flow in path.
I5	IFCFFP	Critical flow check for subcooled regime when IFCF on Card 1011 is 1 = 0 No critical flow check = 1 Critical flow check
F6	AMCFP	Minimum area for critical flow check (ft^2)
F7	FTL	Flow path length (ft). If F1= 0.0, then F7 must not be 0.0.

596 179

Leak Flow Paths (Type 7)

Card Series 4401-4600

These flow paths must follow the momentum-governed paths.

44NN, I1, I2, I3, F4, F5, F6, F7, F8, F9

I1	NTYPE	Type 7
I2	NUP	From node
I3	NDOWN	To node
F4	ZOD	4D = -1.0 Henry-Fauske/Moody tables used with F_Z = 44.0 = 0.0 Henry-Fauske tables used with F_Z = 45.4 = 1.0 Moody tables used with F_Z = 44.0 = 2.0 Homogeneous tables used with F_Z = 42.77
F5	TA	Area (ft^2)
F6	CC1	Discharge coefficient if $h < h_f$
F7	CC2	Discharge coefficient if $h = h_f$
F8	CC3	Discharge coefficient if $h > h_f$ and quality <1.0
F9	CC4	Discharge coefficient if $h > h_f$ and quality = 1.0

There is a linear interpolation between CC2 and CC3 which is a function of the quality.

Drag Coefficients (Optional)

Card Series 4801-4900

4801, $I1_1$, $F2_1$,...., $F19_1$,....,$I1_n$, $F2_n$,....,$F19_n$ ($n \leq 20$)

I1	NDC	flow path number
F2	CF1	constant , coefficients, and exponents for calculating the drag coefficient* if $W \geq 0.0$
F3	CF2	
F4	CF3	
F5	CF4	
F6	CF5	
F7	CF6	
F8	CF7	
F9	CF8	
F10	CF9	
F11	CR1	constant, coefficients, and exponents for calculating the drag coefficient* if $W < 0.0$
F12	CR2	
F13	CR3	
F14	CR4	
F15	CR5	
F16	CR6	
F17	CR7	
F18	CR8	
F19	CR9	

$$K_{drag} = CF1 + CF2\ Re^{CF3} + CF4\ Re^{CF5} + CF6\ Re^{CF7} + CF8\ Re^{CF9} \quad (W \geq 0.0)$$

$$K_{drag} = CR1 + CR2\ Re^{CR3} + CR4\ Re^{CR5} + CR6\ Re^{CR7} + CR8\ Re^{CR9} \quad (W < 0.0)$$

$$*DRAG = \frac{k|W|W\ SPV}{2gA}$$

where: DRAG = drag force (lbf)

A = flow area (ft^2)

SPV = specific volume (ft^3/lbm)

W = flow rate (lbm/sec)

g = 32.171bm-ft/lbf-sec^2

596 181

Modification of Upstream and Downsteam Elevation for Flow Path n (OPTIONAL)

Card Series 4601 - 4800

4901, $I1_1$, $F2_1$, $F3_1$,...,$I1_n$, $F2_n$, $F3_n$

I1	J	Flow path number (corresponds to a consecutive numbering of the flow paths as edited)
F2	ZOUT	Upsteam elevation (ft)
F3	ZIN	Downstream elevation (ft)

One array of three parameters must be supplied for each modified flow path.

Variable Flow Area vs. Pressure Table (Necessary for type 9 flow paths)

Card Series 4941 - 4970

4941, $F1_1$, $F2_1$, $F1_2$, $F2_2$,...,$F1_n$, $F2_n$ ($2 \leq$ pairs ≤ 50)

F1	WFB	Flow area (ft^2)
F2	WFB	Pressure (psia)

There may be several type 9 flow paths but only one table.

Variable Flow Area vs. Time Table (Necessary for type 10 flow paths)

Card Series 4971 - 5000

4971, $F1_1$, $F2_1$, $F1_2$, $F2_2$,...,$F1_n$, $F2_n$ ($2 \leq$ pairs ≤ 50)

F1	WFT	Flow area (ft^2)
F2	WFT	Time (sec)

There may be several type 10 flow paths but only one table.

Reactor Core Parameters

All 5000 and 6000 Card Series are omitted if there are no heated core nodes. There is a maximum of 20 heated core nodes.

General Core Options

Card Series 5001 - 5010

5001, I1, I2, I3, I4, I5, I6, I7, I8, I9, I10, I11, I12, I13

I1	NRZ	Number of radial zones in the core
I2	NAZ	Number of axial zones in the core
I3	ITCLHG	= 1 Use table of T_{ℓ}(°F) vs. kw/ft
		= 2 Use table of gap conductance (BTU/hr-ft^2-°F) vs. kw/ft.
I4	NOP	Geometry option for subregions for temperature distribution
		= 1 Subregions have equal thickness
		= 2 Subregions have equal volume
I5	NYZIR	Zirc water reaction option
		= 0 No Zr-H_2O calculation
		= 1 ZR-H_2O calculation
I6	NZRSL	Steam limited option for Zr-H_2O reaction
		= 0 Not limited
		= 1 Limited
I7	ITHOM	Nucleate boiling heat transfer correlation option
		= 0 Jens-Lottes
		= 1 Thom

596 183

I8	MDELT	$T_{surface} - T_{SAT} \geq 300°F$ criterion
		= 0 Criterion not activated
		= 1 Criterion is activated
I9	NUCB	Stay in pre-DNB regime except when in heat transfer to steam
		= 0 No
		= 1 Yes
I10	NOGOBAK	Return to nucleate boiling
		= 1 No
I11	IFDRG	Stable film boiling correlation option
		= 1 Dougall-Roshenow
		= 2 Groeneveld
		= 3 Modified Dougall-Roshenow
I12	IFDBMC	Heat transfer to steam correlation option
		= 1 Dittus-Boelter
		= 2 McEligot
I13	ILEVY	Modified Levy correlation
		= 1 Use in DNB calculation
		= 2 Do not use in DNB calculation

596 184

General Core Information

Card Series 5011 - 5020

5011, F1, F2, F3, F4, F5, F6, F7, F8, F9, F10, F11, F12

F1	CAKWFT	Core average kw/ft
F2	HCIN	Core inlet enthalpy (BTU/lb)
F3	RIC	Pellet radius and gap (ft)
F4	ZL2	Clad thickness (ft)
F5	DENSM	Density of fuel (lbm/ft^3)
F6	FZBJ	Baker-Just multiplication factor for $Zr-H_2O$ reaction (fraction of $Zr-H_2O$ energy used)
F7	ZXTO	Initial thickness of clad reacted in $Zr-H_2O$ reaction (ft)
F8	SQUAL	Minimum value of quality at which steam correlation will be used
F9	BRX	Minimum heat transfer coefficient for film boiling ($BTU/hr-ft^2-°F$)
F10	H3	Minimum heat transfer coefficient for post DNB regimes ($BTU/hr-ft^2-°F$)
F11	DNBQMN	Minimum DNB heat flux (BTU/ft^2-hr)
F12	DNBRMN	DNB heat flux ratio (a value of 1.0 should be assumed)

596 185

Radial Region Information (Core)

Card Series 5021 - 5030

5021, Fl_1, Fl_2,..,Fl_5, (Max. of 5 radial regions allowed)

Fl	FRODS	Number of fuel rods per radial region

Centerline Temperature or Gap Conductance vs. kw/ft Tables

Card Series 5031 - 5040

5031, Fl_1, $F2_1$,...,Fl_n, $F2_n$ ($2 \leq n \leq 10$)

Fl	TCHGA	Centerline temperature (°F) or gap conductance (BTU/hr-ft^2-°F) for axial nodes below the peak power node
F2	TCHGA	kw/ft

Card Series 5041 - 5050

5041, Fl_1, $F2_1$,...,Fl_n, $F2_n$ ($2 \leq n \leq 10$)

Fl	TCHGH	Centerline temperature (°F) or gap conductance (BTU/hr-ft^2-°F) for axial nodes at and above peak power node
F2	TCHGH	kw/ft

596 186

Core Nodal Parameters

Card Series 5101 - 5120

5101, $F1_1$, $F2_1$, $F3_1$, $F4_1$, ..., $(1 \leq n \leq 20)$

$F1_n$, $F2_n$, $F3_n$, $F4_n$

F1	ZL5	Core length (ft)
F2	FLA	Flow area (ft^2)
F3	RF	Radial fission physics factor
F4	AF	Axial fission physics factor

596 187

Polynomial or Lyons' Fit for Calculating k for UO_2

Card Series 5211 - 5220

5211, F1, F2, F3, F4, F5, F6, F7

F1	CKUO2Z
F2	CKUO2A
F3	CKUO2B
F4	CKUO2C
F5	CKUO2D
F6	CKUO2E
F7	CKUO2F

If CKUO2Z is input 0.0, Lyons' thermal conductivity function is used for calculating k^*_{UO2} where

$$k_{UO2} = \frac{CKUO2A}{CKUO2B+T} + CKUO2C\ (459.69 + T)^3$$

Values for CKUO2D, CKUO2E, CKUO2F must be input as 0.0.

If CKUO2Z is not 0.0 a polynomial fit is used for calculating k^*_{UO2} where

CKUO2Z	=	Coefficient of T° for calculating k_{UO2}
CKUO2A	=	Coefficient of T^1 for calculating k_{UO2}
CKUO2B	=	Coefficient of T^2 for calculating k_{UO2}
CKUO2C	=	Coefficient of T^3 for calculating k_{UO2}
CKUO2D	=	Coefficient of T^4 for calculating k_{UO2}
CKUO2E	=	Coefficient of T^5 for calculating k_{UO2}
CKUO2F	=	Coefficient of T^6 for calculating k_{UO2}

*k_{UO2} calculation in units of BTU/hr-ft-°F

596 188

Conductivity and Volumetric Heat Capacity

Card Series 5221 - 5230

5221, $I1_1$, $F2_1$, $F3_1$,...,$F1_n$, $F2_n$, $F3_n$ $(1 \leq n \leq 6)$

I1	J	Material number
F2	CKM	Conductivity, k (BTU/hr-ft-°F)
F3	RHOCP	Volumetric heat capacity, ρCp (BTU/ft^3-°F)

CKM and RHOCP are set equal to 0.0 if no values are supplied. When the value is 0.0 the code internally calculates the value. The gap material (region #3) requires an input value for RHOCP. One array of 3 numbers must be supplied for any material number. The material number identifications are as follows:

1. UO_2
2. ZR
3. gap

Material Region Information

Card Series 5301 - 5320

5301, $I1_1$, $I2_1$, $F3_1$, $F4_1$,...,$I1_n$, $I2_n$, $F3_n$, $F4_n$ $(1 \leq n \leq 10)$

I1	MT	Material number of region
I2	NSR	Number of subregions in region
F3	FHG	Fraction of material which generates heat
F4	ROUT	Outer radius of region (ft)

Lateral Flow Path K-Factor Coefficients

Card Series 5921 - 5930

5921, $I1_1$, $F2_1$, $F3_1$, $F4_1$,..., $I1_n$, $F2_n$, $F3_n$, $F4_n$ ($n \leq 16$)

I1	NLAT	Flow path number of lateral path
F2	BALAT	Coefficient A
F3	BBLAT	Coefficient B
F4	BCLAT	Coefficient C

Scram Parameters (Core)

Omit if no core is specified.

Care Series 6001

6001, F1, F2, F3, F4, F5, F6, F7, I8, I9

F1	S(1)	Level shutdown (ft)
F2	S(2)	Level time delay (sec)
F3	S(3)	Pressure shutdown (psia)
F4	S(4)	Pressure time delay (sec)
F5	S(5)	Time delay after rupture (sec)
F6	S(6)	Overpower shutdown (fraction)
F7	S(7)	Overpower time delay (sec)
I8	NS	Level detector volume
I9	NSP	Pressure detector volume

Heat Generation vs. Time Table

Card Series 6011 - 6020

6011, $F1_1$, $F2_1$,..., $F1_n$, $F2_n$ ($2 \leq$ pairs ≤ 50)

F1	QDK	Normalized heat generation
F2	QDK	Time (sec)

596 190

Steam Generators:

Steam Generator Shutdown Parameters (General)

Card Series 7001 - 7010

7001, F1, F2, F3, F4, F5, F6, F7, I8, I9

F1	SG(1)	Level shutdown (ft)
F2	SG(2)	Level time delay (sec)
F3	SG(3)	Pressure shutdown (psia)
F4	SG(4)	Pressure time delay (sec)
F5	SG(5)	Time delay after rupture (sec)
F6	SG(6)	Overpower shutdown (fraction)
F7	SG(7)	Overpower time delay (sec)
I8	NSGD	Level detector volume (node number)
I9	NSGDP	Pressure detector volume (node number)

Normalized Heat Load vs. Time Table (General)

Card Series 7011 - 7020

7011, $F1_1$, $F2_1$, ,...,$F1_n$, $F2_n$ ($2 \leq$ pairs ≤ 20)

F1	QSG	Normalized heat load
F2	QSG	Time (sec)

Heat Transfer Multiplier (General) (OPTIONAL)

Card Series 7021 - 7030

7021, $F1_1$, $F2_1$,...,$F1_n$, $F2_n$ ($2 \leq$ pairs ≤ 20)

F1	HTMP	Heat transfer multiplier, normalized
F2	HTMP	[redacted]

596 191[5]

If not input multiplier is set equal to 1.0.

Secondary Node Information

Card Series 7201 - 7210

7201, $I1_1$, $F2_1$,..., $I1_n$, $F2_n$, $(1 \leq n \leq 2)$

NQSGZ = # of steam generato

I1	NSEC	Secondary node
F2	HFEED	Feed enthalpy (BTU/lb)

Primary Node Information

Card Series 7211 - 7220: Primary node data for first steam generator node

Card Series 7221 - 7230: Primary node data for second steam generator node

7211, $I1_1$, $F2_1$, $F3_1$,...,$I1_n$, $F2_n$, $F3_n$ $(1 \leq n \leq 9)$

I1	NSG	Primary node
F2	STMUL	Multiplier on heat transfer coefficient when heat transfer is from secondary to primary
F3	XOLPS	Fractional tube length (length of node/active tube length)

Steam Generator Boundary Conditions

Card Series 7231 - 7240

7231, $F1_1$, $F2_1$, $F3_1$,...,$F1_n$, $F2_n$, $F3_n$ $(1 \leq n \leq 2)$

F1	TISG	Steam generator inlet temperature, ^oF
F2	TOSG	Steam generator outlet temperature, ^oF
F3	PCNTSG	Fraction of core heat transfer rate distributed to the steam generator

Note: $\sum_{n=1}^{NQSGZ}$ PCNTSG $= 1.0 \pm 10^{-4}$

where NQSGZ = number of steam generators

596 192

ain Coolant Pumps

ated Pump Conditions

ard Series 8001 - 8005

he rated pump conditions should be the conditions associated with the

ump head and torque tables (Card series 8021 - 8180).

he first pump path should always be that of a single-loop pump and all

ther pump paths will ratio the flow by the respective areas.

8001, F1, F2, F3, F4, F5, F6, F7, F8, F9, F10.

F1	RLFR	Rated loop flow rate (for a single loop) (lbs/sec)
F2	RPHD	Rated pump head (ft)
F3	RPD	Rated pump density (lbs/ft^3)
F4	PSPED	Rated pump speed (rad/sec)
F5	RPHT	Rated pump hydraulic torque (ft-lb)
F6	PINER	Pump inertia ($lb\text{-}ft^2$)
F7	DARTRK	Design torque for anti-reverse device (ft-lb)
F8	TWIFR	Constant for friction and windage torque (ft-lb)
F9	RPHDF	Fractional tolerance of operating to rated pump head
F10	PSPEDI	Reference pump speed (rad/sec)

596 193

Pump Shutdown Parameters

Card Series 8006 - 8010

8006, F1, F2, F3, F4, F5, I5

F1	PC(1)	Pressure shutdown (psia)
F2	PC(2)	Pressure time delay (sec)
F3	PC(3)	Time delay after rupture (sec)
F4	PC(4)	Overpower shutdown (fraction)
F5	PC(5)	Overpower time delay (sec)
I6	NPC	Pressure detector volume (node number)

Electrical Torque as a Function of Speed

Time

Card Series 8011 - 8020

8011, $F1_1$, $F2_1$, $F1_2$, $F2_2$,...,$F1_n$, $F2_n$ ($2 \leq pairs \leq 20$)

F1	PSET	Electrical torque (ft-lb)
F2	PSET	Pump speed (rad/sec)

Pump Homologous Curves (Torque) (OPTIONAL)

Card Series 8021 - 8030

Normal operation; positive flow, positive speed

Table of β/α^2 as a function of ν/α^* for $\nu/\alpha \leq 1$

8021, F1, F2,..., F11

F1	BAN
:	
F11	BAN

596 194

*when ν/α is positive, ν/α has values of: 0.0, 0.1, 0.2,...,1.0 for all tables

when ν/α is negative, ν/α has values of: 0.0, -0.1, -0.2,...,-1.0 for all tables

Card Series 8031 - 8040

Normal operation; positive flow, positive speed

Table of β/ν^2 as a function of α/ν for $\nu/\alpha > 1$

8031, F1, F2,...,F11

F1	BVN
⋮	
F11	BVN

Card Series 8041 - 8050

Energy dissipation; negative flow, positive speed

Table of β/α^2 as a function of ν/α for $|\nu/\alpha| \leq 1$

8041, F1, F2, ...,F11

F1	BAD
⋮	
F11	BAD

Card Series 8051 - 8060

Energy dissipation; negative flow, positive speed

Table of β/ν^2 as a function of α/ν for $|\nu/\alpha| > 1$

8051, F1, F2, ..., F11

F1	BVD
F11	BVD

Card Series 8061 - 8070

Turbine operation; negative flow, negative speed

Table of β/α^2 as a function of ν/α for $|\nu/\alpha| \leq 1$

596 195

8061, F1, F2, ..., F11

F1 BAT
:
F11 BAT

Card Series 8071 - 8080

Turbine operation; negative flow, negative speed

Table of β/ν^2 as a function of α/ν for $|\nu/\alpha| > 1$.

8071, F1, F2, ..., F11

F1 BVT
:
F11 BVT

Card Series 8141 - 8150

Abnormal Pump: positive flow, negative speed

Table of β/α^2 as a function of ν/α for $|\nu/\alpha| \leq 1$

8141, F1, F2,...,F11

F1 BAR
:
F11 BAR

Card Series 8151 - 8160

Abnormal pump: positive flow, negative speed

Table of β/ν^2 as a function of α/ν for $|\nu/\alpha| > 1$

8151, F1, F2, ..., F11

F1 BVR
:
F11 BVR

Pump Homologous Curves (Head) (OPTIONAL)

Card Series 8081 - 8090

Normal operation; positive flow, positive speed

Table of h/α^2 as a function of ν/α for $\nu/\alpha \leq 1$

8081, F1, F2,...,F11

F1 HAN
:
F11 HAN

Card Series 8091 - 8100

Normal operation; positive flow, positive speed

Table of h/ν^2 as a function of α/ν for $\nu/\alpha > 1$

8091, F1, F2, ...,F11

F1 HVN
:
F11 HVN

Card Series 8101 - 8110

Energy dissipation; negative flow, positive speed

Table of h/α^2 as a function of ν/α for $|\nu/\alpha| \leq 1$

8101, F1, F2,...,F11

F1 HAD
:
F11 HAD

596 197

Card Series 8111 - 8120

Energy dissipation; negative flow, positive speed

Table of h/v^2 as a function of α/v for $|v/\alpha| > 1$

8111, F1, F2, ..., F11

F1 HVD
:
F11 HVD

Card Series 8121 - 8130

Turbine operation; negative flow, negative speed

Table of h/α^2 as a function of v/α for $|v/\alpha| \leq 1$

8121, F1, F2,..., F11

F1 HAT
:
F11 HAT

Card Series 8131 - 8140

Turbine operation; negative flow, negative speed

Table of h/v^2 as a function of α/v for $|v/\alpha| > 1$

8131, F1, F2, ..., F11

F1 HVT
:
F11 HVT

596 198

Card Series 8161 - 8170

Abnormal Pump: positive flow, negative speed

Table of h/α^2 as a function of ν/α for $|\nu/\alpha| \leq 1$

8161, F1, F2,..., F11

F1 HAR
.
.
F11 HAR

Card Series 8171 - 8180

Abnormal Pump: positive flow, negative speed

Table of h/ν^2 as a function of α/ν for $|\nu/\alpha| > 1$

8171, F1, F2, ..., F11

F1 HVR
.
.
F11 HVR

596 199

Pump Heat Degradation Multiplier (OPTIONAL)

Card Series 8201 - 8210

8201, $F1_1$, $F2_1$, ..., $F1_n$, $F2_n$ ($2 \leq n \leq 20$)

F1	HMUL	Multiplier (head)
F2	HMUL	Void fraction

Pump Hydraulic Torque Degradation Multiplier (OPTIONAL)

Card Series 8211 - 8220

8211, $F1_1$, $F2_1$,..., $F1_n$, $F2_n$ ($2 \leq n \leq 20$)

F1	TMUL	Multiplier (torque)
F2	TMUL	Void fraction

Difference Homologous Curves (Head)

Card Series 8301 - 8400

8301, F1, F2,..., F88

a) Normal operation; positive flow, positive speed

Table of $(h/\alpha^2)_{TP}$ as a function of ν/α for $\nu/\alpha \leq 1$

F1 - F11 HANANC

b) Normal operation; positive flow, positive speed

Table of $(h/\nu^2)_{TP}$ as a function of α/ν for $\nu/\alpha > 1$

F12 - F22 HVNANC

c) Energy dissipation; negative flow, positive speed

Table of $(h/\alpha^2)_{TP}$ as a function of ν/α for $|\nu/\alpha| \leq 1$

F23 - F33 HADANC

d) Energy dissipation; negative flow, positive speed

Table of $(h/\nu^2)_{TP}$ as a function of α/ν for $|\nu/\alpha| > 1$

F34 - F44 HVDANC

e) Turbine operation; negative flow, negative speed

Table of $(h/\alpha^2)_{TP}$ as a function of ν/α for $|\nu/\alpha| \leq 1$

F45 - F55 HATANC

f) Turbine operation; negative flow, negative speed

Table of $(h/\nu^2)_{TP}$ as a function of α/ν for $|\nu/\alpha| > 1$

F56 - F66 HVTANC

g) Abnormal pump; positive flow, negative speed

Table of $(h/\alpha^2)_{TP}$ as a function of ν/α for $|\nu/\alpha| \leq 1$

F67 - F77 HARANC

596 201

h) Abnormal pump; positive flow, negative speed

Table of $(h/v^2)_{TP}$ as a function of α/v for $|v/\alpha| > 1$

F78 - F88 HVRANC

A.2 REFERENCES FOR APPENDIX A

A-1 Combustion Engineering, Inc., "CEFLASH-4A: A Fortran-IV Digital Computer Program for Reactor Blowdown Analysis", CENPD-133-P, August 1974 (Proprietary).

A-2 Combustion Engineering, Inc., "CEFLASH-4A: A Fortran-IV Digital Computer Program for Reactor Blowdown Analysis (Modifications)", CENPD-133-P, Supplement 2, February, 1975 (Proprietary).

A-3 Letter A. E. Scherer, Licensing Manager (C-E), to D. F. Ross, Assistant Director of Reactor Safety Division of Systems Safety, LD-76-026, March, 1976 (Proprietary).

Appendix B

COMMENTS ON DECOMPRESSION THERMODYNAMICS

The Combustion Engineering blowdown loads procedure considers the primary coolant fluid, not immediately adjacent to the break, to be in a state of thermodynamic equilibrium during the blowdown. This appendix presents justification for this assumption based on results of large scale blowdown experiments.

B.1 INTRODUCTION

In the decompression of a constant-volume system initially containing a fluid at an elevated subcooled thermodynamic state, the pressure inside the system will begin to decrease once a break from the system to the ambient environment has been exposed. For a system in thermal equilibrium the system pressure will drop rapidly to the liquid saturation pressure and then decrease at the saturation value. Pressure decreases below saturation are prohibited by the nucleation and growth of vapor bubbles which expand to produce additional fluid volume within the system. This is the likely sequence of events for a typical PWR. For small scale systems undergoing locally rapid decompressions, substantially in excess of that expected for a PWR, this may no longer be true. The physical mechanisms governing bubble nucleation and growth may prevent the fluid from expanding sufficiently. Consequently the fluid may pass through a series of metastable thermodynamic states before attaining equilibrium.

In the prediction of PWR blowdown loads, the possible existence of metastable states becomes of concern, since the water in a nonequilibrium state may decompress below its saturation pressure. This behavior can, in turn, effect the unbalanced pressure and flow distribution within the reactor, and ultimately impact on the subsequent structural analyses.

It is the purpose of this section to demonstrate via a comparison of large and small scale blowdown experiments, that nonequilibrium behavior will not occur during a PWR decompression.

B.2 DISCUSSION

Although it has been demonstrated that nonequilibrium behavior can exist for water under certain conditions, it is of concern whether these effects are present for an actual PWR during the blowdown phase of a LOCA. Results of large scale experiments with representative break area to RPV volume ratios indicate that this will not occur for a PWR.

The existence of nonequilibrium thermodynamic states during a rapid decompression has been documented for small scale experimental facilities. Edwards and O'Brien (Reference B-1) and later Banerjee et. al. (Reference B-2) have observed a brief pressure "undershoot" phenomenon during the blowdown of an adiabatic pipe with one end closed. The nonequilibrium behavior was noted to be most pronounced at the pipe closed end. This nonequilibrium behavior was attributed by Edwards (Reference B-1) and Banerjee (Reference B-2) to a delay in bubble nucleation. Once bubbles nucleate and grow the decompression begins to reverse and ultimately a state of thermodynamic equilibirum is achieved.

Nonequilibrium thermodynamic behavior has been reported in a recent experiment conducted by Science, Systems and Software Inc. (Reference B-3). The test, employed a 1/25th scale simulation of a reactor pressure vessel and downcomer. In an analysis of data from this test, Hirt et. al. (Reference B-3) concluded that analytical-experimental agreement could only be obtained when accounting for physical bubble growth mechanisms (thermodynamic nonequilibrium). By assuming that bubbles, once nucleated, grow through heat transfer from the bulk liquid, reasonable agreement with data was obtained.

The above experiments represent but a few of the many tests which have indicated the thermodynamic nonequilibrium aspects of water subjected to a sudden decompression. All these experiments have one common feature. That is, their break areas were large relative to the system volumes. For example, the break area to volume ratio in the Edwards pipe experiment was .075 ft^{-1}. This is to be compared with $\sim$.002 ft^{-1} for a typical double ended PWR full offset shear blowdown. Thus, the small scale experiments would exhibit a more violent decompression than that expected for the larger PWR.

A more reasonable assessment of nonequilibrium characteristics may be obtained by reviewing recent large scale blowdown experiments In this section two large scale blowdown experiments are considered. These are the Loss-of-Fluid-Test L1-2 (LOFT) (References B-4 and B-5) and the Containment-Systems-Experiment (CSE) test B-75 (Reference B-6). The reactor pressure vessel volumes employed in the LOFT and CSE experiments are 108 ft^3 and 140 ft^3 respectively. Break areas for both experiments were selected to provide representative break area to volume ratios. The break area to volume ratio for LOFT is $\simeq$.0016 ft^{-1} and CSE is .001 ft^{-1}. In both situations subcooled blowdown experiments were conducted successfully and no nonequilibrium effects were observed within the vessel. The significance of these observations can be seen more clearly with reference to Table B-1. Table B-1 presents representative rates of decompression for a C-E PWR, LOFT Test L1-2, CSE test B-75, the Edwards pipe test and the Science, Systems and Software Inc. downcomer experiment. PWR characteristic decompression rates have been taken from CEFLASH-4B predictions for the C-E System 80 downcomer. Measurement locations for the various experiments are located in Table B-1 in parentheses. LOFT and CSE decompression rates were evaluated based on internal fluid pressure vessel measurements. Decompression rates for the small scale experiments have been selected at positions of observed nonequilibrium behavior. As a consequence of break sizing, the C-E PWR and large scale blowdowns indicated similar decompression rates.

Both small scale experiments exhibit local decompression rates two orders of magnitude greater than the C-E PWR. Therefore, the observed nonequilibrium behavior for small scale experiments cannot be a priori assumed to apply for a PWR. In fact, results of representative large scale blowdown tests indicates that decompression of C-E PWR's can be well computed assuming thermodynamic equilibrium.

An experimental-analytical comparison of data from LOFT Test L1-2 and C-E modeling procedures are presented in Section 3 of the text.

B.3 REFERENCES FOR APPENDIX B

B-1 Edwards, A. R., O'Brien, T. P., "Studies of Phenomena Connected with the Depressurization of Water Reactors", Journal of the British Nuclear Energy Society, Vol. 9, No. 2, March 1966.

B-2 Banerjee, S., et. al., "Transient Two-Phase Flow and Heat Transfer During Blowdown from Subcooled Conditions with Heat Addition", AIChE paper No. 24, presented at 15th National Heat Transfer Conference, San Francisco, August 10-13, 1975

B-3 Hirt, C. W., et. al., "A Comparison of SOLA-FLX Calculations with Experiments at Systems, Science and Software", LA-NUREG-6752-MS, March 1977

B-4 Robinson, H. C., "LOFT Systems and Test Description (Loss-of-Coolant Experiments Using a Core Simulator)", TREE-NUREG-1019, November 1976

B-5 Schulz, G. L., Manager LOFT Data Systems Branch, letter to R. E. Schneider (C-E), "Transmittal of L1-2 Experimental Data", GLS-38-77, April 18, 1977

B-6 Allemann, R. T. et. al., "Coolant Blowdown Studies of a Reactor Vessel Containing a Simulated Core", BNWL-1524, June 1971

596 206

TABLE B-1

COMPARISON OF DEPRESSURIZATION RATES

WITH TYPICAL PWR DOWNCOMER PREDICTIONS

[3,5]

* FOR EXACT LOCATIONS OF TRANSDUCERS CONSULT REFERENCES B-1, B-3, B-4, AND B-6 FOR THEIR RESPECTIVE TESTS

APPENDIX C

SUPPLEMENTARY INFORMATION ON LOFT ANALYSIS

This appendix presents information supplementary to the LOFT L1-2 analysis. The information covers two topics. In the first portion of this appendix the basis for the selection of the LOFT L1-2 experiment for use in the verification of the C-E blowdown loads methodology is presented. The second section presents the CEFLASH 4B LOFT L1-2 zero time edit.

C.1 LOFT L1-2: BASIS FOR SELECTION

Prior to selecting the LOFT L1-2 test for comparison to analytical results, a review was conducted of the applicability of the available blowdown test information. This review has already been presented to the NRC in Reference C-1. The experiments considered are presented in the following table.

Table C-1

BLOWDOWN EXPERIMENTS REVIEWED

FACILITY	TEST DESIGNATION	REFERENCE	YEAR
Loss-of-Fluid-Test (LOFT)	L1-2	C-2	1976
Containment Systems Experiment (CSE)	B-63	C-3	1970
Containment Systems Experiment (CSE)	B-75	C-3	1970
LOFT Semiscale MOD-1	S-02-6	C-4	1975
LOFT Semiscale MOD-1	S-02-8	C-5	1975

LOSS-OF-FLUID-TEST (LOFT) L1-2

This test employs modern (1976) testing and data recording procedures. These procedures have been developed over several years of previous testing, at Idaho, with the Semiscale series of tests.

This test includes a simulated reactor vessel and a system loop with a pump and a steam generator. Hence, it is more representative of a PWR than the CSE tests which are roughly the same scale as LOFT L1-2 but which have no system loop.

One of the measurement locations in LOFT test L1-2 has two adjacent pressure taps in order to indicate the range of measurement accuracies.

Future tests on the LOFT facility should be useful for confirming blowdown loads predictions.

CONTAINMENT SYSTEMS EXPERIMENT (CSE) TESTS B-63 AND B-75

These tests were performed at Battelle, Northwest in 1970. The facility has been inoperative for several years and the original staff has been dispersed thus making it difficult to resolve questions.

The test facility consisted of a large scale vessel volume comparable to LOFT. However, there was no system loop connected to the vessel. In this sense, the LOFT test is more representative of a PWR.

Combustion Engineering completed an analytical-experimental comparison of CSE test B-75 in 1972. The computer codes employed for the analyses were WATERHAMMER and CEFLASH-4 (a predecessor of the present CEFLASH-4B). The analytical models as well as the results of the comparisons were documented in Reference C-6 (Figures 3.2, 3.3, 3.4, and 3.5). For that analysis it was shown that both WATERHAMMER and CEFLASH-4 predicted the general trend of the results.

596 209

As the CSE and LOFT L1-2 vessel are roughly comparable in size, the advantages of having an external loop and being a more modern test make LOFT L1-2 preferable for a blowdown loads analysis.

LOFT SEMISCALE MOD-1 TESTS S-02-6 AND S-02-8

These tests are small in scale and possess total liquid volumes of about 7 ft^3. The liquid volume in the simulated vessel is only about 3.5 ft^3.

A close look at these experiments shows that the vessel annulus is so small in diameter, relative to its height, that it is effectively a one-dimensional geometry. Hence, pressure differences circumferentially, which are the basis for the blowdown loads contribution to the vessel supports, will not be significant for this test. This can be seen by comparing the dimensions for LOFT, LOFT semiscale and a C-E PWR as shown in Table C-2.

It is seen from Table C-2 that the two-dimensional nature of a PWR downcomer is approximated with the LOFT L1-2 dimensions. However, it is significantly distorted with those of the MOD-1 semiscale. In fact, the MOD-1 semiscale core barrel is so long relative to its circumference that it is effectively a one-dimensional geometry. That is, the decompression wave will rapidly traverse the circumference (<1 msec) causing the pressure distribution in this direction to rapidly equalize. The only significant pressure distribution will be in the axial direction - effectively one-dimension.

For a PWR, the blowdown loads contribution to the forces on the vessel supports results primarily from the circumferential distribution. Thus, the MOD-1 semiscale tests are not appropriate to shed light on this effect.

Table C-2 identifies various features of these experiments and show comparisons to a C-E PWR.

596 210

Table C-2

FEATURES OF BLOWDOWN EXPERIMENTS

ITEM	LOFT L1-2	MOD-1 SEMISCALE	CSE	C-E PWR
SCALE	medium	small	medium	full
vessel volume(ft^3)	108.	3.5	140.	5800 ft^3
TWO-DIMENSIONAL ANNULUS	Yes	No	Yes	Yes
Core barrel height (ft)	16.96	17.0	10.	31.53
Core barrel circumference(ft)	8.64	1.76	11.	42.72
Ratio: height/circumference	1.95	9.66	0.91	0.74
REPRESENTATIVE INITIAL CONDITIONS	Yes	Yes	Yes B-63 No B-75	-
TEST DATE(State of Art)	1975	1974	1970	-
STAFF AVAILABLE to ANSWER QUESTIONS	Yes	Yes	No	-
WILL BE USED FOR FUTURE TESTS	Yes	No	No	-

C.2 LOFT L1-2 CEFLASH-4B ZERO TIME EDIT

This section presents the CEFLASH-4b zero time edit for the LOFT L1-2 "detailed" model described in section 3.3 of the text. Nodal parameters (nodal volumes, masses, pressures, internal energies, etc.) are presented on pages C-6 thru C-9. Flowpath quantities (pressure drops, flow rates, etc.) are shown on pages C-10 thru C-19. For a detailed description of the node-flowpath network, the reader is referred to Figure 3-3 and Tables 3-2 and 3-3 of the text.

596 211

C.3 REFERENCES FOR APPENDIX C

C-1 Scherer, A. E., Licensing Manager (C-E), letter to K. Kneil, Chief Light Water Reactors Branch No. 2, Attachment 1 to LD-77-03, April 7, 1977 (proprietary).

C-2 Robinson, H. C., "LOFT Systems and Test Description (Loss-of-Coolant-Experiments using a Core Simulator)", TREE-NUREG-1019, November, 1976.

C-3 Allemann, R. T., et. al., "Coolant Blowdown Studies of a Reactor Vessel Containing a Simulated Core", BNWL-1524, June 1971.

C-4 Collins, B. L., Crapo, H. S., Sackett, K. E., "Experimental Data Report for Semi-Scale Mod-1 Test S-02-6 (Blowdown Heat Transfer Test)", TREE-NUREG-1037, January, 1977.

C-5 Crapo, H. S., Sackett, K. E., "Experiment Data Report for Semi-Scale Mod-1 Test S-02-8 (Blowdown Heat Transfer Test)", ANCR-NUREG-1238, August 1976.

C-6 Combustion Engineering, Inc., "Dynamic Analysis of Reactor Vessel Internals under Loss-of-Coolant-Accident Condition with Application of Analysis to C-E 800 MWe Class Reactors," CENPD-42, August, 1972 (proprietary).

LOFT L1-2 ZERO TIME EDIT

COMBUSTION ENGINEERING CEFLASH4B VERSION 11 03 1976 76308

PAGE 1 OF OUTPUT 1 TIME STEP 0 TIME 0. SECONDS STEP SIZE 5.0000E-05 SECONDS

LOFT L1-2 EXPERIMENTAL COMPARISON

JOB NO NLS6FQD RUN DATE 08/25/77 RUN BEGUN 11.32.35 CPS USED 4.55800

TOTAL POWER
0.

PUMP	FLOW PATH	SPEED RAD/SEC	NET TORQ FT LB	HYD TORQ FT LB	FR+WI TORQ FT LB	ELEC TORQ FT LB	HEAD PSI	VOID FRAC
1	17	2.4286E+02	-3.8393E-03	2.3085E+02	8.6325E+00	2.3948E+02	4.8104E+01	0.
2	18	2.4286E+02	-3.8393E-03	2.3085E+02	8.6325E+00	2.3948E+02	4.8104E+01	0.

CONTAINMENT NODE	LEAK FLOW PATH		ENTHALPY BTU/LB	FLOW LBS/SEC	ENERGY BTU/SEC	INTEGRAL FLOW LBS	INTEGRAL ENERGY BTU	
65	99		5.3606E+02	0.	0.	0.	0.	
65	100		5.3606E+02	0.	0.	0.	0.	
65	99	100					0.	0.

LEAK FLOW PATHS

FLOW PATH	DISCHARGE COEFF	JUNCT THRUST LBS	THROAT THRUST LBS	MOMENTUM THRUST LBS	JCT + MOM THRUST LBS	THR + MOM THRUST LBS
99	[ ]	[3]				
100						

C-6

5961 2/3

CE	PRESSURE PSI	TOTAL MASS LBS	LIQUID MASS LBS	STEAM MASS LBS	BUBBLE MASS LBS	LIQUID ENTHALPY BTU/LB	STEAM ENTHALPY BTU/LB	TWO PHASE ENTHALPY BTU/LB	TWO PHASE VOID FRAC	AVERAGE FLOW LBS/SEC	NODE
1	2.2842E+03	6.9153E+01	6.9153E+01	0.	0.	5.3606E+02	5.3606E+02	5.3606E+02	0.	5.5940E+02	1
2	2.2833E+03	9.7034E+01	9.7034E+01	0.	0.	5.3606E+02	5.3606E+02	5.3606E+02	0.	5.5940E+02	2
3	2.2823E+03	4.3935E+02	4.3935E+02	0.	0.	5.3606E+02	5.3606E+02	5.3606E+02	0.	5.5940E+02	3
4	2.2811E+03	5.5970E+02	5.5970E+02	0.	0.	5.3606E+02	5.3606E+02	5.3606E+02	0.	5.5940E+02	4
5	2.2800E+03	3.3980E+02	3.3980E+02	0.	0.	5.3606E+02	5.3606E+02	5.3606E+02	0.	5.5940E+02	5
6	2.2786E+03	1.9406E+02	1.9406E+02	0.	0.	5.3606E+02	5.3606E+02	5.3606E+02	0.	5.5940E+02	6
7	2.2737E+03	4.0968E+02	4.0968E+02	0.	0.	5.3606E+02	5.3606E+02	5.3606E+02	0.	5.5940E+02	7
8	2.2729E+03	2.0409E+02	2.0409E+02	0.	0.	5.3606E+02	5.3606E+02	5.3606E+02	0.	0.	8
9	2.2721E+03	2.5256E+02	2.5256E+02	0.	0.	5.3606E+02	5.3606E+02	5.3606E+02	0.	0.	9
10	2.2645E+03	4.5295E+02	4.5295E+02	0.	0.	5.3606E+02	5.3606E+02	5.3606E+02	0.	5.8880E+02	10
11	2.2551E+03	4.5872E+02	4.5872E+02	0.	0.	5.3606E+02	5.3606E+02	5.3606E+02	0.	0.	11
12	2.2726E+03	1.7090E+02	1.7090E+02	0.	0.	5.3606E+02	5.3606E+02	5.3606E+02	0.	5.8880E+02	12
13	2.2731E+03	1.7091E+02	1.7091E+02	0.	0.	5.3606E+02	5.3606E+02	5.3606E+02	0.	0.	13
14	2.2721E+03	3.1047E+02	3.1047E+02	0.	0.	5.3606E+02	5.3606E+02	5.3606E+02	0.	5.8880E+02	14
15	2.2679E+03	2.7767E+02	2.7767E+02	0.	0.	5.3606E+02	5.3606E+02	5.3606E+02	0.	5.8880E+02	15
16	2.2548E+03	1.2071E+03	1.2071E+03	0.	0.	5.3606E+02	5.3606E+02	5.3606E+02	0.	5.8880E+02	16
17	2.2487E+03	1.2070E+03	1.2070E+03	0.	0.	5.3606E+02	5.3606E+02	5.3606E+02	0.	5.8880E+02	17
18	2.2377E+03	5.7129E+02	5.7129E+02	0.	0.	5.3606E+02	5.3606E+02	5.3606E+02	0.	5.8880E+02	18
19	2.2656E+03	2.7394E+02	2.7394E+02	0.	0.	5.3606E+02	5.3606E+02	5.3606E+02	0.	2.9440E+02	19
20	2.2656E+03	1.9041E+02	1.9041E+02	0.	0.	5.3606E+02	5.3606E+02	5.3606E+02	0.	2.9440E+02	20
21	2.2483E+03	4.3017E+02	4.3017E+02	0.	0.	5.3606E+02	5.3606E+02	5.3606E+02	0.	5.8880E+02	21
22	2.2700E+03	8.7691E+02	7.9374E+02	8.3163E+01	8.3163E+01	7.0566E+02	1.1158E+03	7.4458E+02	3.7458E-01	0.	22
23	2.2764E+03	3.2815E+02	3.2815E+02	0.	0.	5.3606E+02	5.3606E+02	5.3606E+02	0.	0.	23
24	2.2805E+03	2.3729E+02	2.3729E+02	0.	0.	5.3606E+02	5.3606E+02	5.3606E+02	0.	0.	24
25	2.2739E+03	2.5826E+01	2.5826E+01	0.	0.	5.3606E+02	5.3606E+02	5.3606E+02	0.	0.	25
26	2.2750E+03	3.5051E+01	3.5051E+01	0.	0.	5.3606E+02	5.3606E+02	5.3606E+02	0.	0.	26
27	2.2734E+03	1.8477E+01	1.8477E+01	0.	0.	5.3606E+02	5.3606E+02	5.3606E+02	0.	0.	27
28	2.2705E+03	5.1743E+02	5.1743E+02	0.	0.	5.3606E+02	5.3606E+02	5.3606E+02	0.	0.	28
29	2.2705E+03	5.1743E+02	5.1743E+02	0.	0.	5.3606E+02	5.3606E+02	5.3606E+02	0.	0.	29
30	2.2734E+03	2.5601E+02	2.5601E+02	0.	0.	5.3606E+02	5.3606E+02	5.3606E+02	0.	0.	30
31	2.2834E+03	3.7884E+01	3.7884E+01	0.	0.	5.3606E+02	5.3606E+02	5.3606E+02	0.	9.8133E+01	31
32	2.2834E+03	3.7884E+01	3.7884E+01	0.	0.	5.3606E+02	5.3606E+02	5.3606E+02	0.	9.8133E+01	32
33	2.2834E+03	3.7884E+01	3.7884E+01	0.	0.	5.3606E+02	5.3606E+02	5.3606E+02	0.	9.8133E+01	33
34	2.2834E+03	3.7884E+01	3.7884E+01	0.	0.	5.3606E+02	5.3606E+02	5.3606E+02	0.	9.8133E+01	34
35	2.2834E+03	3.7884E+01	3.7884E+01	0.	0.	5.3606E+02	5.3606E+02	5.3606E+02	0.	9.8133E+01	35
36	2.2834E+03	3.7884E+01	3.7884E+01	0.	0.	5.3606E+02	5.3606E+02	5.3606E+02	0.	9.8133E+01	36
37	2.2822E+03	6.0689E+01	6.0689E+01	0.	0.	5.3606E+02	5.3606E+02	5.3606E+02	0.	9.8133E+01	37
38	2.2822E+03	6.0689E+01	6.0689E+01	0.	0.	5.3606E+02	5.3606E+02	5.3606E+02	0.	9.8133E+01	38
39	2.2822E+03	6.0689E+01	6.0689E+01	0.	0.	5.3606E+02	5.3606E+02	5.3606E+02	0.	9.8133E+01	39
40	2.2822E+03	6.0689E+01	6.0689E+01	0.	0.	5.3606E+02	5.3606E+02	5.3606E+02	0.	9.8133E+01	40
41	2.2822E+03	6.0689E+01	6.0689E+01	0.	0.	5.3606E+02	5.3606E+02	5.3606E+02	0.	9.8133E+01	41
42	2.2822E+03	6.0689E+01	6.0689E+01	0.	0.	5.3606E+02	5.3606E+02	5.3606E+02	0.	9.8133E+01	42
43	2.2806E+03	8.1936E+01	8.1936E+01	0.	0.	5.3606E+02	5.3606E+02	5.3606E+02	0.	9.8133E+01	43
44	2.2806E+03	8.1936E+01	8.1936E+01	0.	0.	5.3606E+02	5.3606E+02	5.3606E+02	0.	9.8133E+01	44
45	2.2806E+03	8.1936E+01	8.1936E+01	0.	0.	5.3606E+02	5.3606E+02	5.3606E+02	0.	9.8133E+01	45
46	2.2806E+03	8.1936E+01	8.1936E+01	0.	0.	5.3606E+02	5.3606E+02	5.3606E+02	0.	9.8133E+01	46
47	2.2806E+03	8.1936E+01	8.1936E+01	0.	0.	5.3606E+02	5.3606E+02	5.3606E+02	0.	9.8133E+01	47

LOFT L1-2 ZERO TIME EDIT

COMBUSTION ENGINEERING CEFLASH4B VERSION 11 03 1976 76308

PAGE 3 OF OUTPUT 1 TIME STEP 0 TIME 0. SECONDS STEP SIZE 5.0000E-05 SECONDS

NODE	PRESSURE PSI	TOTAL MASS LBS	LIQUID MASS LBS	STEAM MASS LBS	BUBBLE MASS LBS	LIQUID ENTHALPY BTU/LB	STEAM ENTHALPY BTU/LB	TWO PHASE ENTHALPY BTU/LB	TWO PHASE VOID FRAC	AVERAGE FLOW LBS/SEC	NODE
49	2.2805E+03	3.9187E+01	3.9187E+01	0.	0.	5.3606E+02	5.3606E+02	5.3606E+02	0.	2.4533E+02	49
50	2.2805E+03	6.7809E+01	6.7809E+01	0.	0.	5.3606E+02	5.3606E+02	5.3606E+02	0.	5.8480E+02	50
51	2.2805E+03	3.9187E+01	3.9187E+01	0.	0.	5.3606E+02	5.3606E+02	5.3606E+02	0.	2.4533E+02	51
52	2.2805E+03	3.9187E+01	3.9187E+01	0.	0.	5.3606E+02	5.3606E+02	5.3606E+02	0.	1.4720E+02	52
53	2.2805E+03	6.7809E+01	6.7809E+01	0.	0.	5.3606E+02	5.3606E+02	5.3606E+02	0.	9.8133E+01	53
54	2.2805E+03	3.9187E+01	3.9187E+01	0.	0.	5.3606E+02	5.3606E+02	5.3606E+02	0.	1.4720E+02	54
55	2.2796E+03	2.9270E+01	2.9270E+01	0.	0.	5.3606E+02	5.3606E+02	5.3606E+02	0.	0.	55
56	2.2796E+03	2.9270E+01	2.9270E+01	0.	0.	5.3606E+02	5.3606E+02	5.3606E+02	0.	0.	56
57	2.2796E+03	2.9270E+01	2.9270E+01	0.	0.	5.3606E+02	5.3606E+02	5.3606E+02	0.	0.	57
58	2.2796E+03	2.9270E+01	2.9270E+01	0.	0.	5.3606E+02	5.3606E+02	5.3606E+02	0.	0.	58
59	2.2796E+03	2.9270E+01	2.9270E+01	0.	0.	5.3606E+02	5.3606E+02	5.3606E+02	0.	0.	59
60	2.2796E+03	2.9270E+01	2.9270E+01	0.	0.	5.3606E+02	5.3606E+02	5.3606E+02	0.	0.	60
61	2.2793E+03	8.4149E+01	8.4149E+01	0.	0.	5.3606E+02	5.3606E+02	5.3606E+02	0.	2.9400E+01	61
62	2.2707E+03	2.8350E+02	2.8350E+02	0.	0.	5.3606E+02	5.3606E+02	5.3606E+02	0.	0.	62
63	2.2805E+03	1.3457E+02	1.3457E+02	0.	0.	5.3606E+02	5.3606E+02	5.3606E+02	0.	0.	63
64	2.2739E+03	9.5801E+01	9.5801E+01	0.	0.	5.3606E+02	5.3606E+02	5.3606E+02	0.	0.	64
65	1.4700E+01	6.1521E+06	6.1521E+06	0.	0.	1.0000E+02	1.0000E+02	1.0000E+02	0.	0.	65

NODE	VELOCITY SQUARED SQFT/SQSEC	MIXTURE VOLUME CUFT	LIQUID VOLUME CUFT	TOTAL HEAT BTU/SEC	VIS DIS HEAT BTU/SEC	TOTAL ENERGY BTU	INTERNAL ENERGY BTU	NODE TEMP DEG F	NODAL DENSITY LBS/CUFT	NODE
1	1.5422E+01	1.4564E+00	1.4564E+00	0.	1.8355E-01	3.6455E+04	3.6455E+04	5.4002E+02	4.7483E+01	1
2	1.1215E+01	2.0436E+00	2.0436E+00	0.	1.4219E-01	5.1154E+04	5.1153E+04	5.4002E+02	4.7482E+01	2
3	1.2624E+01	9.2531E+00	9.2531E+00	0.	3.2358E-02	2.3162E+05	2.3161E+05	5.4002E+02	4.7481E+01	3
4	1.2424E+01	1.1788E+01	1.1788E+01	0.	2.4790E-02	2.9507E+05	2.9506E+05	5.4002E+02	4.7480E+01	4
5	1.2824E+01	7.1567E+00	7.1567E+00	0.	3.8891E-01	1.7914E+05	1.7913E+05	5.4002E+02	4.7480E+01	5
6	3.2024E+01	4.1000E+00	4.1000E+00	0.	6.5542E-01	1.0262E+05	1.0262E+05	5.4002E+02	4.7477E+01	6
7	2.2214E+01	8.6294E+00	8.6294E+00	0.	4.0838E-01	2.1599E+05	2.1598E+05	5.4002E+02	4.7475E+01	7
8	0.	4.2989E+00	4.2989E+00	0.	0.	1.0760E+05	1.0760E+05	5.4002E+02	4.7475E+01	8
9	0.	5.3200E+00	5.3200E+00	0.	0.	1.3316E+05	1.3315E+05	5.4002E+02	4.7474E+01	9
10	3.1176E+00	9.5392E+00	9.5392E+00	0.	1.6060E-01	2.3877E+05	2.3877E+05	5.4002E+02	4.7483E+01	10
11	0.	9.6608E+00	9.6608E+00	0.	0.	2.4182E+05	2.4182E+05	5.4002E+02	4.7483E+01	11
12	2.5283E+02	3.5999E+00	3.5999E+00	0.	1.4966E+00	9.0106E+04	9.0101E+04	5.4002E+02	4.7475E+01	12
13	0.	3.5999E+00	3.5999E+00	0.	0.	9.0106E+04	9.0101E+04	5.4002E+02	4.7475E+01	13
14	3.3004E+02	6.5397E+00	6.5397E+00	0.	3.0878E+00	1.6369E+05	1.6368E+05	5.4002E+02	4.7474E+01	14
15	2.9676E+02	5.8492E+00	5.8492E+00	0.	7.2168E+00	1.4644E+05	1.4643E+05	5.4002E+02	4.7471E+01	15
16	3.8476E+01	2.5933E+01	2.5933E+01	0.	1.2185E+01	6.3651E+05	6.3647E+05	5.4002E+02	4.7462E+01	16
17	3.6482E+01	2.5933E+01	2.5933E+01	0.	1.2162E+01	6.3649E+05	6.3644E+05	5.4002E+02	4.7458E+01	17
18	2.9704E+02	1.2040E+01	1.2040E+01	0.	5.2032E+00	3.0128E+05	3.0124E+05	5.4002E+02	4.7450E+01	18
19	2.5273E+02	5.7699E+00	5.7699E+00	0.	8.0497E-01	1.4443E+05	1.4443E+05	5.4002E+02	4.7484E+01	19
20	2.5273E+02	4.0100E+00	4.0100E+00	0.	6.4140E-02	1.0038E+05	1.0037E+05	5.4002E+02	4.7484E+01	20
21	3.2992E+02	9.0597E+00	9.0597E+00	0.	1.0104E+00	2.2678E+05	2.2677E+05	5.4002E+02	4.7482E+01	21
22	0.	3.4448E+01	2.1542E+01	0.	0.	6.3847E+05	6.3844E+05	6.5810E+02	2.5459E+01	22
23	0.	6.9115E+00	6.9115E+00	0.	0.	1.7300E+05	1.7299E+05	5.4002E+02	4.7478E+01	23
24	0.	4.9978E+00	4.9978E+00	0.	0.	1.2510E+05	1.2509E+05	5.4002E+02	4.7480E+01	24
25	0.	5.4400E-01	5.4400E-01	0.	0.	1.3616E+04	1.3616E+04	5.4002E+02	4.7475E+01	25
26	0.	7.3828E-01	7.3828E-01	0.	0.	1.8479E+04	1.8478E+04	5.4002E+02	4.7476E+01	26
27	0.	3.8920E-01	3.8920E-01	0.	0.	9.7415E+03	9.7410E+03	5.4002E+02	4.7475E+01	27
28	0.	1.0899E+01	1.0899E+01	0.	0.	2.7281E+05	2.7279E+05	5.4002E+02	4.7473E+01	28
29	0.	1.0899E+01	1.0899E+01	0.	0.	2.7281E+05	2.7279E+05	5.4002E+02	4.7473E+01	29
30	0.	5.3925E+00	5.3925E+00	0.	0.	1.3497E+05	1.3497E+05	5.4002E+02	4.7475E+01	30
31	6.5948E+01	7.9364E-01	7.9364E-01	0.	1.2645E-02	1.9866E+04	1.9865E+04	5.4002E+02	4.7482E+01	31
32	6.5948E+01	7.9364E-01	7.9364E-01	0.	1.2645E-02	1.9866E+04	1.9865E+04	5.4002E+02	4.7482E+01	32
33	6.5948E+01	7.9364E-01	7.9364E-01	0.	1.2645E-02	1.9866E+04	1.9865E+04	5.4002E+02	4.7482E+01	33
34	6.5948E+01	7.9364E-01	7.9364E-01	0.	1.2645E-02	1.9866E+04	1.9865E+04	5.4002E+02	4.7482E+01	34
35	6.5948E+01	7.9364E-01	7.9364E-01	0.	1.2645E-02	1.9866E+04	1.9865E+04	5.4002E+02	4.7482E+01	35
36	6.5948E+01	7.9364E-01	7.9364E-01	0.	1.2645E-02	1.9866E+04	1.9865E+04	5.4002E+02	4.7482E+01	36
37	6.5950E+01	1.2782E+00	1.2782E+00	0.	7.6425E-03	3.1994E+04	3.1993E+04	5.4002E+02	4.7481E+01	37
38	6.5950E+01	1.2782E+00	1.2782E+00	0.	7.6425E-03	3.1994E+04	3.1993E+04	5.4002E+02	4.7481E+01	38
39	6.5950E+01	1.2782E+00	1.2782E+00	0.	7.6425E-03	3.1994E+04	3.1993E+04	5.4002E+02	4.7481E+01	39
40	6.5950E+01	1.2782E+00	1.2782E+00	0.	7.6425E-03	3.1994E+04	3.1993E+04	5.4002E+02	4.7481E+01	40
41	6.5950E+01	1.2782E+00	1.2782E+00	0.	7.6425E-03	3.1994E+04	3.1993E+04	5.4002E+02	4.7481E+01	41
42	6.5950E+01	1.2782E+00	1.2782E+00	0.	7.6425E-03	3.1994E+04	3.1993E+04	5.4002E+02	4.7481E+01	42
43	6.5953E+01	1.7257E+00	1.7257E+00	0.	2.5094E-02	4.3196E+04	4.3194E+04	5.4002E+02	4.7480E+01	43
44	6.5953E+01	1.7257E+00	1.7257E+00	0.	2.5106E-02	4.3196E+04	4.3194E+04	5.4002E+02	4.7480E+01	44
45	6.5953E+01	1.7257E+00	1.7257E+00	0.	2.5094E-02	4.3196E+04	4.3194E+04	5.4002E+02	4.7480E+01	45
46	6.5953E+01	1.7257E+00	1.7257E+00	0.	2.5094E-02	4.3196E+04	4.3194E+04	5.4002E+02	4.7480E+01	46
47	6.5953E+01	1.7257E+00	1.7257E+00	0.	2.5094E-02	4.3196E+04	4.3194E+04	5.4002E+02	4.7480E+01	47
48	6.5953E+01	1.7257E+00	1.7257E+00	0.	2.5094E-02	4.3196E+04	4.3194E+04	5.4002E+02	4.7480E+01	48

LOFT L1-2 ZERO TIME EDIT

COMBUSTION ENGINEERING CEFLASH4B VERSION 11 03 1976 76308

PAGE 5 OF OUTPUT 1 TIME STEP 0 TIME 0. SECONDS STEP SIZE 5.0000E-05 SECONDS

NODE	VELOCITY SQUARED SQFT/SQSEC	MIXTURE VOLUME CUFT	LIQUID VOLUME CUFT	TOTAL HEAT BTU/SEC	VIS DIS HEAT BTU/SEC	TOTAL ENERGY BTU	INTERNAL ENERGY BTU	NODE TEMP DEG F	NODAL DENSITY LBS/CUFT	NODE
49	4.4365E+01	8.2534E-01	8.2534E-01	0.	1.9253E-02	2.0659E+04	2.0658E+04	5.4002E+02	4.7480E+01	49
50	2.5554E+02	1.4282E+00	1.4282E+00	0.	1.7504E-01	3.5749E+04	3.5747E+04	5.4002E+02	4.7480E+01	50
51	4.4365E+01	8.2534E-01	8.2534E-01	0.	1.9253E-02	2.0659E+04	2.0658E+04	5.4002E+02	4.7480E+01	51
52	1.5972E+01	8.2534E-01	8.2534E-01	0.	1.9196E-02	2.0659E+04	2.0658E+04	5.4002E+02	4.7480E+01	52
53	7.0965E+00	1.4282E+00	1.4282E+00	0.	1.9157E-02	3.5749E+04	3.5747E+04	5.4002E+02	4.7480E+01	53
54	1.5972E+01	8.2534E-01	8.2534E-01	0.	1.9196E-02	2.0659E+04	2.0658E+04	5.4002E+02	4.7480E+01	54
55	0.	6.1647E-01	6.1647E-01	0.	0.	1.5431E+04	1.5430E+04	5.4002E+02	4.7479E+01	55
56	0.	6.1647E-01	6.1647E-01	0.	0.	1.5431E+04	1.5430E+04	5.4002E+02	4.7479E+01	56
57	0.	6.1647E-01	6.1647E-01	0.	0.	1.5431E+04	1.5430E+04	5.4002E+02	4.7479E+01	57
58	0.	6.1647E-01	6.1647E-01	0.	0.	1.5431E+04	1.5430E+04	5.4002E+02	4.7479E+01	58
59	0.	6.1647E-01	6.1647E-01	0.	0.	1.5431E+04	1.5430E+04	5.4002E+02	4.7479E+01	59
60	0.	6.1647E-01	6.1647E-01	0.	0.	1.5431E+04	1.5430E+04	5.4002E+02	4.7479E+01	60
61	2.1444E+01	1.7724E+00	1.7723E+00	0.	3.5024E-01	4.4363E+04	4.4361E+04	5.4002E+02	4.7479E+01	61
62	0.	5.9718E+00	5.9718E+00	0.	0.	1.4947E+05	1.4946E+05	5.4002E+02	4.7473E+01	62
63	0.	2.8342E+00	2.8342E+00	0.	0.	7.0943E+04	7.0939E+04	5.4002E+02	4.7480E+01	63
64	0.	2.0179E+00	2.0179E+00	0.	0.	5.0509E+04	5.0506E+04	5.4002E+02	4.7475E+01	64
65	0.	1.0000E+05	1.0000E+05	0.	0.	6.1534E+08	6.1494E+08	1.3208E+02	6.1521E+01	65

FLOW PATH	FRICTION K FACTOR DIMENSLESS	GEOM FWD K FACTOR DIMENSLESS	GEOM RVS K FACTOR DIMENSLESS	L/D DIMENSLESS	INLET ELEVATION FT	OUTLET ELEVATION FT	DIFFERENCE ELEVATION FT
1	1.6396E+00	5.2800E+00	5.2800E+00	1.4278E+02	8.5516E+00	9.1475E+00	-5.9585E-01
2	3.0423E-01	6.9000E-01	6.9000E-01	3.6447E+01	9.1475E+00	1.0844E+01	-1.6963E+00
3	1.7967E-01	0.	0.	2.1217E+01	1.0844E+01	1.4041E+01	-3.1977E+00
4	1.7112E-01	0.	0.	2.0761E+01	1.4041E+01	1.6916E+01	-2.8745E+00
5	4.7788E-01	3.8800E+00	3.8800E+00	7.2173E+01	1.6916E+01	1.8989E+01	-2.0727E+00
6	1.2455E+00	7.0470E+00	7.0470E+00	1.5758E+02	1.8989E+01	2.2000E+01	-3.0113E+00
7	2.0700E-02	0.	0.	1.5783E+00	2.2000E+01	2.4458E+01	-2.4580E+00
8	0.	1.0000E+00	1.0300E+00	0.	2.4458E+01	2.7138E+01	-2.6800E+00
9	1.0296E-01	1.5660E-01	1.5660E-01	1.9632E+01	2.2000E+01	2.2000E+01	0.
10	0.	1.5660E-01	1.5660E-01	0.	2.2000E+01	2.2000E+01	0.
11	0.	1.5110E-01	1.5110E-01	0.	2.2000E+01	2.2000E+01	0.
12	5.4753E-01	1.1650E-01	1.1850E-01	7.7519E+01	2.2000E+01	2.2000E+01	0.
13	6.0321E-01	9.8210E-01	9.8210E-01	9.5568E+01	2.2000E+01	2.2000E+01	0.
14	1.8301E+01	3.0500E+01	3.0500E+01	2.4789E+03	2.2000E+01	2.4477E+01	-2.4771E+00
15	6.7202E+00	0.	0.	4.5822E+02	2.4477E+01	2.4477E+01	0.
16	3.2720E+00	5.4600E+00	5.4600E+00	4.5811E+02	2.4477E+01	1.7773E+01	6.7040E+00
17	2.2500E-02	7.8400E-01	7.8400E-01	2.7326E+00	1.7773E+01	2.2000E+01	-4.2270E+00
18	2.2500E-02	7.8400E-01	7.8400E-01	2.7326E+00	1.7773E+01	2.2000E+01	-4.2270E+00
19	1.2826E+00	2.8400E-01	2.8400E-01	1.6726E+02	2.2000E+01	2.2000E+01	0.
20	6.8902E-02	2.9330E-01	2.9330E-01	1.1416E+01	2.2000E+01	2.2000E+01	0.
21	8.0272E-02	2.3640E+00	2.3640E+00	1.1365E+01	2.2000E+01	2.2000E+01	0.
22	1.5000E-01	3.8520E+01	3.7270E+01	3.5461E+00	2.2000E+01	2.8669E+01	-6.6690E+00
23	5.0000E-02	2.9000E+02	2.9000E+02	4.4444E+00	2.8669E+01	2.8669E+01	0.
24	1.0000E-01	2.9320E+01	3.9410E+01	2.1157E+00	2.8669E+01	2.1881E+01	6.7880E+00
25	4.7500E-02	4.9000E+01	4.7000E+01	8.5387E+00	2.1881E+01	1.8803E+01	3.0780E+00
26	2.6600E-01	1.3200E+00	1.7400E+00	1.7843E+01	1.8803E+01	2.2514E+01	-3.7110E+00
27	1.0000E-01	1.1400E+00	1.1400E+00	8.0446E+00	2.2000E+01	2.2000E+01	0.
28	1.5100E-01	2.2500E+00	2.2500E+00	1.0102E+01	2.3833E+01	2.2000E+01	1.8330E+00
29	3.1564E-01	1.0160E+00	1.0160E+00	3.9236E+01	7.5660E+00	8.5516E+00	-9.8565E-01
30	1.0000E-04	0.	0.	4.9098E-01	6.2000E+00	7.5660E+00	-1.3660E+00
31	5.3207E-01	2.6600E-01	2.6600E-01	5.1298E+01	9.5395E+00	7.5660E+00	1.9735E+00
32	5.3207E-01	2.6600E-01	2.6600E-01	5.1298E+01	9.5395E+00	7.5660E+00	1.9735E+00
33	5.3207E-01	2.6600E-01	2.6600E-01	5.1298E+01	9.5395E+00	7.5660E+00	1.9735E+00
34	5.3207E-01	2.6600E-01	2.6600E-01	5.1298E+01	9.5395E+00	7.5660E+00	1.9735E+00
35	5.3207E-01	2.6600E-01	2.6600E-01	5.1298E+01	9.5395E+00	7.5660E+00	1.9735E+00
36	5.3207E-01	2.6600E-01	2.6600E-01	5.1298E+01	9.5395E+00	7.5660E+00	1.9735E+00
37	5.7789E-02	5.9300E-01	5.9300E-01	6.5119E+00	1.2917E+01	9.5395E+00	3.3771E+00
38	5.7789E-02	5.9300E-01	5.9300E-01	6.5119E+00	1.2917E+01	9.5395E+00	3.3771E+00
39	5.7789E-02	5.9300E-01	5.9300E-01	6.5119E+00	1.2917E+01	9.5395E+00	3.3771E+00
40	5.7789E-02	5.9300E-01	5.9300E-01	6.5119E+00	1.2917E+01	9.5395E+00	3.3771E+00
41	5.7789E-02	5.9300E-01	5.9300E-01	6.5119E+00	1.2917E+01	9.5395E+00	3.3771E+00
42	5.7789E-02	5.9300E-01	5.9300E-01	6.5119E+00	1.2917E+01	9.5395E+00	3.3771E+00
43	6.0444E-02	7.4090E-01	7.4090E-01	6.8110E+00	1.7812E+01	1.2917E+01	4.8959E+00
44	6.0444E-02	7.4090E-01	7.4090E-01	6.8110E+00	1.7812E+01	1.2917E+01	4.8959E+00
45	6.0444E-02	7.4090E-01	7.4090E-01	6.8110E+00	1.7812E+01	1.2917E+01	4.8959E+00
46	6.0444E-02	7.4090E-01	7.4090E-01	6.8110E+00	1.7812E+01	1.2917E+01	4.8959E+00
47	6.0444E-02	7.4090E-01	7.4090E-01	6.8110E+00	1.7812E+01	1.2917E+01	4.8959E+00
48	6.0444E-02	7.4090E-01	7.4090E-01	6.8110E+00	1.7812E+01	1.2917E+01	4.8959E+00

LOFT L1-2 ZERO TIME EDIT

COMBUSTION ENGINEERING CEFLASH4B VERSION 11 03 1976 76308

PAGE 7 OF OUTPUT 1 TIME STEP 0 TIME 0. SECONDS STEP SIZE 5.0000E-05 SECONDS

FLOW PATH	FRICTION K FACTOR DIMENSLESS	GEOM FWD K FACTOR DIMENSLESS	GEOM RVS K FACTOR DIMENSLESS	L/D DIMENSLESS	INLET ELEVATION FT	OUTLET ELEVATION FT	DIFFERENCE ELEVATION FT
49	2.9600E-01	2.9640E-01	2.9640E-01	3.3428E+01	2.2000E+01	1.7812E+01	4.1875E+00
50	2.9595E-01	2.9640E-01	2.9640E-01	3.3461E+01	2.2000E+01	1.7812E+01	4.1875E+00
51	2.9600E-01	2.9640E-01	2.9640E-01	3.3428E+01	2.2000E+01	1.7812E+01	4.1875E+00
52	2.9636E-01	2.9640E-01	2.9640E-01	3.3395E+01	2.2000E+01	1.7812E+01	4.1875E+00
53	2.9606E-01	2.9640E-01	2.9640E-01	3.3361E+01	2.2000E+01	1.7812E+01	4.1875E+00
54	2.9636E-01	2.9640E-01	2.9640E-01	3.3395E+01	2.2000E+01	1.7812E+01	4.1875E+00
55	0.	2.0000E-01	2.0000E-01	0.	2.3733E+01	2.2000E+01	1.7330E+00
56	0.	2.0000E-01	2.0000E-01	0.	2.3733E+01	2.2000E+01	1.7330E+00
57	0.	2.0000E-01	2.0000E-01	0.	2.3733E+01	2.2000E+01	1.7330E+00
58	0.	2.0000E-01	2.0000E-01	0.	2.3733E+01	2.2000E+01	1.7330E+00
59	0.	2.0000E-01	2.0000E-01	0.	2.3733E+01	2.2000E+01	1.7330E+00
60	0.	2.0000E-01	2.0000E-01	0.	2.3733E+01	2.2000E+01	1.7330E+00
61	1.0000E-04	0.	0.	4.5815E+00	2.3733E+01	2.3733E+01	0.
62	1.0000E-04	0.	0.	4.5815E+00	2.3733E+01	2.3733E+01	0.
63	1.0000E-04	0.	0.	4.5815E+00	2.3733E+01	2.3733E+01	0.
64	1.0000E-04	0.	0.	4.5815E+00	2.3733E+01	2.3733E+01	0.
65	1.0000E-04	0.	0.	4.5815E+00	2.3733E+01	2.3733E+01	0.
66	1.0000E-04	0.	0.	4.5815E+00	2.3733E+01	2.3733E+01	0.
67	5.7790E-04	0.	0.	5.9310E-02	2.2000E+01	2.2000E+01	0.
68	5.2012E-03	0.	0.	4.2850E-01	2.2000E+01	2.2000E+01	0.
69	5.2012E-03	0.	0.	4.2850E-01	2.2000E+01	2.2000E+01	0.
70	5.7790E-04	0.	0.	5.9310E-02	2.2000E+01	2.2000E+01	0.
71	2.0805E-04	0.	0.	2.3649E-02	2.2000E+01	2.2000E+01	0.
72	2.0805E-04	0.	0.	2.3649E-02	2.2000E+01	2.2000E+01	0.
73	1.0000E-04	0.	0.	4.5856E+00	1.7812E+01	1.7812E+01	0.
74	1.0000E-04	0.	0.	4.5856E+00	1.7812E+01	1.7812E+01	0.
75	1.0000E-04	0.	0.	4.5856E+00	1.7812E+01	1.7812E+01	0.
76	1.0000E-04	0.	0.	4.5856E+00	1.7812E+01	1.7812E+01	0.
77	1.0000E-04	0.	0.	4.5856E+00	1.7812E+01	1.7812E+01	0.
78	1.0000E-04	0.	0.	4.5856E+00	1.7812E+01	1.7812E+01	0.
79	1.0000E-04	0.	0.	4.5856E+00	1.2917E+01	1.2917E+01	0.
80	1.0000E-04	0.	0.	4.5856E+00	1.2917E+01	1.2917E+01	0.
81	1.0000E-04	0.	0.	4.5856E+00	1.2917E+01	1.2917E+01	0.
82	1.0000E-04	0.	0.	4.5856E+00	1.2917E+01	1.2917E+01	0.
83	1.0000E-04	0.	0.	4.5856E+00	1.2917E+01	1.2917E+01	0.
84	1.0000E-04	0.	0.	4.5856E+00	1.2917E+01	1.2917E+01	0.
85	1.0000E-04	0.	0.	4.5856E+00	9.5395E+00	9.5395E+00	0.
86	1.0000E-04	0.	0.	4.5856E+00	9.5395E+00	9.5395E+00	0.
87	1.0000E-04	0.	0.	4.5856E+00	9.5395E+00	9.5395E+00	0.
88	1.0000E-04	0.	0.	4.5856E+00	9.5395E+00	9.5395E+00	0.
89	1.0000E-04	0.	0.	4.5856E+00	9.5395E+00	9.5395E+00	0.
90	1.0000E-04	0.	0.	4.5856E+00	9.5395E+00	9.5395E+00	0.
91	1.7500E+00	4.2300E+00	4.2300E+00	1.5714E+02	2.7000E+01	2.2000E+01	5.0000E+00
92	1.5400E-01	2.0800E+00	1.0400E+00	1.0[illegible]E+01	2.3833E+01	2.2000E+01	1.8330E+00
93	1.0000E-04	0.	0.	7.6401E+00	2.2660E+01	2.2000E+01	0.

FLOW PATH	FRICTION K FACTOR DIMENSLESS	GEOM FWD K FACTOR DIMENSLESS	GEOM RVS K FACTOR DIMENSLESS	L/D DIMENSLESS	INLET ELEVATION FT	OUTLET ELEVATION FT	DIFFEREN+E ELEVATION FT
97	1.6720E-01	7.3200E+00	3.0000E+00	1.3811E+01	2.2000E+01	2.2000E+01	0.
98	4.8000E-02	2.9980E+01	1.5000E+01	3.9678E+00	2.2000E+01	2.2000E+01	0.

COMBUSTION ENGINEERING CEFLASH4B VERSION 11 03 1976 76308

PAGE 9 OF OUTPUT 1 TIME STEP 0 TIME 0. SECONDS STEP SIZE 5.0000E-05 SECONDS

FLOW PATH	FLOW LBS/SEC	TOT ELEV PRES DROP PSI	FRICTION PRES DROP PSI	MOMENTUM PRES DROP PSI	LOSS PRES DROP PSI	L/A/144G X DW/DT PSI	SPECIFIC VOLUME CUFT/LB	FLOW INTEGRAL LBS	NODAL PRES DROP CHECK PSI	CRITICAL FLOW	PATH
1	5.5940E+02	-1.9154E-01	1.1222E-01	2.2423E-01	3.6141E-01	0.	2.1060E-02	0.	0.		1
2	5.5940E+02	-9.2707E-01	1.8186E-02	-7.5067E-03	4.1246E-02	0.	2.1061E-02	0.	1.1102E-16		2
3	5.5940E+02	-1.1814E+00	1.1491E-02	2.3231E-06	0.	0.	2.1061E-02	0.	1.4279E-16		3
4	5.5940E+02	-7.1615E-01	1.1244E-02	1.4164E-06	0.	0.	2.1061E-02	0.	1.1679E-16		4
5	5.5940E+02	-6.4869E-01	3.4542E-01	1.5038E-01	2.8045E+00	0.	2.1062E-02	0.	5.3291E-15		5
6	5.5940E+02	-1.1051E+00	2.5565E-01	9.3807E-06	1.4464E+00	0.	2.1063E-02	0.	3.2484E-15		6
7	0.	-7.3240E-01	0.	0.	0.	0.	2.1064E-02	0.	3.4932E-05		7
8	0.	-8.2750E-01	0.	0.	0.	0.	2.1064E-02	0.	6.9562E-05		8
9	5.5940E+02	-5.4035E-01	1.1885E-01	2.8701E-05	1.8077E-01	0.	2.1064E-02	0.	-3.3701E-15		9
10	0.	-5.4035E-01	0.	0.	0.	0.	2.1064E-02	0.	4.8108E-05		10
11	0.	2.4822E-01	0.	0.	0.	0.	2.1064E-02	0.	1.7926E-05		11
12	5.8880E+02	8.2652E-01	9.2582E-01	3.7913E-01	2.0037E+01	0.	2.1064E-02	0.	3.5527E-15		12
13	5.8880E+02	-2.1424E-01	1.7843E+00	-3.4113E-01	2.6126E+00	0.	2.1065E-02	0.	5.3291E-15		13
14	5.8860E+02	-2.4265E+00	4.5223E+00	-1.8617E+00	7.5365E+00	0.	2.1067E-02	0.	1.2790E-13		14
15	5.8880E+02	2.2210E-04	6.0912E+00	3.5418E-05	0.	0.	2.1070E-02	0.	3.1020E-14		15
16	5.8860E+02	2.9203E+00	4.5185E+00	1.6627E+00	7.5401E+00	0.	2.1073E-02	0.	-4.2633E-14		16
17	2.9440E+02	2.5047E-01	1.2608E-02	0.	4.3953E-01	0.	2.1067E-02	0.	-9.1127E-13		17
18	2.9440E+02	2.5047E-01	1.2608E-02	0.	4.3953E-01	0.	2.1067E-02	0.	-9.1127E-13		18
19	2.9440E+02	-3.6911E-02	1.3902E+00	0.	3.0784E-01	0.	2.1060E-02	0.	1.5987E-14		19
20	2.9440E+02	-3.6911E-02	9.9167E-02	1.2714E+00	3.2753E-01	0.	2.1060E-02	0.	-7.1054E-15		20
21	5.8880E+02	4.0647E-05	1.3571E-01	-7.6240E-01	3.9967E+00	0.	2.1061E-02	0.	0.		21
22	0.	-2.8769E+00	0.	0.	0.	0.	2.1064E-02	0.	5.8126E-05		22
23	0.	0.	0.	0.	0.	0.	2.1065E-02	0.	0.		23
24	0.	2.8769E+00	0.	0.	0.	0.	2.1064E-02	0.	-5.8962E-05		24
25	0.	1.6346E+00	0.	0.	0.	0.	2.1063E-02	0.	-3.4997E-05		25
26	0.	-1.1281E+00	0.	0.	0.	0.	2.1062E-02	0.	9.3014E-05		26
27	0.	-3.3138E-05	0.	-7.2746E-02	0.	0.	2.1062E-02	0.	-8.6693E-05		27
28	0.	-3.7425E-03	0.	0.	0.	0.	2.1064E-02	0.	-2.7135E+00		28
29	5.5940E+02	-2.0170E-01	5.6123E-02	-1.5292E-01	1.8080E-01	0.	2.1060E-02	0.	8.8818E-16		29
30	0.	-4.2759E-01	0.	3.1951E-02	0.	0.	2.1060E-02	0.	6.0852E-05		30
31	9.8133E+01	8.5307E-01	4.6583E-02	-3.2560E-01	2.3259E-02	0.	2.1060E-02	0.	-5.3291E-15		31
32	9.8133E+01	8.5307E-01	4.6583E-02	-3.2380E-01	2.3289E-02	0.	2.1060E-02	0.	-5.3291E-15		32
33	9.8133E+01	8.5307E-01	4.6583E-02	-3.2380E-01	2.3289E-02	0.	2.1060E-02	0.	-5.3291E-15		33
34	9.8133E+01	8.5307E-01	4.6583E-02	-3.2380E-01	2.3289E-02	0.	2.1060E-02	0.	-5.3291E-15		34
35	9.8133E+01	8.5307E-01	4.6583E-02	-3.2380E-01	2.3289E-02	0.	2.1060E-02	0.	-5.3291E-15		35
36	9.8133E+01	8.5307E-01	4.6583E-02	-3.2380E-01	2.3289E-02	0.	2.1060E-02	0.	-5.3291E-15		36
37	9.8133E+01	1.3739E+00	1.9529E-02	-1.1559E-05	2.0040E-01	0.	2.1061E-02	0.	4.0052E-15		37
38	9.8133E+01	1.3739E+00	1.9529E-02	-1.1559E-05	2.0040E-01	0.	2.1061E-02	0.	4.0052E-15		38
39	9.8133E+01	1.3739E+00	1.9529E-02	-1.1559E-05	2.0040E-01	0.	2.1061E-02	0.	4.0052E-15		39
40	9.8133E+01	1.3739E+00	1.9529E-02	-1.1559E-05	2.0040E-01	0.	2.1061E-02	0.	4.0052E-15		40
41	9.8133E+01	1.3739E+00	1.9529E-02	-1.1559E-05	2.0040E-01	0.	2.1061E-02	0.	4.0052E-15		41
42	9.8133E+01	1.3739E+00	1.9529E-02	-1.1559E-05	2.0040E-01	0.	2.1061E-02	0.	4.0052E-15		42
43	9.8133E+01	1.3739E+00	2.0427E-02	-1.5864E-05	2.5034E-01	0.	2.1061E-02	0.	7.0929E-16		43
44	9.8133E+01	1.3739E+00	2.0427E-02	-1.5864E-05	2.5034E-01	0.	2.1061E-02	0.	7.0929E-16		44
45	9.8133E+01	1.3739E+00	2.0427E-02	-1.5864E-05	2.5034E-01	0.	2.1061E-02	0.	7.0929E-16		45
46	9.8133E+01	1.3739E+00	2.0427E-02	-1.5864E-05	2.5034E-01	0.	2.1061E-02	0.	7.0929E-16		46
47	9.8133E+01	1.3739E+00	2.0427E-02	-1.5864E-05	2.5034E-01	0.	2.1061E-02	0.	7.0929E-16		47

FLOW PATH	FLOW LBS/SEC	TOT ELEV PRES DROP PSI	FRICTION PRES DROP PSI	MOMENTUM PRES DROP PSI	LOSS PRES DROP PSI	L/A/144G X DP/DT PSI	SPECIFIC VOLUME CUFT/LB	FLOW INTEGRAL LBS	NODAL PRES DROP CHECK PSI	CRITICAL FLOW	PATH
49	9.8133E+01	6.0702E-01	1.0025E-01	2.3650E-01	1.0017E-01	0.	2.1061E-02	0.	0.		49
50	9.8133E+01	6.0702E-01	1.0035E-01	2.3650E-01	1.0017E-01	0.	2.1061E-02	0.	-1.7764E-15		50
51	9.8133E+01	6.0702E-01	1.0025E-01	2.3650E-01	1.0017E-01	0.	2.1061E-02	0.	0.		51
52	9.8133E+01	6.0702E-01	1.0015E-01	2.3650E-01	1.0017E-01	0.	2.1061E-02	0.	8.8818E-16		52
53	9.8133E+01	6.0702E-01	1.0005E-01	2.3650E-01	1.0017E-01	0.	2.1061E-02	0.	4.4409E-15		53
54	9.8133E+01	6.0702E-01	1.0015E-01	2.3650E-01	1.0017E-01	0.	2.1061E-02	0.	8.8818E-		54
55	0.	8.3544E-01	0.	0.	0.	0.	2.1062E-02	0.	4.0798E-		55
56	0.	8.3544E-01	0.	0.	0.	0.	2.1062E-02	0.	-5.9203E-05		56
57	0.	8.3544E-01	0.	0.	0.	0.	2.1062E-02	0.	4.0798E-05		57
58	0.	8.3544E-01	0.	0.	0.	0.	2.1062E-02	0.	1.4080E-04		58
59	0.	8.3544E-01	0.	0.	0.	0.	2.1062E-02	0.	2.4080E-04		59
60	0.	8.3544E-01	0.	0.	0.	0.	2.1062E-02	0.	1.4080E-04		60
61	0.	0.	0.	0.	0.	0.	2.1062E-02	0.	0.		61
62	0.	0.	0.	0.	0.	0.	2.1062E-02	0.	0.		62
63	0.	0.	0.	0.	0.	0.	2.1062E-02	0.	0.		63
64	0.	0.	0.	0.	0.	0.	2.1062E-02	0.	0.		64
65	0.	0.	0.	0.	0.	0.	2.1062E-02	0.	0.		65
66	0.	0.	0.	0.	0.	0.	2.1062E-02	0.	0.		66
67	1.4720E+02	2.2764E-10	9.9998E-05	5.1273E-10	0.	0.	2.1062E-02	0.	-1.2504E-15		67
68	4.9067E+01	2.2764E-10	1.0000E-04	5.6969E-11	0.	0.	2.1062E-02	0.	2.1402E-17		68
69	4.9067E+01	2.2764E-10	1.0000E-04	5.6969E-11	0.	0.	2.1062E-02	0.	2.1402E-17		69
70	1.4720E+02	2.2764E-10	9.9998E-05	5.1273E-10	0.	0.	2.1062E-02	0.	-1.2504E-15		70
71	2.4533E+02	2.2764E-10	1.0000E-04	1.4242E-09	0.	0.	2.1062E-02	0.	-9.6658E-16		71
72	2.4533E+02	2.2764E-10	1.0000E-04	1.4242E-09	0.	0.	2.1062E-02	0.	-9.6658E-16		72
73	0.	0.	0.	0.	0.	0.	2.1061E-02	0.	0.		73
74	0.	0.	0.	0.	0.	0.	2.1061E-02	0.	0.		74
75	0.	0.	0.	0.	0.	0.	2.1061E-02	0.	0.		75
76	0.	0.	0.	0.	0.	0.	2.1061E-02	0.	0.		76
77	0.	0.	0.	0.	0.	0.	2.1061E-02	0.	0.		77
78	0.	0.	0.	0.	0.	0.	2.1061E-02	0.	0.		78
79	0.	0.	0.	0.	0.	0.	2.1061E-02	0.	0.		79
80	0.	0.	0.	0.	0.	0.	2.1061E-02	0.	0.		80
81	0.	0.	0.	0.	0.	0.	2.1061E-02	0.	0.		81
82	0.	0.	0.	0.	0.	0.	2.1061E-02	0.	0.		82
83	0.	0.	0.	0.	0.	0.	2.1061E-02	0.	0.		83
84	0.	0.	0.	0.	0.	0.	2.1061E-02	0.	0.		84
85	0.	0.	0.	0.	0.	0.	2.1061E-02	0.	0.		85
86	0.	0.	0.	0.	0.	0.	2.1061E-02	0.	0.		86
87	0.	0.	0.	0.	0.	0.	2.1061E-02	0.	0.		87
88	0.	0.	0.	0.	0.	0.	2.1061E-02	0.	0.		88
89	0.	0.	0.	0.	0.	0.	2.1061E-02	0.	0.		89
90	0.	0.	0.	0.	0.	0.	2.1061E-02	0.	0.		90
91	0.	2.0570E+00	0.	0.	0.	0.	3.9242E-02	0.	-7.7067E-02		91
92	0.	5.7443E-01	0.	0.	0.	0.	2.1062E-02	0.	-1.6183E-03		92
93	0.	4.3450E-06	0.	0.	0.	0.	2.1061E-02	0.	2.9960E-01		93
94	0.	-4.3450E-06	0.	0.	0.	0.	2.1061E-02	0.	-2.9960E-01		94
95	2.9400E+01	-4.3499E+00	6.0185E-01	1.7709E-05	0.	0.	2.1061E-02	0.	1.2974E-14		95
96	2.9400E+01	-1.1450E+00	5.3096E+00	4.7154E-02	0.	0.	2.1063E-02	0.	1.0725E-13		96

LOFT L1-2 ZERO TIME EDIT

COMBUSTION ENGINEERING CEFLASH4B VERSION 11 03 1976 76308

PAGE 11 OF OUTPUT 1 TIME STEP 0 TIME 0. SECONDS STEP SIZE 5.0000E-05 SECONDS

FLOW PATH	FLOW LBS/SEC	TOT ELEV PRES DROP PSI	FRICTION PRES DROP PSI	MOMENTUM PRES DROP PSI	LOSS PRES DROP PSI	L/A/144G X DW/DT PSI	SPECIFIC VOLUME CUFT/LB	FLOW INTEGRAL LBS	NODAL PRES DROP CHECK PSI	CRITICAL FLOW	PATH
97	0.	1.4574E-02	0.	0.	0.	0.	2.1061E-02	0.	1.4574E-02		97
98	0.	8.7796E-02	0.	0.	0.	0.	2.1064E-02	0.	8.7796E-02		98
99	0.						2.1061E-02	0.			99
100	0.						2.1064E-02	0.			100

FLOW PATH	PIPE ENTHALPY BTU/LB	PIPE QUALITY	K FACTOR FRC OR LAT DIMENSLESS	AV CORE OR EXIT TEMP DEG F	FLOW SQ X SPEC VOL LBFT3/SEC2	STEAM INTEGRAL LBS	PATH ELEV PRES DROP PSI	VEL SQ / 2 G J BTU/LB	PATH
1	5.3600E+02	0.	1.6396E+00	5.4002E+02	6.5904E+03	0.	-1.9647E-01	1.2082E-03	1
2	5.3600E+02	0.	3.0423E-01	5.4002E+02	6.5905E+03	0.	-5.5931E-01	1.8264E-04	2
3	5.3600E+02	0.	1.7487E-01	5.4002E+02	6.5906E+03	0.	-1.0544E+00	2.5616E-04	3
4	5.3600E+02	0.	1.7112E-01	5.4002E+02	6.5907E+03	0.	-9.4779E-01	2.5617E-04	4
5	5.3600E+02	0.	4.7788E-01	5.4002E+02	6.5909E+03	0.	-6.8339E-01	2.5619E-04	5
6	5.3600E+02	0.	1.2455E+00	5.4002E+02	6.5913E+03	0.	-9.9281E-01	4.3956E-04	6
7	5.3600E+02	0.	2.0700E-02	5.4002E+02	0.	0.	-8.1037E-01	0.	7
8	5.3600E+02	0.	0.	5.4002E+02	0.	0.	-8.8355E-01	0.	8
9	5.3600E+02	0.	1.0296E-01	5.4002E+02	6.5915E+03	0.	0.	4.5006E-03	9
10	5.3600E+02	0.	0.	5.4002E+02	0.	0.	0.	0.	10
11	5.3600E+02	0.	0.	5.4002E+02	0.	0.	0.	0.	11
12	5.3600E+02	0.	5.4753E-01	5.4002E+02	7.3026E+03	0.	0.	4.9863E-03	12
13	5.3600E+02	0.	6.6321E-01	5.4002E+02	7.3029E+03	0.	0.	6.5930E-03	13
14	5.3600E+02	0.	1.8301E+01	5.4002E+02	7.3038E+03	0.	-8.1652E-01	6.5947E-03	14
15	5.3600E+02	0.	6.7202E+00	5.4002E+02	7.3048E+03	0.	0.	3.5350E-03	15
16	5.3600E+02	0.	3.2720E+00	5.4002E+02	7.3057E+03	0.	2.2092E+00	3.5359E-03	16
17	5.3600E+02	0.	2.2500E-02	5.4002E+02	1.8259E+03	0.	-1.3933E+00	1.6487E-03	17
18	5.3600E+02	0.	2.2500E-02	5.4002E+02	1.8259E+03	0.	-1.3933E+00	1.6487E-03	18
19	5.3600E+02	0.	1.2626E+00	5.4002E+02	1.8253E+03	0.	0.	4.9441E-03	19
20	5.3600E+02	0.	8.8502E-02	5.4002E+02	1.8253E+03	0.	0.	4.9441E-03	20
21	5.3600E+02	0.	8.0272E-02	5.4002E+02	7.3015E+03	0.	0.	6.5907E-03	21
22	5.3600E+02	0.	1.5000E-01	5.4002E+02	0.	0.	-2.1986E+00	0.	22
23	5.3600E+02	0.	5.0000E-02	5.4002E+02	0.	0.	0.	0.	23
24	5.3600E+02	0.	1.0000E-01	5.4002E+02	0.	0.	2.2379E+00	0.	24
25	5.3600E+02	0.	9.7500E-02	5.4002E+02	0.	0.	1.0148E+00	0.	25
26	5.3600E+02	0.	2.0800E-01	5.4002E+02	0.	0.	-1.2235E+00	0.	26
27	5.3600E+02	0.	1.0000E-01	5.4002E+02	0.	0.	0.	0.	27
28	5.3600E+02	0.	1.5100E-01	5.4002E+02	0.	0.	6.0430E-01	0.	28
29	5.3600E+02	0.	3.1504E-01	5.4002E+02	904E+03	0.	-3.2501E-01	1.1709E-04	29
30	5.3600E+02	0.	1.0000E-04	5.4002E+02		0.	-4.5043E-01	0.	30
31	5.3600E+02	0.	5.3207E-01	5.4002E+	2.0282E+02	0.	6.5074E-01	1.3173E-03	31
32	5.3600E+02	0.	5.3207E-01	5.4002E+	2.0282E+02	0.	6.5074E-01	1.3173E-03	32
33	5.3600E+02	0.	5.3207E-01	5.4002E	2.0282E+02	0.	6.5074E-01	1.3173E-03	33
34	5.3600E+02	0.	5.3207E-01	5.4002E+	2.0282E+02	0.	6.5074E-01	1.3173E-03	34
35	5.3600E+02	0.	5.3207E-01	5.4002E+0	2.0282E+02	0.	6.5074E-01	1.3173E-03	35
36	5.3600E+02	0.	5.3207E-01	5.4002E+02	2.0282E+02	0.	6.5074E-01	1.3173E-03	36
37	5.3600E+02	0.	5.7789E-02	5.4002E+02	2.0282E+02	0.	1.1135E+00	1.3174E-03	37
38	5.3600E+02	0.	5.7789E-02	5.4002E+02	2.0282E+02	0.	1.1135E+00	1.3174E-03	38
39	5.3600E+02	0.	5.7789E-02	5.4002E+02	2.0282E+02	0.	1.1135E+00	1.3174E-03	39
40	5.3600E+02	0.	5.7789E-02	5.4002E+02	2.0282E+02	0.	1.1135E+00	1.3174E-03	40
41	5.3600E+02	0.	5.7789E-02	5.4002E+02	2.0282E+02	0.	1.1135E+00	1.3174E-03	41
42	5.3600E+02	0.	5.7789E-02	5.4002E+02	2.0282E+02	0.	1.1135E+00	1.3174E-03	42
43	5.3600E+02	0.	6.0444E-02	5.4002E+02	2.0282E+02	0.	1.0143E+00	1.3174E-03	43
44	5.3600E+02	0.	6.0444E-02	5.4002E+02	2.0282E+02	0.	1.0143E+00	1.3174E-03	44
45	5.3600E+02	0.	6.0444E-02	5.4002E+02	2.0282E+02	0.	1.0143E+00	1.3174E-03	45
46	5.3600E+02	0.	6.0444E-02	5.4002E+02	2.0282E+02	0.	1.0143E+00	1.3174E-03	46
47	5.3600E+02	0.	6.0444E-02	5.4002E+02	2.0282E+02	0.	1.0143E+00	1.3174E-03	47
48	5.3600E+02	0.	6.0444E-02	5.4002E+02	2.0282E+02	0.	1.0143E+00	1.3174E-03	48

LOFT L1-2 ZERO TIME EDIT

COMBUSTION ENGINEERING CEFLASHAR VERSION 11 03 1976 76308

PAGE 15 OF OUTPUT 1 TIME STEP 0 TIME 0. SECONDS STEP SIZE 5.0000E-05 SECONDS

FLOW PATH	PIPE ENTHALPY BTU/LB	PIPE QUALITY	K FACTOR FRC OR LAT DIMENSLESS	AV CORE OR EXIT TEMP DEG F	FLOW SQ X SPEC VOL LBF**2/SEC2	STEAM INTEGRAL LBS	PATH ELEV PRES DROP PSI	VEL SQ / 2 G J BTU/LB	PATH
49	5.3802E+02	0.	2.9666E-01	5.4002E+02	2.0283E+02	0.	1.3807E+00	3.9549E-04	49
50	5.3800E+02	0.	2.9695E-01	5.4002E+02	2.0283E+02	0.	1.3807E+00	3.9549E-04	50
51	5.3800E+02	0.	2.9666E-01	5.4002E+02	2.0283E+02	0.	1.3807E+00	3.9549E-04	51
52	5.3800E+02	0.	2.9636E-01	5.4002E+02	2.0283E+02	0.	1.3807E+00	3.9549E-04	52
53	5.3800E+02	0.	2.9606E-01	5.4002E+02	2.0283E+02	0.	1.3807E+00	3.9549E-04	53
54	5.3800E+02	0.	2.9636E-01	5.4002E+02	2.0283E+02	0.	1.3807E+00	3.9549E-04	54
55	5.3800E+02	0.	0.	5.4002E+02	0.	0.	5.7140E-01	0.	55
56	5.3800E+02	0.	0.	5.4002E+02	0.	0.	5.7140E-01	0.	56
57	5.3800E+02	0.	0.	5.4002E+02	0.	0.	5.7140E-01	0.	57
58	5.3800E+02	0.	0.	5.4002E+02	0.	0.	5.7140E-01	0.	58
59	5.3800E+02	0.	0.	5.4002E+02	0.	0.	5.7140E-01	0.	59
60	5.3800E+02	0.	0.	5.4002E+02	0.	0.	5.7140E-01	0.	60
61	5.3800E+02	0.	1.0000E-04	5.4002E+02	0.	0.	0.	0.	61
62	5.3800E+02	0.	1.0000E-04	5.4002E+02	0.	0.	0.	0.	62
63	5.3800E+02	0.	1.0000E-04	5.4002E+02	0.	0.	0.	0.	63
64	5.3800E+02	0.	1.0000E-04	5.4002E+02	0.	0.	0.	0.	64
65	5.3800E+02	0.	1.0000E-04	5.4002E+02	0.	0.	0.	0.	65
66	5.3800E+02	0.	1.0000E-04	5.4002E+02	0.	0.	0.	0.	66
67	5.3800E+02	0.	5.7790E-04	5.4002E+02	4.5636E+02	0.	0.	6.7456E-04	67
68	5.3800E+02	0.	5.2012E-03	5.4002E+02	5.0706E+01	0.	0.	7.4952E-05	68
69	5.3800E+02	0.	5.2012E-03	5.4002E+02	5.0706E+01	0.	0.	7.4952E-05	69
70	5.3800E+02	0.	5.7790E-04	5.4002E+02	4.5636E+02	0.	0.	6.7456E-04	70
71	5.3800E+02	0.	2.0905E-04	5.4002E+02	1.2676E+03	0.	0.	1.8737E-03	71
72	5.3800E+02	0.	2.0905E-04	5.4002E+02	1.2676E+03	0.	0.	1.8737E-03	72
73	5.3800E+02	0.	1.0000E-04	5.4002E+02	0.	0.	0.	0.	73
74	5.3800E+02	0.	1.0000E-04	5.4002E+02	0.	0.	0.	0.	74
75	5.3800E+02	0.	1.0000E-04	5.4002E+02	0.	0.	0.	0.	75
76	5.3800E+02	0.	1.0000E-04	5.4002E+02	0.	0.	0.	0.	76
77	5.3800E+02	0.	1.0000E-04	5.4002E+02	0.	0.	0.	0.	77
78	5.3800E+02	0.	1.0000E-04	5.4002E+02	0.	0.	0.	0.	78
79	5.3800E+02	0.	1.0000E-04	5.4002E+02	0.	0.	0.	0.	79
80	5.3800E+02	0.	1.0000E-04	5.4002E+02	0.	0.	0.	0.	80
81	5.3800E+02	0.	1.0000E-04	5.4002E+02	0.	0.	0.	0.	81
82	5.3800E+02	0.	1.0000E-04	5.4002E+02	0.	0.	0.	0.	82
83	5.3800E+02	0.	1.0000E-04	5.4002E+02	0.	0.	0.	0.	83
84	5.3800E+02	0.	1.0000E-04	5.4002E+02	0.	0.	0.	0.	84
85	5.3800E+02	0.	1.0000E-04	5.4002E+02	0.	0.	0.	0.	85
86	5.3800E+02	0.	1.0000E-04	5.4002E+02	0.	0.	0.	0.	86
87	5.3800E+02	0.	1.0000E-04	5.4002E+02	0.	0.	0.	0.	87
88	5.3800E+02	0.	1.0000E-04	5.4002E+02	0.	0.	0.	0.	88
89	5.3800E+02	0.	1.0000E-04	5.4002E+02	0.	0.	0.	0.	89
90	5.3800E+02	0.	1.0000E-04	5.4002E+02	0.	0.	0.	0.	90
91	7.4465E+02	9.4602E-02	1.2105E+00	6.5817E+02	0.	0.	8.8482E-01	0.	91
92	5.3800E+02	0.	1.5400E-01	5.4002E+02	0.	0.	6.0437E-01	0.	92
93	5.3800E+02	0.	1.0000E-04	5.4002E+02	0.	0.	0.	0.	93

PAGE 14 OF OUTPUT 1 TIME STEP 0 TIME 0. SECONDS STEP SIZE 5.0000E-05 SECONDS

FLOW PATH	PIPE ENTHALPY BTU/LM	PIPE QUALITY	K FACTOR FRC OR LAT DIMENSLESS	AV CORE OR EXIT TEMP DEG F	FLOW SQ X SPEC VOL LBFT3/SEC2	STEAM INTEGRAL LBS	PATH ELEV PRES DROP PSI	VEL SQ / 2 G J BTU/LB	PATH
97	5.3606E+02	0.	1.6720E-01	5.4002E+02	0.	0.	0.	0.	97
98	5.3606E+02	0.	4.8000E+02	5.4002E+02	0.	0.	0.	0.	98
99	5.3606E+02	0.		5.4002E+02	0.	0.		0.	99
100	5.3606E+02	0.		5.4002E+02	0.	0.		0.	100

APPENDIX D

CEFLASH-4B LOFT SENSITIVITY STUDY

This appendix presents the results of an extensive CEFLASH-4B sensitivity study performed on two computer model simulations of the LOFT L1-2 experiment. The purpose of this investigation is to determine the best modeling procedures to be applied to the CEFLASH-4B LOFT analysis.

D.1 DESCRIPTION OF CEFLASH-4B MODELS

The LOFT facility was simulated using two CEFLASH-4B computer models. The models were identical in the treatment of all LOFT piping with the exception of the piping downstream of the designated break planes. The CEFLASH-4B LOFT "break plane" model lumped all piping downstream of the break planes as a single volume (NODE 63). This model tacitly assumes the LOFT designated break planes to experience critical flow from the instant of blowdown. In fact, by neglecting the presence of the high pressures in the piping between the break planes and the Quick Opening Blowdown Valves (QOBV's), the critical flow was imposed more quickly than was realistic. Therefore, this model was used only for parametric sensitivities and to confirm modeling assumptions. The node-flowpath diagram for this model is presented in Figure D-1.

The second CEFLASH-4B model elaborated upon the "break plane" model by treating the connecting piping between the hot and cold leg break planes and pressure suppression tank as discrete nodes. These nodes are designated as nodes 63 and 64 in the node-flowpath network in Figure D-2. This modeling initiates the break opening at the outlet of the Quick Opening Blowdown Valves. Thus leaving the flow at the break plane free to accelerate to its maximum value in accordance with the conservation laws.

Descriptions of the node and flowpath arrangement for the "break plane" and "detailed" downstream piping model are presented in Tables D-1 and D-2. Additional details of path and nodal parameters for the "detailed" model can be found in the zero time edit presented in Appendix C.

D.2 STUDIES WITH THE LOFT L1-2 "DETAILED" MODEL

D.2.1 Loop Temperature Distribution

LOFT computer models employing a "best-estimate" nonisothermal loop temperature distribution and a 540°F isothermal loop were compared. The "best-estimate" temperature distribution is shown in Table D-3. This distribution is based on experimental pre-rupture measurements at discrete loop positions (Reference D-1).

Figure D-3 presents a typical comparison of predicted pressures obtained with both models. [

[3]

]

D.2.2 Critical Flow Model and Discharge Coefficient at the QOBV

The sensitivity of blowdown pressure history to the critical flow model formulation and the critical flow discharge coefficient at the Quick Opening Blowdown Valve (QOBV) was investigated by varying characteristics of the break flowpaths of the base LOFT model. The sensitivity of the critical flow formulation was established by comparing the predictions of the C-E[[3]
]correlation (a nonequilibrium procedure) with those of the homogeneous equilibrium formulation. The discharge coefficient sensitivity was determined using the base critical flow correlation[
] [3]

Typical comparisons from both studies are presented in Figures D-4 and D-5. Changing break flow correlations results in[
[3]
]

596 228

D.2.3 Quick Opening Blowdown Valve Opening Time

The opening time for the QOBV's has been recorded to vary from 17 msec (hot leg) to 28 msec (cold leg). Since the cold leg opening has the more profound effect on the system, a 28 msec QOBV opening time was selected to describe the break behavior of the LOFT Test L1-2. The sensitivity of this assumption was investigated by comparing these results with an alternate opening time derived from the average (22.5 msec) of the hot and cold leg break opening times.

[

] A typical comparison is presented in Figure D-6. [3]

D.2.4 Calculational Time Step

A sensitivity study was conducted to confirm the calculational time step used in the LOFT experimental comparison. Two time steps,[ ]seconds [3] and[ ]seconds were investigated. [[3]

] Typical results from this study are shown in Figure D-7 and D-8. Predictions obtained by reducing the time step by a factor of two demonstrated excellent agreement with the [ ]second time step [3] computation. Thus, the[ ]second time step was used for purposes [3] of this calculation.

D.3 STUDIES WITH THE CEFLASH-4B "BREAK PLANE" MODEL

D.3.1 Break Plane Area Opening Time

The purpose of this study was to establish the influence of the assumed break opening characteristics on the LOFT system decompression. Total break opening times spanned the range from 3.6 milliseconds to twenty (20) milliseconds. The lower number represents the estimated time necessary to expose an area equivalent to the orifice area (.09 ft^2) based on LOFT QOBV measured opening times. The upper limit was taken near the nominal QOBV opening time.

Representative comparisons of absolute and differential pressure for the above limits of opening times are presented in Figures D-9 thru D-11 and D-12, respectively. The longer opening times demonstrate the slower and smoother decompression. Spikes and bumps noted for the 3.6 msec opening time case become slope changes for a 20 msec opening time. Similarly, differential pressures predicted for the shorter opening time are of higher frequency content and greater magnitude than those predicted for a 20 millisecond opening.

The selection of a break opening time has a substantial influence on the predicted pressure fine structure, with the more slowly opening breaks resulting in a smoother, slower initial decompression. This observation supports the position presented in the text, that accounting for the early break processes will smooth the predicted pressure decay, thereby further improving the experimental-analytical comparison.

D.3.2 Reflood Assist Bypass Modeling

The LOFT facility has been designed with a Reflood Assist Bypass (RAB) system (See Figure 44 of Reference D-2). The purpose of this system is to provide LOFT with a higher core reflood rate capability during the reflood phase of a LOCA than does occur in a PWR. However, for the blowdown phase of the LOCA the system is valved shut. Those portions of the system remaining in direct contact with the blowdown loop behave as two "dead ends". In this analysis these "dead ends" have been each represented by a single node and flowpath. The RAB is atypical of standard C-E PWR plant designs. Therefore, the sensitivity of LOFT predictions to RAB modeling was of considerable interest.

In order to assess the importance of this region, to the overall CEFLASH-4B prediction of LOFT, the associated RAB cold leg flowpath fluid inertia was varied from 0.1 ft^{-1} to 10^8 ft^{-1}. These values were selected as bounding cases. The smaller inertia value assumes the RAB fluid is essentially lumped into the adjacent volume. The larger value indicates a near infinite inertia, and consequently results in poor communication between the RAB and the adjacent node.

Representative comparisons of pressures predicted with the two limiting RAB models are presented in Figures D-13 and D-14. Figure D-13 displays the downcomer pressures in node 48.[

[3]

]

[

[3]

]

D.4 COMPARISON OF "BREAK PLANE" AND "DETAILED" MODEL PREDICTIONS

This section presents comparisons of predictions obtained using the "break plane" model and the "detailed" LOFT model. For both cases critical flow at the respective break positions were evaluated using the C-E[[3]
]correlation with a[ ]multiplier. [3]

Representative comparisons are presented in Figures D-15 thru D-17. Differences between the two predictive models can be seen. In all cases, the "detailed" model results in smoother pressure predictions. This is a consequence of the increased spacial detail used to represent the piping downstream of the LOFT break planes. The more realistic, "detailed", model is presented in the text (Section 3) as the base case for the LOFT data comparison.

D.5 REFERENCES FOR APPENDIX D

D-1 Robinson, H. C., "Experiment Data Report for LOFT Test L1-2", TREE-NUREG-1026, July 1976.

D-2 Robinson, H. C., "LOFT Systems and Test Description (Loss-of-Coolant Experiments Using a Core Simulator)", TREE-NUREG-1019, Nov. 1976.

596 231

TABLE D-1

CEFLASH-4B LOFT L1-2 NODAL DESCRIPTION(1),(2) FOR DETAILED AND BREAK PLANE MODELS

NODE NO.	DESCRIPTION
[	]

[3]

TABLE D-1 (Cont'd.)

CEFLASH-4B LOFT L1-2 NODAL DESCRIPTION FOR DETAILED AND BREAK PLANE MODELS

NODE NO.	DESCRIPTION
[	]

[3]

TABLE D-1 (Cont'd.)

CEFLASH-4B LOFT L1-2 NODAL DESCRIPTION FOR DETAILED AND BREAK PLANE MODELS

NODE NO.	DESCRIPTION
[	] [3]

(1) Piping section numbers refer to the identification in Tables VI and XIV of Reference D-2

(2) Nodal Descriptions apply to both the break plane and detailed model unless otherwise specified

596 234

TABLE D-2

CEFLASH-4B LOFT L1-2 FLOWPATH DESCRIPTION FOR DETAILED AND BREAK PLANE MODELS (1)

FLOWPATH NUMBER	DESCRIPTION
[3]	

TABLE D-2 (Cont'd)

CEFLASH-4B LOFT L1-2 FLOWPATH DESCRIPTION FOR DETAILED AND BREAK PLANE MODELS

FLOWPATH NUMBER	DESCRIPTION
[	] [3]

TABLE D-2 (Cont'd.)

CEFLASH-4B LOFT L1-2 FLOWPATH DESCRIPTION FOR DETAILED AND BREAK PLANE MODELS

FLOWPATH NUMBER	DESCRIPTION
[	] [3]

TABLE D-2 (Cont'd.)

CEFLASH-4B LOFT L1-2 FLOWPATH DESCRIPTION FOR DETAILED AND BREAK PLANE MODELS

FLOWPATH NUMBER	DESCRIPTION
[	]

(1) Flowpath Descriptions apply to both the detailed and break plane models unless otherwise specified.

596 238

TABLE D-3

BEST-ESTIMATE LOFT TEMPERATURE DISTRIBUTION*

NODE NO.(S)	TEMPERATURE °F
1-10	538
11	536
12	538
13	536
14-21	540
22 (pressurizer)	654
23	528
24	540
25-30	536
31-61	538
62	528
63	536
65 (suppression tank)	70

596 239

* Distribution developed from data presented in Reference D-1.

Figure D-1
CEFLASH-4B: BREAK PLANE MODEL

[3,5]

Figure D-2

Figure D-3

EFFECT OF ISOTHERMAL LOOP
ASSUMPTION ON CEFLASH-4B PREDICTED PRESSURES
DETAILED MODEL
(CORE SIMULATOR: NODE 7)

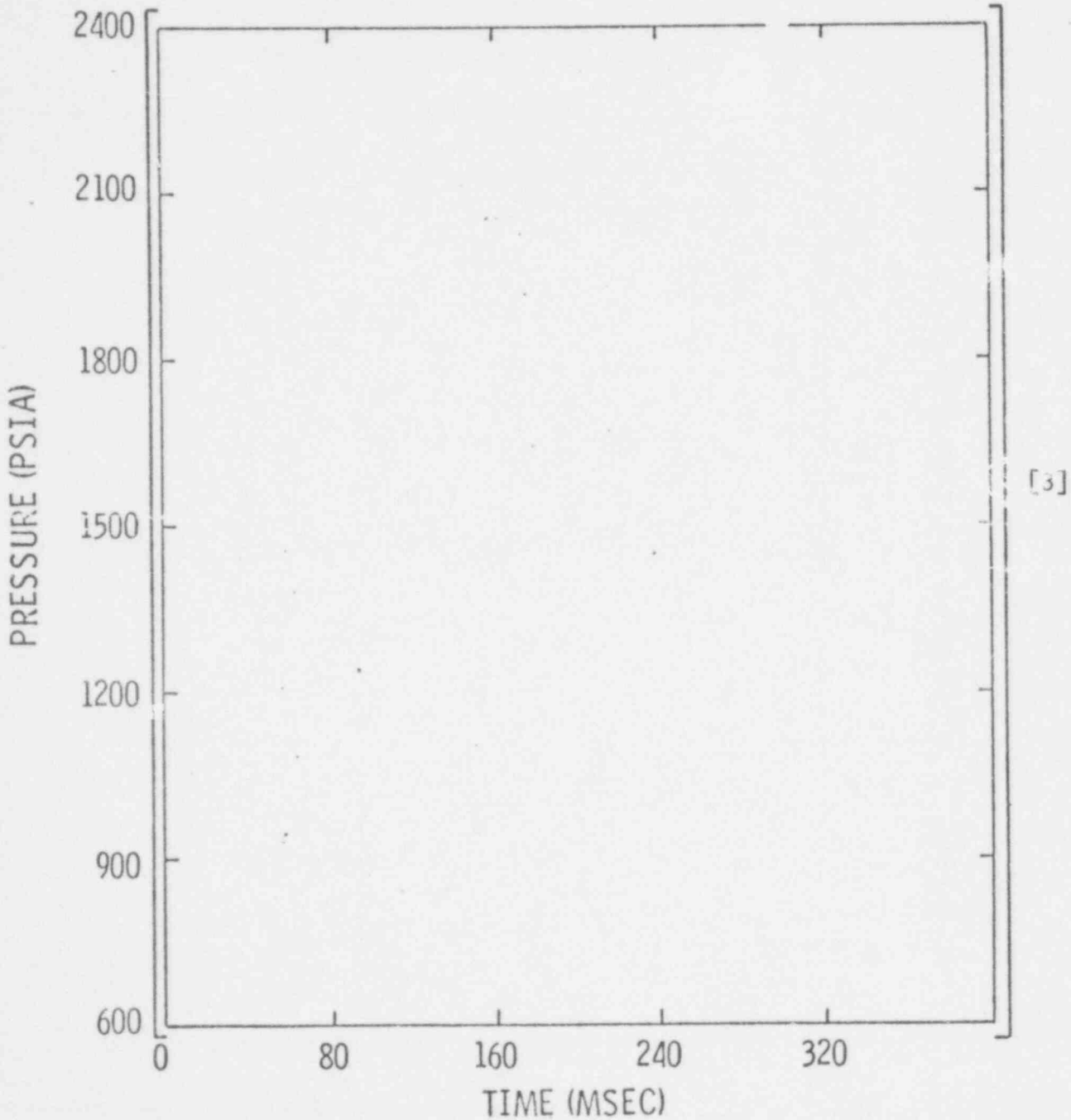

596 242

Figure D-4

INFLUENCE OF CRITICAL FLOW CORRELATION
ON PREDICTED PRESSURE DECAY
DETAILED MODEL
(CORE SIMULATOR: NODE 7)

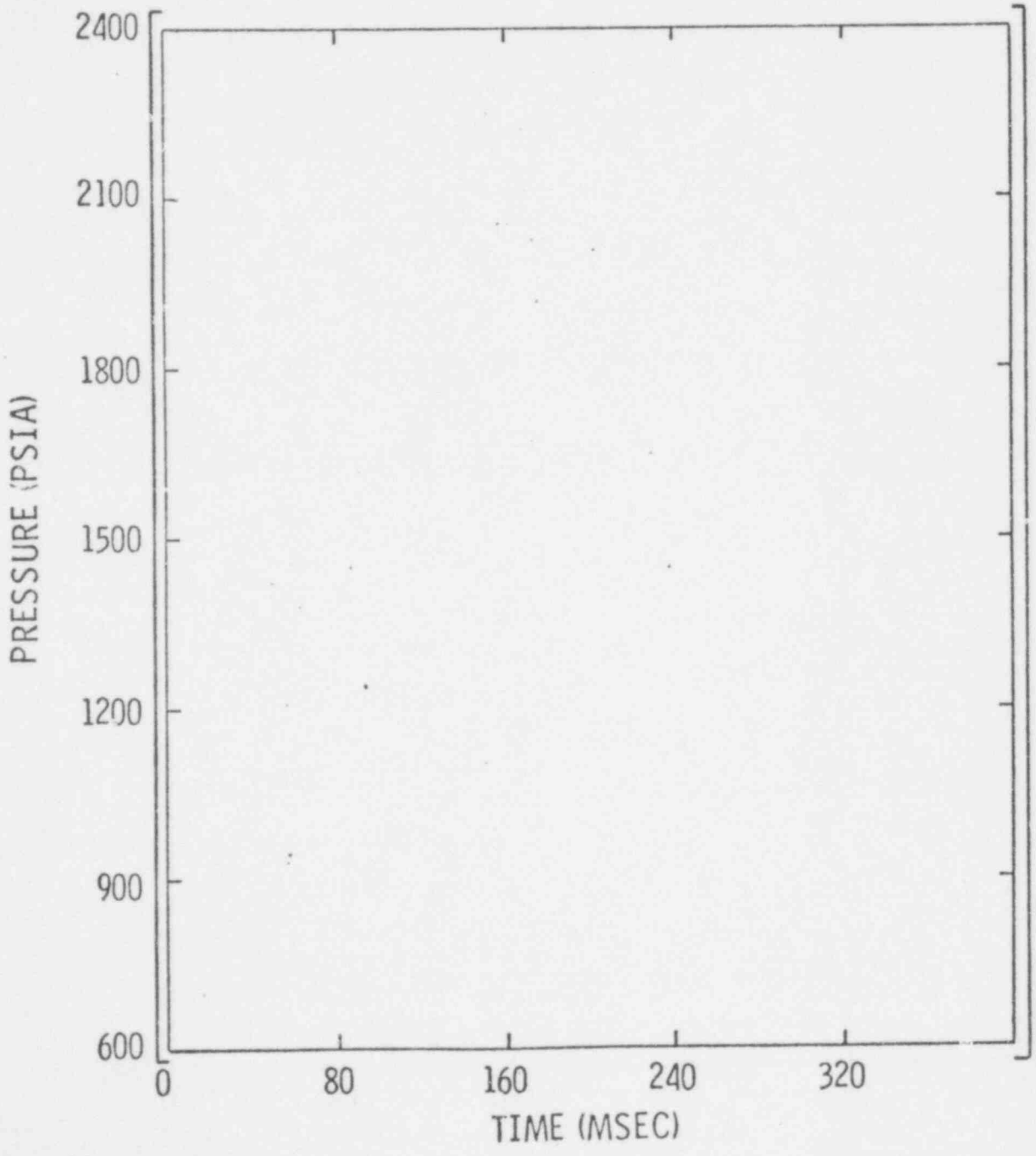

Figure D-5

EFFECT OF VARYING THE DISCHARGE COEFFICIENT
AT THE QOBV ON THE CEFLASH-4B PREDICTED PRESSURE DECAY
DETAILED MODEL
(DOWNCOMER: NODE 47)

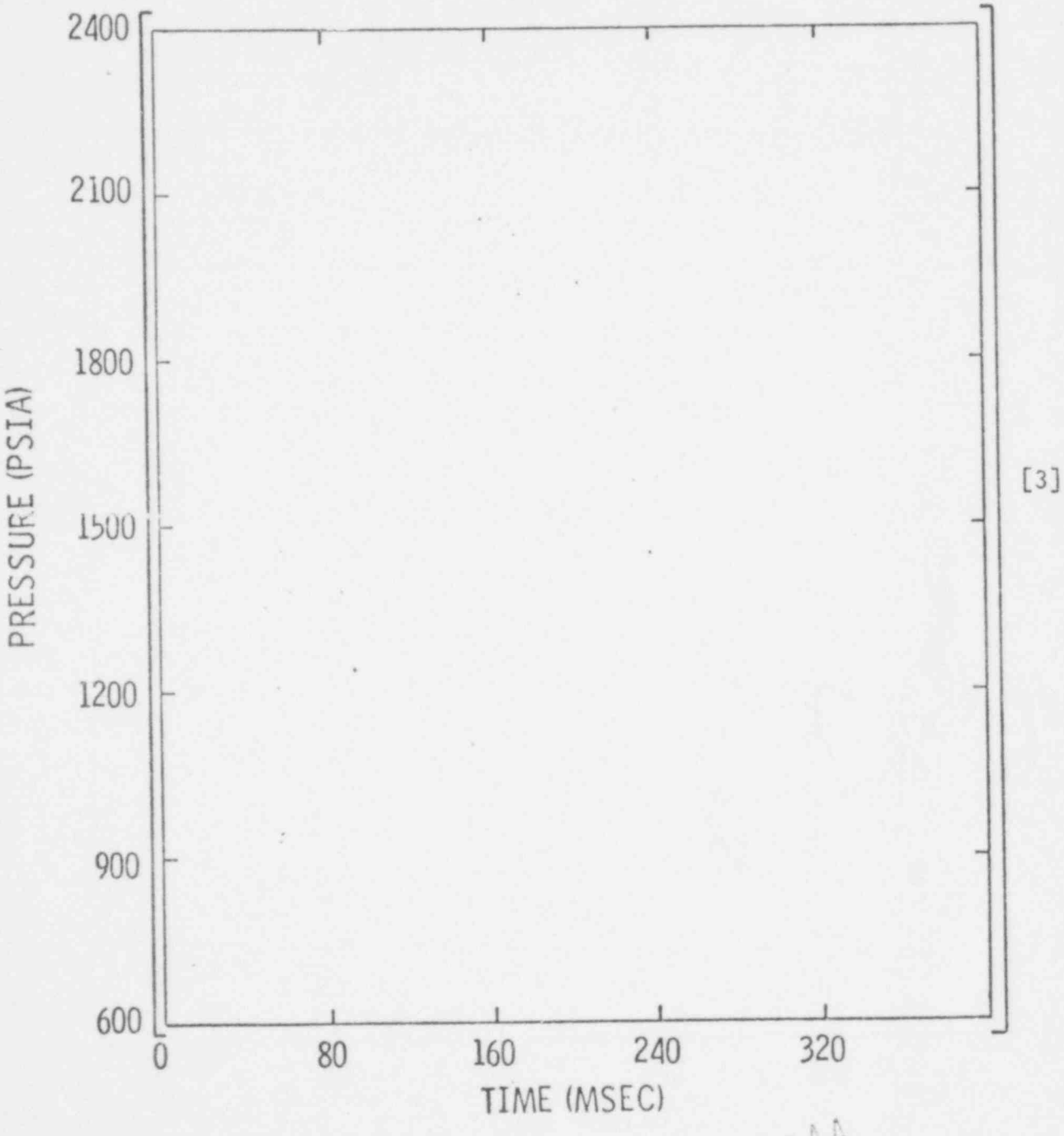

[3]

Figure D-6

SENSITIVITY OF CEFLASH-4B
PREDICTED PRESSURES TO ASSUMED QOBV
OPENING TIME
DETAILED MODEL
(CORE SIMULATOR: NODE 7)

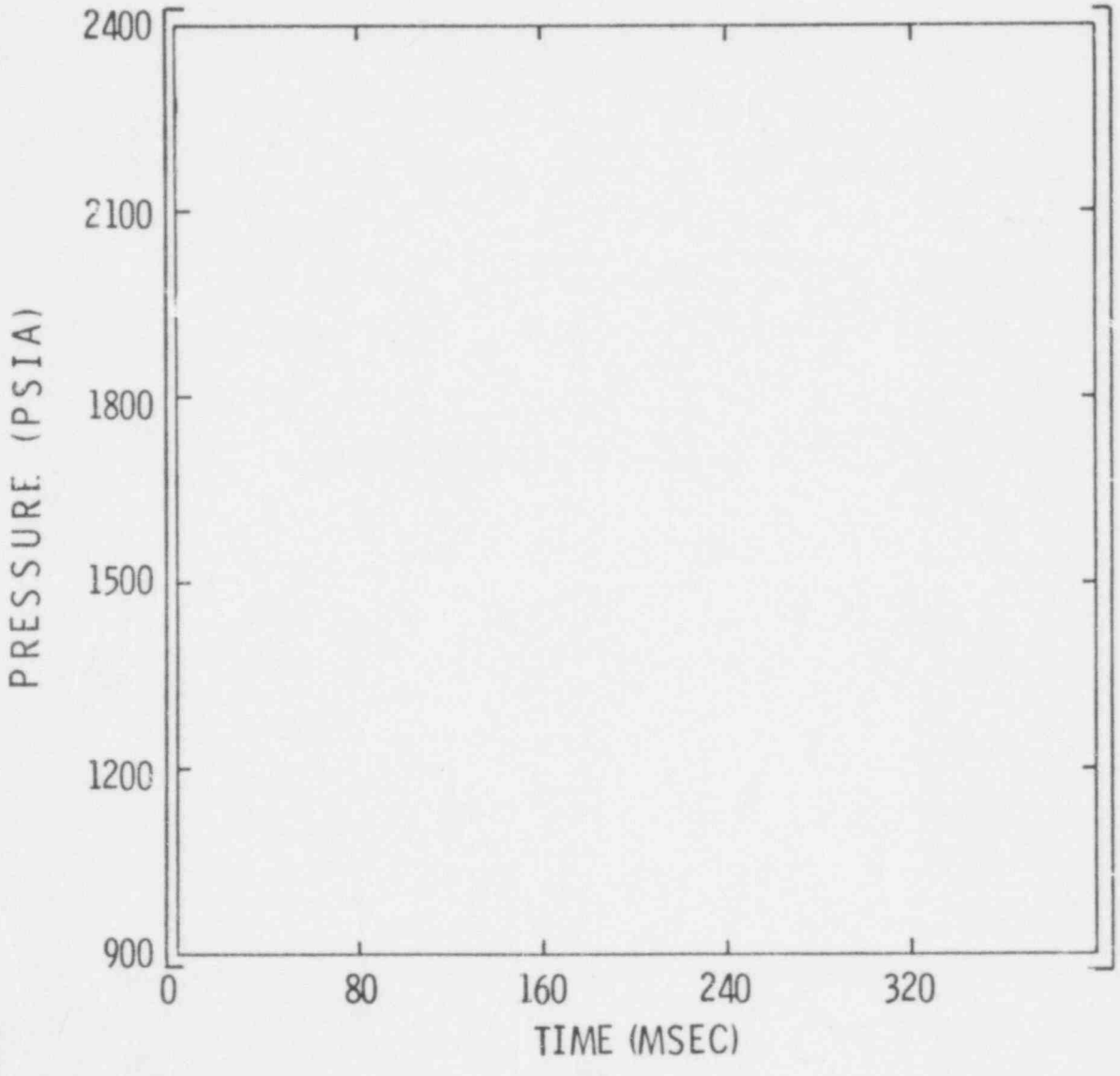

[3]

Figure D-7

LOFT CALCULATIONAL TIME STEP STUDY
DETAILED MODEL
(PRESSURE UPSTREAM OF COLD LEG BREAK
PLANE: NODE 24)

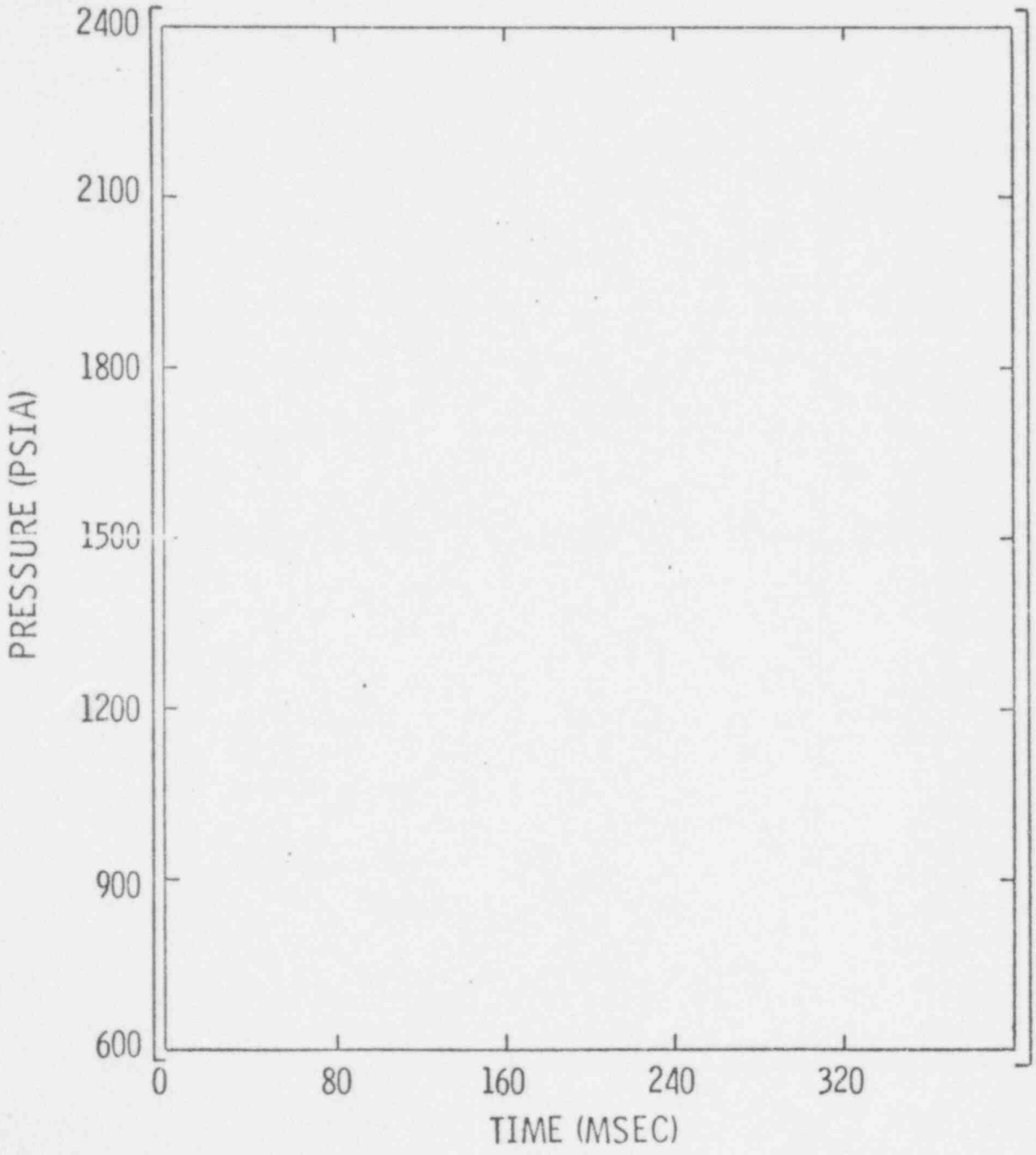

[3]

Figure D-8

LOFT CALCULATIONAL TIME STEP STUDY
DETAILED MODEL
(PRESSURE AT INLET PLENUM: NODE 10)

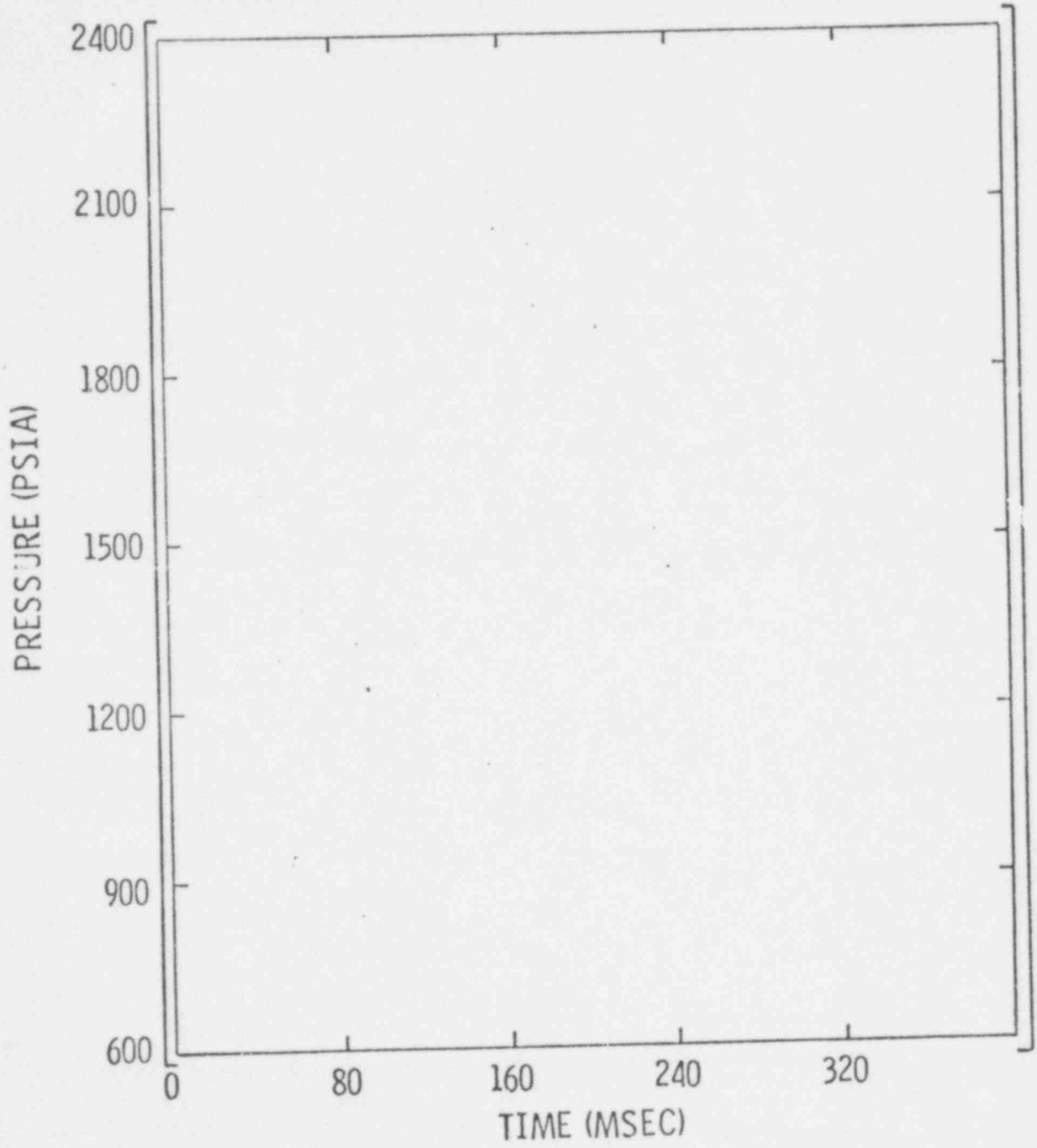

[3]

Figure D-9

INFLUENCE OF BREAK OPENING TIME ON CEFLASH-4B
LOFT MODEL PREDICTIONS
BREAK PLANE MODEL
(PRIMARY LOOP PIPING: NODE 21)

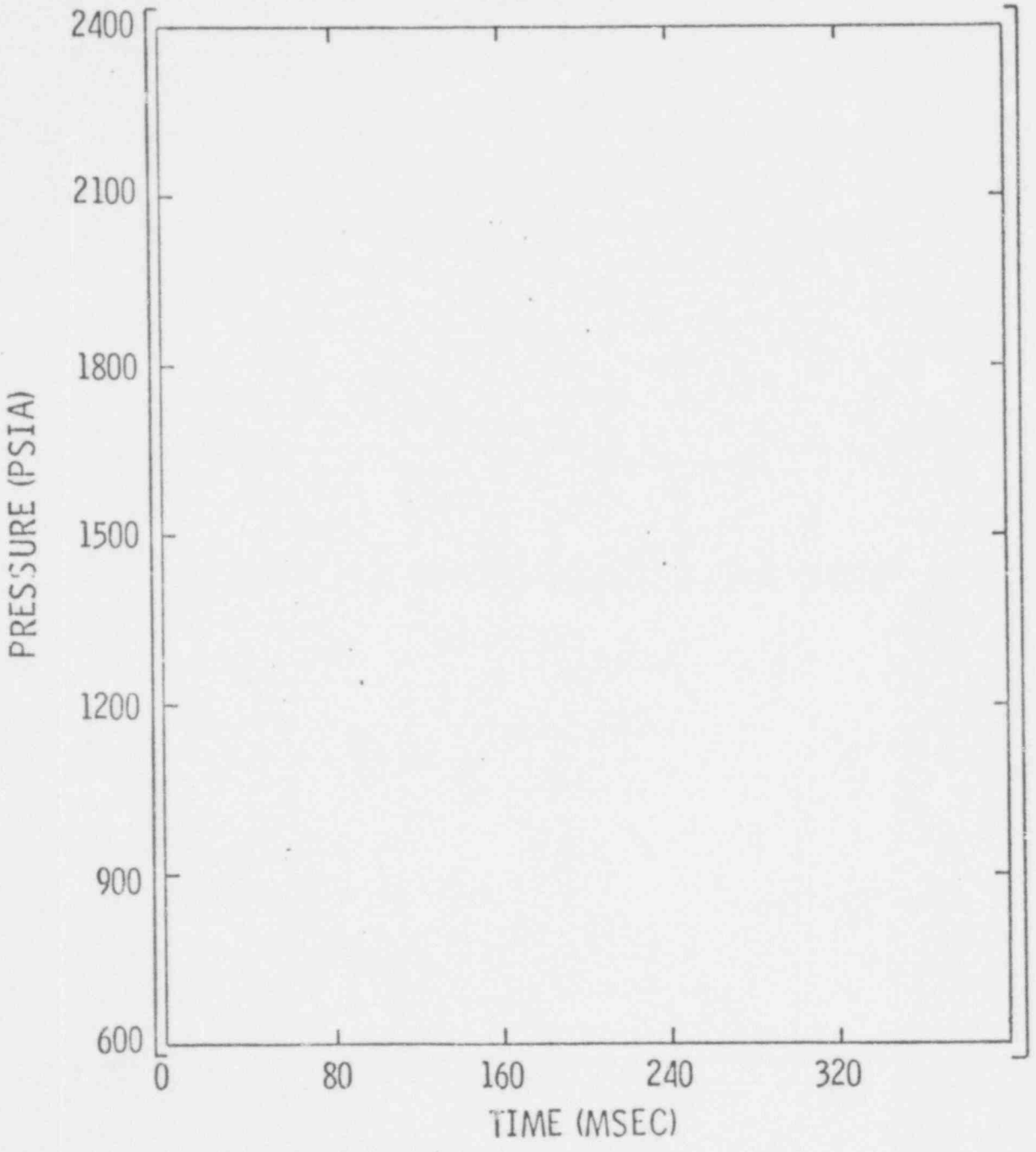

[3]

Figure D-10

INFLUENCE OF BREAK OPENING TIME ON CEFLASH-4B
LOFT MODEL PREDICTIONS
BREAK PLANE MODEL
(DOWNCOMER DISTRIBUTOR ANNULUS: NODE 53)

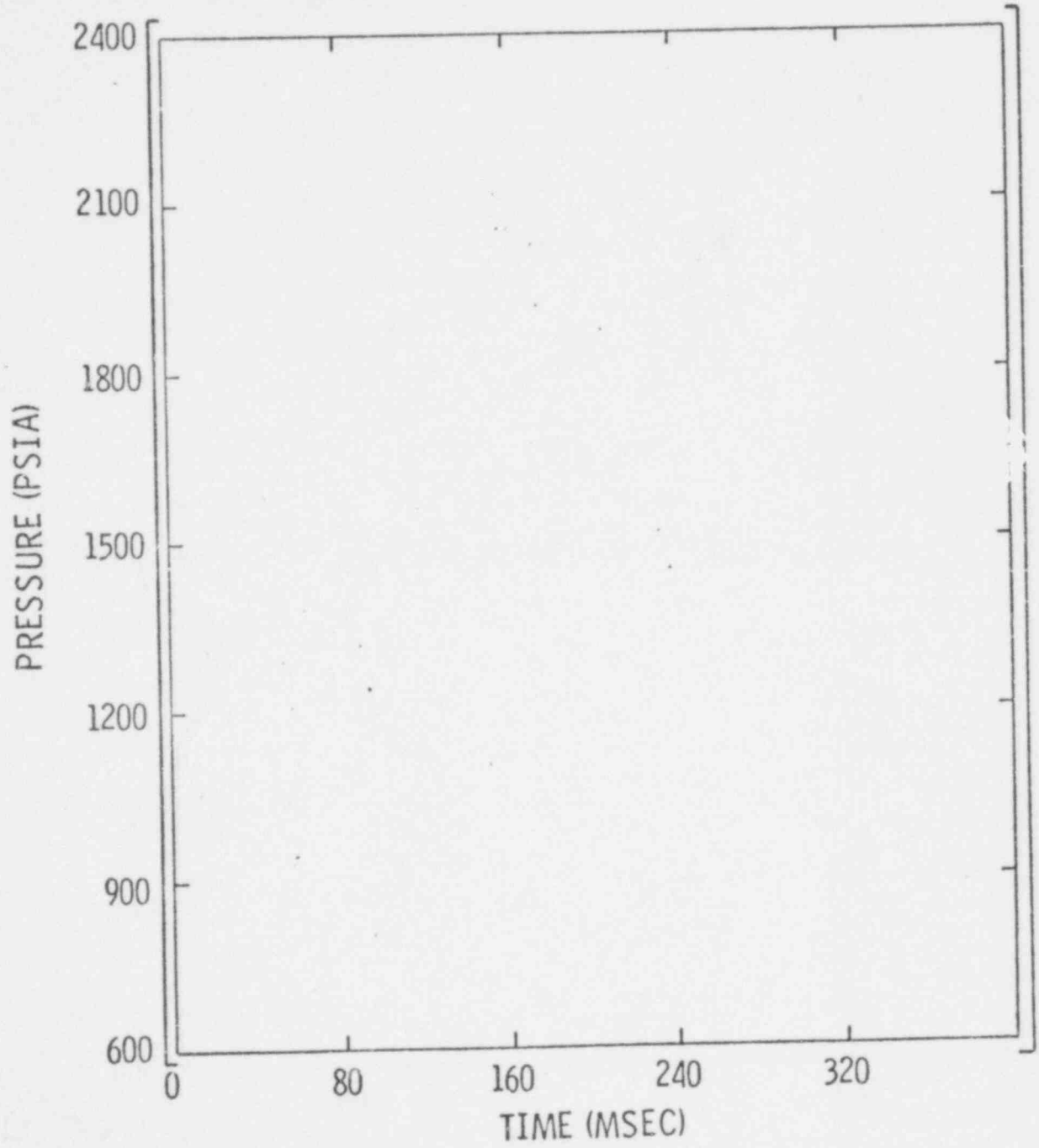

[3]

Figure D-11

INFLUENCE OF BREAK OPENING TIME ON CEFLASH-4B
LOFT MODEL PREDICTIONS
BREAK PLANE MODEL
(CORE SIMULATOR: NODE 6)

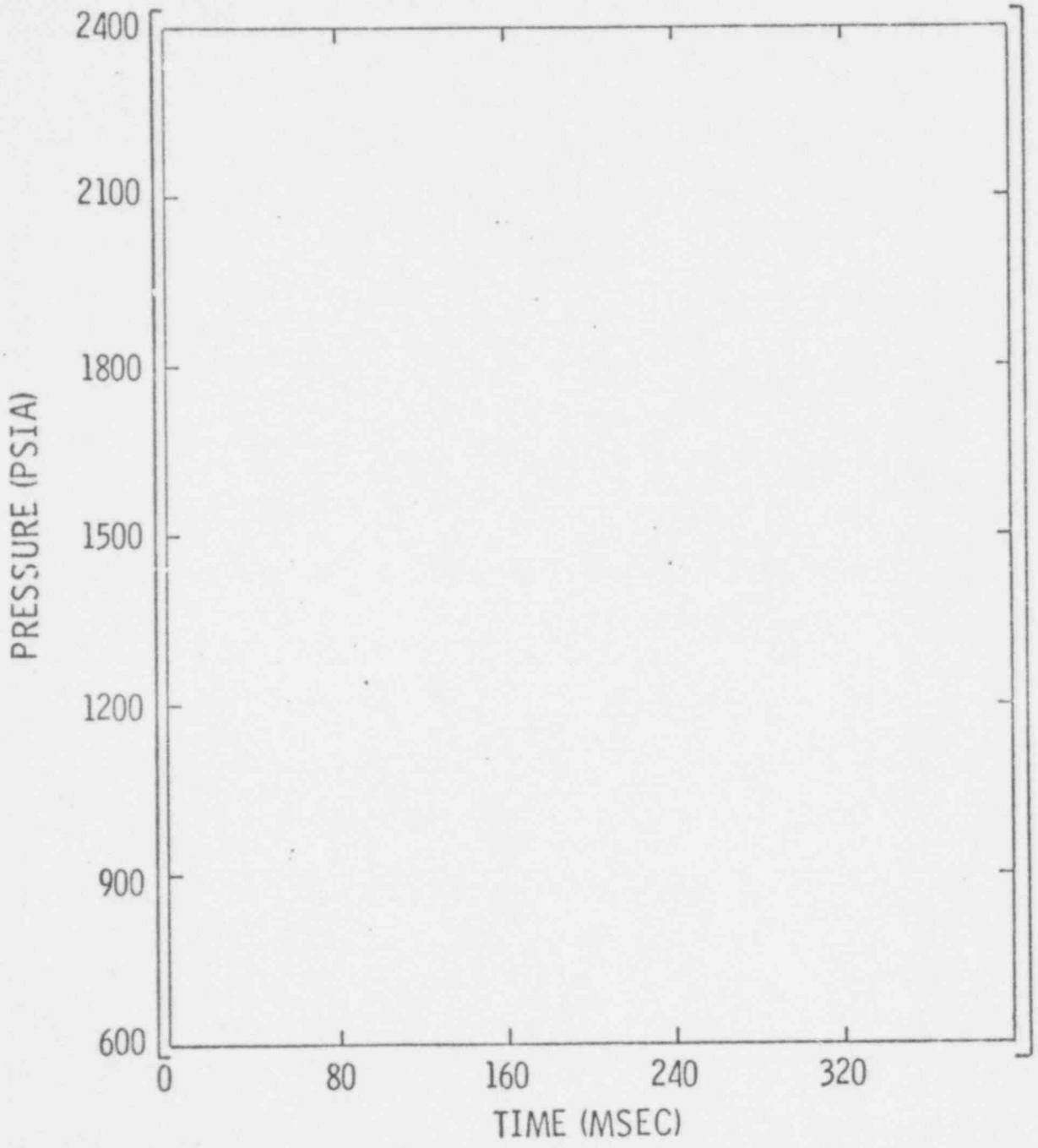

[3]

596 250

Figure D-12

INFLUENCE OF BREAK OPENING TIME ON CEFLASH-4B
LOFT MODEL PREDICTIONS
BREAK PLANE MODEL
(PRESSURE DROP AROUND CORE BARREL: P_{53}-P_{50})

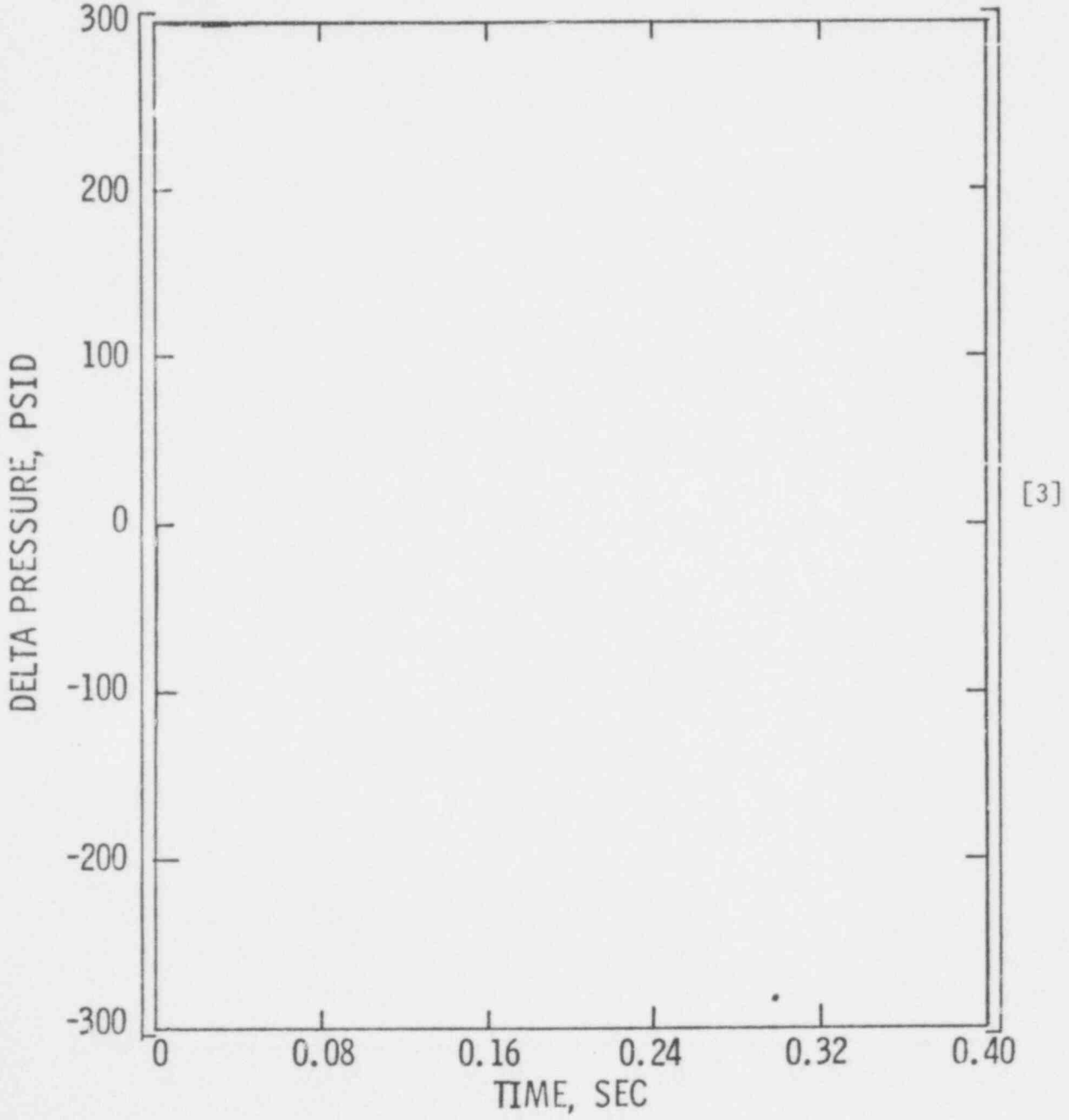

[3]

Figure D-13

INFLUENCE OF REFLOOD ASSIST BYPASS INERTIA
ON PREDICTED LOFT PRESSURE DECAY
BREAK PLANE MODEL
(DOWNCOMER PRESSURE: NODE 48)

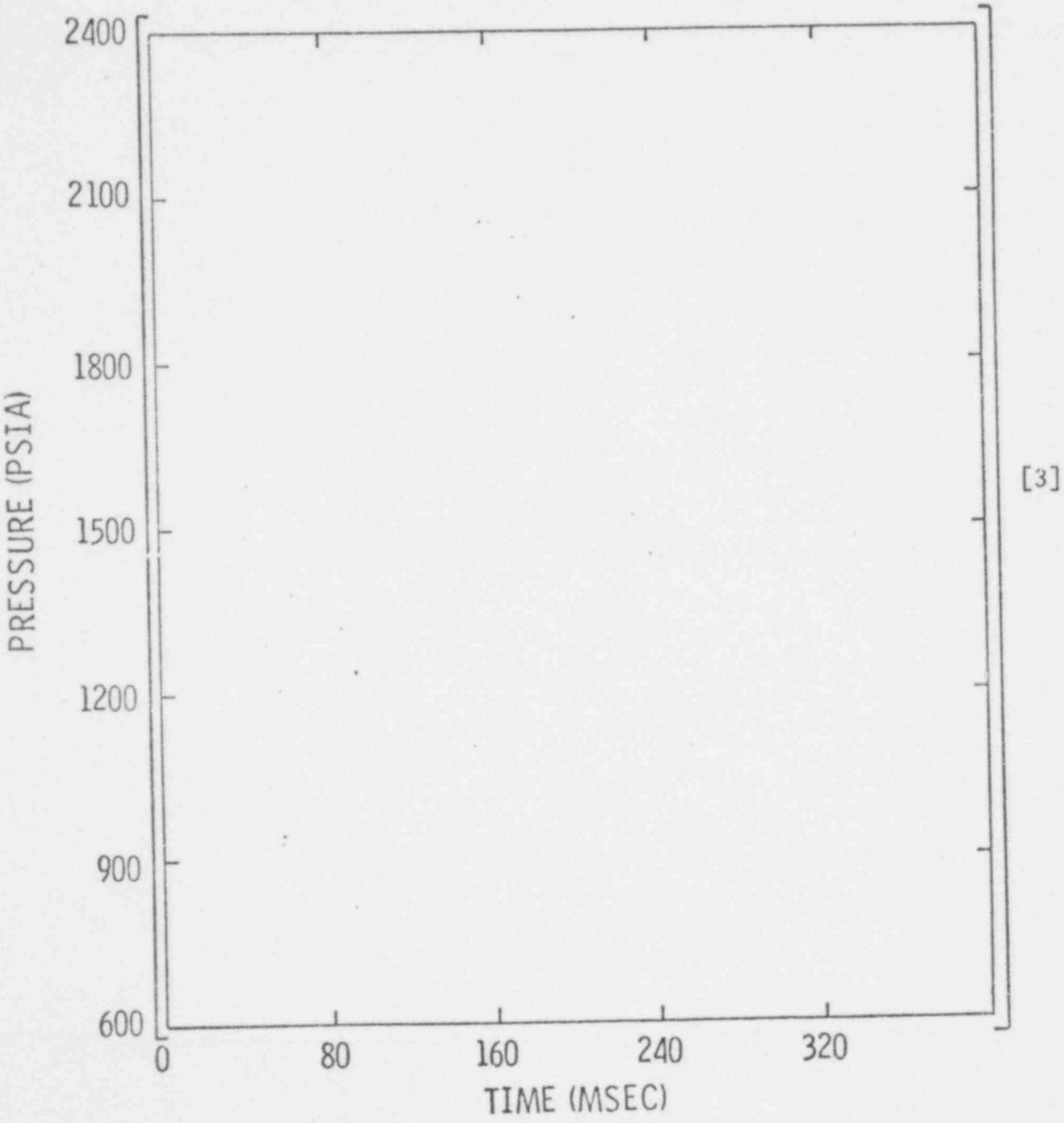

Figure D-14

INFLUENCE OF REFLOOD ASSIST BYPASS INERTIA
ON PREDICTED LOFT PRESSURE DECAY
BREAK PLANE MODEL
(DOWNCOMER PRESSURE: NODE 33)

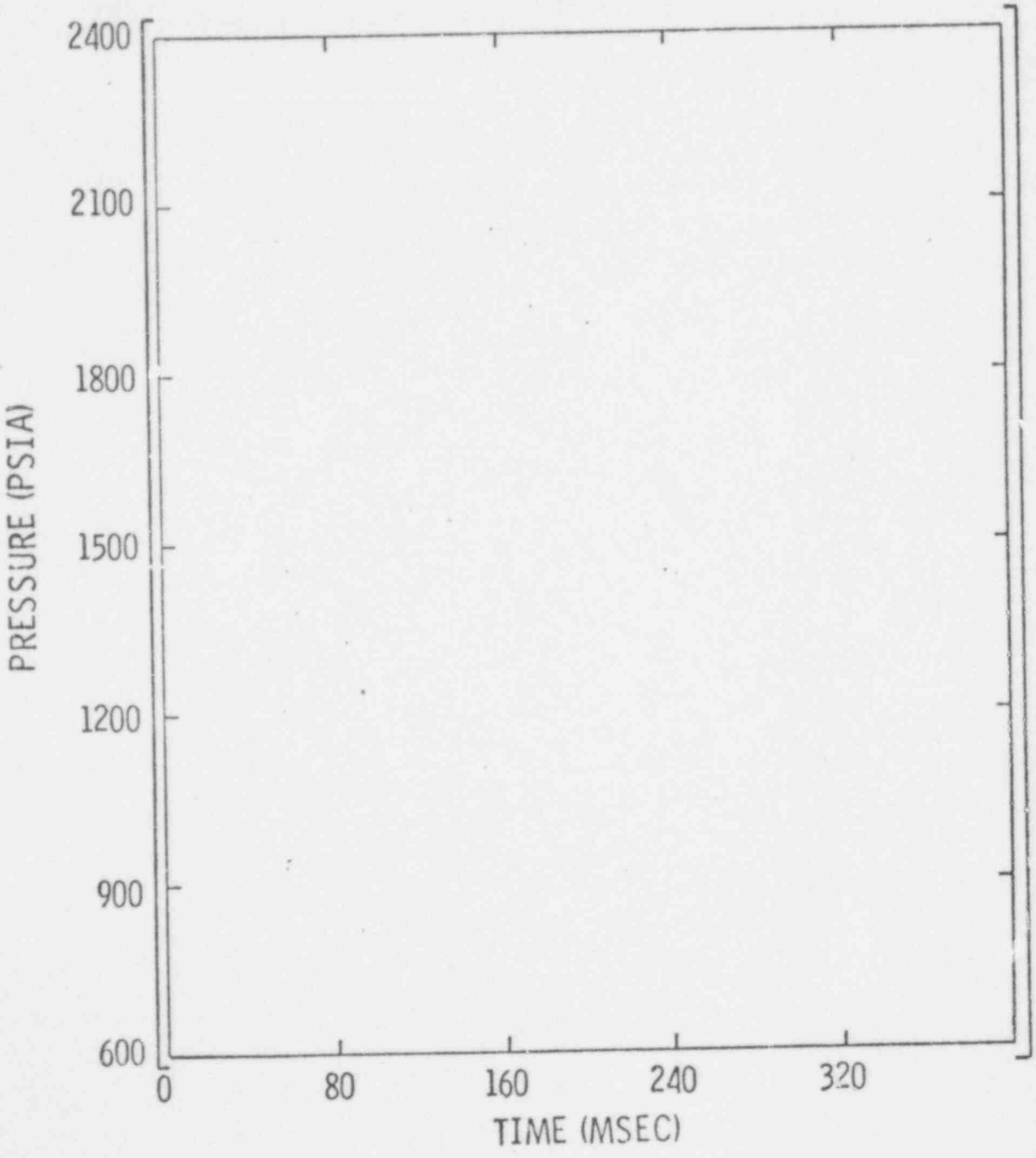

Figure D-15

COMPARISON OF CEFLASH-4B "BREAK PLANE"
AND DETAILED MODELS
(PIPING UPSTREAM OF COLD LEG BREAK: NODE 24)

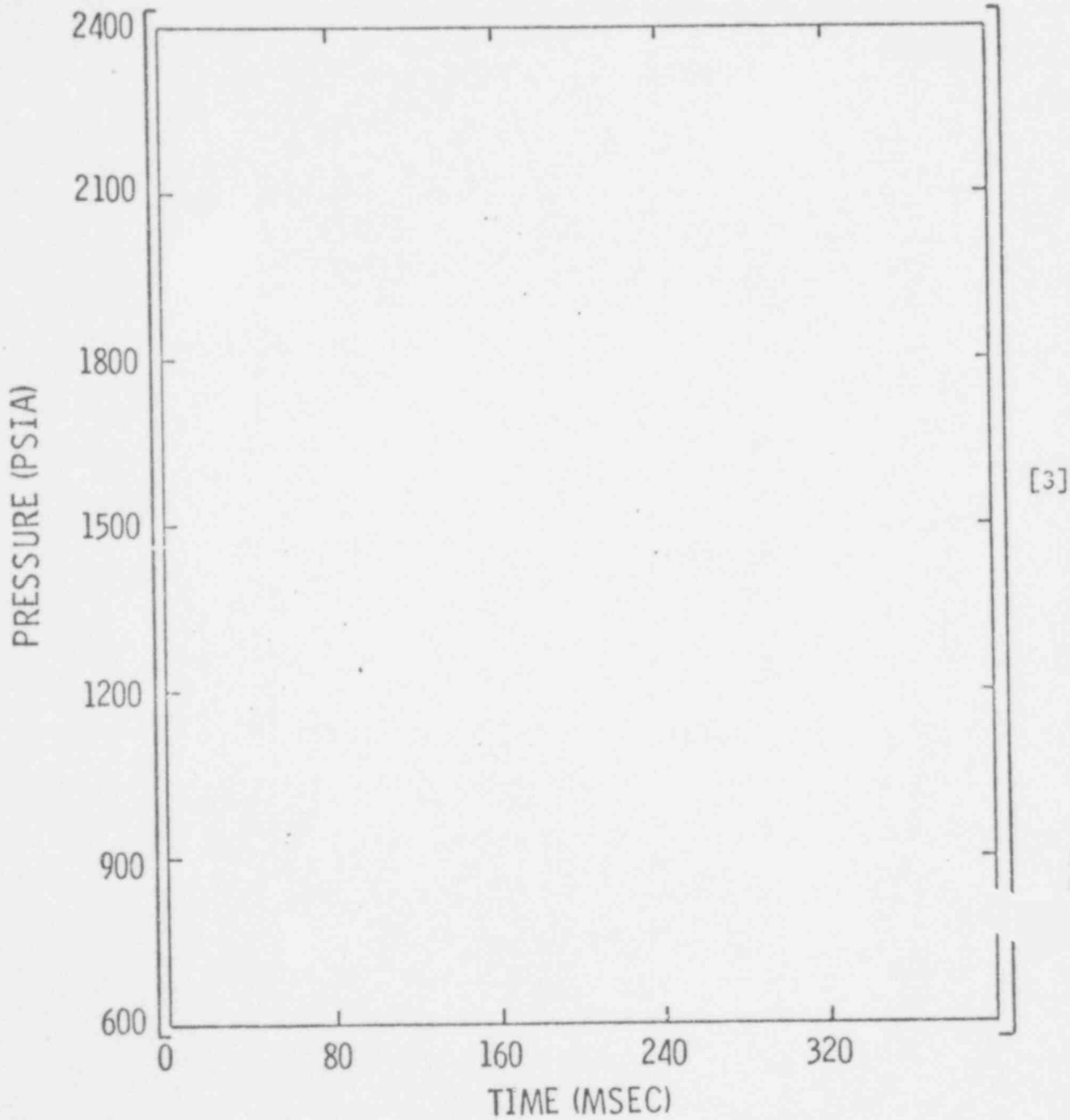

Figure D-16

COMPARISON OF PRESSURE PREDICTIONS
FOR "BREAK PLANE" AND "DETAILED" MODELS
(HOT LEG PIPING: NODE 30)

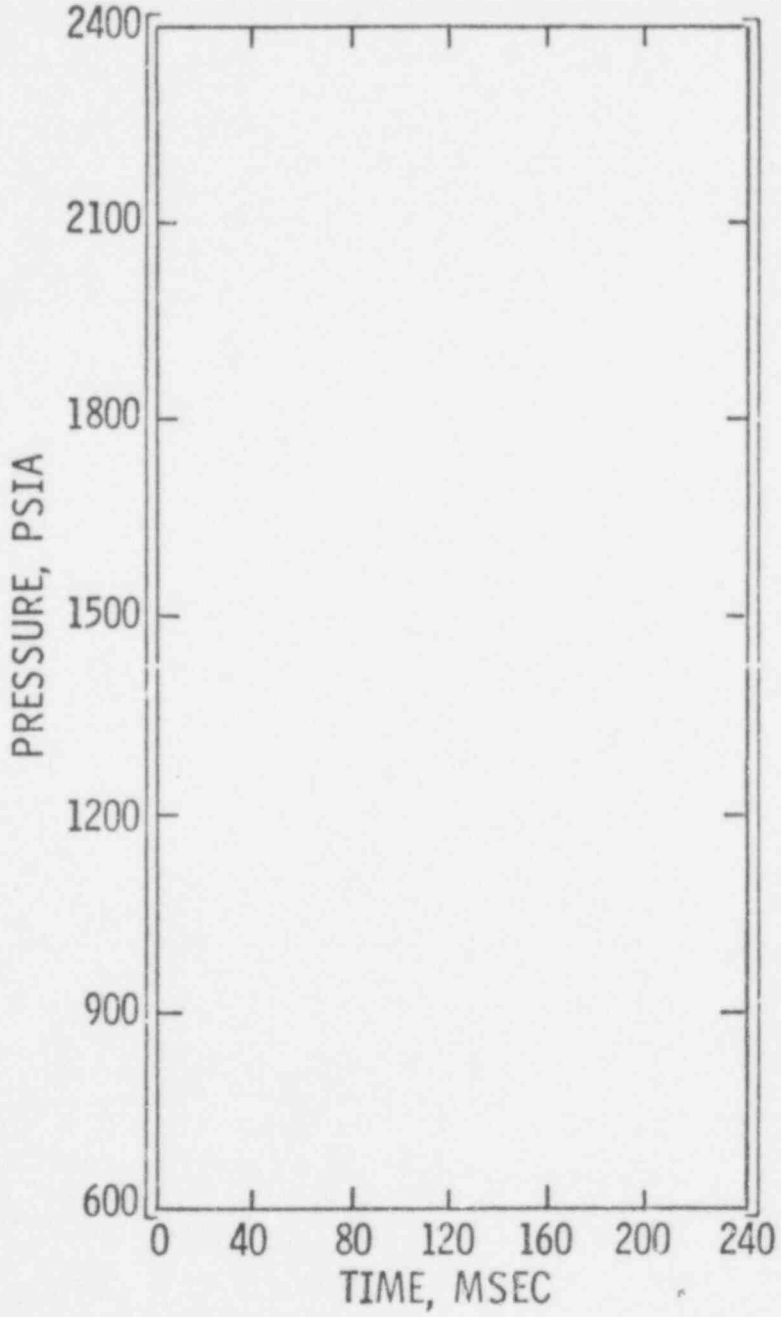

[3]

Figure D-17

COMPARISON OF PRESSURE PREDICTIONS
FOR "BREAK PLANE" AND "DETAILED" MODELS
(DOWNCOMER: NODE 35)

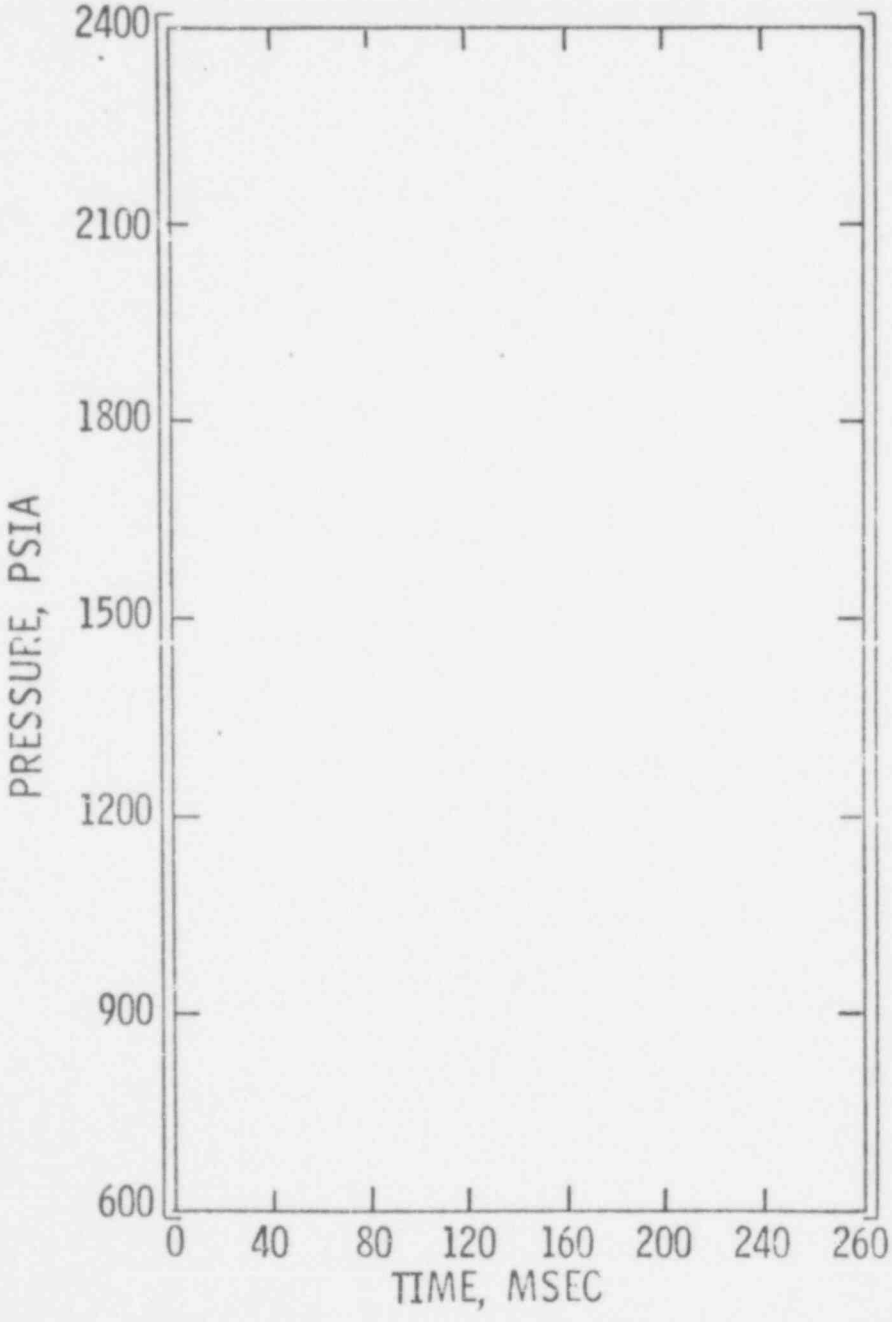

[3]

SUPPLEMENT 1

RESPONSES TO NRC QUESTIONS ON CENPD-252-P

RESPONSES TO NRC QUESTIONS ON CENPD-252-P

Table of Contents

.0 Introduction

This supplement provides responses to the Reference 1.0-1 NRC questions. This information is intended to supplement the text of the topical report. In preparing the NRC approved version of this supplement, the presentation has been ordered to be consistent with Reference 1.0-1 and as suggested by the NRC in Reference 1.0-2 computer listings requested in questions 2.4 and 2.5 have been omitted.

References for Section 1.0

1.0-1 Letter from K. Kniel to A. E. Scherer dated May 10, Subject: Request for Additional Information on CENPD-252-P.

1.0-2 Letter from R. L. Baer to A. E. Scherer dated Feb. 12, 1979, Subject: Staff Evaluation Report of Topical Report CENPD-252-P.

.0 RESPONSES TO NRC QUESTIONS

Question 1.1

he modeling of a PWR to obtain blowdown induced forces in a reactor vessel equires that the downcomer annulus be modeled in at least two dimensions o allow for the analysis of the hydraulic loads. The CEFLASH-4B computer rogram solves the one-dimensional form of the conservation equations. In he framework of these equations, a method is applied to a PWR region to odel the multi-dimensional geometry. Present a detailed description of this ethod and describe how volume, length and flow area are treated in the model evelopment.

esponse

ombustion Engineering, Inc., accounts for the presence of the blowdown loads through detailed two dimensional segmentation of the PWR downcomer annulus. In articular, the procedure subdivides the downcomer annulus into[ ] olume nodes[ ] reference .1-1). While at each elevation the nodes are equally spaced circumferentially, the xial node sizes are determined based on physical PWR boundaries. [

everal guidelines are followed for positioning flowpath junctions within odes. First of all, flowpath junctions are positioned at axial elevations orresponding to internal core barrel locations. This allows a meaningful alculation of core barrel radial pressure differences. All flowpaths within he same circumferential row are positioned at the same elevation. In addition, flowpath junction is specified at the core barrel upper and lower flanges.

596 260

This defines the flowpath junctions within the upper and lowermost control volumes. At the nozzle elevation, the flowpath junction is located at the nozzle centerline elevation. This procedure minimizes the flowpath length and resistance that the entering decompression wave must traverse before its influence is felt inside the annulus. Consequently, the depressurization of the downcomer node adjacent to the break is enhanced and the peak core barrel load is maximized. The remainder of the flowpath junctions are positioned towards the center of their respective nodes.

In developing fluid volumes for the above [ ] nodes, detailed reactor pressure vessel internal information is used to assure that only fluid mass is considered. For example, the volumes of the hot leg penetrations and metallic volume of snubber core stops, etc. are subtracted from the unobstructed downcomer fluid volume. Unobstructed volumes are treated by simply including all the fluid mass within the control volume node.

Flowpath parameters such as flow areas, momentum flux areas, and flowpath inertias are determined based solely on geometric considerations. Flow areas for circumferential flowpaths are determined by taking the flow area perpendicular to the flowpath. Axial downcomer flowpath flow areas are treated in an analogous manner. Flowpath inertias are then defined as the flowpath length (length from flowpath junction to flowpath junction) divided by the corresponding flowpath flow area. Momentum flux flow areas represents the local flow area at the particular flowpath junction. In general, for circumferential paths momentum flow upstream and downstream flow areas are the same. Momentum flux flow areas for axial paths will differ when the paths trasverse elevations where the annulus downcomer width changes.

The development of friction loss factors also are based on system geometry through representative flowpath length-to-hydraulic diameter ratios. Friction coefficients are calculated on a flow varying basis. All resistance factors used in these models are based on scale model flow test data or are derived from standard handbooks.

Reference

1.1-1 Combustion Engineering Inc., "Method for the Analysis of Blowdown Induced Forces in a Reactor Vessel", CENPD-252-P, Dec., 1977.

Question 1.2

The modeling of a PWR includes a number of transition regions where the geometry and multi-dimensional aspects may be important. Examples of these regions are (1) from the inlet nozzle to the downcomer annulus, (2) from the downcomer annulus to the vessel lower plenum, (3) from the lower plenum to the core region, (4) from the core region to the upper plenum (and upper head), and (5) from the upper plenum to the outlet nozzles. Describe the procedures used to model these regions and address the important geometric effects being considered. For example, in the lower plenum all the downcomer nodes connect to a single volume. It is therefore assumed, by the model, that no radial pressure difference exist across the lower core plate, when in fact such differences should exist for a cold leg break. This effect is therefore not considered. Provide the justification for ignoring this effect. Extend this to the upper plenum for a hot leg break.

Response

The procedure for modeling reactor transition regions is based upon the following rules:

1. Node boundaries are located at the positions of abrupt area change.
2. Nodal volumes are determined from the free fluid volume within the defined control region.
3. Node and flowpath elevation parameters are based on engineering drawings of the specific reactor system.
4. Flowpath inertia is determined from geometric lengths and areas obtained from engineering drawings and associated parameter lists. The relationship for evaluating the flowpath geometric inertia $\left(\frac{L}{A}\Big|_{FLOWPATH}\right)$ is as follows:

$$\frac{L}{A}\Big|_{FLOWPATH} = \sum_{i=1}^{N} \frac{L_i}{A_i}$$

where N is the number of area transitio s

A_i is the area of a given region i

L_i is the length of region i

5. Friction and geometric pressure losses across the transition region are input as component pressure drops obtained, primarily, from PWR scale model experiments (for the RPV) or other standard design methods for primary loop piping and fittings.

596 262

As can be seen from the above, it is sought to obtain a realistic description of these transition regions. Modeling relies on careful definition of system geometry and on the results of steady state hydraulic flow tests.

The use of these rules as they apply to the various transition regions (and non-transition regions as well) is generally straight forward. The following paragraphs present a brief description of the key modeling features of the transition regions.

(1) Inlet nozzle to the downcomer annulus

As the fluid enters the RPV downcomer from an inlet nozzle the flow changes direction and character from being predominantly one dimensional to two dimensional. To model this transition region, a nodal interface is selected at the intersection of the inlet nozzle and downcomer annulus. The total inlet nozzle is modeled as a single node. The connecting flowpath is along the nozzle centerline elevation. Geometric parameters such as lengths and flow areas are obtained from detailed engineering drawings. The flowpath geometric losses are distributed between the inlet flowpath and the flowpath connecting the annulus node at the nozzle elevation with the lower annulus nodes.

(2) The downcomer annulus to the vessel lower plenum

In the Combustion Engineering, Inc. Blowdown Loads Model, the [ ] lowest downcomer nodes are connected via [ ] corresponding flowpaths to a single node representing the upper portion of the lower plenum (upper lower plenum). For the C-E System 80 PWR design this node includes all the fluid between the instrumentation plate and the lower support structure bottom plate. The natural interface between the downcomer annulus and the lower plenum is the Core Support Barrel (CSB) flow skirt. In developing this system, momentum and inertia contributions to the various flowpaths are based on an equal division of the upper lower plenum node into [ ] "pie-like" segments. Each of the lower downcomer nodes is connected to the single inlet plenum node, assuming each path is influenced by its adjacent [ ] plenum segment. All flowpaths start in the annulus at the bottom of the CSB lower flange elevation a at the reactor vessel centerline.

In selecting a single node representation for the lower plenum region, the detailed propagation characteristics of incoming pressure waves across the plate radius cannc be ascertained. However, the physical consequences of this assumption are minimal. During a cold leg break decompression waves propagate from the broken nozzle around

he downcomer annulus. As these waves progress through the downcomer the wave front eakens and becomes approximately symmetrical with respect to the core support arrel. (For example, for a System 80 full offset shear inlet break the peak ifference between the absolute pressures at two annulus locations 180° apart at he bottom of the CSB (flow skirt region) occurs at ~10 msec. after rupture and is 00 psi. The difference is to be compared with a greater than 600 psi pressure ifference at the nozzle centerline elevation. Seventy milliseconds after blowdown his asymmetry reduces to under 20 psi.) Ultimately the symmetrical wave front passes hrough the flow skirt and into the lower plenum. The propagation of this wave along he radius of the lower core support structure is computed using a single node plenum odel. This procedure hypothesizes the lower core support structure (LCSS) to have a ingle flow hole at its center. That is, pressure waves must propagate to the center of he inlet plenum before they may proceed through the remainder of the reactor vessel. n reality substantial plate perforations and flow areas exist across the extent of the late outboard regions (especially for the lower core support structure). These holes llow numerous pathways for pressure waves to travel. Since the plat thickness (~4") is uch less than the radial flowpath length, local axial loads should in reality dissipate n less than 0.1 milliseconds. By using a single node lower plenum the current C-E rocedure does not account for this benefit in plate load reduction.

3) Lower plenum to the core region

he transition from the lower plenum to the core region is accomplished using an inter- ediate node to represent the fluid contained within the lower core support structure LCSS), between the inlet plenum and lower inactive core region. Node interfaces are onveniently identified at the bottom of the lower plate of the lower core support tructure and at the top of the upper plate of the LCSS for the lower plenum and lower nactive core respectively. Flow is assumed to be one dimensional in this region. eometric paramters such as lengths and flow areas are obtained from detailed engineering rawings and associated parameter lists.

4) Core region to upper plenum (and upper head)

he fuel alignment plate divides the core region from the upper plenum. This transition is odeled using two nodes. The lower node represents the top inactive core and the upper node imulates the RPV outlet plenum. The top inactive core node extends to the lower face of he fuel alignment plate. Pressure losses across the plate are based on flow test data.

he upper head region located above the UGS top plate is divided into three nodes.

. The lower portion of the upper guide structure plenum (this node extends from the bottom of the UGS top plate to the midplane of the UGS assembly).

596 264

b. The upper portion of the upper UGS plenum (this node extends from the midplane of the UGS assembly to the UGS flange elevation).

c. Top head (includes the RPV fluid volume above the UGS flange elevation).

The transition in the upper head occurs between the RPV outlet plenum and the lower portion of the upper guide structure plenum. These plena are separated by the UGS top plate. During a blowdown the predominant flow would be from the UGS upper plenum into the RPV outlet plenum. Pressure losses across the upper plate are based on flow test data. Geometrical factors necessary to describe this region are based on parameter lists and engineering drawings.

(5) Upper plenum to outlet nozzle

In the model the total upper guide structure (UGS) between the UGS plate and the fuel alignment plate (FAP) is modeled as a single node. It is in this region that the flow exiting from the core changes direction to flow out through the hot leg nozzles. The transition to the hot leg nozzles is modeled by having the plenum node boundaries terminate at its physical interface with the hot leg nozzle. The modeling of the hot leg nozzle is dependent upon the type of break under consideration. For hot leg break transients both hot leg nozzles are treated as individual nodes with flowpath junctions ending at the nozzle terminus. In modeling cold leg breaks, the hot leg nozzle volumes are lumped into the hot leg piping nodes. In both cases, the pressure losses resulting from the flow turning, CEA shroud crossflow and plenum-nozzle area change were established from scale model flow test data.

It has been noted that the upper plenum adjacent to the hot leg nozzles has been modeled as a single node. In the CEFLASH-4B model during a hot leg break any fluid traversing the plate must proceed in a radial direction from the RPV center line to the break location before any axial wave transmission across the plate occurs. In actuality, outboard plate holes in both the upper guide structure (UGS) and fuel alignment plates provide wave pathways distributed along the plate radius through which an incoming rarefaction wave may dissipate. As was demonstrated in part (2) of this response, by preventing axial wave transport until the wave reaches the node center, the net load on the plate will tend to be artifically increased. An analogous argument holds true for FAP and UGS top plates loads during a cold leg break.

The basic modeling procedures and guidelines presented in this analysis are general. In certain instances where specific information is given, this data is utilized. As a result of differences in geometry and/or design between various PWR's, blowdown loads modeling may have small variations in node and flowpath definitions.

Question 1.3

The CEFLASH-4B computer code does not account for non-equilibrium affects, except empirically at the break location. The affects of non-equilibrium would be a reduction in the local pressure below saturation. This would result in a larger pressure difference than is currently assumed. Accordingly, provide justification for not considering non-equilibrium affects in the primary coolant system. This argument is to be extended beyond comparisons with experimental data and should include discussions of break open time, fluid conditions and nucleation, and any other system parameters which may affect the blowdown analysis.

Response

Appendix B of the topical report presents a discussion based on experimental observations that demonstrates non-equilibrium behavior (in particular, the "pressure undershoot" phenomenon) will not occur in a PWR. This was accomplished by reviewing results of large and small scale blowdown tests. Test depressurization rates were evaluated and related to their respective non-equilibrium contribution to the blowdown pressure transient. Larger test facilities exhibited decompression rates similar to those expected for PWRs, with no non-equilibrium behavior (except in the immediate vicinity of the broken nozzle). Based on these results it was concluded in Appendix B that the peak CEFLASH-4B predicted downcomer decompression rate (for LOCA's including a double ended guillotine break) will not be sufficient to cause non-equilibrium behavior.

In order to establish the above conclusion it was necessary to relate the predicted CEFLASH-4B depressurization rates with experimental data. The fact that the analytical-experimental results can be related in this manner may be seen from analytical comparisons for both large and small scale blowdown experiments. Typical CEFLASH-4B test comparisons with a large scale blowdown test (LOFT test L1-2) are presented in Section 3.0 of the topical report. An analytical comparison to the small scale "Edward's Pipe" experiment (NRC standard problem #1) is presented in reference 1.3-1. This later comparison was performed with CEFLASH-4, a less extensive version of the CEFLASH-4B code. Both comparisons demonstrated the CEFLASH-4 type codes can provide good predictions of the subcooled decompression and depressurization rates.

Additional Considerations

To further illustrate that non-equilibrium affects are negligible, it is useful to compare analytical predictions of a hypothetical non-equilibrium imparted impulse to the initial lateral (equilibrium) impulse imparted to the Core Support Barrel (CSB) at the nozzle centerline elevation. The nozzle elevation is selected for comparison, since non-equilibrium effects will be greatest at that location.

Based on a two dimensional analytical study performed by Los Alamos (references 1.3-2, 1.3-3) and funded by the NRC, it was demonstrated that, during a large cold leg break, the non-equilibrium pressure pulse transmitted to the downcomer annulus will be small. To estimate this effect, Los Alamos used the SOLA-DF computer code modified to account for non-equilibrium bubble nucleation. (A description of their non-equilibrium flashing model is presented in Reference 1.3-2) The Los Alamos analysis employed a geometry similar to that of the NRC sample blowdown problem 2.3 (reference 1.3-4), with a total double-ended break area of 9 ft^2. (This break area is ~4 times greater than the maximum CE mechanistic break leak area). It was further assumed that the break occurs instantaneously. Similarly sized breaks for CE plants would take ~18 milliseconds to develop. The System 80 mechanistic break of 350 in^2 (2.43 ft^2) requires five (5) milliseconds to fully open.

Using the above model, Los Alamos predicted the maximum peak non-equilibrium pressure undershoot transmitted to the downcomer fluid in the vicinity of the CSB to be ~160 psi. The duration of the predicted undershoot was <1 msec. To estimate the significance of the transmitted pressure pulse it is possible to compare the total impulse associated with the non-equilibrium undershoot to the total (equilibrium) impulse imparted to the CSB at the nozzle centerline elevation. To maximize the predicted non-equilibrium impulse for the present investigation (and simplify the analysis) it was assumed that the pulse is triangular and the pulse duration is equal to 1 msec. The local projected area of the CSB was taken to be the projected area of the CEFLASH-4B nozzle elevation downcomer node [ ] (see section 4.4.2 of Reference 1.3-5).

The resulting non-equilibrium impulse becomes 326 lb_f-sec. The initial impulse imparted to the core barrel at the nozzle elevation for a typical mechanistic break LOCA is, from Table 4-7 of the topical report (break node study), 4.0907×10^4 lb_f-sec. Comparing these impulses on a local basis, the predicted non-equilibrium impulse will contribute less than 0.8% of the initial CSB impulse at the nozzle centerline elevation. This ratio will further reduce if the comparison were to be made for the same break area transient. As pointed out earlier, the Los Alamos study assumes an instantaneous 9 ft^2 break while the reference PWR used in this study was exposed to a break of only 2.43 ft^2 occurring over 5 milliseconds. The above comparison has been made on a local core barrel basis. Non-equilibrium effects are highly localized and therefore will not significantly propagate through the downcomer, Thus, their relative contribution to the total CSB load is expected to be negligible.

Based on the preceding discussions presented here and additional information presented in Appendix B of the topical report it is seen that non-equilibrium behavior is not expected to occur in the unlikely event of a PWR LOCA. Therefore, it is concluded that in light of the inherent conservatisms in the CE methodology (see Question 1.4), the neglect of non-equilibrium behavior will not affect the ability of Combustion Engineering, Inc., to conservatively calculate the loads impinging on various reactor component structures.

References for Question 1.3

1.3-1 CENPD-103, "Standard Problem Analysis:. Problem No. 1-Blowdown of a Straight Pipe Filled with Pressurized Water", Combustion Engineering, Inc., May, 1973.

1.3-2 LA-NUREG-6842-PR, "Nuclear Reactor Safety Quarterly Progress Report: January 1-March 31, 1977, J. F. Jackson, June 1977.

1.3-3 NRC Staff, "NRC MULTIFLEX Review", (Presentation made by the NRC Staff to ACRS), May 25, 1977, Los Angeles.

1.3-4 K. Kniel (Chief Light Water Reactors Branch No. 2) letter to A. E. Scherer (CE), Request for Additional Information on CENPD-252-P, May, 1978.

1.3-5 Combustion Engineering, Inc., "Method for the Analysis of Blowdown Induced Forces in a Reactor Vessel", CENPD-252-P, Dec., 1977.

596 270

Question 1.4

Provide a qualitative assessment of the amount of conservativeness in the PWR licensing calculation. Address the uncertainties of the input data and assumptions used to perform the analyses. Describe how uncertainties affect the overall assessment of the structural integrity of the various PWR components.

Response

There are several assumptions in the Combustion Engineering, Inc., methodology which contribute to the overall conservative prediction of blowdown loads. These assumptions are:

1. all PWR walls and plates are rigid
2. the break flow acceleration is instantaneous
3. the break flow area is developed following the instantaneous formation of a through-wall crack (Reference 1.4-3).

The current procedure is to assume all fluid boundaries are rigid and at rest. Thus, fluid-structure interaction phenomena are not included in the CEFLASH-4B analysis of the subcooled blowdown. This assumption results in a substantial overestimate of the expected component pressure differences. Typical calculations of this effect have been documented (Reference 1.4-1, 1.4-2). Reference 1.4-1 demonstrated that by including the fluid-structure interaction of the core support barrel (CSB) and annulus downcomer fluid the horizontal blowdown loads across the CSB would reduce by ~30%. Similar load reductions (~20%) were obtained by KWU using the KRAFT code with a simple PWR structural representation (Reference 1.4-2).

Another conservatism associated with the break model is that CEFLASH-4B assumes that the discharge flow out through the breach is instantaneously at its critical limit. In actuality, the fluid in the pipe possesses a finite inertia and must accelerate from its initial (pre-rupture) flow rate to the choke plane mass efflux rate. This unrealistic treatment increases the early system mass outflow and decompression which, in turn, artifically increases the loadings across various internal structures. This effect is not expected to be large.

596 271

The break flow area used in the blowdown loads analysis is determined as outlined in Reference 1.4-3. In these studies CE conservatively postulates the nozzle break to arise as a consequence of the instantaneous formation of a through-wall crack around the pipe circumference. (For details regarding these treatment the reader is referred to Reference 1.4-3.) In postulating the nozzle to rupture in this manner, break areas in excess of that physically possible are computed. The use of this larger break area results in a calculated break mass outflow of greater magnitude than could occur. As a consequence of this increased system mass outflow the system pressure falls more rapidly, resulting in an overestimate of various component loadings.

The input data used to perform a blowdown loads analysis includes system geometry (flow areas, lengths, volumes, etc.), pressure loss factors, and initial operating conditions. In blowdown loads analyses the above parameters are selected based on their nominal values. For application to blowdown loads the parameters most significantly affecting the calculated loads are the system's dimensions. These parameters are well defined and are used to determine the system inertias, fluid volumes, flowpath lengths and flow areas. Uncertainties associated with geometric input arises primarily from specified tolerances which are typically small (for example in manufacturing a CE core barrel the tolerance on the diameter is <.4% of specification). Resistance factor uncertainties are greater than those associated with geometric parameters. However, wave transport during the early blowdown period is primarily influenced by the fluid inertia (strongly dependent on system geometry) with the K factors providing a small contribution to the overall decompression. The most significant initial condition input parameter is the system pressure. The system pressure is closely controlled by the pressurizer and it variation is distributed uniformly throughout the system. This variation has a negli effect on the evaluation of fluid properties.

The overall result of the Combustion Engineering, Inc., treatment is to predict LOCA induced blowdown loads of greater magnitude than would be expected on a physical basis. Therefore, the blowdown loads methodology presented in the text of the topical report is conservative for application to reactor structural analyses. However, it should be noted that the conservatisms in the blowdown loads calculation do not necessarily translate into equivalent conservatism for the structural response analyses which employ reactor vessel blowdown pressure differences as only a portion of their input.

ased on the above discussion of the various assumptions and conservatisms, t is our judgement that the predicted pressure loads are approximately 50% igher than expected in reality. The overall assessment of the structural ntegrity for the combined effects of blowdown loads and other forcing functions caused by the postulated pipe break is beyond the scope of topical report CENPD-252-P which is under the subject review.

References

1.4-1 Stolz, J. F., Chief Light Water Reactors Branch No. 1, Division of Project Management, Letter to C. Eicheldinger (W), "Evaluation of Westinghouse Topical Reports" WCAP-8708(P) and WCAP 8709(NP), June 17, 1977.

1.4-2 Watzinger, J., Gruber, P., Winkler, F., "Prediction of Forces on Pressurized Water Reactor Vessel Internals Following a Loss of Coolant Accident", presented at CREST Meeting, Munich, October, 1972.

1.4-3 CENPD-168-A, Design Basis Pipe Breaks for the Combustion Engineering Two Loop Coolant System", Plant Engineering, September, 1976.

596 273

uestion 2.1 (Problem No. 1)

two-dimensional sheet of water (see Figure 2.1-1), of unit thickness, is at pressure of 2100 psia and a temperature of 544°F. The fluid is at rest everywhere. A small region, of radius equal to 0.5 ft. is suddenly relieved to a pressure of 1700 psia, at time equals zero, and held constant at 1700 psia. Provide plots of pressure and fluid velocity along the 0°, 45°, and 90° references as a function of distance, for at least 5 feet from the center of the relived region at times equal to 0.25, 0.50, 0.75, 1.00 and 1.25 milliseconds.

Response

ANALYTICAL MODEL

The above system geometry describes a 10 ft. x 10 ft. quadrant of a pressurized sheet of water (Figure 2.1-1) of unit thickness which is relieved to a lower pressure through a small circular opening (diameter= 1.0 ft.) located at the center of the region. A review of the problem has revealed that a subcooled decompression wave (based on isentropic saturation conditions) would travel less than 5.0 ft. in the desired 1.25 millisecond time frame. Hence, it is not necessary to represent the entire region as shown on Figure 2.1-1 For the present analysis, a 7.0 ft region (measured from the origin) was modeled. This provides an additional point for pressure prediction beyond the wave front which confirms that the CEFLASH-4B computer code does not predict a decompression beyond 5.0 ft. In order to obtain pressure and flow rate data along the 0° and 90° axes as stated in the problem, nodes must be located along these axes. For this problem, it was deemed advantageous to use all nodes of equal size, if possible. This requirement, coupled with node center to center flow path connections results in those nodes along the axes having equal volumes on either side of the 0° or 90° lines. This increased the total system volume

596 274

beyond that specified in the problem. This difficulty was resolved by representing a full four quadrant system even though a symmetric solution is expected.

The region shown in Figure 2.1-1 was modeled as a flat sheet of water of unit (1 ft.) thickness using a 7 x 7 nodal grid. The assumption of modeling the region as a flate plate eliminates the consideration of elevation differences between nodes. The CEFLASH-4B network diagram of this system is presented in Figure 2.2-2. Each node (control volume) has dimensions of 2 ft. x 2 ft. x 1 ft. thick. The flow paths connect node centers to node centers with lengths of 2 ft. and an associated L/A of 1.0 $ft.^{-1}$ with the exception of flow paths 1, 4, 7 and 52. These paths connect the central "leak" node (node 1) to the rest of the region. Paths 1, 4, 7 and 52 have a length of 1.5 ft. which reflects the transport distance from the outer boundary of the relieved area to the connecting node center. The paths have an associated L/A of 0.75 $ft.^{-1}$ The central node is connected to an arbitrarily large (20,000 $ft.^3$) containment volume (node 50) through a 0.7854 $ft.^2$ (1 ft. diameter circle) flow area. Nodes 1 and 50 are assumed to be at 1700 psia at time zero. Nodes 2-49 are initially at 2100 psia. The pressure in node 1 cannot be maintained at 1700 psia over all time periods, as requested, since there is more mass inflow into the node than outflow for a short period of time. However, by assuming virtually instantaneous communication (L/A= 10^{-6} $ft.^{-1}$) between the "leak node" (node 1) and the containment node (node 50) the pressure in node 1 will increase to 1732 psia (0.25 msec) and decline slowly (1727 psia at 1.25 msec) over the remaining duration of the transient.

A listing of the CEFLASH-4B input as outlined above is provided in Table 2.1-1.

RESULTS

Results of pressure and flow rate versus distance at times of 0.25, 0.50, 0.75, 1.00 and 1.25 milliseconds are given on Figures 2.1-3 through 2.1-7. Each of these figures illustrate the instantaneous pressure and flow fields along the extent of the reference lines (0°, 45° and 90°). It is seen from these figures that the disturbance propagates in a symmetric radial fashion from the decompressed control node.

596

Figure 2.1-1

LAYOUT OF PROBLEM 2.1

SYMMETRIC PLANAR DECOMPRESSION

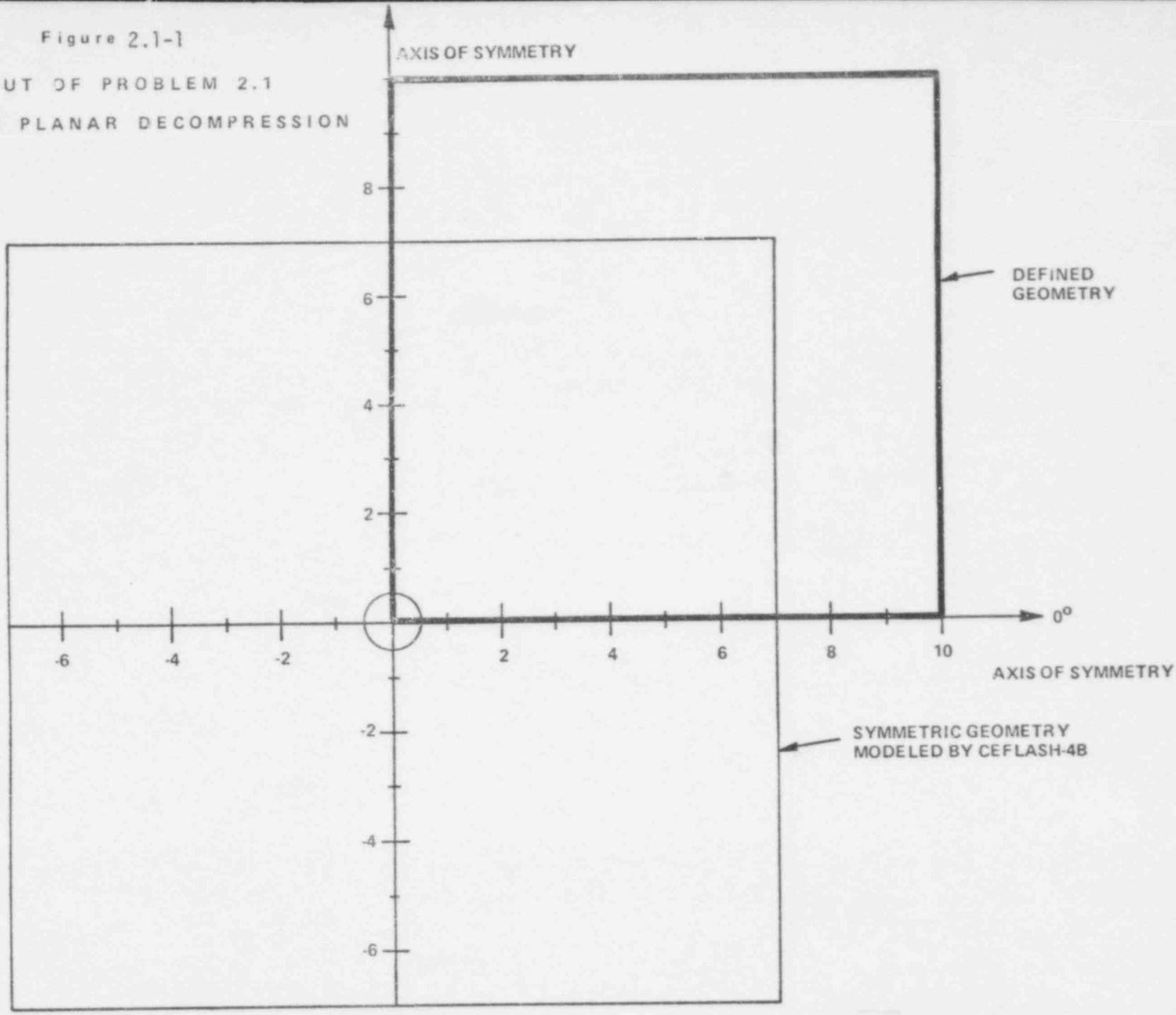

Figure 2.1-2

CEFLASH-4B MODEL FOR PLANAR DECOMPRESSION

PROBLEM 2.1

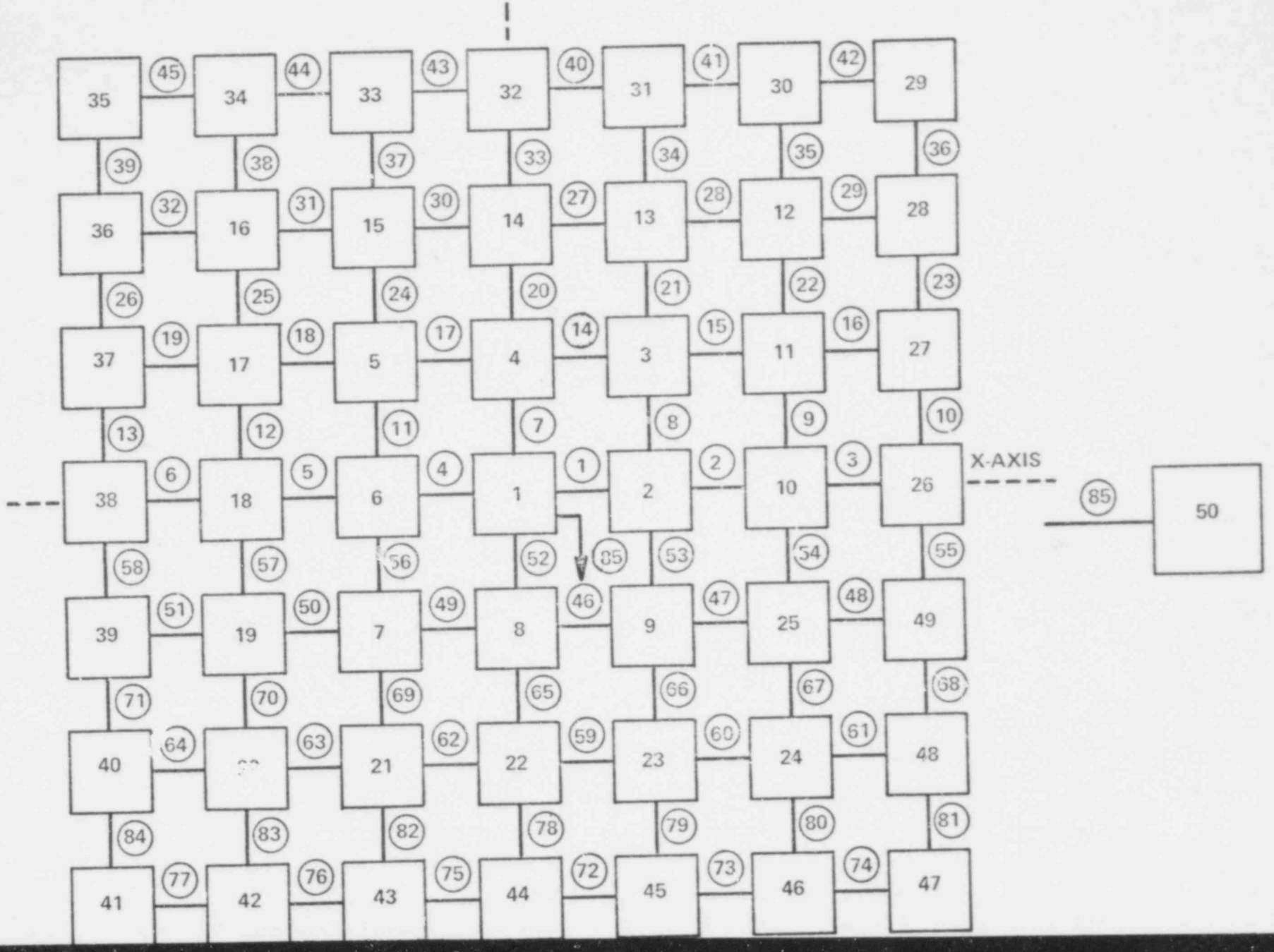

FIGURE 2.1-3
RESULTS OF SYMMETRIC PLANAR DECOMPRESSION AT 0.25 MSEC.

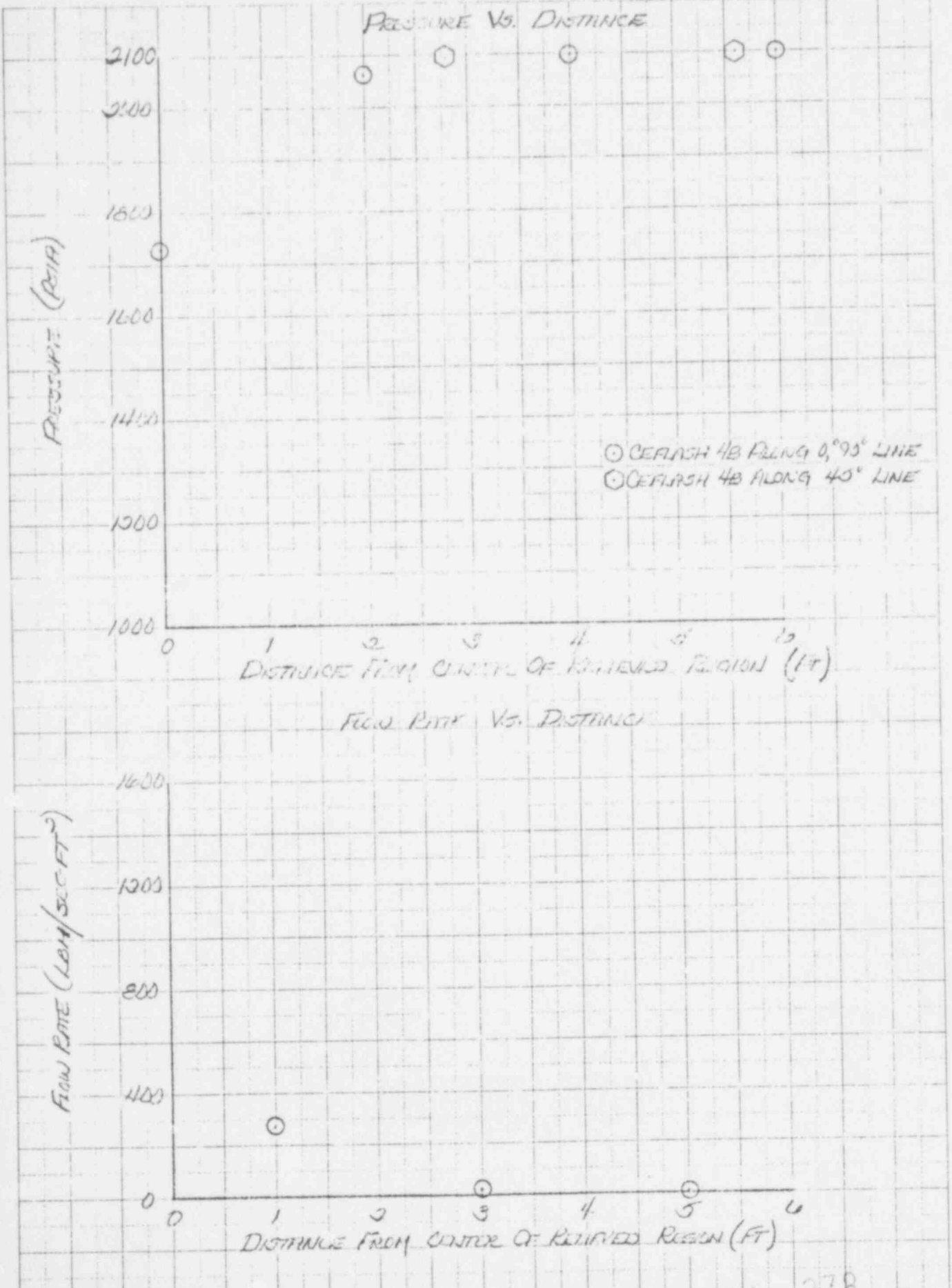

FIGURE 2.1-4
RESULTS OF SYMMETRIC PLANAR DECOMPRESSION AT 0.50 MSEC.

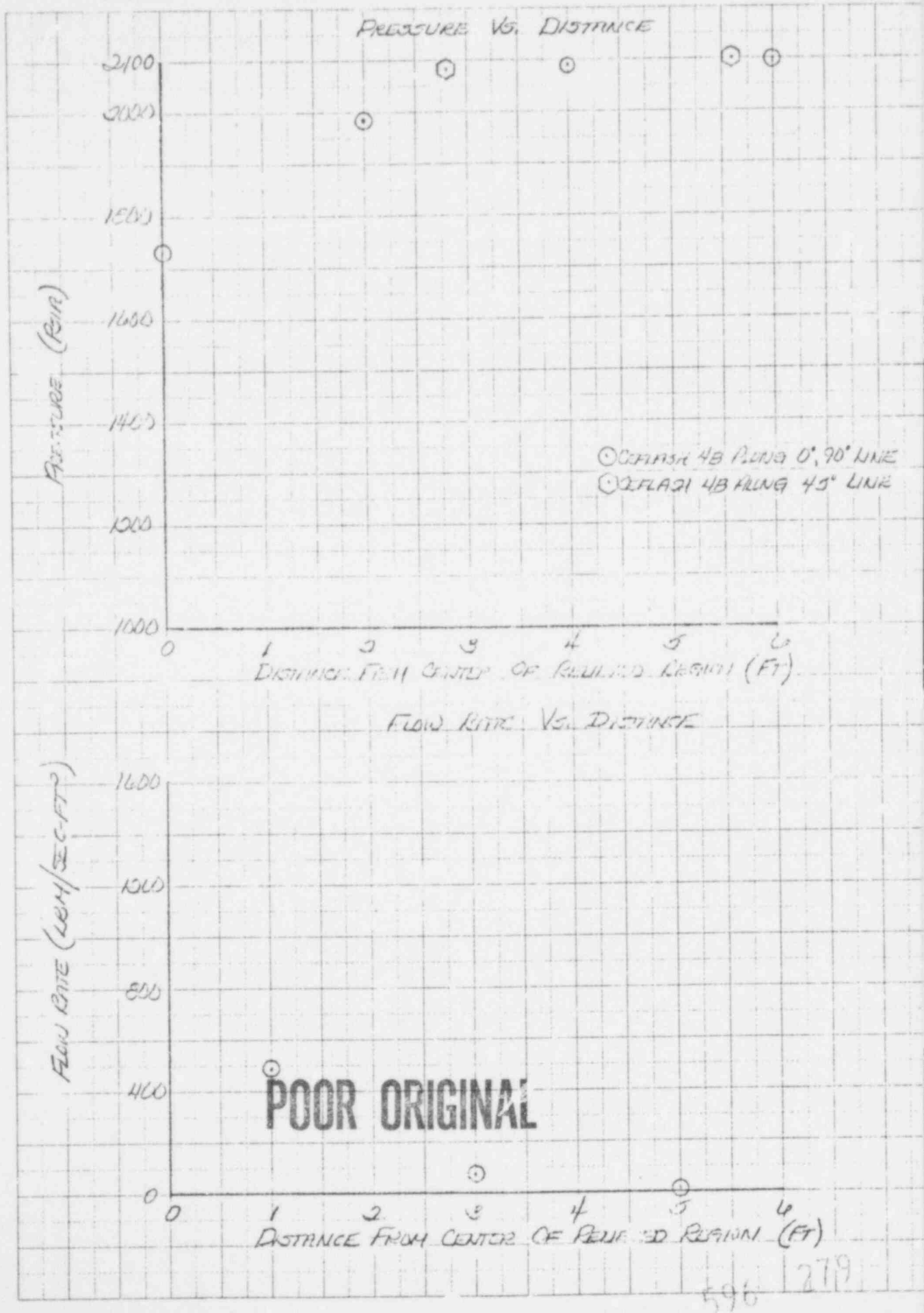

596 279

FIGURE 2.1-5
RESULTS OF SYMMETRIC PLANAR DECOMPRESSION AT 0.75 MSEC.

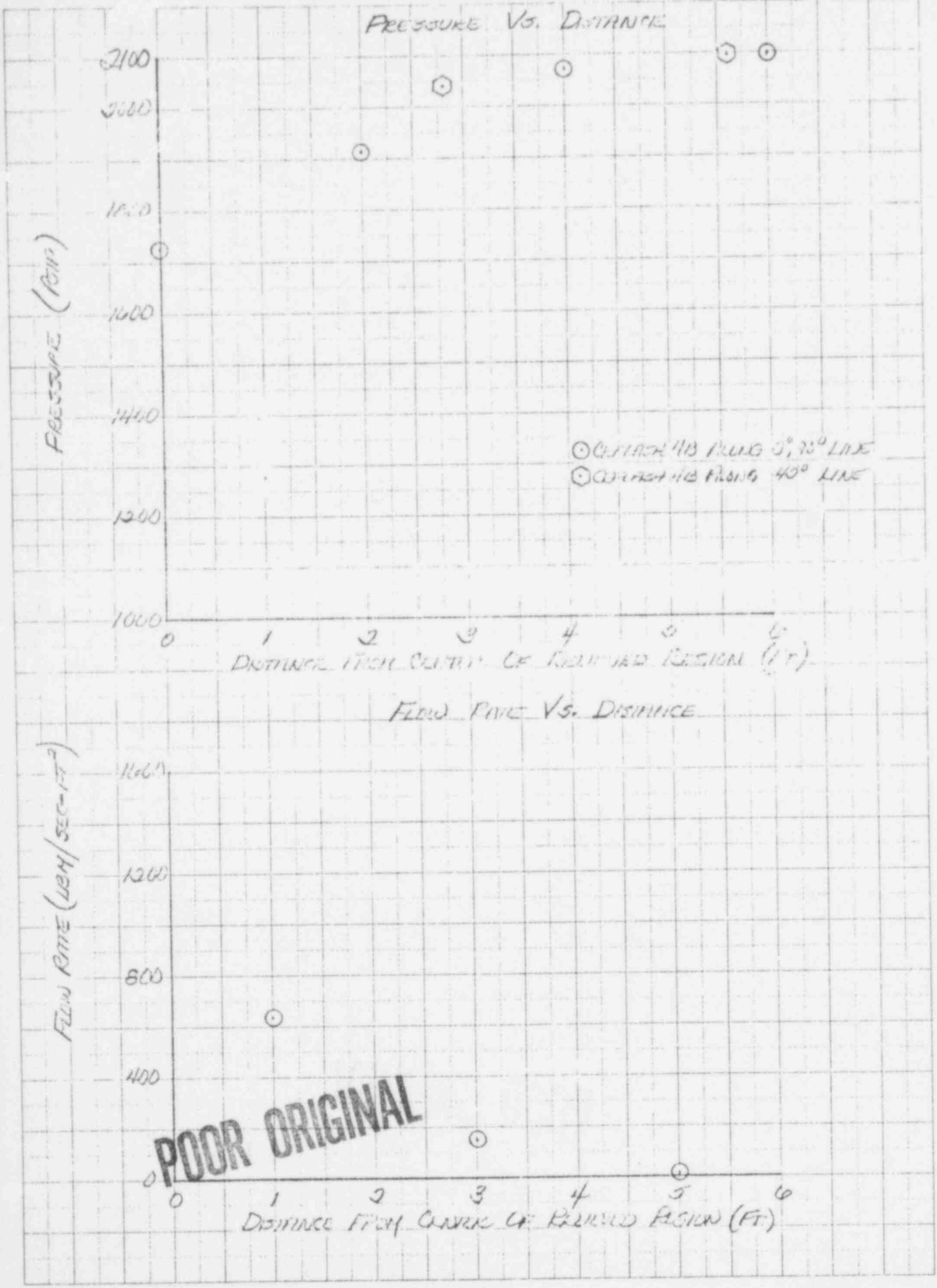

FIGURE 2.1-6

RESULTS OF SYMMETRIC PLANAR DECOMPRESSION AT 1.00 MSEC

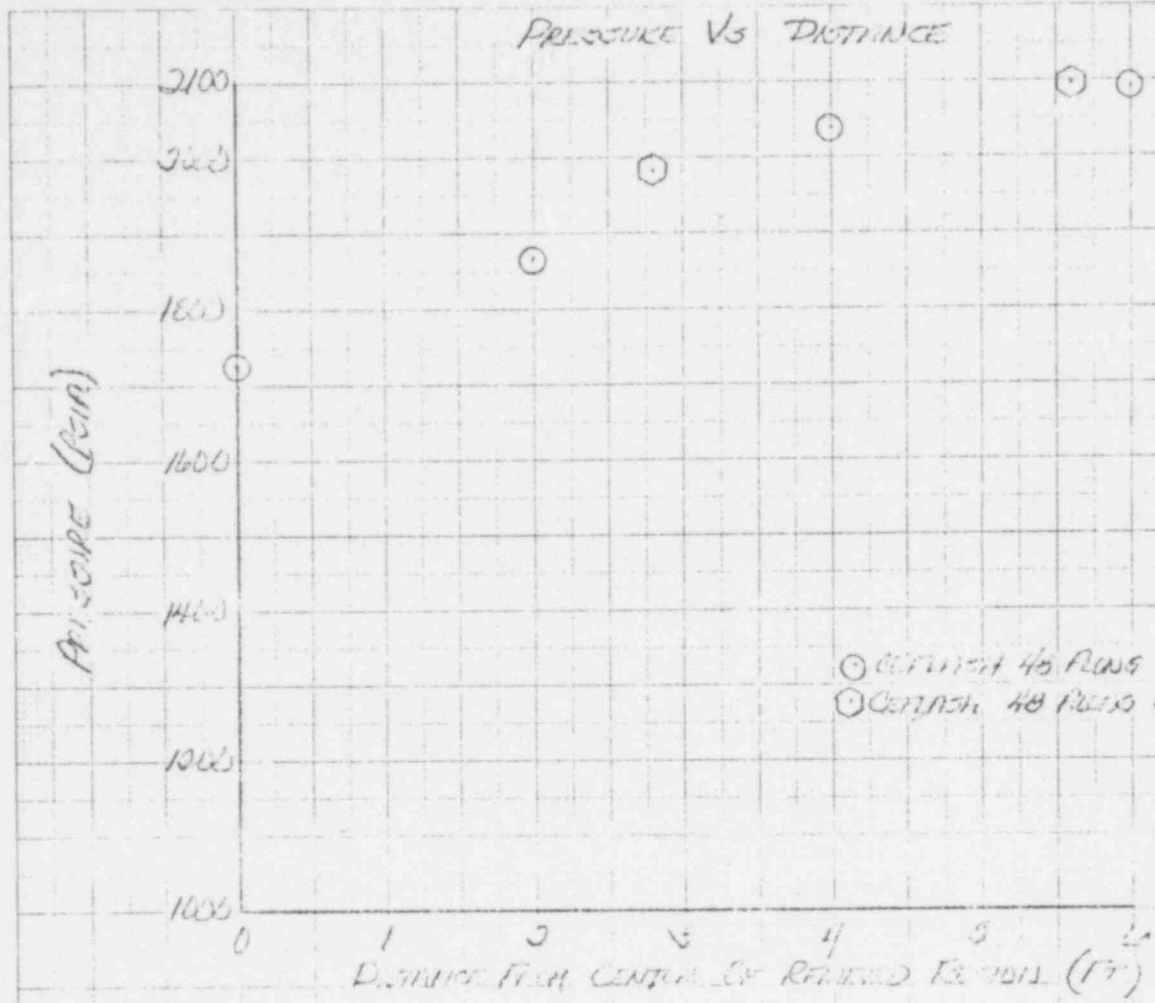

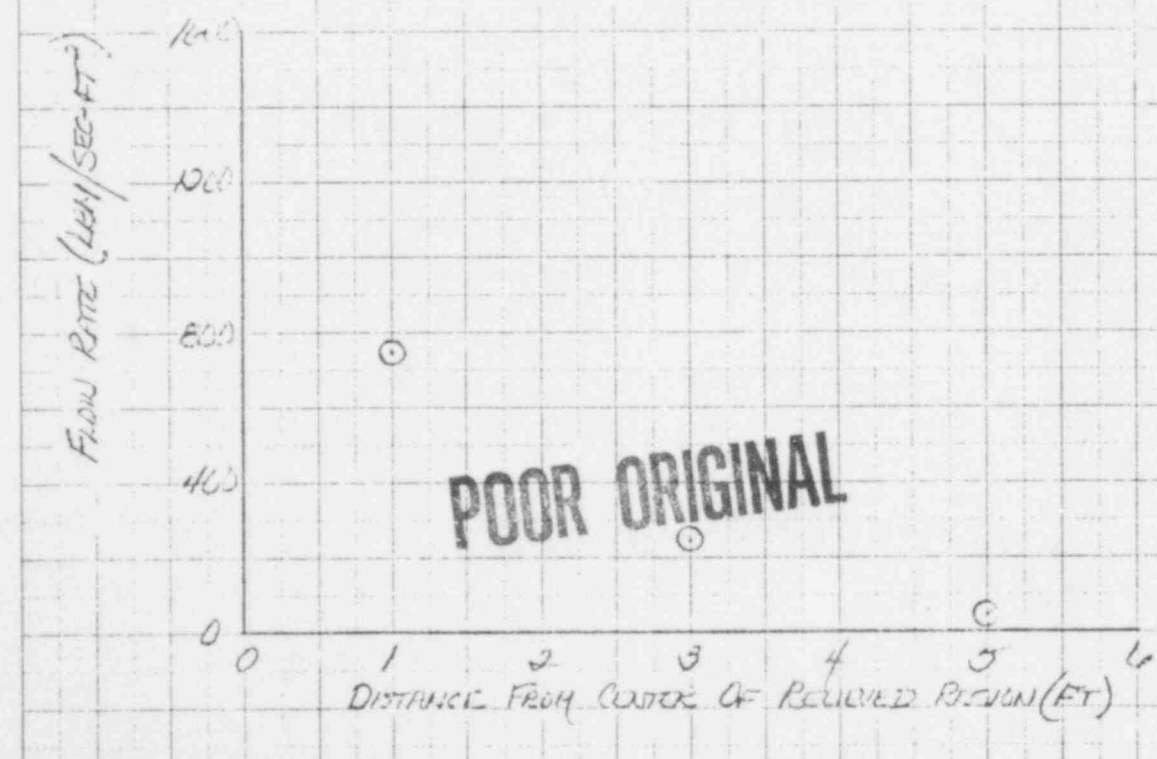

FIGURE 2.1-7
RESULTS OF SYMMETRIC PLANAR DECOMPRESSION AT 1.25 MSEC.

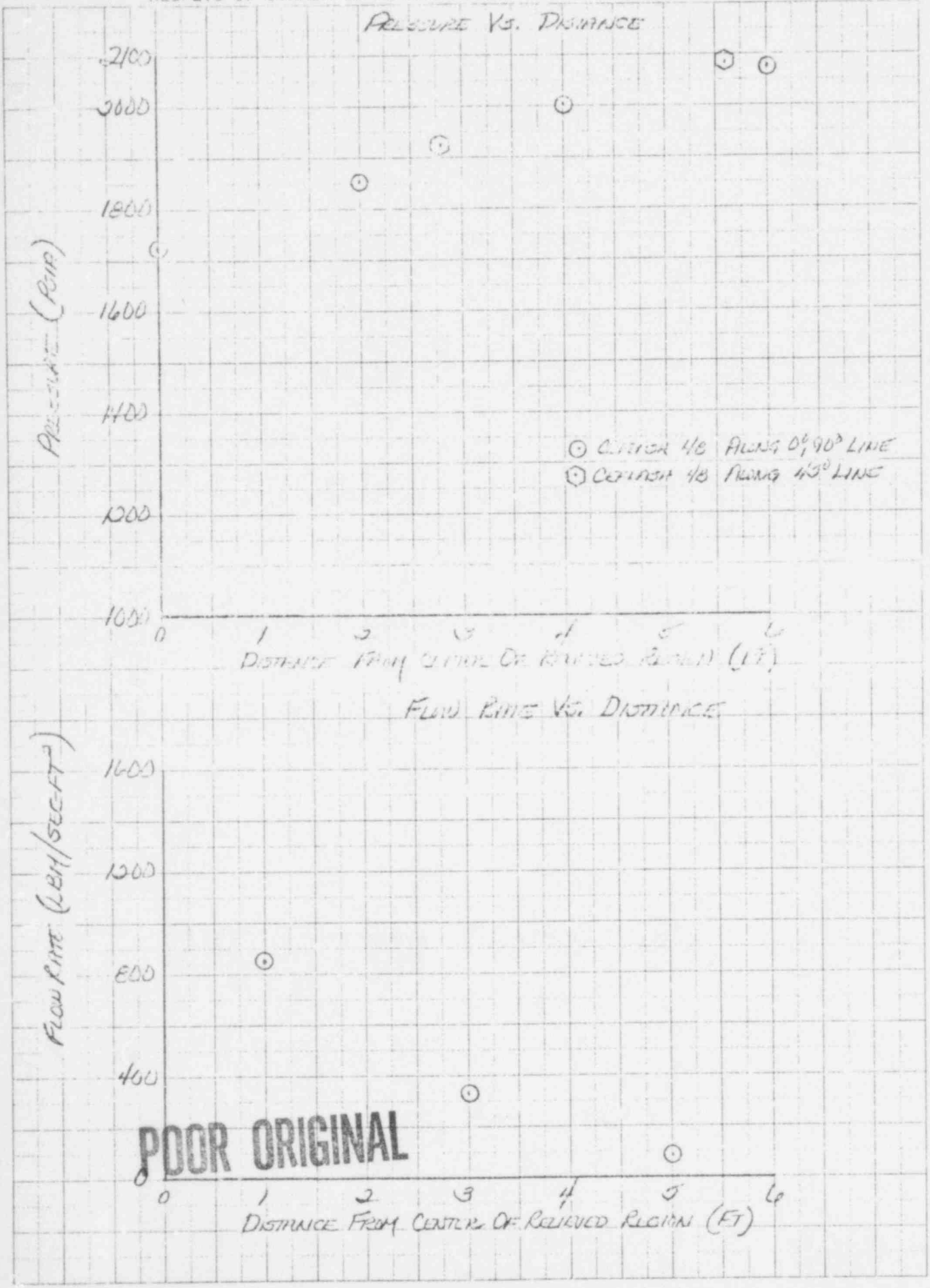

TABLE 2.1-1

CEFLASH- [illegible] PROBLEM
INPUT LISTING AND
ZERO TIME EDIT

COMBUSTION ENGINEERING CEFLASH4B VERSION 11 03 1976 76308

JOB NO KLRCWYT RUN DATE 07/07/78 RUN BEGUN 14.16.15 CPS USED 2.17200

A2 GENERAL INFORMATION AND OPTION INFORMATION

END TIME	RUPT TIME	LEAK OPENS	REF ELEV	PSEUDO P F	MAX STEPS	MAX EDITS
3.0000E-03	1.0000E+00	1.0000E+00	0.	0.	80000	1000

OPTIONS SELECTED

IFMX	1	MOMENTUM TERM USED IN FLOW PATHS SELECTED CARD SERIES 41NN
IFTAX	3	THOM CORRELATION
IFKC	2	FLOW VARYING FRICTION FACTOR
IFCF	1	CRITICAL FLOW CHECK TYPE 5 PLUS PATHS SELECTED CARD SERIES 41NN
IFBL	0	DO NOT BALANCE SYSTEM

OPTION FOR LEAK TABLES SELECTED BY VALUE OF L/D FOR FIRST LEAK FLOW PATH

PATH	L/D	TABLES USED
85	0.	HENRY-FAUSKE

TIME STEP TABLE

USE	UNTIL	STEPS PER PRINT
5.0000E-05	3.0000E-03	1

COMBUSTION ENGINEERING CEFLASH4B VERSION 11 05 1976 76308

5. CONTROL VOLUMES

CODE	AREA	HEIGHT	EXIT ELEV	INLET ELEV	BOTTM ELEV	FLOW AREA
1	4.0000E+00	1.0000E+00	0.	0.	-5.0000E-01	2.0000E+00
2	4.0000E+00	1.0000E+00	0.	0.	-5.0000E-01	2.0000E+00
3	4.0000E+00	1.0000E+00	0.	0.	-5.0000E-01	2.0000E+00
4	4.0000E+00	1.0000E+00	0.	0.	-5.0000E-01	2.0000E+00
5	4.0000E+00	1.0000E+00	0.	0.	-5.0000E-01	2.0000E+00
6	4.0000E+00	1.0000E+00	0.	0.	-5.0000E-01	2.0000E+00
7	4.0000E+00	1.0000E+00	0.	0.	-5.0000E-01	2.0000E+00
8	4.0000E+00	1.0000E+00	0.	0.	-5.0000E-01	2.0000E+00
9	4.0000E+00	1.0000E+00	0.	0.	-5.0000E-01	2.0000E+00
10	4.0000E+00	1.0000E+00	0.	0.	-5.0000E-01	2.0000E+00
11	4.0000E+00	1.0000E+00	0.	0.	-5.0000E-01	2.0000E+00
12	4.0000E+00	1.0000E+00	0.	0.	-5.0000E-01	2.0000E+00
13	4.0000E+00	1.0000E+00	0.	0.	-5.0000E-01	2.0000E+00
14	4.0000E+00	1.0000E+00	0.	0.	-5.0000E-01	2.0000E+00
15	4.0000E+00	1.0000E+00	0.	0.	-5.0000E-01	2.0000E+00
16	4.0000E+00	1.0000E+00	0.	0.	-5.0000E-01	2.0000E+00
17	4.0000E+00	1.0000E+00	0.	0.	-5.0000E-01	2.0000E+00
18	4.0000E+00	1.0000E+00	0.	0.	-5.0000E-01	2.0000E+00
19	4.0000E+00	1.0000E+00	0.	0.	-5.0000E-01	2.0000E+00
20	4.0000E+00	1.0000E+00	0.	0.	-5.0000E-01	2.0000E+00
21	4.0000E+00	1.0000E+00	0.	0.	-5.0000E-01	2.0000E+00
22	4.0000E+00	1.0000E+00	0.	0.	-5.0000E-01	2.0000E+00
23	4.0000E+00	1.0000E+00	0.	0.	-5.0000E-01	2.0000E+00
24	4.0000E+00	1.0000E+00	0.	0.	-5.0000E-01	2.0000E+00
25	4.0000E+00	1.0000E+00	0.	0.	-5.0000E-01	2.0000E+00
26	4.0000E+00	1.0000E+00	0.	0.	-5.0000E-01	2.0000E+00
27	4.0000E+00	1.0000E+00	0.	0.	-5.0000E-01	2.0000E+00
28	4.0000E+00	1.0000E+00	0.	0.	-5.0000E-01	2.0000E+00
29	4.0000E+00	1.0000E+00	0.	0.	-5.0000E-01	2.0000E+00
30	4.0000E+00	1.0000E+00	0.	0.	-5.0000E-01	2.0000E+00
31	4.0000E+00	1.0000E+00	0.	0.	-5.0000E-01	2.0000E+00
32	4.0000E+00	1.0000E+00	0.	0.	-5.0000E-01	2.0000E+00
33	4.0000E+00	1.0000E+00	0.	0.	-5.0000E-01	2.0000E+00
34	4.0000E+00	1.0000E+00	0.	0.	-5.0000E-01	2.0000E+00
35	4.0000E+00	1.0000E+00	0.	0.	-5.0000E-01	2.0000E+00
36	4.0000E+00	1.0000E+00	0.	0.	-5.0000E-01	2.0000E+00
37	4.0000E+00	1.0000E+00	0.	0.	-5.0000E-01	2.0000E+00
38	4.0000E+00	1.0000E+00	0.	0.	-5.0000E-01	2.0000E+00
39	4.0000E+00	1.0000E+00	0.	0.	-5.0000E-01	2.0000E+00
40	4.0000E+00	1.0000E+00	0.	0.	-5.0000E-01	2.0000E+00
41	4.0000E+00	1.0000E+00	0.	0.	-5.0000E-01	2.0000E+00
42	4.0000E+00	1.0000E+00	0.	0.	-5.0000E-01	2.0000E+00
43	4.0000E+00	1.0000E+00	0.	0.	-5.0000E-01	2.0000E+00
44	4.0000E+00	1.0000E+00	0.	0.	-5.0000E-01	2.0000E+00
45	4.0000E+00	1.0000E+00	0.	0.	-5.0000E-01	2.0000E+00
46	4.0000E+00	1.0000E+00	0.	0.	-5.0000E-01	2.0000E+00
47	4.0000E+00	1.0000E+00	0.	0.	-5.0000E-01	2.0000E+00
48	4.0000E+00	1.0000E+00	0.	0.	-5.0000E-01	2.0000E+00
49	4.0000E+00	1.0000E+00	0.	0.	-5.0000E-01	2.0000E+00
50	1.0000E+02	2.0000E+02	-1.0000E+02	5.0000E-01	-1.0000E+02	1.0000E+02

Table 2.1-1 (continued)

COMBUSTION ENGINEERING CEFLASH4B VERSION 11 03 1976 76308

N	PROPERTIES PRESSURE	ENTH SURC	LEVEL TPH
1	1.700nE+03	5.3997E+02	0.
2	2.100nE+03	5.3997E+02	0.
3	2.100nE+03	5.3997E+02	0.
4	2.100nE+03	5.3997E+02	0.
5	2.100nE+03	5.3997E+02	0.
6	2.100nE+03	5.3997E+02	0.
7	2.100nE+03	5.3997E+02	0.
8	2.100nE+03	5.3997E+02	0.
9	2.100nE+03	5.3997E+02	0.
10	2.100nE+03	5.3997E+02	0.
11	2.100nE+03	5.3997E+02	0.
12	2.100nE+03	5.3997E+02	0.
13	2.100nE+03	5.3997E+02	0.
14	2.100nE+03	5.3997E+02	0.
15	2.100nE+03	5.3997E+02	0.
16	2.100nE+03	5.3997E+02	0.
17	2.100nE+03	5.3997E+02	0.
18	2.100nE+03	5.3997E+02	0.
19	2.100nE+03	5.3997E+02	0.
20	2.100nE+03	5.3997E+02	0.
21	2.100nE+03	5.3997E+02	0.
22	2.100nE+03	5.3997E+02	0.
23	2.100nE+03	5.3997E+02	0.
24	2.100nE+03	5.3997E+02	0.
25	2.100nE+03	5.3997E+02	0.
26	2.100nE+03	5.3997E+02	0.
27	2.100nE+03	5.3997E+02	0.
28	2.100nE+03	5.3997E+02	0.
29	2.100nE+03	5.3997E+02	0.
30	2.100nE+03	5.3997E+02	0.
31	2.100nE+03	5.3997E+02	0.
32	2.100nE+03	5.3997E+02	0.
33	2.100nE+03	5.3997E+02	0.
34	2.100nE+03	5.3997E+02	0.
35	2.100nE+03	5.3997E+02	0.
36	2.100nE+03	5.3997E+02	0.
37	2.100nE+03	5.3997E+02	0.
38	2.100nE+03	5.3997E+02	0.
39	2.100nE+03	5.3997E+02	0.
40	2.100nE+03	5.3997E+02	0.
41	2.100nE+03	5.3997E+02	0.
42	2.100nE+03	5.3997E+02	0.
43	2.100nE+03	5.3997E+02	0.
44	2.100nE+03	5.3997E+02	0.
45	2.100nE+03	5.3997E+02	0.
46	2.100nE+03	5.3997E+02	0.
47	2.100nE+03	5.3997E+02	0.
48	2.100nE+03	5.3997E+02	0.
49	2.100nE+03	5.3997E+02	0.

C. FLOW PATHS

PATH	TYPE	NODE FROM	NODE TO	WO	SUM L/A	AREA	DIAMETER	HOM FLOW AREA UP	HOM FLOW AREA DOWN	FRICTION K OR DELTA P	GEOM FWD K OR DELTA P	GEOM RVS K OR DELTA P
1	8	1	2	0.	7.5000E-01	2.0000E+00	2.0000E+00	2.0000E+00	2.0000E+00	2.2500E-02	0.	0.
2	8	2	10	0.	1.0000E+00	2.0000E+00	2.0000E+00	2.0000E+00	2.0000E+00	3.0000E-02	0.	0.
3	8	10	26	0.	1.0000E+00	2.0000E+00	2.0000E+00	2.0000E+00	2.0000E+00	3.0000E-02	0.	0.
4	8	1	6	0.	7.5000E-01	2.0000E+00	2.0000E+00	2.0000E+00	2.0000E+00	2.2500E-02	0.	0.
5	8	6	18	0.	1.0000E+00	2.0000E+00	2.0000E+00	2.0000E+00	2.0000E+00	3.0000E-02	0.	0.
6	8	18	38	0.	1.0000E+00	2.0000E+00	2.0000E+00	2.0000E+00	2.0000E+00	3.0000E-02	0.	0.
7	8	1	4	0.	7.5000E-01	2.0000E+00	2.0000E+00	2.0000E+00	2.0000E+00	2.2500E-02	0.	0.
8	8	2	3	0.	1.0000E+00	2.0000E+00	2.0000E+00	2.0000E+00	2.0000E+00	3.0000E-02	0.	0.
9	8	10	11	0.	1.0000E+00	2.0000E+00	2.0000E+00	2.0000E+00	2.0000E+00	3.0000E-02	0.	0.
10	8	26	27	0.	1.0000E+00	2.0000E+00	1.6000E+00	2.0000E+00	2.0000E+00	3.7500E-02	0.	0.
11	2	6	5	0.	1.0000E+00	2.0000E+00	2.0000E+00	2.0000E+00	2.0000E+00	3.0000E-02	0.	0.
12	8	18	17	0.	1.0000E+00	2.0000E+00	2.0000E+00	2.0000E+00	2.0000E+00	3.0000E-02	0.	0.
13	8	38	37	0.	1.0000E+00	2.0000E+00	1.6000E+00	2.0000E+00	2.0000E+00	3.7500E-02	0.	0.
14	8	4	3	0.	1.0000E+00	2.0000E+00	2.0000E+00	2.0000E+00	2.0000E+00	3.0000E-02	0.	0.
15	8	3	11	0.	1.0000E+00	2.0000E+00	2.0000E+00	2.0000E+00	2.0000E+00	3.0000E-02	0.	0.
16	8	11	27	0.	1.0000E+00	2.0000E+00	2.0000E+00	2.0000E+00	2.0000E+00	3.0000E-02	0.	0.
17	8	4	5	0.	1.0000E+00	2.0000E+00	2.0000E+00	2.0000E+00	2.0000E+00	3.0000E-02	0.	0.
18	8	5	17	0.	1.0000E+00	2.0000E+00	2.0000E+00	2.0000E+00	2.0000E+00	3.0000E-02	0.	0.
19	8	17	37	0.	1.0000E+00	2.0000E+00	2.0000E+00	2.0000E+00	2.0000E+00	3.0000E-02	0.	0.
20	8	4	14	0.	1.0000E+00	2.0000E+00	2.0000E+00	2.0000E+00	2.0000E+00	3.0000E-02	0.	0.
21	8	3	13	0.	1.0000E+00	2.0000E+00	2.0000E+00	2.0000E+00	2.0000E+00	3.0000E-02	0.	0.
22	8	11	12	0.	1.0000E+00	2.0000E+00	2.0000E+00	2.0000E+00	2.0000E+00	3.0000E-02	0.	0.
23	2	27	28	0.	1.0000E+00	2.0000E+00	1.6000E+00	2.0000E+00	2.0000E+00	3.7500E-02	0.	0.
24	8	5	15	0.	1.0000E+00	2.0000E+00	2.0000E+00	2.0000E+00	2.0000E+00	3.0000E-02	0.	0.
25	8	17	16	0.	1.0000E+00	2.0000E+00	1.6000E+00	2.0000E+00	2.0000E+00	3.7500E-02	0.	0.
26	8	37	36	0.	1.0000E+00	2.0000E+00	2.0000E+00	2.0000E+00	2.0000E+00	3.0000E-02	0.	0.
27	8	14	13	0.	1.0000E+00	2.0000E+00	2.0000E+00	2.0000E+00	2.0000E+00	3.0000E-02	0.	0.
28	8	13	12	0.	1.0000E+00	2.0000E+00	2.0000E+00	2.0000E+00	2.0000E+00	3.0000E-02	0.	0.
29	8	12	28	0.	1.0000E+00	2.0000E+00	2.0000E+00	2.0000E+00	2.0000E+00	3.0000E-02	0.	0.
30	8	14	15	0.	1.0000E+00	2.0000E+00	2.0000E+00	2.0000E+00	2.0000E+00	3.0000E-02	0.	0.
31	8	15	16	0.	1.0000E+00	2.0000E+00	2.0000E+00	2.0000E+00	2.0000E+00	3.0000E-02	0.	0.
32	8	16	36	0.	1.[illegible]00E+00	2.0000E+00	2.0000E+00	2.0000E+00	2.0000E+00	3.0000E-02	0.	0.
33	8	14	32	0.	1.0000E+00	2.0000E+00	2.0000E+00	2.0000E+00	2.0000E+00	3.0000E-02	0.	0.
34	8	13	31	0.	1.0000E+00	2.0000E+00	2.0000E+00	2.0000E+00	2.0000E+00	3.0000E-02	0.	0.
35	8	12	30	0.	1.0000E+00	2.0000E+00	2.0000E+00	2.0000E+00	2.0000E+00	3.0000E-02	0.	0.
36	3	28	29	0.	1.0000E+00	2.0000E+00	1.6000E+00	2.0000E+00	2.0000E+00	3.7500E-02	0.	0.
37	8	15	33	0.	1.0000E+00	2.0000E+00	2.0000E+00	2.0000E+00	2.0000E+00	3.0000E-02	0.	0.
38	8	16	34	0.	1.0000E+00	2.0000E+00	2.0000E+00	2.0000E+00	2.0000E+00	3.0000E-02	0.	0.
39	8	36	35	0.	1.0000E+00	2.0000E+00	1.6000E+00	2.0000E+00	2.0000E+00	3.7500E-02	0.	0.
40	8	32	31	0.	1.0000E+00	2.0000E+00	1.6000E+00	2.0000E+00	2.0000E+00	3.7500E-02	0.	0.
41	8	31	30	0.	1.0000E+00	2.0000E+00	1.6000E+00	2.0000E+00	2.0000E+00	3.7500E-02	0.	0.
42	8	30	29	0.	1.0000E+00	2.0000E+00	1.6000E+00	2.0000E+00	2.0000E+00	3.7500E-02	0.	0.
43	8	32	33	0.	1.0000E+00	2.0000E+00	1.6000E+00	2.0000E+00	2.0000E+00	3.7500E-02	0.	0.
44	8	33	34	0.	1.0000E+00	2.0000E+00	1.6000E+00	2.0000E+00	2.0000E+00	3.7500E-02	0.	0.
45	8	34	35	0.	1.0000E+00	2.0000E+00	1.6000E+00	2.0000E+00	2.0000E+00	3.7500E-02	0.	0.
46	8	8	9	0.	1.0000E+00	2.0000E+00	2.0000E+00	2.0000E+00	2.0000E+00	3.0000E-02	0.	0.
47	8	9	25	0.	1.0000E+00	2.0000E+00	2.0000E+00	2.0000E+00	2.0000E+00	3.0000E-02	0.	0.
48	8	25	49	0.	1.0000E+00	2.0000E+00	2.0000E+00	2.0000E+00	2.0000E+00	3.0000E-02	0.	0.
49	8	8	7	0.	1.0000E+00	2.0000E+00	2.0000E+00	2.0000E+00	2.0000E+00	3.0000E-02	0.	0.

POOR ORIGINAL

596 286

Table 2.1-1 (continued)

COMBUSTION ENGINEERING CEFLASH4B VERSION 11 03 1976 76308

C. FLOW PATHS

PATH	TYPE	NODE FROM	NODE TO	WO	SUM L/A	AREA	DIAMETER	MOM FLOW AREA UP	MOM FLOW AREA DOWN	FRICTION K OR DELTA P	GEOM FWD K OR DELTA P	GEOM RVS K OR DELTA P
50	8	7	19	0.	1.0000E+00	2.0000E+00	2.0000E+00	2.0000E+00	2.0000E+00	3.0000E-02	0.	0.
51	8	19	39	0.	1.0000E+00	2.0000E+00	2.0000E+00	2.0000E+00	2.0000E+00	3.0000E-02	0.	0.
52	8	1	8	0.	7.5000E-01	2.0000E+00	2.0000E+00	2.0000E+00	2.0000E+00	2.2500E-02	0.	0.
53	8	2	9	0.	1.0000E+00	2.0000E+00	2.0000E+00	2.0000E+00	2.0000E+00	3.0000E-02	0.	0.
54	8	10	25	0.	1.0000E+00	2.0000E+00	2.0000E+00	2.0000E+00	2.0000E+00	3.0000E-02	0.	0.
55	8	26	49	0.	1.0000E+00	2.0000E+00	1.6000E+00	2.0000E+00	2.0000E+00	3.7500E-02	0.	0.
56	8	6	7	0.	1.0000E+00	2.0000E+00	2.0000E+00	2.0000E+00	2.0000E+00	3.0000E-02	0.	0.
57	8	18	19	0.	1.0000E+00	2.0000E+00	2.0000E+00	2.0000E+00	2.0000E+00	3.0000E-02	0.	0.
58	8	38	39	0.	1.0000E+00	2.0000E+00	1.6000E+00	2.0000E+00	2.0000E+00	3.7500E-02	0.	0.
59	8	22	23	0.	1.0000E+00	2.0000E+00	2.0000E+00	2.0000E+00	2.0000E+00	3.0000E-02	0.	0.
60	8	23	24	0.	1.0000E+00	2.0000E+00	2.0000E+00	2.0000E+00	2.0000E+00	3.0000E-02	0.	0.
61	8	24	48	0.	1.0000E+00	2.0000E+00	2.0000E+00	2.0000E+00	2.0000E+00	3.0000E-02	0.	0.
62	8	22	21	0.	1.0000E+00	2.0000E+00	2.0000E+00	2.0000E+00	2.0000E+00	3.0000E-02	0.	0.
63	8	21	20	0.	1.0000E+00	2.0000E+00	2.0000E+00	2.0000E+00	2.0000E+00	3.0000E-02	0.	0.
64	8	20	40	0.	1.0000E+00	2.0000E+00	2.0000E+00	2.0000E+00	2.0000E+00	3.0000E-02	0.	0.
65	8	8	22	0.	1.0000E+00	2.0000E+00	2.0000E+00	2.0000E+00	2.0000E+00	3.0000E-02	0.	0.
66	8	9	23	0.	1.0000E+00	2.0000E+00	2.0000E+00	2.0000E+00	2.0000E+00	3.0000E-02	0.	0.
67	8	25	24	0.	1.0000E+00	2.0000E+00	2.0000E+00	2.0000E+00	2.0000E+00	3.0000E-02	0.	0.
68	8	49	48	0.	1.0000E+00	2.0000E+00	1.6000E+00	2.0000E+00	2.0000E+00	3.7500E-02	0.	0.
69	8	7	21	0.	1.0000E+00	2.0000E+00	2.0000E+00	2.0000E+00	2.0000E+00	3.0000E-02	0.	0.
70	8	19	20	0.	1.0000E+00	2.0000E+00	2.0000E+00	2.0000E+00	2.0000E+00	3.0000E-02	0.	0.
71	8	39	40	0.	1.0000E+00	2.0000E+00	1.6000E+00	2.0000E+00	2.0000E+00	3.7500E-02	0.	0.
72	8	44	45	0.	1.0000E+00	2.0000E+00	1.6000E+00	2.0000E+00	2.0000E+00	3.7500E-02	0.	0.
73	8	45	46	0.	1.0000E+00	2.0000E+00	1.6000E+00	2.0000E+00	2.0000E+00	3.7500E-02	0.	0.
74	8	46	47	0.	1.0000E+00	2.0000E+00	1.6000E+00	2.0000E+00	2.0000E+00	3.7500E-02	0.	0.
75	8	44	43	0.	1.0000E+00	2.0000E+00	1.6000E+00	2.0000E+00	2.0000E+00	3.7500E-02	0.	0.
76	8	43	42	0.	1.0000E+00	2.0000E+00	1.6000E+00	2.0000E+00	2.0000E+00	3.7500E-02	0.	0.
77	8	42	41	0.	1.0000E+00	2.0000E+00	1.6000E+00	2.0000E+00	2.0000E+00	3.7500E-02	0.	0.
78	8	22	44	0.	1.0000E+00	2.0000E+00	2.0000E+00	2.0000E+00	2.0000E+00	3.0000E-02	0.	0.
79	8	23	45	0.	1.0000E+00	2.0000E+00	2.0000E+00	2.0000E+00	2.0000E+00	3.0000E-02	0.	0.
80	8	24	46	0.	1.0000E+00	2.0000E+00	2.0000E+00	2.0000E+00	2.0000E+00	3.0000E-02	0.	0.
81	8	48	47	0.	1.0000E+00	2.0000E+00	1.6000E+00	2.0000E+00	2.0000E+00	3.7500E-02	0.	0.
82	8	21	43	0.	1.0000E+00	2.0000E+00	2.0000E+00	2.0000E+00	2.0000E+00	3.0000E-02	0.	0.
83	8	20	42	0.	1.0000E+00	2.0000E+00	2.0000E+00	2.0000E+00	2.0000E+00	3.0000E-02	0.	0.
84	8	40	41	0.	1.0000E+00	2.0000E+00	1.6000E+00	2.0000E+00	2.0000E+00	3.7500E-02	0.	0.
85	8	1	50	0.	1.0000E-06	7.8540E-01	1.0000E+00	4.0000E+00	1.0000E+02	3.0000E-02	0.	0.

PATH	TYPE	L/D	AREA	DISCHARGE COEFF	DISCHARGE COEFF	DISCHARGE COEFF	DISCHARGE COEFF
86	0	0					

Table 2.1-1 (continued)

COMBUSTION ENGINEERING CEFLASH4B VERSION 11 03 1976 76308

OPTIONS BY FLOW PATHS

FLOW PATH	MOMENTUM FLUX	CRITICAL FLOW	MIN AREA CRIT FLOW	LENGTH
1	4	1	2.0000E+00	1.5000E+00
2	4	1	2.0000E+00	2.0000E+00
3	4	1	2.0000E+00	2.0000E+00
4	4	1	2.0000E+00	1.5000E+00
5	4	1	2.0000E+00	2.0000E+00
6	4	1	2.0000E+00	2.0000E+00
7	4	1	2.0000E+00	1.5000E+00
8	4	1	2.0000E+00	2.0000E+00
9	4	1	2.0000E+00	2.0000E+00
10	4	1	2.0000E+00	2.0000E+00
11	4	1	2.0000E+00	2.0000E+00
12	4	1	2.0000E+00	2.0000E+00
13	4	1	2.0000E+00	2.0000E+00
14	4	1	2.0000E+00	2.0000E+00
15	4	1	2.0000E+00	2.0000E+00
16	4	1	2.0000E+00	2.0000E+00
17	4	1	2.0000E+00	2.0000E+00
18	4	1	2.0000E+00	2.0000E+00
19	4	1	2.0000E+00	2.0000E+00
20	4	1	2.0000E+00	2.0000E+00
21	4	1	2.0000E+00	2.0000E+00
22	4	1	2.0000E+00	2.0000E+00
23	4	1	2.0000E+00	2.0000E+00
24	4	1	2.0000E+00	2.0000E+00
25	4	1	2.0000E+00	2.0000E+00
26	4	1	2.0000E+00	2.0000E+00
27	4	1	2.0000E+00	2.0000E+00
28	4	1	2.0000E+00	2.0000E+00
29	4	1	2.0000E+00	2.0000E+00
30	4	1	2.0000E+00	2.0000E+00
31	4	1	2.0000E+00	2.0000E+00
32	4	1	2.0000E+00	2.0000E+00
33	4	1	2.0000E+00	2.0000E+00
34	4	1	2.0000E+00	2.0000E+00
35	4	1	2.0000E+00	2.0000E+00
36	4	1	2.0000E+00	2.0000E+00
37	4	1	2.0000E+00	2.0000E+00
38	4	1	2.0000E+00	2.0000E+00
39	4	1	2.0000E+00	2.0000E+00
40	4	1	2.0000E+00	2.0000E+00
41	4	1	2.0000E+00	2.0000E+00
42	4	1	2.0000E+00	2.0000E+00
43	4	1	2.0000E+00	2.0000E+00
44	4	1	2.0000E+00	2.0000E+00
45	4	1	2.0000E+00	2.0000E+00
46	4	1	2.0000E+00	2.0000E+00
47	4	1	2.0000E+00	2.0000E+00
48	4	1	2.0000E+00	2.0000E+00
49	4	1	2.0000E+00	2.0000E+00
50	4	1	2.0000E+00	2.0000E+00
51	4	1	2.0000E+00	2.0000E+00

Table 2.1-1 (continued)

COMBUSTION ENGINEERING CEFLASH4B VERSION 11 03 1976 76308

FLOW PATH	OPTIONS BY FLOW PATHS MOMENTUM FLUX	CRITICAL FLOW	MIN AREA CRIT FLOW	LENGTH
52	4	1	2.0000E+00	1.5000E+00
53	4	1	2.0000E+00	2.0000E+00
54	4	1	2.0000E+00	2.0000E+00
55	4	1	2.0000E+00	2.0000E+00
56	4	1	2.0000E+00	2.0000E+00
57	4	1	2.0000E+00	2.0000E+00
58	4	1	2.0000E+00	2.0000E+00
59	4	1	2.0000E+00	2.0000E+00
60	4	1	2.0000E+00	2.0000E+00
61	4	1	2.0000E+00	2.0000E+00
62	4	1	2.0000E+00	2.0000E+00
63	4	1	2.0000E+00	2.0000E+00
64	4	1	2.0000E+00	2.0000E+00
65	4	1	2.0000E+00	2.0000E+00
66	4	1	2.0000E+00	2.0000E+00
67	4	1	2.0000E+00	2.0000E+00
68	4	1	2.0000E+00	2.0000E+00
69	4	1	2.0000E+00	2.0000E+00
70	4	1	2.0000E+00	2.0000E+00
71	4	1	2.0000E+00	2.0000E+00
72	4	1	2.0000E+00	2.0000E+00
73	4	1	2.0000E+00	2.0000E+00
74	4	1	2.0000E+00	2.0000E+00
75	4	1	2.0000E+00	2.0000E+00
76	4	1	2.0000E+00	2.0000E+00
77	4	1	2.0000E+00	2.0000E+00
78	4	1	2.0000E+00	2.0000E+00
79	4	1	2.0000E+00	2.0000E+00
80	4	1	2.0000E+00	2.0000E+00
81	4	1	2.0000E+00	2.0000E+00
82	4	1	2.0000E+00	2.0000E+00
83	4	1	2.0000E+00	2.0000E+00
84	4	1	2.0000E+00	2.0000E+00
85	4	1	1.0000E+00	1.0000E+00

QUESTION 2.2 (Problem No. 2)

A two-dimensional sheet of water (see Figure 2.2-1), of unit thickness is at a pressure of 2100 psia and a temperature of 544°F. The fluid is at rest everywhere. An obstruction, 2 feet in diameter, is present. A 2 foot diameter region is suddenly relieved to a pressure of 1700 psia, at time equals zero, and held constant at 1700 psia. The problem is intended to be equivalent to a typical PWR downcomer annulus in geometry (un-wrapped) and to evaluate the effects of the hot leg nozzle extension which penetrates the downcomer region.

Provide plots of pressure and fluid velocity along the x-axis at distances of 5 feet above, 3 feet above, 3 feet below, 6 feet below, and 10 feet below the center of the relieved region, and at the centerline of the relieved region. Provide plots of pressure and fluid velocity along the y-axis at distance of 2 feet, 4 feet, 8 feet, and 10 feet from the center of the relieved region, and at the centerline of the relieved region. The data is to provided at 0.5, 1.0, 1.5, 2.0, 2.5, and 3.0 milliseconds.

RESPONSE

Analytical Model

This problem simulates a reactor vessel downcomer with the hot leg nozzle extension into the annulus taken into account. An 18 ft. long x 11 ft. wide flat sheet of water of unit (1 ft.) thickness as shown on Figure 2.2-1 was modeled using the CEFLASH-4B computer code. A 58 node and 94 flow path network arrangement was developed, which is given in the diagram on Figure 2.2-2.

The problem as stated above describes an unwrapped downcomer geometry which is symmetric about the y-axis. A node size of 2 ft. x 2 ft. x 1 ft. thick was used to model this region. The axis of symmetry would divide full size (2 ft. 2 ft. x 1 ft. nodes along the centerline of the sheet of water in half if the entire region were to be modeled. Since symmetry is accounted for in this model formulation, these nodes are represented as one-half the width (2 ft.x 1 ft.x 1ft.) of the remaining nodes.

The region around the hot leg nozzle extension was modeled by four separate nodes. These four nodes each account for one quarter of the volume between a full size node circumscribed about the nozzle extension and the volume occupied by the nozzle itself. These four nodes are connected to the adjacent control volumes (nodes) as shown on Figure 2.2-2.

The "leak" node (node 1) is connected to an arbitrarily large (20,000 ft^3) containment volume(node 55) through a 1.571 $ft.^2$ (area of semicircle with radius 1 ft) flow area. Further nodal descriptions are presented in Table 2.2-1.

Flow paths are used to connect node centers to node centers except when prevented due to the problem formulation. The pressure and flow rate information was requested at unequal intervals along the x-axis which prohibited the use of flow paths with uniform lengths.

Flow paths 1, 6 and 28 connect the outer boundary of the "leak" node (node 1) to their respective adjacent nodes in order to account for the transport distance associated with the relieved region.

Flow paths 3, 4, 9 and 31 connect the nodes around the hot leg nozzle extension to the surrounding nodes. These paths end at the outer boundary of the obstruction. More flow path definitions can be found in Table 2.2-2. Nodes 1 and 55 are assumed to be at 1700 psia at time zero. All remaining nodes are initially at 2100 psia. As in problem 2.1, the pressure in node 1 cannot be maintained at 1700 psia over all time periods. However, by assuming instantaneous communication ($L/A = 10^{-6}$ ft^{-1}) between the "leak" node (node 1) and the containment node (node 55) the pressure in node 1 approximates 1700 psia over the 3.0 millisecond transient.

A complete listing of the CEFLASH-4B input is presented in Table 2.2-3.

RESULTS

The requested plots of pressure and flow rate at times of 0.5, 1.0, 1.5, 2.0, 2.5, and 3.0 milliseconds are provided on Figures 2.2-3 through 2.2-14.

The data is presented as instantaneous "snapshots" of the pressure and flow fields on the 18 ft. x 11 ft. grid established in the problem formulation and shown on Figure 2.2-1. The pressure disturbance is seen on the figures to propogate radially outward from the "leak" location during the first 1.5 milliseconds at which time the decompression has reached the hot leg nozzle extension. At 2.0 milliseconds, the pressure disturbance has reflected off the obstruction and is traveling back toward the break as a decompression wave. By 3.0 milliseconds, the disturbance has traveled virtually throughout the sheet of water and has started to approach an equilibrium position (1700 psia) near the break location.

TABLE 2.2-1

CEFLASH-4B NODE DESCRIPTION FOR PROBLEM 2.2

NODE NO.	DESCRIPTION
1	"Leak" node, half-size (2 ft^3) node from 1 ft below to 1 ft above x-axis
2, 3	Full size (4 ft^3) nodes from 1 ft below to 1 ft above x-axis
4, 56-58	Nodes containing 1/4 the volume difference between a full size no and a 2 ft dia. obstruction located from 1 ft below to 1 ft above
5, 6	Full size nodes from 1 ft below to 1 ft above x-axis
7	Half-size node from 1 ft above to 3 ft above x-axis
8-12	Full size nodes from 1 ft above to 3 ft above x-axis
13	Half-size node from 3 ft above to 5 ft above x-axis
14-18	Full size nodes from 3 ft above to 5 ft above x-axis
19	Half-size node from 1 ft below to 3 ft below x-axis
20-24	Full size nodes from 1 ft below to 3 ft below x-axis
25	Half-size node from 3 ft below to 5 ft below x-axis
26-30	Full size nodes from 3 ft below to 5 ft below x-axis
31	Half-size node from 5 ft below to 7 ft below x-axis
32-36	Full size nodes from 5 ft below to 7 ft below x-axis
37	Half-size node from 7 ft below to 9 ft below x-axis

TABLE 2.2-1 (CONT'D)

CEFLASH-4B NODE DESCRIPTION FOR PROBLEM 2.2

NODE NO.	DESCRIPTION
38-42	Full size nodes from 7 ft below to 9 ft below x-axis
43	Half-size node from 9 ft below to 11 ft below x-axis
44-48	Full size nodes from 9 ft below to 11 ft below x-axis
49	Half-size node from 11 ft below to 13 ft below x-axis
50-54	Full size nodes from 11 ft below to 13 ft below x-axis
55	Containment node

TABLE 2.2-2

CEFLASH-4B FLOW PATH DESCRIPTION FOR PROBLEM 2-2

FLOW PATH NO.	DESCRIPTION
1-5	Horizontal connections along x-axis
6-11	Vertical connections from x-axis to 3 ft above x-axis
12-16	Horizontal connections 3 ft above x-axis
17-22	Vertical connections from 3 ft above to 5 ft above x-axis
23-27	Horizontal connections 5 ft above x-axis
28-33	Vertical connections from x-axis to 3 ft below x-axis
34-38	Horizontal connections 3 ft below x-axis
39-44	Vertical connections from 3 ft below to 4 ft below x-axis
45-49	Horizontal connections 4 ft below x-axis
50-55	Vertical connections from 4 ft below to 6 ft below x-axis
56-60	Horizontal connections 6 ft below x-axis
61-66	Vertical connections from 6 ft below to 8 ft below x-axis
67-71	Horizontal connections 8 ft below x-axis
72-77	Veritcal connections from 8 ft below to 10 ft below x-axis
78-82	Horizontal connections 10 ft below x-axis
83-88	Vertical connections from 10 ft to 12 ft below x-axis
89-93	Horizontal connections 12 ft below x-axis
94	"Leak" path, connection from "Leak" node (Node 1) to containment node (node 55)

TABLE 2.2-3

CEFLASH-4B INPUT FOR PROBLEM 2.2

COMBUSTION ENGINEERING CEFLASH4B VERSION 11 03 1976 76308

JOB NO NLRCW0Z RUN DATE 09/05/78 RUN BEGUN 14.28.50 CPS USED 2.51700

GENERAL INFORMATION AND OPTION INFORMATION

END TIME	ABRT TIME	LEAK OPENS	REF ELEV	PSEUDO P F	MAX STEPS	MAX EDITS
3.0000E+03	1.0000E+00	1.0000E+00	0.	0.	80000	1000

OPTIONS SELECTED

IFMX	1	MOMENTUM TERM USED IN FLOW PATHS SELECTED CARD SERIES 41NN
IFTAX	3	THICK CORRELATION
IFKC	2	FLOW VARYING FRICTION FACTOR
IFCF	1	CRITICAL FLOW CHECK TYPE 5 PLUS PATHS SELECTED CARD SERIES 41NN
IFBL	0	DO NOT BALANCE SYSTEM

OPTION FOR LEAK TABLES SELECTED BY VALUE OF L/D FOR FIRST LEAK FLOW PATH

PATH	L/D	TABLES USED
95	0.	[ ]

TIME STEP TABLE

USE	UNTIL	STEPS PER PRINT
5.0000E+05	3.0000E+03	1

2.2-7

ORIGINAL COPY

967 965

TABLE 2.2-3 (Con't)

CEFLASH-4B INPUT FOR PROBLEM 2.2

COMBUSTION ENGINEERING CEFLASH4B VERSION 11-03-1976 76308

8. CONTROL VOLUMES

NODE	AREA	HEIGHT	EXIT ELEV	INLET ELEV	BOTTM ELEV	FLOW AREA
1	2.0000E+00	1.0000E+00	0.	0.	-5.0000E-01	2.0000E+00
2	4.0000E+00	1.0000E+00	0.	0.	-5.0000E-01	2.0000E+00
3	4.0000E+00	1.0000E+00	0.	0.	-5.0000E-01	2.0000E+00
4	2.1460E+01	1.0000E+00	0.	0.	-5.0000E-01	2.0000E+00
5	4.0000E+00	1.0000E+00	0.	0.	-5.0000E-01	2.0000E+00
6	4.0000E+00	1.0000E+00	0.	0.	-5.0000E-01	2.0000E+00
7	2.0000E+00	1.0000E+00	0.	0.	-5.0000E-01	2.0000E+00
8	4.0000E+00	1.0000E+00	0.	0.	-5.0000E-01	2.0000E+00
9	4.0000E+00	1.0000E+00	0.	0.	-5.0000E-01	2.0000E+00
10	4.0000E+00	1.0000E+00	0.	0.	-5.0000E-01	2.0000E+00
11	4.0000E+00	1.0000E+00	0.	0.	-5.0000E-01	2.0000E+00
12	4.0000E+00	1.0000E+00	0.	0.	-5.0000E-01	2.0000E+00
13	2.0000E+00	1.0000E+00	0.	0.	-5.0000E-01	2.0000E+00
14	4.0000E+00	1.0000E+00	0.	0.	-5.0000E-01	2.0000E+00
15	4.0000E+00	1.0000E+00	0.	0.	-5.0000E-01	2.0000E+00
16	4.0000E+00	1.0000E+00	0.	0.	-5.0000E-01	2.0000E+00
17	4.0000E+00	1.0000E+00	0.	0.	-5.0000E-01	2.0000E+00
18	4.0000E+00	1.0000E+00	0.	0.	-5.0000E-01	2.0000E+00
19	2.0000E+00	1.0000E+00	0.	0.	-5.0000E-01	2.0000E+00
20	4.0000E+00	1.0000E+00	0.	0.	-5.0000E-01	2.0000E+00
21	4.0000E+00	1.0000E+00	0.	0.	-5.0000E-01	2.0000E+00
22	4.0000E+00	1.0000E+00	0.	0.	-5.0000E-01	2.0000E+00
23	4.0000E+00	1.0000E+00	0.	0.	-5.0000E-01	2.0000E+00
24	4.0000E+00	1.0000E+00	0.	0.	-5.0000E-01	2.0000E+00
25	2.0000E+00	1.0000E+00	0.	0.	-5.0000E-01	2.0000E+00
26	4.0000E+00	1.0000E+00	0.	0.	-5.0000E-01	2.0000E+00
27	4.0000E+00	1.0000E+00	0.	0.	-5.0000E-01	2.0000E+00
28	4.0000E+00	1.0000E+00	0.	0.	-5.0000E-01	2.0000E+00
29	4.0000E+00	1.0000E+00	0.	0.	-5.0000E-01	2.0000E+00
30	4.0000E+00	1.0000E+00	0.	0.	-5.0000E-01	2.0000E+00
31	2.0000E+00	1.0000E+00	0.	0.	-5.0000E-01	2.0000E+00
32	4.0000E+00	1.0000E+00	0.	0.	-5.0000E-01	2.0000E+00
33	4.0000E+00	1.0000E+00	0.	0.	-5.0000E-01	2.0000E+00
34	4.0000E+00	1.0000E+00	0.	0.	-5.0000E-01	2.0000E+00
35	4.0000E+00	1.0000E+00	0.	0.	-5.0000E-01	2.0000E+00
36	4.0000E+00	1.0000E+00	0.	0.	-5.0000E-01	2.0000E+00
37	2.0000E+00	1.0000E+00	0.	0.	-5.0000E-01	2.0000E+00
38	4.0000E+00	1.0000E+00	0.	0.	-5.0000E-01	2.0000E+00
39	4.0000E+00	1.0000E+00	0.	0.	-5.0000E-01	2.0000E+00
40	4.0000E+00	1.0000E+00	0.	0.	-5.0000E-01	2.0000E+00
41	4.0000E+00	1.0000E+00	0.	0.	-5.0000E-01	2.0000E+00
42	4.0000E+00	1.0000E+00	0.	0.	-5.0000E-01	2.0000E+00
43	2.0000E+00	1.0000E+00	0.	0.	-5.0000E-01	2.0000E+00
44	4.0000E+00	1.0000E+00	0.	0.	-5.0000E-01	2.0000E+00
45	4.0000E+00	1.0000E+00	0.	0.	-5.0000E-01	2.0000E+00
46	4.0000E+00	1.0000E+00	0.	0.	-5.0000E-01	2.0000E+00
47	4.0000E+00	1.0000E+00	0.	0.	-5.0000E-01	2.0000E+00
48	4.0000E+00	1.0000E+00	0.	0.	-5.0000E-01	2.0000E+00
49	2.0000E+00	1.0000E+00	0.	0.	-5.0000E-01	2.0000E+00
50	4.0000E+00	1.0000E+00	0.	0.	-5.0000E-01	2.0000E+00

TABLE 2.2-3(CONT'D)

CEFLASH-4B INPUT FOR PROBLEM 2.2

COMBUSTION ENGINEERING CEFLASH4B VERSION 11-03-1976 76308

0. CONTROL VOLUMES

NODE	AREA	HEIGHT	EXIT ELEV	INLET ELEV	BOTTM ELEV	FLOW AREA
51	2.0000E+00	1.0000E+00	0.	0.	-5.0000E-01	2.0000E+00
52	4.0000E+00	1.0000E+00	0.	0.	-5.0000E-01	2.0000E+00
53	4.0000E+00	1.0000E+00	0.	0.	-5.0000E-01	2.0000E+00
54	4.0000E+00	1.0000E+00	0.	0.	-5.0000E-01	2.0000E+00
55	1.0000E+02	2.0000E+02	-1.0000E+02	5.0000E-01	-1.0000E+02	1.0000E+02
56	2.1460E-01	1.0000E+00	0.	0.	-5.0000E-01	2.0000E+00
57	2.1460E-01	1.0000E+00	0.	0.	-5.0000E-01	2.0000E+00
58	2.1460E-01	1.0000E+00	0.	0.	-5.0000E-01	2.0000E+00

TABLE 2.2-3(con't)

CEFLASH-4B INPUT FOR PROBLEM 2.2

COMBUSTION ENGINEERING — CEFLASH4B — VERSION 11 03 1976 — 76305

NODAL PROPERTIES

NODE	PRESSURE	ENTH SURC	LEVEL TRH
1	1.700DE+03	5.3997E+02	0.
2	2.100DE+03	5.3997E+02	0.
3	2.100DE+03	5.3997E+02	0.
4	2.100DE+03	5.3997E+02	0.
5	2.100DE+03	5.3997E+02	0.
6	2.100DE+03	5.3997E+02	0.
7	2.100DE+03	5.3997E+02	0.
8	2.100DE+03	5.3997E+02	0.
9	2.100DE+03	5.3997E+02	0.
10	2.100DE+03	5.3997E+02	0.
11	2.100DE+03	5.3997E+02	0.
12	2.100DE+03	5.3997E+02	0.
13	2.100DE+03	5.3997E+02	0.
14	2.100DE+03	5.3997E+02	0.
15	2.100DE+03	5.3997E+02	0.
16	2.100DE+03	5.3997E+02	0.
17	2.100DE+03	5.3997E+02	0.
18	2.100DE+03	5.3997E+02	0.
19	2.100DE+03	5.3997E+02	0.
20	2.100DE+03	5.3997E+02	0.
21	2.100DE+03	5.3997E+02	0.
22	2.100DE+03	5.3997E+02	0.
23	2.100DE+03	5.3997E+02	0.
24	2.100DE+03	5.3997E+02	0.
25	2.100DE+03	5.3997E+02	0.
26	2.100DE+03	5.3997E+02	0.
27	2.100DE+03	5.3997E+02	0.
28	2.100DE+03	5.3997E+02	0.
29	2.100DE+03	5.3997E+02	0.
30	2.100DE+03	5.3997E+02	0.
31	2.100DE+03	5.3997E+02	0.
32	2.100DE+03	5.3997E+02	0.
33	2.100DE+03	5.3997E+02	0.
34	2.100DE+03	5.3997E+02	0.
35	2.100DE+03	5.3997E+02	0.
36	2.100DE+03	5.3997E+02	0.
37	2.100DE+03	5.3997E+02	0.
38	2.100DE+03	5.3997E+02	0.
39	2.100DE+03	5.3997E+02	0.
40	2.100DE+03	5.3997E+02	0.
41	2.100DE+03	5.3997E+02	0.
42	2.100DE+03	5.3997E+02	0.
43	2.100DE+03	5.3997E+02	0.
44	2.100DE+03	5.3997E+02	0.
45	2.100DE+03	5.3997E+02	0.
46	2.100DE+03	5.3997E+02	0.
47	2.100DE+03	5.3997E+02	0.
48	2.100DE+03	5.3997E+02	0.
49	2.100DE+03	5.3997E+02	0.
50	2.100DE+03	5.3997E+02	0.

TABLE 2.2-3 (Con't)

CEFLASH-4B INPUT FOR PROBLEM 2.2

COMBUSTION ENGINEERING CEFLASH4B VERSION 11 03 1976 76308

NODAL PROPERTIES

NODE	PRESSURE	ENTH SUBC	LEVEL TPH
51	2.1000E+03	5.3997E+02	0.
52	2.1000E+03	5.3997E+02	0.
53	2.1000E+03	5.3997E+02	0.
54	2.1000E+03	5.3997E+02	0.
55	1.7000E+03	5.4057E+02	0.
56	2.1000E+03	5.3997E+02	0.
57	2.1000E+03	5.3997E+02	0.
58	2.1000E+03	5.3997E+02	0.

LEAK FLOW PATHS TO CONTAINMENT NODE

NODE	FLOW PATHS
55	0

TABLE 2.2-3 (Con't)

CEFLASH-4B INPUT FOR PROBLEM 2.2

COMBUSTION ENGINEERING — CEFLASH4B — VERSION 11-03-1976 — 76308

C. FLOW PATHS

PATH	TYPE	NODE FROM	NODE TO	NO	SUM L/A	AREA	DIAMETER	NOM FLOW AREA UP	NOM FLOW AREA DOWN	FRICTION K OR DELTA P	GEOM FWD K OR DELTA P	GEOM REV K OR DELTA P
1	8	1	2	0.	5.0000E-01	2.0000E+00	2.0000E+00	2.0000E+00	2.0000E+00	1.5000E-02	0.	0.
2	8	2	3	0.	1.0000E+00	2.0000E+00	2.0000E+00	2.0000E+00	2.0000E+00	3.0000E-02	0.	0.
3	8	3	4	0.	5.0000E-01	2.0000E+00	2.0000E+00	2.0000E+00	2.0000E+00	1.5000E-02	0.	0.
4	8	57	5	0.	5.0000E-01	2.0000E+00	2.0000E+00	2.0000E+00	2.0000E+00	3.0000E-02	0.	0.
5	8	5	6	0.	1.0000E+00	2.0000E+00	2.0000E+00	2.0000E+00	2.0000E+00	3.0000E-02	0.	0.
6	8	1	7	0.	2.0000E+00	1.0000E+00	2.0000E+00	1.0000E+00	1.0000E+00	4.5000E-02	0.	0.
7	8	2	8	0.	1.5000E+00	2.0000E+00	2.0000E+00	2.0000E+00	2.0000E+00	4.5000E-02	0.	0.
8	8	3	9	0.	1.5000E+00	2.0000E+00	2.0000E+00	2.0000E+00	2.0000E+00	3.0000E-02	0.	0.
9	8	56	10	0.	1.0000E+00	2.0000E+00	2.0000E+00	2.0000E+00	2.0000E+00	4.5000E-02	0.	0.
10	8	5	11	0.	1.5000E+00	2.0000E+00	2.0000E+00	2.0000E+00	2.0000E+00	4.5000E-02	0.	0.
11	8	6	12	0.	1.5000E+00	2.0000E+00	2.0000E+00	2.0000E+00	2.0000E+00	3.0000E-02	0.	0.
12	8	7	8	0.	1.0000E+00	2.0000E+00	2.0000E+00	2.0000E+00	2.0000E+00	3.0000E-02	0.	0.
13	8	8	9	0.	1.0000E+00	2.0000E+00	2.0000E+00	2.0000E+00	2.0000E+00	3.0000E-02	0.	0.
14	8	9	10	0.	1.0000E+00	2.0000E+00	2.0000E+00	2.0000E+00	2.0000E+00	3.0000E-02	0.	0.
15	8	10	11	0.	1.0000E+00	2.0000E+00	2.0000E+00	2.0000E+00	2.0000E+00	3.0000E-02	0.	0.
16	8	11	12	0.	2.0000E+00	1.0000E+00	2.0000E+00	1.0000E+00	1.0000E+00	3.0000E-02	0.	0.
17	8	7	13	0.	1.0000E+00	2.0000E+00	2.0000E+00	2.0000E+00	2.0000E+00	3.0000E-02	0.	0.
18	8	8	14	0.	1.0000E+00	2.0000E+00	2.0000E+00	2.0000E+00	2.0000E+00	3.0000E-02	0.	0.
19	8	9	15	0.	1.0000E+00	2.0000E+00	2.0000E+00	2.0000E+00	2.0000E+00	3.0000E-02	0.	0.
20	8	10	16	0.	1.0000E+00	2.0000E+00	2.0000E+00	2.0000E+00	2.0000E+00	3.0000E-02	0.	0.
21	8	11	17	0.	1.0000E+00	2.0000E+00	2.0000E+00	2.0000E+00	2.0000E+00	3.0000E-02	0.	0.
22	8	12	18	0.	1.0000E+00	2.0000E+00	1.5000E+00	2.0000E+00	2.0000E+00	3.7500E-02	0.	0.
23	8	13	14	0.	1.0000E+00	2.0000E+00	1.5000E+00	2.0000E+00	2.0000E+00	3.7500E-02	0.	0.
24	8	14	15	0.	1.0000E+00	2.0000E+00	1.5000E+00	2.0000E+00	2.0000E+00	3.7500E-02	0.	0.
25	8	15	16	0.	1.0000E+00	2.0000E+00	1.5000E+00	2.0000E+00	2.0000E+00	3.7500E-02	0.	0.
26	8	16	17	0.	1.0000E+00	2.0000E+00	1.5000E+00	2.0000E+00	2.0000E+00	3.7500E-02	0.	0.
27	8	17	18	0.	2.0000E+00	1.0000E+00	2.0000E+00	1.0000E+00	1.0000E+00	3.0000E-02	0.	0.
28	8	1	19	0.	1.5000E+00	2.0000E+00	2.0000E+00	2.0000E+00	2.0000E+00	4.5000E-02	0.	0.
29	8	2	20	0.	1.5000E+00	2.0000E+00	2.0000E+00	2.0000E+00	2.0000E+00	4.5000E-02	0.	0.
30	8	3	21	0.	1.0000E+00	2.0000E+00	2.0000E+00	2.0000E+00	2.0000E+00	3.0000E-02	0.	0.
31	8	58	22	0.	1.5000E+00	2.0000E+00	2.0000E+00	2.0000E+00	2.0000E+00	4.5000E-02	0.	0.
32	8	5	23	0.	1.5000E+00	2.0000E+00	2.0000E+00	2.0000E+00	2.0000E+00	4.5000E-02	0.	0.
33	8	6	24	0.	1.0000E+00	2.0000E+00	2.0000E+00	2.0000E+00	2.0000E+00	3.0000E-02	0.	0.
34	8	19	20	0.	1.0000E+00	2.0000E+00	2.0000E+00	2.0000E+00	2.0000E+00	3.0000E-02	0.	0.
35	8	20	21	0.	1.0000E+00	2.0000E+00	2.0000E+00	2.0000E+00	2.0000E+00	3.0000E-02	0.	0.
36	8	21	22	0.	1.0000E+00	2.0000E+00	2.0000E+00	2.0000E+00	2.0000E+00	3.0000E-02	0.	0.
37	8	22	23	0.	1.0000E+00	2.0000E+00	2.0000E+00	2.0000E+00	2.0000E+00	3.0000E-02	0.	0.
38	8	23	24	0.	1.0000E+00	1.0000E+00	2.0000E+00	2.0000E+00	2.0000E+00	1.5000E-02	0.	0.
39	8	10	25	0.	5.0000E-01	2.0000E+00	2.0000E+00	2.0000E+00	2.0000E+00	1.5000E-02	0.	0.
40	8	25	26	0.	5.0000E-01	2.0000E+00	2.0000E+00	2.0000E+00	2.0000E+00	1.5000E-02	0.	0.
41	8	26	27	0.	5.0000E-01	2.0000E+00	2.0000E+00	2.0000E+00	2.0000E+00	1.5000E-02	0.	0.
42	8	27	28	0.	5.0000E-01	2.0000E+00	2.0000E+00	2.0000E+00	2.0000E+00	1.5000E-02	0.	0.
43	8	28	29	0.	5.0000E-01	2.0000E+00	2.0000E+00	2.0000E+00	2.0000E+00	1.5000E-02	0.	0.
44	8	29	30	0.	1.0000E+00	2.0000E+00	2.0000E+00	2.0000E+00	2.0000E+00	3.0000E-02	0.	0.
45	8	25	26	0.	1.0000E+00	2.0000E+00	2.0000E+00	2.0000E+00	2.0000E+00	3.0000E-02	0.	0.
46	8	26	27	0.	1.0000E+00	2.0000E+00	2.0000E+00	2.0000E+00	2.0000E+00	3.0000E-02	0.	0.
47	8	27	28	0.	1.0000E+00	2.0000E+00	2.0000E+00	2.0000E+00	2.0000E+00	3.0000E-02	0.	0.
48	8	28	29	0.	1.0000E+00	2.0000E+00	2.0000E+00	2.0000E+00	2.0000E+00	3.0000E-02	0.	0.

POOR ORIGINAL

2.2-12

5966 301

C. FLOW PATHS

PATH	TYPE	NODE FROM	NODE TO	WO	SUM L/A	AREA	DIAMETER	MOM FLOW AREA UP	MOM FLOW AREA DOWN	FRICTION K OR DELTA P	GEOM FWD K OR DELTA P	GEOM RVS K OR DELTA P
50	8	25	31	0.	2.0000E+00	1.0000E+00	2.0000E+00	1.0000E+00	1.0000E+03	3.0000E-02	0.	0.
51	8	26	32	0.	1.0000E+00	2.0000E+00	2.0000E+00	2.0000E+00	2.0000E+03	3.0000E-02	0.	0.
52	8	27	33	0.	1.0000E+00	2.0000E+00	2.0000E+00	2.0000E+00	2.0000E+03	3.0000E-02	0.	0.
53	8	28	34	0.	1.0000E+00	2.0000E+00	2.0000E+00	2.0000E+00	2.0000E+03	3.0000E-02	0.	0.
54	8	29	35	0.	1.0000E+00	2.0000E+00	2.0000E+00	2.0000E+00	2.0000E+03	3.0000E-02	0.	0.
55	8	30	36	0.	1.0000E+00	2.0000E+00	2.0000E+00	2.0000E+00	2.0000E+03	3.0000E-02	0.	0.
56	8	31	32	0.	1.0000E+00	2.0000E+00	2.0000E+00	2.0000E+00	2.0000E+03	3.0000E-02	0.	0.
57	8	32	33	0.	1.0000E+00	2.0000E+00	2.0000E+00	2.0000E+00	2.0000E+00	3.0000E-02	0.	0.
58	8	33	34	0.	1.0000E+00	2.0000E+00	2.0000E+00	2.0000E+00	2.0000E+03	3.0000E-02	0.	0.
59	8	34	35	0.	1.0000E+00	2.0000E+00	2.0000E+00	2.0000E+00	2.0000E+03	3.0000E-02	0.	0.
60	8	35	36	0.	1.0000E+00	2.0000E+00	2.0000E+00	2.0000E+00	2.0000E+03	3.0000E-02	0.	0.
61	8	31	37	0.	2.0000E+00	1.0000E+00	2.0000E+00	1.0000E+00	1.0000E+03	3.0000E-02	0.	0.
62	8	32	38	0.	1.0000E+00	2.0000E+00	2.0000E+00	2.0000E+00	2.0000E+03	3.0000E-02	0.	0.
63	8	33	39	0.	1.0000E+00	2.0000E+00	2.0000E+00	2.0000E+00	2.0000E+03	3.0000E-02	0.	0.
64	8	34	40	0.	1.0000E+00	2.0000E+00	2.0000E+00	2.0000E+00	2.0000E+03	3.0000E-02	0.	0.
65	8	35	41	0.	1.0000E+00	2.0000E+00	2.0000E+00	2.0000E+00	2.0000E+03	3.0000E-02	0.	0.
66	8	36	42	0.	1.0000E+00	2.0000E+00	2.0000E+00	2.0000E+00	2.0000E+03	3.0000E-02	0.	0.
67	8	37	38	0.	1.0000E+00	2.0000E+00	2.0000E+00	2.0000E+00	2.0000E+03	3.0000E-02	0.	0.
68	8	38	39	0.	1.0000E+00	2.0000E+00	2.0000E+00	2.0000E+00	2.0000E+03	3.0000E-02	0.	0.
69	8	39	40	0.	1.0000E+00	2.0000E+00	2.0000E+00	2.0000E+00	2.0000E+03	3.0000E-02	0.	0.
70	8	40	41	0.	1.0000E+00	2.0000E+00	2.0000E+00	2.0000E+00	2.0000E+03	3.0000E-02	0.	0.
71	8	41	42	0.	1.0000E+00	2.0000E+00	2.0000E+00	2.0000E+00	2.0000E+03	3.0000E-02	0.	0.
72	8	37	43	0.	2.0000E+00	1.0000E+00	2.0000E+00	1.0000E+00	1.0000E+03	3.0000E-02	0.	0.
73	8	38	44	0.	1.0000E+00	2.0000E+00	2.0000E+00	2.0000E+00	2.0000E+03	3.0000E-02	0.	0.
74	8	39	45	0.	1.0000E+00	2.0000E+00	2.0000E+00	2.0000E+00	2.0000E+03	3.0000E-02	0.	0.
75	8	40	46	0.	1.0000E+00	2.0000E+00	2.0000E+00	2.0000E+00	2.0000E+03	3.0000E-02	0.	0.
76	8	41	47	0.	1.0000E+00	2.0000E+00	2.0000E+00	2.0000E+00	2.0000E+03	3.0000E-02	0.	0.
77	8	42	48	0.	1.0000E+00	2.0000E+00	2.0000E+00	2.0000E+00	2.0000E+03	3.0000E-02	0.	0.
78	8	43	44	0.	1.0000E+00	2.0000E+00	2.0000E+00	2.0000E+00	2.0000E+03	3.0000E-02	0.	0.
79	8	44	45	0.	1.0000E+00	2.0000E+00	2.0000E+00	2.0000E+00	2.0000E+03	3.0000E-02	0.	0.
80	8	45	46	0.	1.0000E+00	2.0000E+00	2.0000E+00	2.0000E+00	2.0000E+03	3.0000E-02	0.	0.
81	8	46	47	0.	1.0000E+00	2.0000E+00	2.0000E+00	2.0000E+00	2.0000E+03	3.0000E-02	0.	0.
82	8	47	48	0.	1.0000E+00	2.0000E+00	2.0000E+00	2.0000E+00	2.0000E+00	3.0000E-02	0.	0.
83	8	43	49	0.	2.0000E+00	1.0000E+00	2.0000E+00	1.0000E+00	1.0000E+03	3.0000E-02	0.	0.
84	8	44	50	0.	1.0000E+00	2.0000E+00	2.0000E+00	2.0000E+00	2.0000E+03	3.0000E-02	0.	0.
85	8	45	51	0.	1.0000E+00	2.0000E+00	2.0000E+00	2.0000E+00	2.0000E+03	3.0000E-02	0.	0.
86	8	46	52	0.	1.0000E+00	2.0000E+00	2.0000E+00	2.0000E+00	2.0000E+03	3.0000E-02	0.	0.
87	8	47	53	0.	1.0000E+00	2.0000E+00	2.0000E+00	2.0000E+00	2.0000E+03	3.0000E-02	0.	0.
88	8	48	54	0.	1.0000E+00	2.0000E+00	2.0000E+00	2.0000E+00	2.0000E+03	3.7500E-02	0.	0.
89	8	49	50	0.	1.0000E+00	2.0000E+00	1.6000E+00	2.0000E+00	2.0000E+03	3.7500E-02	0.	0.
90	8	50	51	0.	1.0000E+00	2.0000E+00	1.6000E+00	2.0000E+00	2.0000E+03	3.7500E-02	0.	0.
91	8	51	52	0.	1.0000E+00	2.0000E+00	1.6000E+00	2.0000E+00	2.0000E+03	3.7500E-02	0.	0.
92	8	52	53	0.	1.0000E+00	2.0000E+00	1.6000E+00	2.0000E+00	2.0000E+03	3.7500E-02	0.	0.
93	8	53	54	0.	1.0000E+00	2.0000E+00	1.6000E+00	2.0000E+00	2.0000E+03	3.7500E-02	0.	0.
94	8	1	55	0.	1.0000E-06	1.5708E+00	1.0000E+00	1.0000E+00	1.0000E+02	3.0000E-02	0.	0.

			L/D	AREA	DISCHARGE COEFF	DISCHARGE COEFF	DISCHARGE COEFF	DISCHARGE COEFF
95	0	0						

POOR ORIGINAL

596 302

TABLE 2.2-3 (Con't)

CEFLASH-4B INPUT FOR PROBLEM 2.2

COMBUSTION ENGINEERING CEFLASH4B VERSION 11 03 1976 76308

OPTIONS BY FLOW PATHS

FLOW PATH	MOMENTUM FLUX	CRITICAL FLOW	MIN. AREA CRIT FLOW	LENGTH
1	0	1	2.0000E+00	1.0000E+00
2	0	1	2.0000E+00	2.0000E+00
3	0	1	2.0000E+00	1.0000E+00
4	0	1	2.0000E+00	1.0000E+00
5	0	1	2.0000E+00	2.0000E+00
6	0	1	1.0000E+00	2.0000E+00
7	0	1	2.0000E+00	3.0000E+00
8	0	1	2.0000E+00	3.0000E+00
9	0	1	2.0000E+00	2.0000E+00
10	0	1	2.0000E+00	3.0000E+00
11	0	1	2.0000E+00	3.0000E+00
12	0	1	2.0000E+00	2.0000E+00
13	0	1	2.0000E+00	2.0000E+00
14	0	1	2.0000E+00	2.0000E+00
15	0	1	2.0000E+00	2.0000E+00
16	0	1	1.0000E+00	2.0000E+00
17	0	1	2.0000E+00	2.0000E+00
18	0	1	2.0000E+00	2.0000E+00
19	0	1	2.0000E+00	2.0000E+00
20	0	1	2.0000E+00	2.0000E+00
21	0	1	2.0000E+00	2.0000E+00
22	0	1	2.0000E+00	2.0000E+00
23	0	1	2.0000E+00	2.0000E+00
24	0	1	2.0000E+00	2.0000E+00
25	0	1	2.0000E+00	2.0000E+00
26	0	1	2.0000E+00	2.0000E+00
27	0	1	1.0000E+00	2.0000E+00
28	0	1	2.0000E+00	3.0000E+00
29	0	1	2.0000E+00	3.0000E+00
30	0	1	2.0000E+00	2.0000E+00
31	0	1	2.0000E+00	3.0000E+00
32	0	1	2.0000E+00	3.0000E+00
33	0	1	2.0000E+00	2.0000E+00
34	0	1	2.0000E+00	2.0000E+00
35	0	1	2.0000E+00	2.0000E+00
36	0	1	2.0000E+00	2.0000E+00
37	0	1	2.0000E+00	2.0000E+00
38	0	1	1.0000E+00	1.0000E+00
39	0	1	2.0000E+00	1.0000E+00
40	0	1	2.0000E+00	1.0000E+00
41	0	1	2.0000E+00	1.0000E+00
42	0	1	2.0000E+00	1.0000E+00
43	0	1	2.0000E+00	1.0000E+00
44	0	1	2.0000E+00	2.0000E+00
45	0	1	2.0000E+00	2.0000E+00
46	0	1	2.0000E+00	2.0000E+00
47	0	1	2.0000E+00	2.0000E+00
48	0	1	2.0000E+00	2.0000E+00
49	0	1	2.0000E+00	2.0000E+00
50	0	1	2.0000E+00	2.0000E+00

2.2-14

COMBUSTION ENGINEERING CEFLASH4B VERSION 11 03 1976 76308

OPTIONS BY FLOW PATHS

FLOW PATH	MOMENTUM FLUX	CRITICAL FLOW	MIN AREA CRIT FLOW	LENGTH
52	0	1	2.0000E+00	2.0000E+00
53	0	1	2.0000E+00	2.0000E+00
54	0	1	2.0000E+00	2.0000E+00
55	0	1	2.0000E+00	2.0000E+00
56	0	1	2.0000E+00	2.0000E+00
57	0	1	2.0000E+00	2.0000E+00
58	0	1	2.0000E+00	2.0000E+00
59	0	1	2.0000E+00	2.0000E+00
60	0	1	2.0000E+00	2.0000E+00
61	0	1	1.0000E+00	2.0000E+00
62	0	1	2.0000E+00	2.0000E+00
63	0	1	2.0000E+00	2.0000E+00
64	0	1	2.0000E+00	2.0000E+00
65	0	1	2.0000E+00	2.0000E+00
66	0	1	2.0000E+00	2.0000E+00
67	0	1	2.0000E+00	2.0000E+00
68	0	1	2.0000E+00	2.0000E+00
69	0	1	2.0000E+00	2.0000E+00
70	0	1	2.0000E+00	2.0000E+00
71	0	1	2.0000E+00	2.0000E+00
72	0	1	1.0000E+00	2.0000E+00
73	0	1	2.0000E+00	2.0000E+00
74	0	1	2.0000E+00	2.0000E+00
75	0	1	2.0000E+00	2.0000E+00
76	0	1	2.0000E+00	2.0000E+00
77	0	1	2.0000E+00	2.0000E+00
78	0	1	2.0000E+00	2.0000E+00
79	0	1	2.0000E+00	2.0000E+00
80	0	1	2.0000E+00	2.0000E+00
81	0	1	2.0000E+00	2.0000E+00
82	0	1	2.0000E+00	2.0000E+00
83	0	1	1.0000E+00	2.0000E+00
84	0	1	2.0000E+00	2.0000E+00
85	0	1	2.0000E+00	2.0000E+00
86	0	1	2.0000E+00	2.0000E+00
87	0	1	2.0000E+00	2.0000E+00
88	0	1	2.0000E+00	2.0000E+00
89	0	1	2.0000E+00	2.0000E+00
90	0	1	2.0000E+00	2.0000E+00
91	0	1	2.0000E+00	2.0000E+00
92	0	1	2.0000E+00	2.0000E+00
93	0	1	2.0000E+00	2.0000E+00
94	0	1	1.5700E+00	1.0000E+00

Figure 2.2-1
PLANAR DECOMPRESSION WITH OBSTRUCTION

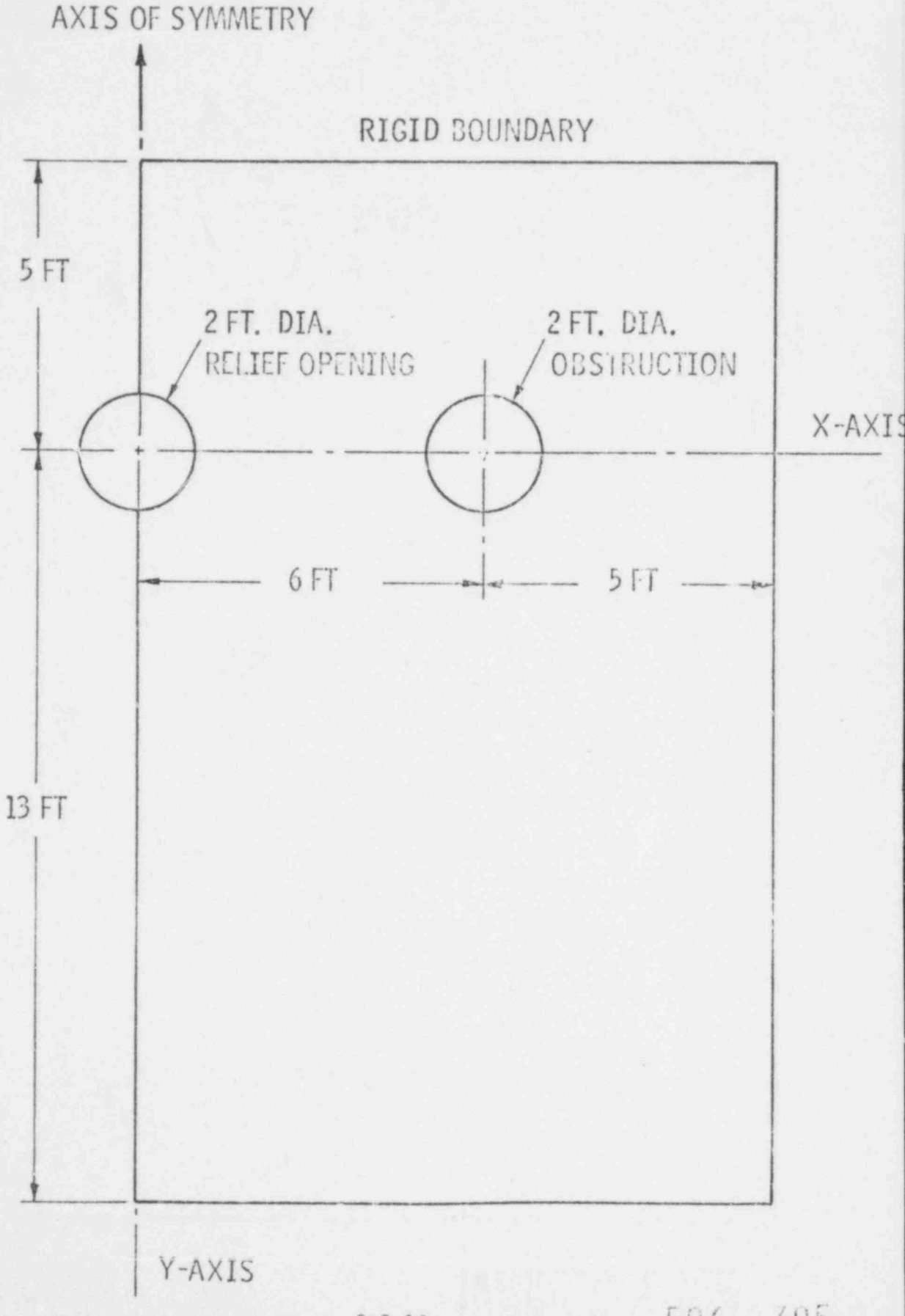

Figure 2.2-2
CEFLASH-4B MODEL FOR PLANAR DECOMPRESSION WITH OBSTRUCTION
PROBLEM 2.2

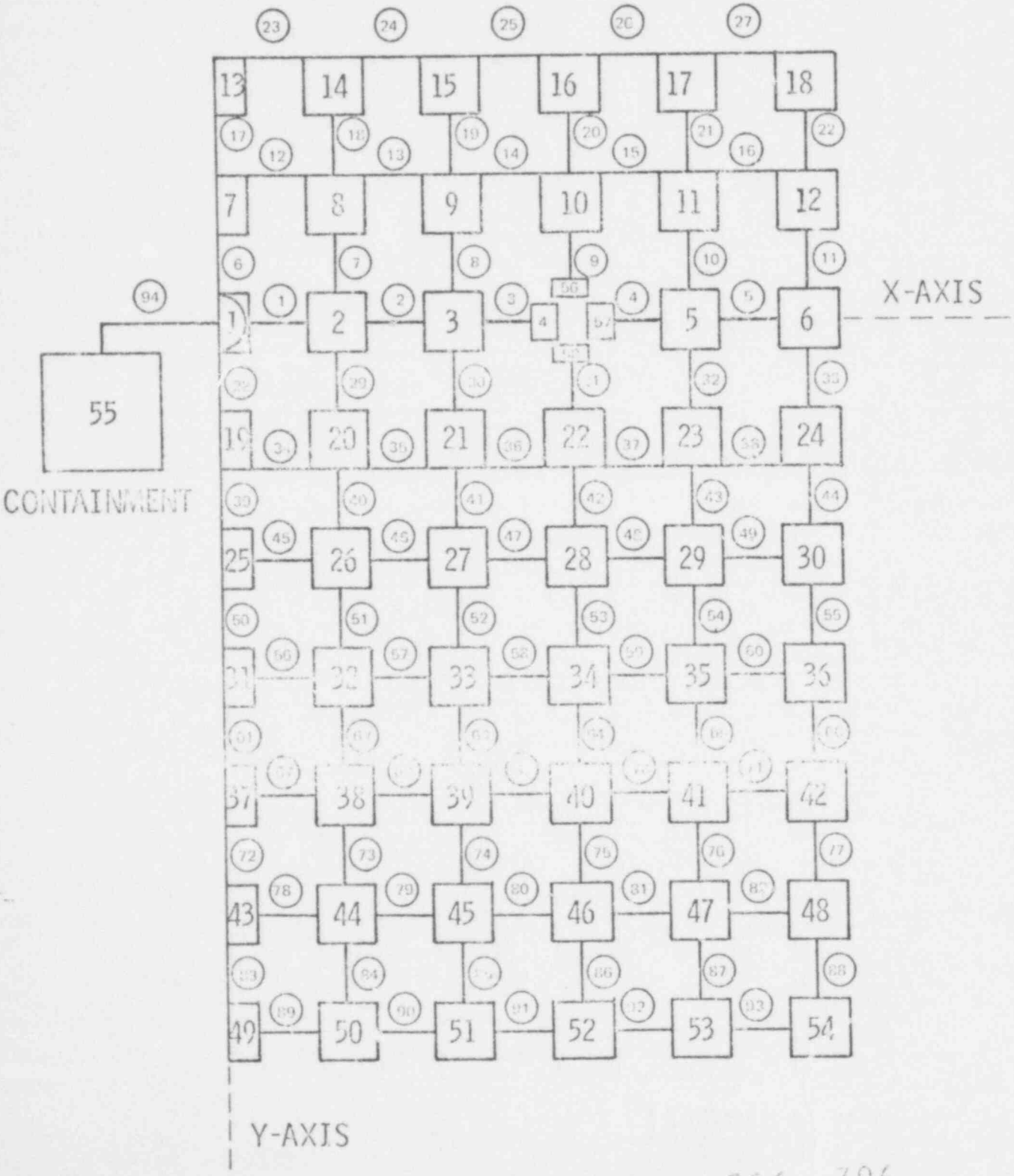

Figure 2.2-3

PLANAR DECOMPRESSION WITH OBSTRUCTION
ABSOLUTE PRESSURE AT 0.5 MSEC

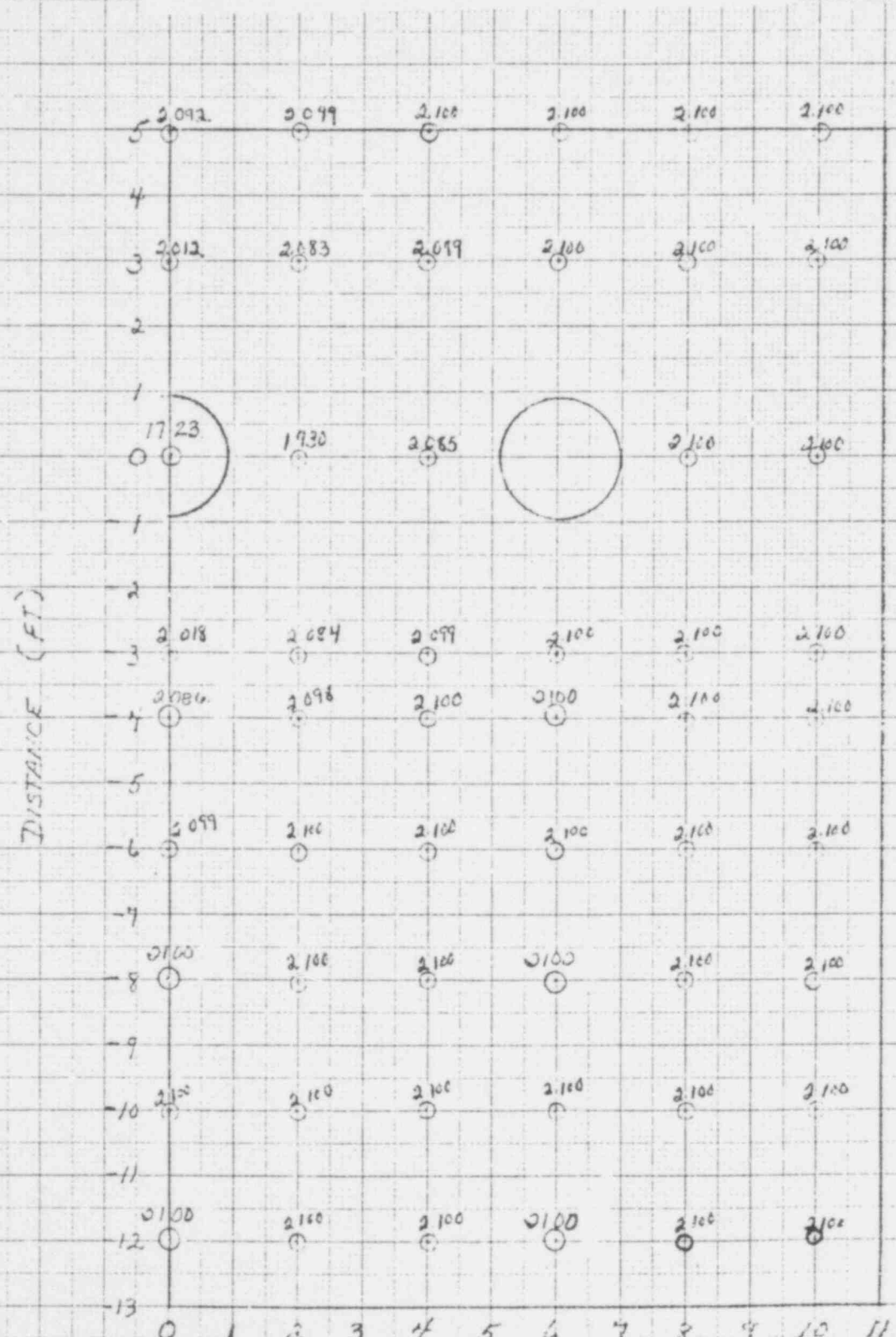

Figure 2.2-4

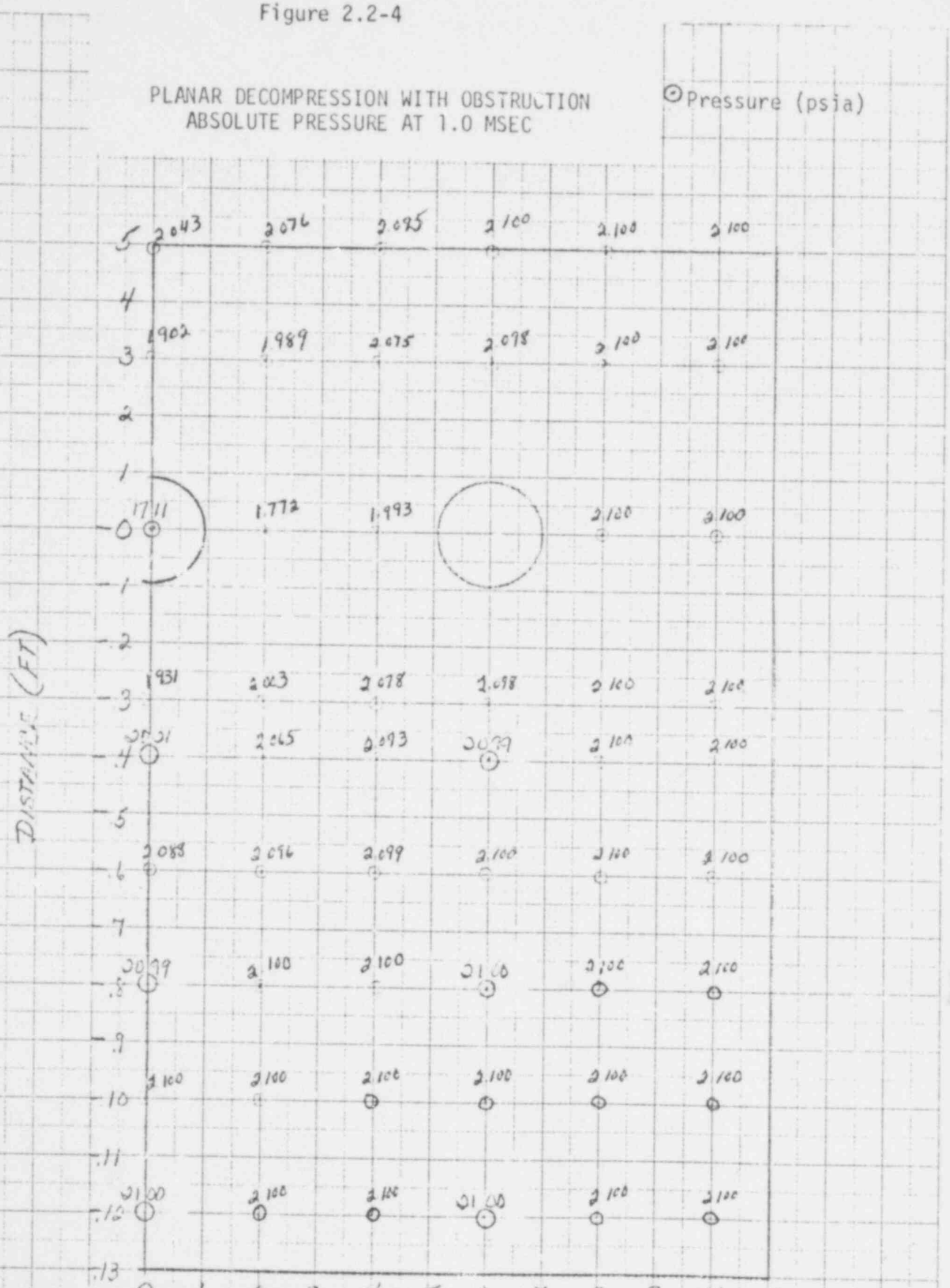

Figure 2.2-5

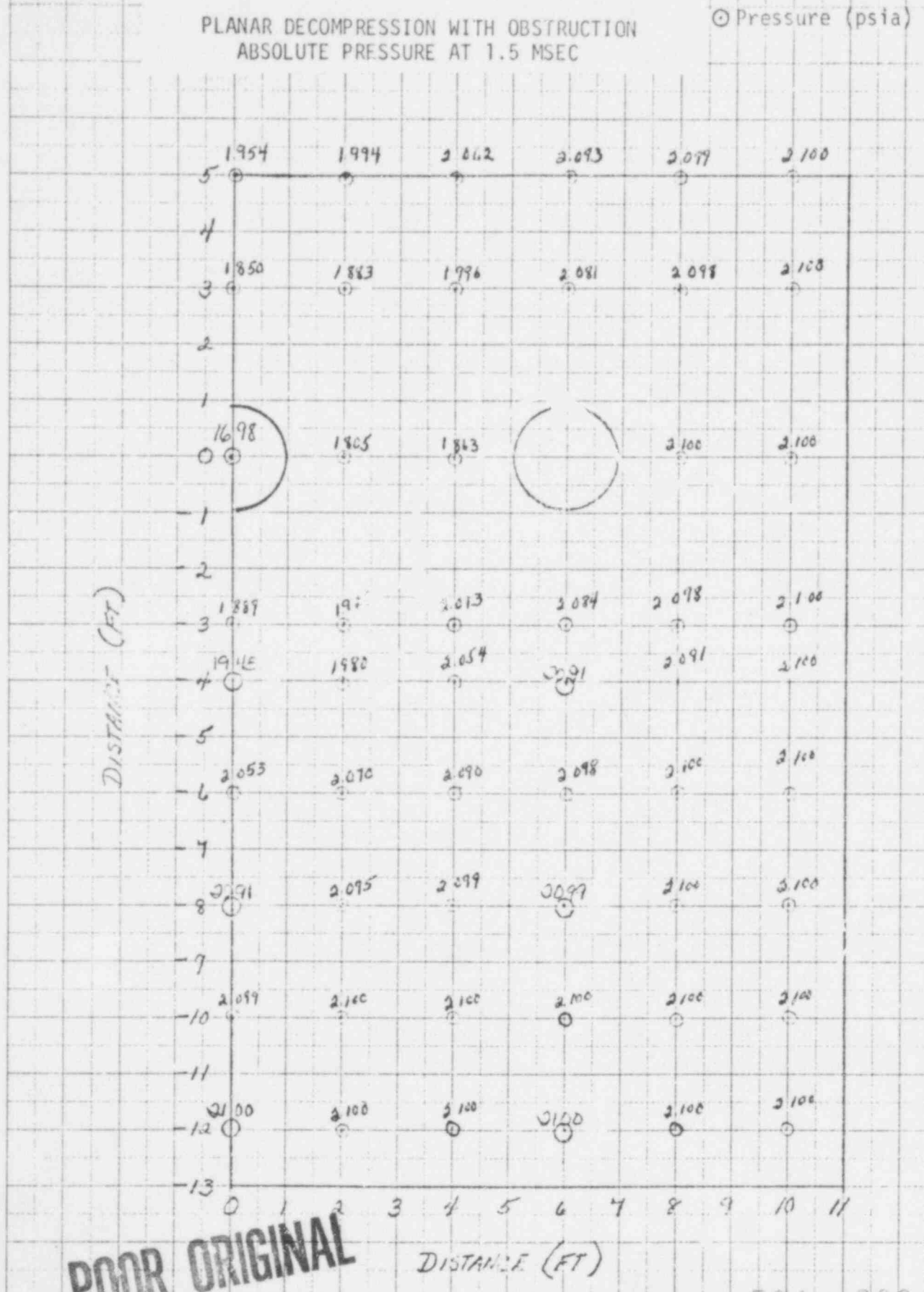

Figure 2.2-6

PLANAR DECOMPRESSION WITH OBSTRUCTION
ABSOLUTE PRESSURE AT 2.0 MSEC

⊙ Pressure (psia)

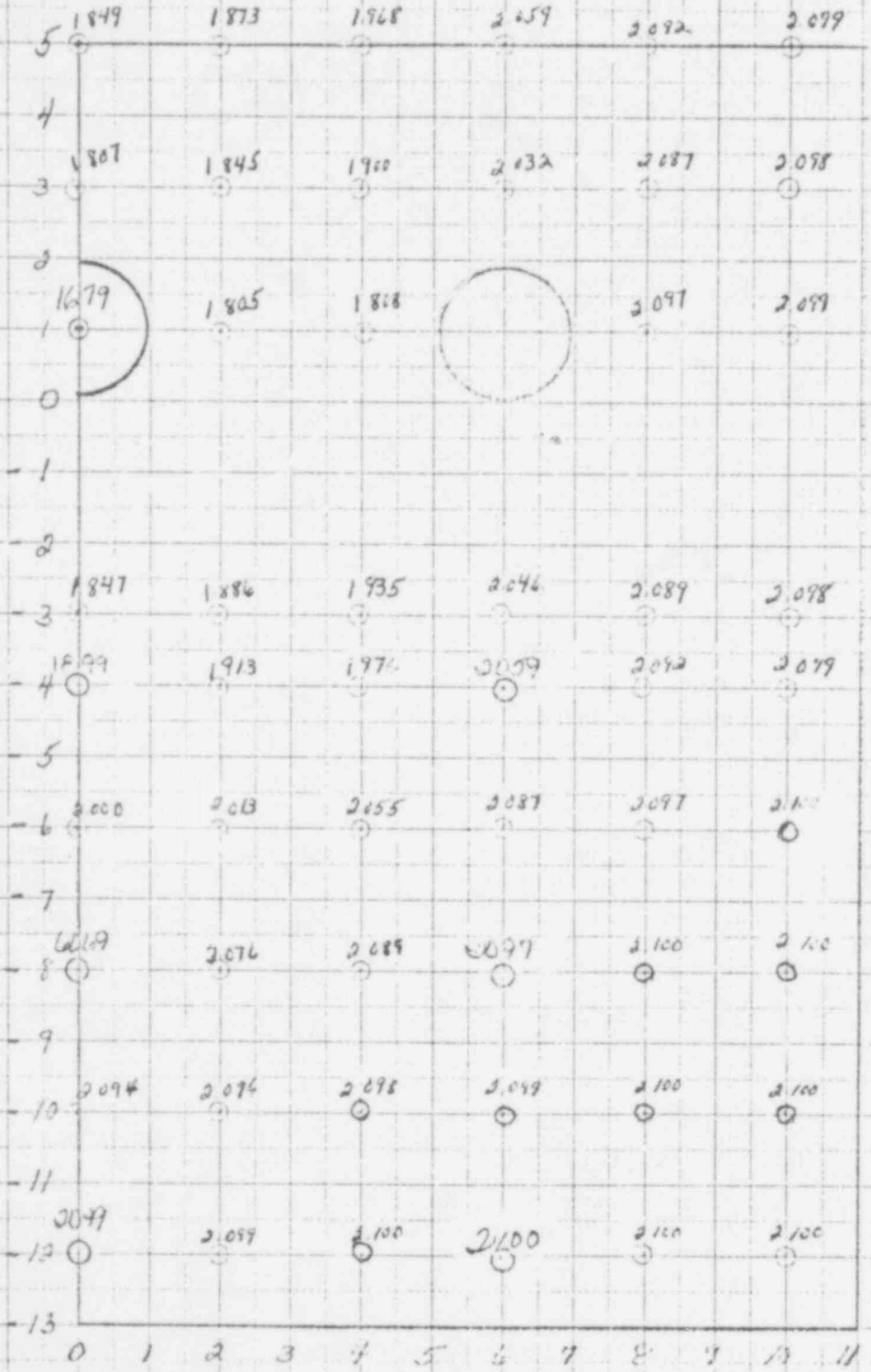

8/22/78 KCD

Figure 2.2-7

PLANAR DECOMPRESSION WITH OBSTRUCTION
ABSOLUTE PRESSURE AT 2.5 MSEC

⊙ Pressure(psia)

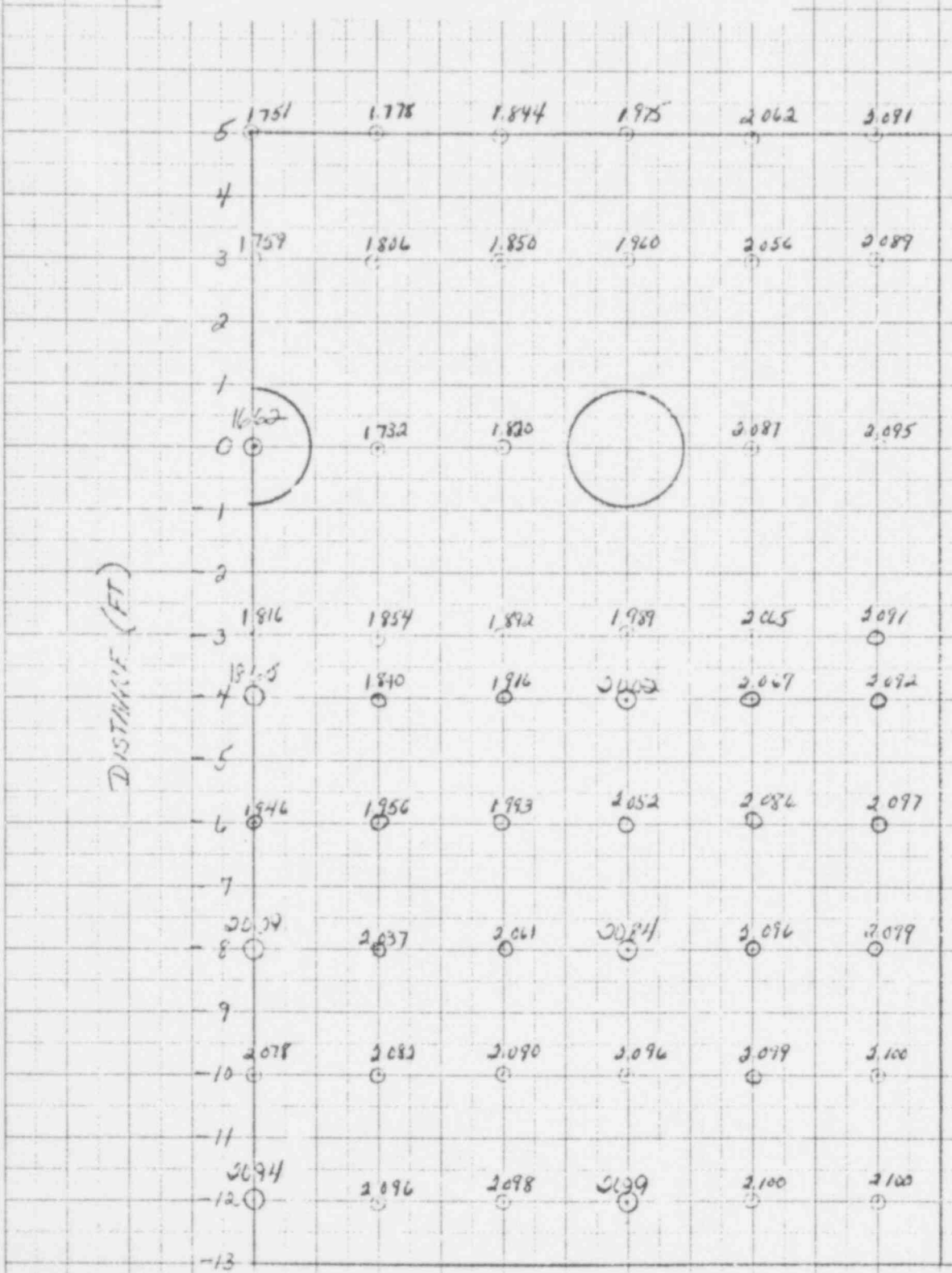

8/28/78 KCA

Figure 2.2-8

PLANAR DECOMPRESSION WITH OBSTRUCTION
ABSOLUTE PRESSURE AT 3.0 MSEC

⊙Pressure (psia)

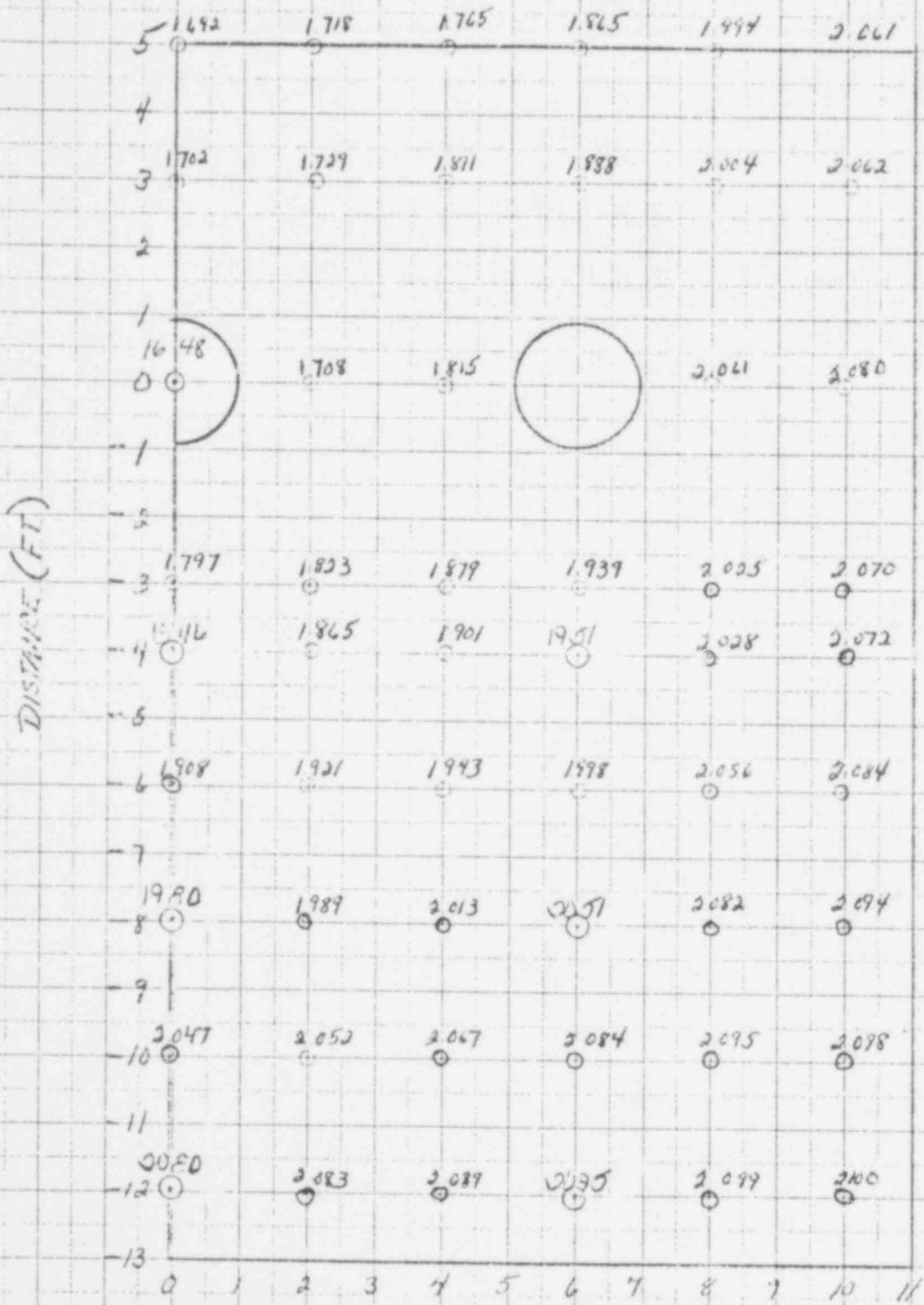

DISTANCE (FT)

8/23/78 AL6

FIGURE 2.2-9

PLANAR DECOMPRESSION WITH OBSTRUCTION
FLOW RATE AT 0.5 MSEC

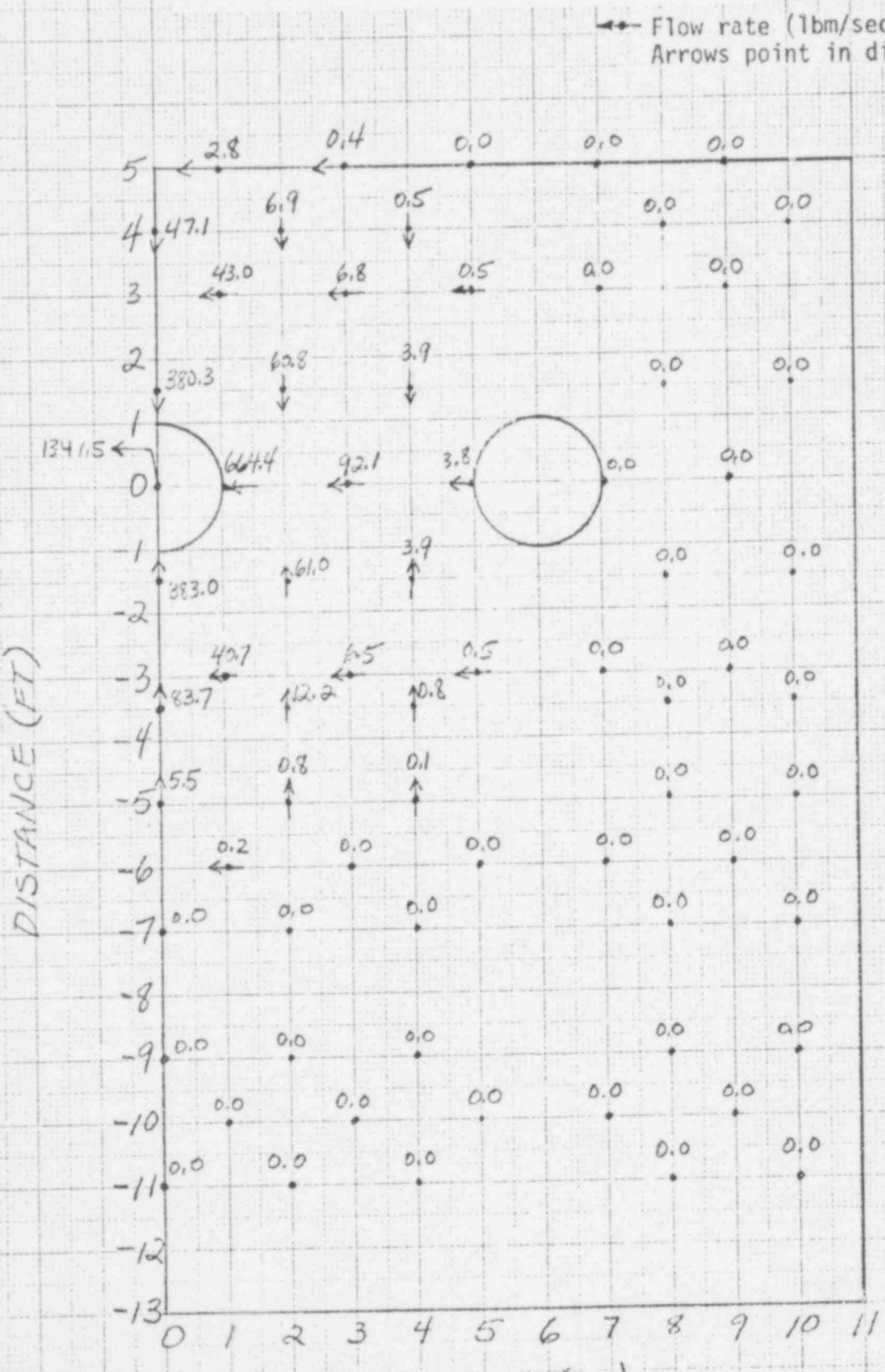

FIGURE 2.2-10

PLANAR DECOMPRESSION WITH OBSTRUCTION
FLOW RATE AT 1.0 MSEC

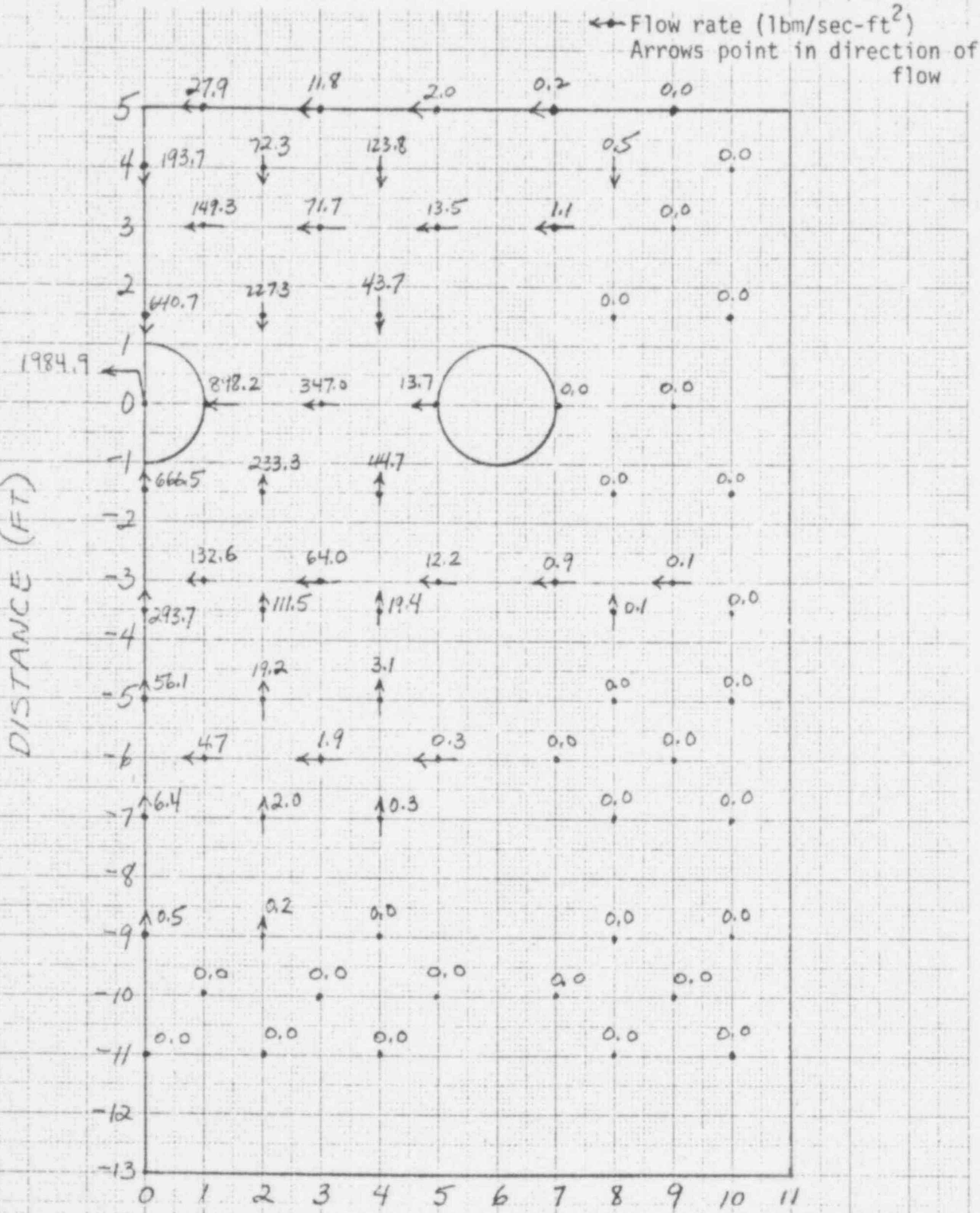

POOR ORIGINAL

596 314

FIGURE 2.2-11

PLANAR DECOMPRESSION WITH OBSTRUCTION
FLOW RATE AT 1.5 MSEC

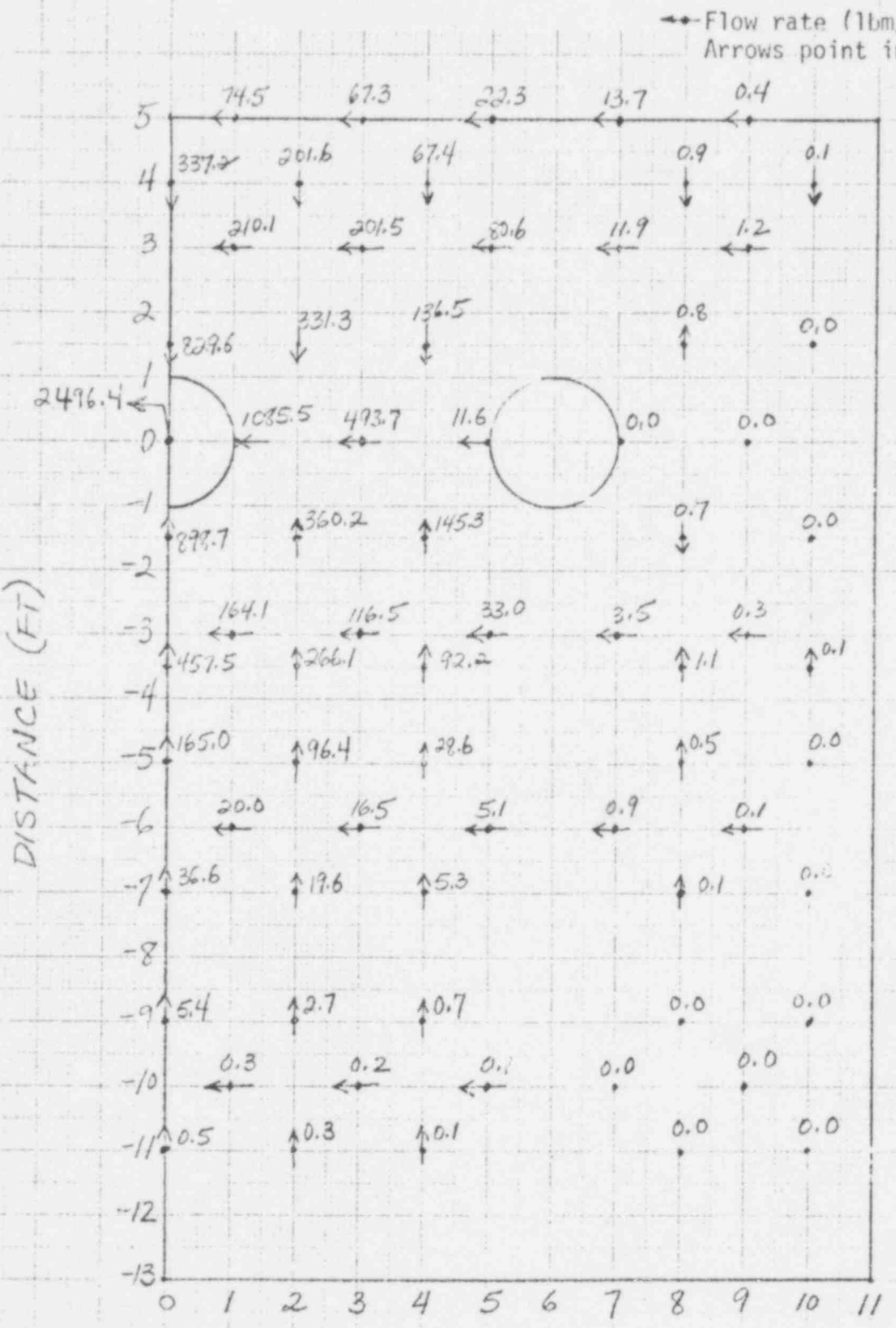

FIGURE 2.2-12

PLANAR DECOMPRESSION WITH OBSTRUCTION
FLOW RATE AT 2.0 MSEC

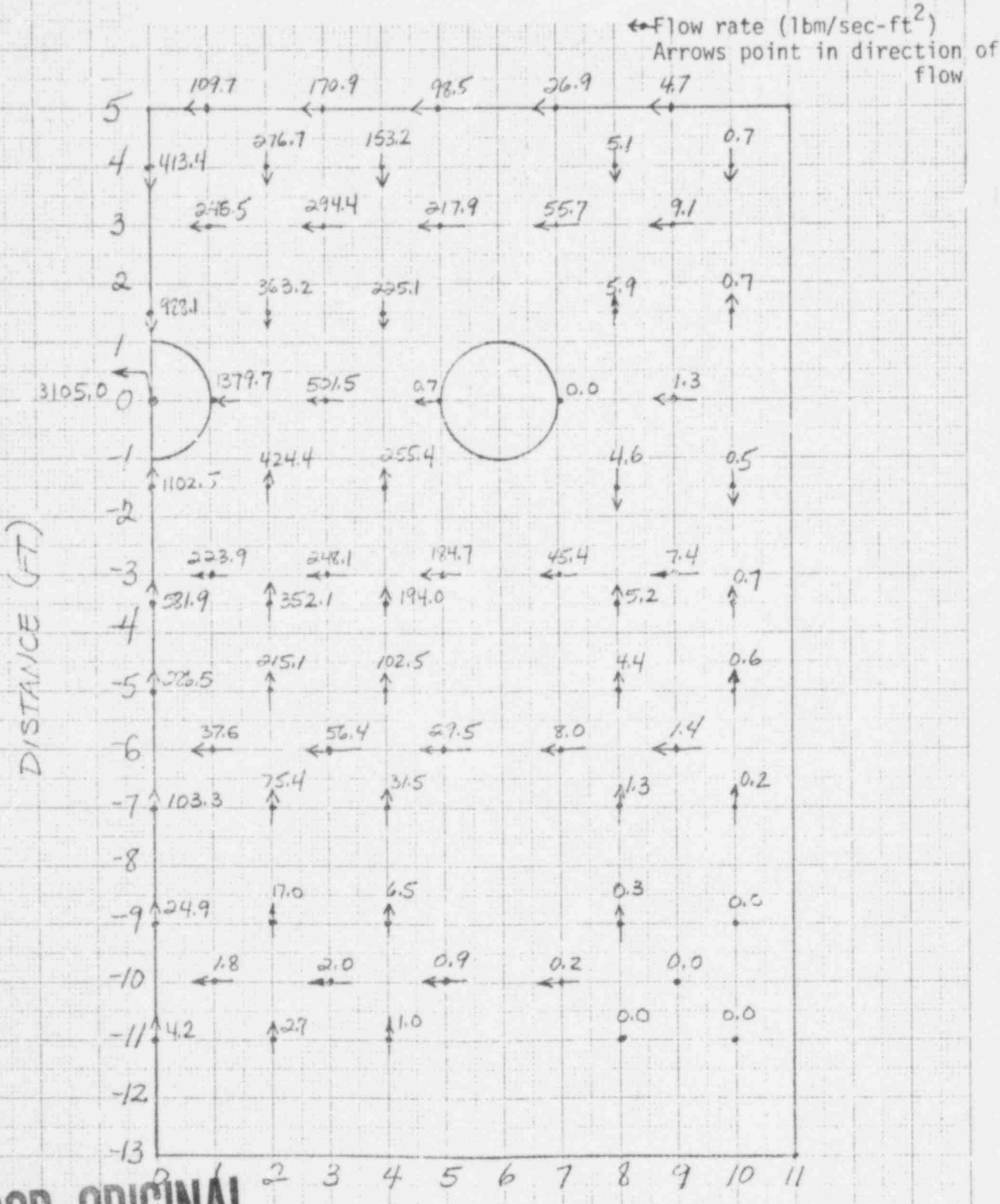

FIGURE 2.2-13

PLANAR DECOMPRESSION WITH OBSTRUCTION
FLOW RATE AT 2.5 MSEC

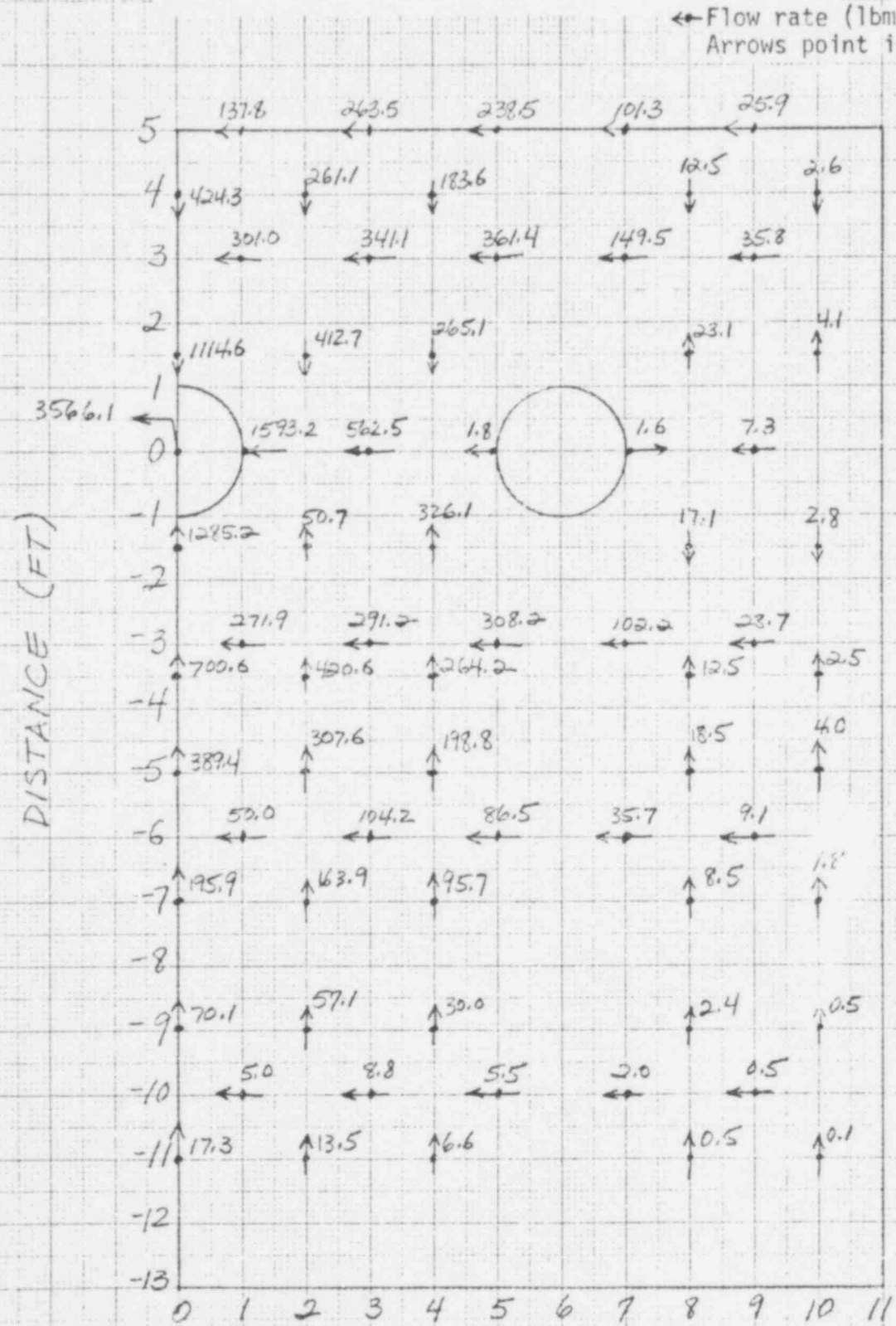

POOR ORIGINAL

DISTANCE (FT)

FIGURE 2.2-14

PLANAR DECOMPRESSION WITH OBSTRUCTION
FLOW RATE AT 3.0 MSEC

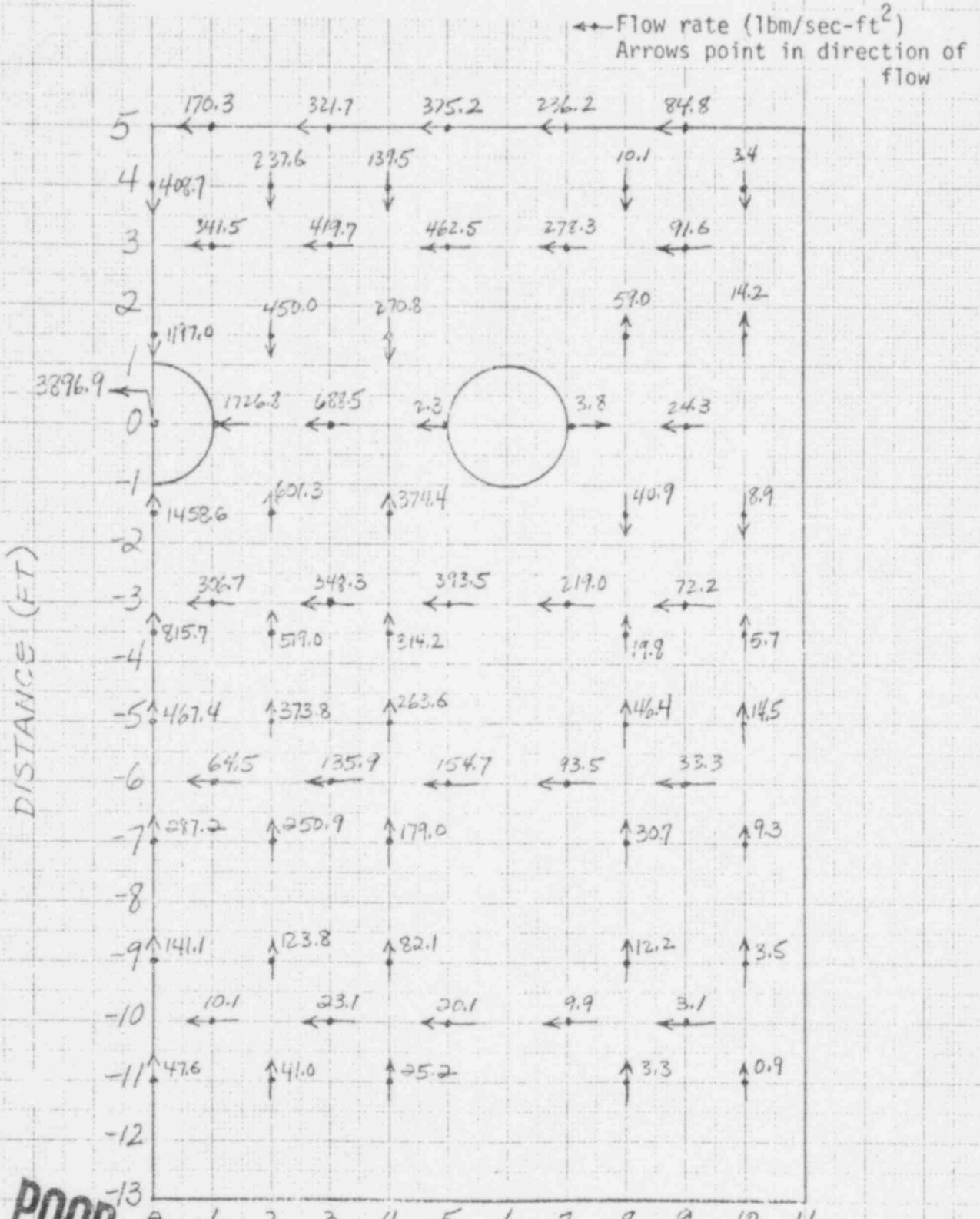

QUESTION 2.3 (Problem No. 3)

A one-dimensional pipe enters a two-dimensional region 0.8 feet thick (see Figure 2.3-1) and of semi-infinite length (no reflections from the boundary). The fluid is water at a pressure of 2100 psia and a temperature of 544°F. The fluid is at rest everywhere. The 2.4 foot diameter region at the top of the pipe is relieved to 1700 psia at time equals zero, and held constant at 1700 psia. This problem is intended to model the nozzle to downcomer interface, where the downcomer has been un-wrapped for simplicity. Neglect the obstruction in the gap.

Provide plots of pressure and fluid velocity along the centerline of the pipe from the relieved region to the lower boundary, and provide plots of pressure and velocity as a function of distance from the centerline of the pipe along the middle of the gap at the 0°, 45°, and 90° references. The data is to be presented at 1.0, 1.25, ..., 2.25, 2.50, and 2.75 milliseconds.

RESPONSE

Analytical Model

The intent of this problem is to simulate the interface between the reactor vessel inlet nozzle and the downcomer annulus. A 2.4 ft. diameter circular pipe, 4 ft. long, is connected to a flat sheet of water 0.8 ft. thick, as shown on Figure 2.3-1. The CEFLASH-4B computer code was used to model this geometry. The network configuration developed for this question consists of 54 nodes and 89 flow paths and is presented on Figure 2.3-2.

Four nodes each, 1 ft. in length, were used to model the RV inlet nozzle part of this problem. These nodes have a cross-sectional area of 4.524 ft.^{2} (circle of radius 1.2 ft.). The two dimensional region, which simulates the gap between the inside of the reactor vessel and the outside of the core support barrel, is modeled by 49 nodes of equal size in a 7 x 7 node grid. Each node is 2.4 ft. x 2.4 ft. x 0.8 ft. thick. There are no obstructions present in the gap region. The nodes representing the nozzle and gap have volumes of 4.524 ft.^{3} and 4.608 ft.^{3}, respectively.

Node 1, located at the end of the nozzle, is connected to an arbitrarily

596 319

large (20,000 ft.^{3}) containment volume (node 54) through the 2.4 ft. diameter opening.

The flow paths in the gap region connect node centers to node centers with lengths of 2.4 ft. and an associated L/A of 1.25 ft.$^{-1}$ except for paths 40, 46, 47 and 53. These paths connect the central node (node 29) in the gap to the adjacent nodes. Paths 40, 46, 47 and 53 have a length of 1.2 ft. which reflect the transport distance from the outer boundary of the nozzle to the adjacent node centers. The L/A for these flow paths is 0.625 ft.$^{-1}$.

Flow paths 1 - 4 connect the end of the inlet nozzle to the middle of the gap region. Node centers are joined along the centerline of the nozzle (pipe) except for node 1, where flow path 1 terminates at the end of the nozzle. Path 4 accounts for the sudden contraction loss associated with the flow from the gap region into the pipe.

Nodes 1 and 54 are specified to be at 1700 psia at time zero. Nodes 2 - 53 are initially at 2100 psia. The pressure in node 1 cannot be maintained at 1700 psia over all time periods, since there is more mass inflow into the node than outflow for a short period of time. Assuming virtually instantaneous communication (L/A = 10^{-10} ft.$^{-1}$) between the "leak" node (node 1) and the containment node (node 54), the pressure increases to 1732 psia in node 1 at the start of the transient and remains constant at 1732 psia over the duration of the transient.

A complete listing of the CEFLASH-4B input is presented in Table 2.3-1.

RESULTS

Plots of pressure and flow rate along the centerline of the pipe are presented on Figures 2.3-3 through 2.3-10. Pressure data as a function of distance along the middle of the gap region at the 0°, 45° and 90° references are shown on Figures 2.3-11 through 2.3-18. Flow rate data as a function of distance along the middle of the gap region along the 0° and 90° references are shown on Figures 2.3-11 through 2.3-18. Flow rate data are not presented along the 45° reference line since this information cannot be explicitly provided by an x-y grid arrangement. These figures provide "snapshots" of the system transient at the requested times of 1.0, 1.25,. ., 2.25, 2.50 and 2.75 milliseconds.

The pressure disturbance has traveled to the center of the gap region (node 29) at 1.25 milliseconds. A symmetric decompression is seen to develop in the gap region. This can be seen on Figures 2.3-11 through 2.3-18. At 2.0 milliseconds, the pressure disturbance has reflected from the nozzle-downcomer interface as a compression and has begun to travel toward the break location. This reflection through the pipe is most evident at 2.50 and 2.75 milliseconds (see Figures 2.3-9 and 2.3-10, respectively). The decompression continues to traverse the gap region in a symmetric radial manner during this time period.

596 321

TABLE 2.3-1

CEFLASH-4B INPUT FOR PROBLEM 2.3

COMBUSTION ENGINEERI CEFLASH4B VERSION 11-03 1976 76308

JOB NO NLRCNAV RUN DATE 09/1 '8 RUN BEGUN 09.11.29 CPS USED 2.34900

A. GENERAL INFORMATION AND OPTION INFO TION

END TIME	RUPT TIME	LEAK OPENS	F ELEV	PSEUDO P F	MAX STEPS	MAX EDITS
3.0000E+03	1.0000E+00	1.0000E+00		0.	80000	1000

OPTIONS SELECTED

IFMK	1	MOMENTUM TERM USED IN FLO PATHS SELECTED CARD SERIES 4INN
IFTAB	3	THOM CORRELATION
IFKC	2	FLOW VARYING FRICTION FACTOR
IFCF	1	CRITICAL FLOW CHECK TYPE 5 PLUS PATHS SELECTED CARD SERIES 4INN
IFBL	0	DO NOT BALANCE SYSTEM

OPTION FOR LEAK TABLES SELECTED BY VALUE OF L/D FOR FIRST LEAK FLOW PATH

PATH	L/D	TABLES USED
90	0.	[ ]

TIME STEP TABLE

USE	UNTIL	STEPS PER PRINT
5.0000E-05	5.0000E-03	5

8. CONTROL VOLUMES

NODE	AREA	HEIGHT	EXIT ELEV	INLET ELEV	BOTTM ELEV	FLOW AREA
1	4.5240E+00	1.0000E+00	4.0000E+00	3.0000E+00	3.0000E+00	4.5240E+00
2	4.5240E+00	1.0000E+00	3.0000E+00	2.0000E+00	2.0000E+00	4.5240E+00
3	4.5240E+00	1.0000E+00	2.0000E+00	1.0000E+00	1.0000E+00	4.5240E+00
4	4.5240E+00	1.0000E+00	1.0000E+00	0.	0.	4.5240E+00
5	5.7600E+00	8.0000E-01	0.	0.	-4.0000E-01	5.7600E+00
6	5.7600E+00	8.0000E-01	0.	0.	-4.0000E-01	5.7600E+00
7	5.7600E+00	8.0000E-01	0.	0.	-4.0000E-01	5.7600E+00
8	5.7600E+00	8.0000E-01	0.	0.	-4.0000E-01	5.7600E+00
9	5.7600E+00	8.0000E-01	0.	0.	-4.0000E-01	5.7600E+00
10	5.7600E+00	8.0000E-01	0.	0.	-4.0000E-01	5.7600E+00
11	5.7600E+00	8.0000E-01	0.	0.	-4.0000E-01	5.7600E+00
12	5.7600E+00	8.0000E-01	0.	0.	-4.0000E-01	5.7600E+00
13	5.7600E+00	8.0000E-01	0.	0.	-4.0000E-01	5.7600E+00
14	5.7600E+00	8.0000E-01	0.	0.	-4.0000E-01	5.7600E+00
15	5.7600E+00	8.0000E-01	0.	0.	-4.0000E-01	5.7600E+00
16	5.7600E+00	8.0000E-01	0.	0.	-4.0000E-01	5.7600E+00
17	5.7600E+00	8.0000E-01	0.	0.	-4.0000E-01	5.7600E+00
18	5.7600E+00	8.0000E-01	0.	0.	-4.0000E-01	5.7600E+00
19	5.7600E+00	8.0000E-01	0.	0.	-4.0000E-01	5.7600E+00
20	5.7600E+00	8.0000E-01	0.	0.	-4.0000E-01	5.7600E+00
21	5.7600E+00	8.0000E-01	0.	0.	-4.0000E-01	5.7600E+00
22	5.7600E+00	8.0000E-01	0.	0.	-4.0000E-01	5.7600E+00
23	5.7600E+00	8.0000E-01	0.	0.	-4.0000E-01	5.7600E+00
24	5.7600E+00	8.0000E-01	0.	0.	-4.0000E-01	5.7600E+00
25	5.7600E+00	8.0000E-01	0.	0.	-4.0000E-01	5.7600E+00
26	5.7600E+00	8.0000E-01	0.	0.	-4.0000E-01	5.7600E+00
27	5.7600E+00	8.0000E-01	0.	0.	-4.0000E-01	5.7600E+00
28	5.7600E+00	8.0000E-01	0.	0.	-4.0000E-01	5.7600E+00
29	5.7600E+00	8.0000E-01	4.0000E-01	0.	-4.0000E-01	5.7600E+00
30	5.7600E+00	8.0000E-01	0.	0.	-4.0000E-01	5.7600E+00
31	5.7600E+00	8.0000E-01	0.	0.	-4.0000E-01	5.7600E+00
32	5.7600E+00	8.0000E-01	0.	0.	-4.0000E-01	5.7600E+00
33	5.7600E+00	8.0000E-01	0.	0.	-4.0000E-01	5.7600E+00
34	5.7600E+00	8.0000E-01	0.	0.	-4.0000E-01	5.7600E+00
35	5.7600E+00	8.0000E-01	0.	0.	-4.0000E-01	5.7600E+00
36	5.7600E+00	8.0000E-01	0.	0.	-4.0000E-01	5.7600E+00
37	5.7600E+00	8.0000E-01	0.	0.	-4.0000E-01	5.7600E+00
38	5.7600E+00	8.0000E-01	0.	0.	-4.0000E-01	5.7600E+00
39	5.7600E+00	8.0000E-01	0.	0.	-4.0000E-01	5.7600E+00
40	5.7600E+00	8.0000E-01	0.	0.	-4.0000E-01	5.7600E+00
41	5.7600E+00	8.0000E-01	0.	0.	-4.0000E-01	5.7600E+00
42	5.7600E+00	8.0000E-01	0.	0.	-4.0000E-01	5.7600E+00
43	5.7600E+00	8.0000E-01	0.	0.	-4.0000E-01	5.7600E+00
44	5.7600E+00	8.0000E-01	0.	0.	-4.0000E-01	5.7600E+00
45	5.7600E+00	8.0000E-01	0.	0.	-4.0000E-01	5.7600E+00
46	5.7600E+00	8.0000E-01	0.	0.	-4.0000E-01	5.7600E+00
47	5.7600E+00	8.0000E-01	0.	0.	-4.0000E-01	5.7600E+00
48	5.7600E+00	8.0000E-01	0.	0.	-4.0000E-01	5.7600E+00
49	5.7600E+00	8.0000E-01	0.	0.	-4.0000E-01	5.7600E+00
50	5.7600E+00	8.0000E-01	0.	0.	-4.0000E-01	5.7600E+00

TABLE 2.3-1 (CONT'D)

COMBUSTION ENGINEERING CEFLASH4B VERSION 11 03 1976 76308

8. CONTROL VOLUMES

NODE	AREA	HEIGHT	EXIT ELEV	INLET ELEV	BOTTM ELEV	FLOW AREA
51	5.7600E+00	8.0000E+01	0.	0.	-4.0000E+01	5.7600E+00
52	5.7600E+00	8.0000E+01	0.	0.	-4.0000E+01	5.7600E+00
53	5.7600E+00	8.0000E+01	0.	0.	-4.0000E+01	5.7600E+00
54	1.0000E+02	2.0000E+02	-1.0000E+02	4.4000E+00	-1.0000E+02	1.0000E+02

596

724

COMBUSTION ENGINEERING CEFLASH4B VERSION-11-03-1976 76308

NODAL PROPERTIES

NODE	PRESSURE	ENTH SUBC	LEVEL TPH
1	1.7000E+03	5.3997E+02	0.
2	2.1000E+03	5.3997E+02	0.
3	2.1000E+03	5.3997E+02	0.
4	2.1000E+03	5.3997E+02	0.
5	2.1000E+03	5.3997E+02	0.
6	2.1000E+03	5.3997E+02	0.
7	2.1000E+03	5.3997E+02	0.
8	2.1000E+03	5.3997E+02	0.
9	2.1000E+03	5.3997E+02	0.
10	2.1000E+03	5.3997E+02	0.
11	2.1000E+03	5.3997E+02	0.
12	2.1000E+03	5.3997E+02	0.
13	2.1000E+03	5.3997E+02	0.
14	2.1000E+03	5.3997E+02	0.
15	2.1000E+03	5.3997E+02	0.
16	2.1000E+03	5.3997E+02	0.
17	2.1000E+03	5.3997E+02	0.
18	2.1000E+03	5.3997E+02	0.
19	2.1000E+03	5.3997E+02	0.
20	2.1000E+03	5.3997E+02	0.
21	2.1000E+03	5.3997E+02	0.
22	2.1000E+03	5.3997E+02	0.
23	2.1000E+03	5.3997E+02	0.
24	2.1000E+03	5.3997E+02	0.
25	2.1000E+03	5.3997E+02	0.
26	2.1000E+03	5.3997E+02	0.
27	2.1000E+03	5.3997E+02	0.
28	2.1000E+03	5.3997E+02	0.
29	2.1000E+03	5.3997E+02	0.
30	2.1000E+03	5.3997E+02	0.
31	2.1000E+03	5.3997E+02	0.
32	2.1000E+03	5.3997E+02	0.
33	2.1000E+03	5.3997E+02	0.
34	2.1000E+03	5.3997E+02	0.
35	2.1000E+03	5.3997E+02	0.
36	2.1000E+03	5.3997E+02	0.
37	2.1000E+03	5.3997E+02	0.
38	2.1000E+03	5.3997E+02	0.
39	2.1000E+03	5.3997E+02	0.
40	2.1000E+03	5.3997E+02	0.
41	2.1000E+03	5.3997E+02	0.
42	2.1000E+03	5.3997E+02	0.
43	2.1000E+03	5.3997E+02	0.
44	2.1000E+03	5.3997E+02	0.
45	2.1000E+03	5.3997E+02	0.
46	2.1000E+03	5.3997E+02	0.
47	2.1000E+03	5.3997E+02	0.
48	2.1000E+03	5.3997E+02	0.
49	2.1000E+03	5.3997E+02	0.
50	2.1000E+03	5.3997E+02	0.

TABLE 2.3-1 (CONT'D)

COMBUSTION ENGINEERING CEFLASH4B VERSION-11-03-1976 76308

NODAL PROPERTIES

NODE	PRESSURE	ENTH SUBC	LEVEL TPH
51	2.1000E+03	5.3997E+02	0.
52	2.1000E+03	5.3997E+02	0.
53	2.1000E+03	5.3997E+02	0.
54	1.7000E+03	5.4057E+02	0.

LEAK FLOW PATHS TO CONTAINMENT NODE

NODE	FLOW PATHS
54	0

C. FLOW PATHS

PATH	TYPE	NODE FROM	NODE TO	WQ	SUM L/A	AREA	DIAMETER	MOM FLOW AREA UP	MOM FLOW AREA DOWN	FRICTION K OR DELTA P	GEOM FWD K OR DELTA P	GEOM RVS K OR DELTA P
1	8	1	2	0.	3.3150E+01	4.5240E+00	2.4000E+00	4.5240E+00	4.5240E+00	1.8800E+02	1.0000E+00	5.0000E+01
2	8	2	3	0.	2.2100E+01	4.5240E+00	2.4000E+00	4.5240E+00	4.5240E+00	1.2500E+02	0.	0.
3	8	3	4	0.	2.2100E+01	4.5240E+00	2.4000E+00	4.5240E+00	4.5240E+00	1.2500E+02	0.	0.
4	8	4	29	0.	1.9890E+01	4.5240E+00	2.4000E+00	4.5240E+00	5.7600E+00	1.1300E+02	1.0000E+00	5.0000E+01
5	8	5	6	0.	1.2500E+00	1.9200E+00	1.6000E+00	1.9200E+00	1.9200E+00	3.7500E+02	0.	0.
6	8	6	7	0.	1.2500E+00	1.9200E+00	1.6000E+00	1.9200E+00	1.9200E+00	3.7500E+02	0.	0.
7	8	7	8	0.	1.2500E+00	1.9200E+00	1.6000E+00	1.9200E+00	1.9200E+00	3.7500E+02	0.	0.
8	8	8	9	0.	1.2500E+00	1.9200E+00	1.6000E+00	1.9200E+00	1.9200E+00	3.7500E+02	0.	0.
9	8	9	10	0.	1.2500E+00	1.9200E+00	1.6000E+00	1.9200E+00	1.9200E+00	3.7500E+02	0.	0.
10	8	10	11	0.	1.2500E+00	1.9200E+00	1.6000E+00	1.9200E+00	1.9200E+00	3.7500E+02	0.	0.
11	8	5	12	0.	1.2500E+00	1.9200E+00	1.6000E+00	1.9200E+00	1.9200E+00	3.7500E+02	0.	0.
12	8	6	13	0.	1.2500E+00	1.9200E+00	1.6000E+00	1.9200E+00	1.9200E+00	3.7500E+02	0.	0.
13	8	7	14	0.	1.2500E+00	1.9200E+00	1.6000E+00	1.9200E+00	1.9200E+00	3.7500E+02	0.	0.
14	8	8	15	0.	1.2500E+00	1.9200E+00	1.6000E+00	1.9200E+00	1.9200E+00	3.7500E+02	0.	0.
15	8	9	16	0.	1.2500E+00	1.9200E+00	1.6000E+00	1.9200E+00	1.9200E+00	3.7500E+02	0.	0.
16	8	10	17	0.	1.2500E+00	1.9200E+00	1.6000E+00	1.9200E+00	1.9200E+00	3.7500E+02	0.	0.
17	8	11	18	0.	1.2500E+00	1.9200E+00	1.6000E+00	1.9200E+00	1.9200E+00	3.7500E+02	0.	0.
18	8	12	13	0.	1.2500E+00	1.9200E+00	1.6000E+00	1.9200E+00	1.9200E+00	3.7500E+02	0.	0.
19	8	13	14	0.	1.2500E+00	1.9200E+00	1.6000E+00	1.9200E+00	1.9200E+00	3.7500E+02	0.	0.
20	8	14	15	0.	1.2500E+00	1.9200E+00	1.6000E+00	1.9200E+00	1.9200E+00	3.7500E+02	0.	0.
21	8	15	16	0.	1.2500E+00	1.9200E+00	1.6000E+00	1.9200E+00	1.9200E+00	3.7500E+02	0.	0.
22	8	16	17	0.	1.2500E+00	1.9200E+00	1.6000E+00	1.9200E+00	1.9200E+00	3.7500E+02	0.	0.
23	8	17	18	0.	1.2500E+00	1.9200E+00	1.6000E+00	1.9200E+00	1.9200E+00	3.7500E+02	0.	0.
24	8	12	19	0.	1.2500E+00	1.9200E+00	1.6000E+00	1.9200E+00	1.9200E+00	3.7500E+02	0.	0.
25	8	13	20	0.	1.2500E+00	1.9200E+00	1.6000E+00	1.9200E+00	1.9200E+00	3.7500E+02	0.	0.
26	8	14	21	0.	1.2500E+00	1.9200E+00	1.6000E+00	1.9200E+00	1.9200E+00	3.7500E+02	0.	0.
27	8	15	22	0.	1.2500E+00	1.9200E+00	1.6000E+00	1.9200E+00	1.9200E+00	3.7500E+02	0.	0.
28	8	16	23	0.	1.2500E+00	1.9200E+00	1.6000E+00	1.9200E+00	1.9200E+00	3.7500E+02	0.	0.
29	8	17	24	0.	1.2500E+00	1.9200E+00	1.6000E+00	1.9200E+00	1.9200E+00	3.7500E+02	0.	0.
30	8	18	25	0.	1.2500E+00	1.9200E+00	1.6000E+00	1.9200E+00	1.9200E+00	3.7500E+02	0.	0.
31	8	19	20	0.	1.2500E+00	1.9200E+00	1.6000E+00	1.9200E+00	1.9200E+00	3.7500E+02	0.	0.
32	8	20	21	0.	1.2500E+00	1.9200E+00	1.6000E+00	1.9200E+00	1.9200E+00	3.7500E+02	0.	0.
33	8	21	22	0.	1.2500E+00	1.9200E+00	1.6000E+00	1.9200E+00	1.9200E+00	3.7500E+02	0.	0.
34	8	22	23	0.	1.2500E+00	1.9200E+00	1.6000E+00	1.9200E+00	1.9200E+00	3.7500E+02	0.	0.
35	8	23	24	0.	1.2500E+00	1.9200E+00	1.6000E+00	1.9200E+00	1.9200E+00	3.7500E+02	0.	0.
36	8	24	25	0.	1.2500E+00	1.9200E+00	1.6000E+00	1.9200E+00	1.9200E+00	3.7500E+02	0.	0.
37	8	19	26	0.	1.2500E+00	1.9200E+00	1.6000E+00	1.9200E+00	1.9200E+00	3.7500E+02	0.	0.
38	8	20	27	0.	1.2500E+00	1.9200E+00	1.6000E+00	1.9200E+00	1.9200E+00	3.7500E+02	0.	0.
39	8	21	28	0.	1.2500E+00	1.9200E+00	1.6000E+00	1.9200E+00	1.9200E+00	3.7500E+02	0.	0.
40	8	22	29	0.	6.2500E-01	1.9200E+00	1.6000E+00	1.9200E+00	1.9200E+00	1.8800E+02	0.	0.
41	8	23	30	0.	1.2500E+00	1.9200E+00	1.6000E+00	1.9200E+00	1.9200E+00	3.7500E+02	0.	0.
42	8	24	31	0.	1.2500E+00	1.9200E+00	1.6000E+00	1.9200E+00	1.9200E+00	3.7500E+02	0.	0.
43	8	25	32	0.	1.2500E+00	1.9200E+00	1.6000E+00	1.9200E+00	1.9200E+00	3.7500E+02	0.	0.
44	8	26	27	0.	1.2500E+00	1.9200E+00	1.6000E+00	1.9200E+00	1.9200E+00	3.7500E+02	0.	0.
45	8	27	28	0.	1.2500E+00	1.9200E+00	1.6000E+00	1.9200E+00	1.9200E+00	1.8800E+02	0.	0.
46	8	28	29	0.	6.2500E-01	1.9200E+00	1.6000E+00	1.9200E+00	1.9200E+00	1.8800E+02	0.	0.
47	8	29	30	0.	1.2500E+00	1.9200E+00	1.6000E+00	1.9200E+00	1.9200E+00	3.7500E+02	0.	0.
48	8	30	31	0.	1.2500E+00	1.9200E+00	1.6000E+00	1.9200E+00	1.9200E+00	3.7500E+02	0.	0.
49	8	31	32	0.	1.2500E+00	1.9200E+00	1.6000E+00	1.9200E+00	1.9200E+00	3.7500E+02	0.	0.

COMBUSTION ENGINEERING CEFLASH4B VERSION 11 03 1976 76308

C. FLOW PATHS

PATH	TYPE	NODE FROM	NODE TO	WO	SUM L/A	AREA	DIAMETER	HOM FLOW AREA UP	HOM FLOW AREA DOWN	FRICTION K OR DELTA P	GEOM FWD K OR DELTA P	GEOM RVS K OR DELTA P
50	8	26	33	0.	1.2500E+00	1.9200E+00	1.6000E+00	1.9200E+00	1.9200E+00	3.7500E-02	0.	0.
51	8	27	34	0.	1.2500E+00	1.9200E+00	1.6000E+00	1.9200E+00	1.9200E+00	3.7500E-02	0.	0.
52	8	28	35	0.	1.2500E+00	1.9200E+00	1.6000E+00	1.9200E+00	1.9200E+00	3.7500E-02	0.	0.
53	8	29	36	0.	6.2500E-01	1.9200E+00	1.6000E+00	1.9200E+00	1.9200E+00	1.8800E-02	0.	0.
54	8	30	37	0.	1.2500E+00	1.9200E+00	1.6000E+00	1.9200E+00	1.9200E+00	3.7500E-02	0.	0.
55	8	31	38	0.	1.2500E+00	1.9200E+00	1.6000E+00	1.9200E+00	1.9200E+00	3.7500E-02	0.	0.
56	8	32	39	0.	1.2500E+00	1.9200E+00	1.6000E+00	1.9200E+00	1.9200E+00	3.7500E-02	0.	0.
57	8	33	34	0.	1.2500E+00	1.9200E+00	1.6000E+00	1.9200E+00	1.9200E+00	3.7500E-02	0.	0.
58	8	34	35	0.	1.2500E+00	1.9200E+00	1.6000E+00	1.9200E+00	1.9200E+00	3.7500E-02	0.	0.
59	8	35	36	0.	1.2500E+00	1.9200E+00	1.6000E+00	1.9200E+00	1.9200E+00	3.7500E-02	0.	0.
60	8	36	37	0.	1.2500E+00	1.9200E+00	1.6000E+00	1.9200E+00	1.9200E+00	3.7500E-02	0.	0.
61	8	37	38	0.	1.2500E+00	1.9200E+00	1.6000E+00	1.9200E+00	1.9200E+00	3.7500E-02	0.	0.
62	8	38	39	0.	1.2500E+00	1.9200E+00	1.6000E+00	1.9200E+00	1.9200E+00	3.7500E-02	0.	0.
63	8	33	40	0.	1.2500E+00	1.9200E+00	1.6000E+00	1.9200E+00	1.9200E+00	3.7500E-02	0.	0.
64	8	34	41	0.	1.2500E+00	1.9200E+00	1.6000E+00	1.9200E+00	1.9200E+00	3.7500E-02	0.	0.
65	8	35	42	0.	1.2500E+00	1.9200E+00	1.6000E+00	1.9200E+00	1.9200E+00	3.7500E-02	0.	0.
66	8	36	43	0.	1.2500E+00	1.9200E+00	1.6000E+00	1.9200E+00	1.9200E+00	3.7500E-02	0.	0.
67	8	37	44	0.	1.2500E+00	1.9200E+00	1.6000E+00	1.9200E+00	1.9200E+00	3.7500E-02	0.	0.
68	8	38	45	0.	1.2500E+00	1.9200E+00	1.6000E+00	1.9200E+00	1.9200E+00	3.7500E-02	0.	0.
69	8	39	46	0.	1.2500E+00	1.9200E+00	1.6000E+00	1.9200E+00	1.9200E+00	3.7500E-02	0.	0.
70	8	40	41	0.	1.2500E+00	1.9200E+00	1.6000E+00	1.9200E+00	1.9200E+00	3.7500E-02	0.	0.
71	8	41	42	0.	1.2500E+00	1.9200E+00	1.6000E+00	1.9200E+00	1.9200E+00	3.7500E-02	0.	0.
72	8	42	43	0.	1.2500E+00	1.9200E+00	1.6000E+00	1.9200E+00	1.9200E+00	3.7500E-02	0.	0.
73	8	43	44	0.	1.2500E+00	1.9200E+00	1.6000E+00	1.9200E+00	1.9200E+00	3.7500E-02	0.	0.
74	8	44	45	0.	1.2500E+00	1.9200E+00	1.6000E+00	1.9200E+00	1.9200E+00	3.7500E-02	0.	0.
75	8	45	46	0.	1.2500E+00	1.9200E+00	1.6000E+00	1.9200E+00	1.9200E+00	3.7500E-02	0.	0.
76	8	40	47	0.	1.2500E+00	1.9200E+00	1.6000E+00	1.9200E+00	1.9200E+00	3.7500E-02	0.	0.
77	8	41	48	0.	1.2500E+00	1.9200E+00	1.6000E+00	1.9200E+00	1.9200E+00	3.7500E-02	0.	0.
78	8	42	49	0.	1.2500E+00	1.9200E+00	1.6000E+00	1.9200E+00	1.9200E+00	3.7500E-02	0.	0.
79	8	43	50	0.	1.2500E+00	1.9200E+00	1.6000E+00	1.9200E+00	1.9200E+00	3.7500E-02	0.	0.
80	8	44	51	0.	1.2500E+00	1.9200E+00	1.6000E+00	1.9200E+00	1.9200E+00	3.7500E-02	0.	0.
81	8	45	52	0.	1.2500E+00	1.9200E+00	1.6000E+00	1.9200E+00	1.9200E+00	3.7500E-02	0.	0.
82	8	46	53	0.	1.2500E+00	1.9200E+00	1.6000E+00	1.9200E+00	1.9200E+00	3.7500E-02	0.	0.
83	8	47	48	0.	1.2500E+00	1.9200E+00	1.6000E+00	1.9200E+00	1.9200E+00	3.7500E-02	0.	0.
84	8	48	49	0.	1.2500E+00	1.9200E+00	1.6000E+00	1.9200E+00	1.9200E+00	3.7500E-02	0.	0.
85	8	49	50	0.	1.2500E+00	1.9200E+00	1.6000E+00	1.9200E+00	1.9200E+00	3.7500E-02	0.	0.
86	8	50	51	0.	1.2500E+00	1.9200E+00	1.6000E+00	1.9200E+00	1.9200E+00	3.7500E-02	0.	0.
87	8	51	52	0.	1.2500E+00	1.9200E+00	1.6000E+00	1.9200E+00	1.9200E+00	3.7500E-02	0.	0.
88	8	52	53	0.	1.2500E+00	1.9200E+00	1.6000E+00	1.9200E+00	1.9200E+00	3.7500E-02	0.	0.
89	8	1	54	0.	1.0000E+10	4.5240E+00	2.4000E+00	2.4000E+00	1.0000E+02	0.	1.0000E+00	5.0000E-01

	L/D	AREA	DISCHARGE COEFF	DISCHARGE COEFF	DISCHARGE COEFF	DISCHARGE COEFF
90	0	0				

596

328

COMBUSTION ENGINEERING — CEFLASH4B — VERSION 11-03-1976 — 76308

OPTIONS BY FLOW PATHS

FLOW PATH	MOMENTUM FLUX	CRITICAL FLOW	MIN AREA CRIT FLOW	LENGTH
1	1	1	4.5240E+00	1.5000E+00
2	1	1	4.5240E+00	1.0000E+00
3	1	1	4.5240E+00	1.0000E+00
4	1	1	4.5240E+00	9.0000E-01
5	4	1	1.9200E+00	2.4000E+00
6	4	1	1.9200E+00	2.4000E+00
7	4	1	1.9200E+00	2.4000E+00
8	4	1	1.9200E+00	2.4000E+00
9	4	1	1.9200E+00	2.4000E+00
10	4	1	1.9200E+00	2.4000E+00
11	4	1	1.9200E+00	2.4000E+00
12	4	1	1.9200E+00	2.4000E+00
13	4	1	1.9200E+00	2.4000E+00
14	4	1	1.9200E+00	2.4000E+00
15	4	1	1.9200E+00	2.4000E+00
16	4	1	1.9200E+00	2.4000E+00
17	4	1	1.9200E+00	2.4000E+00
18	4	1	1.9200E+00	2.4000E+00
19	4	1	1.9200E+00	2.4000E+00
20	4	1	1.9200E+00	2.4000E+00
21	4	1	1.9200E+00	2.4000E+00
22	4	1	1.9200E+00	2.4000E+00
23	4	1	1.9200E+00	2.4000E+00
24	4	1	1.9200E+00	2.4000E+00
25	4	1	1.9200E+00	2.4000E+00
26	4	1	1.9200E+00	2.4000E+00
27	4	1	1.9200E+00	2.4000E+00
28	4	1	1.9200E+00	2.4000E+00
29	4	1	1.9200E+00	2.4000E+00
30	4	1	1.9200E+00	2.4000E+00
31	4	1	1.9200E+00	2.4000E+00
32	4	1	1.9200E+00	2.4000E+00
33	4	1	1.9200E+00	2.4000E+00
34	4	1	1.9200E+00	2.4000E+00
35	4	1	1.9200E+00	2.4000E+00
36	4	1	1.9200E+00	2.4000E+00
37	4	1	1.9200E+00	2.4000E+00
38	4	1	1.9200E+00	2.4000E+00
39	4	1	1.9200E+00	2.4000E+00
40	4	1	1.9200E+00	1.2000E+00
41	4	1	1.9200E+00	2.4000E+00
42	4	1	1.9200E+00	2.4000E+00
43	4	1	1.9200E+00	2.4000E+00
44	4	1	1.9200E+00	2.4000E+00
45	4	1	1.9200E+00	2.4000E+00
46	4	1	1.9200E+00	1.2000E+00
47	4	1	1.9200E+00	1.2000E+00
48	4	1	1.9200E+00	2.4000E+00
49	4	1	1.9200E+00	2.4000E+00
50	4	1	1.9200E+00	2.4000E+00
51	4	1	1.9200E+00	2.4000E+00

TABLE 2.3-1 (CONT'D)

COMBUSTION ENGINEERING CEFLASH4B VERSION 11-03 1976 76308

OPTIONS BY FLOW PATHS

FLOW PATH	MOMENTUM FLUX	CRITICAL FLOW	MIN AREA CRIT FLOW	LENGTH
52	0	1	1.9200E+00	2.4000E+00
53	0	1	1.9200E+00	1.2000E+00
54	0	1	1.9200E+00	2.4000E+00
55	0	1	1.9200E+00	2.4000E+00
56	0	1	1.9200E+00	2.4000E+00
57	0	1	1.9200E+00	2.4000E+00
58	0	1	1.9200E+00	2.4000E+00
59	0	1	1.9200E+00	2.4000E+00
60	0	1	1.9200E+00	2.4000E+00
61	0	1	1.9200E+00	2.4000E+00
62	0	1	1.9200E+00	2.4000E+00
63	0	1	1.9200E+00	2.4000E+00
64	0	1	1.9200E+00	2.4000E+00
65	0	1	1.9200E+00	2.4000E+00
66	0	1	1.9200E+00	2.4000E+00
67	0	1	1.9200E+00	2.4000E+00
68	0	1	1.9200E+00	2.4000E+00
69	0	1	1.9200E+00	2.4000E+00
70	0	1	1.9200E+00	2.4000E+00
71	0	1	1.9200E+00	2.4000E+00
72	0	1	1.9200E+00	2.4000E+00
73	0	1	1.9200E+00	2.4000E+00
74	0	1	1.9200E+00	2.4000E+00
75	0	1	1.9200E+00	2.4000E+00
76	0	1	1.9200E+00	2.4000E+00
77	0	1	1.9200E+00	2.4000E+00
78	0	1	1.9200E+00	2.4000E+00
79	0	1	1.9200E+00	2.4000E+00
80	0	1	1.9200E+00	2.4000E+00
81	0	1	1.9200E+00	2.4000E+00
82	0	1	1.9200E+00	2.4000E+00
83	0	1	1.9200E+00	2.4000E+00
84	0	1	1.9200E+00	2.4000E+00
85	0	1	1.9200E+00	2.4000E+00
86	0	1	1.9200E+00	2.4000E+00
87	0	1	1.9200E+00	2.4000E+00
88	0	1	1.9200E+00	2.4000E+00
89	0	1	4.5240E+00	1.0000E+01

MODIFICATION OF UPSTREAM AND DOWNSTREAM ELEVATION FOR FLOW PATH N

FLOW PATH	UPSTREAM ELEVATION	DOWNSTREAM ELEVATION
1	4.4000E+00	2.9000E+00
2	2.9000E+00	1.9000E+00
3	1.9000E+00	9.0000E-01
6	9.0000E-01	0.
40	0.	0.
48	0.	0.

596

350

Figure 2.3-1
LAYOUT OF PROBLEM 2.3
RV NOZZLE TO DOWNCOMER INTERFACE SIMULATION

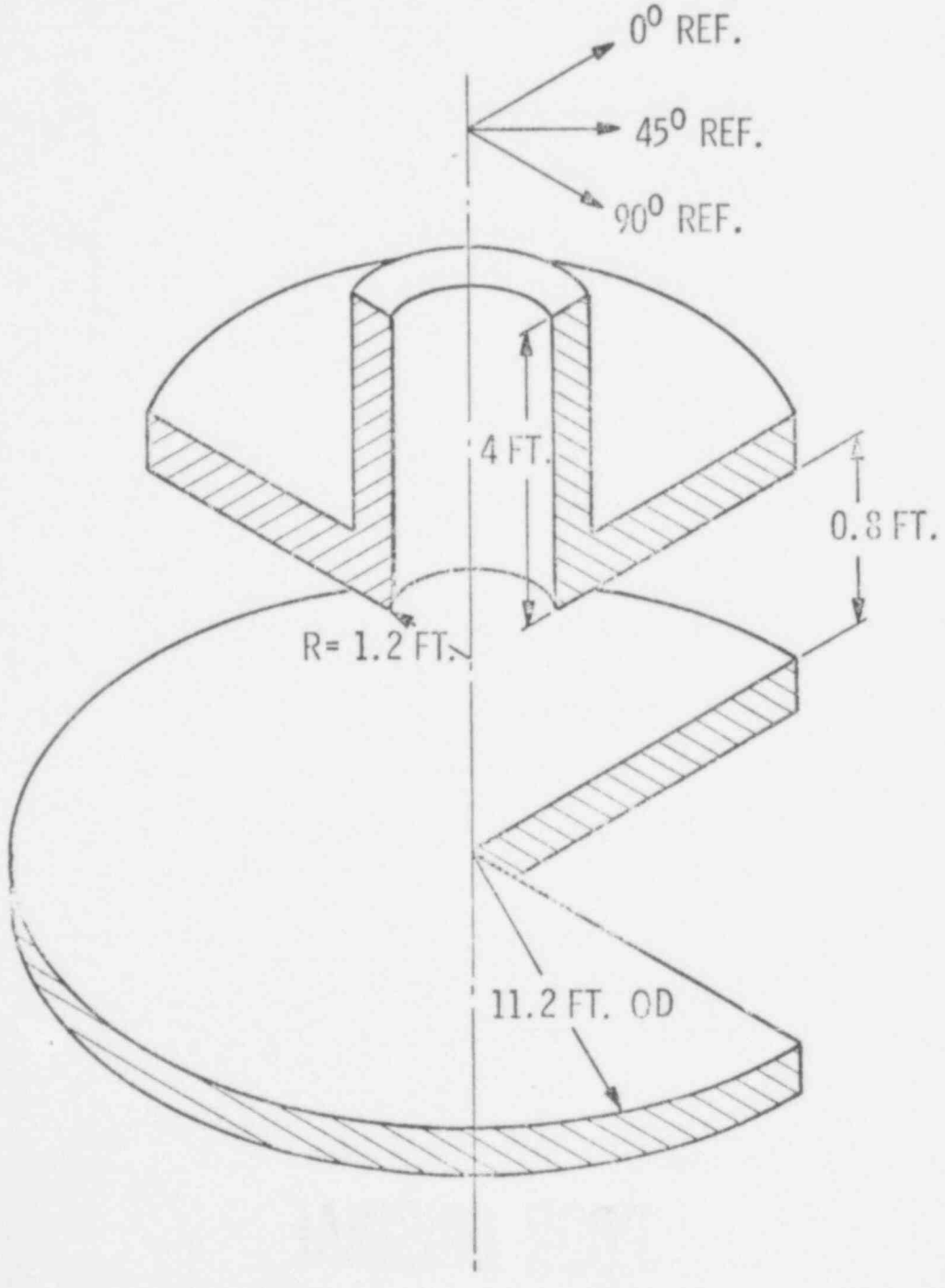

596 331

Figure 2.3-2
CEFLASH-4B MODEL FOR NOZZLE TO DOWNCOMER
INTERFACE PROBLEM
PROBLEM 2.3

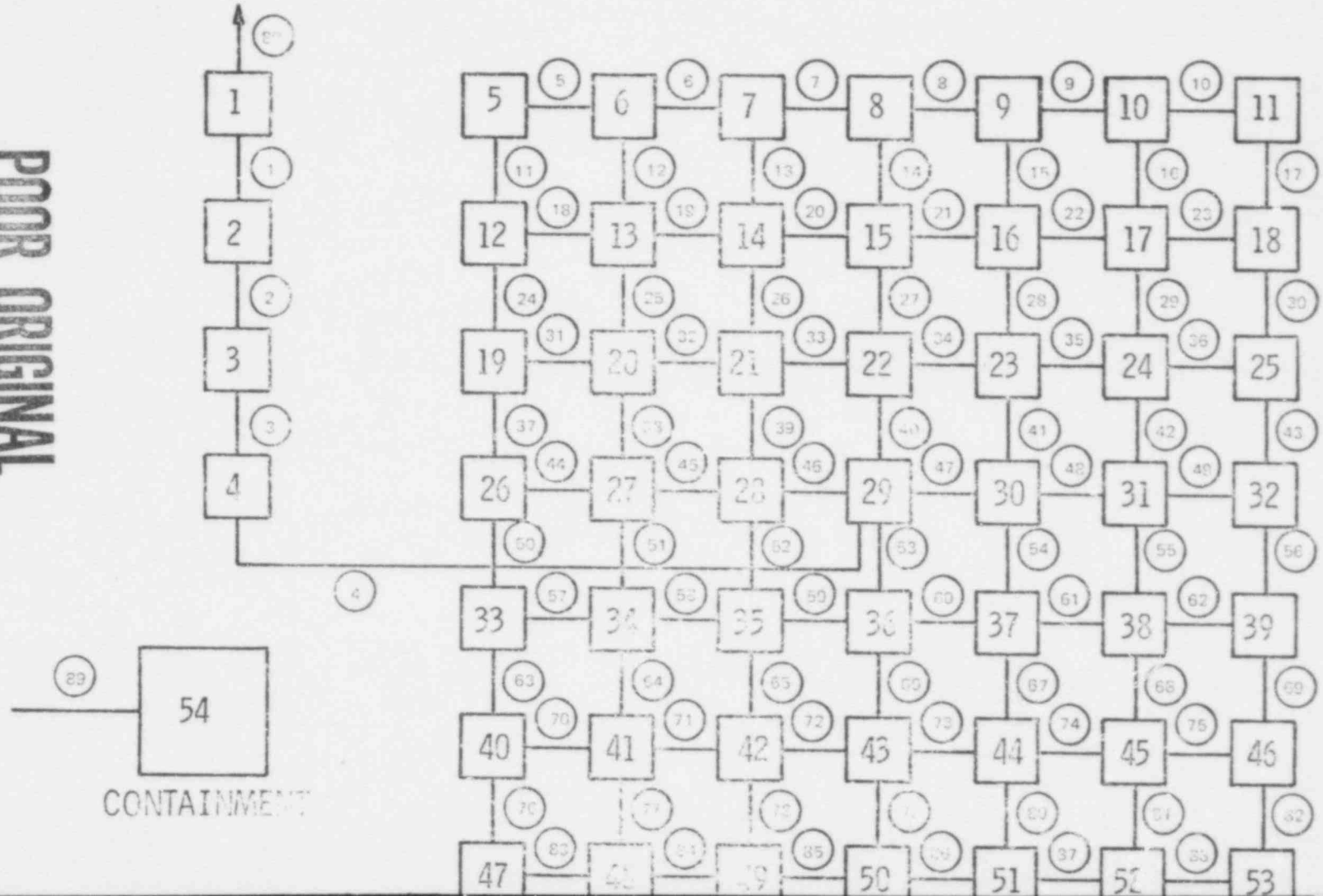

FIGURE 2.3-3
NOZZLE TO DOWNCOMER INTERFACE PROBLEM
PRESSURE AND FLOW RATE ALONG CENTERLINE
OF PIPE AT 1.0 MSEC

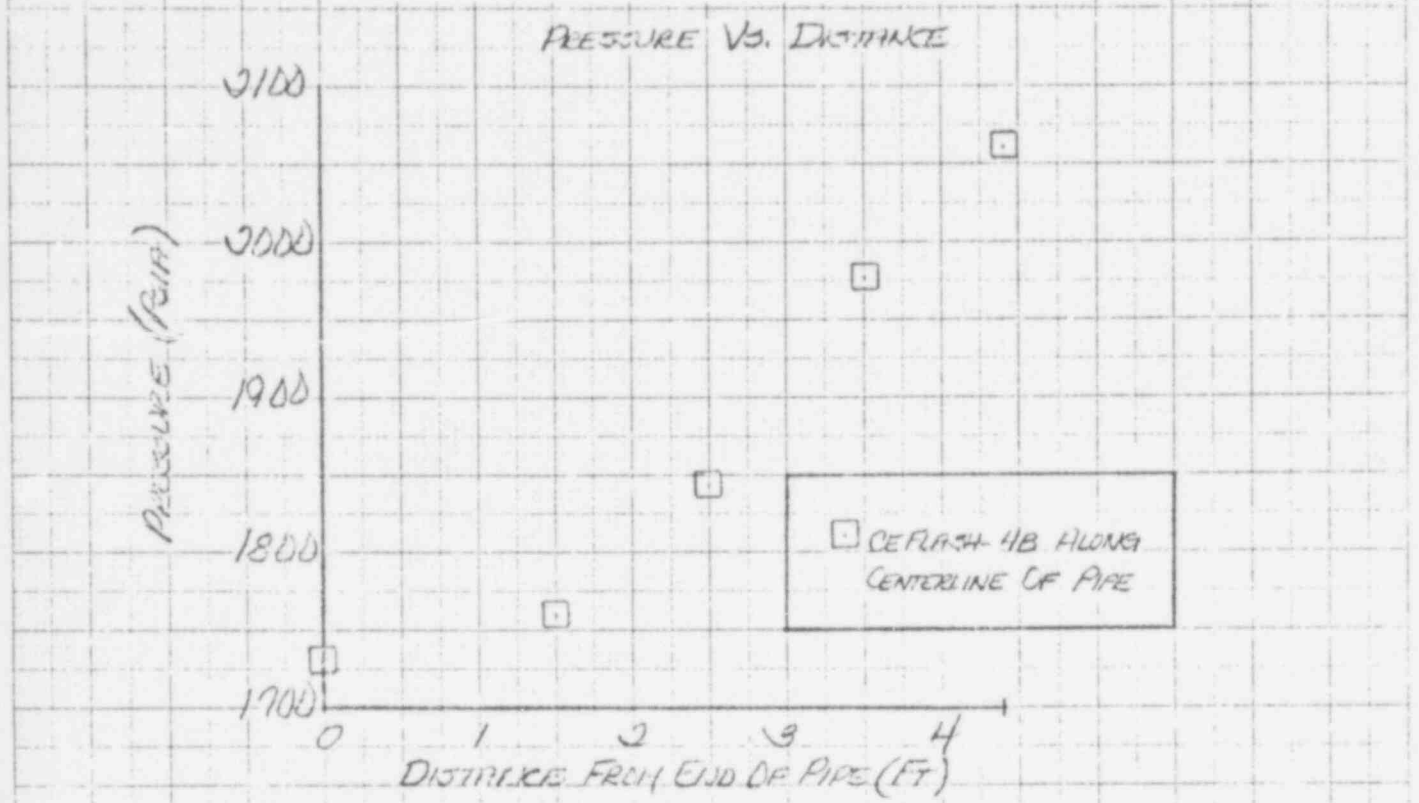

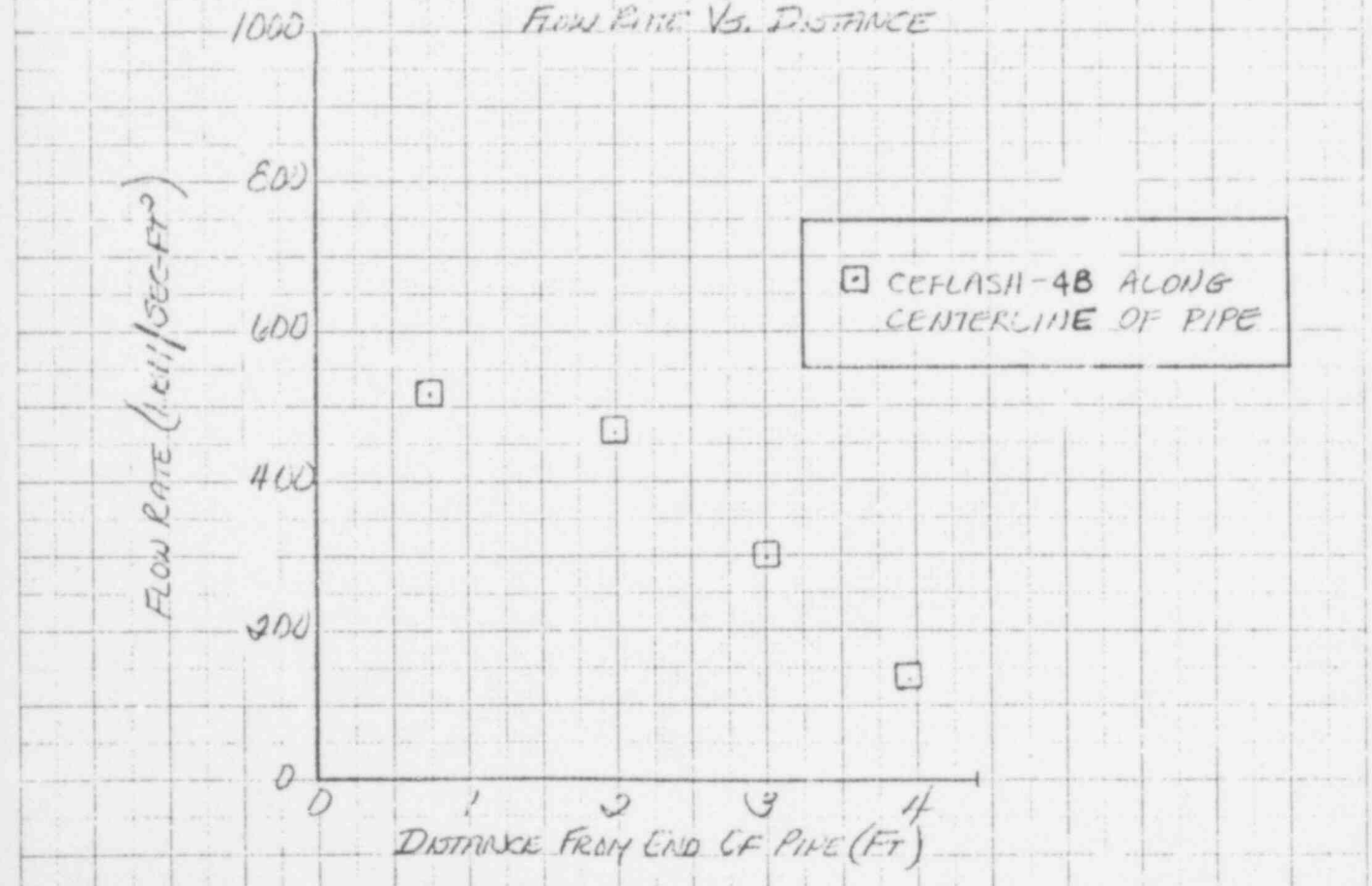

FIGURE 2.3-4

NOZZLE TO DOWNCOMER INTERFACE PROBLEM
PRESSURE AND FLOW RATE ALONG CENTERLINE
OF PIPE AT 1.25 MSEC

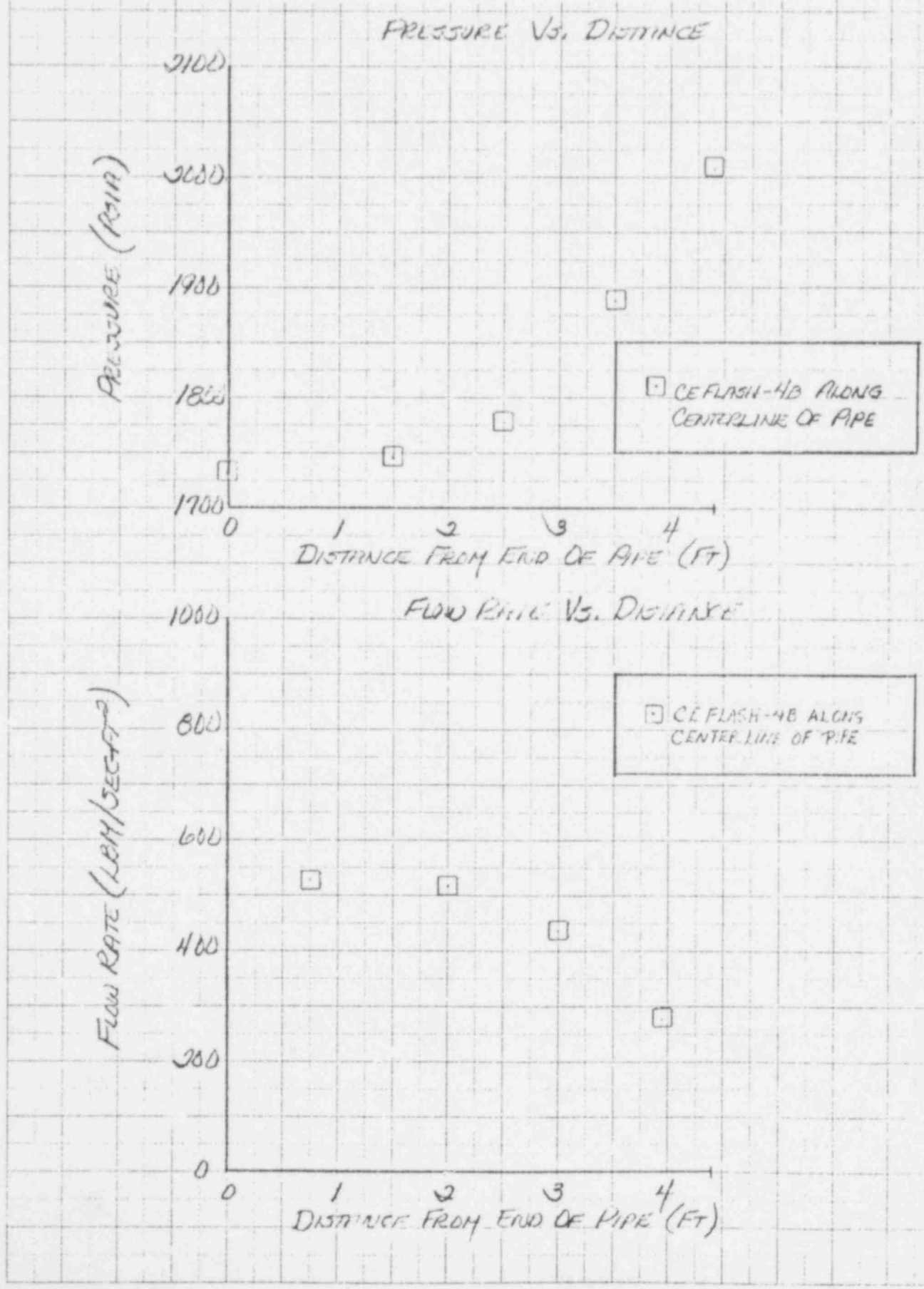

FIGURE 2.3-5

NOZZLE TO DOWNCOMER INTERFACE PROBLEM
PRESSURE AND FLOW RATE ALONG CENTERLINE
OF PIPE AT 1.50 MSEC

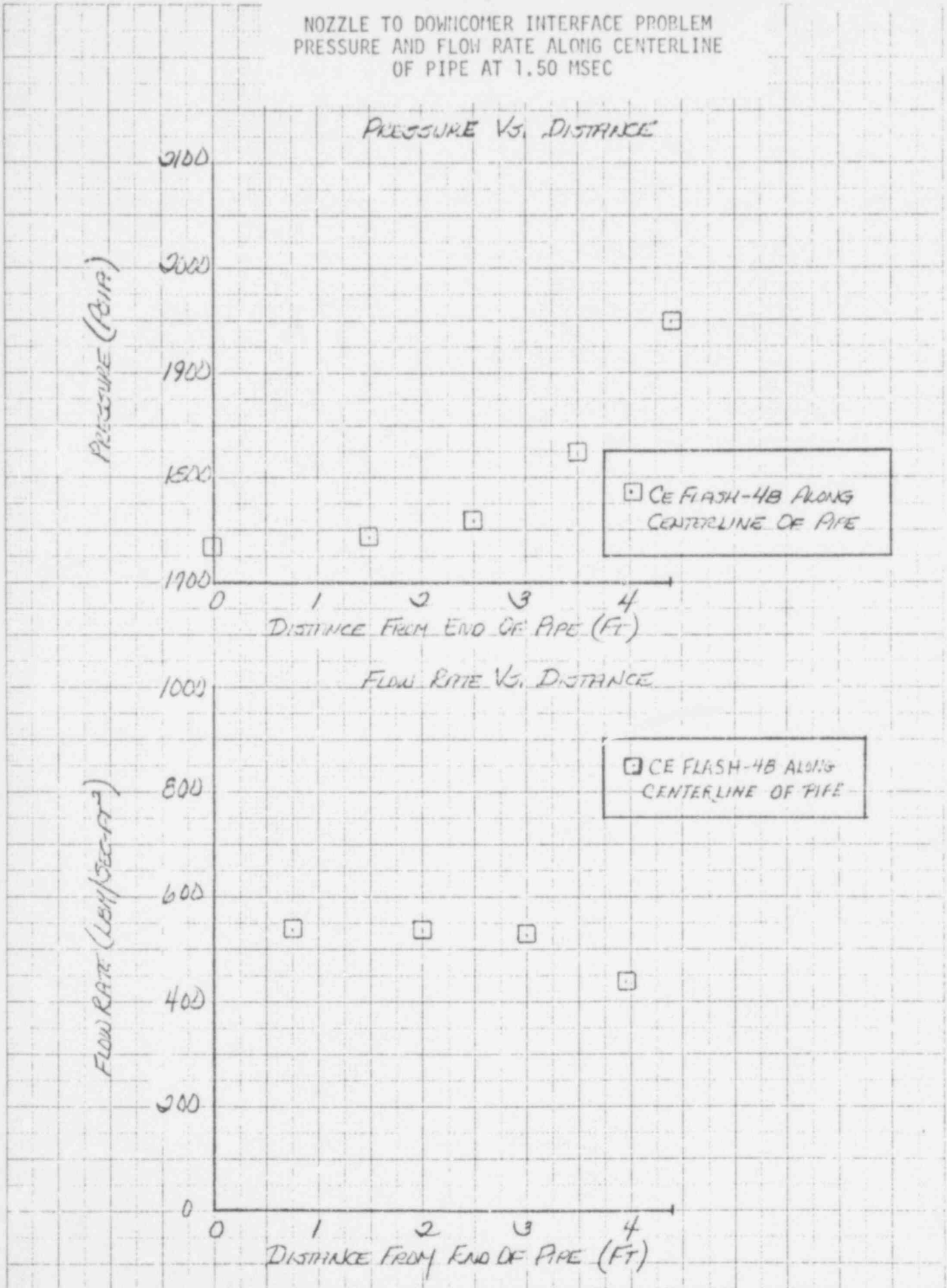

596 335

FIGURE 2.3-6

NOZZLE TO DOWNCOMER INTERFACE PROBLEM
PRESSURE AND FLOW RATE ALONG CENTERLINE
OF PIPE AT 1.75 MSEC

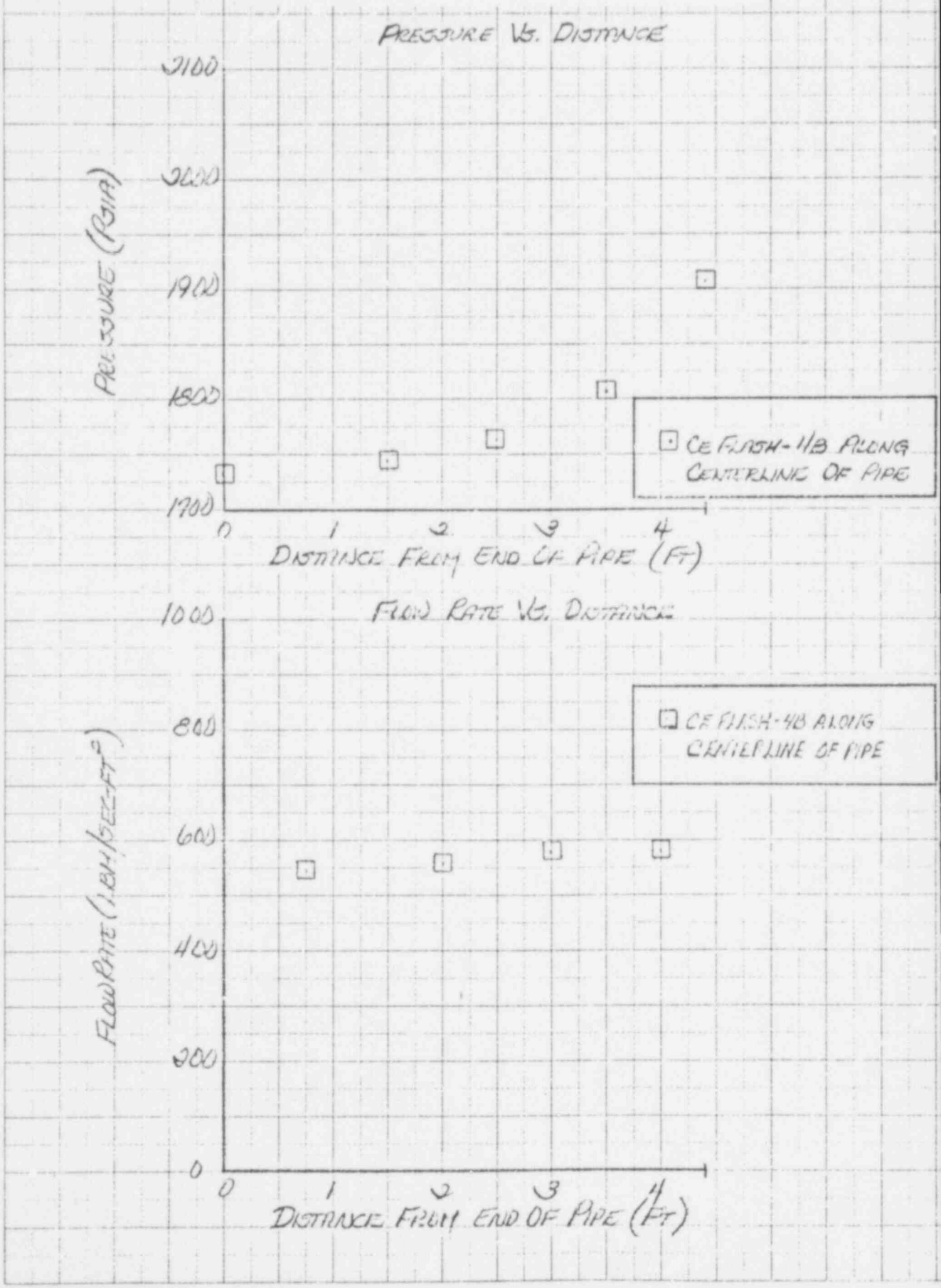

FIGURE 2.3-7

NOZZLE TO DOWNCOMER INTERFACE PROBLEM
PRESSURE AND FLOW RATE ALONG CENTERLINE
OF PIPE AT 2.0 MSEC

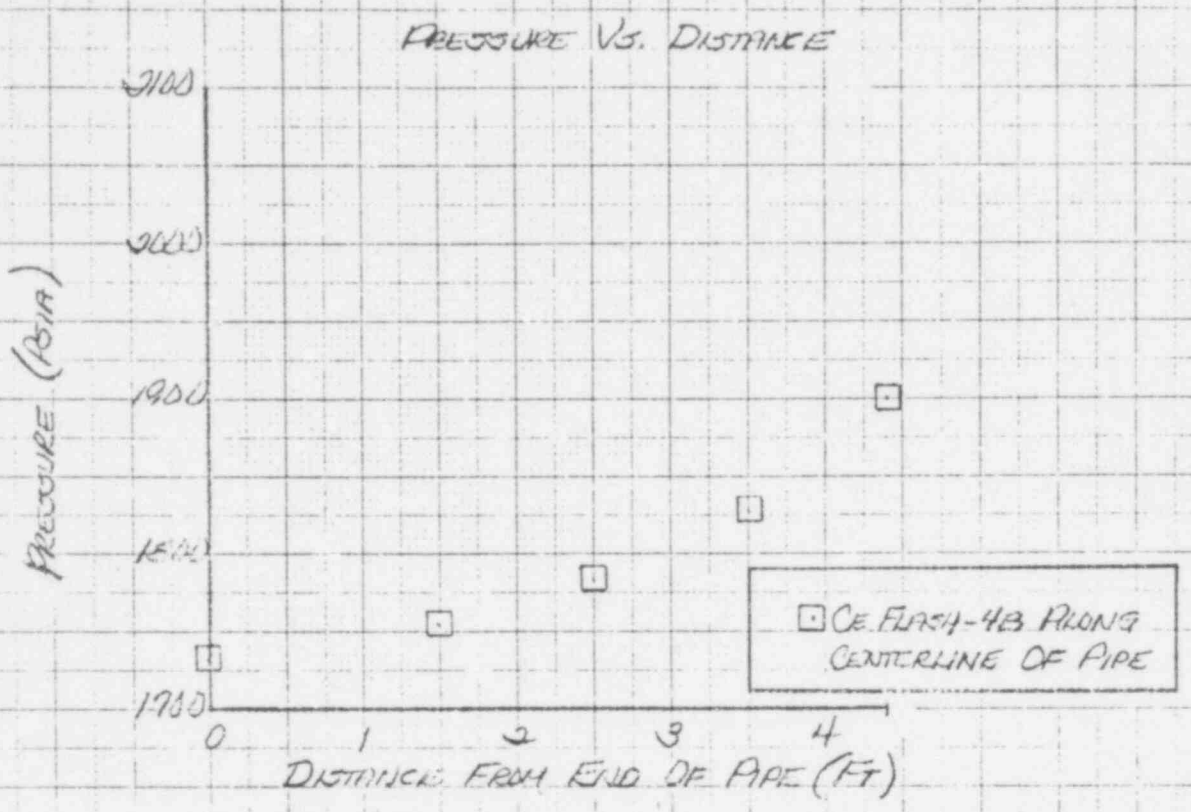

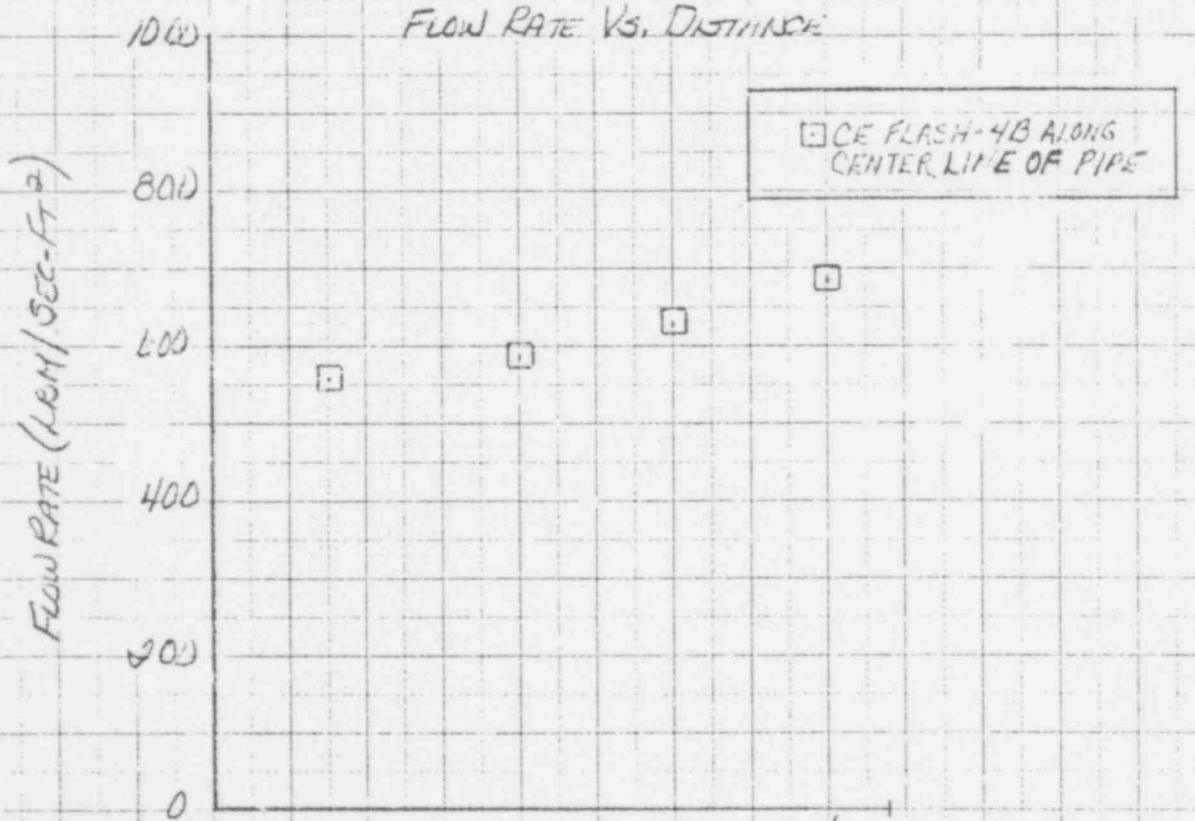

546 337

FIGURE 2.3-8

NOZZLE TO DOWNCOMER INTERFACE PROBLEM
PRESSURE AND FLOW RATE ALONG CENTERLINE
OF PIPE AT 2.25 MSEC

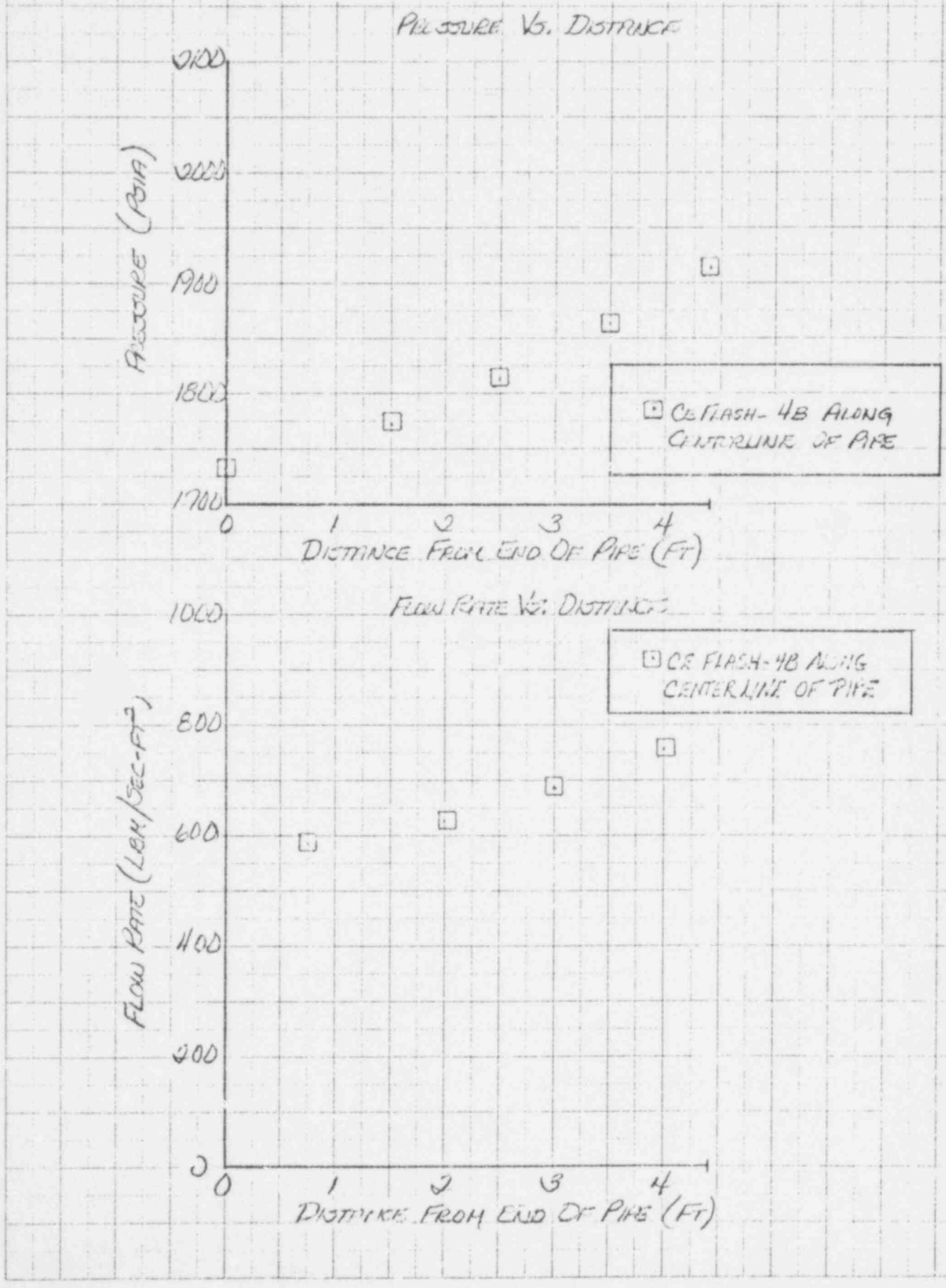

FIGURE 2.3-9

NOZZLE TO DOWNCOMER INTERFACE PROBLEM
PRESSURE AND FLOW RATE ALONG CENTERLINE
OF PIPE AT 2.50 MSEC

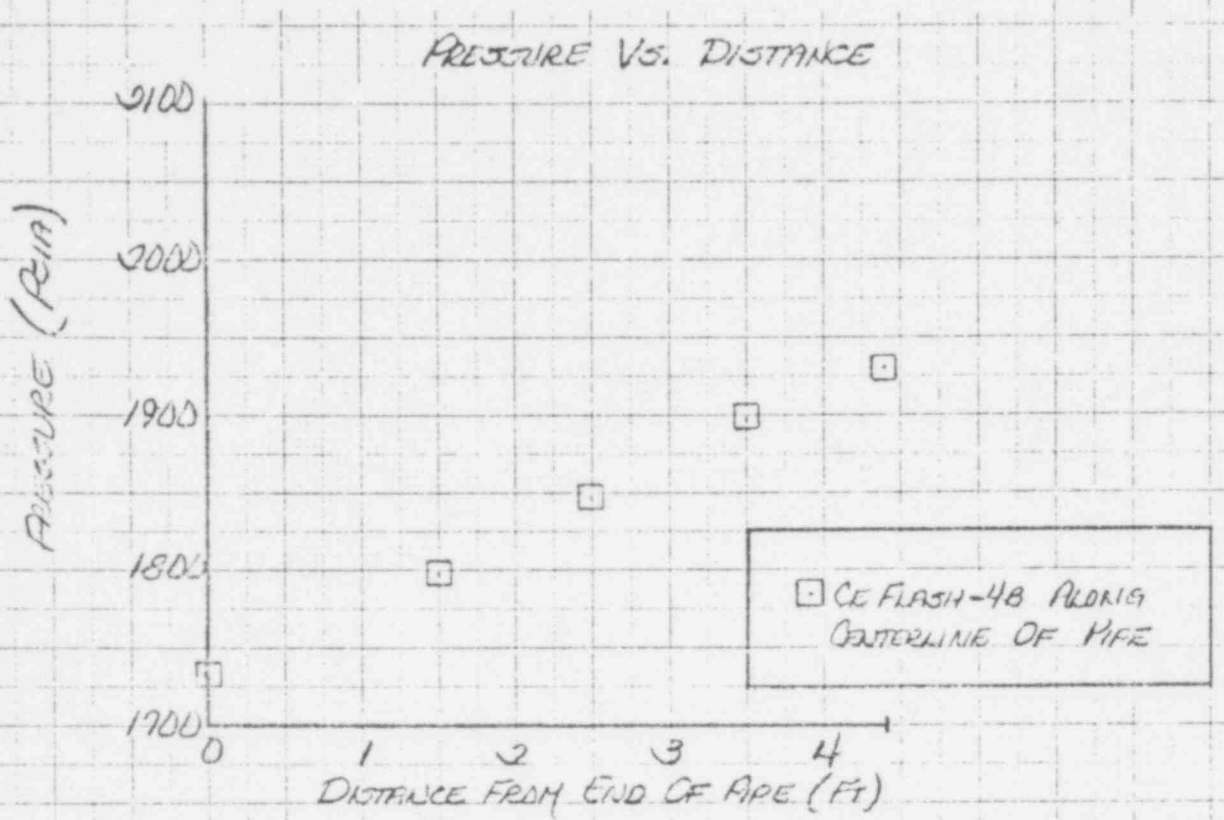

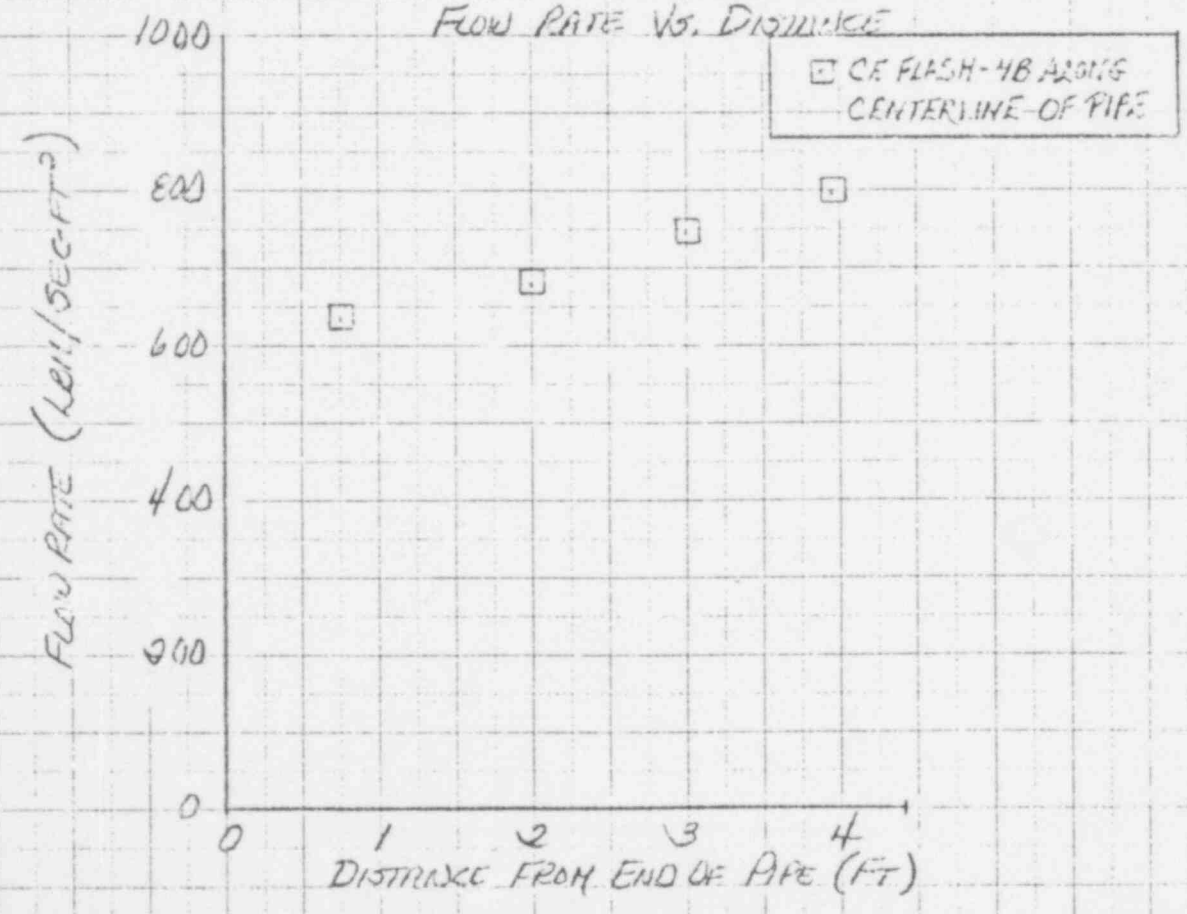

FIGURE 2.3-10

NOZZLE TO DOWNCOMER INTERFACE PROBLEM
PRESSURE AND FLOW RATE ALONG CENTERLINE
OF PIPE AT 2.75 MSEC

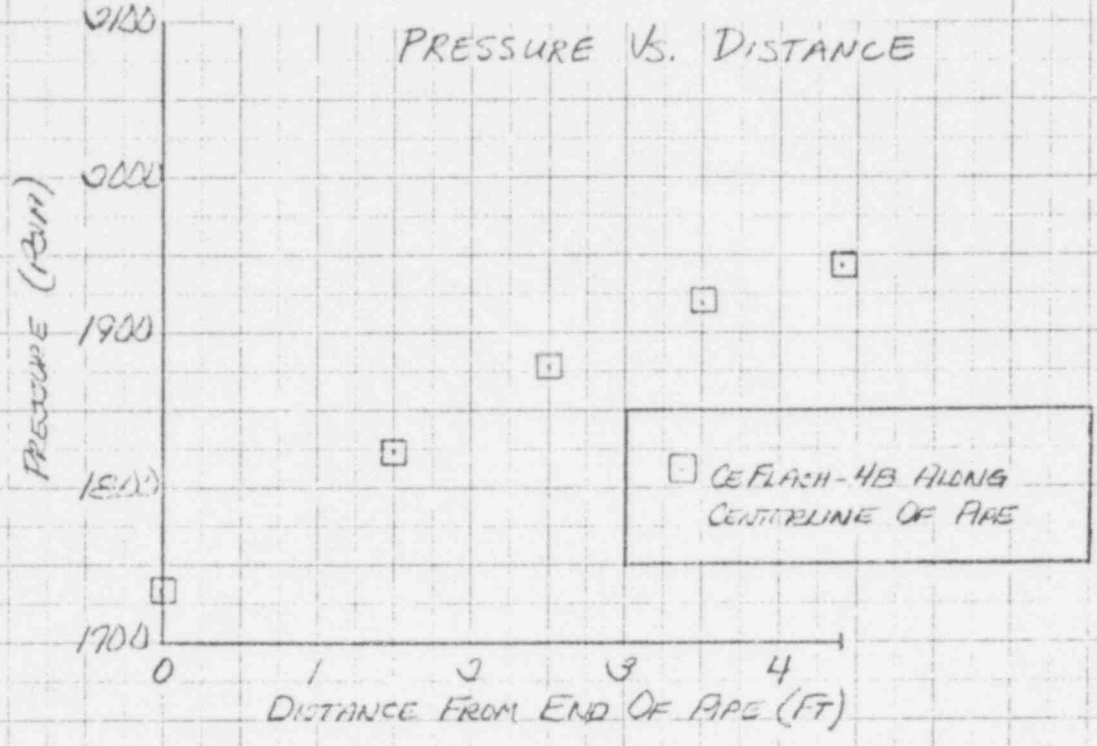

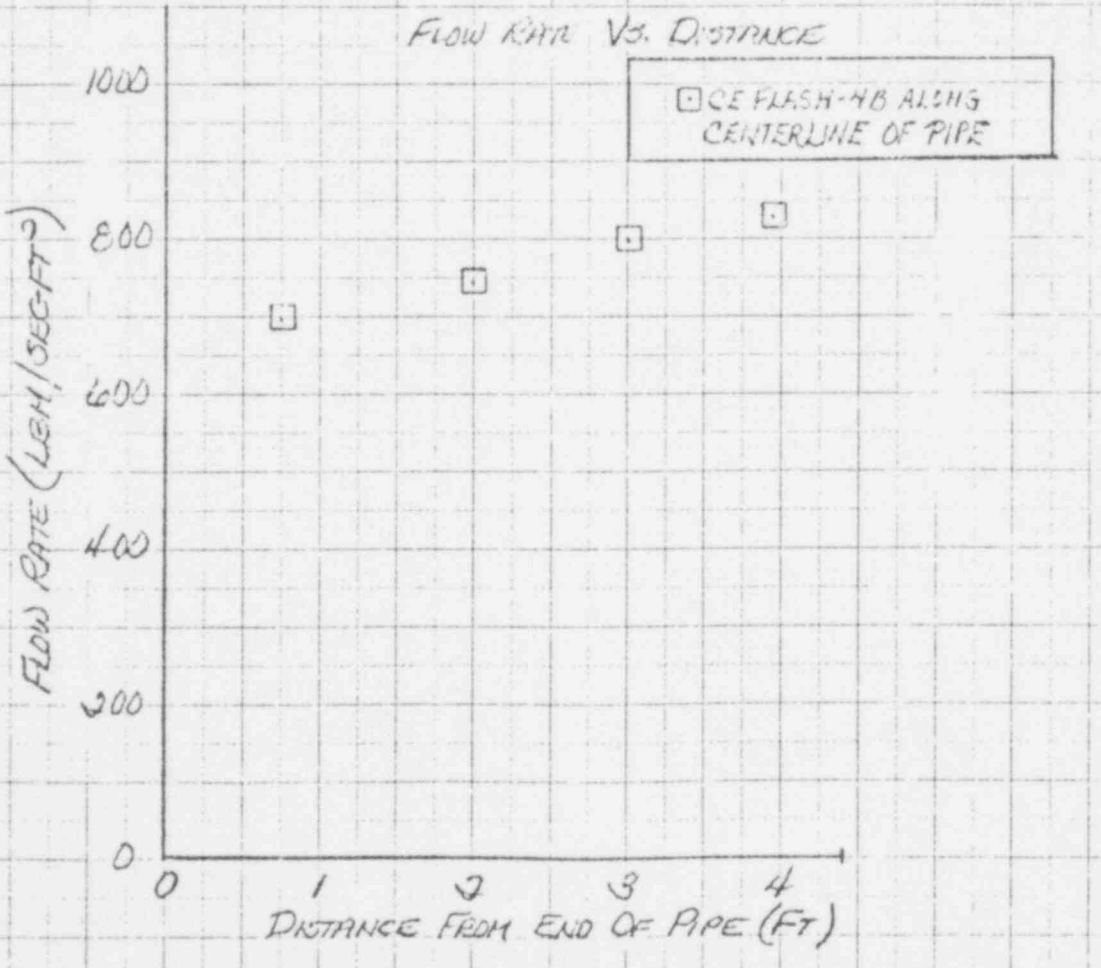

FIGURE 2.3-11

NOZZLE TO DOWNCOMER INTERFACE PROBLEM
PRESSURE AND FLOW RATE ALONG CENTER
OF THE GAP REGION AT 1.0 MSEC

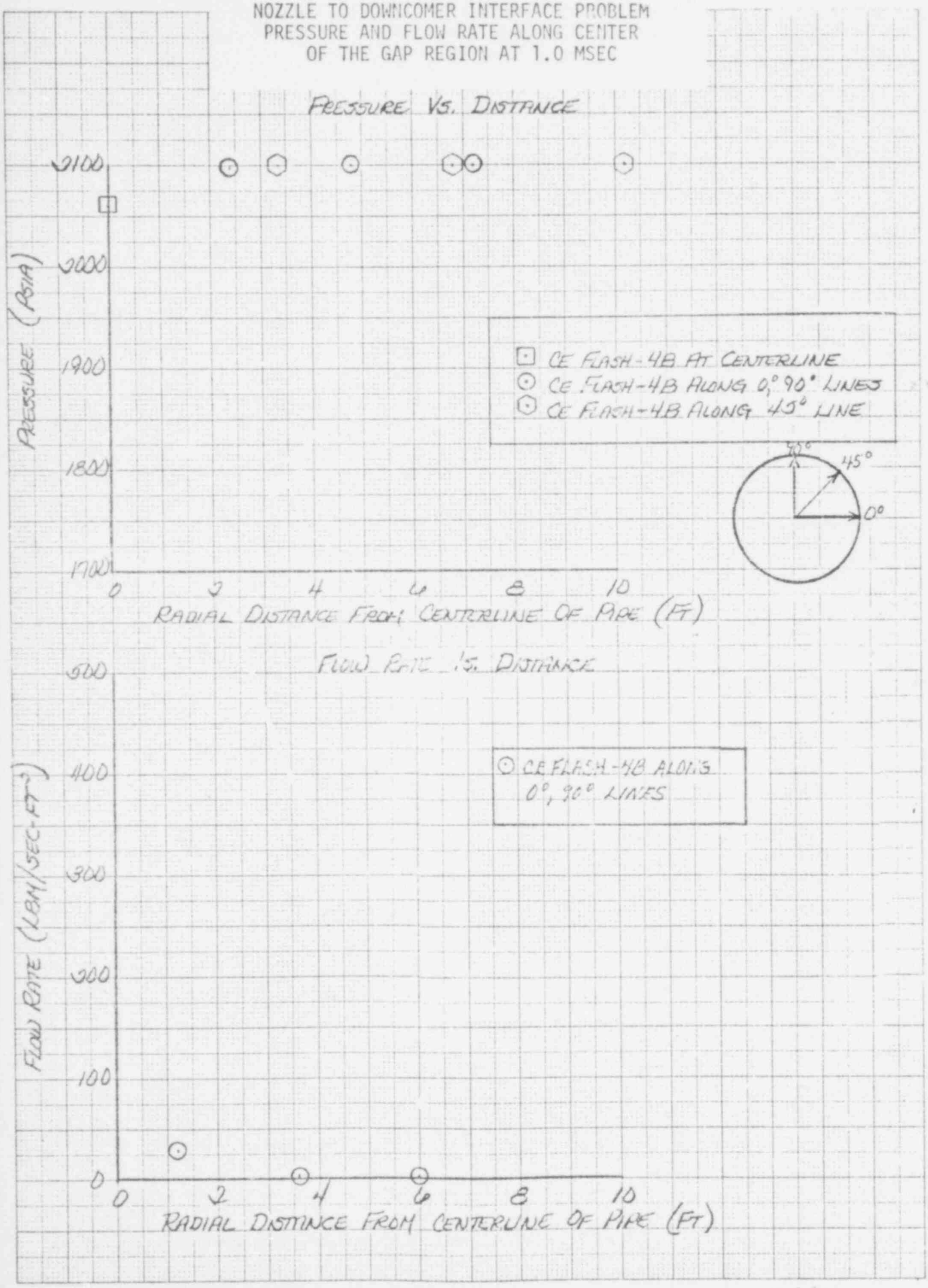

596 341

FIGURE 2.3-12

NOZZLE TO DOWNCOMER INTERFACE PROBLEM
PRESSURE AND FLOW RATE ALONG CENTER
OF THE GAP REGION AT 1.25 MSEC

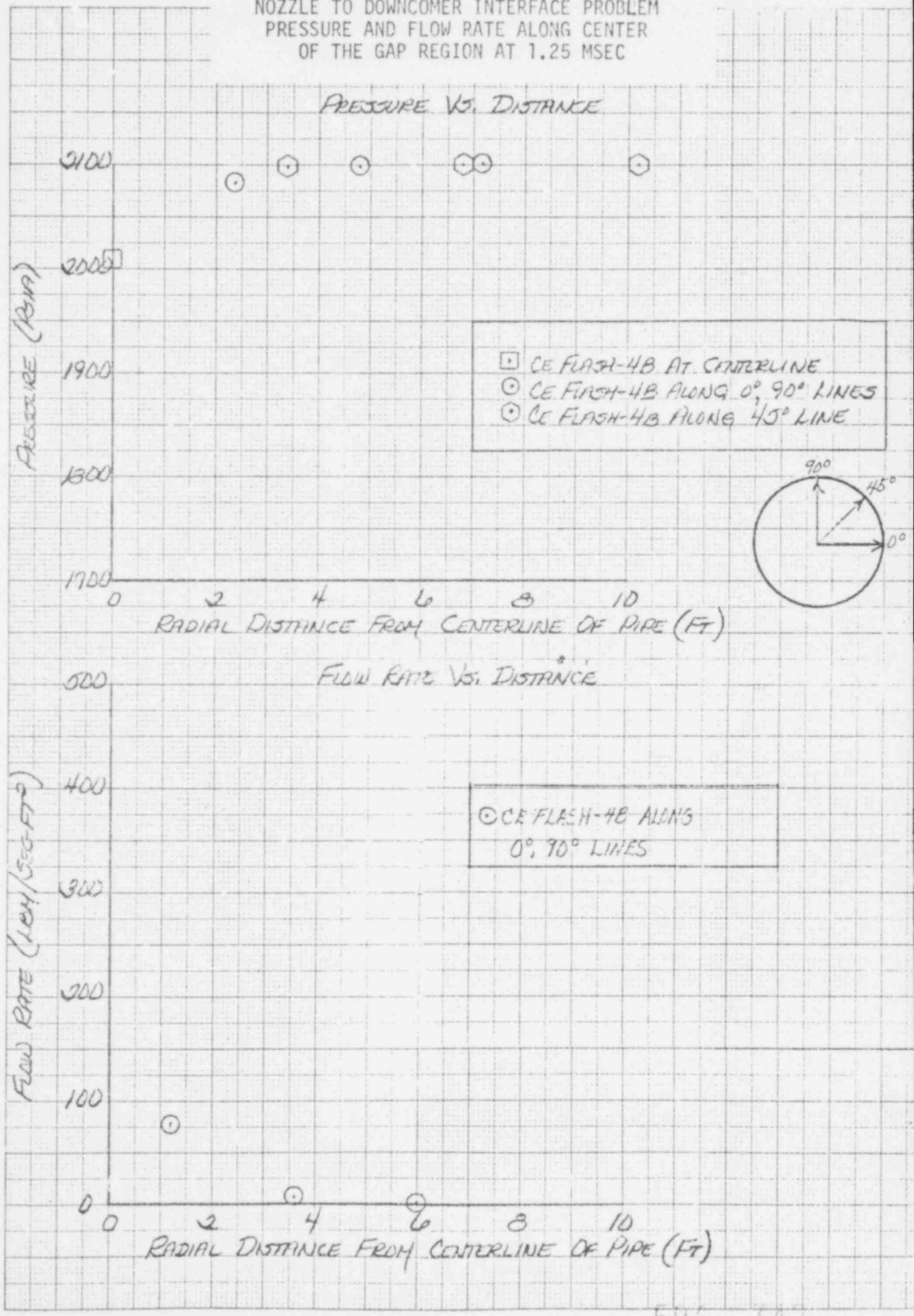

FIGURE 2.3-13

NOZZLE TO DOWNCOMER INTERFACE PROBLEM
PRESSURE AND FLOW RATE ALONG CENTER
OF THE GAP REGION AT 1.50 MSEC

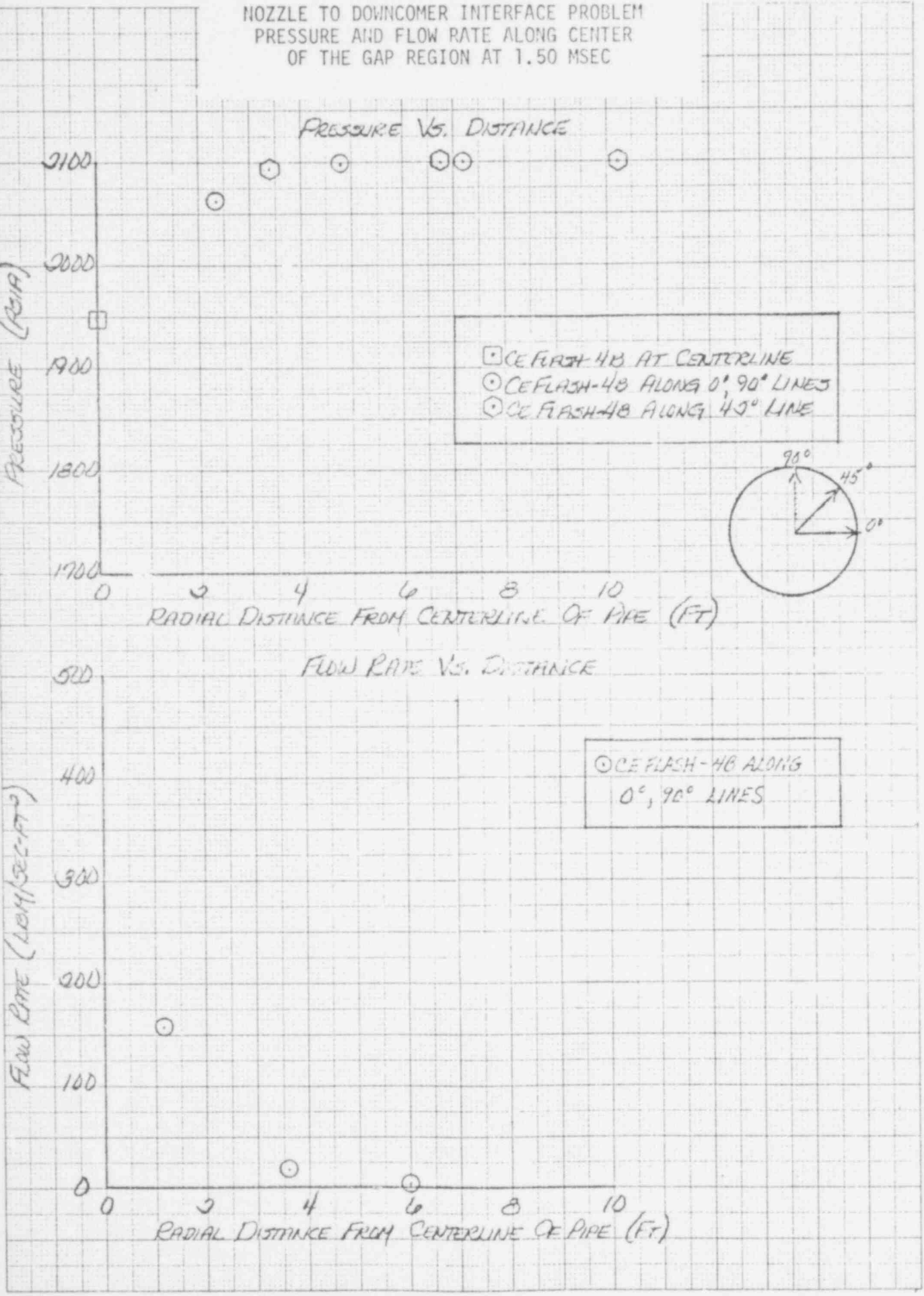

596 343

FIGURE 2.3-14

NOZZLE TO DOWNCOMER INTERFACE PROBLEM
PRESSURE AND FLOW RATE ALONG CENTER
OF THE GAP REGION AT 1.75 MSEC

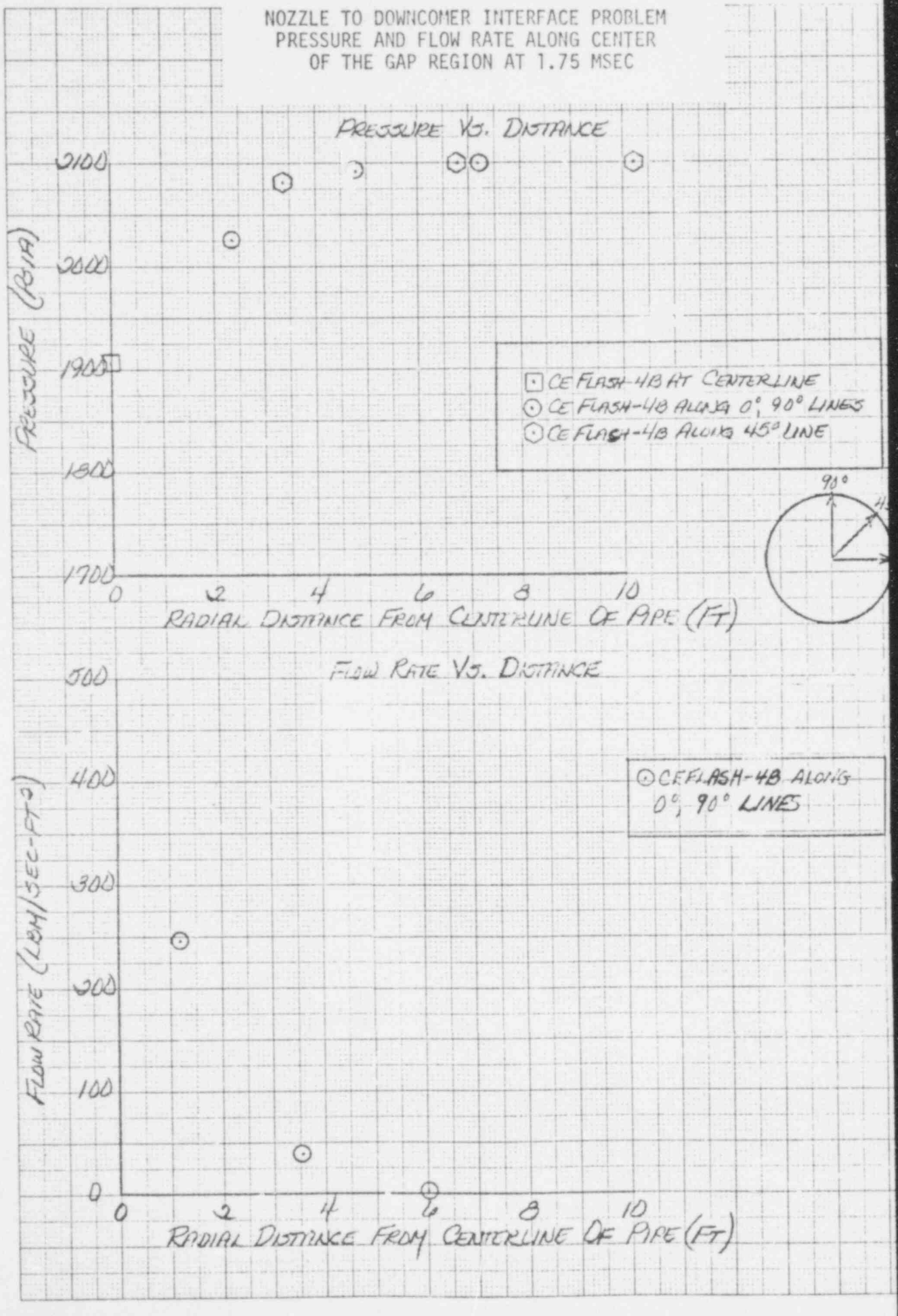

596 344

FIGURE 2.3-15

NOZZLE TO DOWNCOMER INTERFACE PROBLEM
PRESSURE AND FLOW RATE ALONG CENTER
OF THE GAP REGION AT 2.0 MSEC

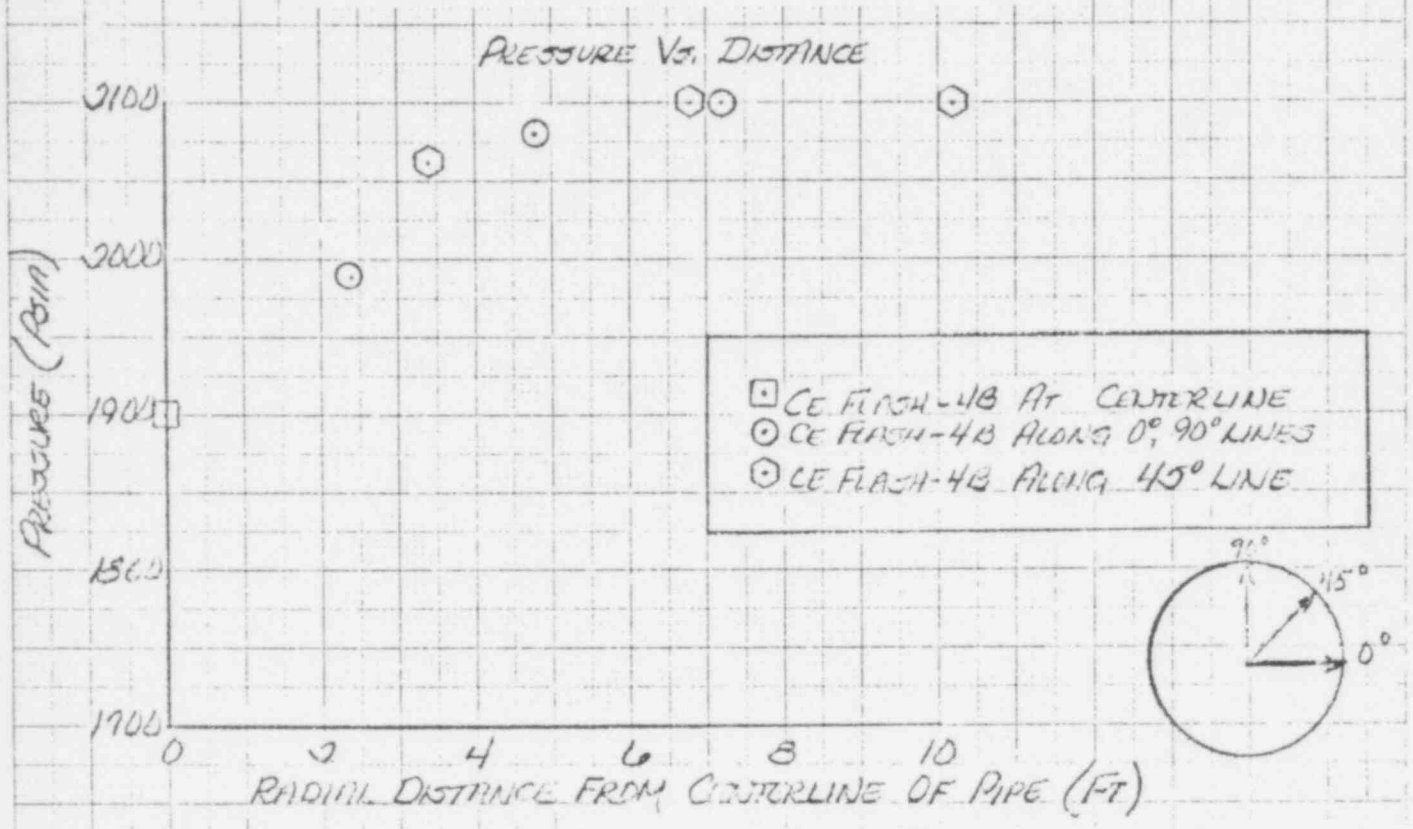

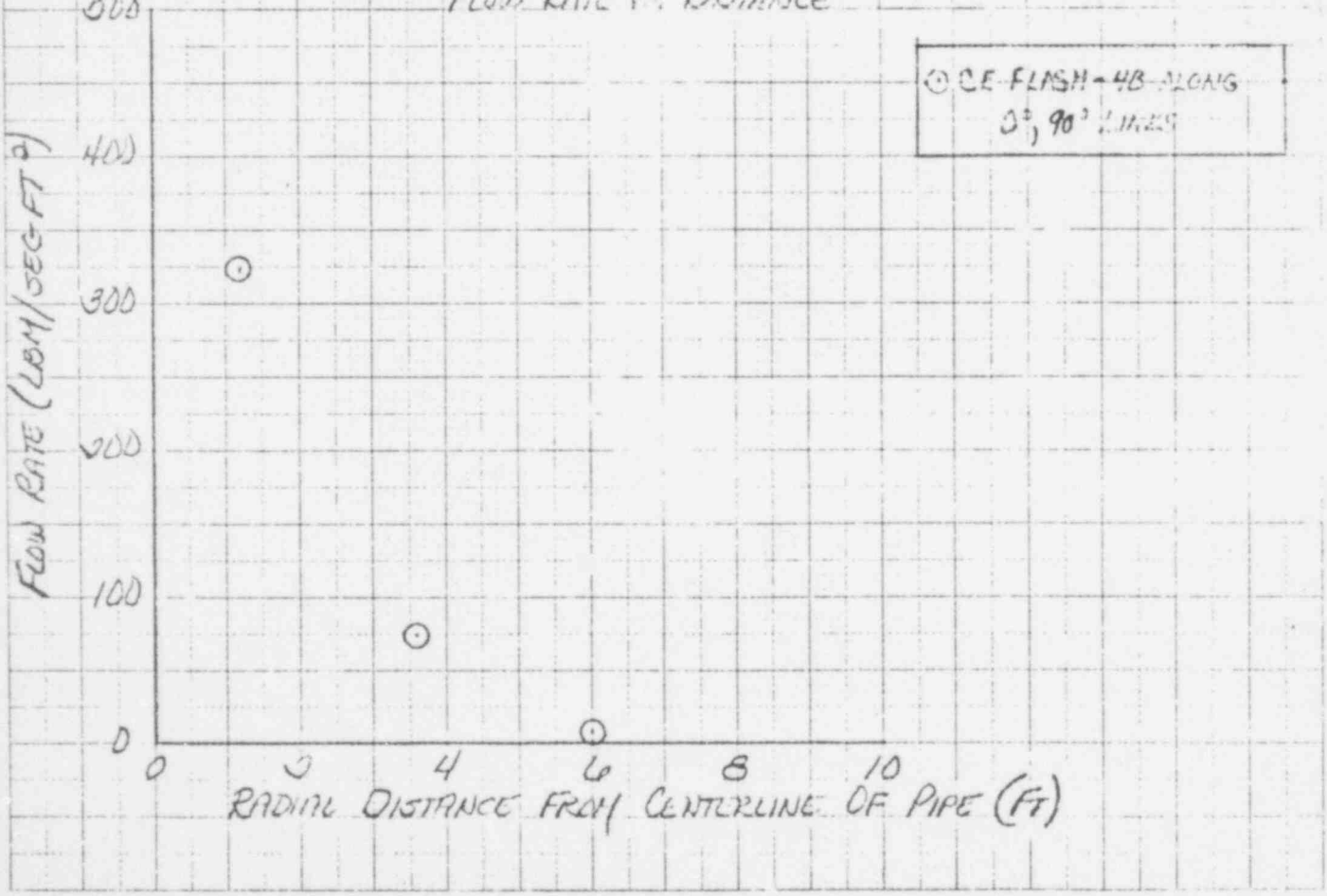

596 345

FIGURE 2.3-16

NOZZLE TO DOWNCOMER INTERFACE PROBLEM
PRESSURE AND FLOW RATE ALONG CENTER
OF THE GAP REGION AT 2.25 MSEC

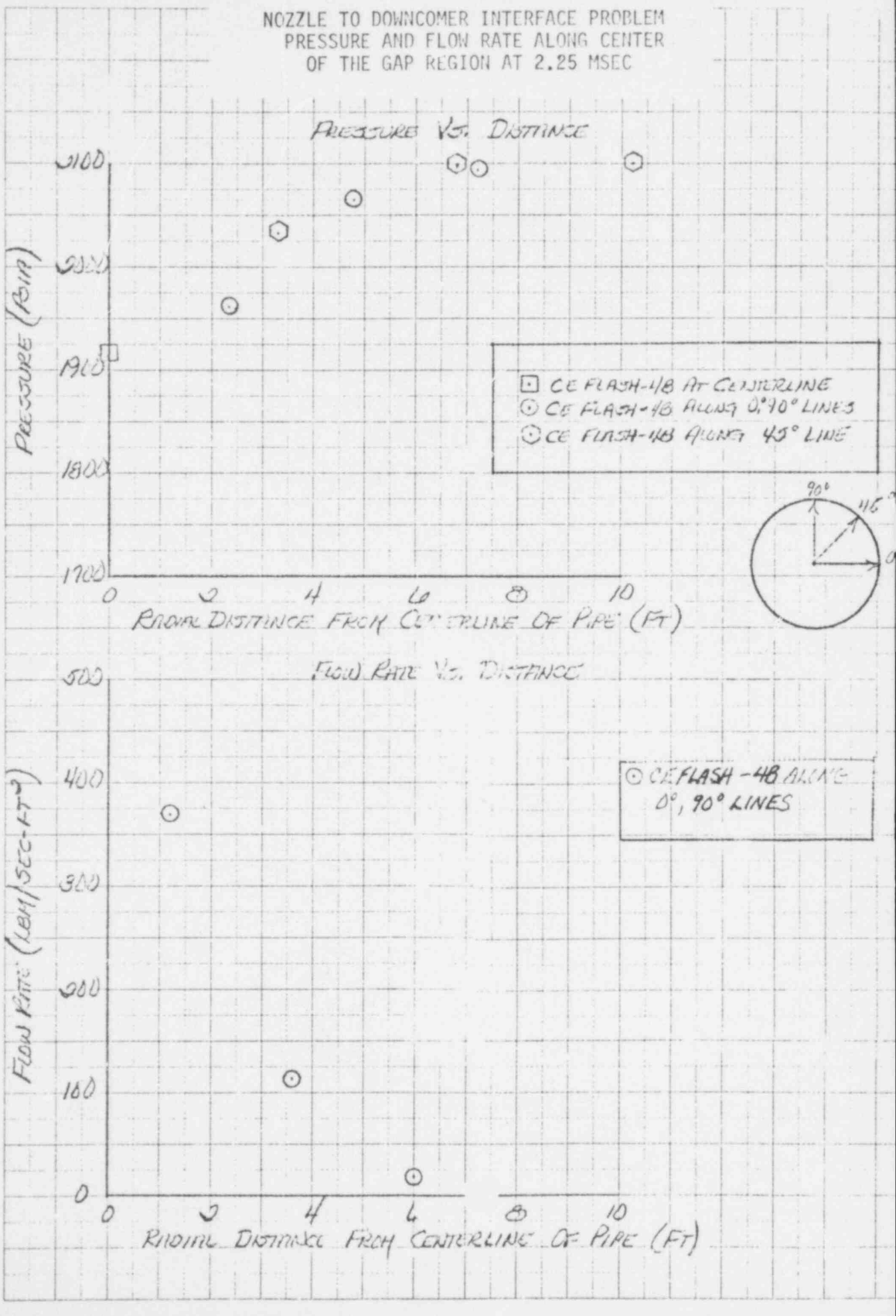

596 346

FIGURE 2.3-17

NOZZLE TO DOWNCOMER INTERFACE PROBLEM
PRESSURE AND FLOW RATE ALONG CENTER
OF THE GAP REGION AT 2.50 MSEC

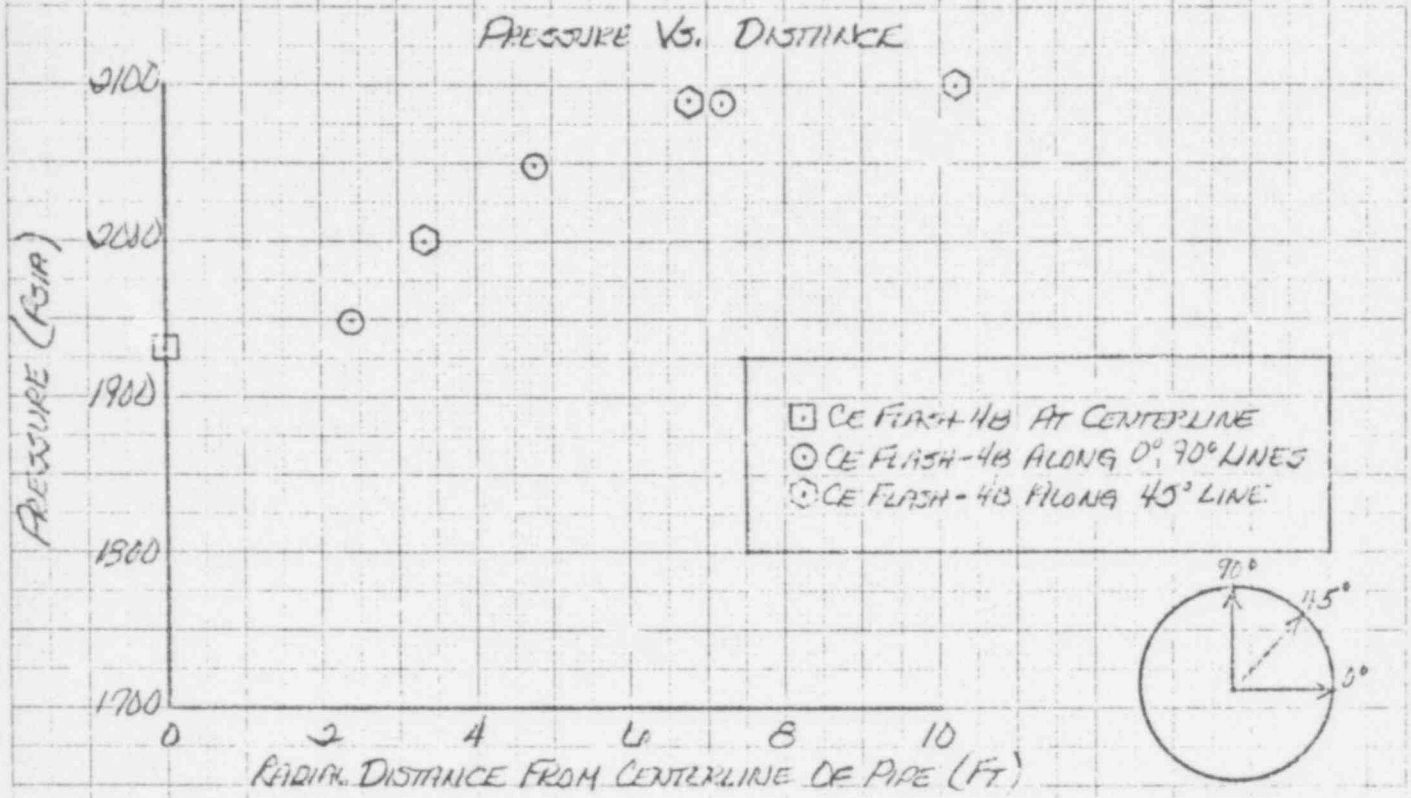

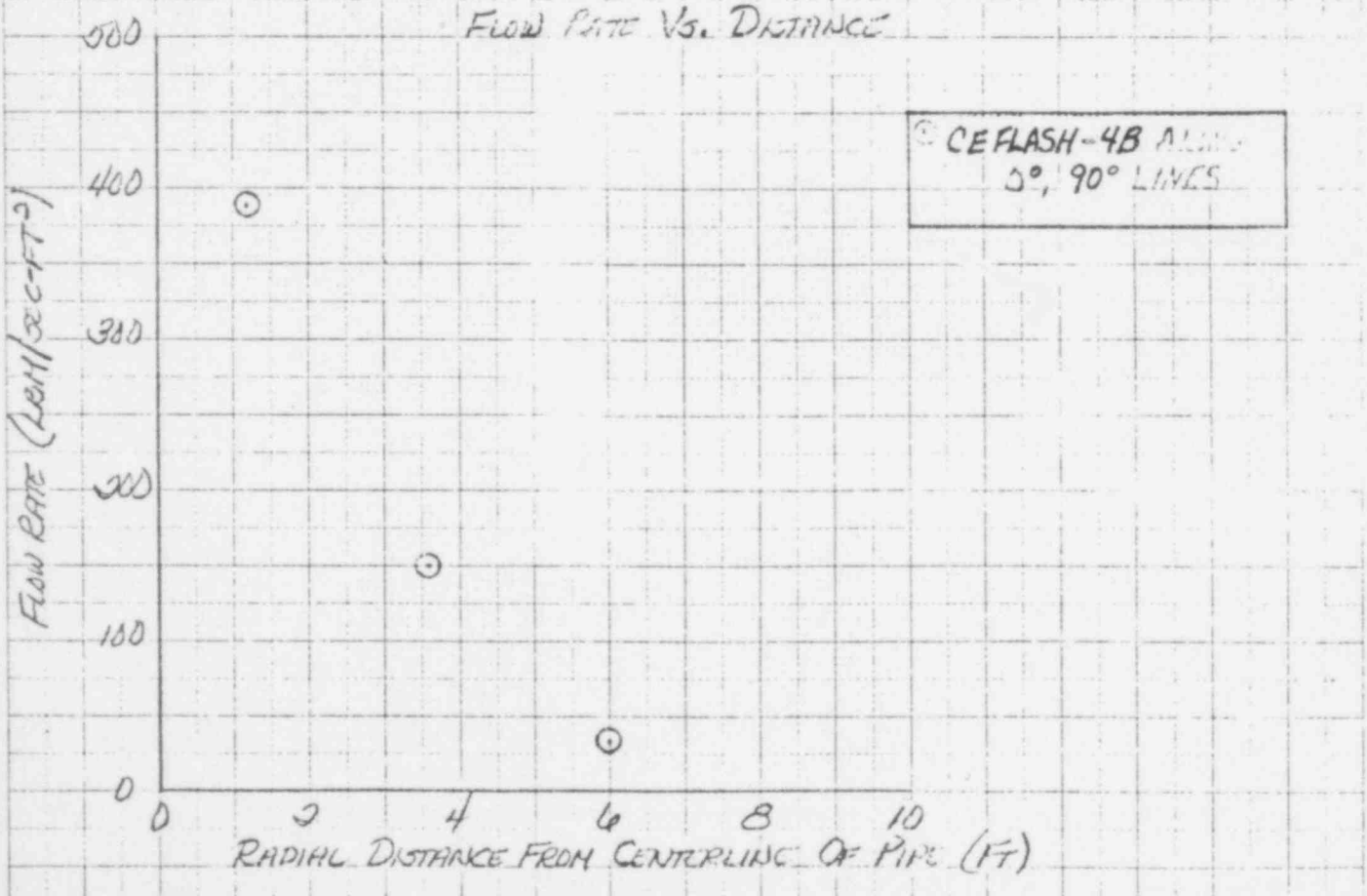

FIGURE 2.3-18

NOZZLE TO DOWNCOMER INTERFACE PROBLEM
PRESSURE AND FLOW RATE ALONG CENTER
OF THE GAP REGION AT 2.75 MSEC

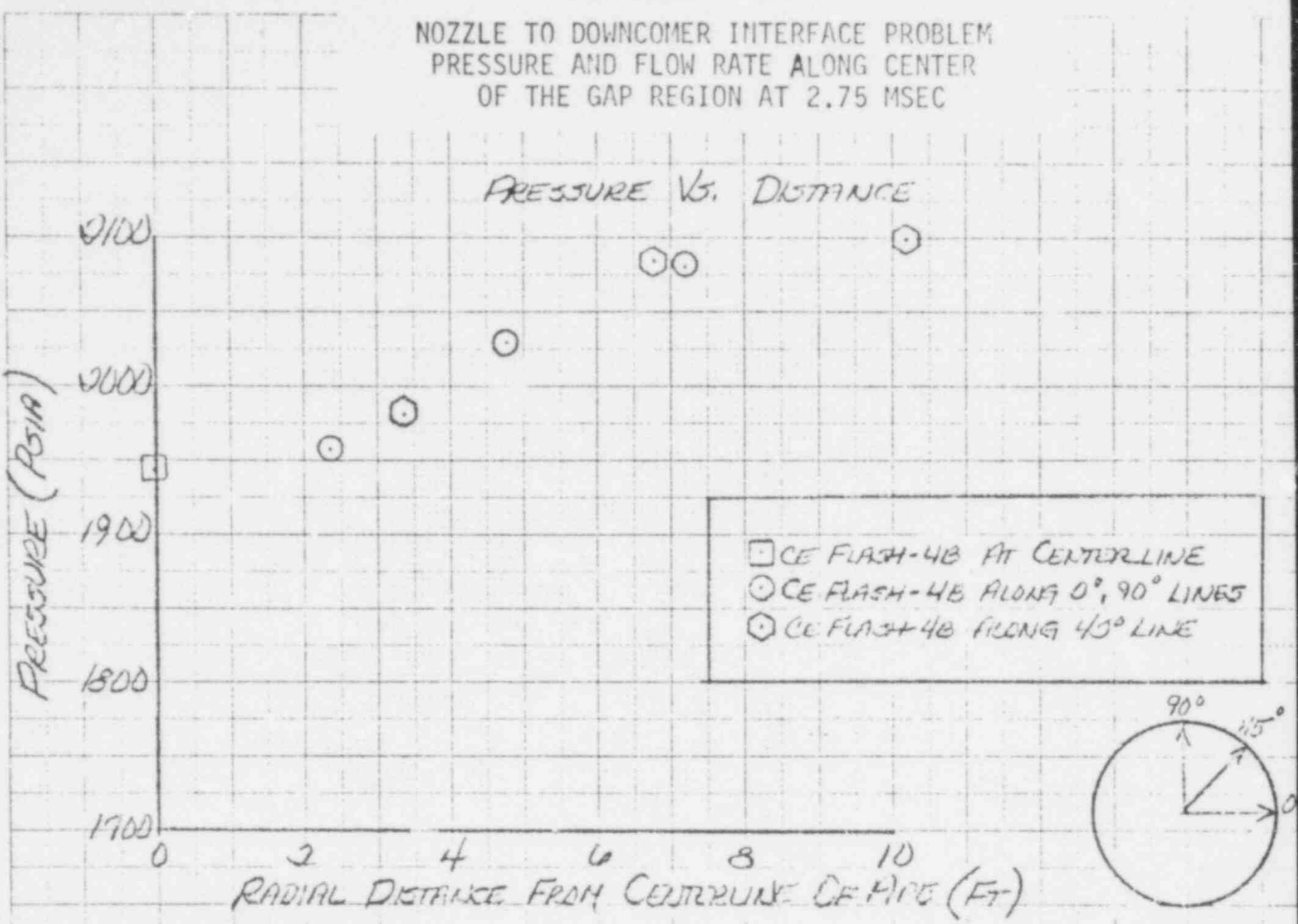

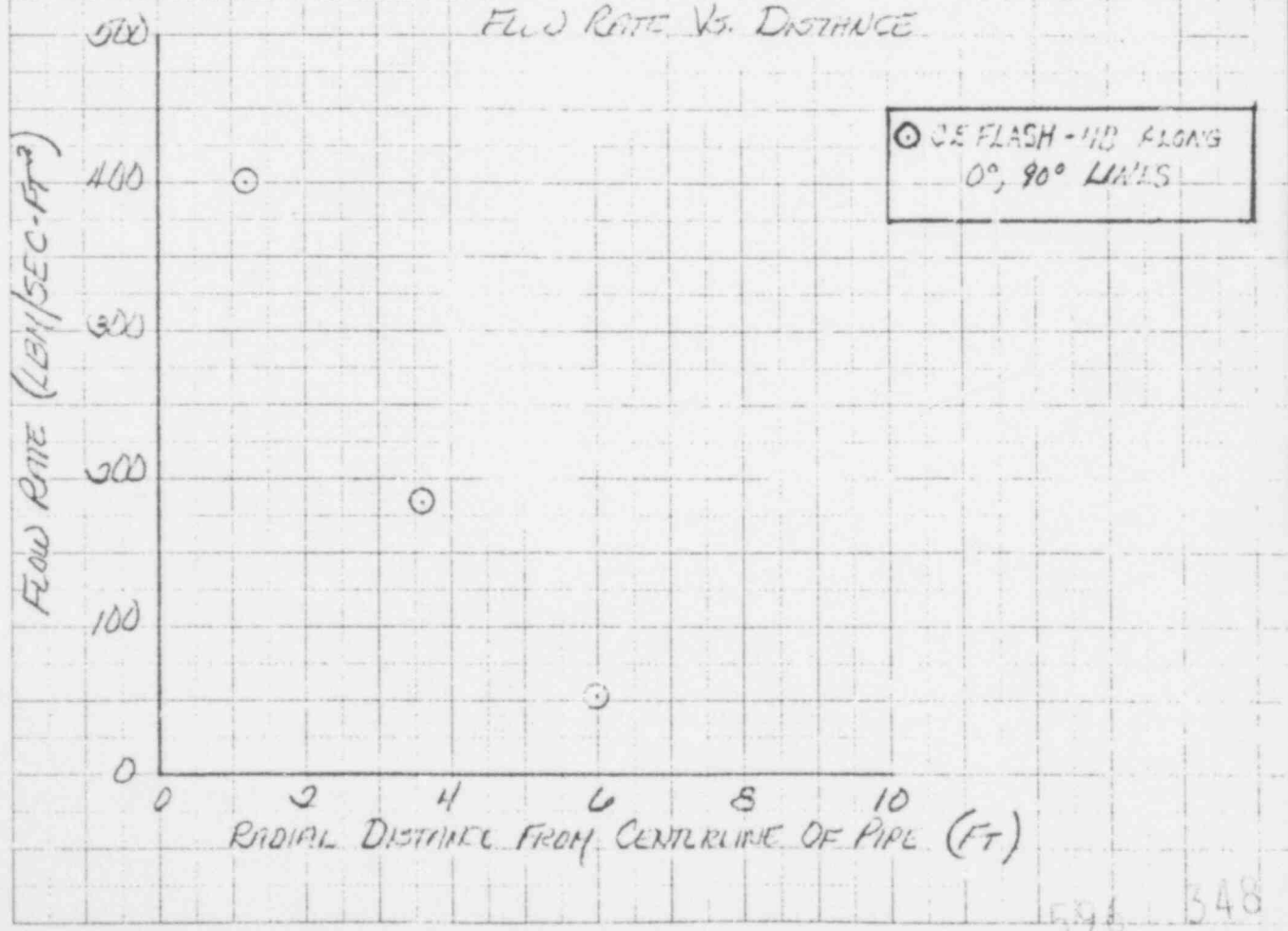

5.4.6-548

Question 2.4

2.4 Three annulus models have been analyzed in CENPD-252-P. The following additional information is to be provided for each model:

(a) Complete CEFLASH-4B listing of the input data through time step zero.

(b) A plot of the spacially integrated total hydraulic load, summation of dp*A, on the core support barrel. The positive force is defined as towards the broken nozzle.

With reference to the integrated loads, provide justification for the annulus model to be used for licensing calculations.

Response

(a) CEFLASH-4B INPUT

The complete CEFLASH-4B input listings and zero time code edits are presented in Tables 2.4-1 through 2.4-3 for the [ ]. For convenience, the node-flowpath models corresponding to these listings are shown in Figures 2.4-1 to 2.4-3. These figures differ slightly (by the addition of an extra break path) from the annulus models presented in figures 4-12, 4-13 and 4-14 of the topical report and should replace them.

(b) SPACIALLY INTEGRATED TOTAL HYDRAULIC LOAD

A plot of the spacially integrated total hydraulic load on the core support barrel (CSB) for the three annulus models is presented in Figure 2.4-4. The spacial integration has been performed using standard structural design procedures described in reference 2.4-1. In these analyses the positive force has been defined (as required) towards the broken nozzle. As can be seen from the figure all models are in close agreement. The initial peak loads calculated by the three models are found to be within ~3% (the highest load being predicted with the [ ] downcomer annulus model). The percentage difference increases

376 249

at later times, with the[ ]model generally predicting the higher loads. All models predict CSB loads to dissipate approximately 70 milliseconds after blowdown. It may also be noted that the loading frequency characteristics on the core barrel are similar for all models, particularly at the early period following blowdown.

Based on the above comparison and comparisons presented in Section 4 of the topical report it can be seen that all annulus models presented provide good agreement with one another in the prediction of transient pressure and the consequent core support barrel loading. However, for purposes of blowdown loads design applications, CE has selected to use the[ ]node[ ]annulus representation. The added detail of the[ ]node model will provide slightly more accurate loads predictions, than either of the simpler representation

Reference

2.4-1. Combustion Engineering, Inc., "Dynamic Analysis of Reactor Vessel Internals Under Loss-of-Coolant-Accident Conditions with Application of Analysis to CE 800 MWe Class Reactors", CENPD-42, August 1972 (proprietary).

596 350

[3,5]

FIGURE 2.4-1

DOWNCOMER ANNULUS MODEL

Figure 2.4-2

DOWNCOMER ANNULUS MODEL

[3,5

FIGURE 2.4-5

DOWNCOMER ANNULUS MODEL

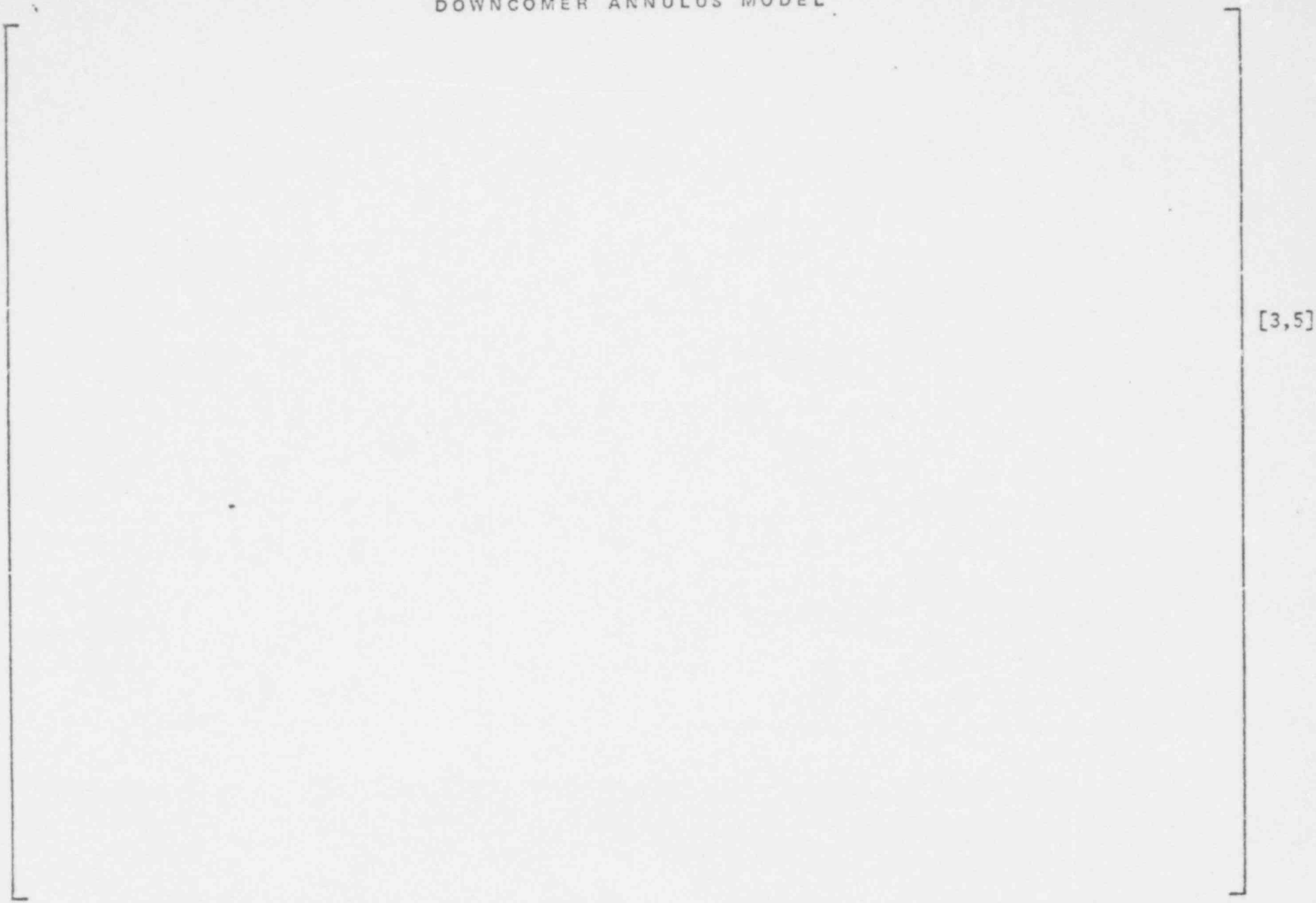

[3,5]

Figure 2.4-4
ANNULUS STUDY
COMPARISON OF INTEGRATED CORE SUPPORT BARREL LOADS
(RESOLVED PARALLEL TO BROKEN NOZZLE)

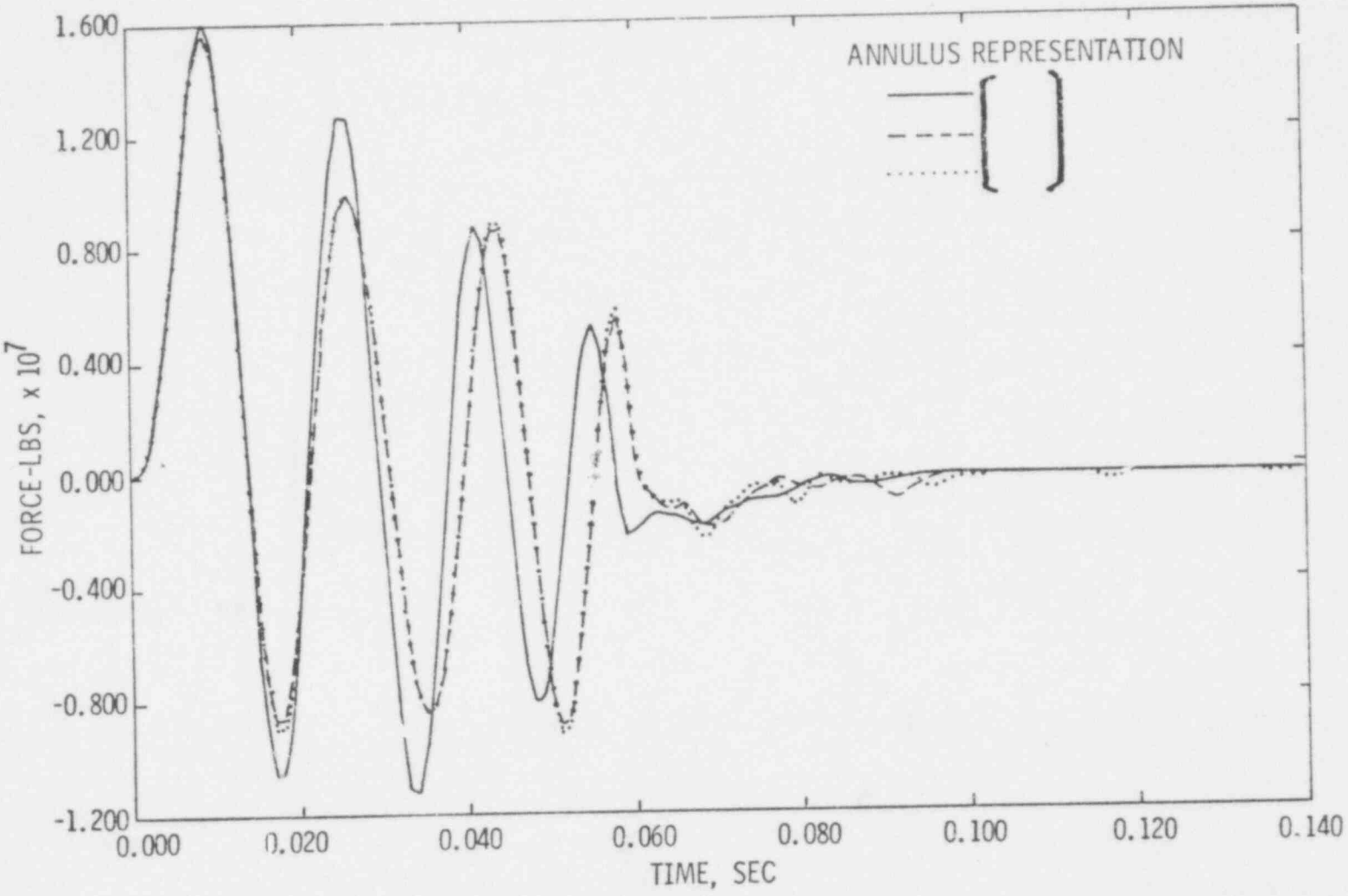

AS REQUESTED BY THE NRC (SEE SECTION 1.0 OF THIS SUPPLEMENT), ASSOCIATED PROPRIETARY COMPUTER LISTINGS DESCRIBING THE CEFLASH-4B COMPUTER MODEL (TABLES 2.4-1 THROUGH 2.4-3) HAVE BEEN OMITTED.

Question 2.5

2.5 Three nozzle models have been analyzed in CENPD-252-P. The following additional information is to be provided for each model:

(a) A description of the volume and junction data associated with the nozzle from the break to the downcomer interface.

(b) A plot of the spacially integrated total hydraulic data, summation of dp*A on the core support barrel. The positive force is defined as towards the broken nozzle. With respect to the integrated loads, provide justification for the nozzle model to be used for licensing calculations.

Response

(a) Model Description

This section provides supplemental information for the topical report break nodalization study. For completeness an input listing and zero time edit for the one, two and three node break nozzle models are presented in Tables 2.5-1, 2.5-2 and 2.5-3 respectively. A summary of the break volume and junction data for the three models are shown in Tables 2.5-4 to 2.5-6. A node flowpath diagram for the base break node case is presented in Figure 2.5-1.

(b) Core Support Barrel Hydraulic Load

Figure 2.5-2 presents the predicted total integrated hydraulic load on the core support barrel for all three break node models. The positive force is defined towards the broken nozzle. All predictions agree very closely indicating that the single node RPV nozzle model is adequate for an accurate prediction of the net core support barrel hydraulic load. This conclusion, has been made previously, (in section 4 of the topical report) based on similarly close agreement found among the three models in the prediction of absolute pressures and pressure differences.

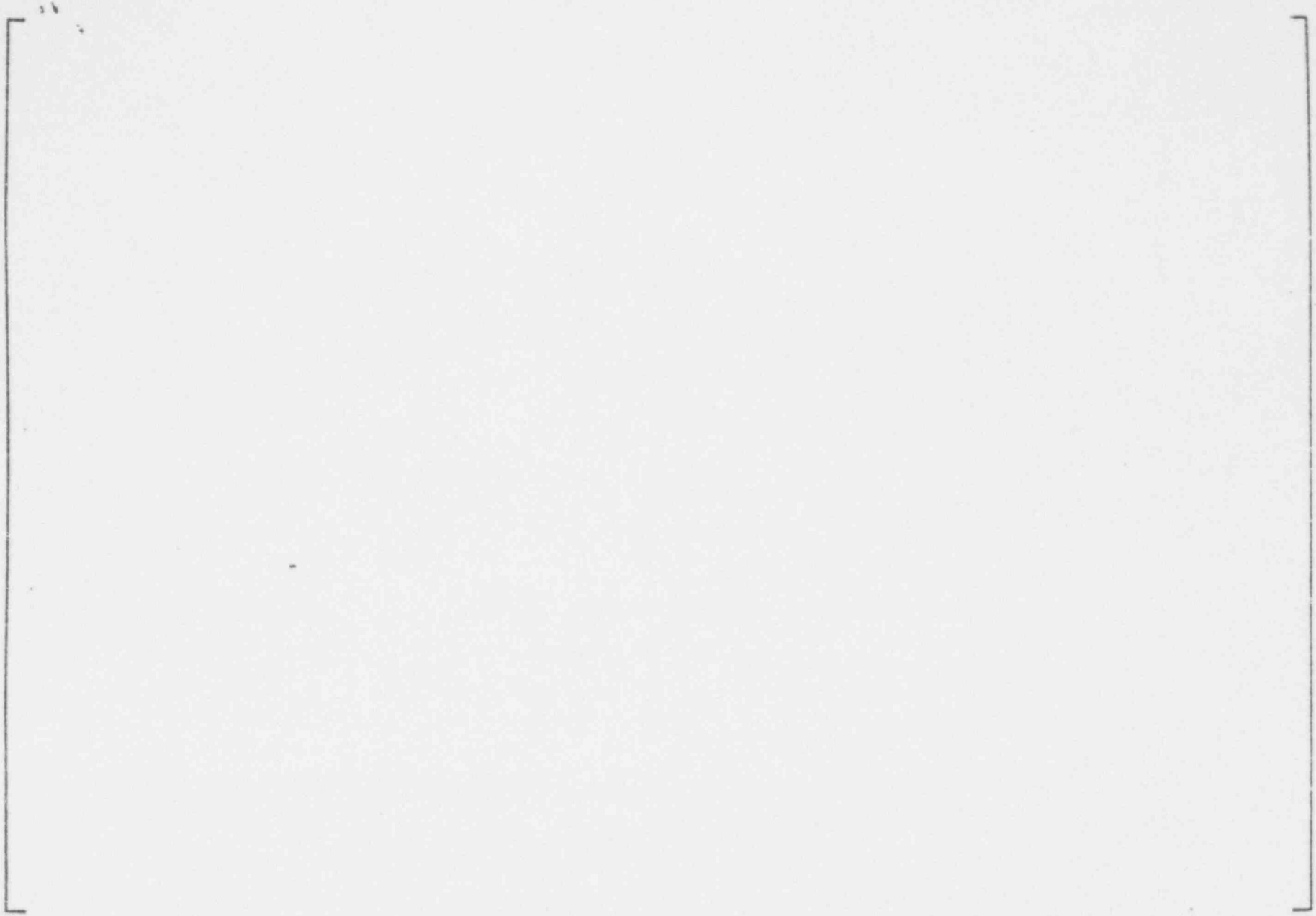

Figure 2.5-1
PARAMETER STUDY BASE MODEL

Figure 2.5-2

BREAK NODE STUDY

COMPARISON OF TOTAL PREDICTED INTEGRATED LATERAL LOADS ON THE CORE SUPPORT BARREL

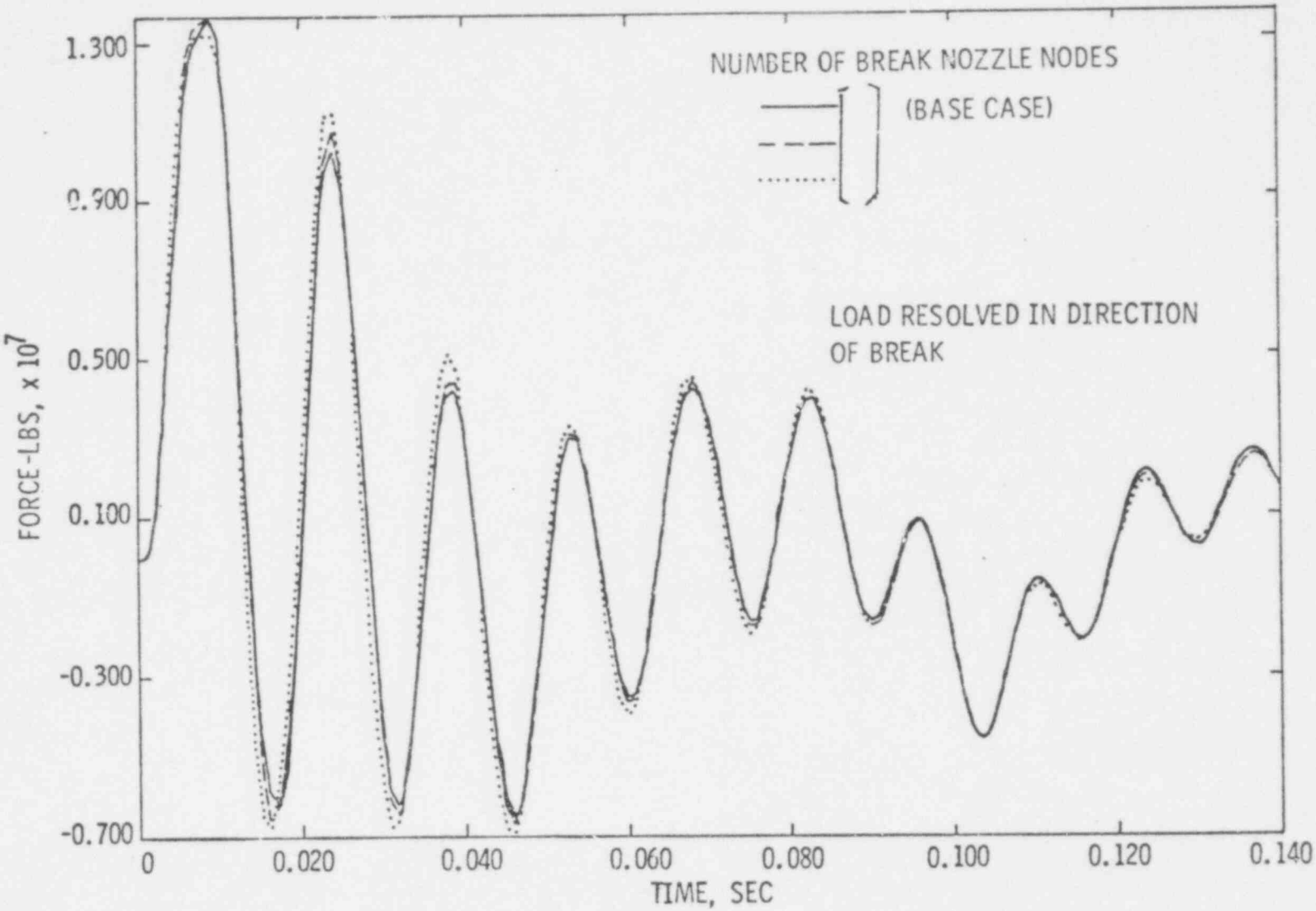

AS REQUESTED BY THE NRC (SEE SECTION 1.0 OF THIS SUPPLEMENT) ASSOCIATED PROPRIETARY COMPUTER LISTINGS (TABLES 2.5-1 THROUGH 2.5-3, PAGES 2.5-4 TO 2.5-89) DESCRIBING THE CEFLASH-4B COMPUTER MODEL HAVE BEEN OMITTED.

TABLE 2.5-4

BREAK NODE STUDY

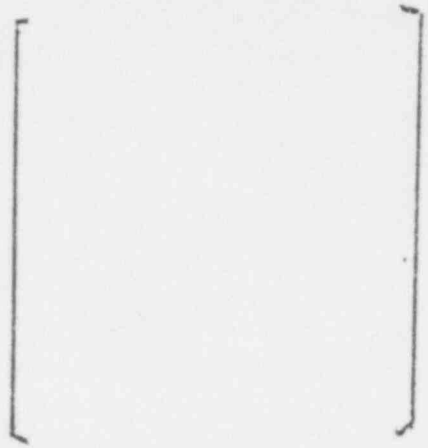

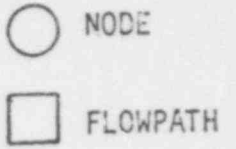

NODE DESCRIPTION

NODE NUMBER	DESCRIPTION	VOLUME (ft^3)

JUNCTION DATA

FLOWPATH NUMBER	FLOW AREA (ft^2)	FLOWPATH INERTIA (1/ft)	HYDRAULIC DIAMETER (ft)	MOMENTUM FLUX AREAS(ft^2)		ΔP LOSS(psi)		FLOWPATH LENGTH (ft)
				UPSTREAM	DOWNSTREAM	FORWARD	REVERSE	

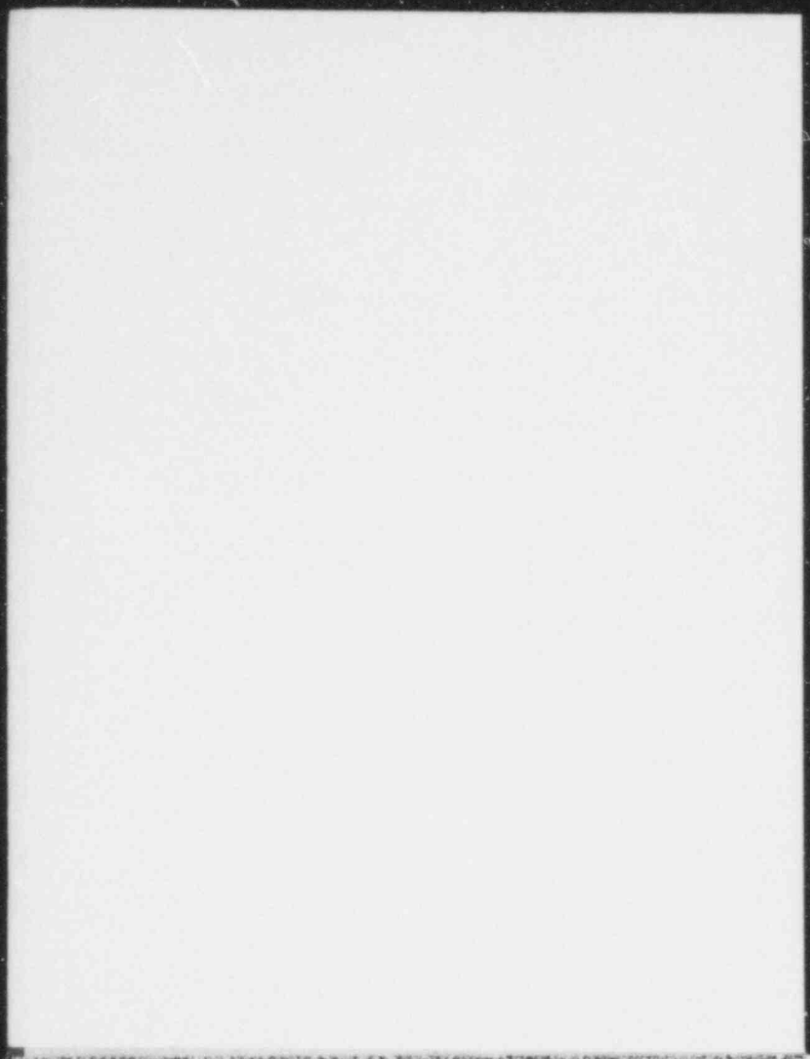

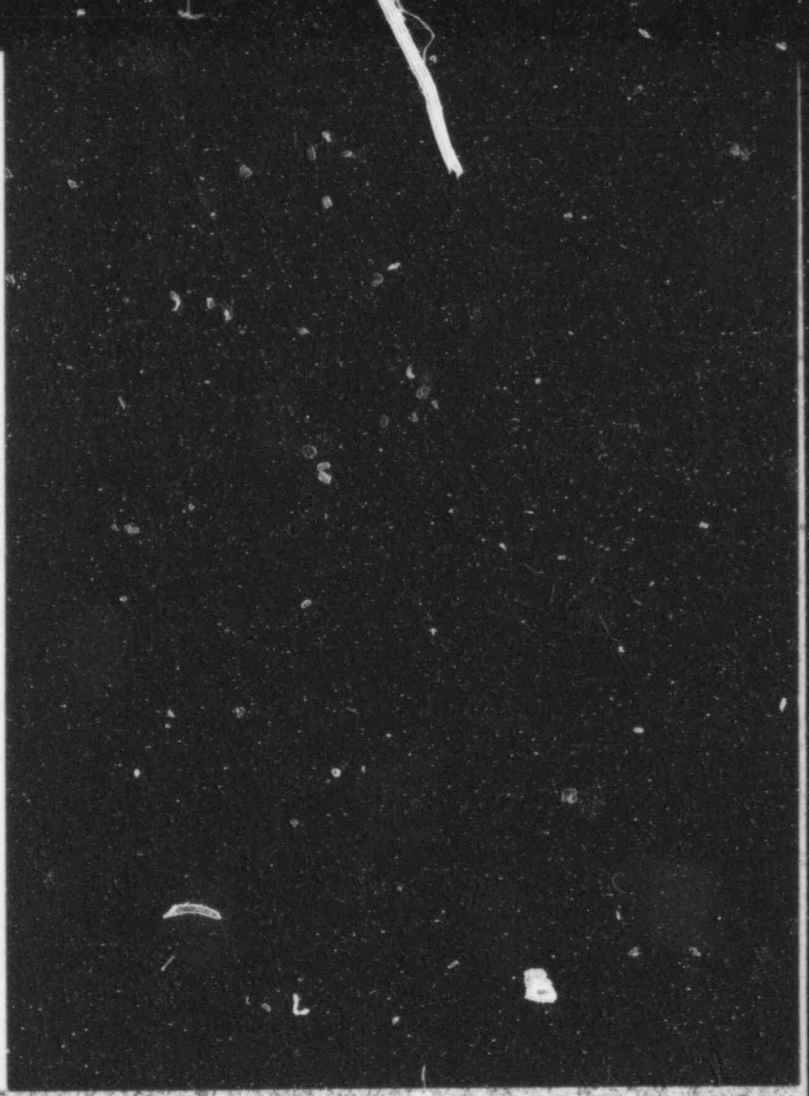

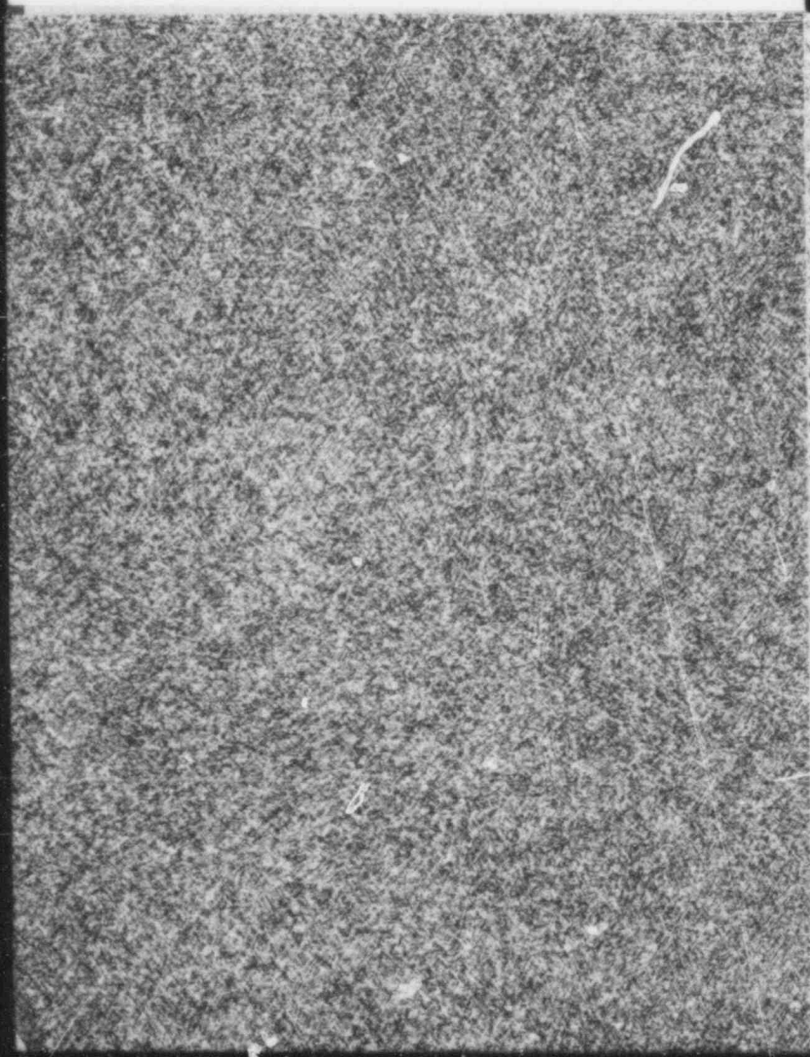

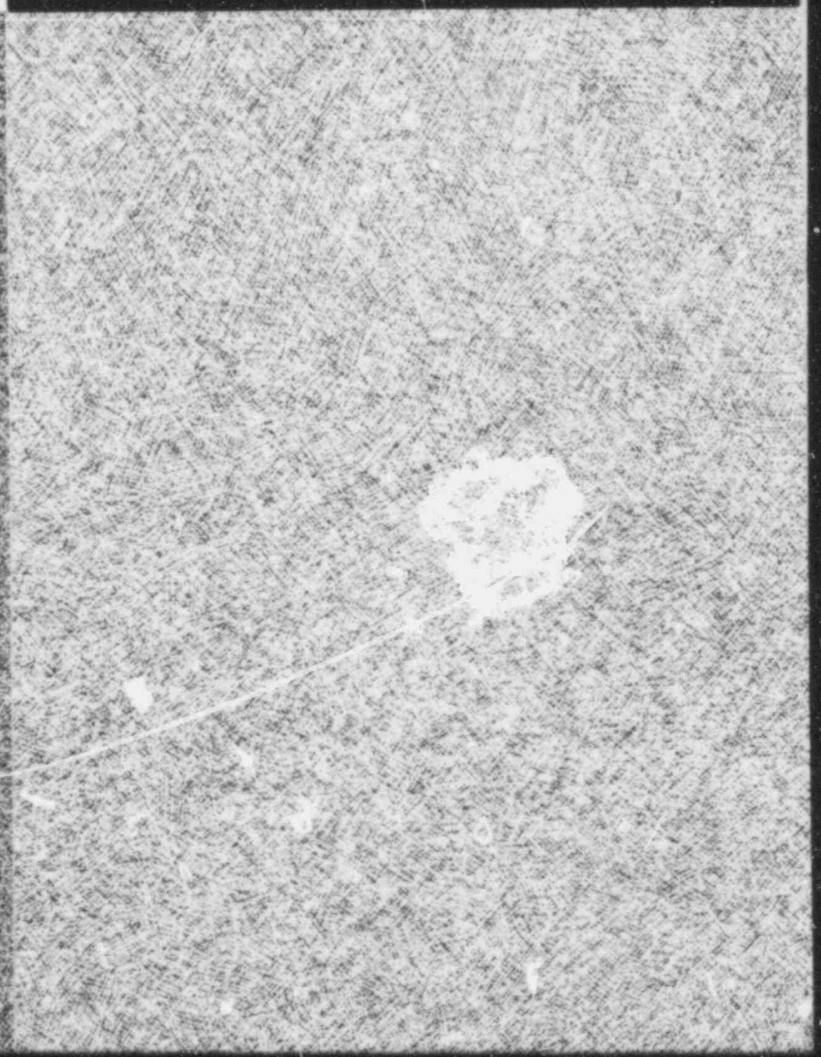

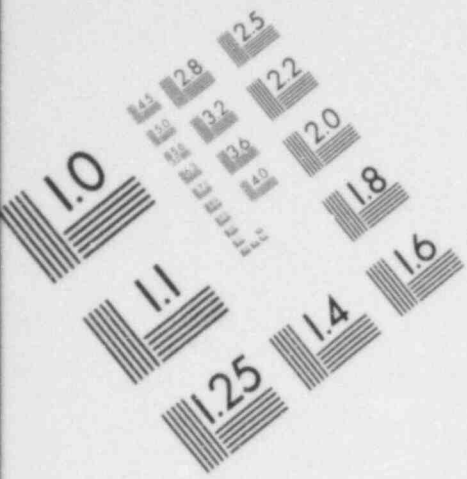

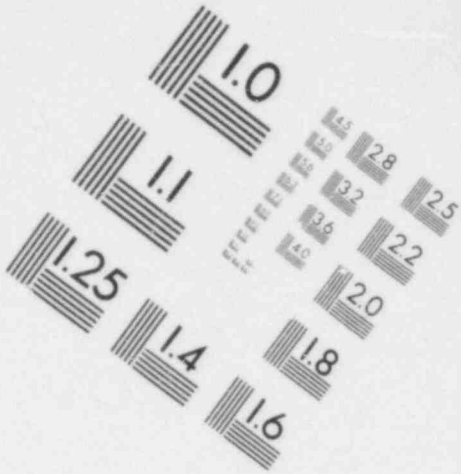

IMAGE EVALUATION TEST TARGET (MT-3)

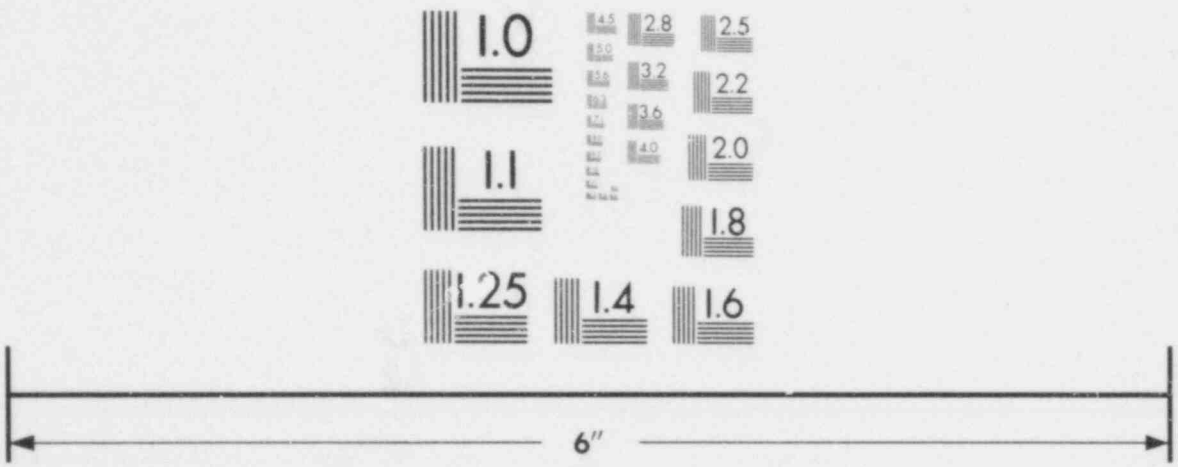

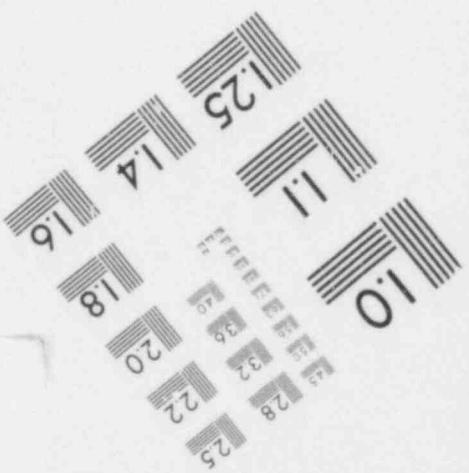

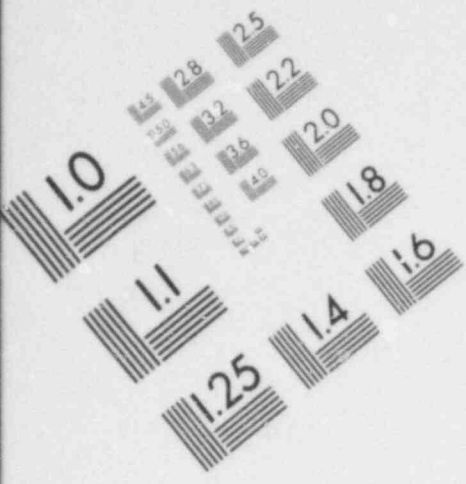

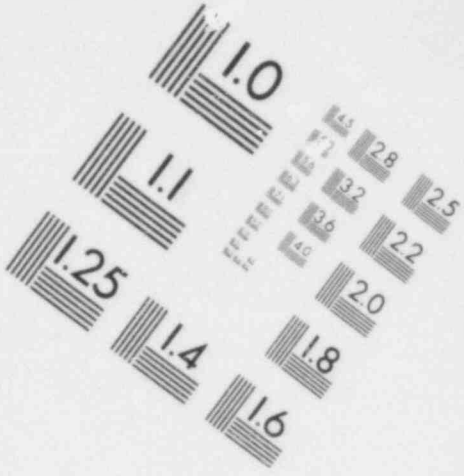

IMAGE EVALUATION TEST TARGET (MT-3)

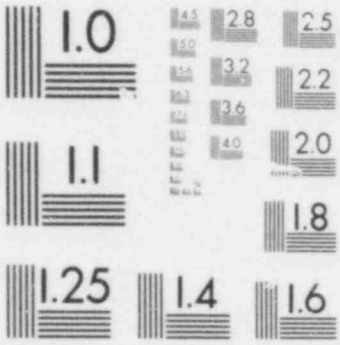

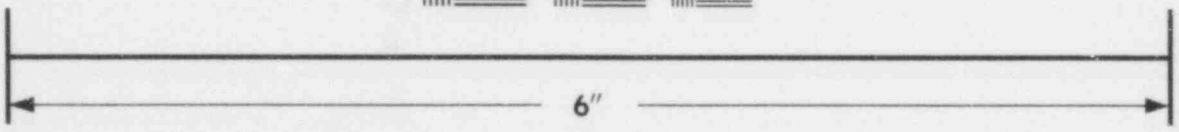

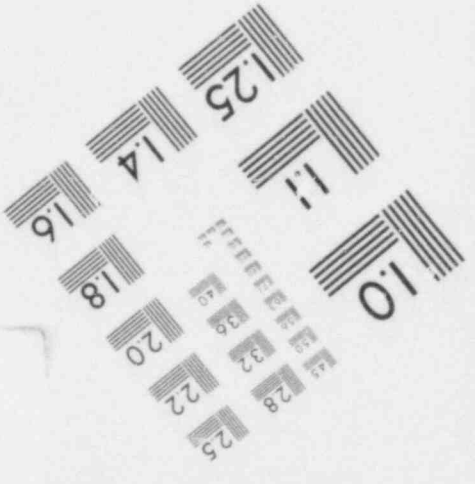

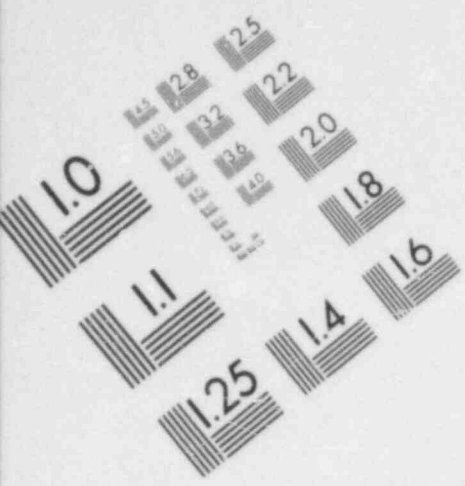

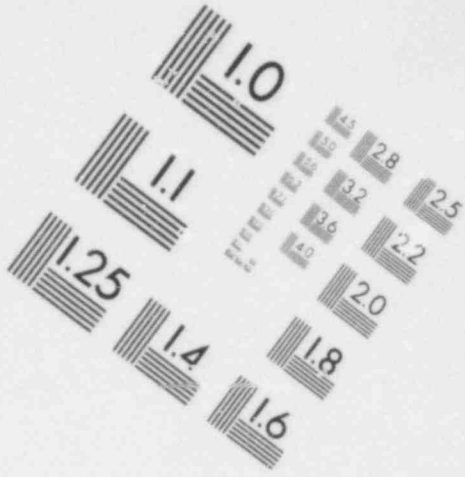

IMAGE EVALUATION TEST TARGET (MT-3)

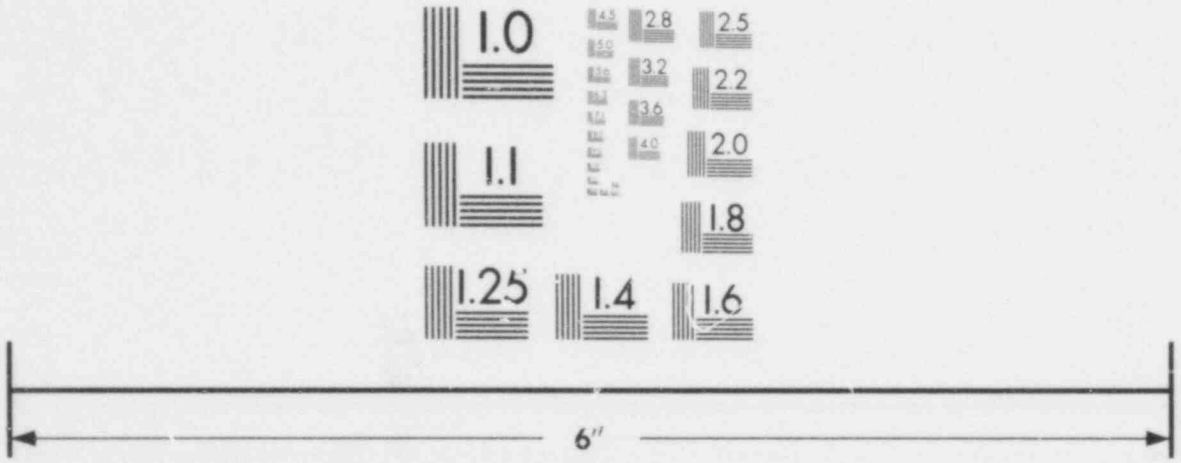

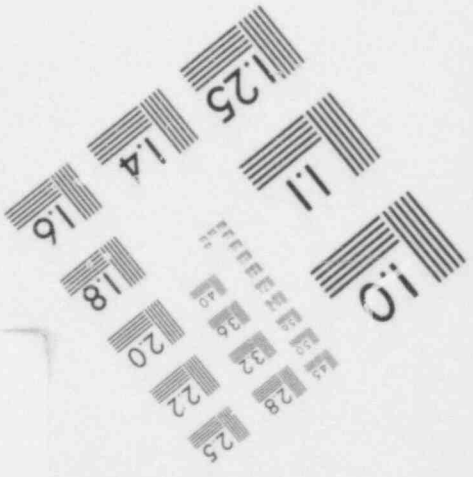

BREAK NODE STUDY

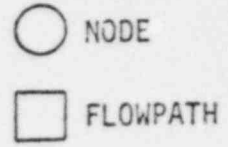

NODE DESCRIPTION

NODE NUMBER	DESCRIPTION	VOLUME (ft^3)

JUNCTION DATA

FLOWPATH NUMBER	FLOW AREA (ft^2)	FLOW INERTIA ($1/ft$)	HYDRAULIC DIAMETER (ft)	MOMENTUM FLUX AREAS (ft^2)		ΔP LOSS(psi)		FLOWPATH LENGTH (ft)
				UPSTREAM	DOWNSTREAM	FORWARD	REVERSE	

TABLE 2.5-6

BREAK NODE STUDY

○ NODE

□ FLOWPATH

NODE DESCRIPTION

NODE NUMBER	NODE DESCRIPTION	VOLUME (ft^3)
[redacted]		

JUNCTION DATA

FLOWPATH NUMBER	FLOW AREA(ft^2)	FLOWPATH INERTIA (1/ft)	HYDRAULIC DIAMETER (ft)	MOMENTUM FLUX AREAS (ft^2)		ΔP LOSS (psi)		FLOWPATH LENGTH (ft)
				UPSTREAM	DOWNSTREAM	FORWARD	REVERSE	
[redacted]								

2.5-92

594 465

202

QUESTION 2.6

2.6 The following plotted data is to be provided for the audit PWR analysis for a 350 square inch guillotine failure of the cold leg piping near the reactor pressure vessel inlet nozzle. A 5 millisecond break opening time is assumed. A 100 millisecond analysis is required. A complete listing of the CEFLASH-4B input data through time step zero is also to be provided.

(a) At each axial location in the downcomer region, provide plots of differential pressure from a location 180° from the nozzle centerline to the nozzle centerline. Identify each node.

(b) Pressure plots at the following locations. Identify each node.

1. Vessel side break
2. Pump side break
3. Nozzle to downcomer interface, broken loop
4. Vessel lower plenum
5. Core region
6. Vessel upper plenum
7. 180° from broken nozzle, at nozzle centerline in downcomer
8. Steam generator outlet plenum, broken loop
9. Pump discharge pressure, broken loop
10. 180° from broken nozzle, at lowest axial elevation.

(c) Differential pressure plot at the following locations. Identify each node.

1. Across reactor assembly
2. Across broken loop pump
3. Across broken loop steam generator
4. Across intact loop steam generator
5. From broken loop inlet nozzle to broken loop outlet nozzle (across the reactor pressure vessel).

597 083

(d) Mass flow rate plots at the following locations. Identify each junction.

1. Vessel side break
2. Pump side break
3. Core inlet

(e) Integrated load on core support barrel in the plane of the break (x-direction) and perpendicular to the break plane (y-direction).

Response

For purposes of blowdown loads methods analysis verification, the C-E audit PWR has been selected to be the C-E System 80 plant. A complete listing of the CEFLASH-4B blowdown loads input data has been previously forwarded to the NRC (Ref.2.6-1). The nodal diagram corresponding to the input listing and zero time edit is shown in Figure 5-3 of reference 2.6-3. The following paragraphs and attached figures (2.6-1 to 2.6-30) presents the requested blowdown information for a sample CEFLASH-4B System 80 350 in^2 cold leg break.

(a) DIFFERENTIAL PRESSURE PLOTS FROM A LOCATION 180° FROM THE NOZZLE CENTERLINE TO THE NOZZLE CENTERLINE.

The differential pressure around the System 80 core support barrel (CSB) is presented in Figures 2.6-1 through 2.6-6. The figures are arranged according to axial location with the downcomer node at the upper UGS elevation first (Figure 2.6-1) and the downcomer node just upstream of the lower plenum (CSB lower flange elevation) last (Figure 2.6-6). The asymmetric pressure differences around the core support barrel are located as follows:

Downcomer elevation	Nodes	Figure #
Bottom of UGS upper flange	14-17	2.6-1
UGS (4.66 ft. above nozzle centerline)	20-23	2.6-2
Nozzle centerline	26-29	2.6-3
Core region (8.3[illegible] ft. below nozzle centerline)	32-35	2.6-4
Core region (14.61 ft. below nozzle centerline)	38-41	2.6-5
Flow skirt (19.5 ft. below nozzle centerline)	44-47	2.6-6

It is seen from the figures that the peak asymmetric pressure differences occur at the nozzle centerline elevation (Figure 2.6-3). Loading histories are given to 200 milliseconds.

(b) PRESSURE PLOTS

1. Vessel Side Break

The absolute pressure time history at the ruptured reactor vessel inlet nozzle (node 65) (vessel side break) i shown in Figure 2.6-7.

2. Pump Side Break

The absolute pressure time history at the pump side of the break (node 64) is presented in Figure 2.6-8.

3. Nozzle to Downcomer Interface

To represent the pressure at the nozzle-downcomer interface, the downcomer node adjacent to the broken nozzle (node 29)is used. The absolute pressure time history of downcomer node 29 is presented in Figure 2.6-9.

4. Vessel Lower Plenum

The vessel lower plenum pressure transient is presented in Figure 2.6-10. In the C-E model the lower plenum is divided into two nodes an "upper-lower plenum" (node 10) and a "lower-lower plenum" (node 9). The plot shows the transient pressure decay at node 10.

5. Core Region

The absolute pressure time histories for the core region nodes are presented in Figures 2.6-11 to 2.6-15. All pressure traces are similar. The lower inactive core [illegible] transient is shown in Figure 2.6-11. The pressure decay in the three active core nodes (nodes 1, 2 and 3) are displayed in Figures 2.6-12 thru 2.6-14. The upper inactive core (node 4) pressure history is shown in Figure 2.6-15.

6. Vessel Upper Plenum

The pressure decay in the reactor pressure vessel outlet plenum (node 5)is presented in Figure 2.6-16.

7. Downcomer: Nozzle Centerline Elevation (180° from Broken Nozzle)
The pressure in the downcomer 180° from the broken nozzle at the centerline elevation (node 26) is presented in Figure 2.6-17.

8. Steam Generator Outlet Plenum,Broken Loop
The pressure time history at the broken loop steam generator outlet plenum (node 60) is shown in Figure 2.6-18.

9. Pump Discharge Pressure, Broken Loop
The pump discharge pressure in the broken loop (node 63) is presented in Figure 2.6-19.

10. Downcomer: Lowest Axial Elevation (180° from Broken Nozzle)
The downcomer pressure at the CSB flange elevation (node 44) 180° away from the broken nozzle circumferential location is presented in Figure 2.6-20.

(c) DIFFERENTIAL PRESSURE PLOTS

1. Across Reactor Assembly
The core axial pressure drop (from bottom of inactive core (node 12) to top of inactive core (node 4))is presented in Figure 2.6-21. A positive pressure drop is defined to indicate the pressure at the core bottom (node 12) exceeds the pressure at the top inactive core (node 4).

2. Across Broken Loop Pump
The pressure difference across the pump in the ruptured loop is defined by the pressure difference between nodes 62 and 63. This pressure difference is presented in Figure 2.6-22.

3. Across Broken Loop Steam Generator
The pressure drop across the broken loop steam generator (inlet steam generator plenum (node 58) to outlet steam generator plenum (node 60)) is presented in Figure 2.6-23.

597 007

4. Across Intact Loop Steam Generator

The pressure drop across the steam generator (inlet steam generator plenum (node 52) to outlet steam generator plenum (node 54)) for the intact loop is presented in Figure 2.6-24.

5. Across Reactor Pressure Vessel

The transient pressure drop across the reactor pressure vessel (pressure at the broken cold leg nozzle (node 65) less the pressure at the hot leg nozzle (node 57)) is presented in Figure 2.6-25.

(d) MASS FLOW

1. Vessel Side Break

The transient mass flow out of the vessel side of the ruptured nozzle (as given by the flow through flowpath 107) is presented in Figure 2.6-26.

2. Pump Side Break

Mass flow through flowpath 105 (pump side of the broken nozzle) is presented in Figure 2.6-27.

3. Core Inlet

Mass flow at the entrance to the active core (flowpath 1) is presented in Figure 2.6-28.

(e) Integrated Load on Core Support Barrel

The load on the core support barrel (CSB) is calculated using procedures of reference 2.6-2. The integrated CSB load resolved in the direction of the break (x-direction) is presented in Figure 2.6-29. The integrated CSB load resolved perpendicular to the break direction (y-direction) is presented in Figure 2.6-30.

596 019

REFERENCES FOR 2.6

1. Scherer, A. E. (C-E), letter to Baer, R., Chief, Light Water Reactor, Branch 2, Division of Project Management, USNRC, June 13, 1978.

2. Combustion Engineering, Inc., "Topical Report on Dynamic Analysis of Reactor Vessel Internals Under Loss-of-Coolant Accident Conditions with Application of Analysis to C-E 800 MWe Class Reactors", CENPD-42, August, 1972 (proprietary).

3. Combustion Engineering, Inc., "Blowdown Analysis Method: Method for the Analysis of Blowdown Induced Forces in a Reactor Vessel", CENPD-252-P (Proprietary), December, 1977.

FIGURE 2.6-1

SYSTEM 80 350 SQ. INCH-INLET BREAK
PRESSURE DIFFERENCE AROUND CORE SUPPORT BARREL
(NODES 14-17)

(UPPER PLENUM ELEVATION)

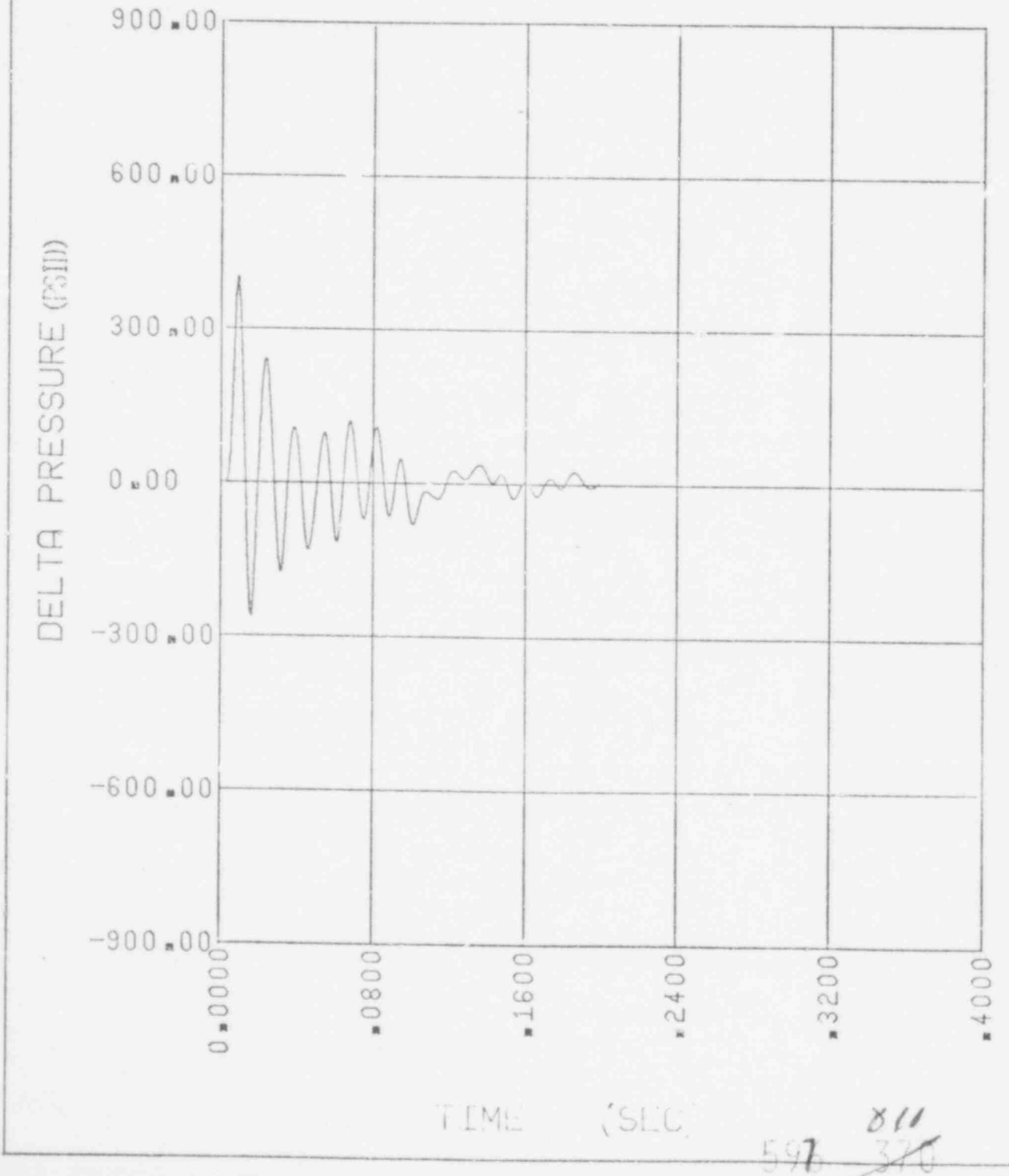

811
597 370

FIGURE 2.6-2

SYSTEM 80 350 SQ. INCH-INLET BREAK
PRESSURE DIFFERENCE AROUND CORE SUPPORT BARREL
(NODES 20-23)
(4.66 FT. ABOVE NOZZLE CENTERLINE ELEVATION)

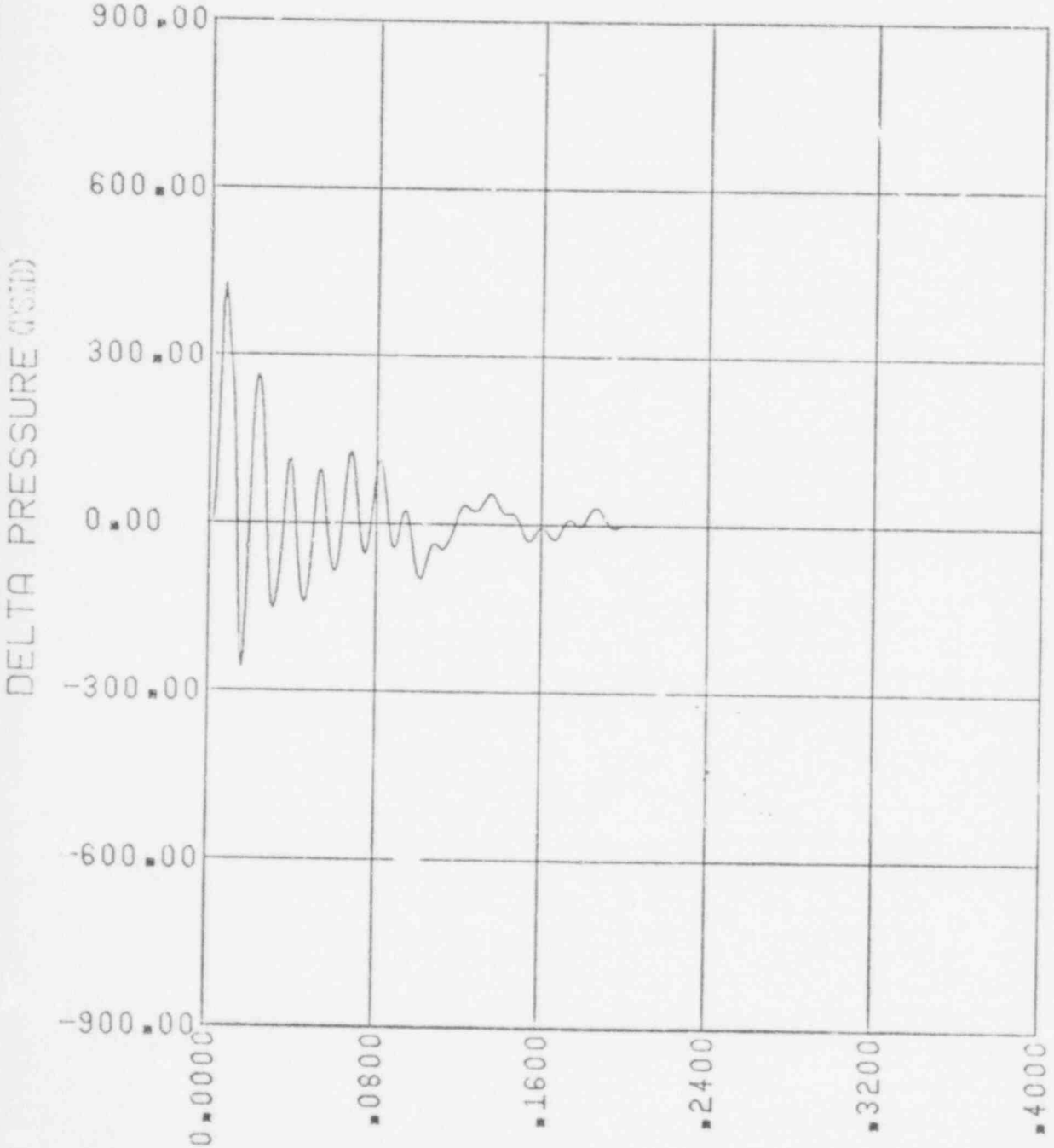

FIGURE 2.6-3

SYSTEM 80 350 SQ. INCH-INLET BREAK

PRESSURE DIFFERENCE AROUND CORE SUPPORT BARREL

(NODES 26-29)

(NOZZLE CENTERLINE ELEVATION)

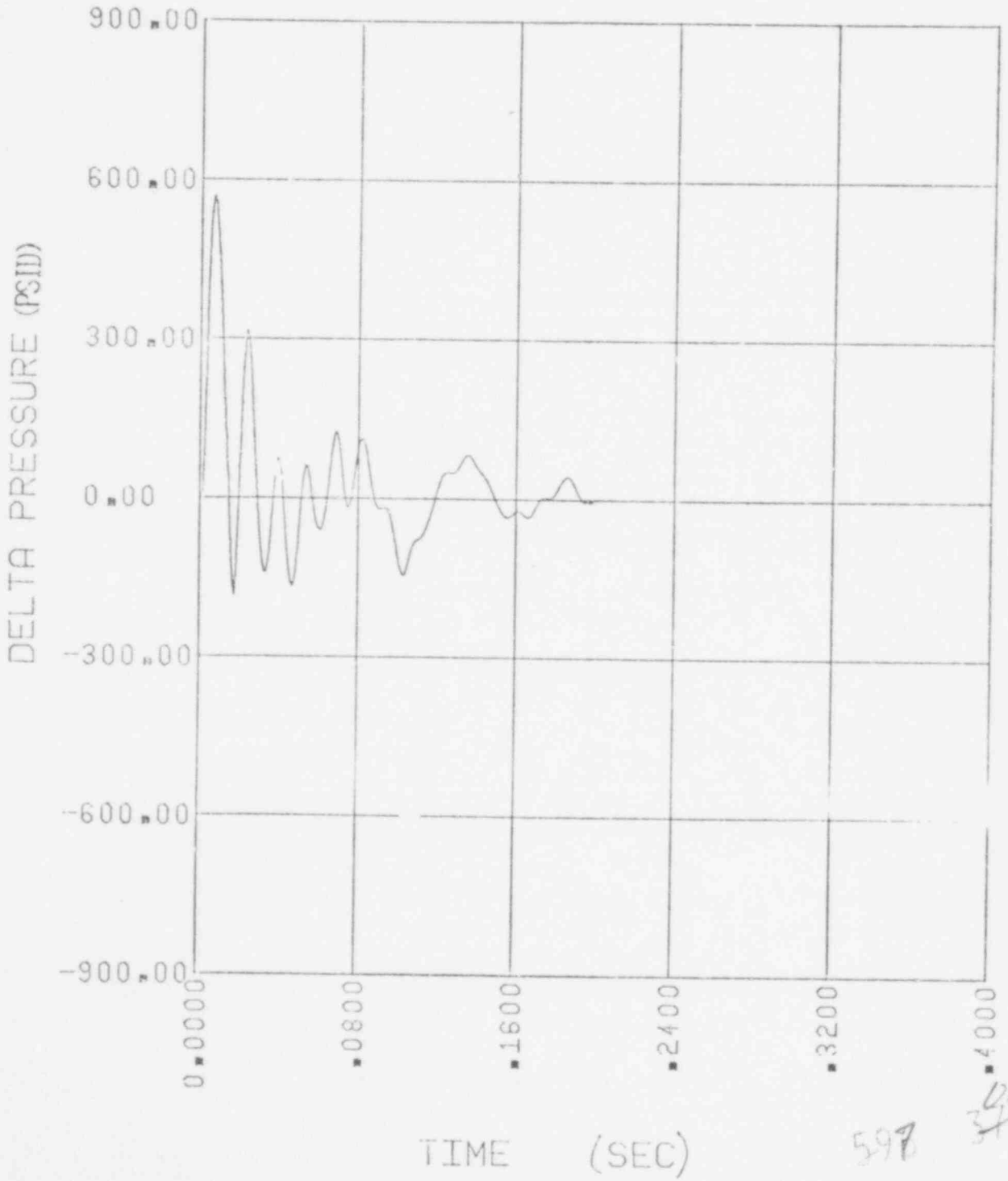

FIGURE 2.6-4

SYSTEM 80 350 SQ. INCH-INLET BREAK

PRESSURE DIFFERENCE AROUND CORE SUPPORT BARREL

(NODES 32-35)

(8.36 FT. BELOW NOZZLE CENTERLINE ELEVATION)

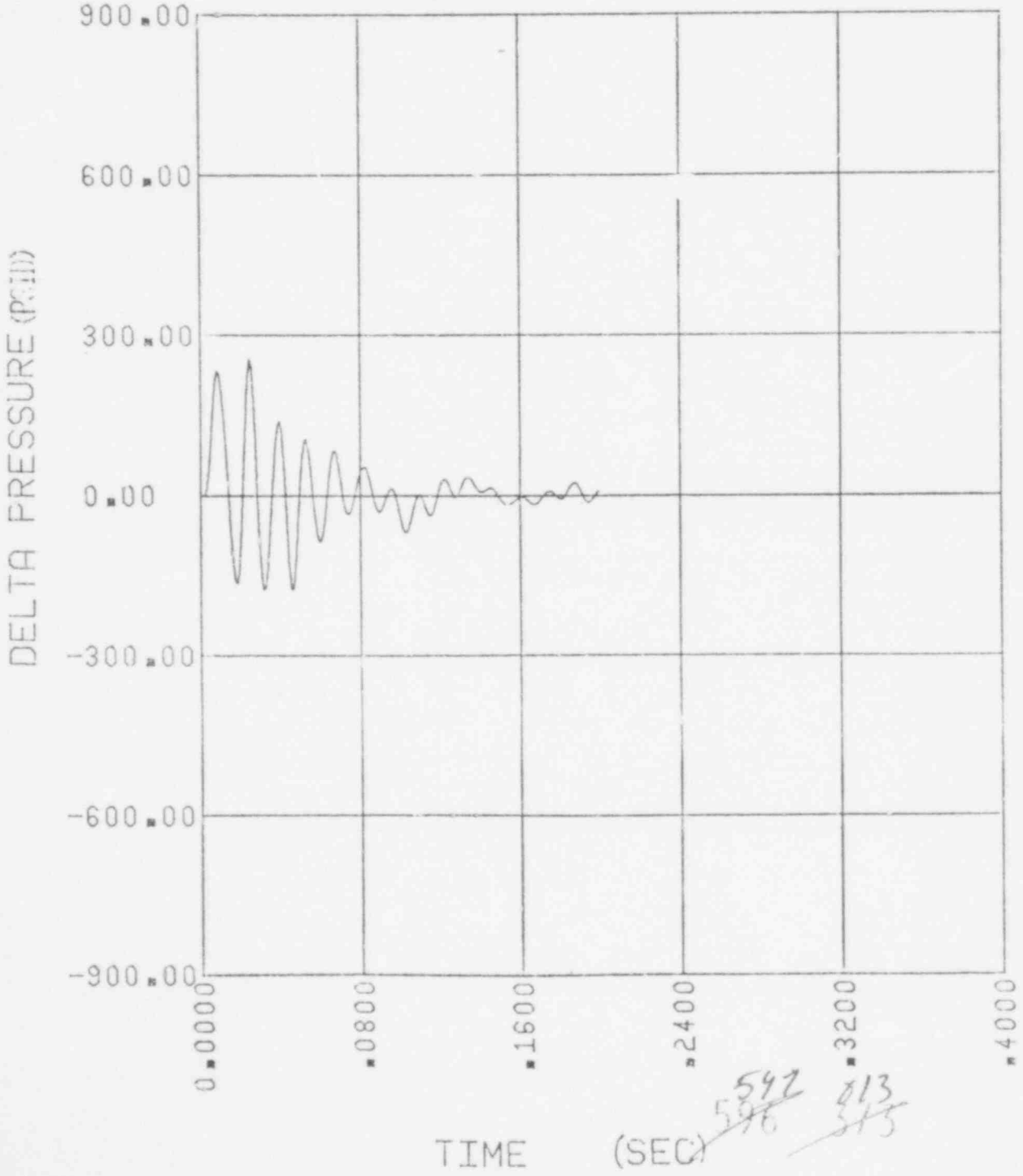

542 813

FIGURE 2.6-5

SYSTEM 80 350 SQ. INCH-INLET BREAK

PRESSURE DIFFERENCE AROUND CORE SUPPORT BARREL

(NODES 38-41)

(14.61 FT. BELOW NOZZLE CENTERLINE ELEVATION)

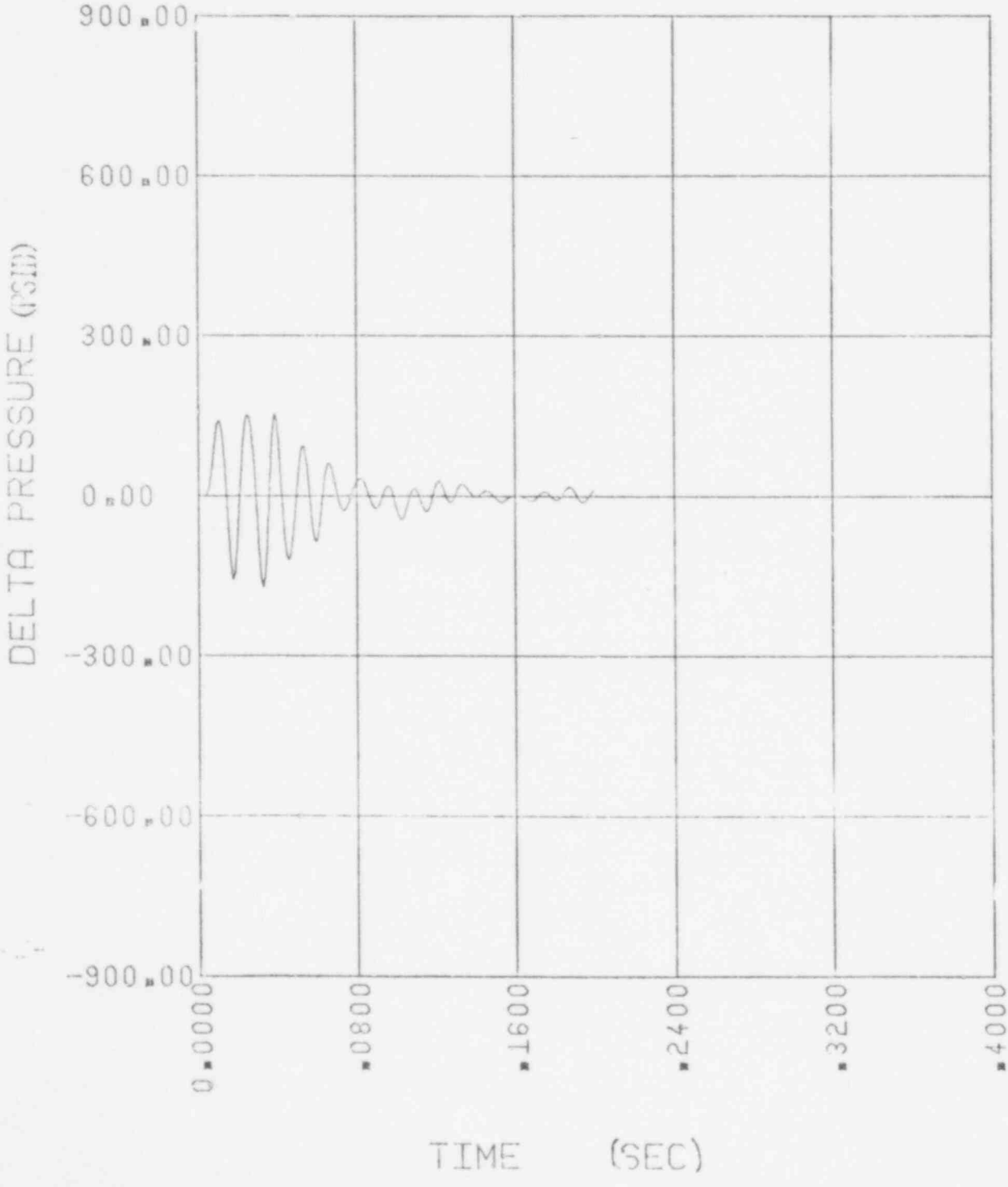

~~596 374~~

596 014

FIGURE 2.6-6

SYSTEM 80 350 SQ. INCH-INLET BREAK -

PRESSURE DIFFERENCE AROUND CORE SUPPORT BARREL

(NODES 44-47)

(FLOW SKIRT REGION: 19.5 FT. BELOW NOZZLE CENTERLINE ELEVATION)

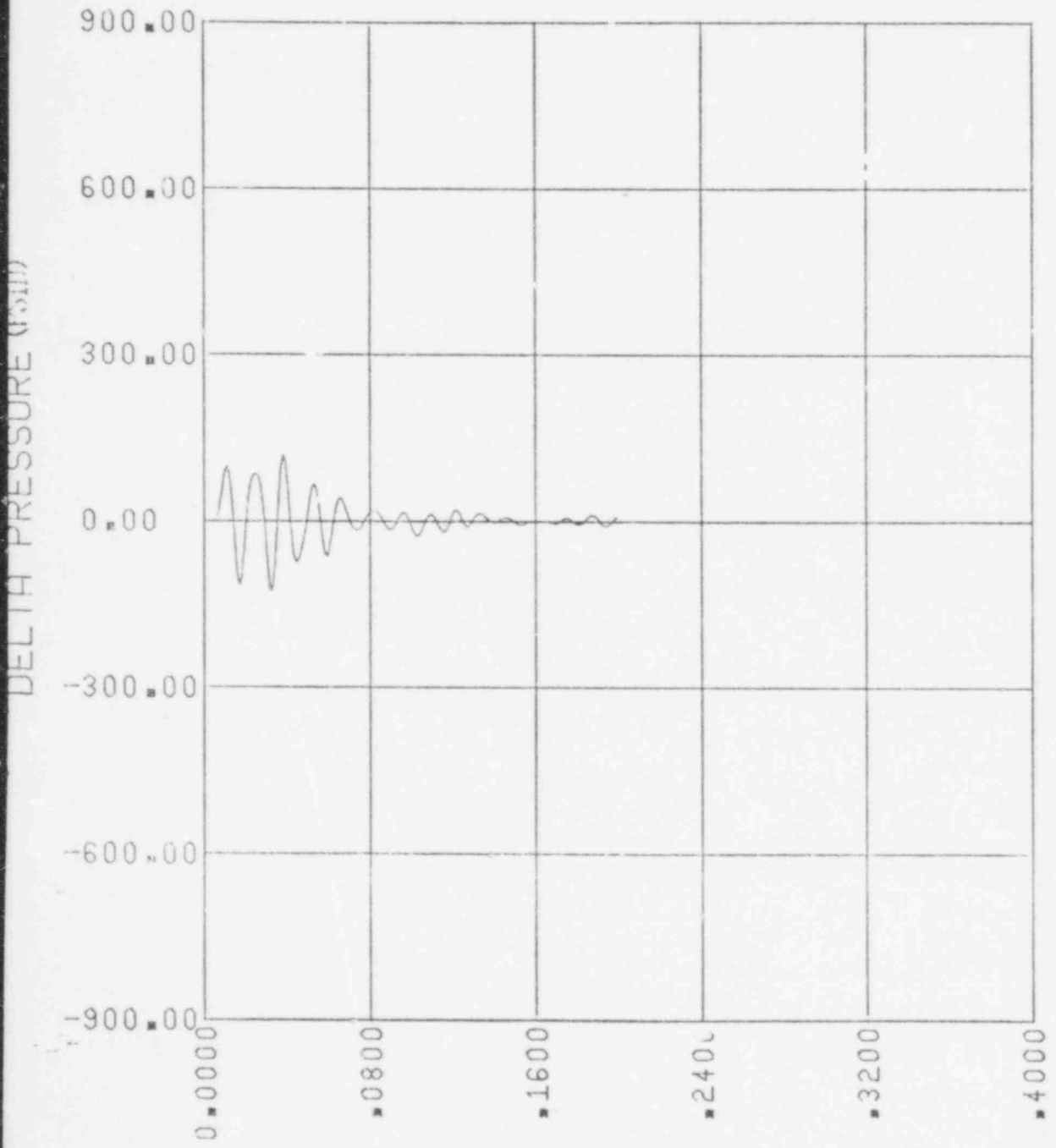

597 615

~~596~~ ~~575~~

FIGURE 2.6-7

SYSTEM 80 350 SQ. INCH-INLET BREAK

ABSOLUTE PRESSURE TIME HISTORY: REACTOR VESSEL INLET NOZZLE (NODE 65)

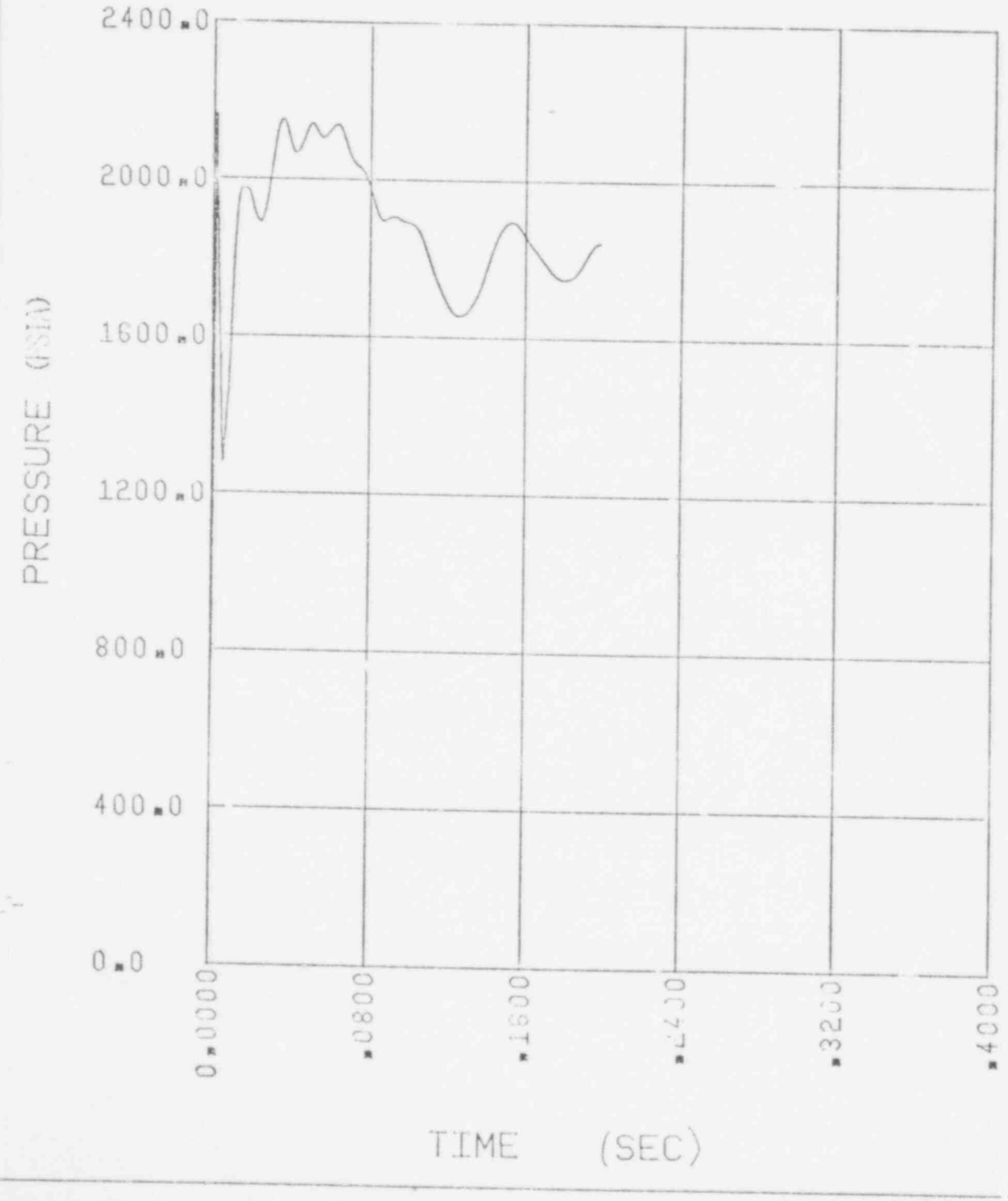

594 376
546 516

FIGURE 2.6-8

SYSTEM 80 350 SQ. INCH-INLET BREAK

ABSOLUTE PRESSURE TIME HISTORY:PUMP SIDE BREAK

(NODE 64)

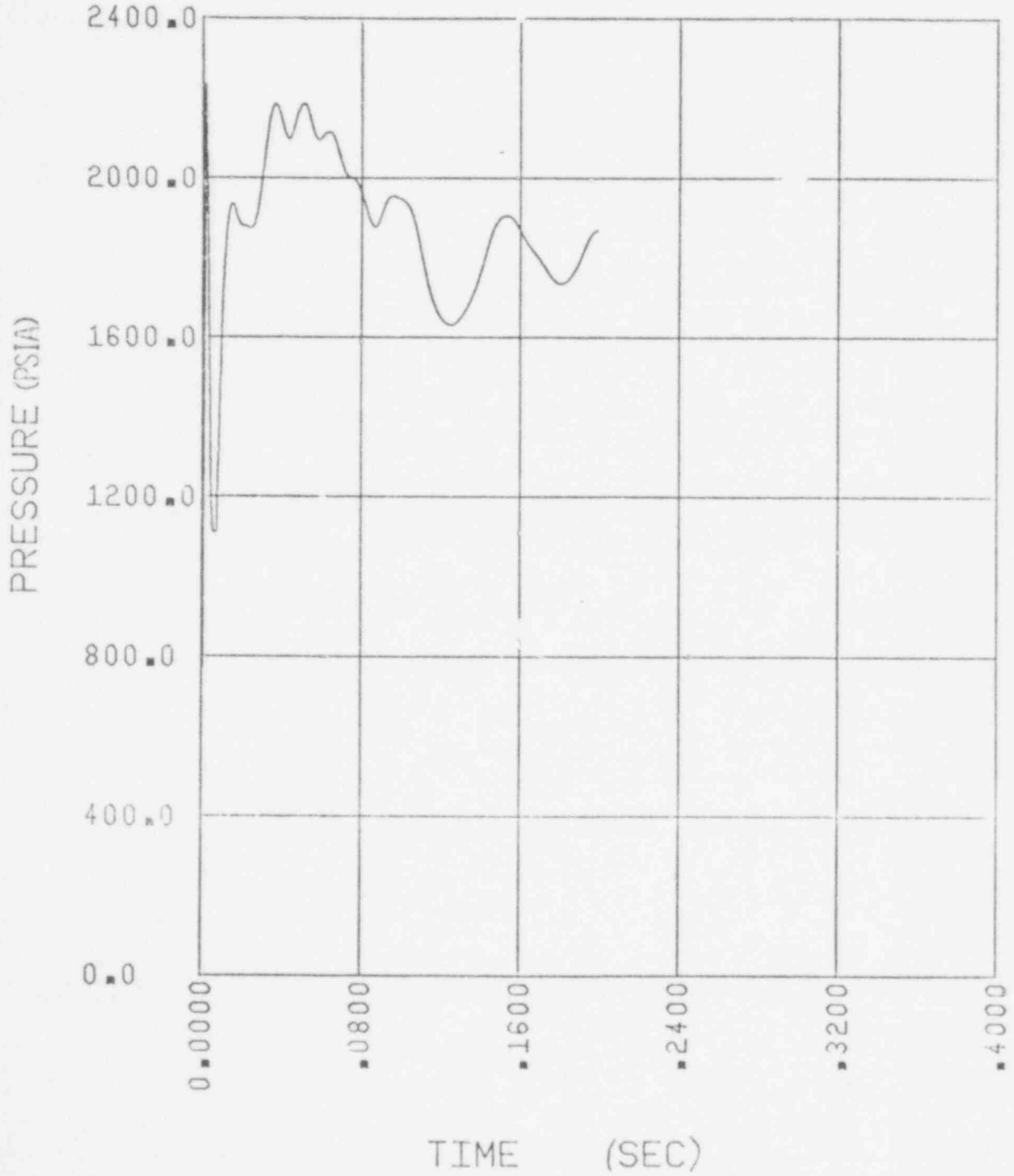

598 377

017

FIGURE 2.6-9

SYSTEM 80 350 SQ. INCH-INLET BREAK

ABSOLUTE PRESSURE TIME HISTORY: BROKEN NOZZLE-

DOWNCOMER INTERFACE (NOZZLE CENTERLINE ELEVATION)

(NODE 29)

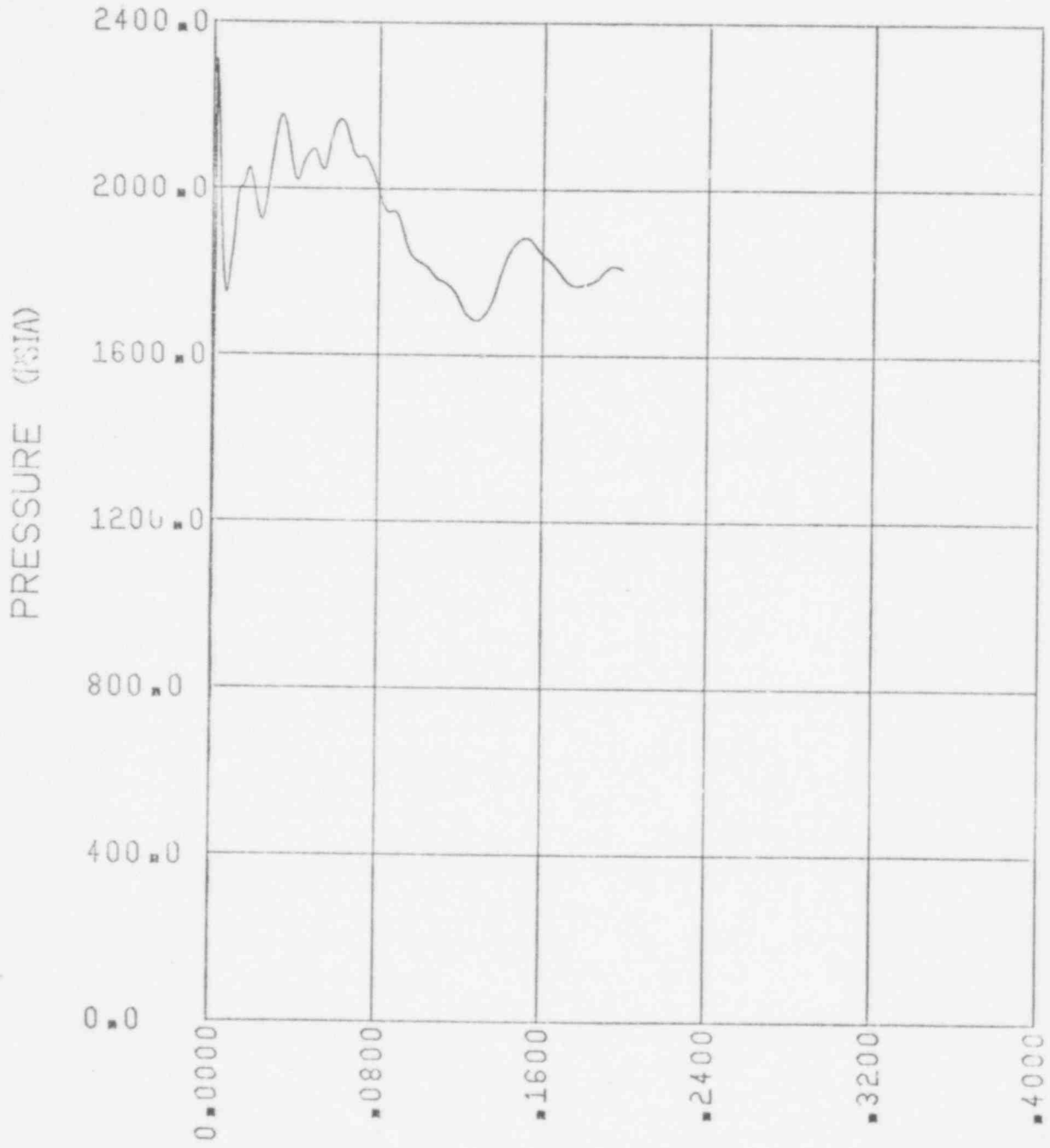

FIGURE 2.6-10

SYSTEM 80 350 SQ. INCH-INLET BREAK

ABSOLUTE PRESSURE TIME HISTORY: VESSEL LOWER PLENUM

(NODE 10)

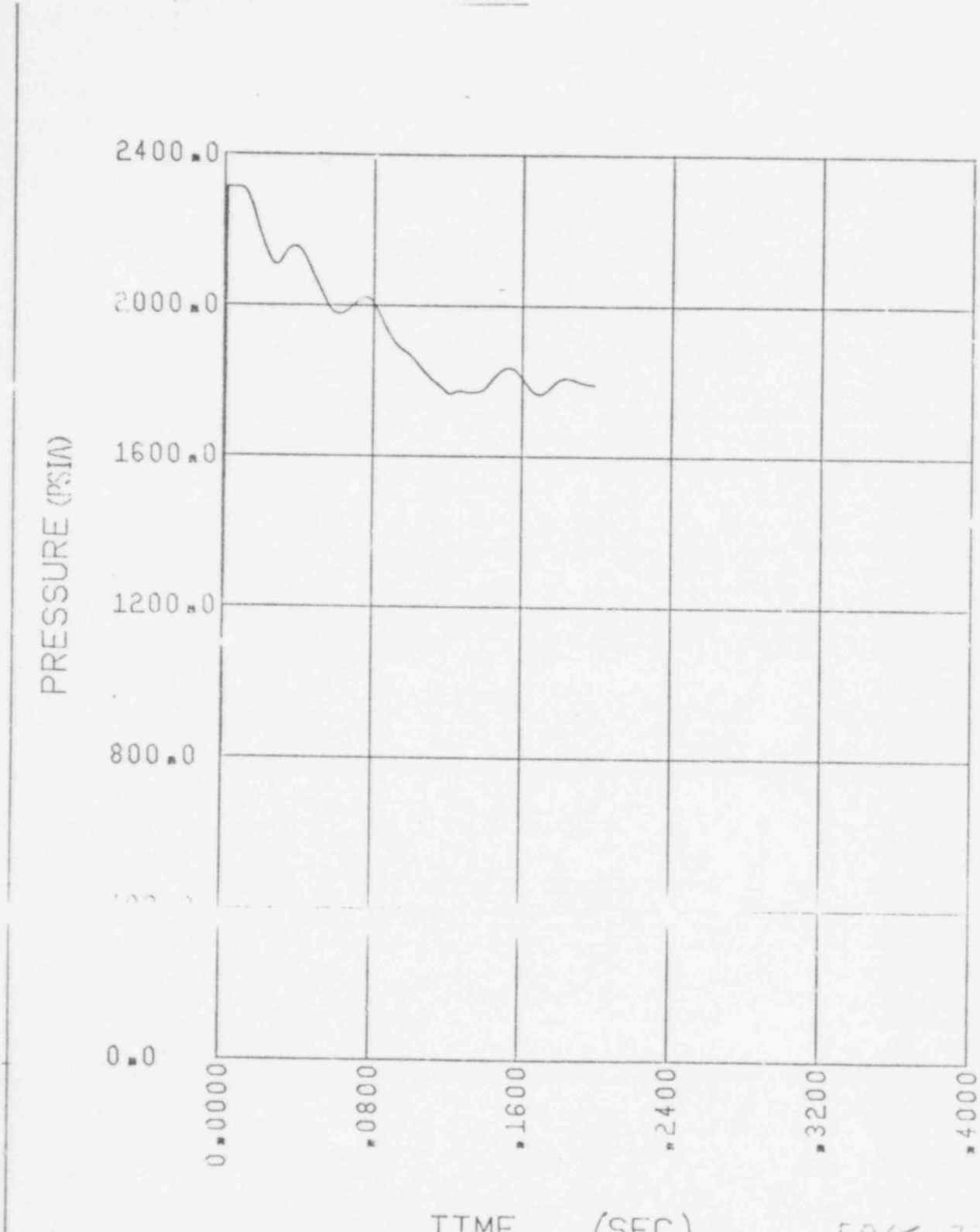

596 379

567 019

FIGURE 2.6-11

SYSTEM 80 350 SQ. INCH-INLET BREAK

ABSOLUTE PRESSURE TIME HISTORY: LOWER INACTIVE CORE

(NODE 12)

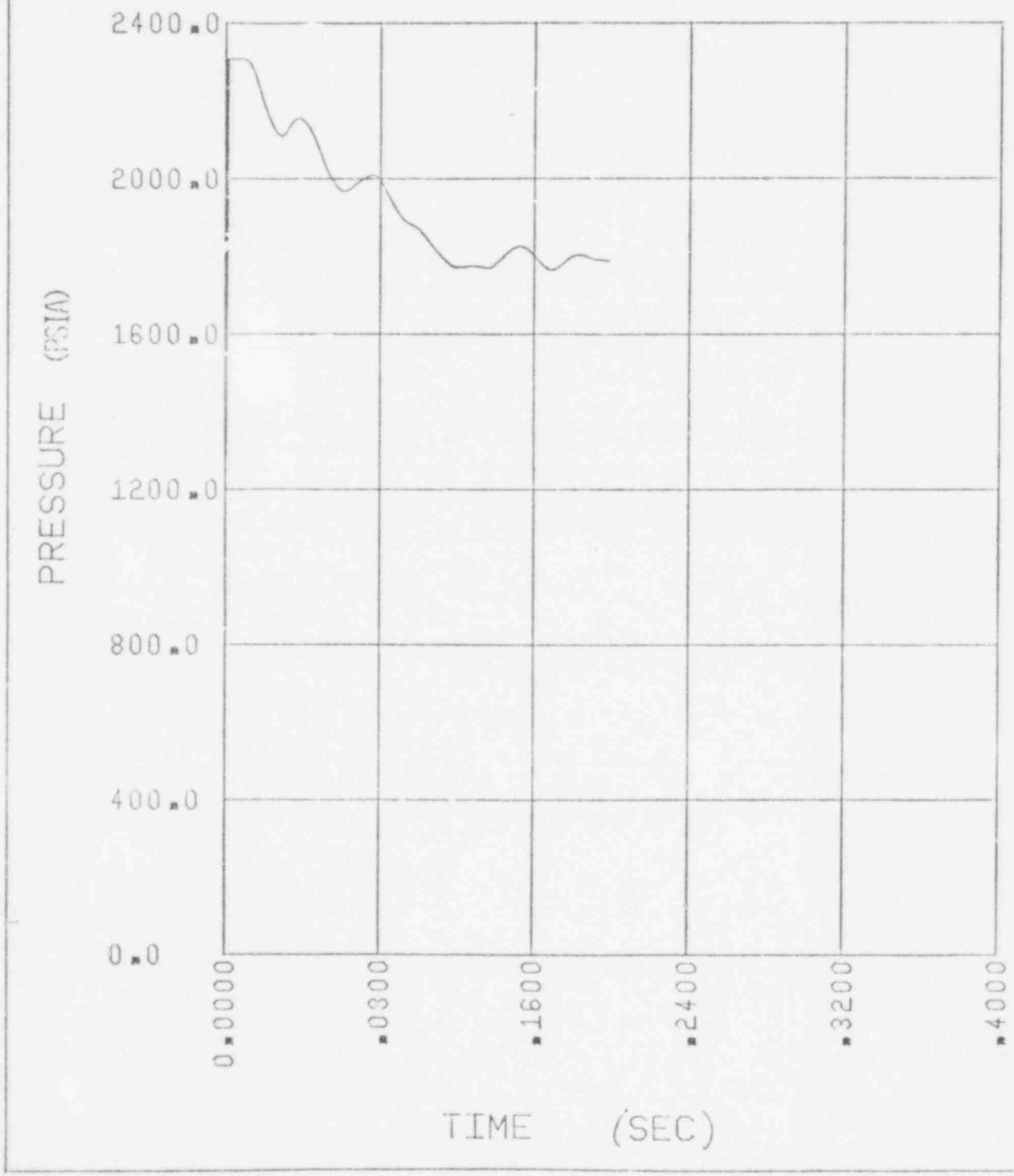

596 380
597 120

FIGURE 2.6-12

SYSTEM 80 350 SQ. INCH INLET BREAK

ABSOLUTE PRESSURE TIME HISTORY: ONE-THIRD ACTIVE CORE

(NODE 1)

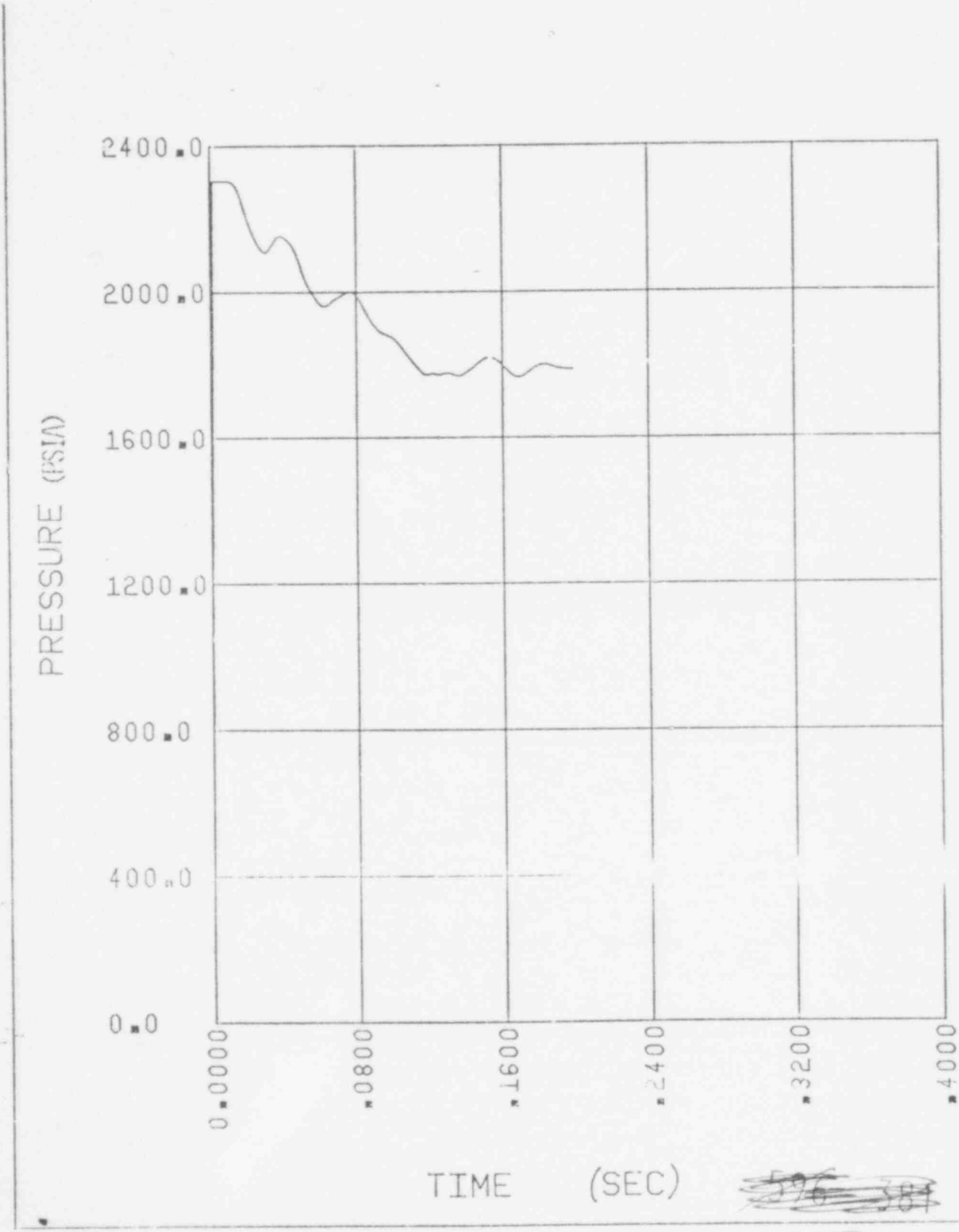

597
021

FIGURE 2.6-13

SYSTEM 80 350 SQ. INCH-INLET BREAK
ABSOLUTE PRESSURE TIME HISTORY:ONE-THIRD ACTIVE CORE
(NODE 2)

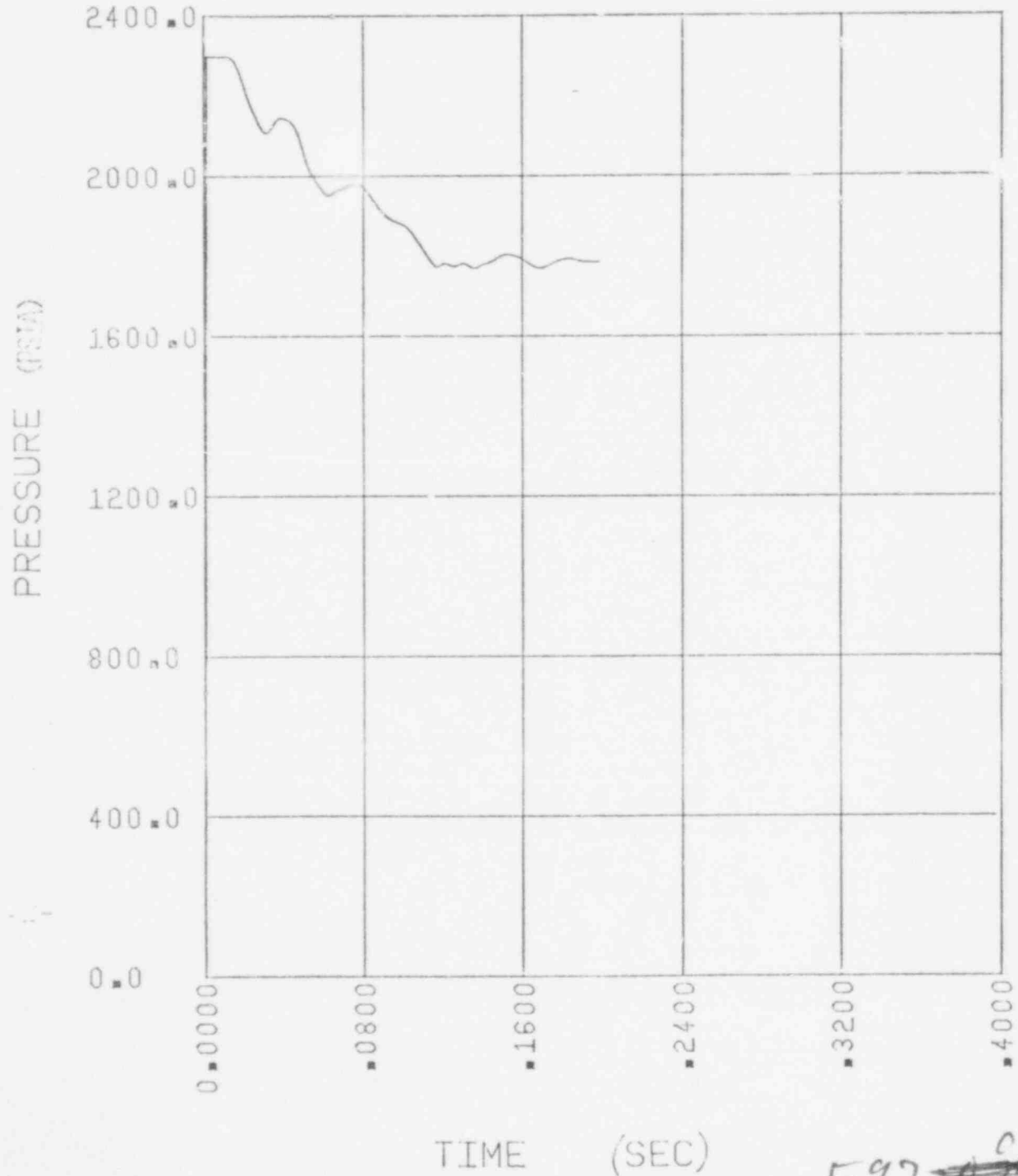

597 C22

596 393

FIGURE 2.6-14

SYSTEM 80 350 SQ. INCH-INLET BREAK

ABSOLUTE PRESSURE TIME HISTORY:ONE-THIRD ACTIVE CORE

(NODE 3)

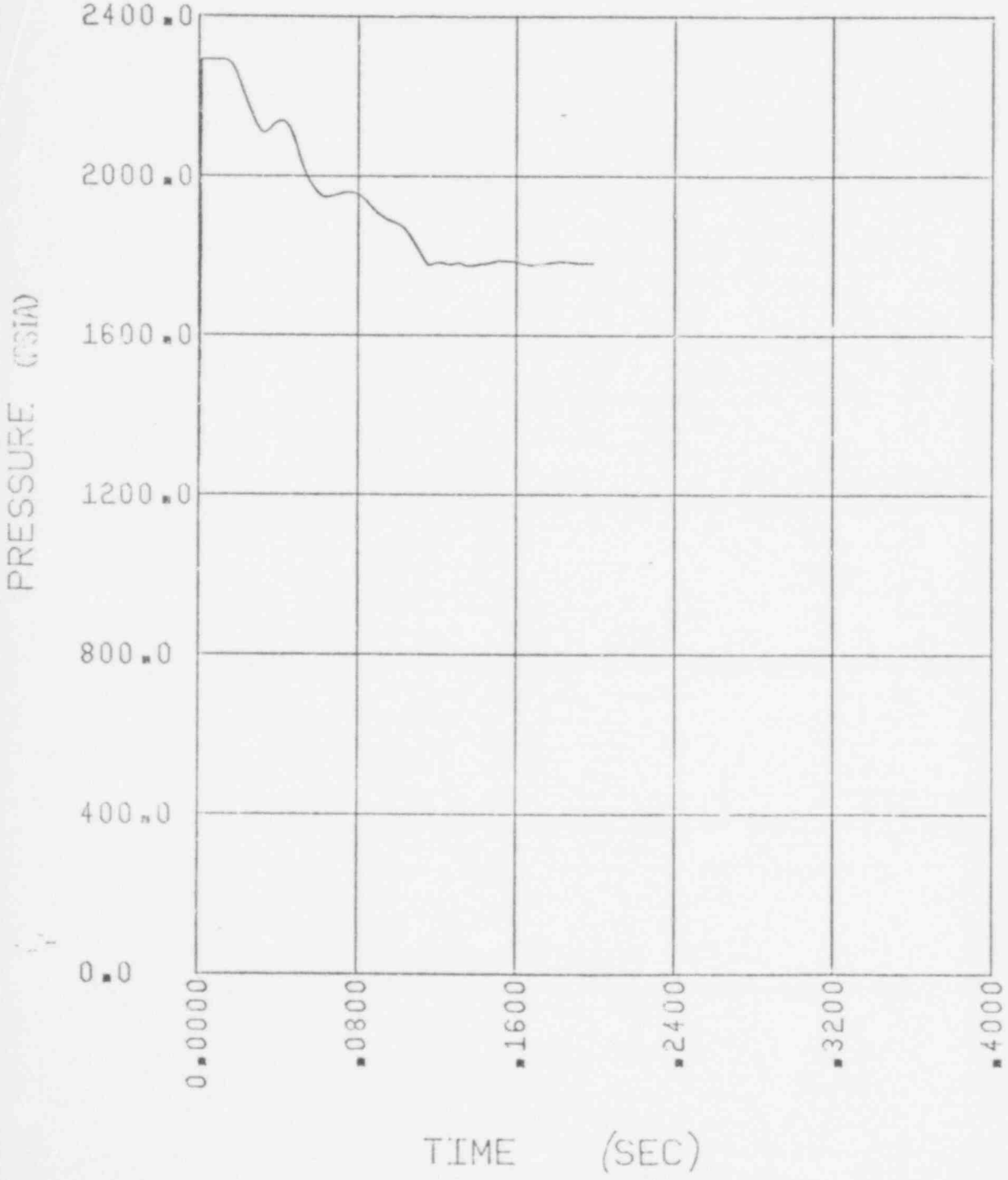

597 023

596 584

FIGURE 2.6-15

SYSTEM 80 350 SQ. INCH-INLET BREAK
ABSOLUTE PRESSURE TIME HISTORY:UPPER INACTIVE CORE
(NODE 4)

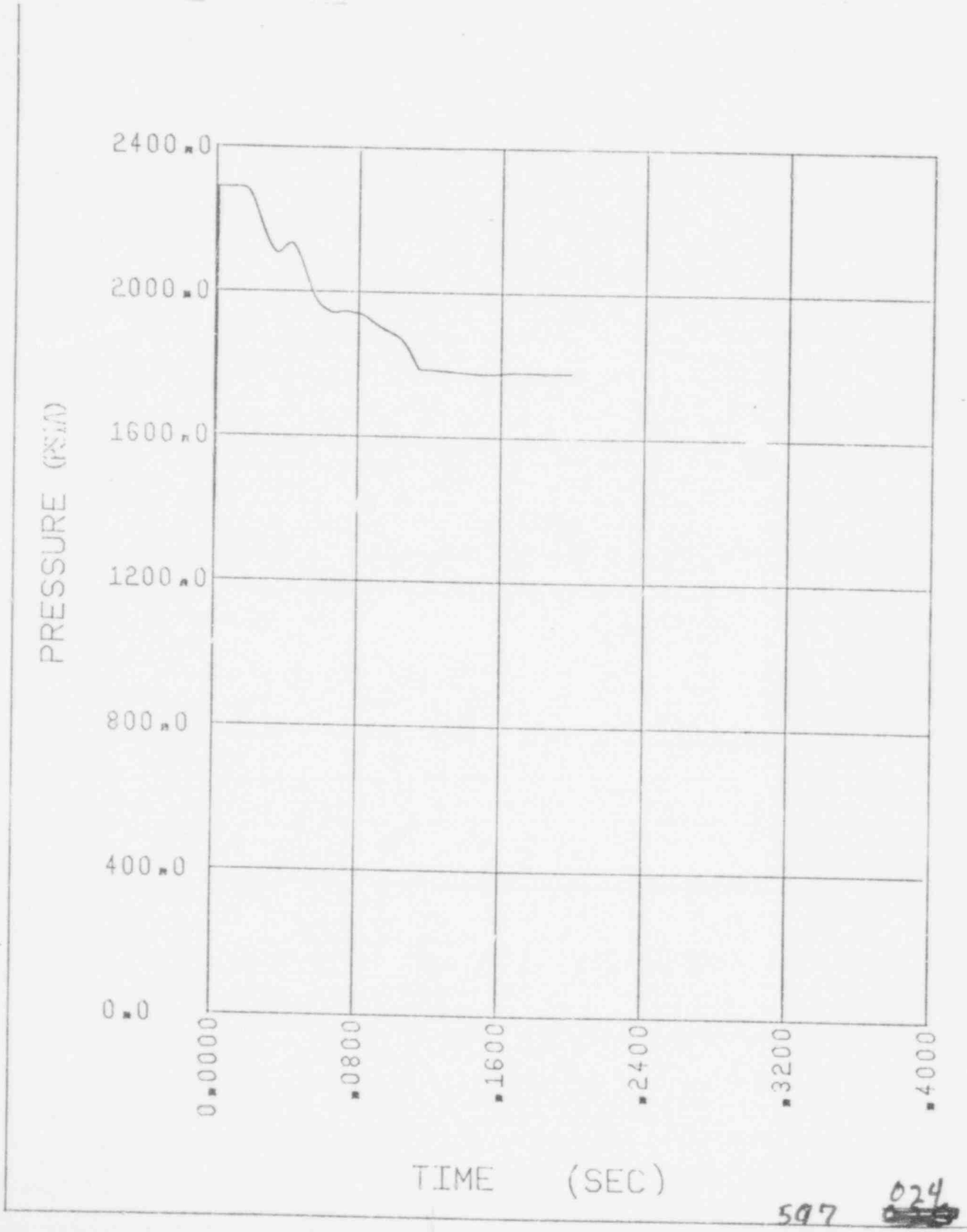

597 024
~~596~~ 385

FIGURE 2.6-16

SYSTEM 80 350 SQ. INCH-INLET BREAK
ABSOLUTE PRESSURE TIME HISTORY: RPV OUTLET PLENUM
(NODE 5)

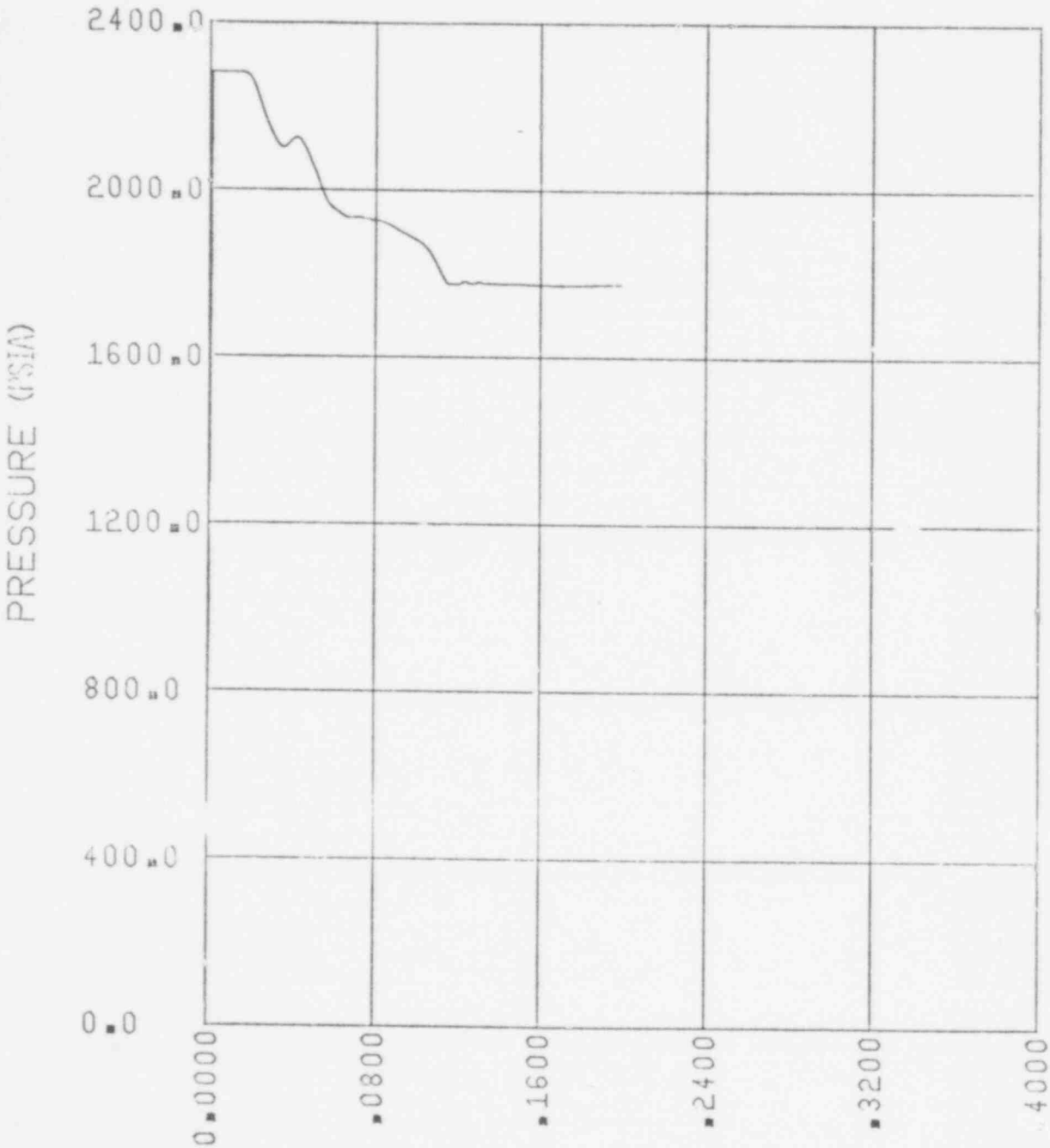

597 025
2

596 386

FIGURE 2.6-17

SYSTEM 80 350 SQ. INCH-INLET BREAK

ABSOLUTE PRESSURE TIME HISTORY: DOMICOFER NODE-NOZZLE CENTERLINE ELEVATIO

180 DEGREES FROM BROKEN NOZZLE (NODE 26)

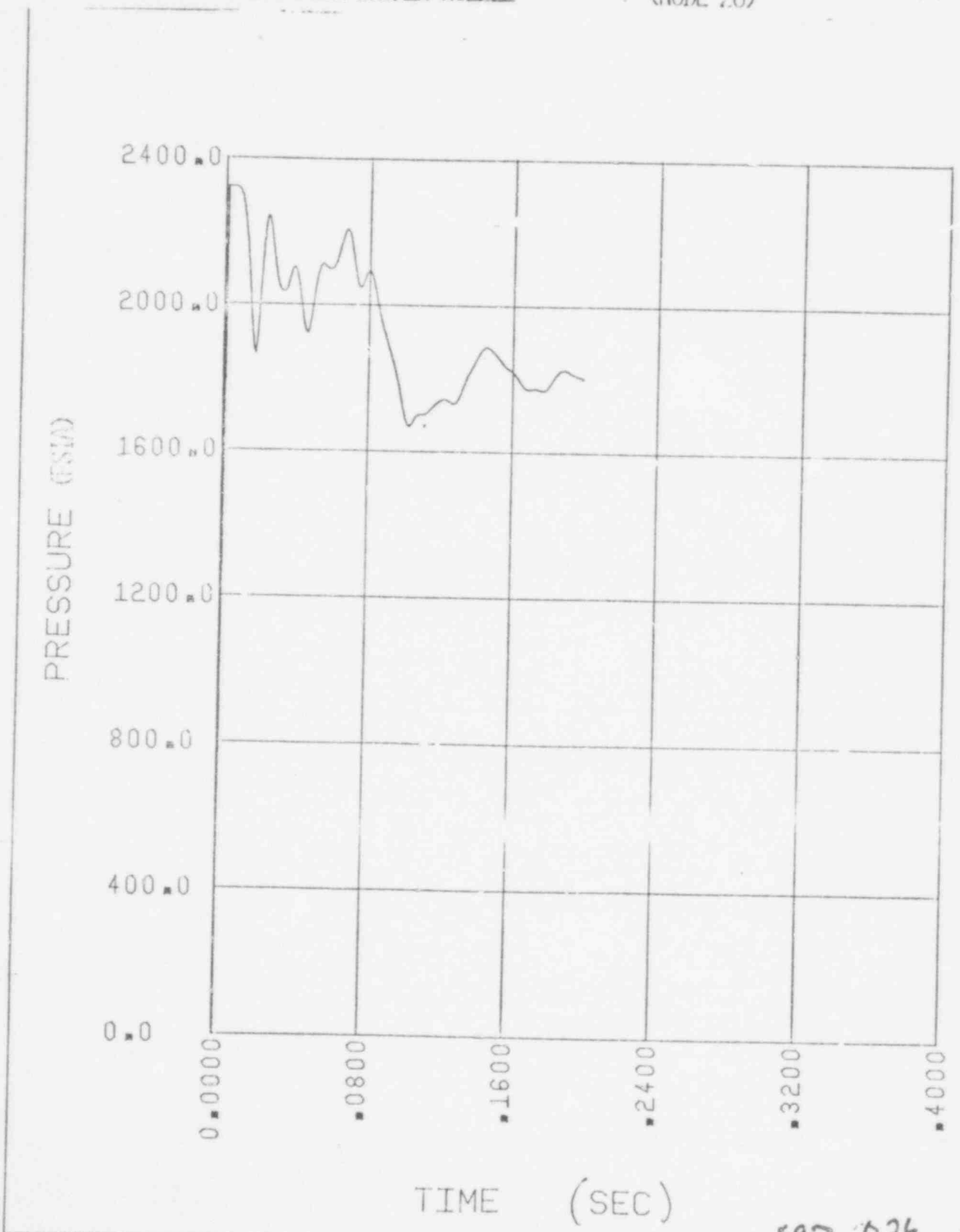

597 026

FIGURE 2.6-18

SYSTEM 80 350 SQ. INCH-INLET BREAK

ABSOLUTE PRESSURE TIME HISTORY: STEAM GENERATOR OUTLET PLENUM

(NODE 60)

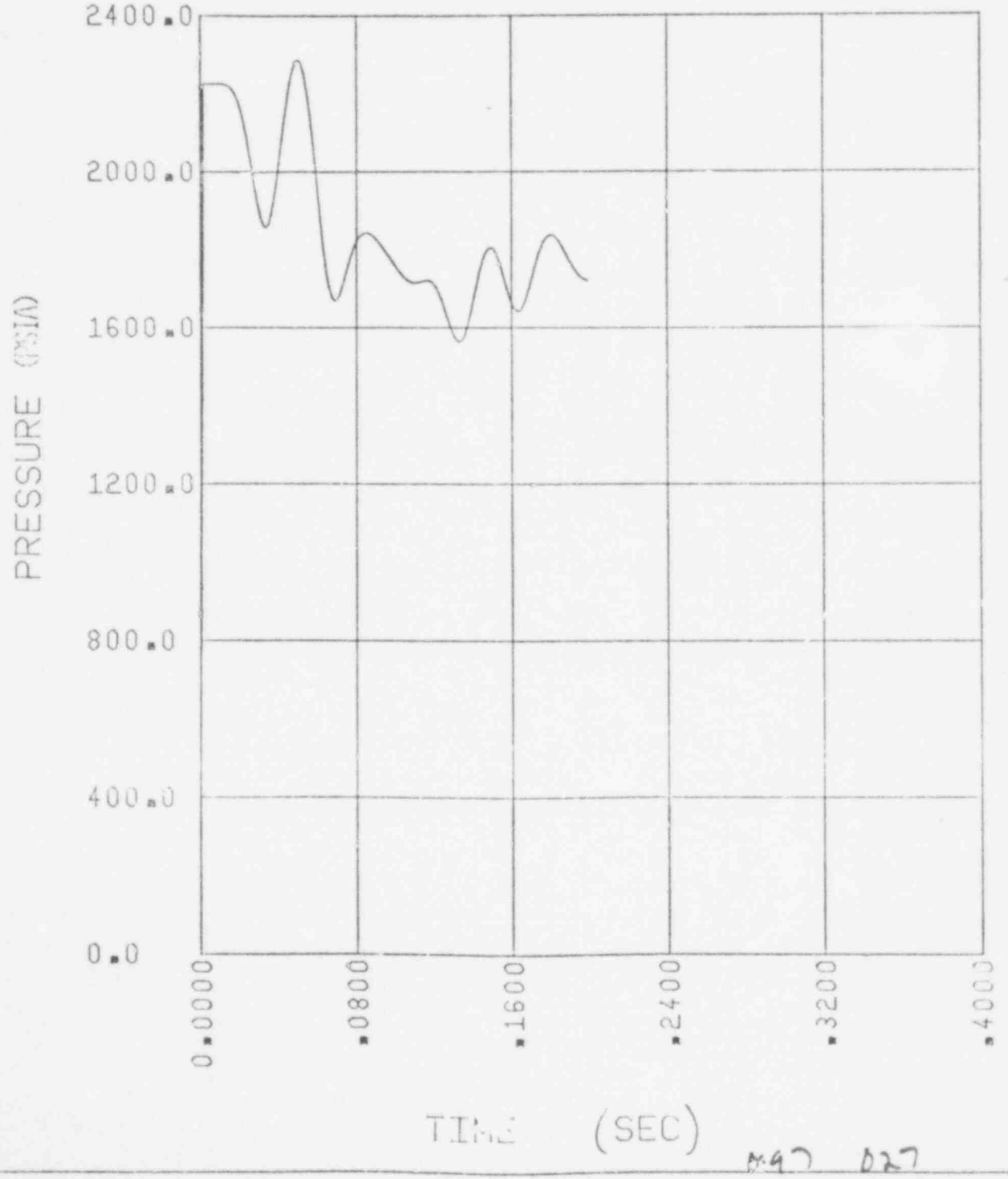

M-97 027

596 388

FIGURE 2.6-19

SYSTEM 80 350 SQ. INCH-INLET BREAK

ABSOLUTE PRESSURE TIME HISTORY: PUMP DISCHARGE LEG

(NODE 63)

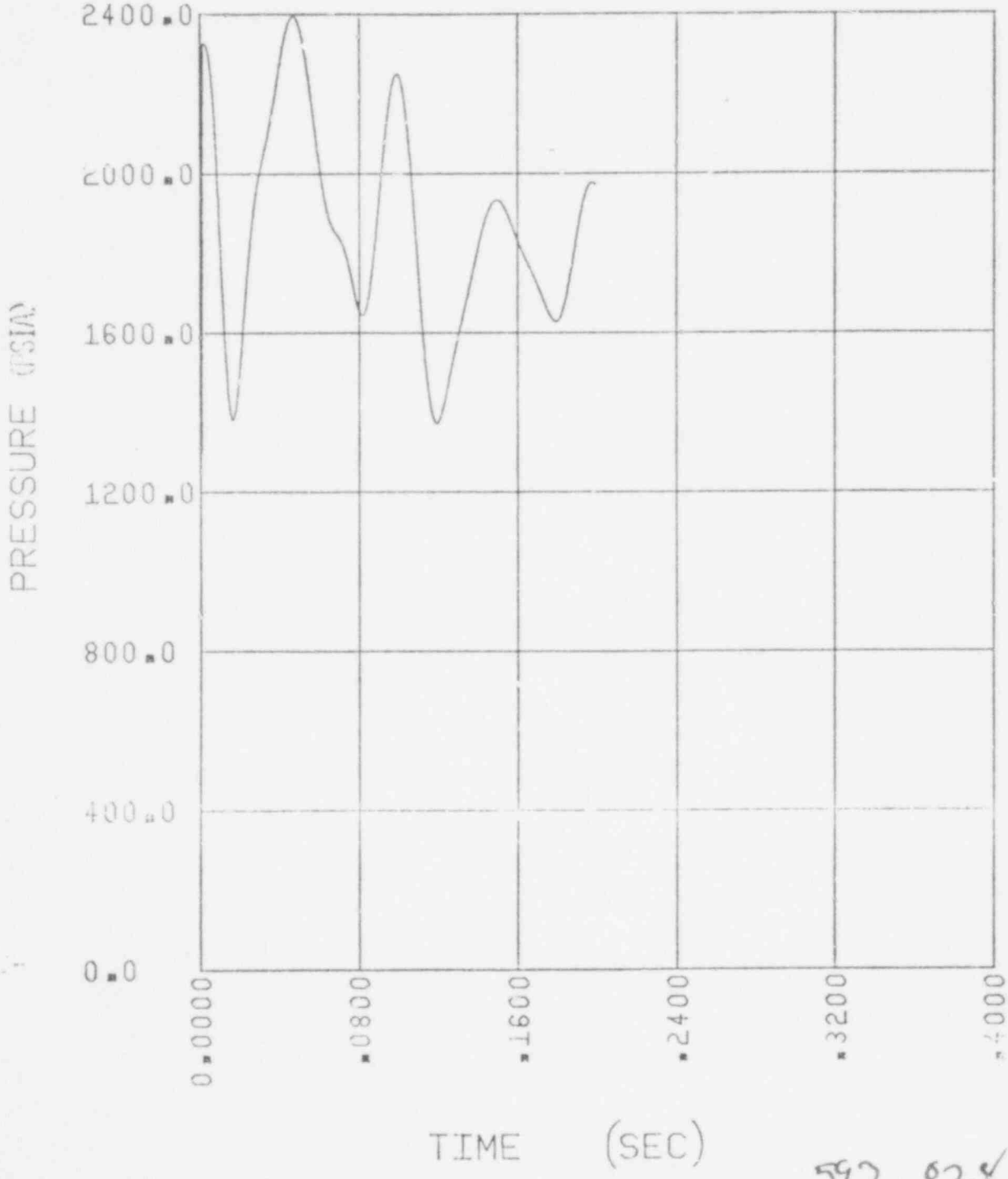

597 624

596 597

FIGURE 2.6-20

SYSTEM 80 350 SQ. INCH-INLET BREAK

ABSOLUTE PRESSURE TIME HISTORY: DOWNCOMER NODE-BOTTOM CSB ELEVATION

180 DEGREES FROM BROKEN NOZZLE (NODE 44)

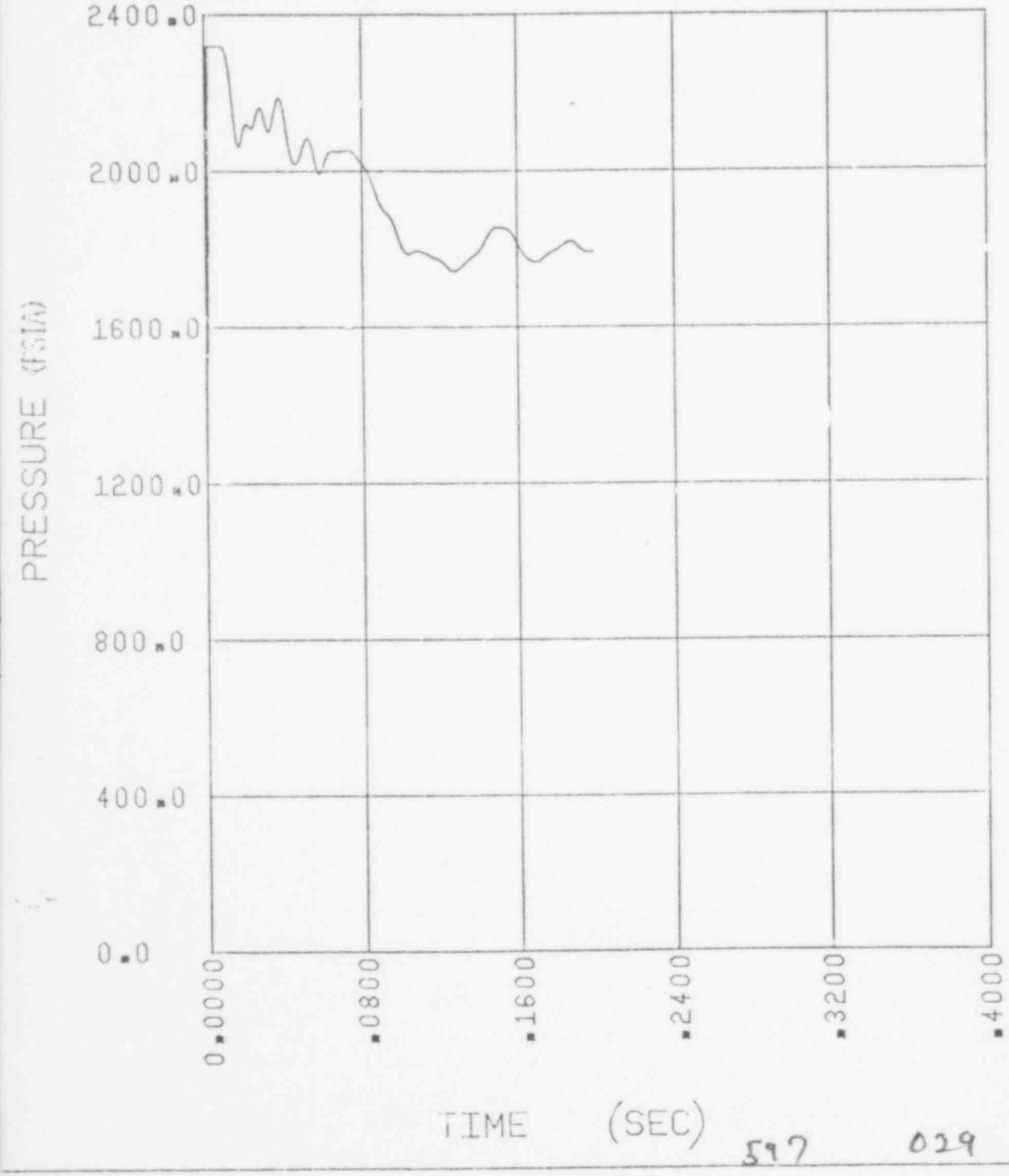

597 029

FIGURE 2.6-21

SYSTEM 80 350 SQ. INCH-INLET BREAK

CORE AXIAL PRESSURE DROP

(NODES 12-4)

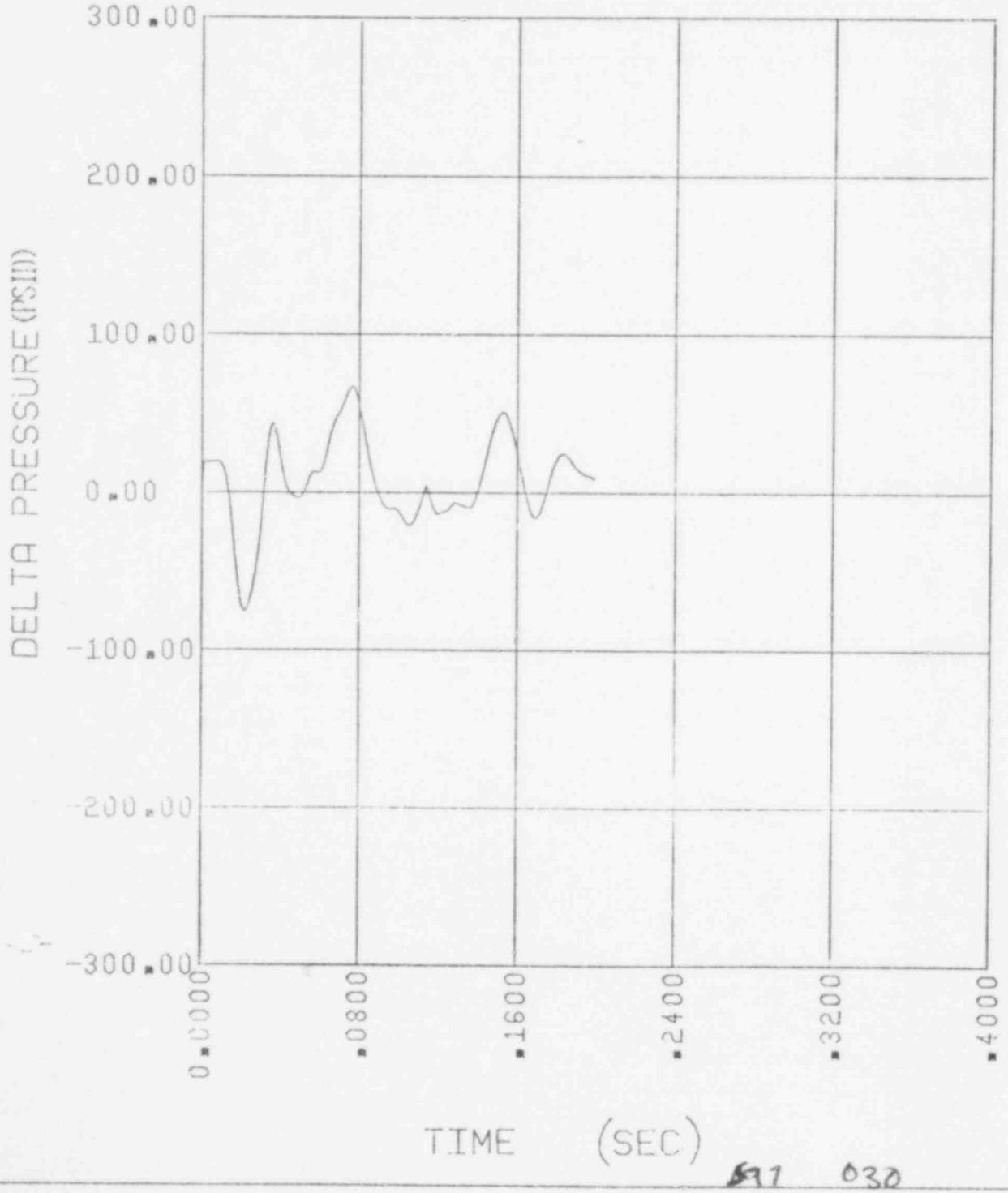

891 030

FIGURE 2.6-22

SYSTEM 80 350 SQ. INCH-INLET BREAK

PRESSURE DIFFERENCE ACROSS PUMP (BROKEN LOOP)

(NODES 62-63)

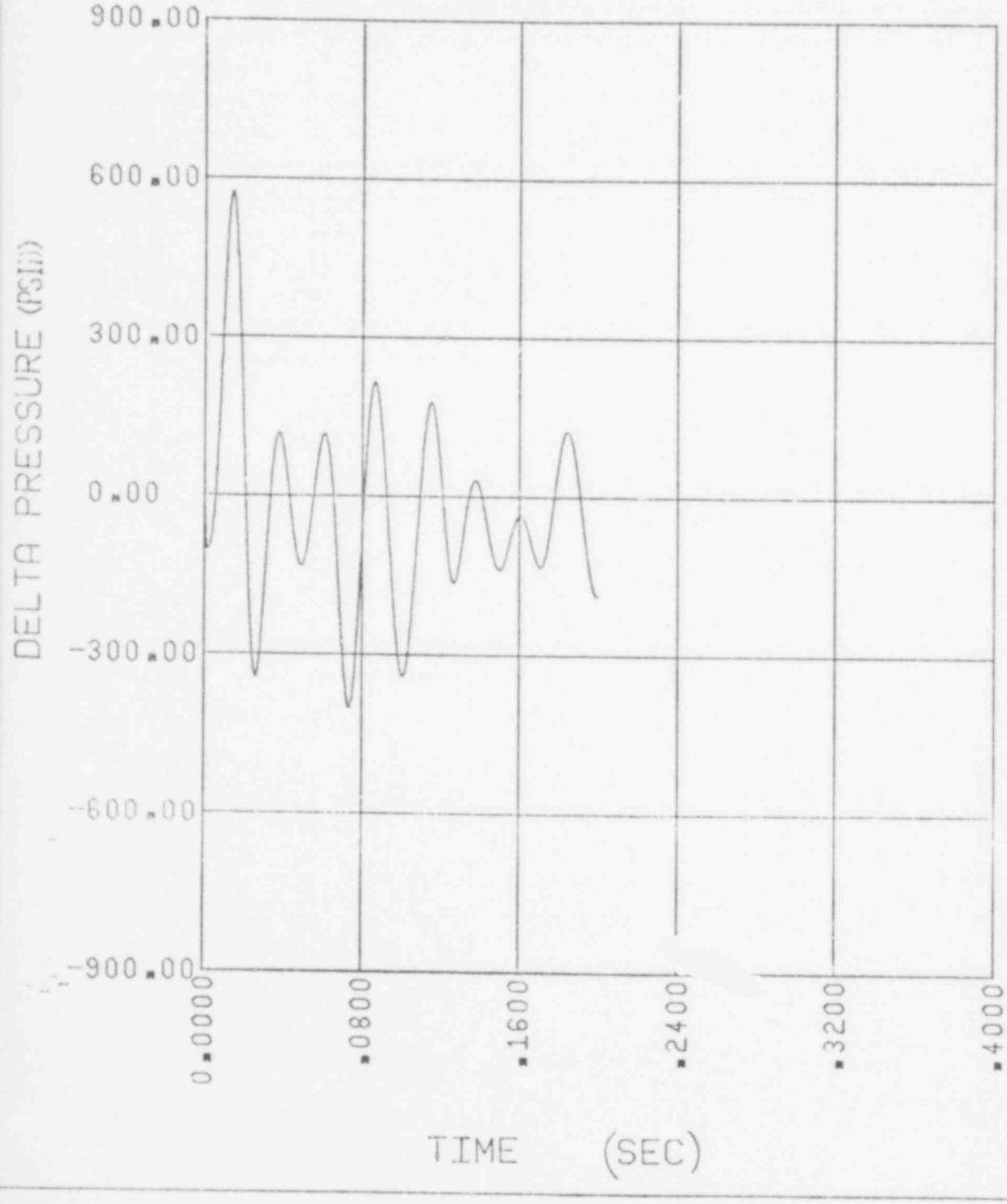

597 031

FIGURE 2.6-23

SYSTEM 80 350 SQ. INCH INLET BREAK

PRESSURE DROP ACROSS BROKEN LOOP STEAM GENERATOR

(NODES 58-60)

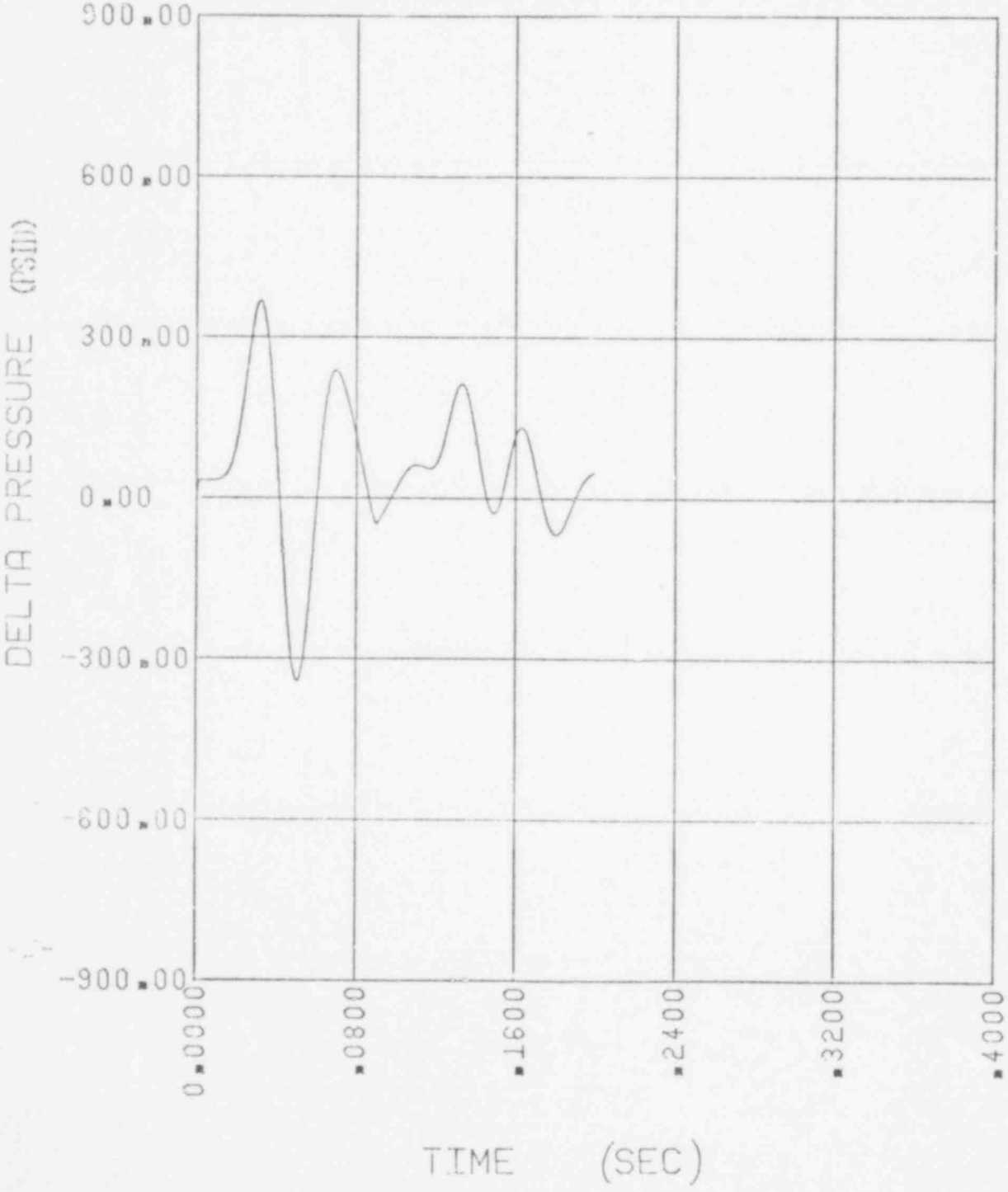

597 032

FIGURE 2.6-24

SYSTEM 80 350 SQ. INCH-INLET BREAK
PRESSURE DROP ACROSS INTACT LOOP STEAM GENERATOR
(NODES 52-54)

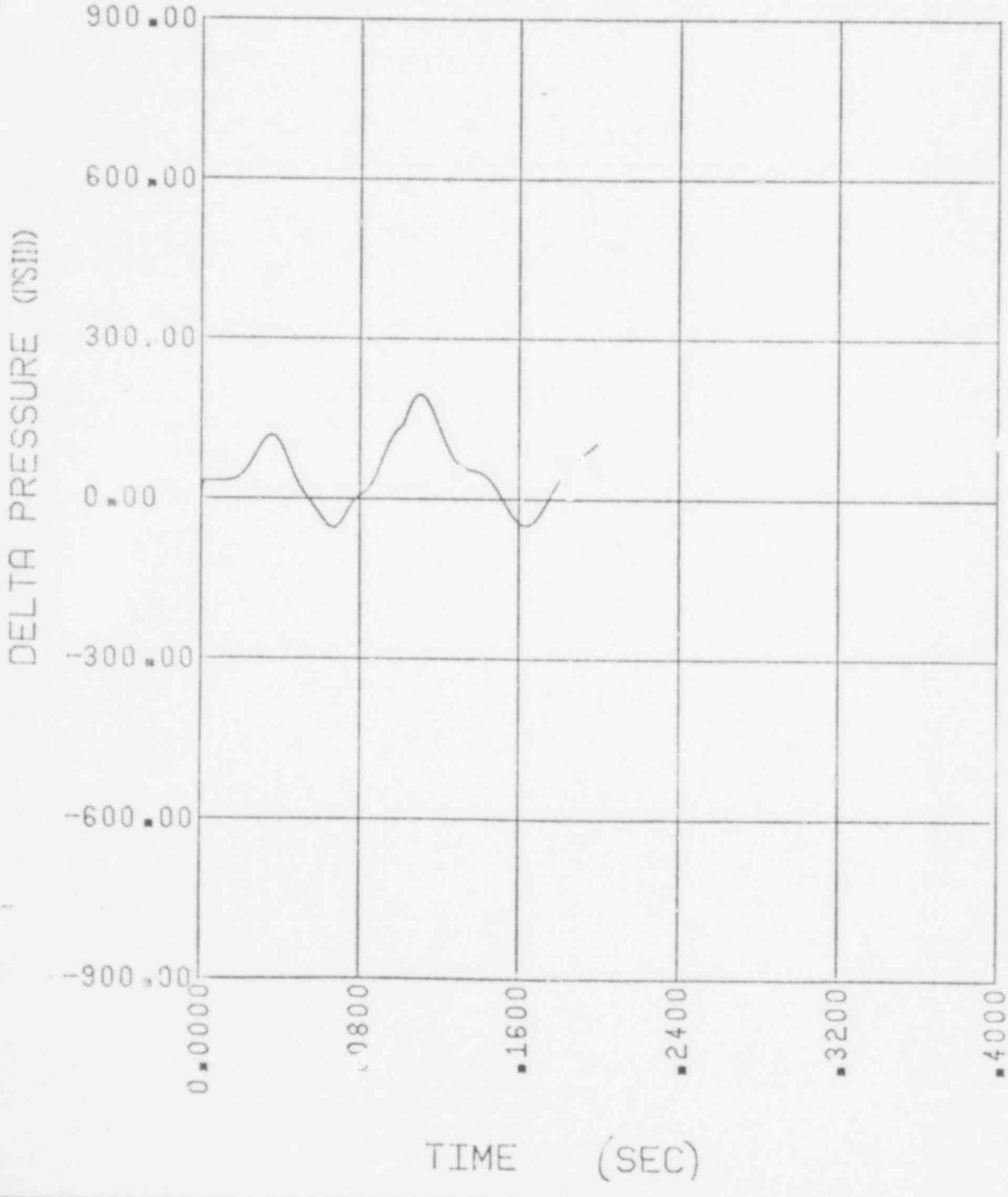

597 033

Figure 2.6-25
SYSTEM 80 350 SQ. INCH-INLET BREAK
PRESSURE DROP ACROSS REACTOR
PRESSURE VESSEL
(NODES 65 - 57)

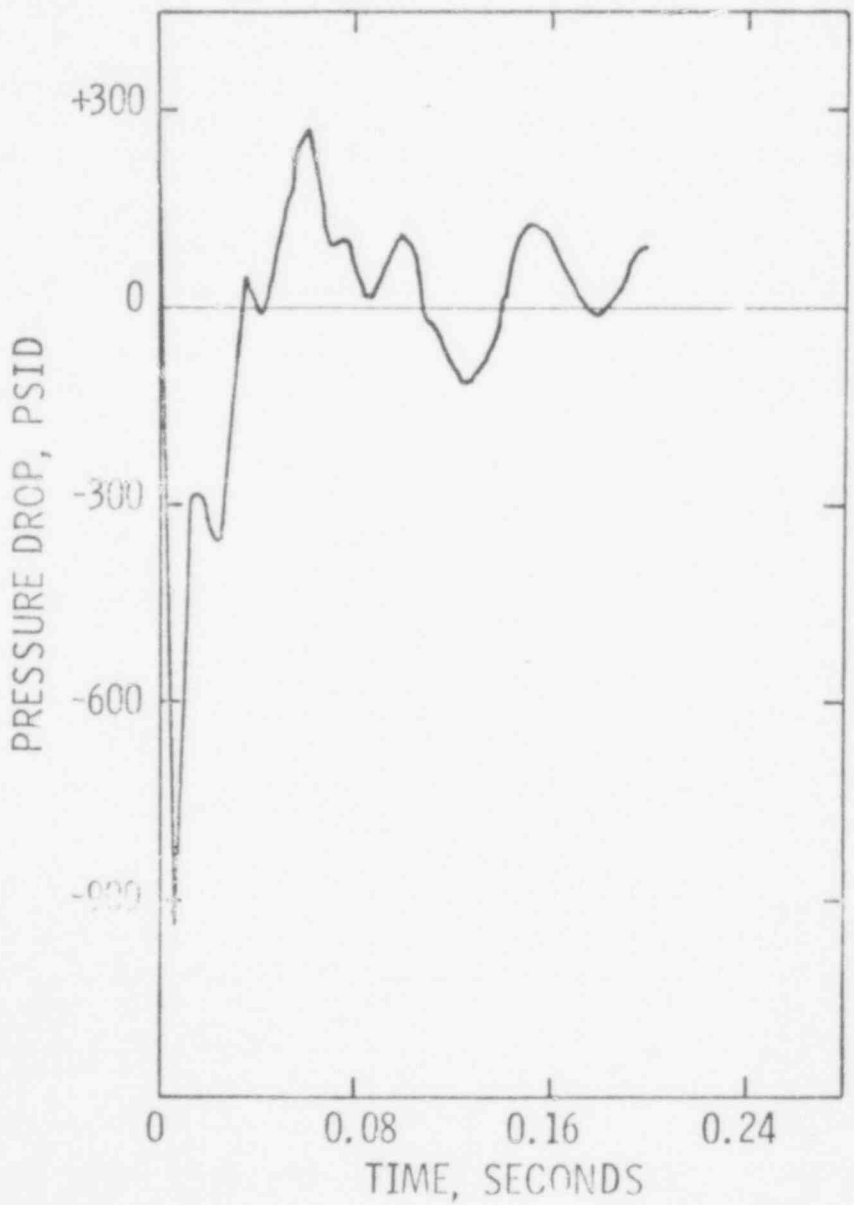

FIGURE 2.6-26

SYSTEM 80 350 SQ. INCH-INLET BREAK

MASS FLOW RATE: VESSEL SIDE BREAK

(PATH 10Y)

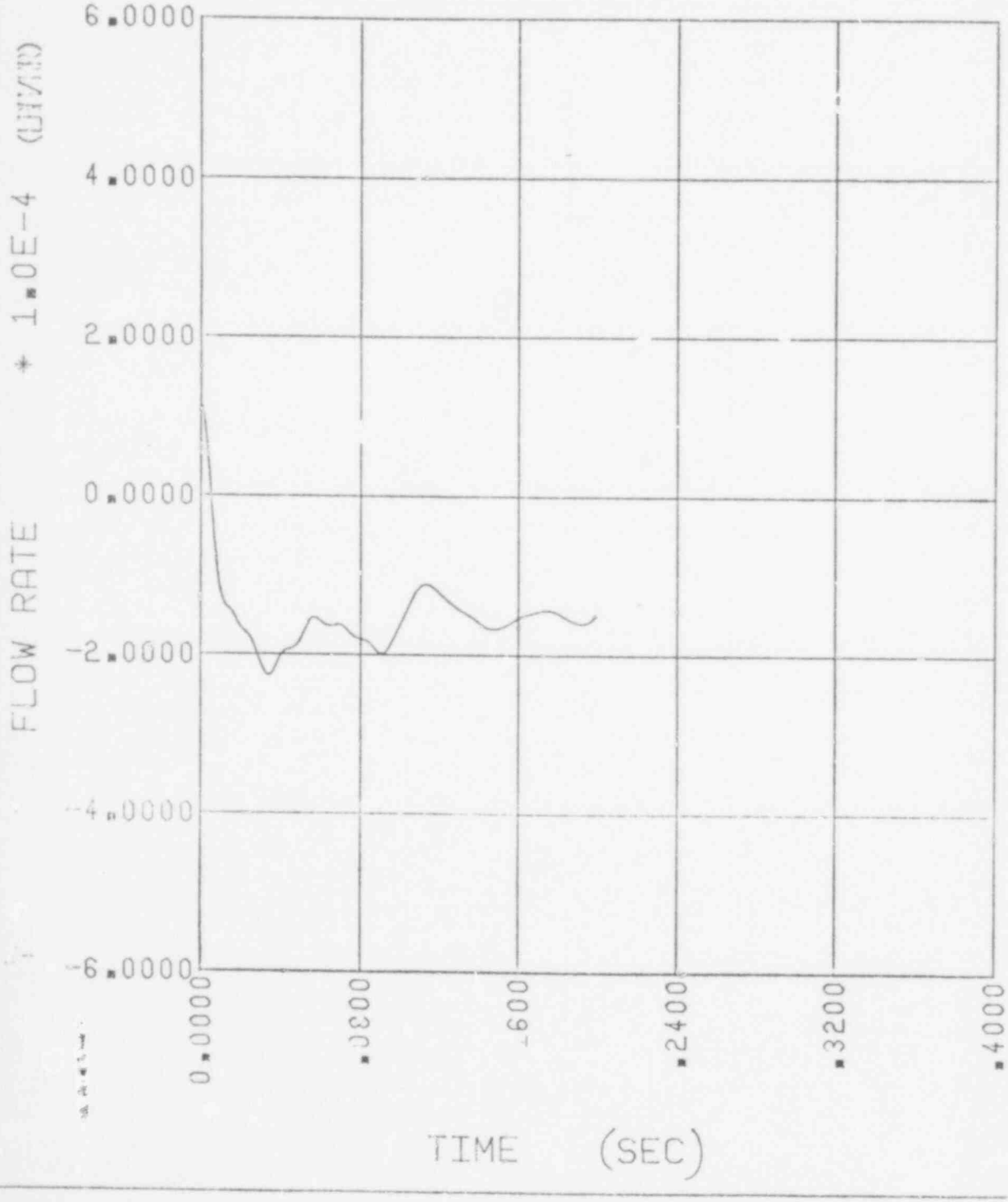

FIGURE 2.6-27

SYSTEM 80 350 SQ. INCH-INLET BREAK

MASS FLOW RATE:PUMP SIDE BREAK

(PATH 105)

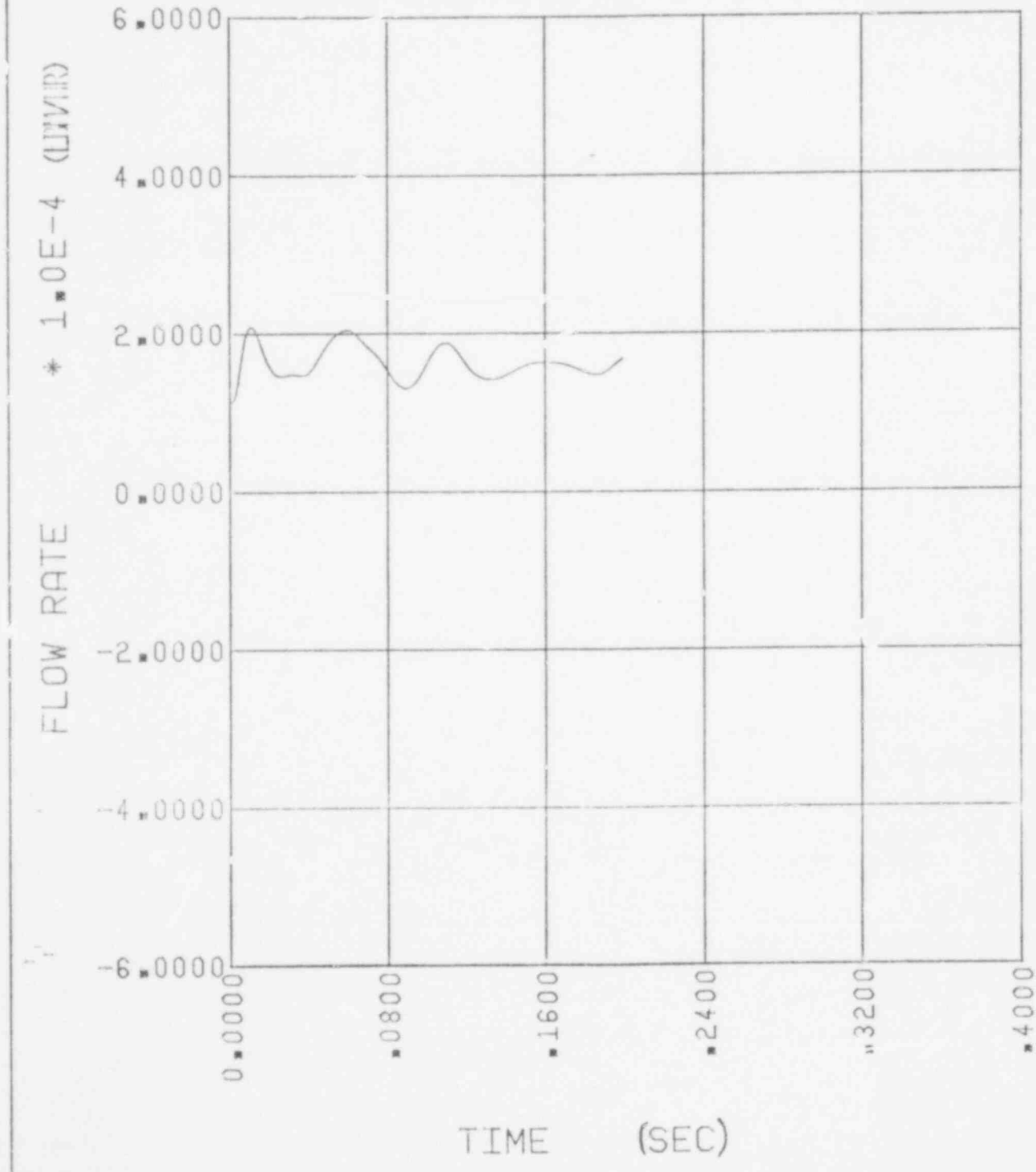

597 036

FIGURE 2.6-28

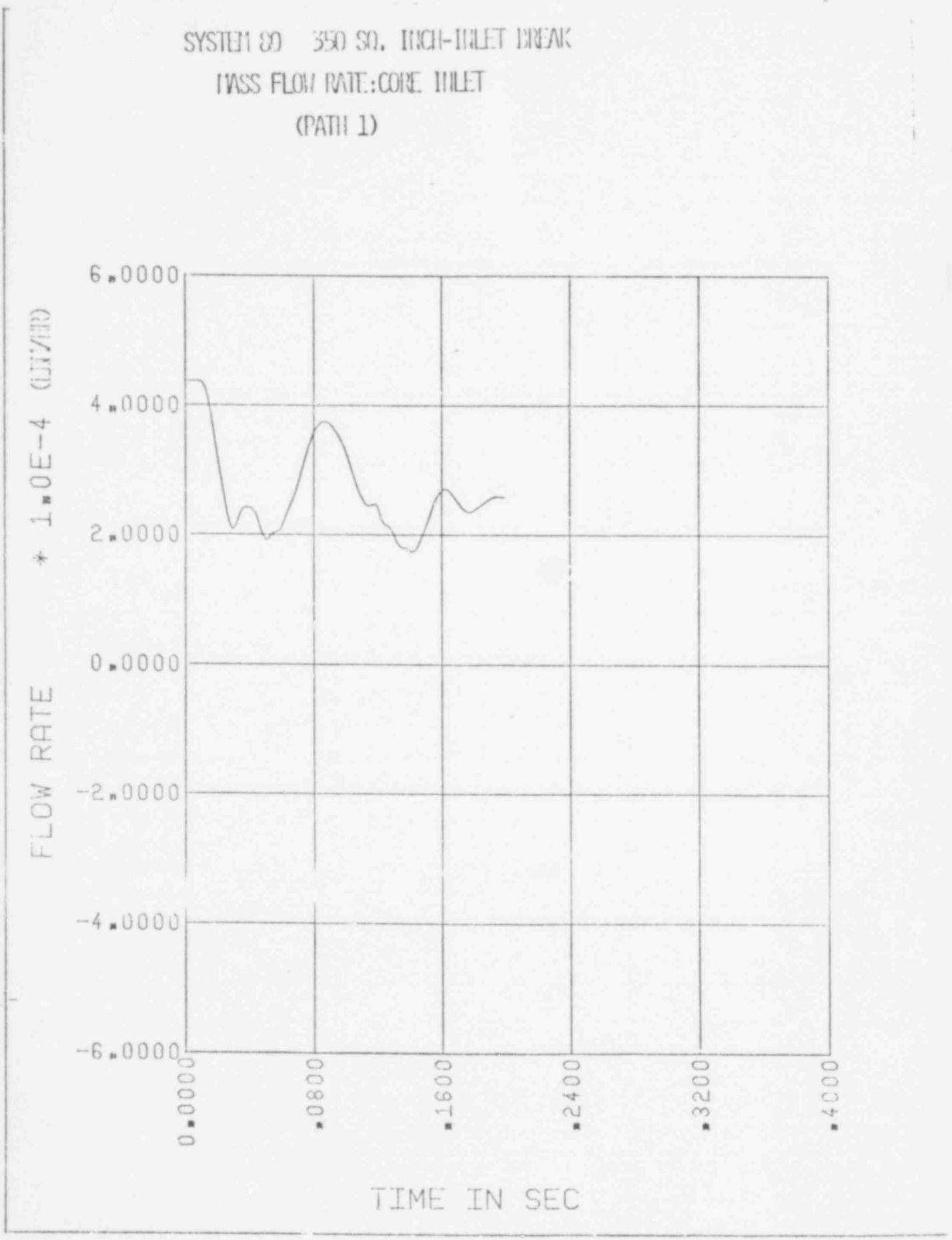

FIGURE 2.6-29
SYSTEM 80 350 IN^2 INLET BREAK
INTEGRATED CORE SUPPORT BARREL LOAD
(IN PLANE OF THE BREAK: x-DIRECTION)

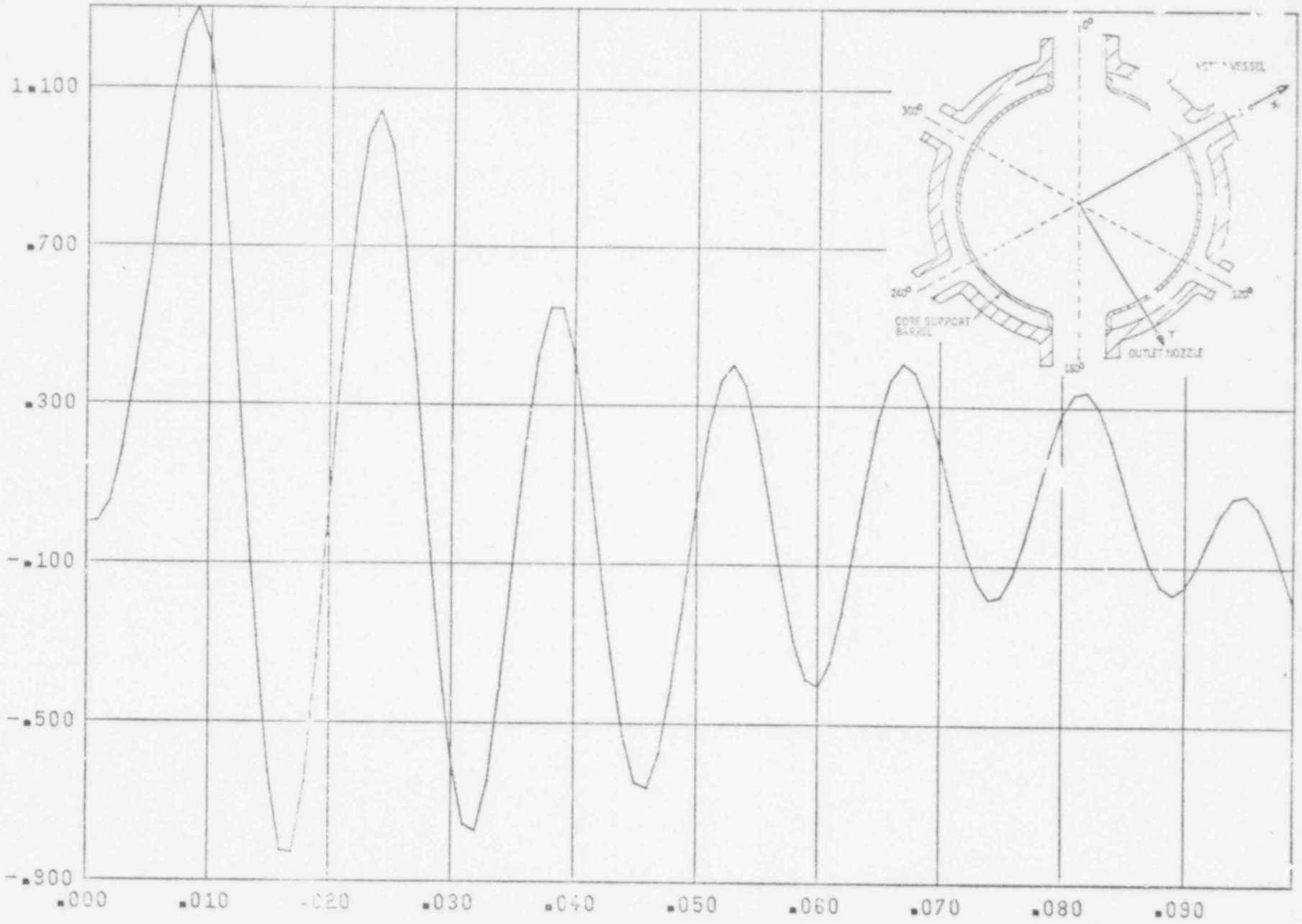

(PERPENDICULAR TO THE BREAK PLANE: y-DIRECTION)

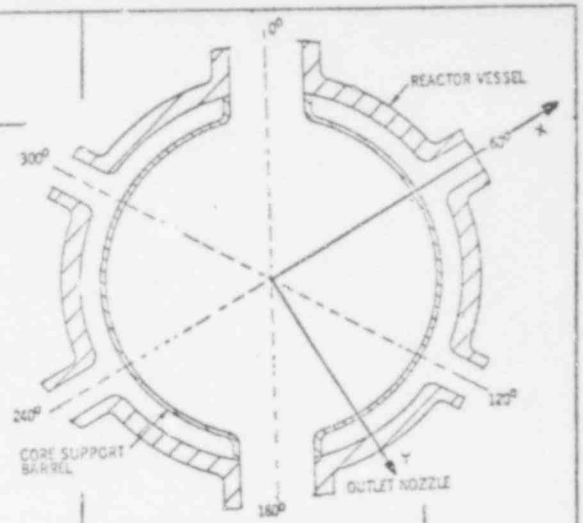

FORCE-LBS
(X10')

1.100
.700
.300
-.100
-.500
-.900

.000 .010 .020 .030 .040 .050 .060 .070 .080 .090

TIME-SEC
(X10 °)

2.6-37

QUESTION 3.1

3.1 The LOFT L1-2 experiment has been analyzed in CENPD-252-P. For the model described in Section 3 of the topical report provide plots of the data listed in Table 3-1. Identify the nodes used. For those cases where the model does not compute data at the specified instrument location, provide the data at the nearest node and identify all nodes. Provide a complete CEFLASH-4B listing of the input data through time step zero for this case.

TABLE 3-1

LOFT L1-2 Data References

Differential Pressure	Absolute Pressure
PdE-BL-5	PE-BL-1
PdE-BL-7	PE-BL-2
PdE-PC-1	PE-BL-3
PdE-PC-2	PE-BL-4
PdE-CS-1	PE-BL-6
	PE-CS-1FF
	PE-PC-1
	PE-PC-2
	PE-PC-3A
	PE-1ST-1FF
	PE-1ST-3FF
	PE-2ST-1FF
	PE-2ST-3FF

Response

This section provides the supplemental CEFLASH-4B LOFT L1-2 input information and CEFLASH-4B data as requested above.

CEFLASH-4B LISTING OF INPUT DATA AND ZERO TIME EDIT

A listing of the basic CEFLASH-4B input parameters is presented in Table 3.1-1. The corresponding time zero edit has already been

presented in Appendix C of the topical report. To aid in the interpretation of the input parameters and data predictions to follow, a nodal diagram (identical to Figure 3-3 of the topical (report) is included as Figure 3.1-1 of this response.

SUPPLEMENTARY PLOTS

The plots of the requested CEFLASH-4B absolute and differential pressure predictions are provided in Figures 3.1-3 thru 3.1-16. The nodes selected for the pressure sensor comparisons are summarized in Tables 3.1-2 and 3.1-3. Sensor locations are shown in Figure 3.1-2. In all instances, the node nearest the desired instrument location was selected for presentation. Node 24 (see Figure 3.1-1) has been selected to be representative of sensor measurements PE-BL-1 and PE-BL-4. Actually Node 24 closely simuates the cold leg DTT* flange location and therefore should be representative of transducer PE-BL-1. PE-BL-4 is located in a small diameter pipe somewhat downstream of PE-BL-1(in the choked flow region upstream of the break orifice).As a consequence of stabi considerations and to keep the basic C-E modeling practice of simulating the broken nozzle with a single CEFLASH-4B node, it was necessary that the small diameter adjacent piping be lumped into Node 24.

*Drag Disc Turbine Transducer

TABLE 3.1-1

LOFT L?-2 CEFLASH-4B MODEL

INPUT DESCRIPTION

COMBUSTION ENGINEERING CEFLASH-4B VERSION 11 03 1976 76308

LOFT L1-2 EXPERIMENTAL COMPARISON

JOB NO NLS6BCS RUN DATE 07/13/77 RUN BEGUN 06.04.34 CPS USED 4.07800

A. GENERAL INFORMATION AND OPTION INFORMATION

END TIME	RUPT TIME	LEAK DRONG	REF ELEV	PSEUDO P F	MAX STEPS	MAX EDITS
1.5000E-01	0.	2.0000E-02	0.	0.	100000	5000

OPTIONS SELECTED

IFMK	1	MOMENTUM TERM USED IN FLOW PATHS SELECTED CARD SERIES 4INN
IFTAX	3	VIRIAL CORRELATION
IFKC	2	FLOW VARYING FRICTION FACTOR
IFCF	1	CRITICAL FLOW CHECK TYPE 5 PLUS PATHS SELECTED CARD SERIES 4INN
IFBL	0	DO NOT BALANCE SYSTEM

OPTION FOR LEAK TABLES SELECTED BY VALUE OF L/D FOR FIRST LEAK FLOW PATH

PATH	L/D	TABLES USED
99	0.	( )

TIME STEP TABLE

USE	UNTIL	STEPS PER PRINT
5.0000E-05	2.0000E-02	10
5.0000E-04	1.5000E-01	10
5.0000E-03	3.0000E-01	25
5.0000E-04	5.4000E-01	25

TABLE 3.1-1 (CONT'D)

LOFT L1-2 CEFLASH-4B MODEL

COMBUSTION ENGINEERING — CEFLASH4B — VERSION 11 03 1976 — 76308

B. CONTROL VOLUMES

NODE	AREA	HEIGHT	EXIT ELEV	INLET ELEV	BOTTM ELEV	FLOW AREA
1	2.3809E+00	6.1170E-01	8.0575E+00	8.2450E+00	8.2450E+00	3.0000E+00
2	3.5106E+00	5.8000E-01	9.4375E+00	8.0576E+00	8.0576E+00	3.5100E+00
3	3.2500E+00	2.0120E+00	1.2230E+01	9.4376E+00	9.4375E+00	3.2900E+00
4	3.2900E+00	3.5030E+00	1.5033E+01	1.2251E+01	1.2230E+01	3.2000E+00
5	3.2950E+00	2.1720E+00	1.8035E+01	1.5034E+01	1.5033E+01	3.2000E+00
6	2.0029E+00	1.9675E+00	1.9272E+01	1.8006E+01	1.8095E+01	2.0000E+00
7	2.5675E+00	3.3610E+00	2.3370E+01	1.9273E+01	1.9270E+01	2.5000E+00
8	1.9347E+00	2.2200E+00	2.5550E+01	2.3350E+01	2.3330E+01	1.5000E+00
9	2.1283E+00	2.5000E+00	2.5555E+01	2.5555E+01	2.5550E+01	2.0000E+00
10	7.0229E+00	[illegible]	8.2450E+00	8.2450E+00	6.0070E+00	7.0300E+00
11	7.7132E+00	1.3524E+00	6.0075E+00	6.0075E+00	5.6000E+00	9.6400E+00
12	5.2940E-01	6.0090E+00	2.2000E+01	2.2000E+01	1.0172E+01	7.0000E-01
13	5.2540E-01	6.0000E+00	2.2000E+01	2.2000E+01	1.0172E+01	7.4700E-01
14	7.6146E+00	9.3230E-01	2.2000E+01	2.2000E+01	2.1531E+01	6.0270E-01
15	3.5450E+00	1.6000E+00	2.2755E+01	2.2000E+01	2.1460E+01	7.2000E-01
16	2.5224E+00	1.0000E+01	3.1670E+01	2.2755E+01	2.1000E+01	2.0000E+00
17	2.5224E+00	1.0000E+01	2.2755E+01	3.1670E+01	2.1000E+01	2.0000E+00
18	2.0720E+00	5.0000E+00	2.1640E+01	2.2755E+01	1.7307E+01	7.2000E-01
19	4.3370E+00	1.3300E+00	2.2000E+01	2.1024E+01	2.1024E+01	3.9200E-01
20	3.0141E+00	1.3300E+00	2.2000E+01	2.1024E+01	2.1024E+01	3.9200E-01
21	9.7175E+00	9.3230E-01	2.2000E+01	2.2000E+01	2.1531E+01	6.0270E-01
22	2.8825E+00	1.2030E+01	2.2457E+01	2.2457E+01	2.2466E+01	2.0000E-02
23	2.6755E+00	2.5000E+00	2.2000E+01	2.2000E+01	2.1620E+01	4.17[illegible]E-01
24	5.3607E+00	9.3200E-01	2.2000E+01	2.2000E+01	2.1534E+01	6.6270E-01
25	1.3430E-01	4.0400E+00	2.2519E+01	1.0000E+01	1.0034E+01	9.0000E-02
26	7.9340E-01	9.2470E-01	1.0003E+01	1.9262E+01	1.8337E+01	6.0270E-01
27	7.6500E-02	4.9379E+00	1.9200E+01	2.4220E+01	1.9200E+01	9.0000E-02
28	1.2800E+00	8.7200E+00	2.4220E+01	3.2344E+01	2.4220E+01	1.1300E+00
29	1.2800E+00	0.7200E+00	3.2314E+01	2.4220E+01	2.4220E+01	1.1300E+00
30	2.0070E+00	2.0000E+00	2.4220E+01	2.2000E+01	2.1534E+01	4.0000E-01
31	3.0677E-01	2.5071E+00	8.2450E+00	1.0033E+01	8.2450E+00	2.5450E-01
32	3.0677E-01	2.5071E+00	8.2450E+00	1.0033E+01	8.2458E+00	2.5450E-01
33	3.0677E-01	2.5071E+00	8.2450E+00	1.0033E+01	8.2450E+00	2.5450E-01
34	3.0677E-01	2.5071E+00	8.2450E+00	1.0033E+01	8.2450E+00	2.5450E-01
35	3.0677E-01	2.5071E+00	8.2450E+00	1.0033E+01	8.2450E+00	2.5450E-01
36	3.0677E-01	2.5071E+00	8.2450E+00	1.0033E+01	8.2450E+00	2.5450E-01
37	3.0676E-01	4.1667E+00	1.0033E+01	1.5000E+01	1.0033E+01	2.5450E-01
38	3.0676E-01	4.1667E+00	1.0033E+01	1.5000E+01	1.0033E+01	2.5450E-01
39	3.0676E-01	4.1667E+00	1.0033E+01	1.5000E+01	1.0033E+01	2.5450E-01
40	3.0676E-01	4.1667E+00	1.0033E+01	1.5000E+01	1.0033E+01	2.5450E-01
41	3.0676E-01	4.1667E+00	1.0033E+01	1.5000E+01	1.0033E+01	2.5450E-01
42	3.0676E-01	4.1667E+00	1.0033E+01	1.5000E+01	1.0033E+01	2.5450E-01
43	3.0679E-01	5.6250E+00	1.5000E+01	2.0625E+01	1.5000E+01	2.5450E-01
44	3.0679E-01	5.6250E+00	1.5000E+01	2.0625E+01	1.5000E+01	2.5450E-01
45	3.0679E-01	5.6250E+00	1.5000E+01	2.0625E+01	1.5000E+01	2.5450E-01
46	3.0679E-01	5.6250E+00	1.5000E+01	2.0625E+01	1.5000E+01	2.5450E-01
47	3.0679E-01	5.6250E+00	1.5000E+01	2.0625E+01	1.5000E+01	2.5450E-01
48	3.0679E-01	[illegible]	[illegible]	[illegible]	[illegible]	[illegible]

POOR ORIGINAL

597 043

TABLE 3.1-1 (CONT'D)

LOFT L1-2 CEFLASH-4B MODEL

COMBUSTION ENGINEERING   CEFLASH4B   VERSION 11.03 1976   76308

B. CONTROL VOLUMES

NODE	AREA	HEIGHT	EXIT ELEV	INLET ELEV	BOTTM ELEV	FLOW AREA
51	4.4031E-01	1.6410E+00	2.0626E+01	[illegible]	[illegible]	[illegible]
52	4.4031E-01	1.6410E+00	[illegible]	[illegible]	[illegible]	[illegible]
53	[illegible]	1.6410E+00	[illegible]	[illegible]	[illegible]	[illegible]
54	4.4031E-01	[illegible]	[illegible]	[illegible]	[illegible]	[illegible]
55	[illegible]	[illegible]	[illegible]	[illegible]	[illegible]	[illegible]
56	[illegible]	[illegible]	[illegible]	[illegible]	[illegible]	[illegible]
57	[illegible]	[illegible]	[illegible]	[illegible]	[illegible]	[illegible]
58	[illegible]	[illegible]	[illegible]	[illegible]	[illegible]	[illegible]
59	[illegible]	[illegible]	2.2467E+01	[illegible]	[illegible]	[illegible]
60	[illegible]	[illegible]	2.2467E+01	[illegible]	[illegible]	2.5450E-01
61	[illegible]	[illegible]	[illegible]	[illegible]	[illegible]	[illegible]
62	2.3117E+00	[illegible]	[illegible]	[illegible]	[illegible]	4.1750E-01
63	[illegible]	[illegible]	[illegible]	[illegible]	[illegible]	[illegible]
64	2.4216E+00	8.3330E-01	2.2000E+01	2.2000E+01	[illegible]	5.0000E-01
65	1.0000E+03	1.0000E+02	2.2000E+01	2.2000E+01	0.	1.0000E+02

POOR ORIGINAL

597 044

TABLE 3.1-1(CONT'D)

LOFT L1-2 CEFLASH-4B MODEL

COMBUSTION ENGINEERING CEFLASH4B VERSION 11 03 1976 76308

NODAL PROPERTIES

NODE	PRESSURE	ENTH SUBC	LEVEL	TPH
1	2.2012E+03	5.3606E+02	0.	
2	2.2033E+03	5.3606E+02	0.	
3	2.2022E+03	5.3606E+02	0.	
4	2.2011E+03	5.3606E+02	0.	
5	2.2004E+03	5.3606E+02	0.	
6	2.2765E+03	5.3606E+02	0.	
7	2.2737E+03	5.3606E+02	0.	
8	2.2729E+03	5.3606E+02	0.	
9	2.2721E+03	5.3606E+02	0.	
10	2.2045E+03	5.3606E+02	0.	
11	2.2050E+03	5.3606E+02	0.	
12	2.2729E+03	5.3606E+02	0.	
13	2.2731E+03	5.3606E+02	0.	
14	2.2721E+03	5.3606E+02	0.	
15	2.2679E+03	[illegible]	0.	
16	2.2540E+03	5.3606E+02	0.	
17	2.2407E+03	5.3606E+02	0.	
18	2.2377E+03	5.3606E+02	0.	
19	2.20[illegible]E+03	5.3606E+02	0.	
20	2.2036E+03	5.3606E+02	0.	
21	2.20[illegible]E+03	5.3606E+02	0.	
22	2.2700E+03	7.036[illegible]E+02	7.5257E+00	
23	2.2704E+03	5.3606E+02	0.	
24	2.2005[illegible]	5.3606E+02	0.	
25	2.2725E+03	[illegible]	0.	
26	2.2750E+03	5.3606E+02	0.	
27	2.2724E+03	5.3606E+02	0.	
28	2.2705E+03	5.3606E+02	0.	
29	2.2705E+03	5.3606E+02	0.	
30	2.2734E+03	5.3606E+02	0.	
31	2.20[illegible]E+03	[illegible]	0.	
32	2.2034E+03	5.3606E+02	0.	
33	2.2034E+03	5.3606E+02	0.	
34	2.2034E+03	5.3606E+02	0.	
35	2.2034E+03	[illegible]	0.	
36	2.2034E+03	5.3606E+02	0.	
37	[illegible]	[illegible]	0.	
38	2.20[illegible]E+03	5.360[illegible]E+02	0.	
39	[illegible]	[illegible]	0.	
40	2.20[illegible]E+03	[illegible]	0.	
41	[illegible]	[illegible]	0.	
42	2.20[illegible]E+03	[illegible]	0.	
43	[illegible]	[illegible]	0.	
44	2.2006E+03	5.360[illegible]E+02	0.	
45	2.2006E+03	5.3606E+02	0.	
46	2.2006E+03	5.3606E+02	0.	
47	2.2006E+03	5.3606E+02	0.	
48	2.2006E+03	5.3606E+02	0.	
49	2.2005E+03	5.3606E+02	0.	

NODAL PROPERTIES

NODE	PRESSURE	ENTH SUBC	LEVEL	TPH
51	[illegible]	5.3606E+02	0.	
52	2.20[illegible]E+03	5.3606E+02	0.	
53	2.2013E+03	5.3606E+02	0.	
54	2.2[illegible]E+03	5.3606E+02	0.	
55	2.27[illegible]E+03	5.3606E+02	0.	
56	2.2796E+03	5.3606E+02	0.	
57	2.27[illegible]E+03	[illegible]	0.	
58	2.27[illegible]E+03	5.3606E+02	0.	
59	2.27[illegible]E+03	[illegible]	0.	
60	2.27[illegible]E+03	5.3606E+02	0.	
61	[illegible]	[illegible]	0.	
62	2.2[illegible]07E+03	5.3606E+02	0.	
63	2.20[illegible]E+03	5.3606E+02	0.	
64	2.2739E+03	5.3606E+02	0.	
65	1.4700E+01	1.0000E+02	0.	

LEAK FLOW PATHS TO CONTAINMENT NODE

NODE	FLOW PATHS
65	99100

POOR ORIGINAL

597 045

C. FLOW PATHS

PATH	TYPE	NODE FROM	NODE TO	WD	SUM L/A	AREA	DIAMETER	MOM FLOW AREA UP	MOM FLOW AREA DOWN	FRICTION K OR DELTA P	GEOM FWD K OR DELTA P	GEOM REV K OR DELTA P
1	8	1	2	5.5940E+02	2.0020E-01	3.2235E+00	4.0720E-01	1.5170E+00	4.1250E+00	0.	5.2000E+00	5.2000E+00
2	8	2	3	5.5940E+02	6.5600E-01	3.4900E+00	2.1510E+00	4.1200E+00	3.2500E+00	0.	6.9670E-01	6.9000E-01
3	8	3	4	5.5940E+02	9.7000E-01	3.2500E+00	2.1800E+00	3.2500E+00	3.2500E+00	0.	0.	0.
4	8	4	5	5.5940E+02	0.7400E-01	3.2500E+00	2.1800E+00	3.2500E+00	3.2500E+00	0.	0.	0.
5	8	5	6	5.5940E+02	4.9900E+00	9.9700E-01	1.8000E+00	3.2500E+00	2.5110E+00	2.5000E-01	3.8800E+00	3.8900E+00
6	8	6	7	5.5940E+02	1.9910E+00	1.6516E+00	1.5200E+00	2.5110E+00	2.5110E+00	0.	7.0470E+00	7.0470E+00
7	8	7	8	0.	9.7000E-01	2.5110E+00	1.7000E+00	2.5110E+00	2.5110E+00	2.0700E-02	0.	0.
8	8	8	9	0.	1.9910E+00	2.0000E+00	1.5000E+00	2.1000E+00	2.5110E+00	0.	1.0000E+00	1.0300E+00
9	0	7	12	5.5940E+02	1.2000E+00	7.6000E-01	5.0000E+00	7.8000E-01	7.8000E-01	0.	1.5600E-01	1.5600E-01
10	8	7	13	0.	1.3000E+00	7.0300E-01	5.0000E+00	7.0300E-01	7.0300E-01	0.	1.5600E-01	1.5600E-01
11	8	13	30	0.	5.5100E+00	6.0300E-01	9.5000E-01	7.0300E-01	6.0270E-01	0.	1.5110E-01	1.5100E-01
12	8	12	14	5.8000E+02	8.9000E+00	6.0270E-01	9.0000E-01	7.0300E-01	6.0270E-01	0.	1.1000E-01	1.1000E-01
13	8	14	15	5.8000E+02	1.0200E+01	5.4430E-01	8.1100E-01	6.0270E-01	6.0270E-01	0.	9.8210E-01	9.8210E-01
14	8	15	16	5.8000E+02	4.4320E+00	1.7000E+00	1.9000E+00	6.0270E-01	9.3200E-01	0.	3.0500E+01	3.0500E+01
15	8	16	17	5.8000E+02	1.6000E+01	9.3200E-01	3.2000E-02	9.3200E-01	9.3200E-01	6.7296E+00	0.	0.
16	8	17	18	5.8000E+02	1.2000E+01	7.5900E-01	9.7200E-01	9.3200E-01	6.0270E-01	0.	5.4600E+00	5.4600E+00
17	2	18	19	2.9440E+02	7.1000E+00	5.9200E-01	7.6000E-01	6.0270E-01	3.9410E-01	2.2500E-02	7.8400E-01	7.8400E-01
18	2	18	20	2.9440E+02	7.1000E+00	5.9200E-01	7.5600E-01	6.0270E-01	3.9410E-01	2.2500E-02	7.8400E-01	7.8400E-01
19	8	19	21	2.9440E+02	1.5000E+01	4.2600E-01	7.7000E-01	3.9410E-01	6.0270E-01	8.1200E-02	2.6400E-01	2.6100E-01
20	8	20	21	2.9440E+02	5.2600E+00	4.2000E-01	7.0000E-01	3.9410E-01	5.7000E-01	3.1000E-02	2.9300E-01	2.9300E-01
21	0	21	50	5.8080E+02	1.8000E+01	6.0270E-01	9.2000E-01	6.0270E-01	6.0270E-01	1.2470E-01	2.3040E+00	2.3600E+00
22	8	30	29	0.	6.3100E+01	3.5000E-01	9.0700E-01	6.0270E-01	1.0000E+00	1.5000E-01	3.0320E+01	3.7200E+01
23	8	29	28	0.	1.4600E+01	1.1000E+00	1.2100E+00	1.0000E+00	1.0000E+00	5.0000E-02	2.9000E+02	2.9000E+02
24	8	28	27	0.	3.2300E+01	4.4400E-01	1.1000E+00	1.0000E+00	9.0000E-02	1.0000E-01	2.9000E+01	3.9010E+01
25	8	27	26	0.	3.7000E+01	1.6000E-01	5.6000E-01	9.0000E-02	1.0000E-01	9.7000E-02	4.9000E+01	4.7000E+01
26	8	26	25	0.	6.7000E+01	9.0000E-02	3.3000E-01	1.0000E-01	9.0000E-02	2.6000E-01	1.3200E+00	1.7400E+00
27	8	53	24	0.	1.0000E+01	6.0270E-01	9.3000E-01	6.0270E-01	6.0270E-01	1.0000E-01	1.1400E+00	1.1400E+00
28	8	62	30	0.	1.7000E+01	4.1750E-01	7.2000E-01	4.1750E-01	4.1750E-01	1.5100E-01	2.2300E+00	2.2500E+00
29	8	10	1	5.5940E+02	3.4110E-01	2.0000E+00	1.5000E+00	4.8000E+00	1.5170E+00	0.	1.0160E+00	1.0160E+00
30	8	11	10	0.	2.4800E-01	6.0000E+00	2.6000E+00	7.4000E+00	4.8000E+00	1.0000E-04	0.	0.
31	8	31	10	9.8133E+01	5.0410E+00	5.0000E-01	6.0000E-01	2.5750E-01	1.2700E+00	0.	2.6600E-01	2.6600E-01
32	8	32	10	9.8133E+01	5.0410E+00	5.0000E-01	6.0000E-01	2.5950E-01	1.2700E+00	0.	2.6600E-01	2.6600E-01
33	8	33	10	9.8133E+01	5.0410E+00	5.0000E-01	6.0000E-01	2.5950E-01	1.2700E+00	0.	2.6600E-01	2.6600E-01
34	8	34	10	9.8133E+01	5.0410E+00	5.0000E-01	6.0000E-01	2.5950E-01	1.2700E+00	0.	2.6600E-01	2.6600E-01
35	8	35	10	9.8133E+01	5.0410E+00	5.0000E-01	6.0000E-01	2.5950E-01	1.2700E+00	0.	2.6600E-01	2.6600E-01
36	8	36	10	9.8133E+01	5.0410E+00	5.0000E-01	6.0000E-01	2.5950E-01	1.2700E+00	0.	2.6600E-01	2.6600E-01
37	8	37	31	9.0133E+01	1.3800E+01	2.5950E-01	6.6000E-01	2.5950E-01	2.5950E-01	0.	5.9200E-01	5.9200E-01
38	8	38	32	9.8133E+01	1.3800E+01	2.5950E-01	6.6000E-01	2.5950E-01	2.5950E-01	0.	5.9300E-01	5.9300E-01
39	8	39	33	9.8133E+01	1.3800E+01	2.5950E-01	6.6000E-01	2.5950E-01	2.5950E-01	0.	5.9300E-01	5.9300E-01
40	8	40	34	9.8133E+01	1.3800E+01	2.5950E-01	6.6000E-01	2.5950E-01	2.5950E-01	0.	5.9300E-01	5.9300E-01
41	8	41	35	9.8133E+01	1.3800E+01	2.5950E-01	6.6000E-01	2.5950E-01	2.5950E-01	0.	5.9300E-01	5.9300E-01
42	8	42	36	9.8133E+01	1.3800E+01	2.5950E-01	6.6000E-01	2.5950E-01	2.5950E-01	0.	5.9300E-01	5.9300E-01
43	8	43	37	9.8133E+01	1.9237E+01	2.5450E-01	6.6000E-01	2.5450E-01	2.5450E-01	0.	7.4090E-01	7.4090E-01
44	8	44	38	9.8133E+01	1.9237E+01	2.5450E-01	6.6000E-01	2.5450E-01	2.5450E-01	0.	7.4090E-01	7.4090E-01
45	8	45	39	9.8133E+01	1.9237E+01	2.5450E-01	6.6000E-01	2.5450E-01	2.5450E-01	0.	7.4090E-01	7.4090E-01
46	8	46	40	9.8133E+01	1.9237E+01	2.5450E-01	6.6000E-01	2.5450E-01	2.5450E-01	0.	7.4090E-01	7.4090E-01
47	8	47	41	9.8133E+01	1.9237E+01	2.5450E-01	6.6000E-01	2.5450E-01	2.5450E-01	0.	7.4090E-01	7.4090E-01
48	8	48	42	9.8133E+01	1.9237E+01	2.5450E-01	6.6000E-01	2.5450E-01	2.5450E-01	0.	7.4090E-01	7.4090E-01
49	8	49	43	9.8133E+01	1.6450E+01	2.5450E-01	6.6000E-01	4.6450E-01	2.5450E-01	0.	2.9640E-01	2.9640E-01

TABLE 3.1-1 (CONT'D)
LOFT L1-2 CEFLASH-4B MODEL

COMBUSTION ENGINEERING — CEFLASH4B — VERSION 11 03 1976 — 76308

C. FLOW PATHS

PATH	TYPE	NODE FROM	NODE TO	WO	SUM L/A	AREA	DIAMETER	MOM FLOW AREA UP	MOM FLOW AREA DOWN	FRICTION K OR DELTA P	GEOM FWD K OR DELTA P	GEOM RVS K OR DELTA P
50	8	50	44	9.8133E+01	1.6450E+01	2.5450E-01	6.6600E-01	4.6450E-01	2.5450E-01	0.	2.9640E-01	2.9640E-01
51	8	51	45	9.8133E+01	1.6450E+01	2.5450E-01	6.6600E-01	4.6450E-01	2.5450E-01	0.	2.9640E-01	2.9640E-01
52	8	52	46	9.8133E+01	1.6450E+01	2.5450E-01	6.6600E-01	4.6450E-01	2.5450E-01	0.	2.9640E-01	2.9640E-01
53	8	53	47	9.8133E+01	1.6450E+01	2.5450E-01	6.6600E-01	4.6450E-01	2.5450E-01	0.	2.9640E-01	2.9640E-01
54	8	54	48	9.8133E+01	1.6450E+01	2.5450E-01	6.6600E-01	4.6450E-01	2.5450E-01	0.	2.9640E-01	2.9640E-01
55	8	55	49	0.	8.7000E+00	3.0000E-01	6.0000E-01	2.5900E-01	4.6450E-01	0.	2.0000E-01	2.0000E-01
56	8	56	50	0.	8.7000E+00	3.0000E-01	6.0000E-01	2.5900E-01	4.6450E-01	0.	2.0000E-01	2.0000E-01
57	8	57	51	0.	8.7000E+00	3.0000E-01	6.0000E-01	2.5900E-01	4.6450E-01	0.	2.0000E-01	2.0000E-01
58	8	58	52	0.	8.7000E+00	3.0000E-01	6.0000E-01	2.5900E-01	4.6450E-01	0.	2.0000E-01	2.0000E-01
59	8	59	53	0.	8.7000E+00	3.0000E-01	6.0000E-01	2.5900E-01	4.6450E-01	0.	2.0000E-01	2.0000E-01
60	8	60	54	0.	8.7000E+00	3.0000E-01	6.0000E-01	2.5900E-01	4.6450E-01	0.	2.0000E-01	2.0000E-01
61	6	55	60	0.	3.0204E+00	5.0460E-01	3.3300E-01	5.0460E-01	5.0460E-01	1.0000E-04	0.	0.
62	8	60	59	0.	3.0204E+00	5.0460E-01	3.3300E-01	5.0460E-01	5.0460E-01	1.0000E-04	0.	0.
63	8	59	58	0.	3.0204E+00	5.0460E-01	3.3300E-01	5.0460E-01	5.0460E-01	1.0000E-04	0.	0.
64	8	58	57	0.	3.0204E+00	5.0460E-01	3.3300E-01	5.0460E-01	5.0460E-01	1.0000E-04	0.	0.
65	8	57	56	0.	3.0204E+00	5.0460E-01	3.3300E-01	5.0460E-01	5.0460E-01	1.0000E-04	0.	0.
66	8	56	55	0.	3.0204E+00	5.0460E-01	3.3300E-01	5.0460E-01	5.0460E-01	1.0000E-04	0.	0.
67	8	49	54	1.4720E+02	2.0000E+00	5.3500E-01	5.0000E-01	5.3500E-01	5.3500E-01	0.	0.	0.
68	8	54	53	4.9067E+01	2.0000E+00	5.3500E-01	5.0000E-01	5.3500E-01	5.3500E-01	0.	0.	0.
69	8	52	53	4.9067E+01	2.0000E+00	5.3500E-01	5.0000E-01	5.3500E-01	5.3500E-01	0.	0.	0.
70	8	51	52	1.4720E+02	2.0000E+00	5.3500E-01	5.0000E-01	5.3500E-01	5.3500E-01	0.	0.	0.
71	8	50	51	2.4533E+02	2.0000E+00	5.3500E-01	5.0000E-01	5.3500E-01	5.3500E-01	0.	0.	0.
72	8	50	49	2.4533E+02	2.0000E+00	5.3500E-01	5.0000E-01	5.3500E-01	5.3500E-01	0.	0.	0.
73	8	43	48	0.	1.6290E+00	9.3700E-01	3.1000E-01	9.3700E-01	9.3700E-01	1.0000E-04	0.	0.
74	8	48	47	0.	1.6290E+00	9.3700E-01	3.1000E-01	9.3700E-01	9.3700E-01	1.0000E-04	0.	0.
75	8	47	46	0.	1.6290E+00	9.3700E-01	3.1000E-01	9.3700E-01	9.3700E-01	1.0000E-04	0.	0.
76	8	46	45	0.	1.6290E+00	9.3700E-01	3.1000E-01	9.3700E-01	9.3700E-01	1.0000E-04	0.	0.
77	8	45	44	0.	1.6290E+00	9.3700E-01	3.1000E-01	9.3700E-01	9.3700E-01	1.0000E-04	0.	0.
78	8	44	43	0.	1.6290E+00	9.3700E-01	3.1000E-01	9.3700E-01	9.3700E-01	1.0000E-04	0.	0.
79	8	37	42	0.	2.1900E+00	6.9900E-01	3.3000E-01	6.9900E-01	6.9900E-01	1.0000E-04	0.	0.
80	8	42	41	0.	2.1900E+00	6.9900E-01	3.3000E-01	6.9900E-01	6.9900E-01	1.0000E-04	0.	0.
81	8	41	40	0.	2.1900E+00	6.9900E-01	3.3000E-01	6.9900E-01	6.9900E-01	1.0000E-04	0.	0.
82	8	40	39	0.	2.1900E+00	6.9900E-01	3.3000E-01	6.9900E-01	6.9900E-01	1.0000E-04	0.	0.
83	8	39	38	0.	2.1900E+00	6.9900E-01	3.3000E-01	6.9900E-01	6.9900E-01	1.0000E-04	0.	0.
84	8	38	37	0.	2.1900E+00	6.9900E-01	3.3000E-01	6.9900E-01	6.9900E-01	1.0000E-04	0.	0.
85	8	31	36	0.	3.5410E+00	4.3120E-01	3.3000E-01	4.3120E-01	4.3120E-01	1.0000E-04	0.	0.
86	8	36	35	0.	3.5410E+00	4.3120E-01	3.3000E-01	4.3120E-01	4.3120E-01	1.0000E-04	0.	0.
87	8	35	24	0.	3.5410E+00	4.3120E-01	3.3000E-01	4.3120E-01	4.3120E-01	1.0000E-04	0.	0.
88	8	34	33	0.	3.5410E+00	4.3120E-01	3.3000E-01	4.3120E-01	4.3120E-01	1.0000E-04	0.	0.
89	8	33	32	0.	3.5410E+00	4.3120E-01	3.3000E-01	4.3120E-01	4.3120E-01	1.0000E-04	0.	0.
90	8	32	31	0.	3.5410E+00	4.3120E-01	3.3000E-01	4.3120E-01	4.3120E-01	1.0000E-04	0.	0.
91	8	22	14	0.	1.3000E+03	1.5000E-02	1.4000E-01	7.0000E+00	3.0000E-02	1.7000E+00	4.2300E+00	4.2300E+00
92	8	23	24	0.	2.0000E+01	4.1770E-01	7.2000E-01	4.1770E-01	4.1770E-01	1.5000E-01	2.0000E+00	1.0400E+00
93	8	13	12	0.	2.1900E+00	1.5770E+00	4.6000E-01	1.5770E+00	1.5770E+00	1.0000E-04	0.	0.
94	8	12	13	0.	2.1900E+00	1.5770E+00	4.6000E-01	1.5770E+00	1.5770E+00	1.0000E-04	0.	0.
95	8	10	61	2.9400E+01	4.5960E+01	1.3370E-01	4.1200E-01	1.3040E-01	1.3040E-01	0.	0.	0.
96	8	61	12	2.9400E+01	4.5960E+01	1.3370E-01	4.1200E-01	1.3040E-01	1.0590E-01	0.	0.	0.
97	8	24	63	0.	3.8350E+01	3.5000E-01	6.2000E-01	6.6370E-01	5.5810E-01	1.6220E-01	3.3360E+00	3.6000E+00

TABLE 3.1-1 (CONT'D)

LOFT L1-2 CEFLASH-4B MODEL

COMBUSTION ENGINEERING CEFLASH4B VERSION 11 03 1976 76308

				L/D	AREA	DISCHARGE COEFF	DISCHARGE COEFF	DISCHARGE COEFF	DISCHARGE COEFF
99	7	63	65	0.	5.5920E-01				
100	7	64	65	0.	5.5920E-01				

TABLE 3.1-1(CONT'D)
LOFT L1-2 CEFLASH-4B MODEL

COMBUSTION ENGINEERING CEFLASH4B VERSION 11.03 1976 76308

OPTIONS BY FLOW PATHS

FLOW PATH	MOMENTUM FLUX	CRITICAL FLOW	MIN AREA CRIT FLOW	LENGTH
1	1	1	1.49[illegible]E+00	5.9[illegible]E-01
2	1	1	1.2[illegible]E+00	1.2[illegible]E+00
3	1	0	3.2[illegible]E+00	3.197[illegible]E+00
4	1	0	3.2[illegible]E+00	2.07[illegible]E+00
5	1	1	1.40[illegible]E-01	2.00[illegible]E+00
6	4	1	4.[illegible]E-01	3.17[illegible]E+00
7	4	0	2.51[illegible]E+00	2.9[illegible]E+00
8	1	0	5.[illegible]E-01	2.[illegible]E+00
9	4	0	7.[illegible]E-01	1.[illegible]E+00
10	4	0	7.[illegible]E-01	1.[illegible]E+00
11	1	0	6.9[illegible]E-01	4.[illegible]E+00
12	1	0	6.[illegible]E-01	6.[illegible]E-00
13	1	0	6.[illegible]E-01	8.[illegible]E+00
14	1	0	6.[illegible]E-01	4.5600E+00
15	1	0	9.[illegible]E-01	0.
16	1	0	6.[illegible]E-01	5.34[illegible]
17	0	1	3.9910E-01	0.
18	0	1	3.9910E-01	0.
19	0	1	3.9910E-01	0.
20	1	1	3.[illegible]E-01	0.
21	1	0	6.[illegible]E-01	0.
22	1	1	9.[illegible]E-02	3.[illegible]E+00
23	1	1	2.[illegible]E-01	5.[illegible]E+00
24	1	1	9.[illegible]E-02	2.[illegible]E+00
25	1	1	1.[illegible]E-01	4.[illegible]E+00
26	1	1	9.[illegible]E-02	6.[illegible]E+00
27	1	1	6.[illegible]E-01	7.[illegible]E+00
28	1	1	4.177[illegible]E-01	7.[illegible]E+00
29	1	1	1.58[illegible]E+00	9.[illegible]E-01
30	1	0	4.[illegible]	1.[illegible]E+00
31	4	0	2.[illegible]E-01	2.[illegible]E+00
32	4	0	2.[illegible]E-01	2.[illegible]E+00
33	4	0	2.[illegible]E-01	2.[illegible]E+00
34	4	0	2.[illegible]E-01	2.[illegible]E+00
35	4	0	2.[illegible]E-01	2.[illegible]E+00
36	4	0	2.[illegible]E-01	2.[illegible]E+00
37	4	0	2.[illegible]E-01	3.[illegible]E+00
38	4	0	2.[illegible]E-01	3.[illegible]E+00
39	4	0	2.[illegible]E-01	3.[illegible]E+00
40	4	0	2.[illegible]E-01	3.[illegible]E+00
41	4	0	2.[illegible]E-01	3.[illegible]E+00
42	4	0	2.[illegible]E-01	3.[illegible]E+00
43	4	0	2.[illegible]E-01	4.[illegible]E+00
44	4	0	2.[illegible]E-01	4.[illegible]E+00
45	4	0	2.[illegible]E-01	4.[illegible]E+00
46	4	0	2.[illegible]E-01	4.[illegible]E+00
47	4	0	2.[illegible]E-01	4.[illegible]E+00
48	4	0	2.[illegible]E-01	4.[illegible]E+00
49	4	0	2.54[illegible]E-01	4.[illegible]E+00

TABLE 3.1-1 (CONT'D)

LOFT L1-2 CEFLASH-4B MODEL

COMBUSTION ENGINEERING CEFLASH4B VERSION 1: 03 1976 76308

OPTIONS BY FLOW PATHS

FLOW PATH	MOMENTUM FLUX	CRITICAL FLOW	MIN AREA CRIT FLOW	LENGTH
52	4	0	2.5[illegible]E-01	4.1[illegible]E+00
53	4	0	2.5[illegible]E-01	4.1[illegible]E+00
54	4	0	2.5[illegible]E-01	4.1[illegible]E+00
55	4	0	2.5[illegible]E-01	3.0[illegible]E+00
56	4	0	2.5[illegible]E-01	3.0[illegible]E+00
57	4	0	2.5[illegible]E-01	3.0[illegible]E+00
58	4	0	2.5[illegible]E-01	3.0[illegible]E+00
59	4	0	2.5[illegible]E-01	3.0[illegible]E+00
60	4	0	2.5[illegible]E-01	3.0[illegible]E+00
61	4	0	5.0[illegible]E-01	1.5[illegible]E+00
62	4	0	5.0[illegible]E-01	1.5270E+00
63	4	0	5.0[illegible]E-01	1.5[illegible]E+00
64	4	0	5.0[illegible]E-01	1.5[illegible]E+00
65	4	0	5.0[illegible]E-01	1.5[illegible]E+00
66	4	0	5.0[illegible]E-01	1.5[illegible]E+00
67	4	0	5.0[illegible]E-01	1.5[illegible]E+00
68	4	0	5.0[illegible]E-01	1.5[illegible]E+00
69	4	0	5.0[illegible]E-01	1.5[illegible]E+00
70	4	0	5.0[illegible]E-01	1.5[illegible]E+00
71	4	0	5.0[illegible]E-01	1.5[illegible]E+00
72	4	0	5.0[illegible]E-01	1.5[illegible]E+00
73	4	0	9.3[illegible]E-01	1.5[illegible]E+00
74	4	0	9.3[illegible]E-01	1.5[illegible]E+00
75	4	0	9.3[illegible]E-01	1.5[illegible]E+00
76	4	0	9.3[illegible]E-01	1.5[illegible]E+00
77	4	0	9.3[illegible]E-01	1.5[illegible]E+00
78	4	0	9.3[illegible]E-01	1.5[illegible]E+00
79	4	0	6.3[illegible]E-01	1.5[illegible]E+00
80	4	0	6.3[illegible]E-01	1.5[illegible]E+00
81	4	0	6.3[illegible]E-01	1.5[illegible]E+00
82	4	0	6.3[illegible]E-01	1.5[illegible]E+00
83	4	0	6.3[illegible]E-01	1.5[illegible]E+00
84	4	0	6.3[illegible]E-01	1.5[illegible]E+00
85	4	0	4.3[illegible]E-01	1.5[illegible]E+00
86	4	0	4.3[illegible]E-01	1.5[illegible]E+00
87	4	0	4.3[illegible]E-01	1.5[illegible]E+00
88	4	0	4.3[illegible]E-01	1.5[illegible]E+00
89	4	0	4.3[illegible]E-01	1.5[illegible]E+00
90	4	0	4.3[illegible]E-01	1.5[illegible]E+00
91	4	1	1.5[illegible]E-02	2.5[illegible]E+01
92	1	1	4.1[illegible]E-01	7.5[illegible]E+00
93	4	1	1.5[illegible]E+00	3.4[illegible]E+00
94	4	1	1.5[illegible]E+00	3.4[illegible]E+00
95	4	1	1.0000E-01	6.6271E+00
96	4	1	1.0000E-01	6.6271E+00
97	1	1	9.0000E-02	8.5631E+00
98	1	1	5.6000E-01	3.4000E+00

TABLE 3.1-1 (CONT'D)
LOFT L1-2 CEFLASH-4B MODEL

COMBUSTION ENGINEERING CEFLASH4B VERSION 11 03 1976 76308

MODIFICATION OF UPSTREAM AND DOWNSTREAM ELEVATION FOR FLOW PATH'N

FLOW PATH	UPSTREAM ELEVATION	DOWNSTREAM ELEVATION
1	8.5516E+00	9.1479E+00
2	9.1479E+00	1.0044E+01
3	1.0844E+01	1.4041E+01
4	1.4041E+01	1.6916E+01
5	1.6916E+01	1.[illegible]E+01
6	1.[illegible]E+01	2.2000E+01
7	2.2000E+01	2.4[illegible]E+01
8	2.44[illegible]E+01	2.71[illegible]E+01
9	2.2000E+01	2.2000E+01
10	2.2000E+01	2.2000E+01
11	2.2000E+01	2.2000E+01
12	2.2000E+01	2.2000E+01
13	2.2000E+01	2.2000E+01
14	2.2000E+01	2.4477E+01
15	2.4477E+01	2.4477E+01
16	2.4477E+01	1.7773E+01
17	1.7773E+01	2.2000E+01
18	1.7773E+01	2.2000E+01
19	2.2000E+01	2.2000E+01
20	2.2000E+01	2.2[illegible]E+01
21	2.2000E+01	2.2000E+01
22	2.2000E+01	2.1[illegible]E+01
23	2.0[illegible]E+01	2.0[illegible]E+01
24	2.0[illegible]E+01	2.1[illegible]E+01
25	2.1[illegible]E+01	1.0[illegible]E+01
26	1.0[illegible]E+01	2.2518E+01
27	2.2000E+01	2.2000E+01
28	2.2[illegible]E+01	2.2[illegible]E+01
29	7.5[illegible]E+00	8.0[illegible]E+00
30	6.2[illegible]E+00	7.5[illegible]E+00
31	9.5[illegible]E+00	7.5[illegible]E+00
32	9.5[illegible]E+00	7.5[illegible]E+00
33	9.5[illegible]E+00	7.5[illegible]E+00
34	9.5[illegible]E+00	7.5[illegible]E+00
35	9.5[illegible]E+00	7.5[illegible]E+00
36	9.5[illegible]E+00	7.5[illegible]E+00
37	1.2917E+01	9.5[illegible]E+00
38	1.2917E+01	9.5[illegible]E+00
39	1.2917E+01	9.5[illegible]E+00
40	1.2917E+01	9.5[illegible]E+00
41	1.2917E+01	9.5[illegible]E+00
42	1.2917E+01	9.5[illegible]E+00
43	1.7013E+01	1.2917E+01
44	1.7813E+01	1.2917E+01
45	1.7813E+01	1.2917E+01
46	1.7013E+01	1.2917E+01
47	1.7813E+01	1.2917E+01
48	1.7813E+01	1.2917E+01

FLOW PATH	UPSTREAM ELEVATION	DOWNSTREAM ELEVATION
50	2.2000E+01	1.7813E+01
51	2.2000E+01	1.7813E+01
52	2.2000E+01	1.7013E+01
53	2.2000E+01	1.7013E+01
54	2.2000E+01	1.7813E+01
55	2.3773E+01	2.2000E+01
56	2.3773E+01	2.2000E+01
57	2.3773E+01	2.2000E+01
58	2.3773E+01	2.2000E+01
59	2.3773E+01	2.2000E+01
60	2.3773E+01	2.2000E+01
61	2.3773E+01	2.2000E+01
62	2.3773E+01	2.3773E+01
63	2.3773E+01	2.3773E+01
64	2.3773E+01	2.3773E+01
65	2.3773E+01	2.3773E+01
66	2.3773E+01	2.3773E+01
67	2.2000E+01	2.2000E+01
68	2.2000E+01	2.2000E+01
69	2.2000E+01	2.2000E+01
70	2.2000E+01	2.2000E+01
71	2.2000E+01	2.2000E+01
72	2.2000E+01	2.2000E+01
73	1.7013E+01	1.7013E+01
74	1.7813E+01	1.7813E+01
75	1.7813E+01	1.7813E+01
76	1.7813E+01	1.7813E+01
77	1.7813E+01	1.7813E+01
78	1.7813E+01	1.7813E+01
79	1.2917E+01	1.2917E+01
80	1.2917E+01	1.2917E+01
81	1.2917E+01	1.2917E+01
82	1.2917E+01	1.2917E+01
83	1.2917E+01	1.2917E+01
84	1.2917E+01	1.2917E+01
85	9.5[illegible]E+00	9.5[illegible]E+00
86	9.5[illegible]E+00	9.5[illegible]E+00
87	9.5[illegible]E+00	9.5[illegible]E+00
88	9.5[illegible]E+00	9.5[illegible]E+00
89	9.5[illegible]E+00	9.5[illegible]E+00
90	9.5[illegible]E+00	9.5[illegible]E+00
91	2.7[illegible]E+01	2.[illegible]E+01
92	2.[illegible]E+01	2.[illegible]E+01
93	2.2[illegible]E+01	2.2[illegible]E+01
94	2.2[illegible]E+01	2.2[illegible]E+01
95	8.24[illegible]E+00	1.49[illegible]E+01
96	1.4872E+01	2.1500E+01
97	2.2000E+01	2.2000E+01
98	2.2000E+01	2.2000E+01

TABLE 3.1-1 (CONT'D)

LOFT L1-2 CEFLASH-4B MODEL

COMBUSTION ENGINEERING CEFLASH4B VERSION 11 03 1976 76308

MAIN COOLANT PUMPS

RATED PUMP INPUT

LOOP FLOW	HEAD	DENSITY	SPEED	HYD TORQ	INERTIA	A-R D TORQ	F + W TORQ	FRAC TOL	INITIAL PUMP SPEED
4.3167E+02	3.0600E+02	3.6750E+01	3.6966E+02	4.6500E+02	3.4000E+01	1.0000E+07	2.0000E+01	4.7759E-01	2.4286E+02

PUMP SHUTDOWN PARAMETERS

PRESSURE SHUTDOWN	PRESSURE TIME DELAY	TIME DELAY AFTER RUPT	OVERPOWER SHUTDOWN	OVERPOWER TIME DELAY	PRESSURE DETECTOR
5.0000E+02	1.0000E+01	1.0000E+01	1.2000E+00	1.0000E+01	50

ELECTRICAL TORQUE VS SPEED

EL TORQUE	SPEED	E. TORQUE	SPEED	EL TORQUE	SPEED	EL TORQUE	SPEED	EL TORQUE	SPEED
2.3948E+02	1.0000E+02	2.3940E+02	3.0000E+02						

HEAD MULTIPLIER EQUALS 0.0

HYDRAULIC TORQUE MULTIPLIER EQUALS 1.0

TABLE 3.1-1 (CONT'D)

LOFT L1-2 CEFLASH-4B MODEL

COMBUSTION ENGINEERING — CEFLASH4B — VERSION 11 03 1976 — 76308

HOMOLOGOUS HEAD AND TORQUE CURVES

UALPHA	BAN	BUN	BAD	BUD	BAT	BUT	HAN	HUN
0.	6.0000E-01	-7.0000E-01	6.0000E-01	1.2[illegible]+00	-4.0000E-01	1.2[illegible]+00	1.3000E+00	-6.0000E-01
1.0000E-01	6.2000E-01	-5.[illegible]-01	6.40[illegible]-01	1.2[illegible]+00	-4.0[illegible]-01	1.1[illegible]+00	1.3[illegible]+00	-6.0000E-01
2.0000E-01	6.4000E-01	-4.[illegible]-01	6.[illegible]-01	1.[illegible]	-3.[illegible]-01	1.1[illegible]+00	1.[illegible]+00	-5.0[illegible]-01
3.0000E-01	6.9000E-01	-3.[illegible]-01	7.9[illegible]-01	1.4[illegible]+00	-3.00[illegible]-01	1.01[illegible]+00	1.3[illegible]+00	-4.0000E-01
4.0000E-01	7.40[illegible]-01	-2.[illegible]-01	0.2[illegible]-01	1.5[illegible]+00	-2.5000E-01	9.[illegible]-01	1.2[illegible]+00	-2.5[illegible]-01
5.0000E-01	8.0[illegible]-01	1.40[illegible]-01	9.5[illegible]-01	1.5[illegible]+00	0.	8.5[illegible]-01	1.2[illegible]+00	-1.0000E-01
6.0000E-01	8.[illegible]-01	3.0[illegible]-01	1.1[illegible]+00	1.[illegible]	0.0000E-02	7.[illegible]-01	1.[illegible]+00	5.0000E-02
7.0000E-01	8.[illegible]-01	4.0[illegible]-01	1.22[illegible]+00	1.7[illegible]+00	1.[illegible]-01	6.[illegible]-01	1.1[illegible]+00	2.0000E-01
8.0000E-01	9.2[illegible]-01	6.[illegible]-01	1.5[illegible]+00	1.7[illegible]+00	2.1[illegible]-01	5.7[illegible]-01	1.11[illegible]+00	4.5000E-01
9.0000E-01	9.[illegible]-01	8.0[illegible]-01	1.70[illegible]+00	1.5[illegible]+00	2.[illegible]-01	4.[illegible]-01	1.1000E+00	7.0000E-01
1.0000E+00	1.0000E+00	1.0000E+00	2.0000E+00	2.0000E+00	3.0000E-01	3.0000E-01	1.0000E+00	1.0000E+00

UALPHA	HAD	HUD	HAT	HUT	BAR	BUR	HAR	HUR
0.	1.4000E+00	9.4000E-01	2.5000E-01	9.4000E-01	-4.5000E-01	-7.0000E-01	2.5000E-01	-6.0000E-01
1.0000E-01	1.4[illegible]+00	1.0[illegible]+00	2.[illegible]-01	9.[illegible]-01	-5.[illegible]-01	-8.1[illegible]-01	2.0[illegible]-01	-7.[illegible]-01
2.0000E-01	1.4[illegible]+00	1.13[illegible]+00	2.[illegible]-01	9.0[illegible]-01	-7.0[illegible]-01	-0.[illegible]-01	1.4000E-01	-0.0[illegible]-01
3.0000E-01	1.5[illegible]+00	1.21[illegible]+00	3.0[illegible]-01	0.[illegible]-01	-9.[illegible]-01	-9.1[illegible]-01	5.0[illegible]-02	-0.[illegible]-01
4.0000E-01	1.6[illegible]+00	1.2[illegible]+00	3.0[illegible]-01	0.7[illegible]-01	-9.[illegible]-01	-9.2[illegible]-01	-5.[illegible]-02	-9.[illegible]-01
5.0000E-01	1.7[illegible]+00	1.[illegible]+00	3.[illegible]-01	0.[illegible]-01	-9.[illegible]-01	-9.[illegible]-01	-1.[illegible]-01	-9.[illegible]-01
6.0000E-01	1.0[illegible]+00	1.[illegible]+00	4.[illegible]-01	0.[illegible]-01	-9.[illegible]-01	-9.[illegible]-01	-3.0[illegible]-01	-9.[illegible]-01
7.0000E-01	1.9[illegible]+00	1.7[illegible]+00	5.[illegible]-01	0.[illegible]-01	-9.[illegible]-01	-9.[illegible]-01	-4.[illegible]-01	-9.[illegible]-01
8.0000E-01	2.0[illegible]+00	1.9[illegible]+00	7.0[illegible]-01	0.[illegible]-01	-9.[illegible]-01	-9.[illegible]-01	-6.[illegible]-01	-9.7[illegible]-01
9.0000E-01	2.2[illegible]+00	2.2[illegible]+00	0.[illegible]-01	9.0[illegible]-01	-9.[illegible]-01	-9.[illegible]-01	-8.[illegible]-01	-9.5[illegible]-01
1.0000E+00	2.5000E+00	2.5000E+00	1.0000E+00	1.0000E+00	-1.0000E+00	-1.0000E+00	-1.0000E+00	-1.0000E+00

ANC HEAD CURVES

UALPHA	HANANC	HUNANC	HADANC	HUDANC	HATANC	HUTANC	HARANC	HURANC
0.	0.	0.	0.	1.0[illegible]-01	0.	.00[illegible]-01	1.0000E-01	1.0000E-01
1.0000E-01	0.2000E-01	-2.0000E-02	-5.0000E-01	9.[illegible]-02	-2.0000E-01	1.2[illegible]-01	9.0[illegible]-02	9.[illegible]-02
2.0000E-01	1.1000E+00	0	-1.[illegible]+00	4.0[illegible]-02	-3.[illegible]-01	1.40[illegible]-01	4.0000E-02	4.0000E-02
3.0000E-01	1.0[illegible]+00	1.[illegible]-01	-2.[illegible]+00	1.[illegible]-02	-5.[illegible]-01	1.[illegible]-01	1.[illegible]	1.00[illegible]-02
4.0000E-01	1.0[illegible]+00	2.[illegible]-01	-2.7[illegible]+00	-2.[illegible]-02	-6.[illegible]-01	1.2[illegible]-01	-2.0[illegible]	-2.[illegible]-02
5.0000E-01	1.0[illegible]+00	3.[illegible]-01	-2.[illegible]+00	-2.0[illegible]-02	-8.0[illegible]-01	0.[illegible]-02	-8.[illegible]-02	-8.[illegible]-02
6.0000E-01	1.0[illegible]+00	4.[illegible]-01	-2.[illegible]+00	-1.[illegible]-01	-9.[illegible]-01	-2.0[illegible]-02	-1.[illegible]-01	-1.[illegible]-01
7.0000E-01	1.0[illegible]+00	5.[illegible]-01	-2.9[illegible]+00	-3.0[illegible]-01	-1.0[illegible]+00	-2.7[illegible]-01	-3.0[illegible]-01	-3.0000E-01
8.0000E-01	9.0000E-01	6.0000E-01	-1.[illegible]+00	-5.0[illegible]-01	-1.2[illegible]+00	-5.0[illegible]-01	-5.0000E-01	-5.0[illegible]-01
9.0000E-01	9.5[illegible]-01	8.0000E-01	-1.25[illegible]+00	-8.[illegible]-01	-1.3[illegible]+00	-9.0[illegible]-01	-8.0000E-01	-8.0000E-01
1.0000E+00	1.0000E+00	1.0000E+00	-1.1800E+00	-1.1800E+00	-1.5000E+00	-1.5000E+00	-1.1800E+00	-1.1800E+00

POOR ORIGINAL

597 053

TABLE 3.1-2

CEFLASH-4B LOFT L1-2 INSTRUMENT-NODE CORRESPONDENCES

(ABSOLUTE PRESSURE)

urement or	Description	CEFLASH-4B Node No.	Figure No.
BL-1	Broken loop cold leg at drag disc turbine transducer (DTT) flange	24	3.1-3
BL-2	Broken loop hot leg at DDT flange	30	3.1-4
BL-3	Broken loop hot leg piping	29	3.1-5
BL-4	Broken loop cold leg in 5" diameter piping (break plane throat)	(24)*	3.1-3
BL-6	Broken loop at steam generator simulator inlet	27	3.1-6
CS-1FF	Core simulator instrument stalk	7	3-6 of topical
PC-1	Intact loop cold leg at DTT flange	21	3.1-7
PC-2	Intact loop hot leg at DTT flange	14	3.1-8
PC-3A	Intact loop cold leg at steam generator outlet DTT flange	18	3.1-9
1ST-1FF	RPV downcomer instrument stalk 21.6" above RV bottom (25° from broken cold leg nozzle)	35	3-5 of topical
1ST-3FF	RPV downcomer instrument stalk 212" above RV bottom (25° from broken cold leg nozzle)	53	3-4 of topical
2ST-1FF	RPV downcomer instrument stalk 21.6" above RV bottom (25° from intact cold leg nozzle)	32	3.1-10
2ST-3FF	RPV downcomer instrument stalk 212" above RV bottom (25° from intact cold leg nozzle)	50	3.1-11

*throat area not modeled discretely. Next nearest neighbor is node 24.

597 054

TABLE 3.1-3

CEFLASH-4B LOFT L1-2 INSTRUMENT-NODE CORRESPONDENCES

(DIFFERENTIAL PRESSURE)

Measurement Sensor	Description	CEFLASH-4B Nodes	Figure No.
PdE-BL-5	Pressure drop across pump simulator	26, 27	3.1-12
PdE-BL-7	Pressure drop within steam generator simulator	27, 29	3.1-13
PdE-PC-1	Pressure drop across intact loop pumps	18, 21	3.1-14
PdE-PC-2	Pressure drop across intact loop steam generator	15, 17	3.1-15
PdE-CS-1	Pressure drop from core simulator instrument stalk to reactor vessel downcomer stalk 2	7, 32	3.1-16

Figure 3.1 - 1
CEFLASH-4B MODEL OF LOFT L1-2

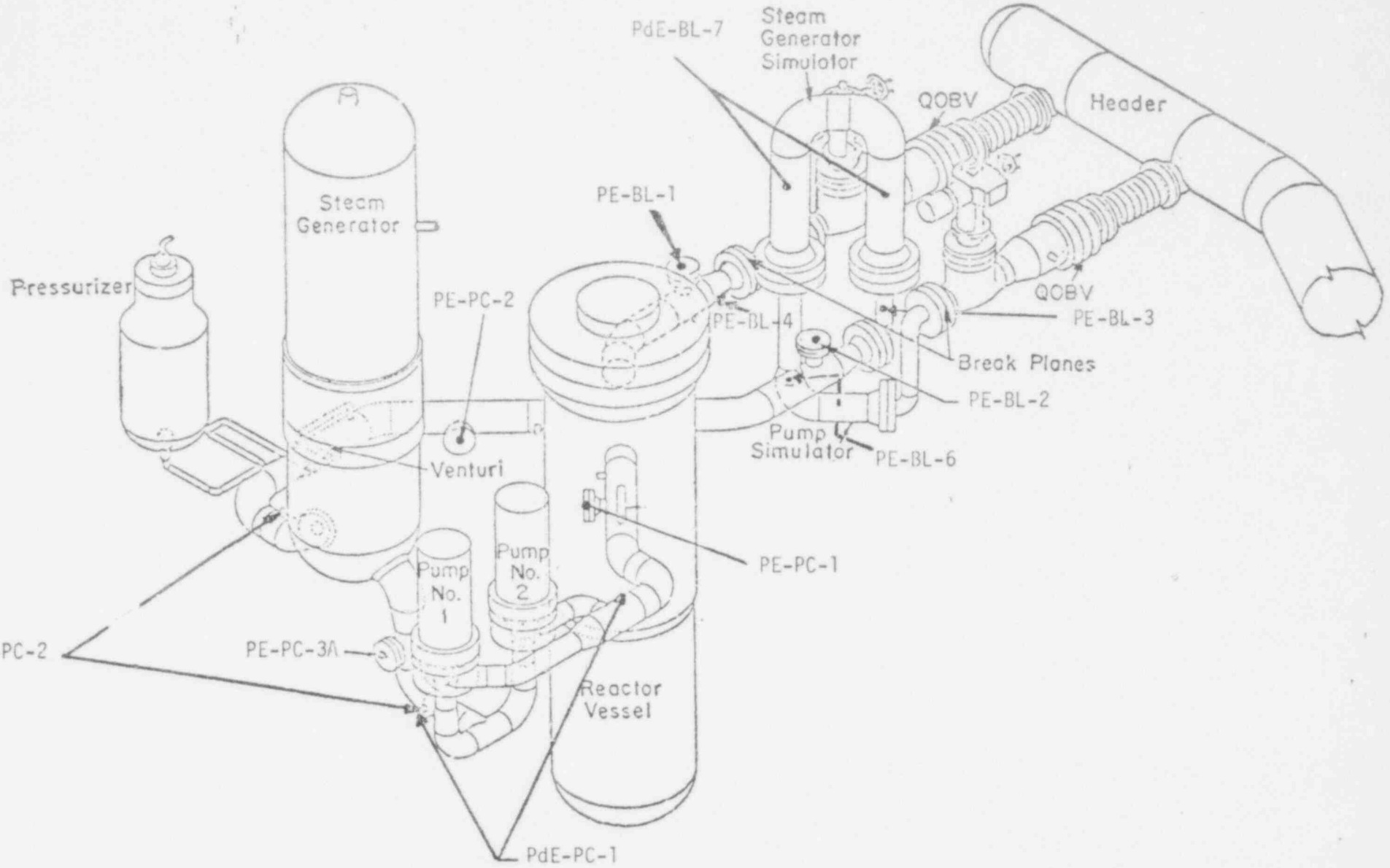

Figure 3.1-2

LOFT LOOP INSTRUMENTATION (COLD LEG BREAK CONFIGURATION)

Figure 3.1-3
CEFLASH-4B PREDICTION OF LOFT L1-2 PRESSURE
SENSOR LOCATION PE-BL-1
(BROKEN LOOP COLD LEG AT DTT FLANGE)

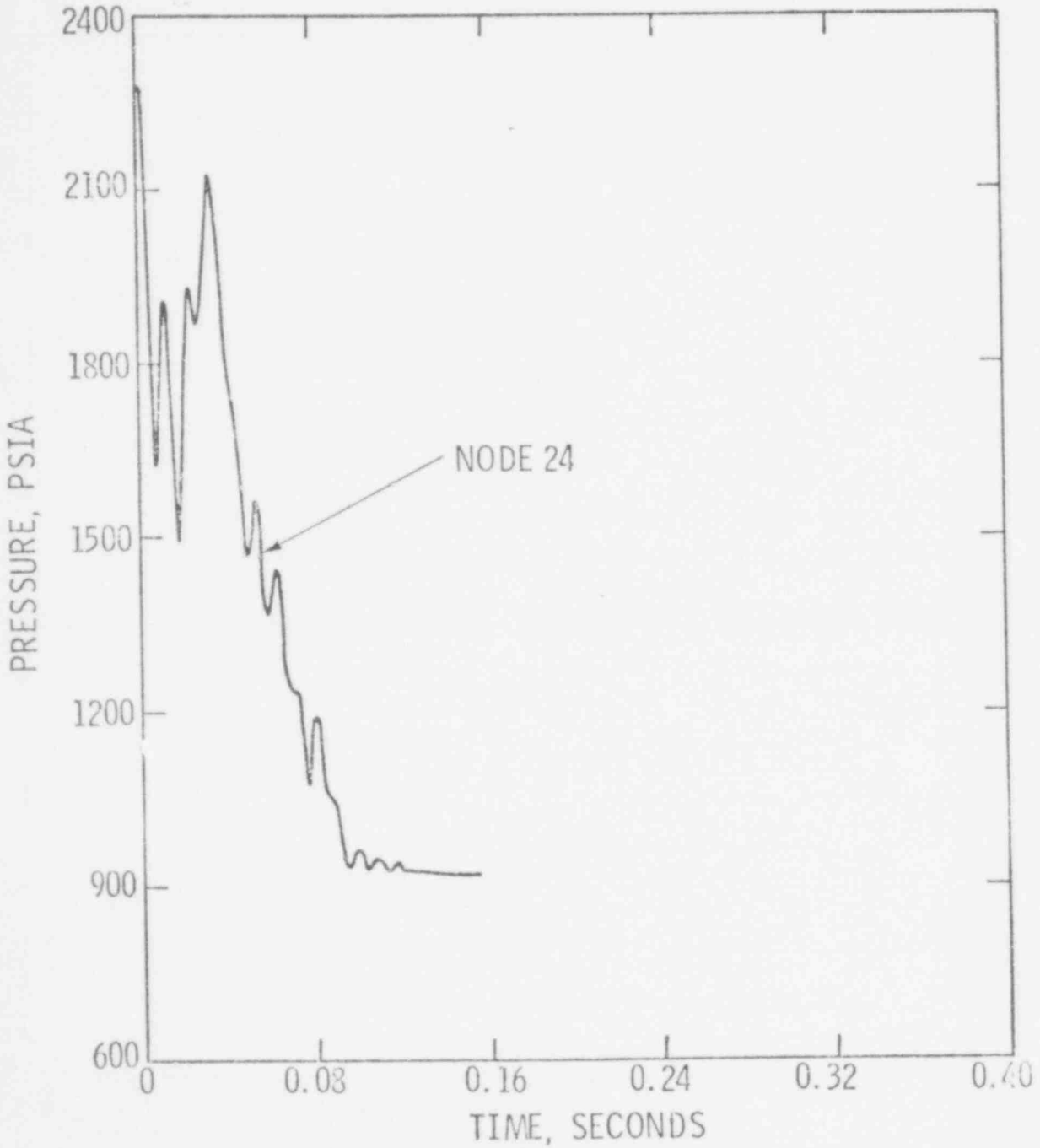

Figure 3.1-4
CEFLASH-4B PREDICTION OF LOFT L1-2 PRESSURE
SENSOR LOCATION PE-BL-2
(BROKEN LOOP HOT LEG AT DTT FLANGE)

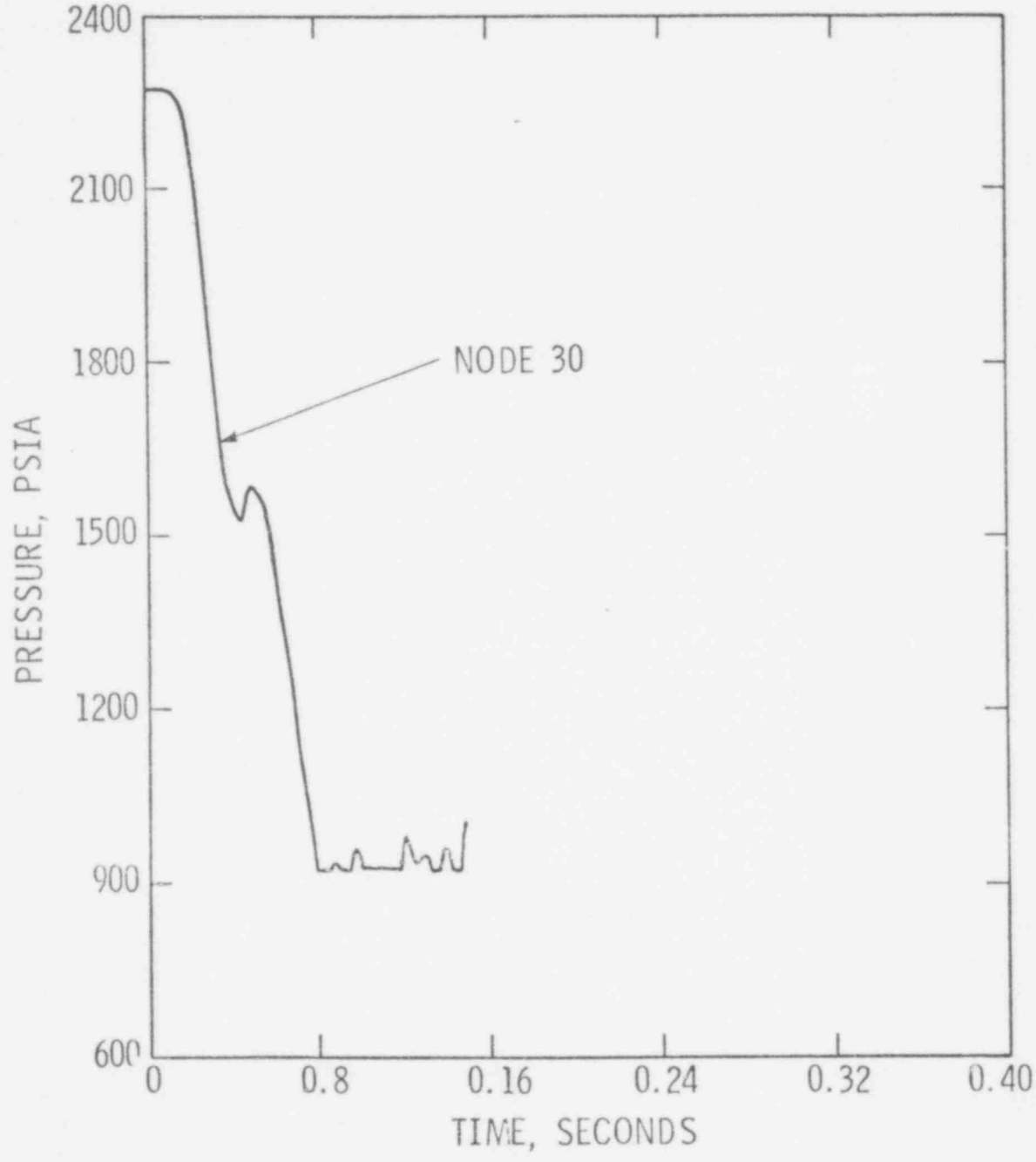

Figure 3.1-5
CEFLASH-4B PREDICTIONS OF LOFT L1-2 PRESSURE
SENSOR LOCATION PE-BL-3
(BROKEN LOOP HOT LEG PIPING)

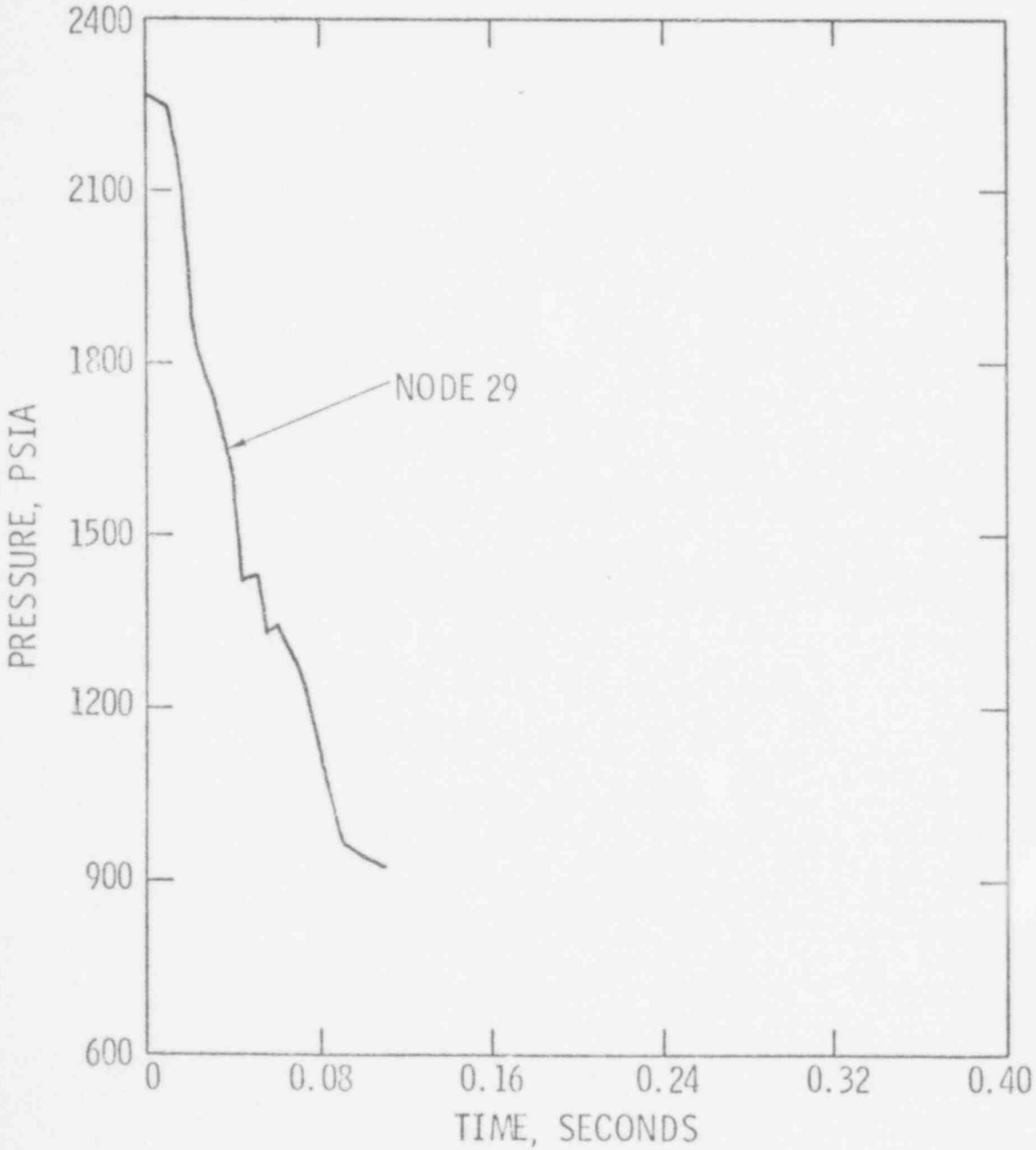

Figure 3.1-6
CEFLASH-4B PREDICTION OF LOFT L1-2 PRESSURE
SENSOR LOCATION PE-BL-6
(BROKEN LOOP AT STEAM GENERATOR SIMULATOR INLET

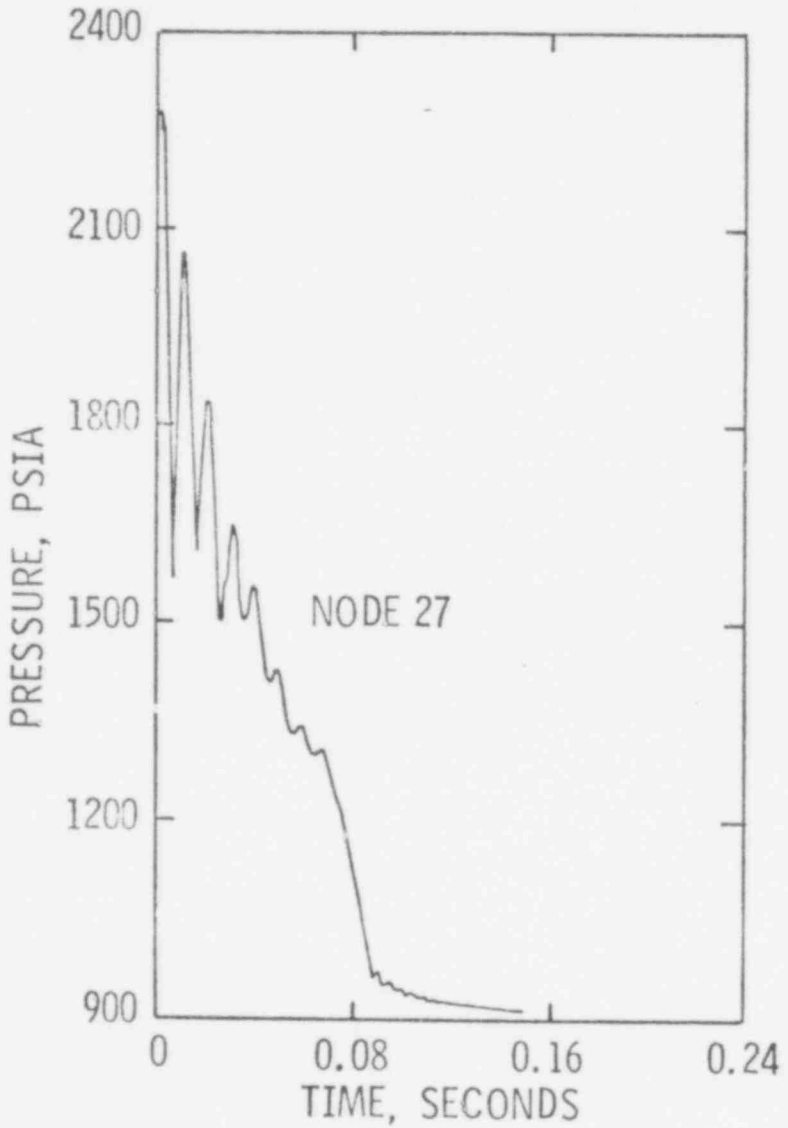

Figure 3.1-7
CEFLASH-4B PREDICTION OF LOFT L1-2 PRESSURE
SENSOR LOCATION PE-PC-1
(INTACT LOOP COLD LEG AT DTT FLANGE)

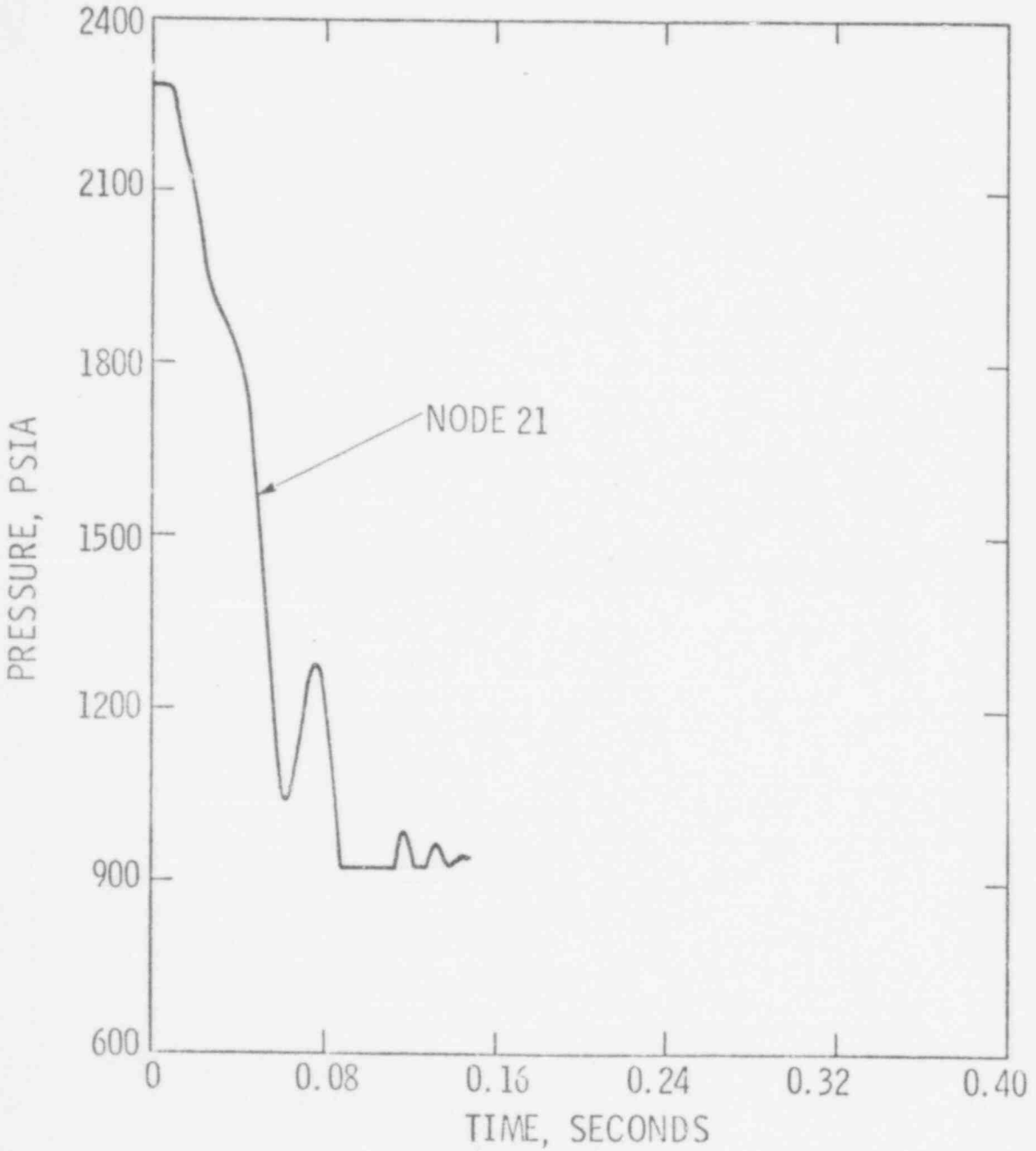

Figure 3.1-8
CEFLASH-4B PREDICTION OF LOFT L1-2 PRESSURE
SENSOR LOCATION PE-PC-2
(INTACT LOOP HOT LEG AT DTT FLANGE)

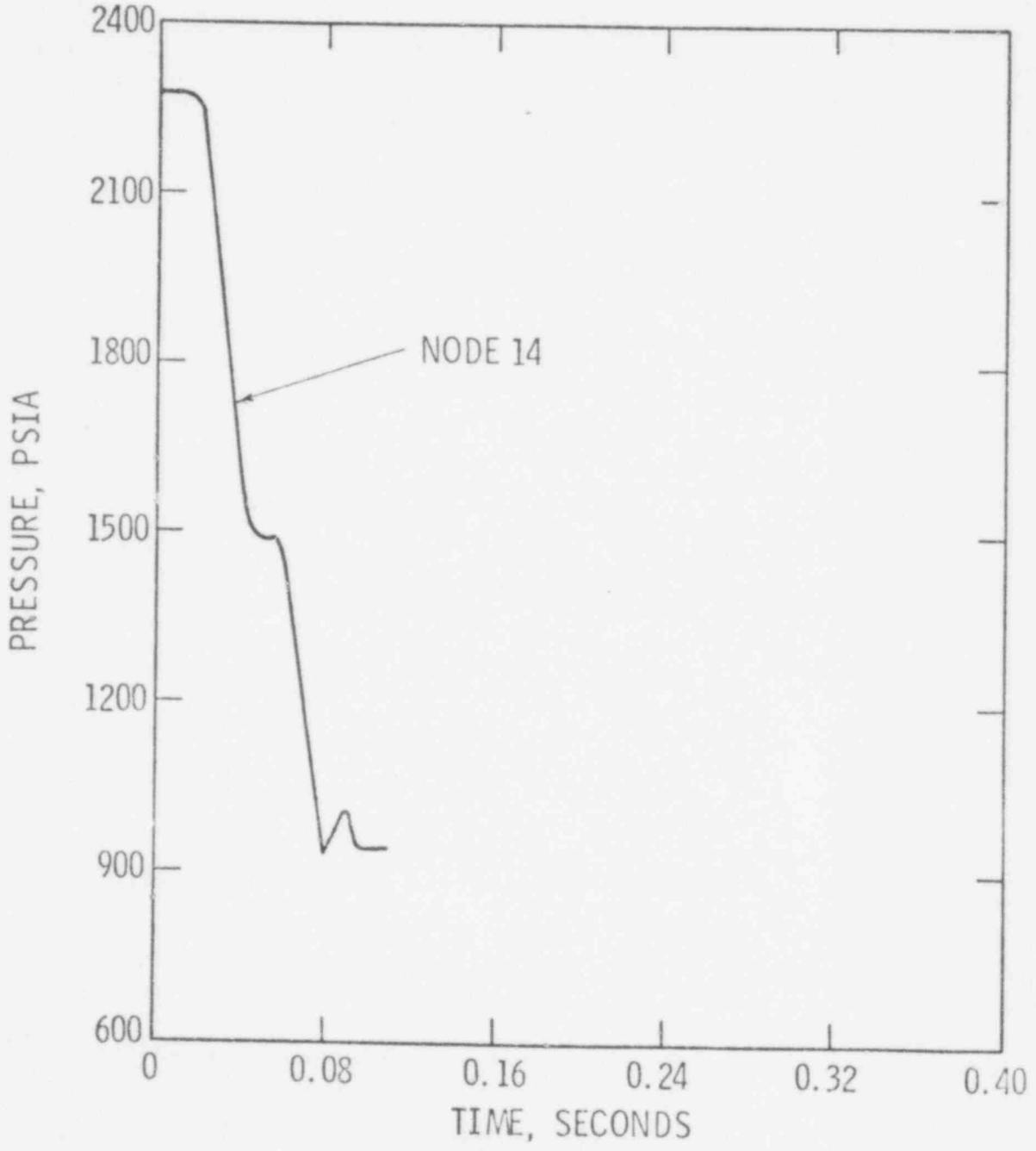

597 063

Figure 3.1-9
CEFLASH-4B PREDICTION OF LOFT L1-2 PRESSURE
SENSOR LOCATION PE-PC-3A
(INTACT LOOP COLD LEG AT STEAM GENERATOR OUTLET
DTT FLANGE)

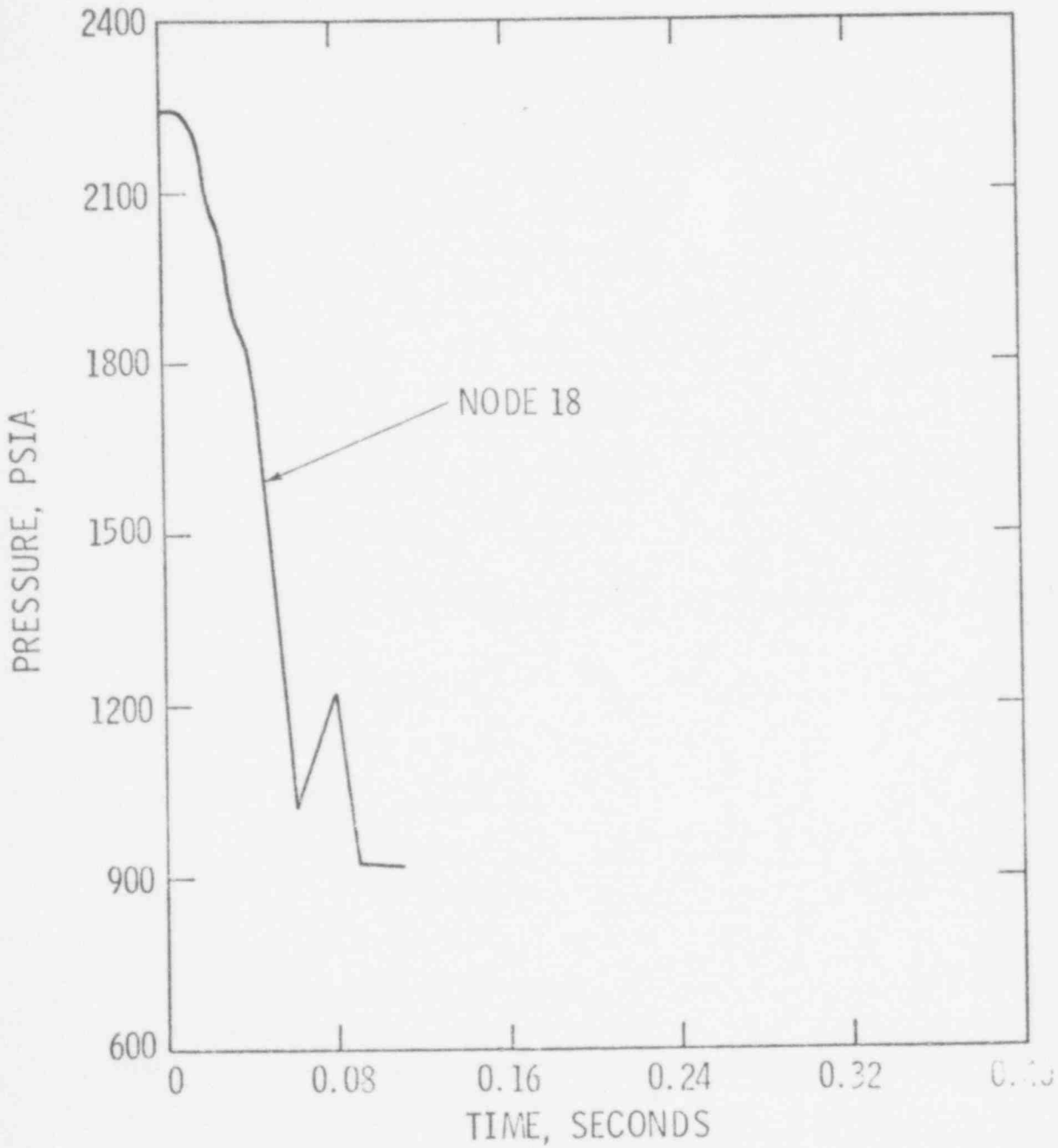

Figure 3.1-10
CEFLASH-4B PREDICTION OF LOFT L1-2 PRESSURE
SENSOR LOCATION PE-2ST-1FF
(RPV DOWNCOMER INSTRUMENT STALK)

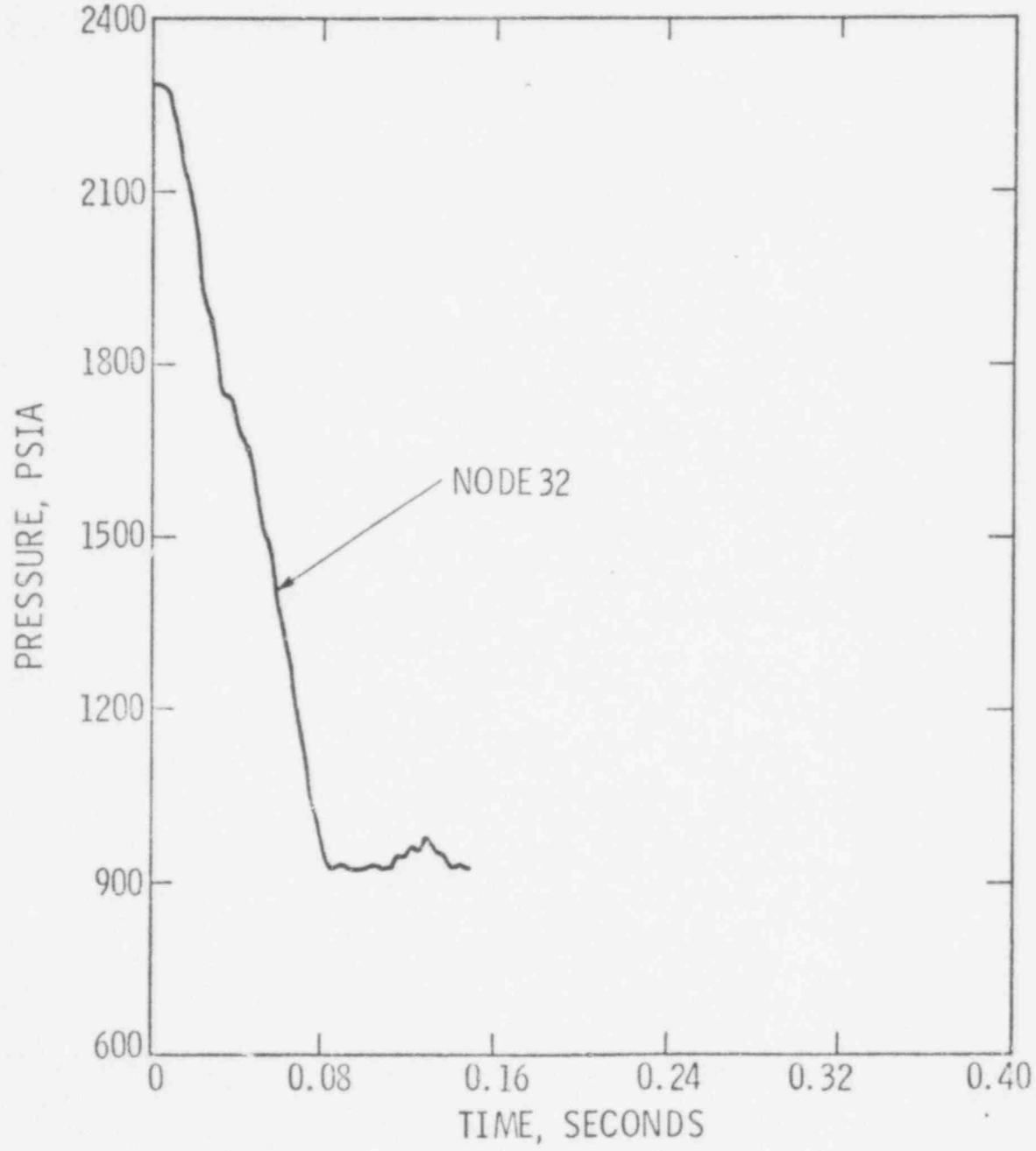

Figure 3.1-11
CEFLASH-4B PREDICTION OF LOFT L1-2 PRESSURE
SENSOR LOCATION PE-2ST-3FF
(RPV DOWNCOMER INSTRUMENT STALK)

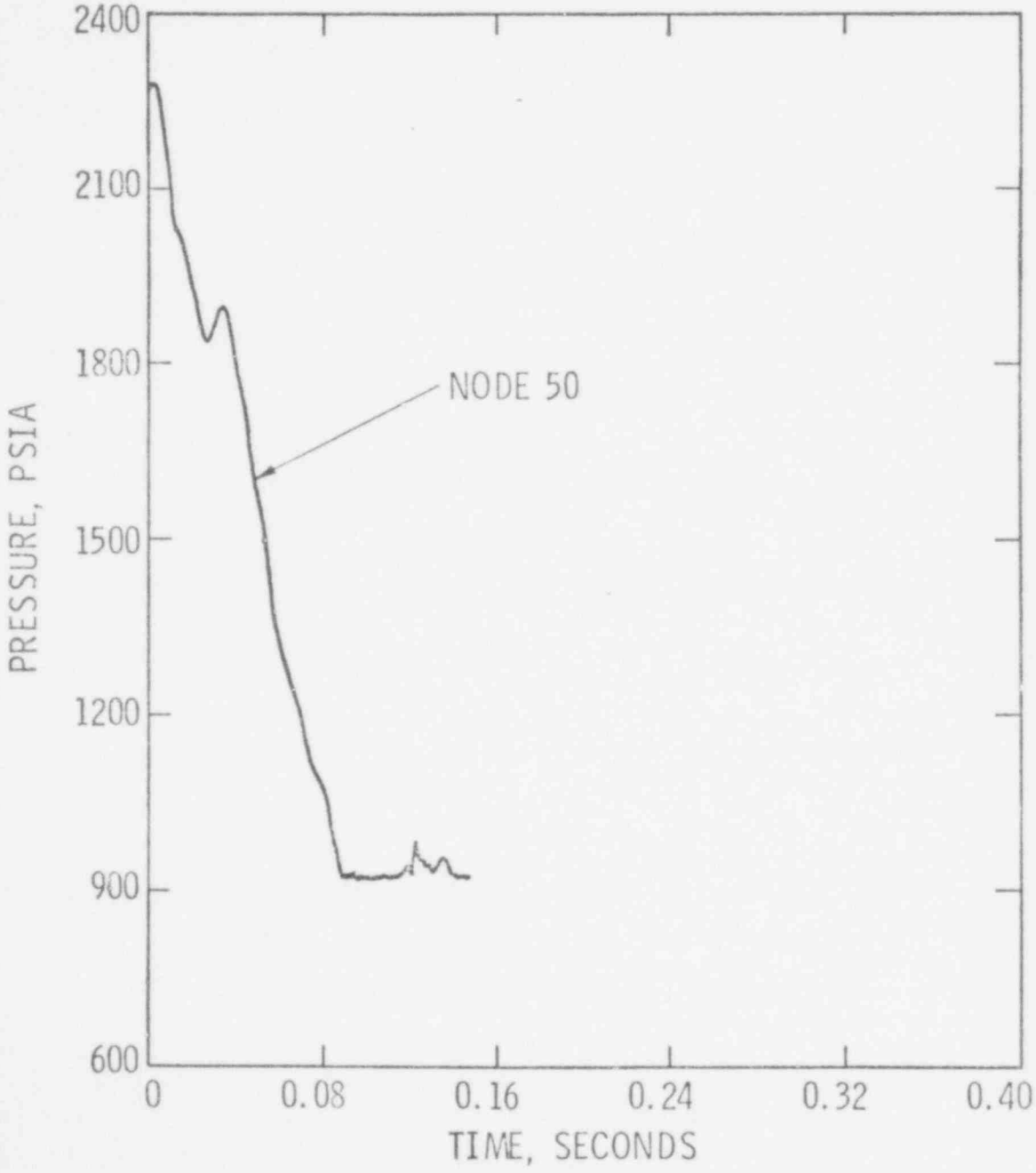

Figure 3.1-12
CEFLASH-4B PREDICTED LOFT L1-2 PRESSURE DROP
PUMP SIMULATOR ΔP (P_{27}-P_{26}) (PdE-BL-5)

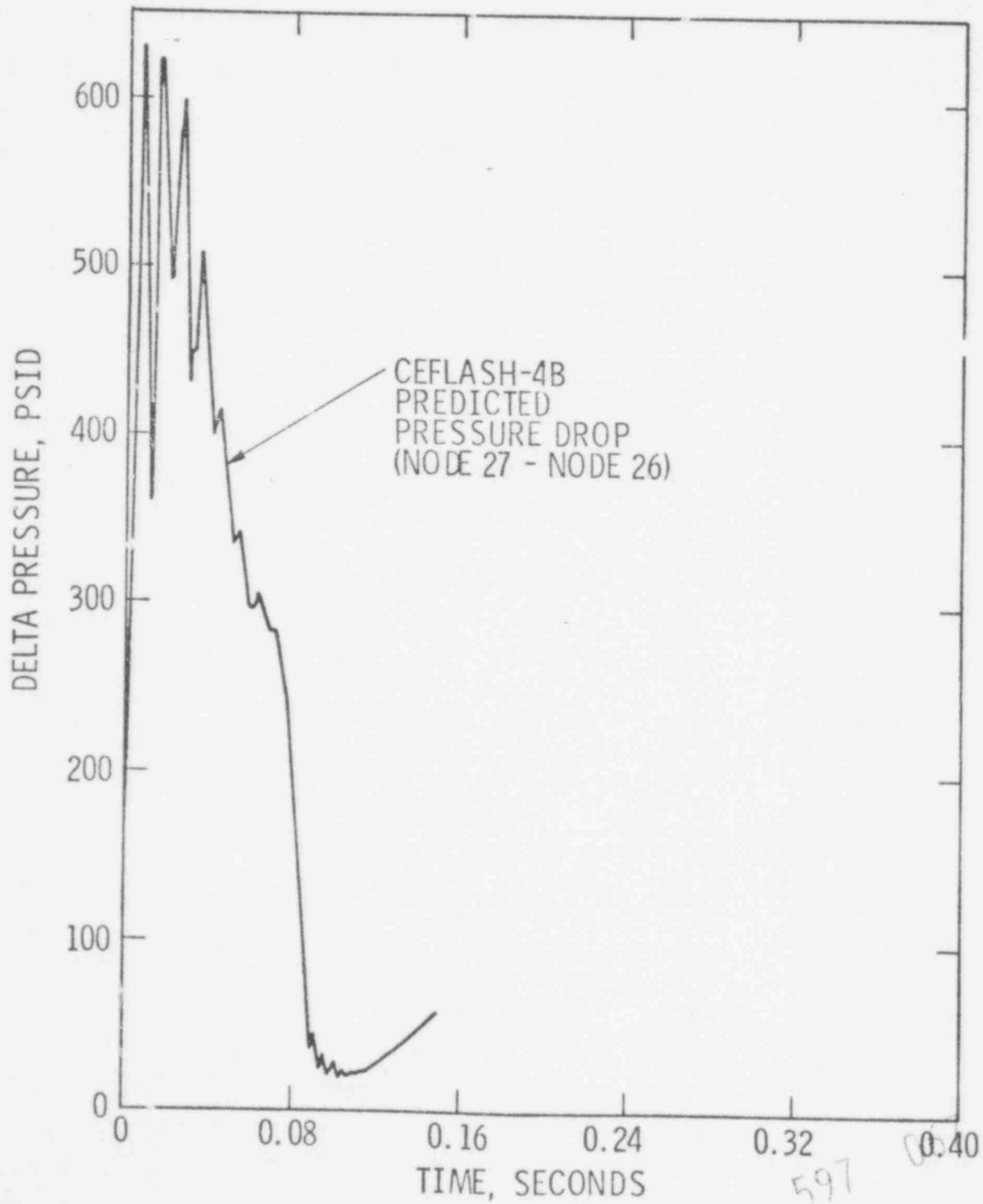

Figure 3.1-13
CEFLASH-4B PREDICTED LOFT L1-2 PRESSURE DROP
WITHIN STEAM GENERATOR SIMULATOR (PdE-BL-7)

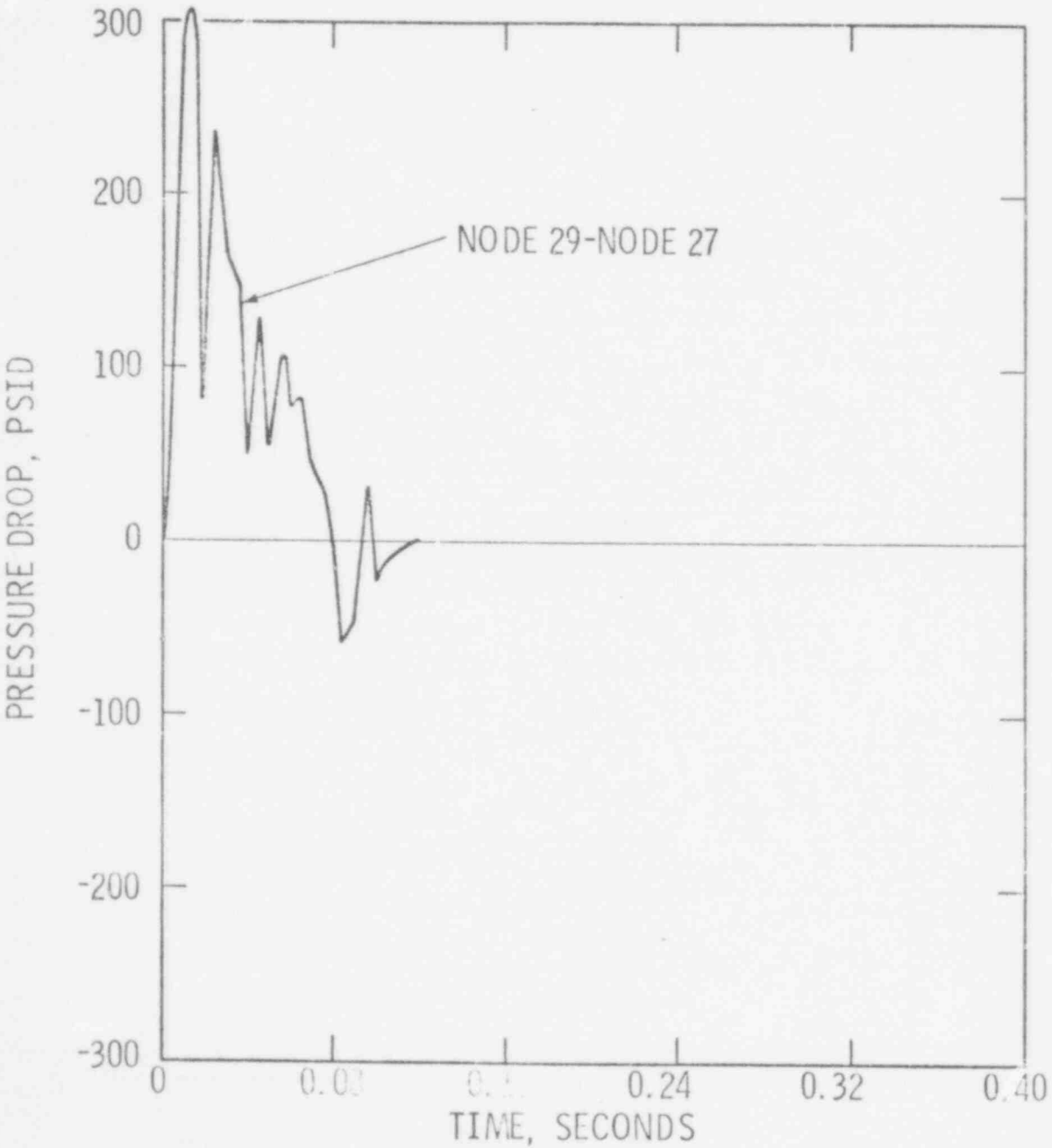

597 068

Figure 3.1-14
CEFLASH-4B LOFT L1-2
PREDICTED PRESSURE DROP
ACROSS PUMPS IN THE INTACT LOOP
(PDE - PC - 1)

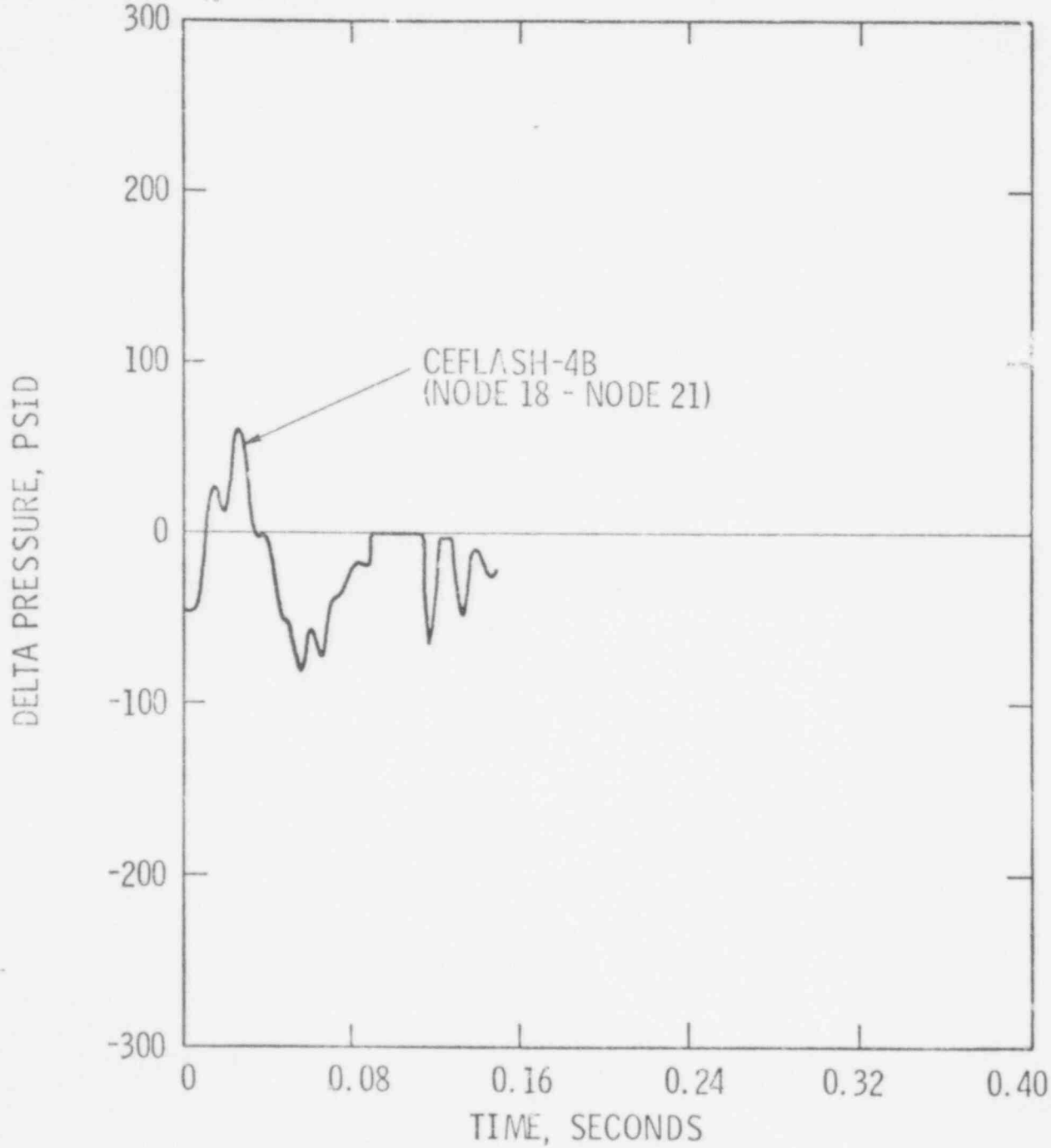

Figure 3.1-15
CEFLASH-4B LOFT L1-2
PREDICTED PRESSURE DROP
ACROSS INTACT LOOP STEAM GENERATOR
(PDE - PC - 2)

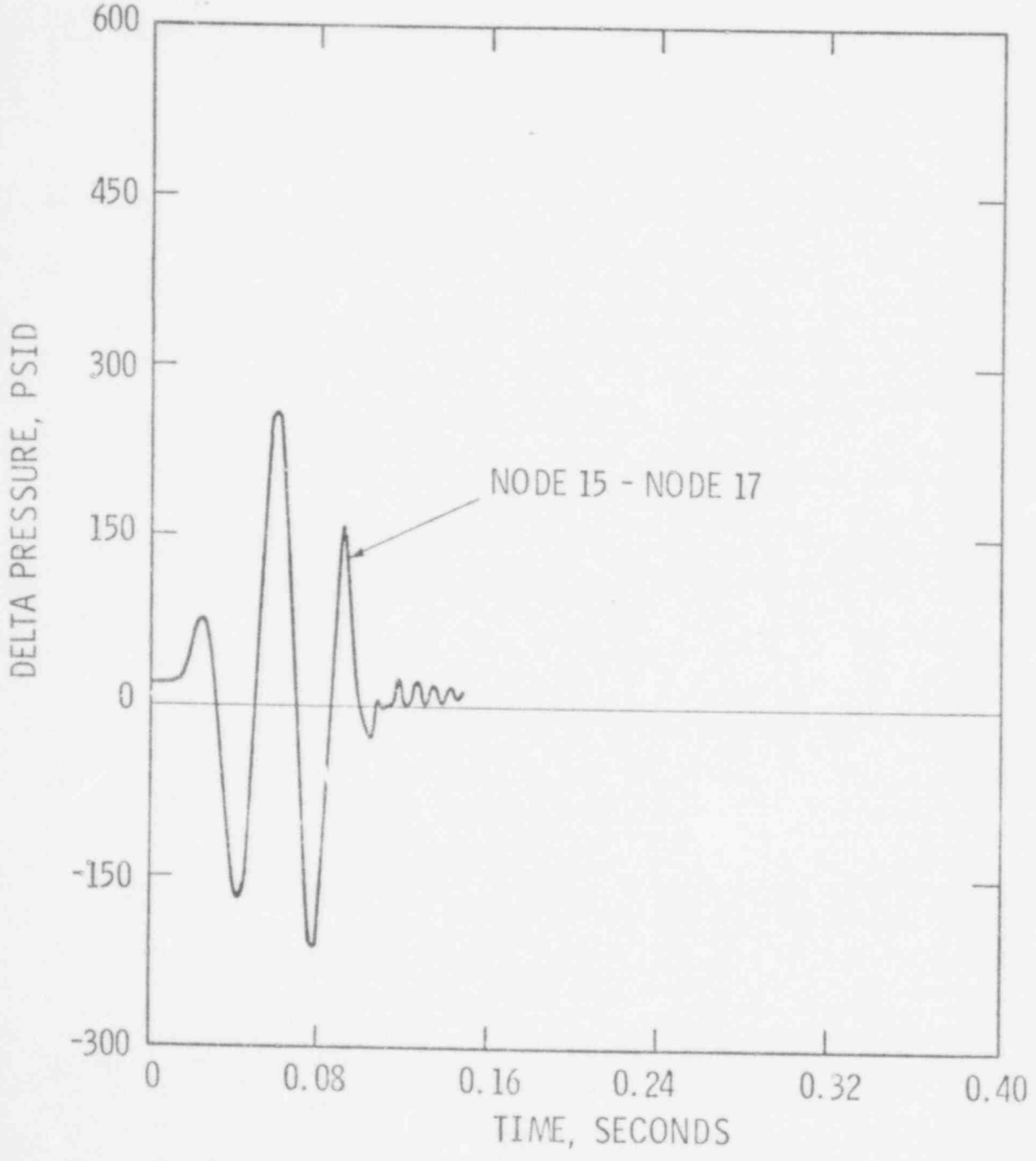

597 070

Figure 3.1-16
CEFLASH-4B PREDICTED PRESSURE DROP
FROM CORE SIMULATOR INSTRUMENT STALK
TO REACTOR VESSEL DOWNCOMER STALK NO. 2

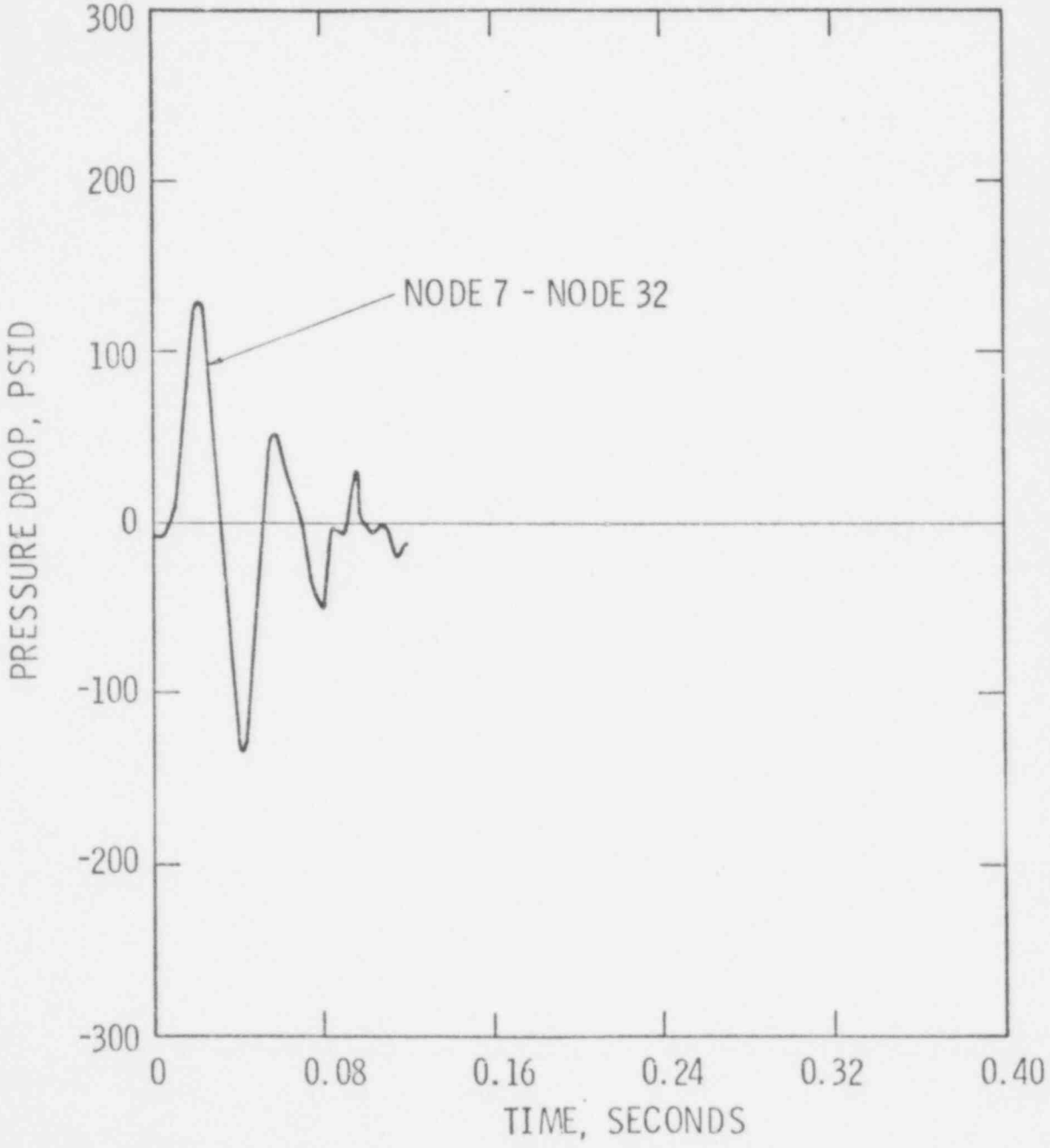

QUESTION 3.2

3.2 The following four systems cover the scale and geometric ranges mentioned above. At least one additional experimental verification analysis is to be performed at this time from the following list. An analysis of the German HDR experiment will be identified at a later date. If Combustion Engineering believes that another system would be of more value to study than one of the below mentioned tests, the NRC will consider that test as a suitable replacement. For the test analyzed, supply noding diagrams of the model and a complete CEFLASH-4B listing of the input data through time step zero.

3.2(a) Containment System Experiments Test B-63 or Test B-75. (See letter from K. Kniel, NRC, to A. E. Scherer, CE, dated October 6, 1976 for required data comparisons).

3.2(b) Semiscale Mod-1 test S-02-6 or Test S-02-8. (See letter from K. Kniel, NRC, to A. E. Scherer, CE, dated October 6, 1976 for required data comparison).

3.2(c) Semiscale Test 711 (Reference: G. H. Hanson, "Subcooled Blowdown Forces on Reactor-System Components: Calculational Method and Experimental Confirmation," IN-1354, Idaho Nuclear Corporation, June 1970).

3.2(d) Semiscale Test 825 (Reference: D. J. Olson, et. al., "Semiscale Blowdown and Emergency Core Cooling (ECC) Project Test Report -- Tests 824 and 825," IN-1481, Idaho Nuclear Corporation, June 1971).

RESPONSE TO QUESTION 3.2

In response to the above mentioned concern of the NRC , Combustion Engineering has performed an analysis of the Containment Systems Experiment (CSE)Test B-75(3.2(a)). The input data for the CSE CEFLASH-4B model has been taken from Reference 3.2-1. Results of the analysis demonstrate reasonable agreement with experimental data.

597 072

CEFLASH-4B Model

The CEFLASH-4B nodal structure of CSE test B-75 used for this study was similar to that employed in Combustion Engineering's earlier CSE study (see Reference 3.2-2). The current node-flowpath network is presented in Figure 3.2-1. This model differs from its predecessor in that a path connecting node 25 to node 5 has been eliminated. The original path was intended to represent a small amount of flow through the central tube of the core plate. More recent information (Ref. 3.2-4)suggests this path has been sealed. Comparisons of nodal pressure predictions obtained with both above mentioned modeling procedures shows the influence of this change to be negligible (See Figure 3.2-26).

A simple nodal structure consisting of [ ] was chosen to represent the CSE downcomer. Nozzles attached to the pressure vessel were modeled as discrete nodes. All nodes were considered isothermal at 500°F.

Flow rates out of the ruptured nozzle were calculated using the [ ] critical flow correlation with a [ ] discharge coefficient. The break opening process was assumed to be linear with a 0.5 millisecond opening time. The total break opening area was given in reference 3.2-1 to be 0.146 ft^2.

Details of the CSE CEFLASH-4B model are presented in the CEFLASH-4B input description (Table 3.2-1) and the CEFLASH-4B zero time edit (Table 3.2-2).

Presentation of Results

Results of the CEFLASH-4B study are presented in Figures 3.2-3 to 3.2-25. A CSE instrumentation layout is shown in Figure 3.2-2. A summary of all the plotted output is presented in Table 3.2-3. As requested by the NRC above and in Reference 3.2-3 the following CEFLASH-4B predictions are presented:

a) All fast response transducer locations listed in Table B-1 of Reference 3.2-1. These plots are contained in Figures 3.2-3 through 3.2-14. When possible, data is superimposed on the CEFLASH-4B prediction. An extra figure, pressure difference at nozzle elevation (NDP), has also been included in this category (Figure 3.2-15).

b) Defined calculated differential pressures 1 through 4 of Reference 3.2-3. These plots are presented in Figures 3.2-16 to 3.2-18.

c) Pressures calculated for each set of points used to obtain the differential pressures requested in a and b above. This information is contained in Figures 3.2-3 to 3.2-8 and 3.2-19 to 3.2-24.

d) Calculated break flow and pressure at the break location. The [ ] calculated break flow is presented in Figure 3.2-25. The pressure at the break location is given by the pressure in Node 10 (Figure 3.2-3).

DISCUSSION OF RESULTS

The CSE tests were performed at Battelle, Northwest in 1970. The facility employed then state-of-the-art fast response pressure instrumentation. The facility has been inoperative for several years and the original staff has been dispersed. This has resulted in difficulties in developing the CSE model and interpreting the data. Nonetheless, the CEFLASH-4B analysis predicts the general trend of the CSE pressure transient. A discussion of the data comparisons is presented in the following paragraphs.

The CEFLASH-4B absolute pressure predictions within the vessel generally indicate a more rapid depressurization in the later portion of the blowdown (>.015 seconds) than is experimentally observed (see Figures 3.2-7 to 3.2-10). This may be a consequence of two salient features of the CEFLASH-4B analysis and/or the CSE experimental procedure. For the analysis these features are the use of a [ ] discharge coefficient in conjunction with the [ ] critical flow model to predict the CSE fluid outflow, and the neglect of fluid structure interaction phenomena. Both of these assumptions have similar consequences on predicted pressures. Use of the standard CE critical flow model to calculate the CSE vessel fluid discharge overpredicts the fluid discharge, and hence produces an excessive pressure decay causing saturation pressures to be predicted ~ 10 msec earlier than measured. Another recent analysis of CSE test B-75, used a 0.40 discharge coefficient (see Reference 3.2-5).

597 074

CEFLASH-4B inherently assumes (see Reference 3.2-6) that the CSE vessel walls are rigid. As a consequence, any physical relief from the depressurization, occurrin as a result of flexure of the CSE core support barrel, cannot be predicted. This is particularly true in the very early blowdown period when large pressure differ ences are induced across the 0.75 inch thick* CSE core support barrel walls. Thi problem has been previously noted by BNWL in their early subcooled blowdown analy (reference 3.2-1). Consequently, CEFLASH-4B predictions would again be observed to indicate a more rapid decay than the experiment.

These factors, as well as instrument and recording errors associated with these early (1970) fast response pressure measurements accounts for discrepancies betwe CSE pressure data and corresponding CEFLASH-4B predictions. In general, the CEFL model predictions are seen to be in reasonable agreement with the CSE data.

CSE pressure vessel pressure drop comparisons are presented in Figures 3.2-11 to 3.2-15. It can be seen from these comparisons that the more rapid fall in pressu results in correspondingly higher predicted component pressure drops. For exampl at the break location the peak radial pressure drop across the core barrel is predicted to be ~40% greater than measured. Similar effects are noted across the core support plate (see Figure 3.2-11).

In order to calculate the required break nozzle pressures (P-04 and P-10), the CSE blowdown line was segmented into 4 nodes (Nodes 1, 4, 10 and 17). Figure 3.2 shows that, at the node immediately adjacent to the discharge orifice (Node 10), a disagreement exists between the pressure sensor P-10 measurement and its CEFLAS 4B prediction. Similar differences have been noted by BNWL and were attributed t calibration errors associated with the P-10 sensor (see Reference 3.2-1).

After the fluid reaches saturation (approximately 20-25 msec after rupture), some numerical difficulties arise in small break node segments. This appears most dramatically as a series of spikes in the predicted node 4 pressure (see Figure 3.2-4). The spikes are transmitted to adjacent nodes with much reduced ma tude. For example, in the downcomer annulus node attached to the blowdown leg the spikes are diminished to ~25 psi pressure bumps (see Figure 3.2-21). These spikes have not been noted in any previous CEFLASH-4B analyses and are considered to be a consequence of instantaneous "overpacking" of node 4. Since the problem

*This is to be compared with the LOFT core support barrel which has a 1.5 inch wall thickness (for roughly the same barrel diameter) and which is further strengthened internal filler ceramics - flow skirt assembly. This system was analyzed by CE in Reference 3.2-6 and did not exhibit significant fluid structure interaction.

occurs late in the transient (after the subcooled blowdown has subsided) it is not considered important in establishing the ability of CEFLASH-4B to predict PWR blowdown loads. Furthermore, the use of small nodes within the broken nozzle is not a standard CE procedure. This methodology has been applied only to CSE, specifically to predict the requested pressures P-04 and P-10 which are located within the discharge nozzle.

Conclusion

A CEFLASH-4B model has been used to predict pressures and flow rates occuring during a CSE vessel decompression. The results show the CEFLASH-4B model to be in reasonable agreement with data. General trends indicate that, when compared to CSE B-75 measurements, CEFLASH-4B pressure predictions are found to fall faster and produce higher component pressure drops.

References to Question 3.2

3.2-1, BNWL-1524, "Coolant Blowdown Studies of a Reactor Simulator Vessel Containing a Simulated-Core,"Allemann, R. T., et. al., June, 1971

3.2-2, CENPD-42, Topical Report on Dynamic Analyses of Reactor Pressure Vessel Internals under Loss-of-Coolant Accident Conditions with Application of Analysis to CE 800 Mwe Class Reactors, Combustion Engineering, Inc., 1972, (proprietary).

3.2-3 Letter from K. Kneil, NRC to A. E. Scherer, C-E, Subject: Reactor Vessel Design Methods, Oct. 6, 1976.

3.2-4 Letter from C. Eicheldinger, Manager Nuclear Safety Dept. (W), to J. Stolz, (NRC), NS-CE-1324, dated December 31, 1976

3.2-5 Letter from J. Taylor, Manager Licensing (B&W) to S. Varga (NRC), Subject: Review of BAW-1032P, dated May 1, 1978

3.2-6 CENPD-252-P, "Blowdown Analysis Method: Method for the Analysis of Blowdown Induced Forces in a Reactor Vessel", Combustion Engineering, Inc., December, 1977.

TABLE 3.2-1

CSE TEST B-75 CEFLASH-4B MODEL
INPUT DESCRIPTION

COMBUSTION ENGINEERING CEFLASH4B VERSION 11 03 1976 76308

*CASE B75 , MAY 23, 1978

JOB NO NLR758E RUN DATE 08/31/78 RUN BEGUN 08.27.24 CPS USED 1.03000

A. GENERAL INFORMATION AND OPTION INFORMATION

END TIME	RUPT TIME	LEAK OPENS	REF ELEV	PSEUDO P F	MAX STEPS	MAX EDITS
4.0000E-02	0.	5.0000E-04	0.	0.	50000	7000

OPTIONS SELECTED

IFMK	1	MOMENTUM TERM USED IN FLOW PATHS SELECTED CARD SERIES 41NN
IFTAX	3	THOM CORRELATION
IFKC	2	FLOW VARYING FRICTION FACTOR
IFCF	1	CRITICAL FLOW CHECK TYPE 5 PLUS PATHS SELECTED CARD SERIES 41NN
IFBL	0	DO NOT BALANCE SYSTEM

OPTION FOR LEAK TABLES SELECTED BY VALUE OF L/D FOR FIRST LEAK FLOW PATH

PATH	L/D	TABLES USED
38	0.	[ ]

TIME STEP TABLE

USE	UNTIL	STEPS PER PRINT
1.0000E-06	7.5000E-03	250
1.0000E-06	5.0000E-02	250

TABLE 3.2-1

CSE TEST B-75 CEFLASH-4B MODEL

INPUT DESCRIPTION

COMBUSTION ENGINEERING CEFLASH4B VERSION 11 03 1976 76308

B. CONTROL VOLUMES

NODE	AREA	HEIGHT	EXIT ELEV	INLET ELEV	BOTTM ELEV	FLOW AREA
1	4.459nE-01	5.6780E-01	1.3845E+01	1.3279E+01	1.3278E+01	4.4590E-01
2	4.363nE-01	5.6354E+00	1.5077E+01	9.4434E+00	9.4424E+00	4.3630E-01
3	7.2663E+00	5.071AE+00	1.5493E+01	1.0424E+01	1.0423E+01	7.2663E+00
4	5.527nE-01	5.6780E-01	1.3845E+01	1.3279E+01	1.3278E+01	5.5270E-01
5	9.6211E+00	5.6780E-01	5.3221E+00	4.6673E+00	4.6663E+00	9.6211E+00
6	2.672nE-01	2.8650E-01	1.3770E+01	1.3485E+01	1.3484E+01	2.6720E-01
7	4.363nE-01	5.6354E+00	1.5077E+01	9.4434E+00	9.4424E+00	4.3630E-01
8	4.363nE-01	5.6355E+00	1.5077E+01	9.4434E+00	9.4424E+00	4.3630E-01
9	4.363nE-01	5.6354E+00	1.5077E+01	9.4434E+00	9.4424E+00	4.3630E-01
10	1.301nE-01	2.917nE-01	1.3569E+01	1.3279E+01	1.3278E+01	1.3010E-01
11	4.363nE-01	3.0416E+00	9.4414E+00	6.4018E+00	6.4018E+00	4.3630E-01
12	5.575nE-01	5.6780E-01	2.2960E+00	1.7302E+00	1.7292E+00	5.5750E-01
13	2.742nE-01	2.8850E-01	4.7256E+00	4.4411E+00	4.4401E+00	2.7420E-01
14	9.596nE+00	2.8650E-01	4.7256E+00	4.4411E+00	4.4401E+00	9.8964E+00
15	4.363nE-01	3.0416E+00	9.4414E+00	6.4018E+00	6.4008E+00	4.3630E-01
16	4.363nE-01	3.0416E+00	9.4414E+00	6.4018E+00	6.4008E+00	4.3630E-01
17	5.388nE-01	5.6780E-01	1.3845E+01	1.3279E+01	1.3278E+01	5.3880E-01
18	4.363nE-01	3.0416E+00	9.4414E+00	6.4018E+00	6.4008E+00	4.3630E-01
19	9.5417E+00	1.1666E+00	6.3997E+00	5.2331E+00	5.2341E+00	9.5417E+00
20	9.6211E+00	1.1666E+00	2.0198E+00	8.5520E-01	8.5420E-01	9.6211E+00
21	5.575nE-01	5.6780E-01	2.2960E+00	1.7302E+00	1.7292E+00	5.5750E-01
22	9.6211E+00	1.8359E+00	4.4391E+00	2.6052E+00	2.6042E+00	9.6211E+00
23	9.6211E+00	1.1666E+00	1.6660E+01	1.5495E+01	1.5494E+01	9.6211E+00
24	1.957nE+00	3.4583E+00	9.8581E+00	6.4018E+00	6.4008E+00	1.9574E+00
25	7.036nE+00	1.4580E-01	6.9622E+00	6.8184E+00	6.8174E+00	7.0369E+00
26	7.036nE+00	2.625nE+00	9.5872E+00	6.9642E+00	6.9632E+00	7.0369E+00
27	7.036nE+00	1.4580E-01	9.7330E+00	9.5892E+00	9.5882E+00	7.0369E+00
28	7.2663E+00	5.035nE-01	1.0422E+01	9.8601E+00	9.8591E+00	7.2663E+00
29	1.0000E+06	1.0000E+06	1.3562E+01	1.3562E+01	0.	1.0000E+06
30	6.8750E-01	5.6780E-01	5.2331E+00	4.6673E+00	4.6683E+00	6.8750E-01
31	3.4920E-01	2.8650E-01	9.4258E+00	9.1413E+00	9.1403E+00	3.4920E-01

TABLE 3.2-1

CSE TEST B-75 CEFLASH-4B MODEL

INPUT DESCRIPTION

COMBUSTION ENGINEERING CEFLASH4B VERSION II 03 1976 76308

NODAL PROPERTIES

NODE	PRESSURE	ENTH SUBC	LEVEL TPH
1	1.0157E+03	4.8779E+02	0.
2	1.0152E+03	4.8779E+02	0.
3	1.0151E+03	4.8779E+02	0.
4	1.0157E+03	4.8779E+02	0.
5	1.0186E+03	4.8779E+02	0.
6	1.0174E+03	4.8779E+02	0.
7	1.0151E+03	4.8779E+02	0.
8	1.0151E+03	4.8779E+02	0.
9	1.0151E+03	4.8779E+02	0.
10	1.0158E+03	4.8779E+02	0.
11	1.0172E+03	4.8779E+02	0.
12	1.0194E+03	4.8779E+02	0.
13	1.0188E+03	4.8779E+02	0.
14	1.0188E+03	4.8779E+02	0.
15	1.0152E+03	4.8779E+02	0.
16	1.0152E+03	4.8779E+02	0.
17	1.0157E+03	4.8779E+02	0.
18	1.0172E+03	4.8779E+02	0.
19	1.0182E+03	4.8779E+02	0.
20	1.0197E+03	4.8779E+02	0.
21	1.0196E+03	4.8779E+02	0.
22	1.0189E+03	4.8779E+02	0.
23	1.0147E+03	4.8779E+02	0.
24	1.0198E+03	4.8779E+02	0.
25	1.0181E+03	4.8779E+02	0.
26	1.0171E+03	4.8779E+02	0.
27	1.0171E+03	4.8779E+02	0.
28	1.0186E+03	4.8779E+02	0.
29	1.4700E+01	7.0000E+01	1.0000E+10
30	1.0186E+03	4.8779E+02	0.
31	1.0172E+03	4.8779E+02	0.

LEAK FLOW PATHS TO CONTAINMENT NODE

NODE	FLOW PATHS
29	38

COMBUSTION ENGINEERING — CEFLASHQB — VERSION 11 03 1976 — 76308

5. FLOW PATHS

PATH	TYPE	NODE FROM	NODE TO	WO	SUM L/A	AREA	DIAMETER	MOM FLOW AREA UP	MOM FLOW AREA DOWN	FRICTION K OR DELTA P	GEOM FWD K OR DELTA P	GEOM RVS K OR DELTA P
1	8	31	11	0.	3.3940E+00	2.5320E-01	5.6800E-01	2.5320E-01	9.2300E-02	3.0000E-02	1.0000E+01	1.0000E+01
2	8	4	10	0.	3.0238E+00	2.5320E-01	5.6800E-01	2.5320E-01	2.5320E-01	2.0220E-02	0.	0.
3	8	17	4	0.	4.8340E+00	2.5320E-01	5.6800E-01	2.5320E-01	2.5320E-01	3.2320E-02	0.	0.
4	8	1	17	0.	4.3609E+00	2.5320E-01	5.6800E-01	2.5320E-01	2.5320E-01	2.9160E-02	0.	0.
5	8	2	1	0.	2.3038E+00	2.5320E-01	5.6800E-01	2.5320E-01	2.5320E-01	1.5410E-02	1.0000E+00	1.9654E+00
6	8	7	2	0.	2.7874E+00	9.3920E-01	1.0940E+00	4.3630E-01	2.9790E-01	2.3940E-02	0.	0.
7	8	8	7	0.	2.7874E+00	9.3920E-01	1.0940E+00	4.3630E-01	2.9790E-01	2.3940E-02	0.	0.
8	8	9	8	0.	2.7874E+00	9.3920E-01	1.0940E+00	4.3630E-01	2.9790E-01	2.3940E-02	0.	0.
9	8	2	9	0.	2.7874E+00	9.3920E-01	1.0940E+00	3.4370E-01	2.9790E-01	2.3940E-02	0.	0.
10	8	18	9	0.	9.9439E+00	4.3630E-01	7.4500E-01	2.0180E-01	1.3840E-01	9.4290E-02	0.	0.
11	8	16	8	0.	9.9439E+00	4.3630E-01	7.4500E-01	2.0180E-01	1.3840E-01	9.4290E-02	0.	0.
12	8	15	7	0.	9.9439E+00	4.3630E-01	7.4500E-01	2.0180E-01	1.3840E-01	9.4290E-02	0.	0.
13	8	11	2	0.	9.9439E+00	4.3630E-01	7.4500E-01	2.0180E-01	1.3840E-01	9.4290E-02	0.	0.
14	8	15	11	0.	5.1647E+00	5.0690E-01	8.0300E-01	2.3450E-01	1.6080E-01	5.2790E-02	0.	0.
15	8	16	15	0.	5.1647E+00	5.0690E-01	8.0300E-01	2.3450E-01	2.3450E-01	5.2790E-02	0.	0.
16	8	18	16	0.	5.1647E+00	5.0690E-01	8.0300E-01	2.3450E-01	2.3450E-01	5.2790E-02	0.	0.
17	8	11	18	0.	5.1647E+00	5.0690E-01	8.0300E-01	2.3450E-01	2.3450E-01	5.2790E-02	0.	0.
18	8	19	18	0.	8.8815E+00	4.3630E-01	7.4500E-01	2.3850E+00	2.0180E-01	8.4200E-02	2.0000E+00	2.0000E+00
19	8	19	16	0.	8.8815E+00	4.3630E-01	7.4500E-01	2.3850E+00	2.0180E-01	8.4200E-02	2.0000E+00	2.0000E+00
20	8	19	15	0.	8.8815E+00	4.3630E-01	7.4500E-01	2.3850E+00	2.0180E-01	8.4200E-02	2.0000E+00	2.0000E+00
21	8	19	11	0.	8.8815E+00	4.3630E-01	7.4500E-01	2.3850E+00	1.5910E-01	8.4200E-02	2.0000E+00	2.0000E+00
22	8	5	19	0.	9.0140E-02	9.6211E+00	3.5000E+00	9.6210E+00	7.9286E+00	3.7200E-03	0.	0.
23	8	30	5	0.	9.9559E+00	2.5320E-01	5.6800E-01	2.5320E-01	2.0470E-01	3.0000E-02	1.0000E+01	1.0000E+01
24	8	14	5	0.	4.3390E-02	9.6211E+00	3.5000E+00	9.6210E+00	9.2992E+00	1.8300E-03	0.	0.
25	8	22	14	0.	1.1030E-01	9.6211E+00	3.5000E+00	9.6210E+00	9.5570E+00	4.5500E-03	0.	0.
26	8	13	14	0.	3.6579E+01	6.4500E-02	2.8600E-01	6.4500E-02	6.4100E-02	3.0000E-02	1.0000E+01	1.0000E+01
27	8	21	20	0.	4.7720E+00	2.5320E-01	5.6800E-01	2.5320E-01	4.8106E+00	3.0000E-02	1.0000E+01	1.0000E+01
28	8	20	22	0.	1.8630E-01	9.6211E+00	3.5000E+00	9.6210E+00	9.6210E+00	7.6800E-03	0.	0.
29	8	12	20	0.	4.7720E+00	2.5320E-01	5.6800E-01	2.5320E-01	4.8106E+00	3.0000E-02	1.0000E+01	1.0000E+01
30	8	24	19	0.	9.2270E-01	1.9574E+00	1.5790E+00	1.9570E+00	1.8265E+00	2.1800E-02	1.0000E+00	1.0000E+00
31	8	6	3	0.	1.0498E+01	6.4500E-02	5.6800E-01	6.4500E-02	6.3900E-02	3.0000E-02	1.0000E+01	1.0000E+01
32	8	26	25	0.	1.7773E+00	7.0368E+00	3.3266E+00	7.0370E+00	7.9790E-02	6.4690E-02	0.	0.
33	8	27	26	0.	1.9690E-01	7.0368E+00	3.3266E+00	7.0370E+00	7.0370E+00	6.4690E-02	0.	0.
34	8	28	27	0.	4.9140E-02	4.5759E+00	2.4167E+00	5.0890E+00	7.0368E+00	3.0000E-03	1.0000E+00	1.0000E+00
35	8	28	24	0.	9.0090E-01	1.9574E+00	1.5790E+00	2.1770E+00	1.9574E+00	2.1220E-02	5.0000E-01	5.0000E-01
36	8	3	28	0.	3.8780E-01	7.2663E+00	3.1670E+00	7.2660E+00	7.2660E+00	9.2600E-03	0.	0.
37	8	23	3	0.	3.1250E-01	7.2663E+00	3.5000E+00	7.2660E+00	7.2023E+00	1.4180E-02	1.5000E+00	1.5000E+00

PATH	TYPE	NODE FROM	NODE TO	L/D	AREA	DISCHARGE COEFF	DISCHARGE COEFF	DISCHARGE COEFF	DISCHARGE COEFF
38	7	10	29	0.	1.4600E-01				

TABLE 3.2-1

CSE TEST B-75 CEFLASH-4B MODEL
INPUT DESCRIPTION

COMBUSTION ENGINEERING CEFLASH4B VERSION 11 03 1976 76308

OPTIONS BY FLOW PATHS

FLOW PATH	MOMENTUM FLUX	CRITICAL FLOW	MIN AREA CRIT FLOW	LENGTH
1	4	1	2.5320E-01	8.5940E-01
2	4	1	1.4680E-01	7.6560E-01
3	4	1	2.5320E-01	1.2240E+00
4	4	1	2.5320E-01	1.1040E+00
5	4	1	2.5320E-01	5.8300E-01
6	4	1	4.3630E-01	2.6190E+00
7	4	1	4.3630E-01	2.6190E+00
8	4	1	4.3630E-01	2.6190E+00
9	4	1	2.5320E-01	2.6190E+00
10	4	1	4.3630E-01	4.3360E+00
11	4	1	4.3630E-01	4.3360E+00
12	4	1	4.3630E-01	4.3360E+00
13	4	1	4.3630E-01	4.3360E+00
14	4	1	4.3630E-01	2.6170E+00
15	4	1	4.3630E-01	2.6170E+00
16	4	1	4.3630E-01	2.6170E+00
17	4	1	4.3630E-01	2.6170E+00
18	4	1	4.3630E-01	3.8700E+00
19	4	1	4.3630E-01	3.8700E+00
20	4	1	4.3630E-01	3.8700E+00
21	4	1	2.5320E-01	3.8700E+00
22	4	1	1.9574E+00	8.6700E-01
23	4	1	7.9790E-02	2.5220E+00
24	4	1	7.9790E-02	4.2700E-01
25	4	1	6.4500E-02	1.0610E+00
26	4	1	6.4500E-02	2.3550E+00
27	4	1	2.5320E-01	1.2090E+00
28	4	1	9.6211E+00	1.7930E+00
29	4	1	2.5320E-01	1.2090E+00
30	4	1	1.9574E+00	1.8060E+00
31	4	1	6.4500E-02	1.3420E+00
32	4	1	7.0368E+00	1.3885E+01
33	4	1	7.0368E+00	1.5000E+00
34	4	1	1.9574E+00	2.7900E-01
35	4	1	1.9574E+00	1.7630E+00
36	4	1	7.2663E+00	2.9330E+00
37	4	1	6.4500E-02	2.6120E+00

TABLE 3.2-2

CSE TEST B-75 CEFLASH-4B MODEL

ZERO TIME EDIT

COMBUSTION ENGINEERING CEFLASH4B VERSION 11 03 1976 76308

PAGE 1 OF OUTPUT 1 TIME STEP 0 TIME 0. SECONDS STEP SIZE 1.0000E-06 SECONDS

*CASE 875 , MAY 23, 1978

JOB NO NLB758E RUN DATE 08/31/78 RUN BEGUN 08.27.24 CPS USED 1.1990

TOTAL POWER
0.

CONTAINMENT NODE	LEAK FLOW PATH	ENTHALPY BTU/LB	FLOW LBS/SEC	ENERGY BTU/SEC	INTEGRAL FLOW LBS	INTEGRAL ENERGY BTU
29	38	4.8779E+02	0.	0.	0.	0.

LEAK FLOW PATHS

FLOW PATH	DISCHARGE COEFF	JUNCT THRUST LBS	THROAT THRUST LBS	MOMENTUM THRUST LBS	JCT + MOM THRUST LBS	THR + MOM THRUST LBS
38	[ ]					

TABLE 3.2-2

CSE TEST B-75 CEFLASH-4B MODEL

ZERO TIME ED T

COMBUSTION ENGINEERING CEFLASH4B VERSION 11 03 1976 76308

PAGE 2 OF OUTPUT 1 TIME STEP 0 TIME 0. SECONDS STEP SIZE 1.0000E-06 SECONDS

NODE	PRESSURE PSI	TOTAL MASS LBS	LIQUID MASS LBS	STEAM MASS LBS	BUBBLE MASS LBS	LIQUID ENTHALPY BTU/LB	STEAM ENTHALPY BTU/LB	TWO PHASE ENTHALPY BTU/LB	TWO PHASE VOID FRAC	AVERAGE FLOW LBS/SEC	NODE
1	1.0157E+03	1.2438E+01	1.2438E+01	0.	0.	4.8779E+02	4.8779E+02	4.8779E+02	0.	0.	1
2	1.0152E+03	1.2079E+02	1.2079E+02	0.	0.	4.8779E+02	4.8779E+02	4.8779E+02	0.	0.	2
3	1.0151E+03	1.8104E+03	1.8104E+03	0.	0.	4.8779E+02	4.8779E+02	4.8779E+02	0.	0.	3
4	1.0157E+03	1.5417E+01	1.5417E+01	0.	0.	4.8779E+02	4.8779E+02	4.8779E+02	0.	0.	4
5	1.0156E+03	[illegible]	[illegible]	0.	0.	4.8779E+02	4.8779E+02	4.8779E+02	0.	0.	5
6	1.0174E+03	3.7608E+00	3.7608E+00	0.	0.	4.8779E+02	4.8779E+02	4.8779E+02	0.	0.	6
7	1.0151E+03	1.2079E+02	1.2079E+02	0.	0.	4.8779E+02	4.8779E+02	4.8779E+02	0.	0.	7
8	1.0151E+03	1.2079E+02	1.2079E+02	0.	0.	4.8779E+02	4.8779E+02	4.8779E+02	0.	0.	8
9	1.0151E+03	1.2079E+02	1.2079E+02	0.	0.	4.8779E+02	4.8779E+02	4.8779E+02	0.	0.	9
10	1.0158E+03	1.8643E+00	1.8643E+00	0.	0.	4.8779E+02	4.8779E+02	4.8779E+02	0.	0.	10
11	1.0172E+03	6.5194E+01	6.5194E+01	0.	0.	4.8779E+02	4.8779E+02	4.8779E+02	0.	0.	11
12	1.0196E+03	1.5551E+01	1.5551E+01	0.	0.	4.8779E+02	4.8779E+02	4.8779E+02	0.	0.	12
13	1.0158E+03	3.8594E+00	3.8594E+00	0.	0.	4.8779E+02	4.8779E+02	4.8779E+02	0.	0.	13
14	1.0188E+03	1.3929E+02	1.3929E+02	0.	0.	4.8779E+02	4.8779E+02	4.8779E+02	0.	0.	14
15	1.0152E+03	6.5192E+01	6.5192E+01	0.	0.	4.8779E+02	4.8779E+02	4.8779E+02	0.	0.	15
16	1.0152E+03	6.5192E+01	6.5192E+01	0.	0.	4.8779E+02	4.8779E+02	4.8779E+02	0.	0.	16
17	1.0157E+03	1.5029E+01	1.5029E+01	0.	0.	4.8779E+02	4.8779E+02	4.8779E+02	0.	0.	17
18	1.0172E+03	6.5194E+01	6.5194E+01	0.	0.	4.8779E+02	4.8779E+02	4.8779E+02	0.	0.	18
19	1.0152E+03	5.4685E+02	5.4685E+02	0.	0.	4.8779E+02	4.8779E+02	4.8779E+02	0.	0.	19
20	1.0197E+03	5.5141E+02	5.5141E+02	0.	0.	4.8779E+02	4.8779E+02	4.8779E+02	0.	0.	20
21	1.0198E+03	1.5551E+01	1.5551E+01	0.	0.	4.8779E+02	4.8779E+02	4.8779E+02	0.	0.	21
22	1.0189E+03	8.6776E+02	8.6776E+02	0.	0.	4.8779E+02	4.8779E+02	4.8779E+02	0.	0.	22
23	1.0147E+03	5.5138E+02	5.5138E+02	0.	0.	4.8779E+02	4.8779E+02	4.8779E+02	0.	0.	23
24	1.0169E+03	3.3255E+02	3.3255E+02	0.	0.	4.8779E+02	4.8779E+02	4.8779E+02	0.	0.	24
25	1.0191E+03	5.0404E+01	5.0404E+01	0.	0.	4.8779E+02	4.8779E+02	4.8779E+02	0.	0.	25
26	1.0171E+03	9.0746E+02	9.0746E+02	0.	0.	4.8779E+02	4.8779E+02	4.8779E+02	0.	0.	26
27	1.0171E+03	5.0403E+01	5.0403E+01	0.	0.	4.8779E+02	4.8779E+02	4.8779E+02	0.	0.	27
28	1.0168E+03	2.0115E+02	2.0115E+02	0.	0.	4.8779E+02	4.8779E+02	4.8779E+02	0.	0.	28
29	1.4700E+01	3.5895E+10	7.6516E+03	3.5895E+10	3.5895E+10	2.0298E+02	1.1586E+03	1.1586E+03	1.0000E+00	0.	29
30	1.0186E+03	1.9178E+01	1.9178E+01	0.	0.	4.8779E+02	4.8779E+02	4.8779E+02	0.	0.	30
31	1.0172E+03	4.9149E+00	4.9149E+00	0.	0.	4.8779E+02	4.8779E+02	4.8779E+02	0.	0.	31

TABLE 3.2-2

CSE TEST B-75 CEFLASH-4B MODEL

ZERO TIME EDIT

COMBUSTION ENGINEERING — CEFLASH4B — VERSION 11 03 1976 — 76308

PAGE 3 OF OUTPUT — TIME STEP 0 — TIME 0. SECONDS — STEP SIZE 1.0000E-04 SECONDS

NODE	VELOCITY SQUARED SQFT/SQSEC	MIXTURE VOLUME CUFT	LIQUID VOLUME CUFT	TOTAL HEAT BTU/SEC	VIS DIS HEAT BTU/SEC	TOTAL ENERGY BTU	INTERNAL ENERGY BTU	NODE TEMP DEG F	NODAL DENSITY LBS/CUFT	NODE
1	0.	2.5318E+01	2.5318E+01	0.	0.	6.0197E+03	6.0195E+03	4.9997E+02	4.9126E+01	1
2	0.	2.4587E+00	2.4587E+00	0.	0.	5.8459E+04	5.8457E+04	4.9997E+02	4.9126E+01	2
3	0.	3.6853E+01	3.6853E+01	0.	0.	8.7622E+05	8.7619E+05	4.9997E+02	4.9126E+01	3
4	0.	3.1382E+01	3.1382E+01	0.	0.	7.4615E+03	7.4612E+03	4.9997E+02	4.9126E+01	4
5	0.	5.4629E+00	5.4629E+00	0.	0.	1.2988E+05	1.2988E+05	4.9997E+02	4.9128E+01	5
6	0.	7.6553E-02	7.6553E-02	0.	0.	1.8201E+03	1.8201E+03	4.9997E+02	4.9127E+01	6
7	0.	2.4587E+00	2.4587E+00	0.	0.	5.8459E+04	5.8457E+04	4.9997E+02	4.9126E+01	7
8	0.	2.4587E+00	2.4587E+00	0.	0.	5.8459E+04	5.8457E+04	4.9997E+02	4.9126E+01	8
9	0.	2.4587E+00	2.4587E+00	0.	0.	5.8459E+04	5.8457E+04	4.9997E+02	4.9126E+01	9
10	0.	3.7950E-02	3.7950E-02	0.	0.	9.0231E+02	9.0227E+02	4.9997E+02	4.9126E+01	10
11	0.	1.3271E+00	1.3271E+00	0.	0.	3.1552E+04	3.1551E+04	4.9997E+02	4.9127E+01	11
12	0.	3.1655E-01	3.1655E-01	0.	0.	7.5261E+03	7.5261E+03	4.9997E+02	4.9128E+01	12
13	0.	7.8553E-02	7.8553E-02	0.	0.	1.8678E+03	1.8678E+03	4.9997E+02	4.9128E+01	13
14	0.	2.8353E+00	2.8353E+00	0.	0.	6.7412E+04	6.7411E+04	4.9997E+02	4.9128E+01	14
15	0.	1.3271E+00	1.3271E+00	0.	0.	3.1551E+04	3.1551E+04	4.9997E+02	4.9126E+01	15
16	0.	1.3271E+00	1.3271E+00	0.	0.	3.1551E+04	3.1551E+04	4.9997E+02	4.9126E+01	16
17	0.	3.0593E-01	3.0593E-01	0.	0.	7.2736E+03	7.2734E+03	4.9997E+02	4.9126E+01	17
18	0.	1.3271E+00	1.3271E+00	0.	0.	3.1552E+04	3.1551E+04	4.9997E+02	4.9127E+01	18
19	0.	1.1131E+01	1.1131E+01	0.	0.	2.6466E+05	2.6465E+05	4.9997E+02	4.9127E+01	19
20	0.	1.1224E+01	1.1224E+01	0.	0.	2.6686E+05	2.6685E+05	4.9997E+02	4.9128E+01	20
21	0.	3.1655E-01	3.1655E-01	0.	0.	7.5261E+03	7.5261E+03	4.9997E+02	4.9128E+01	21
22	0.	1.7663E+01	1.7663E+01	0.	0.	4.1996E+05	4.1995E+05	4.9997E+02	4.9128E+01	22
23	0.	1.1224E+01	1.1224E+01	0.	0.	2.6686E+05	2.6685E+05	4.9997E+02	4.9126E+01	23
24	0.	6.7693E+00	6.7693E+00	0.	0.	1.6094E+05	1.6094E+05	4.9997E+02	4.9127E+01	24
25	0.	1.0260E+00	1.0260E+00	0.	0.	2.4393E+04	2.4393E+04	4.9997E+02	4.9127E+01	25
26	0.	1.8472E+01	1.8472E+01	0.	0.	4.3918E+05	4.3917E+05	4.9997E+02	4.9127E+01	26
27	0.	1.0260E+00	1.0260E+00	0.	0.	2.4394E+04	2.4393E+04	4.9997E+02	4.9127E+01	27
28	0.	4.0946E+00	4.0946E+00	0.	0.	9.7352E+04	9.7349E+04	4.9997E+02	4.9127E+01	28
29	0.	1.0000E+12	1.2918E-04	0.	0.	6.1937E+13	3.8867E+13	2.3497E+02	3.5895E-02	29
30	0.	3.9036E-01	3.9036E-01	0.	0.	9.2811E+03	9.2810E+03	4.9997E+02	4.9128E+01	30
31	0.	1.0005E-01	1.0005E-01	0.	0.	2.3787E+03	2.3786E+03	4.9997E+02	4.9127E+01	31

TABLE 3.2-2

CSE TEST D-75 CEFLASH-4B MODEL
ZERO TIME EDIT

COMBUSTION ENGINEERING CEFLASH4B VERSION 11 03 1976 76308

PAGE 4 OF OUTPUT 1 TIME STEP 0 TIME 0. SECONDS STEP SIZE 1.0000E-06 SECONDS

FLOW PATH	FRICTION K FACTOR DIMENSLESS	GEOM FWD K FACTOR DIMENSLESS	GEOM RVS K FACTOR DIMENSLESS	L/D DIMENSLESS	INLET ELEVATION FT	OUTLET ELEVATION FT	DIFFEREN+E ELEVATION FT
1	3.0000E-02	1.0000E+01	1.0000E+01	1.5130E+00	9.4258E+00	6.4018E+00	3.0240E+00
2	2.0220E-02	0.	0.	1.3479E+00	1.3845E+01	1.3279E+01	5.6600E-01
3	3.2320E-02	0.	0.	2.1549E+00	1.3845E+01	1.3279E+01	5.6600E-01
4	2.9100E-02	0.	0.	1.9437E+00	1.3845E+01	1.3279E+01	5.6600E-01
5	1.5410E-02	1.0004E+00	1.9654E+00	1.0264E+00	1.5077E+01	1.3279E+01	1.7980E+00
6	2.3940E-02	0.	0.	2.3940E+00	1.5077E+01	9.4434E+00	5.6336E+00
7	2.3940E-02	0.	0.	2.3940E+00	1.5077E+01	9.4434E+00	5.6336E+00
8	2.3940E-02	0.	0.	2.3940E+00	1.5077E+01	9.4434E+00	5.6336E+00
9	2.3940E-02	0.	0.	2.3940E+00	1.5077E+01	9.4434E+00	5.6336E+00
10	9.4290E-02	0.	0.	5.8201E+00	9.4414E+00	9.4434E+00	-2.0000E-03
11	9.4290E-02	0.	0.	5.8201E+00	9.4414E+00	9.4434E+00	-2.0000E-03
12	9.4290E-02	0.	0.	5.8201E+00	9.4414E+00	9.4434E+00	-2.0000E-03
13	9.4290E-02	0.	0.	5.8201E+00	9.4414E+00	9.4434E+00	-2.0000E-03
14	5.2790E-02	0.	0.	3.2590E+00	9.4414E+00	6.4018E+00	3.0396E+00
15	5.2790E-02	0.	0.	3.2590E+00	9.4414E+00	6.4018E+00	3.0396E+00
16	5.2790E-02	0.	0.	3.2590E+00	9.4414E+00	6.4018E+00	3.0396E+00
17	5.2790E-02	0.	0.	3.2590E+00	9.4414E+00	6.4018E+00	3.0396E+00
18	8.4200E-02	2.0000E+00	2.0000E+00	5.1946E+00	6.3997E+00	6.4018E+00	-2.1000E-03
19	8.4200E-02	2.0000E+00	2.0000E+00	5.1946E+00	6.3997E+00	6.4018E+00	-2.1000E-03
20	8.4200E-02	2.0000E+00	2.0000E+00	5.1946E+00	6.3997E+00	6.4018E+00	-2.1000E-03
21	8.4200E-02	2.0000E+00	2.0000E+00	5.1946E+00	6.3997E+00	6.4018E+00	-2.1000E-03
22	3.7200E-03	0.	0.	2.4771E-01	5.2341E+00	5.2351E+00	-1.0000E-02
23	3.0000E-02	1.0000E+01	1.0000E+01	4.4401E+00	5.2331E+00	4.6673E+00	5.6580E-01
24	1.8300E-03	0.	0.	1.2200E-01	4.7256E+00	4.6673E+00	5.8300E-02
25	4.5500E-03	0.	0.	3.0314E-01	4.4391E+00	4.4411E+00	-2.0000E-03
26	3.0000E-02	1.0000E+01	1.0000E+01	8.2543E+00	4.7256E+00	4.4411E+00	2.8450E-01
27	3.0000E-02	1.0000E+01	1.0000E+01	2.1285E+00	2.2960E+00	8.5520E-01	1.4408E+00
28	7.6800E-03	0.	0.	5.1227E-01	2.0198E+00	2.6052E+00	-5.8540E-01
29	3.0000E-02	1.0000E+01	1.0000E+01	2.1285E+00	2.2960E+00	8.5520E-01	1.4408E+00
30	2.1800E-02	1.0000E+00	1.0000E+00	1.1438E+00	9.8581E+00	5.2351E+00	4.6230E+00
31	3.0000E-02	1.0000E+01	1.0000E+01	2.3627E+00	1.3770E+01	1.0424E+01	3.3460E+00
32	6.6890E-02	0.	0.	4.1739E+00	9.5872E+00	6.8184E+00	2.7688E+00
33	6.6890E-02	0.	0.	4.6294E-01	9.7330E+00	6.9642E+00	2.7688E+00
34	3.0000E-03	1.0000E+00	1.0000E+00	1.1545E-01	1.0422E+01	9.5892E+00	8.3280E-01
35	2.1220E-02	5.0000E-01	5.0000E-01	1.1165E+00	1.0422E+01	6.4018E+00	4.0202E+00
36	9.2600E-03	0.	0.	9.2611E-01	1.5493E+01	9.8601E+00	5.6329E+00
37	1.4180E-02	1.5000E+00	1.5000E+00	7.4629E-01	1.6660E+01	1.0424E+01	6.2360E+00

CSE TEST B-75 CEFLASH-4B MODEL
ZERO TIME EDIT

COMBUSTION ENGINEERING   CEFLASH4B   VERSION II 03 1976   76308

PAGE 5 OF OUTPUT 1   TIME STEP 0   TIME 0.   SECONDS   STEP SIZE 1.0000E-06 SECONDS

FLOW PATH	FLOW LBS/SEC	TOT ELEV PRES DROP PSI	FRICTION PRES DROP PSI	MOMENTUM PRES DROP PSI	LOSS PRES DROP PSI	L/A/144G X DW/DT PSI	SPECIFIC VOLUME CUFT/LB	FLOW INTEGRAL LBS	NODAL PRES DROP CHECK PSI	CRITICAL FLOW	PATH
1	0.	-5.3220E-03	0.	0.	0.	0.	2.0355E-02	0.	-1.0204E-04		1
2	0.	9.4192E-02	0.	0.	0.	0.	2.0356E-02	0.	-8.7649E-05		2
3	0.	8.1737E-11	0.	0.	0.	0.	2.0356E-02	0.	8.0000E-05		3
4	0.	-8.1733E-11	0.	0.	0.	0.	2.0356E-02	0.	-8.0000E-05		4
5	0.	4.2030E-01	0.	0.	0.	0.	2.0356E-02	0.	1.9918E-04		5
6	0.	-1.4434E-06	0.	0.	0.	0.	2.0356E-02	0.	-1.4230E-01		6
7	0.	1.8422E-05	0.	0.	0.	0.	2.0356E-02	0.	1.8422E-05		7
8	0.	-1.8422E-05	0.	0.	0.	0.	2.0356E-02	0.	-1.8422E-05		8
9	0.	1.4434E-06	0.	0.	0.	0.	2.0356E-02	0.	1.4230E-01		9
10	0.	-1.9225E+00	0.	0.	0.	0.	2.0356E-02	0.	1.4206E-01		10
11	0.	-1.9225E+00	0.	0.	0.	0.	2.0356E-02	0.	-1.3580E+00		11
12	0.	-1.9225E+00	0.	0.	0.	0.	2.0356E-02	0.	-1.3579E+00		12
13	0.	-1.9225E+00	0.	0.	0.	0.	2.0356E-02	0.	-2.4531E-04		13
14	0.	-1.0950E-05	0.	0.	0.	0.	2.0356E-02	0.	-2.0000E+00		14
15	0.	7.1054E-15	0.	0.	0.	0.	2.0356E-02	0.	7.1054E-15		15
16	0.	1.0950E-05	0.	0.	0.	0.	2.0356E-02	0.	2.0000E+00		16
17	0.	2.1316E-14	0.	0.	0.	0.	2.0355E-02	0.	2.1316E-14		17
18	0.	-1.0377E+00	0.	0.	0.	0.	2.0355E-02	0.	-2.0165E-04		18
19	0.	-1.0377E+00	0.	0.	0.	0.	2.0356E-02	0.	1.9998E+00		19
20	0.	-1.0377E+00	0.	0.	0.	0.	2.0356E-02	0.	1.9998E+00		20
21	0.	-1.0377E+00	0.	0.	0.	0.	2.0355E-02	0.	-2.0165E-04		21
22	0.	-3.6798E-01	0.	0.	0.	0.	2.0355E-02	0.	2.9843E-02		22
23	0.	6.8233E-04	0.	0.	0.	0.	2.0355E-02	0.	6.8233E-04		23
24	0.	-1.7314E-01	0.	0.	0.	0.	2.0355E-02	0.	-1.6052E-04		24
25	0.	-9.7744E-02	0.	0.	0.	0.	2.0355E-02	0.	-4.3554E-05		25
26	0.	8.8818E-16	0.	0.	0.	0.	2.0355E-02	0.	8.8818E-16		26
27	0.	9.4230E-02	0.	0.	0.	0.	2.0355E-02	0.	4.3024E-04		27
28	0.	-6.2538E-01	0.	0.	0.	0.	2.0355E-02	0.	-1.8036E-04		28
29	0.	9.4230E-02	0.	0.	0.	0.	2.0355E-02	0.	4.3024E-04		29
30	0.	1.1799E+00	0.	0.	0.	0.	2.0355E-02	0.	-1.1354E-01		30
31	0.	-5.8823E-01	0.	0.	0.	0.	2.0356E-02	0.	1.7298E+00		31
32	0.	8.9554E-01	0.	0.	0.	0.	2.0355E-02	0.	-4.8955E-02		32
33	0.	4.9741E-02	0.	0.	0.	0.	2.0355E-02	0.	4.0627E-05		33
34	0.	2.3492E-01	0.	0.	0.	0.	2.0356E-02	0.	2.1187E-05		34
35	0.	1.9224E-01	0.	0.	0.	0.	2.0356E-02	0.	1.1374E-01		35
36	0.	1.7304E+00	0.	0.	0.	0.	2.0356E-02	0.	2.2021E-04		36
37	0.	3.9771E-01	0.	0.	0.	0.	2.0356E-02	0.	-2.1062E-04		37
38	0.						2.0356E-02	0.			38

POOR ORIGINAL

597 086

TABLE 3.2-2

CSE TEST B-75 CEFLASH-4B MODEL
ZERO TIME EDIT

COMBUSTION ENGINEERING — CEFLASH4B — VERSION 11 03 1976 — 76308

PAGE 6 OF OUTPUT 1 — TIME STEP 0 — TIME 0. SECONDS — STEP SIZE 1.0000E-06 SECONDS

FLOW PATH	PIPE ENTHALPY BTU/LB	PIPE QUALITY	K FACTOR FRC OR LAT DIMENSLESS	AV CORE OR EXIT TEMP DEG F	FLOW SQ X SPEC VOL LBFT3/SEC2	STEAM INTEGRAL LBS	PATH ELEV PRES DROP PSI	VEL SQ / 2 G J BTU/LB	PATH
1	4.8779E+02	0.	3.0000E-02	4.9997E+02	0.	0.	1.0317E+00	0.	1
2	4.8779E+02	0.	2.0220E-02	4.9997E+02	0.	0.	1.9309E+01	0.	2
3	4.8779E+02	0.	3.2320E-02	4.9997E+02	0.	0.	1.9309E+01	0.	3
4	4.8779E+02	0.	2.9160E-02	4.9997E+02	0.	0.	1.9309E+01	0.	4
5	4.8779E+02	0.	1.5410E-02	4.9997E+02	0.	0.	6.1339E+01	0.	5
6	4.8779E+02	0.	2.3940E-02	4.9997E+02	0.	0.	1.9219E+00	0.	6
7	4.8779E+02	0.	2.3940E-02	4.9997E+02	0.	0.	1.9219E+00	0.	7
8	4.8779E+02	0.	2.3940E-02	4.9997E+02	0.	0.	1.9219E+00	0.	8
9	4.8779E+02	0.	2.3940E-02	4.9997E+02	0.	0.	1.9219E+00	0.	9
10	4.8779E+02	0.	9.4290E-02	4.9997E+02	0.	0.	-5.8231E-04	0.	10
11	4.8779E+02	0.	9.4290E-02	4.9997E+02	0.	0.	-5.8230E-04	0.	11
12	4.8779E+02	0.	9.4290E-02	4.9997E+02	0.	0.	-5.8230E-04	0.	12
13	4.8779E+02	0.	9.4290E-02	4.9997E+02	0.	0.	-5.8231E-04	0.	13
14	4.8779E+02	0.	5.2790E-02	4.9997E+02	0.	0.	1.0370E+00	0.	14
15	4.8779E+02	0.	5.2790E-02	4.9997E+02	0.	0.	1.0370E+00	0.	15
16	4.8779E+02	0.	5.2790E-02	4.9997E+02	0.	0.	1.0370E+00	0.	16
17	4.8779E+02	0.	5.2790E-02	4.9997E+02	0.	0.	1.0370E+00	0.	17
18	4.8779E+02	0.	8.4200E-02	4.9997E+02	0.	0.	-7.1844E-04	0.	18
19	4.8779E+02	0.	8.4200E-02	4.9997E+02	0.	0.	-7.1843E-04	0.	19
20	4.8779E+02	0.	8.4200E-02	4.9997E+02	0.	0.	-7.1843E-04	0.	20
21	4.8779E+02	0.	8.4200E-02	4.9997E+02	0.	0.	-7.1844E-04	0.	21
22	4.8779E+02	0.	3.7200E-03	4.9997E+02	0.	0.	2.9681E-02	0.	22
23	4.8779E+02	0.	3.0000E-02	4.9997E+02	0.	0.	1.9303E+01	0.	23
24	4.8779E+02	0.	1.8300E-03	4.9997E+02	0.	0.	1.9990E-02	0.	24
25	4.8779E+02	0.	4.5500E-03	4.9997E+02	0.	0.	-5.8233E-04	0.	25
26	4.8779E+02	0.	3.0000E-02	4.9997E+02	0.	0.	9.7061E-02	0.	26
27	4.8779E+02	0.	3.0000E-02	4.9997E+02	0.	0.	4.9155E+01	0.	27
28	4.8779E+02	0.	7.6800E-03	4.9997E+02	0.	0.	-1.9972E-01	0.	28
29	4.8779E+02	0.	3.0000E-02	4.9997E+02	0.	0.	4.9155E+01	0.	29
30	4.8779E+02	0.	2.1800E-02	4.9997E+02	0.	0.	1.5772E+00	0.	30
31	4.8779E+02	0.	3.0000E-02	4.9997E+02	0.	0.	1.1415E+00	0.	31
32	4.8779E+02	0.	6.4690E-02	4.9997E+02	0.	0.	9.4460E-01	0.	32
33	4.8779E+02	0.	6.4690E-02	4.9997E+02	0.	0.	9.4460E-01	0.	33
34	4.8779E+02	0.	3.0000E-03	4.9997E+02	0.	0.	2.8412E-01	0.	34
35	4.8779E+02	0.	2.1220E-02	4.9997E+02	0.	0.	1.3715E+00	0.	35
36	4.8779E+02	0.	9.2600E-03	4.9997E+02	0.	0.	1.9217E+00	0.	36
37	4.8779E+02	0.	1.4180E-02	4.9997E+02	0.	0.	2.1274E+00	0.	37
38	4.8779E+02	0.		4.9997E+02	0.	0.		0.	38

CEFLASH-4B PLOT SUMMARY

CSE TEST B-75

	SENSOR DESCRIPTION/ LOCATION	SENSOR IDENTIFICATION	CEFLASH-4B NODE/NODES	FIGURE NUMBER	COMPARED WITH DATA
1.	Exit Orifice	P-10	10	3.2-3	Yes
2.	Exit Pipe	P-04	04	3.2-4	Yes
3.	Nozzle R	P-01	07	3.2-5	Yes
4.	Core Near Nozzle A	P-20	11	3.2-6	NA*
5.	Core Opposite Nozzle A	P-21	16	3.2-7	Yes
6.	Center of Core	P-22	25	3.2-8	Yes
7.	Radial Probe Outer	P-13	13	3.2-9	Yes
8.	Radial Probe Inner	P-14	14	3.2-10	Yes
9.	Differential Pressure Across Core Plate	CPDP-2	25/19	3.2-11	Yes
10.	Differential Pressure Across Core Plate	CPDP-4	25/19	3.2-11	Yes
11.	Differential Pressure Across Core Barrel (lower core near break)	CBDP-1	11/25	3.2-12	Yes
12	Differential Pressure Across Core Barrel (break elevation: 90° from break)	CBDP-2	07/03	3.2-13	Yes
13.	Differential Pressure Across Core Barrel (break elevation: 180° from break)	CBDP-3	08/03	3.2-14	Yes
14.	Differential Pressure Across Core Barrel (break location)	NDP	02/03	3.2-15	Yes
15.	Differential Pressure Around Core Barrel at the Break Nozzle Elevation (between break location and 180° from break)	-	02/08	3.2-16	NA

*NA-Not Applicable (No Data Available)

TABLE 3.2-3 (CONT'D)

CEFLASH-4B PLOT SUMMARY

	SENSOR DESCRIPTION/ LOCATION	SENSOR IDENTIFICATION	CEFLASH-4B NODE/NODES	FIGURE NUMBER	COMPARED WITH DATA
16.	Differential Pressure Across Core Barrel at H Nozzle Elevation (location directly below the break and 180° from the break)	-	11/16	3.2-17	NA
17.	Differential Pressure Across Core Barrel at the Core Plate Elevation (location directly below the break nozzle and 180° from the break)	-	11/16	3.2-17	NA
18.	Differential Pressure Across the Core Structure (lower plenum at nozzle S elevation and instrumentation ring)	-	14/23	3.2-18	NA
19.	Pressure in the Instrument ring	-	23	3.2-19	NA
20.	Pressure Below Core Plate	-	19	3.2-20	NA
21.	Pressure in Downcomer Annulus (near break nozzle)	-	02	3.2-21	NA
22.	Pressure in Downcomer Annulus at Broken Nozzle Elevation 180° From Break	-	08	3.2-22	NA
23.	Pressure in Core Region	-	26	3.2-23	NA
24.	Pressure in Upper Guide Structure Region	-	03	3.2-24	NA
25.	Break Flow Rate	-	Path 38	3.2-25	NA
26.	Comparison of CEFLASH-4B CSE Models		16	3.2-26	NA

Figure 3.2-1
CEFLASH-4BMODEL FOR CSE TEST B-75

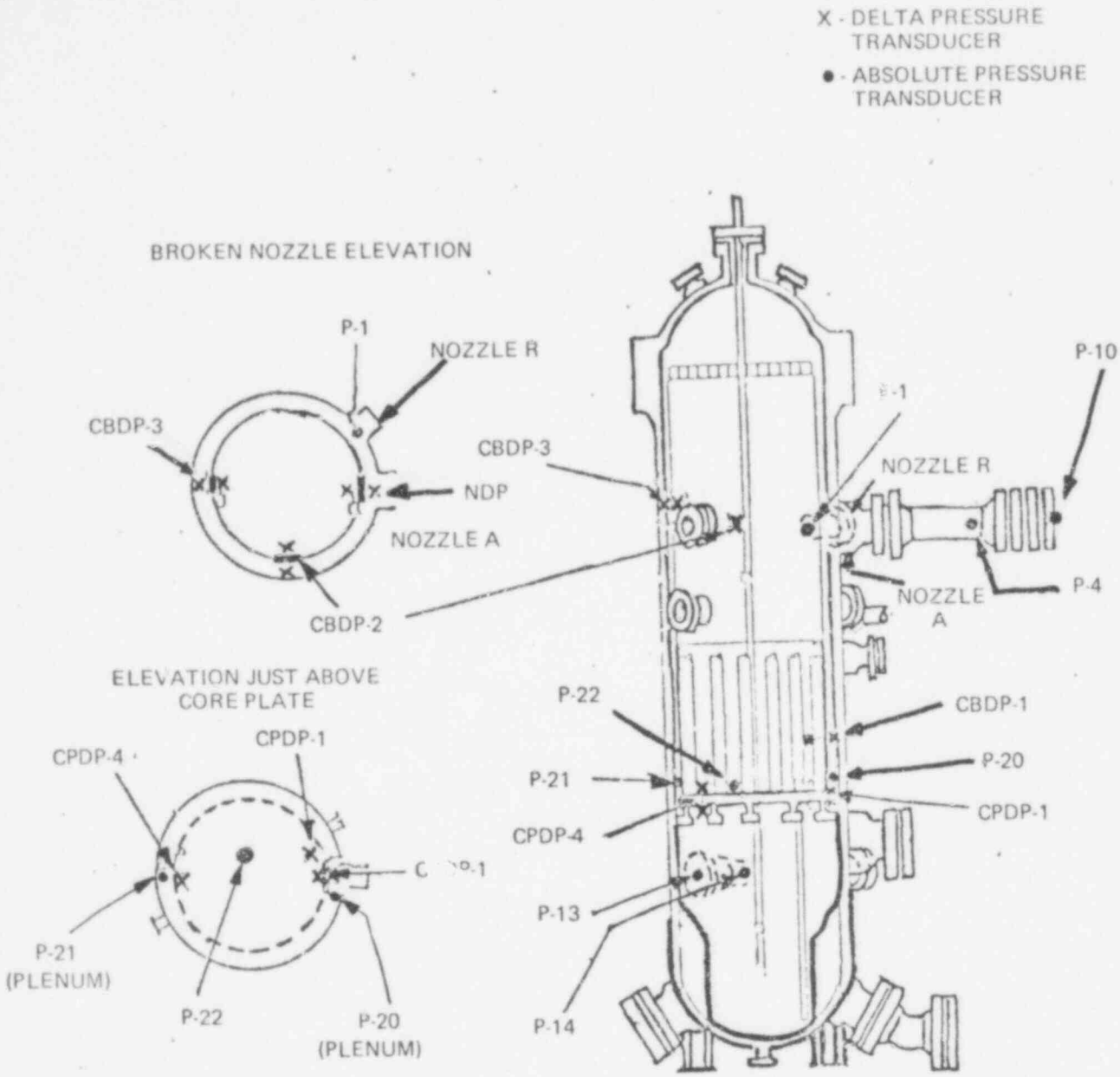

Figure 3.2-2

LOCATION OF CSE SENSORS: PWR RUN SERIES

FIGURE 3.2-3

COMPARISON OF CEFLASH-4B PREDICTIONS
WITH
DATA FROM CSE TEST B-75
PRESSURE AT EXIT ORIFICE (SENSOR P-10)

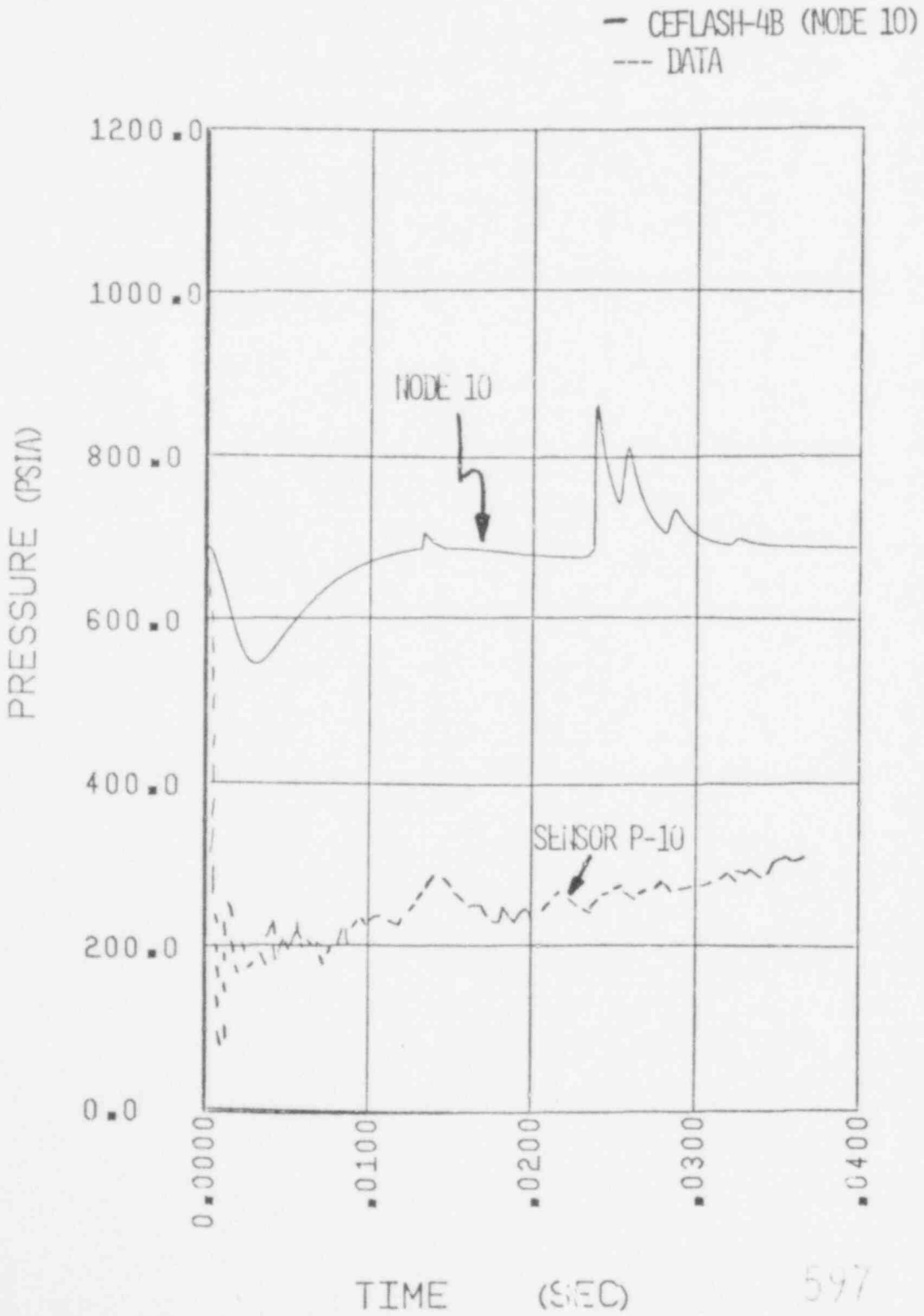

547 092

FIGURE 3.2-4

COMPARISON OF CEFLASH-4B PREDICTIONS
WITH
DATA FROM CSE TEST B-75
PRESSURE IN EXIT PIPE (SENSOR P-04)

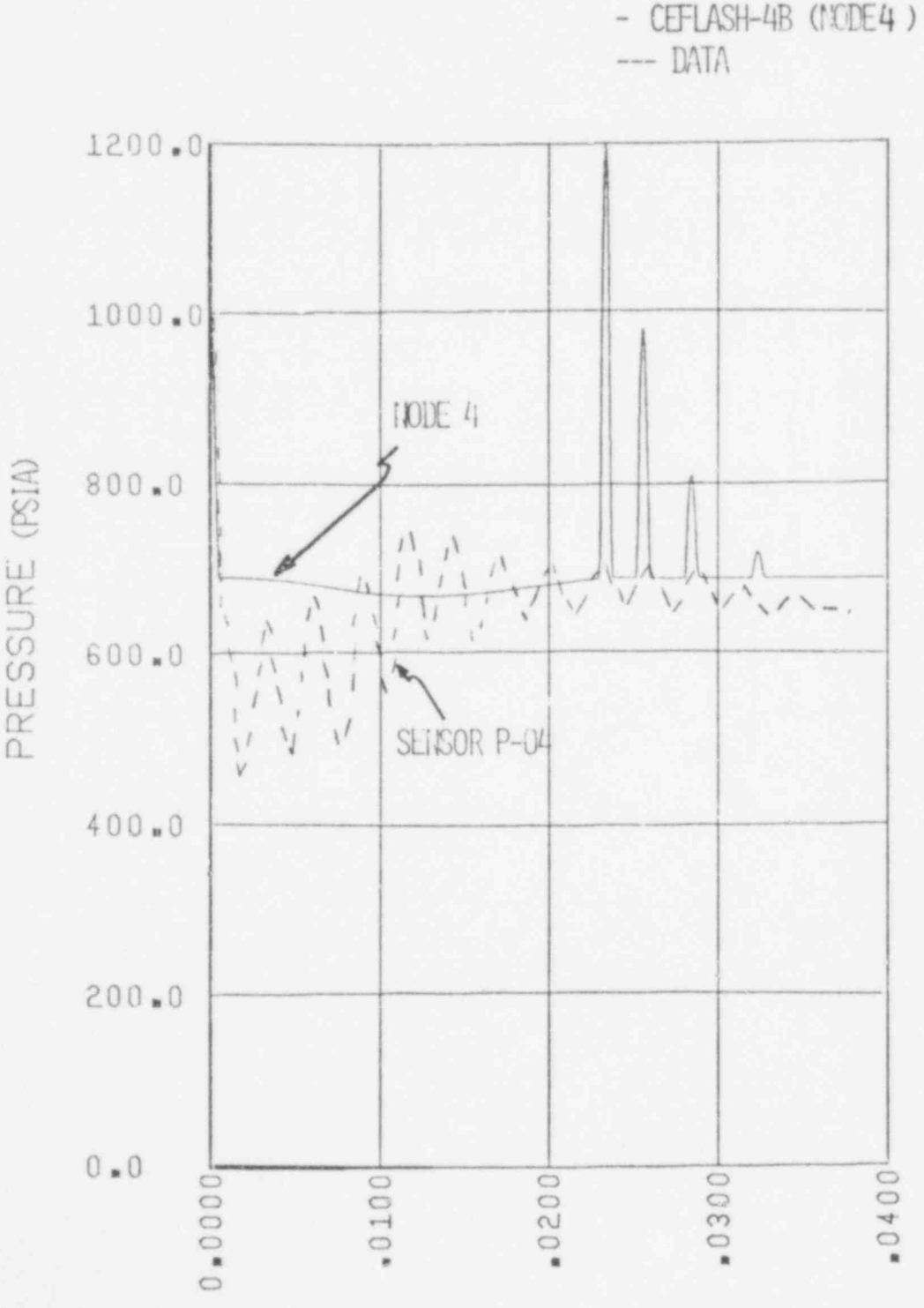

FIGURE 3.2-5

COMPARISON OF CEFLASH-4B PREDICTIONS
WITH
DATA FROM CSE TEST B-75
PRESSURE IN NOZZLE R (SENSOR P-01)

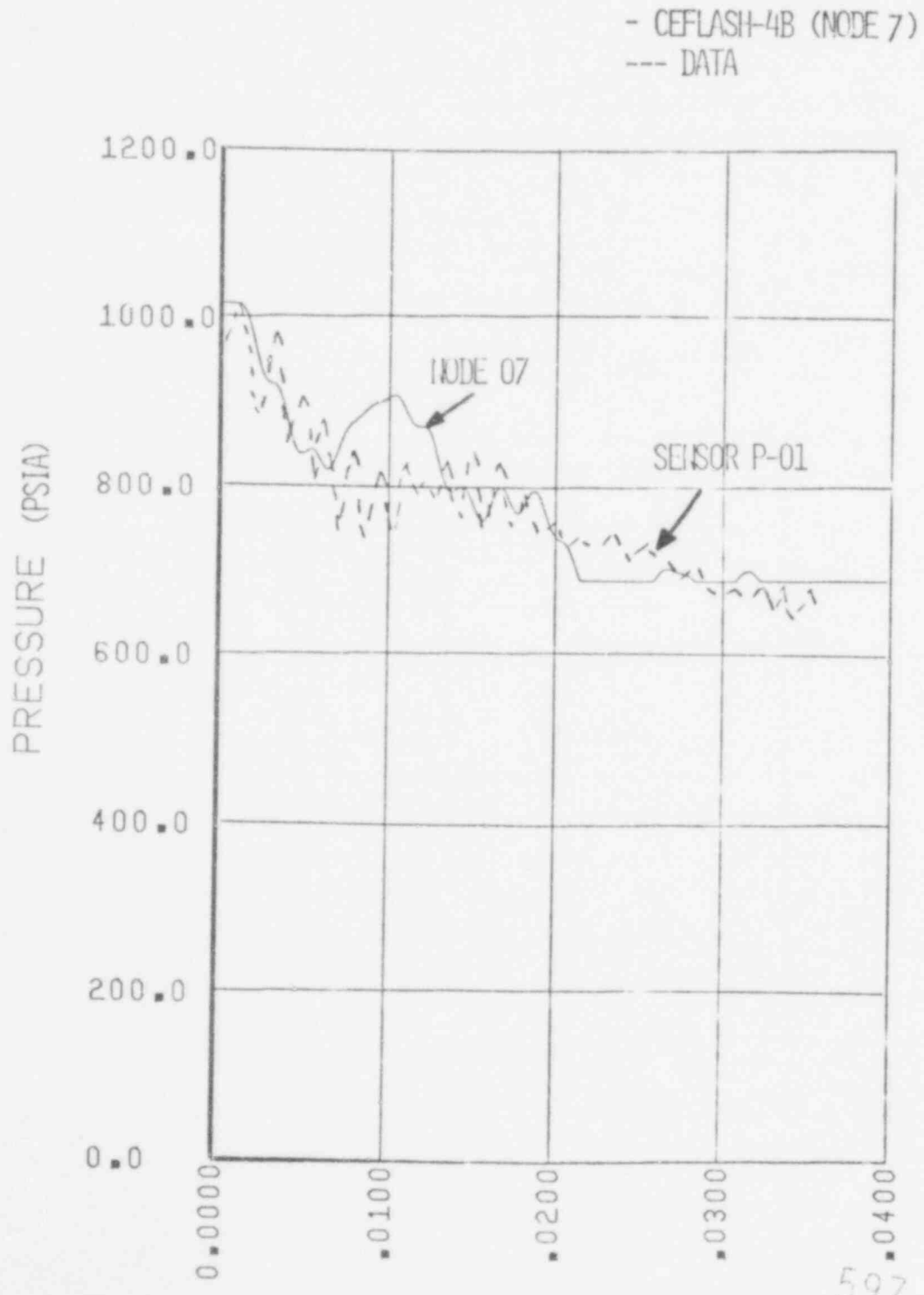

597 094

FIGURE 3.2-6

CEFLASH-4B PREDICTION
CSE TEST B-75

PRESSURE IN DOWNCOMER AT CORE ELEVATION NEAR NOZZLE A
(SENSOR P-20)
(NO DATA AVAILABLE)

- CEFLASH-4B (NODE 11)

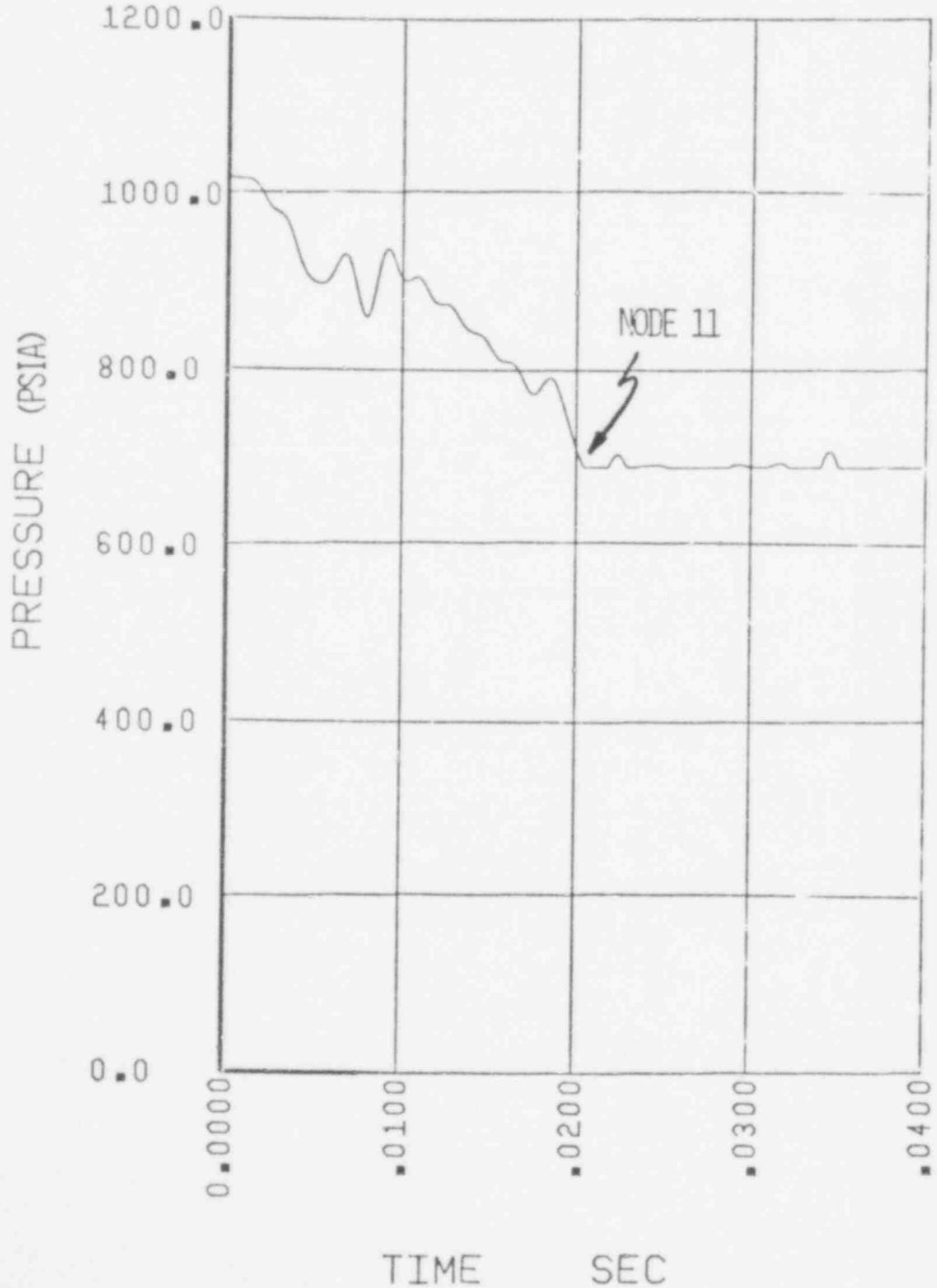

FIGURE 3.2-7

COMPARISON OF CEFLASH-4B PREDICTIONS
WITH
DATA FROM CSE TEST B-75
PRESSURE IN DOWNCOMER AT CORE ELEVATION OPPOSITE NOZZLE A (SENSOR P-21)

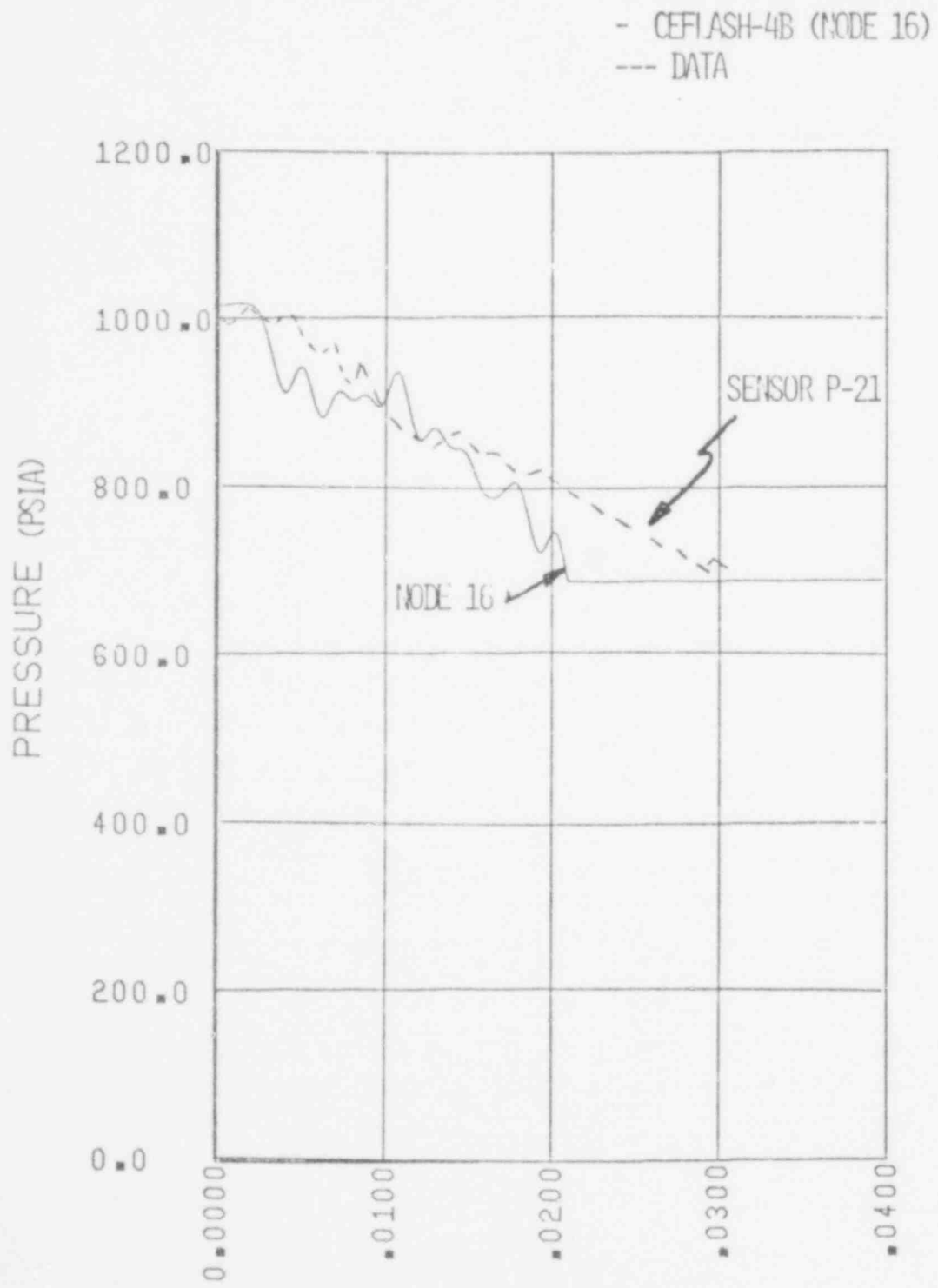

FIGURE 3.2-8

COMPARISON OF CEFLASH-4B PREDICTIONS
WITH
DATA FROM CSE TEST B-75
PRESSURE AT CORE CENTER (SENSOR P-22)

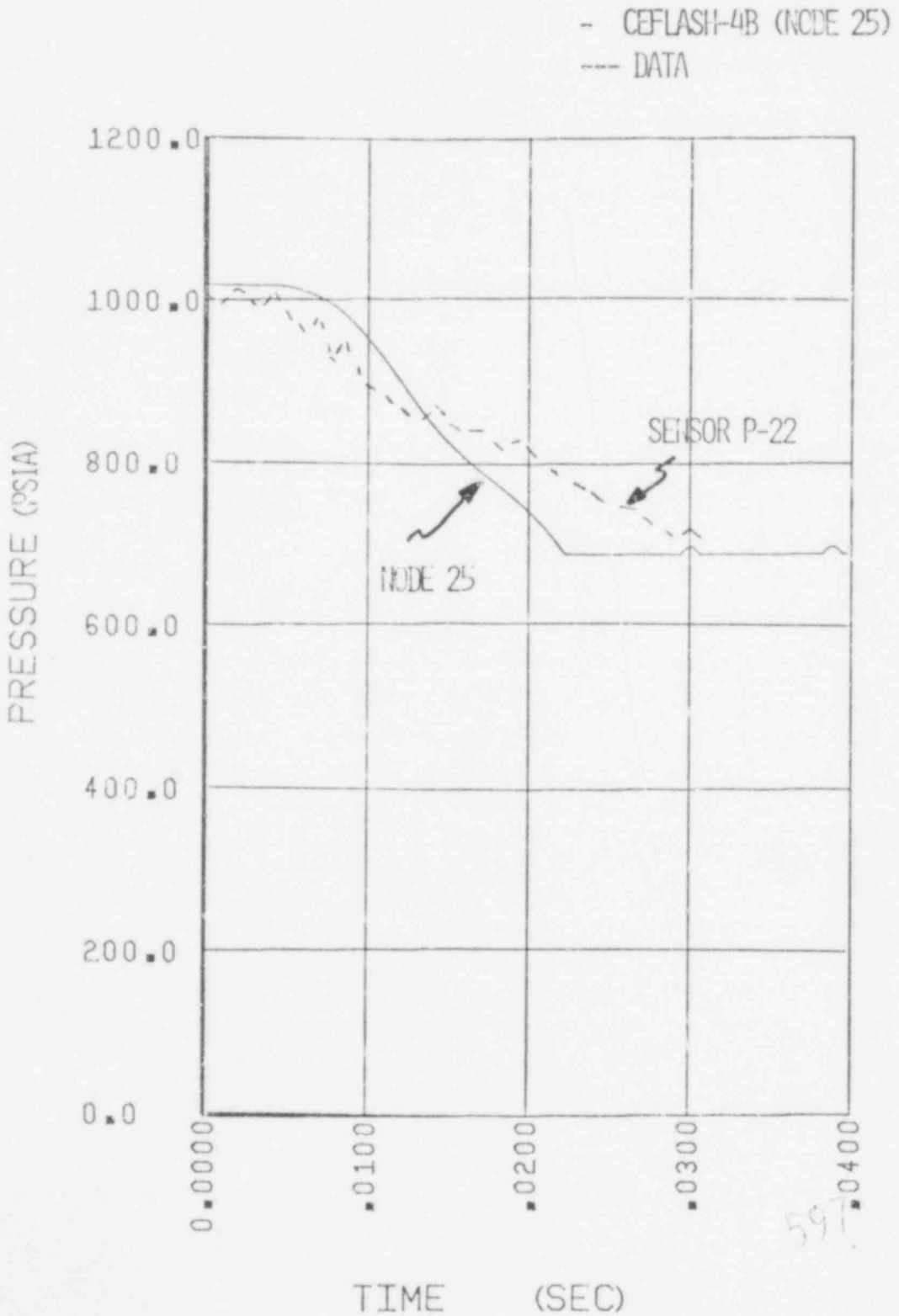

FIGURE 3.2-9

COMPARISON OF CEFLASH-4B PREDICTIONS
WITH
DATA FROM CSE TEST B-75
PRESSURE AT NOZZLE - RADIAL PROBE OUTER (SENSOR P-13)

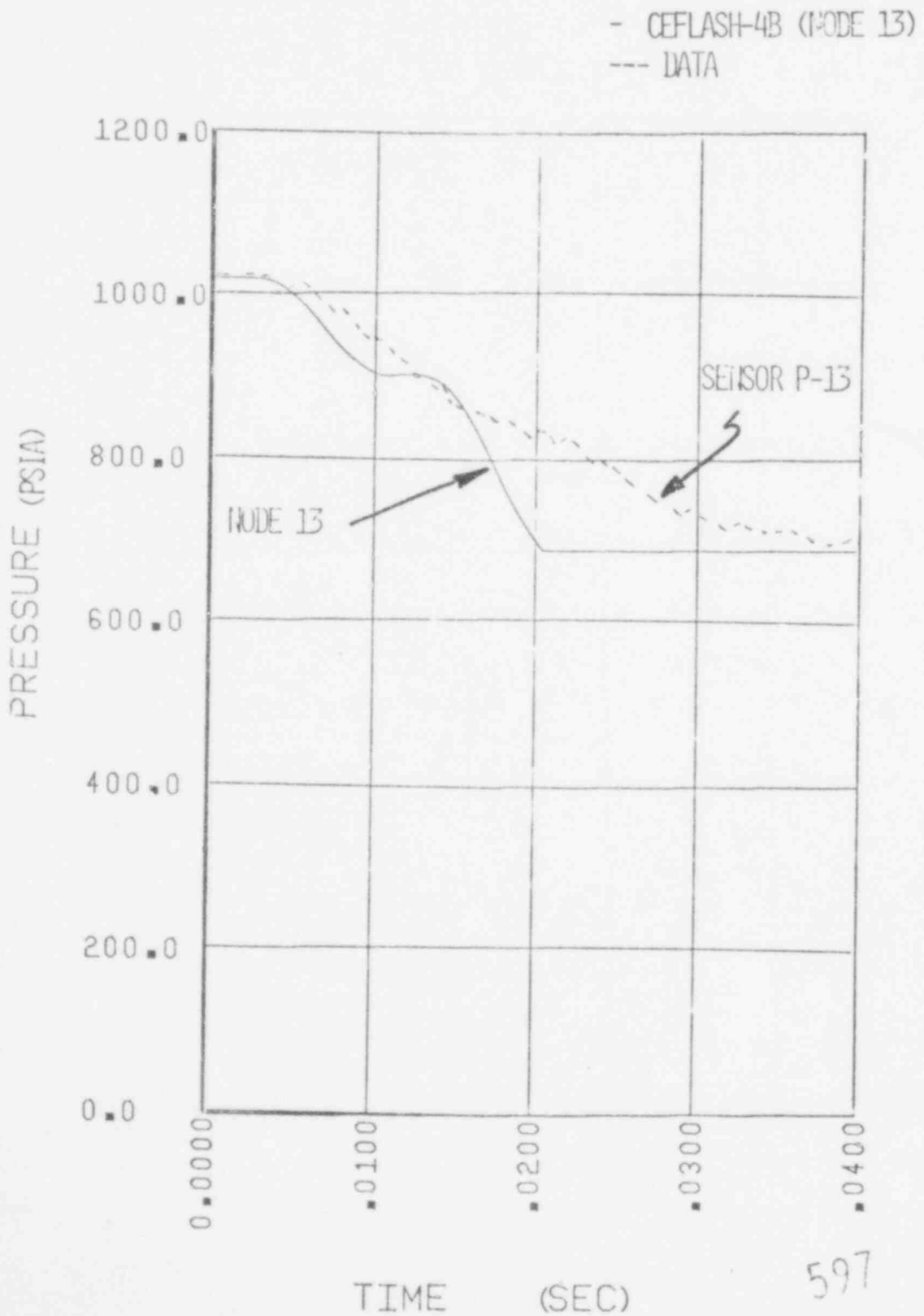

597 093

FIGURE 3.2-10

COMPARISON OF CEFLASH-4B PREDICTIONS
WITH
DATA FROM CSE TEST B-75
PRESSURE AT NOZZLE - RADIAL PROBE INNER (SENSOR P-14)

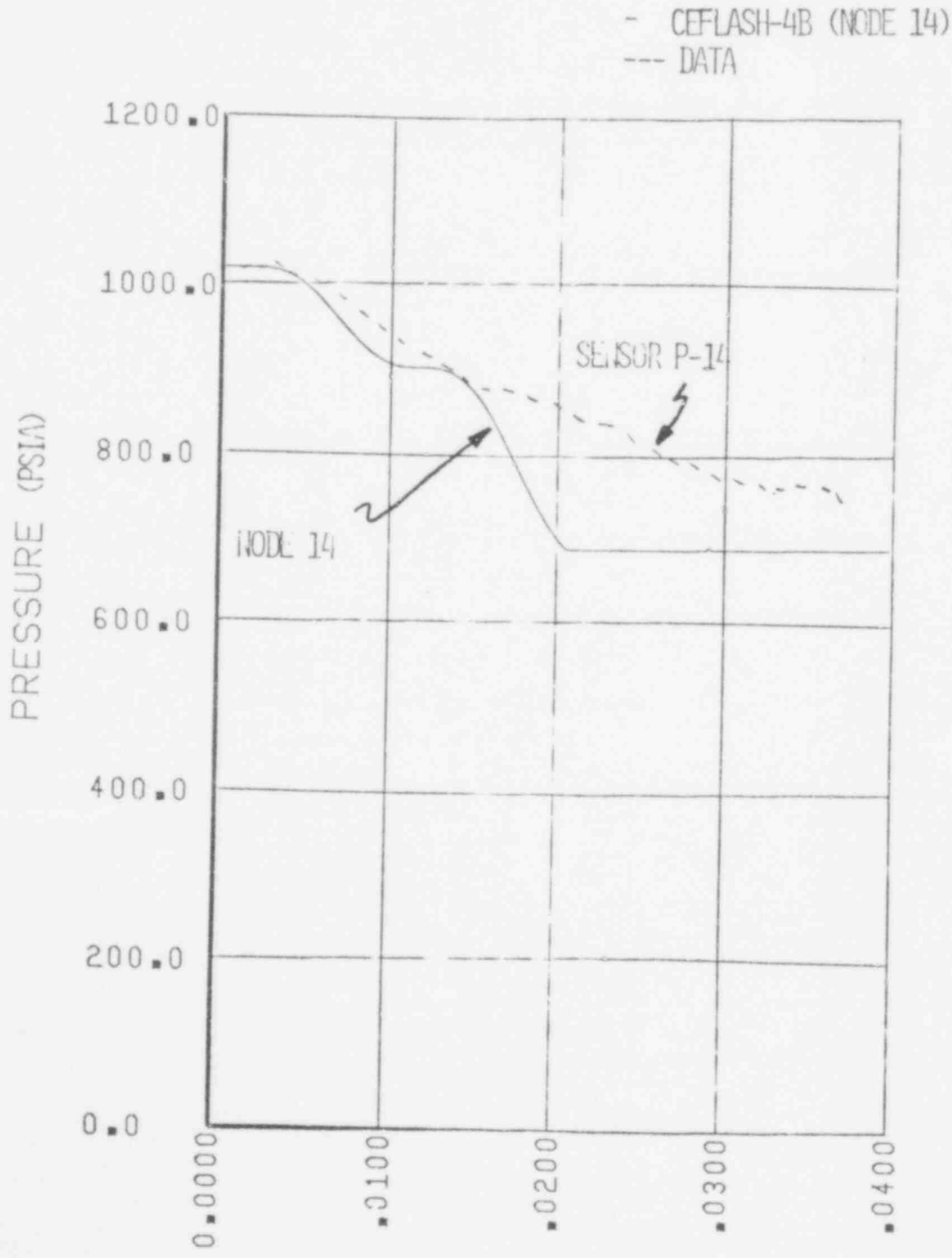

Figure 3.2-11
COMPARISON OF CEFLASH-4B PREDICTIONS WITH DATA
FROM CSE TEST B-75
CORE PLATE PRESSURE DROP
(SENSORS CPDP-2/CPDP-4)

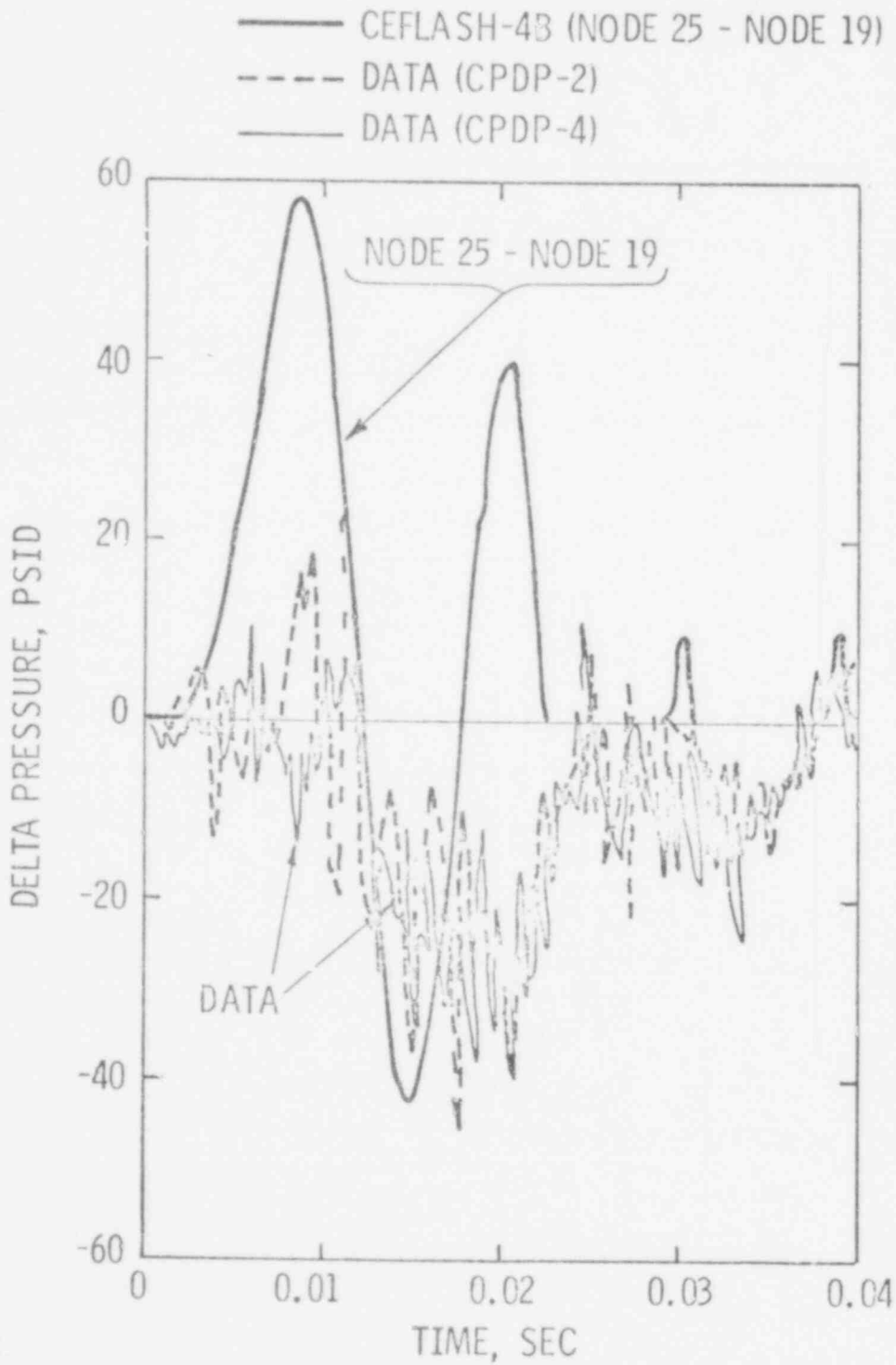

597 100

FIGURE 3.2-12

COMPARISON OF CEFLASH-4B PREDICTIONS
WITH
DATA FROM CSE TEST B-75
RADIAL PRESSURE DIFFERENCE ACROSS CORE BARREL (LOWER CORE NEAR BREAK)
(SENSOR CBDP-1)

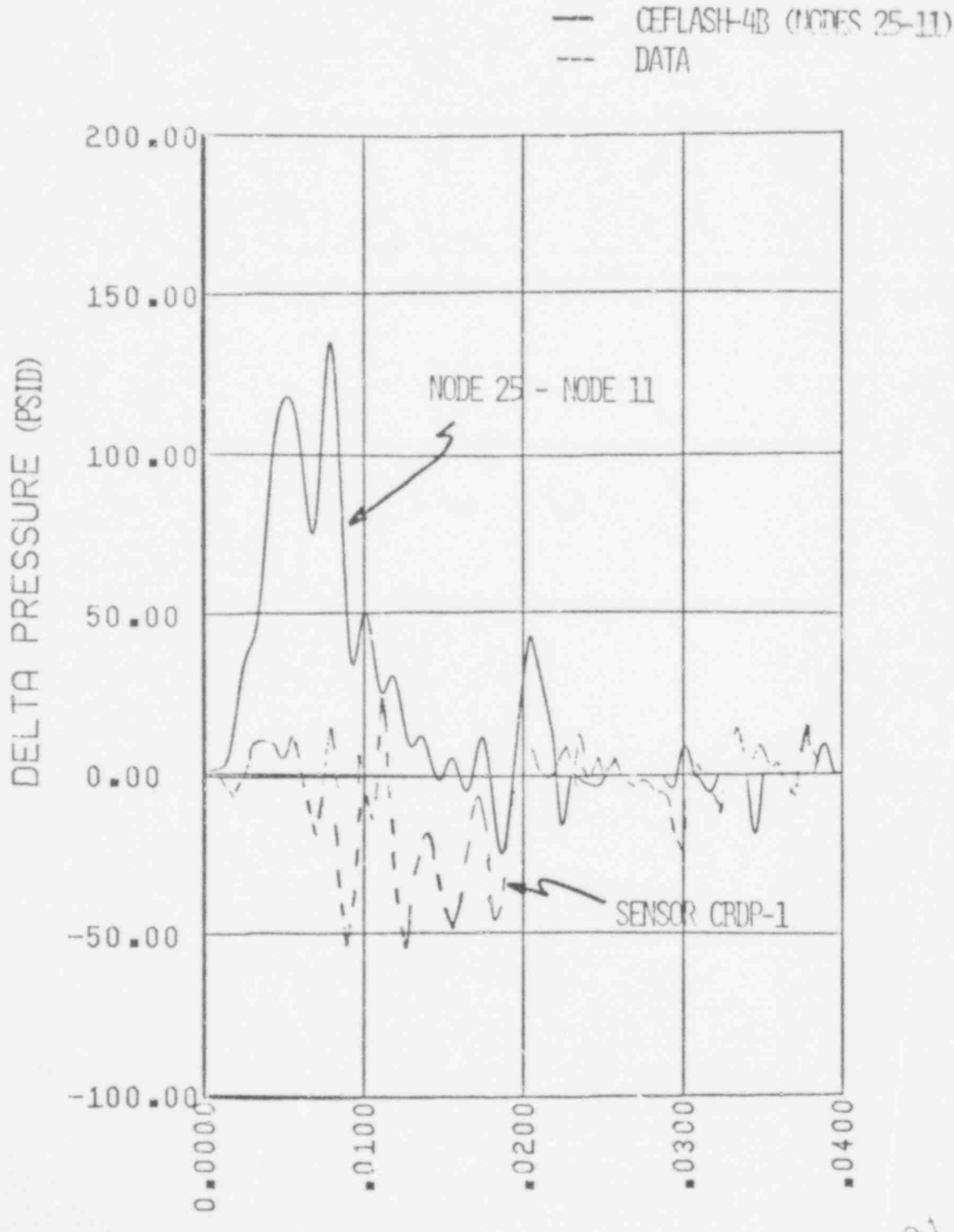

FIGURE 3.2-13

COMPARISON OF CEFLASH-4B PREDICTIONS
WITH
DATA FROM CSE TEST B-75
RADIAL PRESSURE DIFFERENCE ACROSS CORE BARREL
(BREAK ELEVATION: 90° FROM BREAK)
(SENSOR CBDP-2)

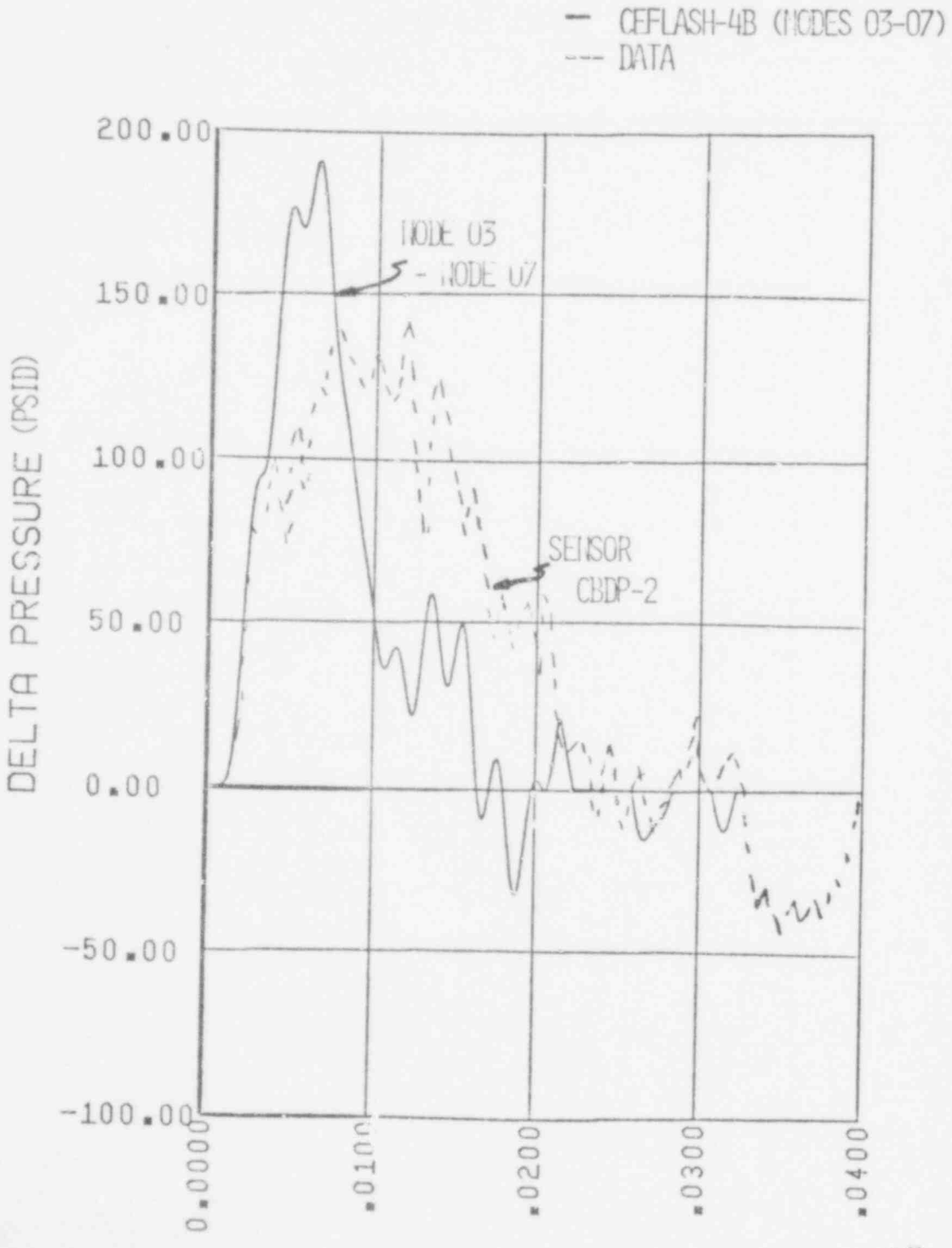

FIGURE 3.2-14

COMPARISON OF CEFLASH-4B PREDICTIONS
WITH
DATA FROM CSE TEST B-75
RADIAL PRESSURE DIFFERENCE ACROSS CORE BARREL
(BREAK ELEVATION: 180° FROM BREAK)
(SENSOR CBDP-3)

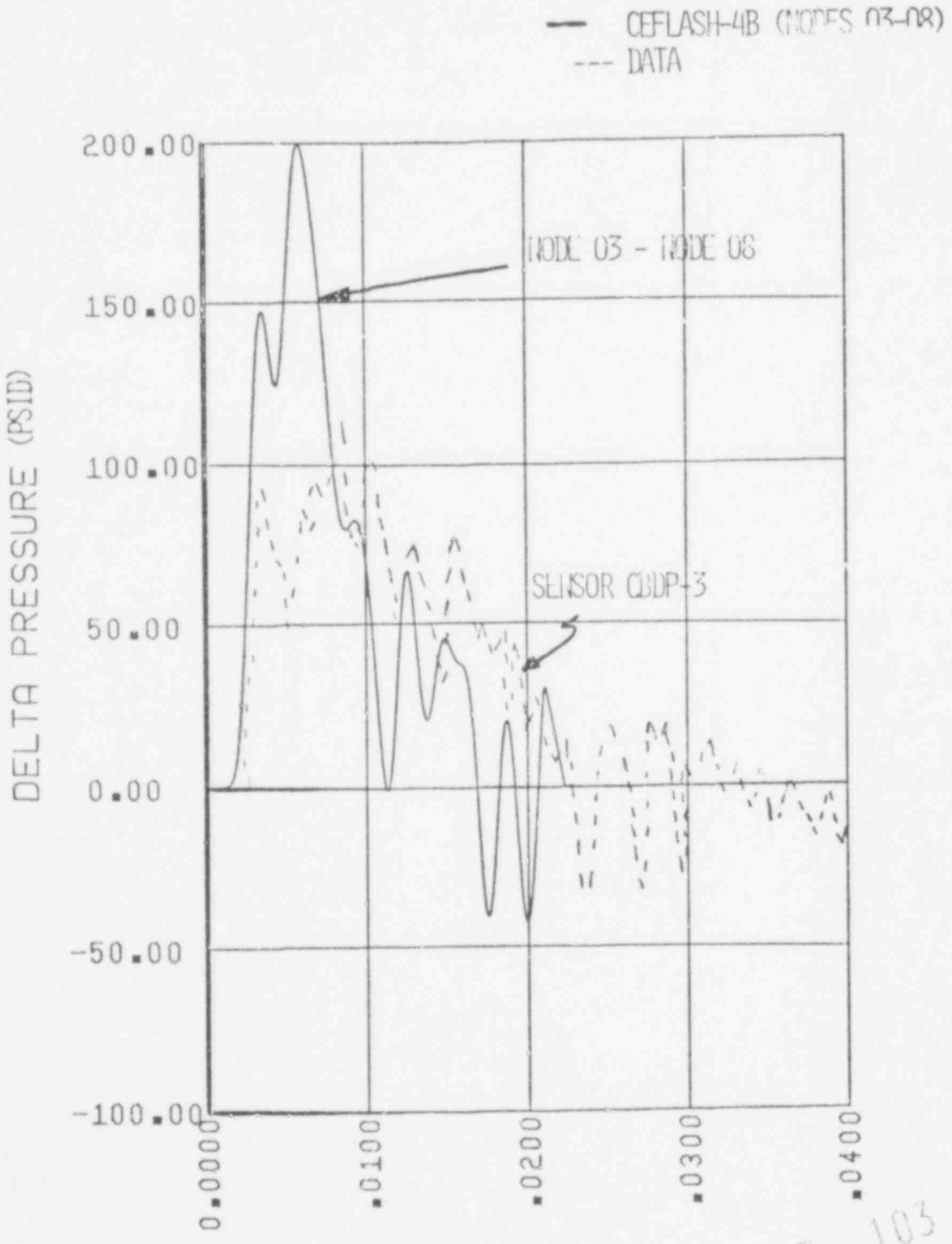

FIGURE 3.2-15

COMPARISON OF CEFLASH-4B PREDICTIONS
WITH
DATA FROM CSE TEST B-75
RADIAL PRESSURE DIFFERENCE ACROSS CORE BARREL (BREAK LOCATION)
(SENSOR NDP)

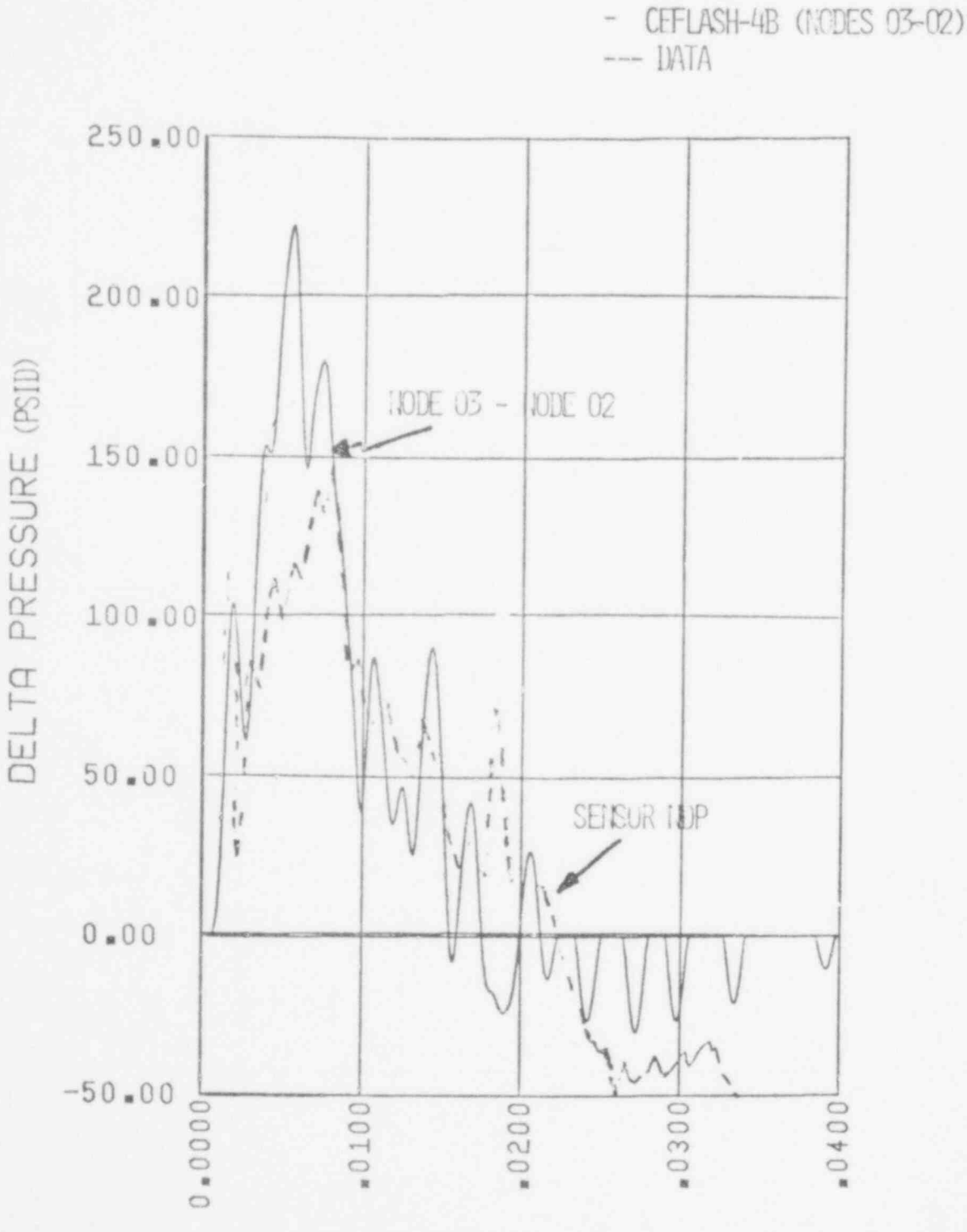

FIGURE 3.2-16

CEFLASH-4B PREDICTION
CSE TEST B-75
PRESSURE DIFFERENCE AROUND CORE BARREL
(NODES 08-02)

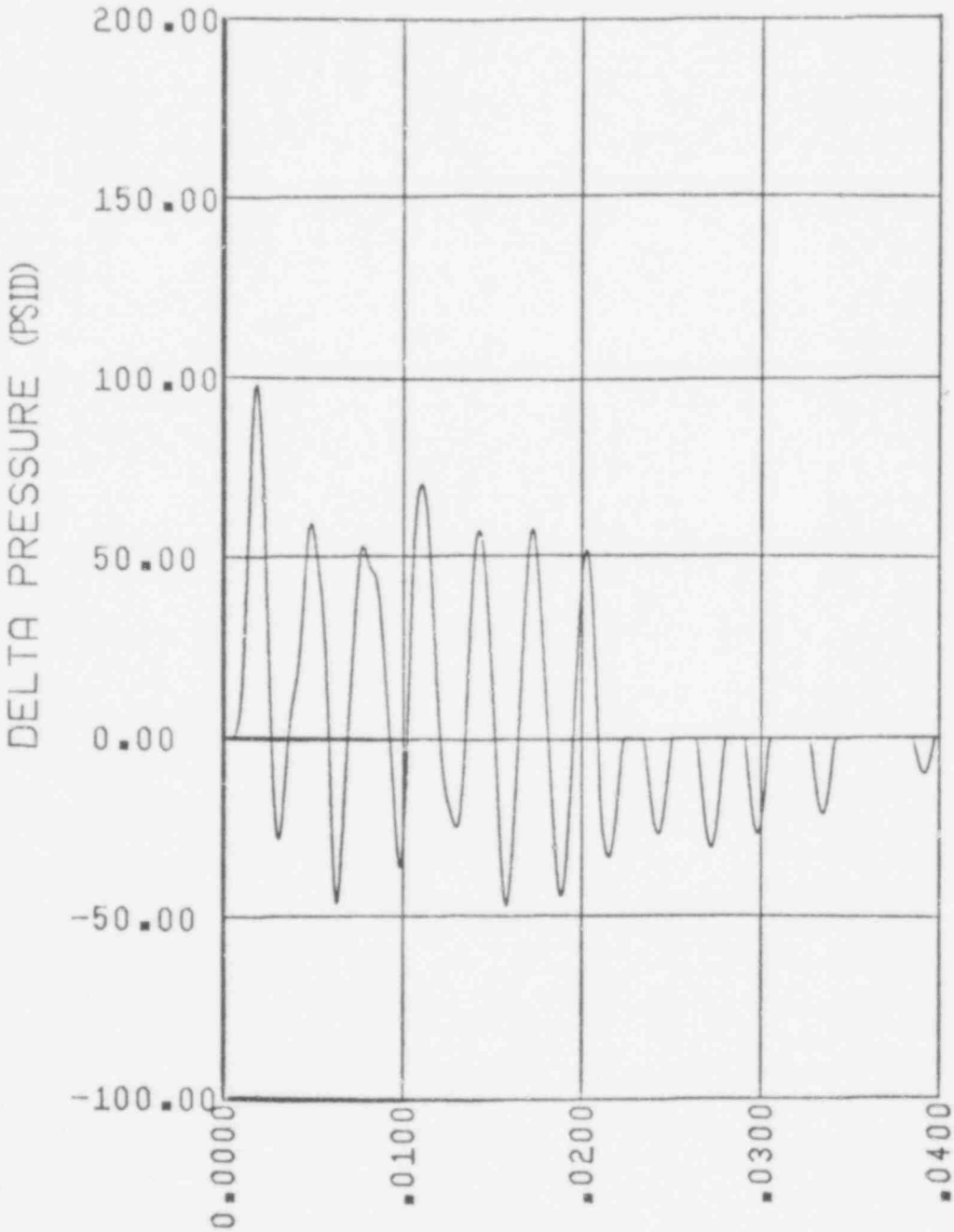

FIGURE 3.2-17

CEFLASH-4B PREDICTION
CSE TEST B-75
PRESSURE DIFFERENCE AROUND CORE BARREL
(NODES 16 - 11)

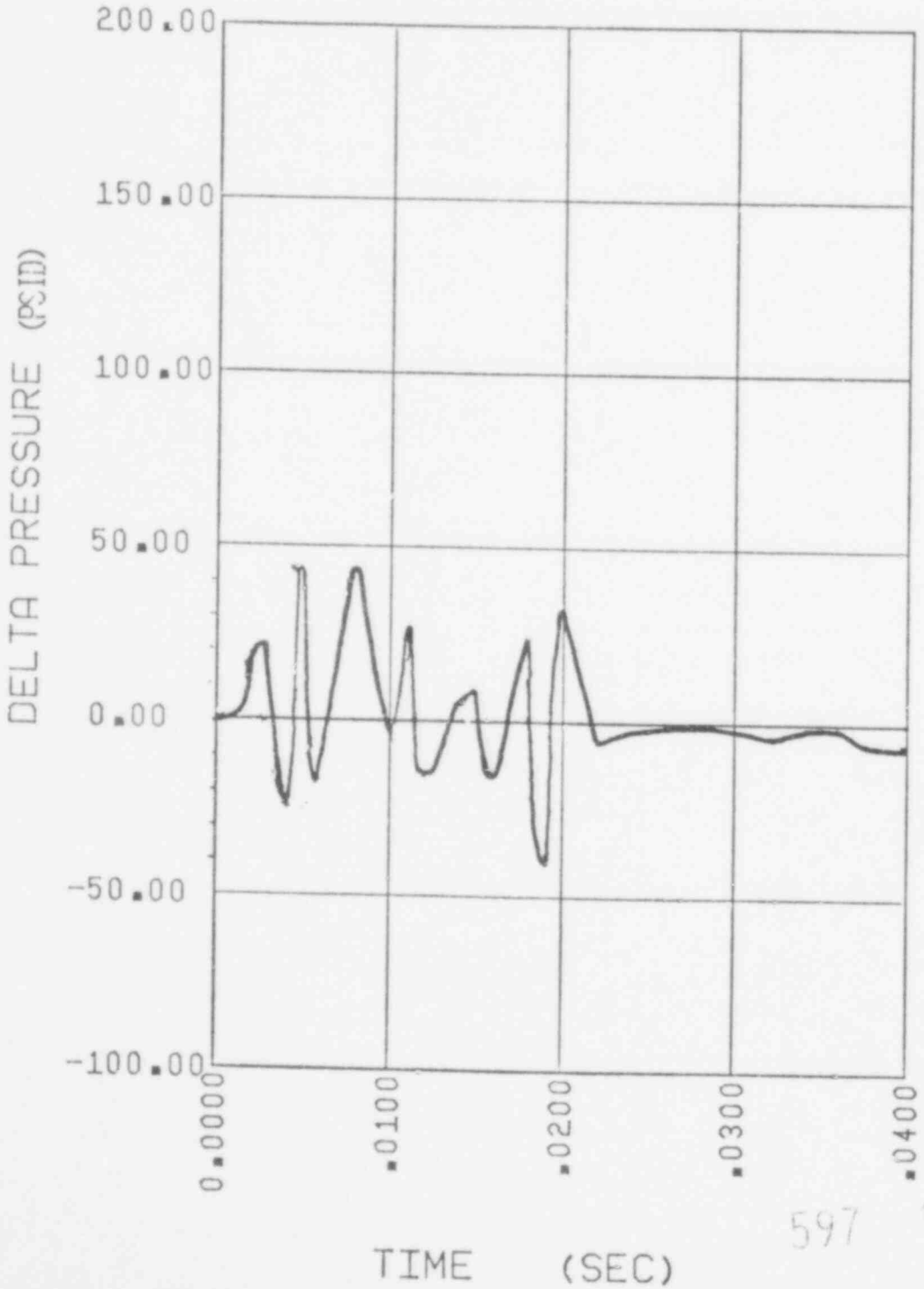

597 106

FIGURE 3.2-18

CEFLASH-4B PREDICTION
CSE TEST B-75
PRESSURE DIFFERENCE ACROSS CORE STRUCTURE
(NODES 23-14)

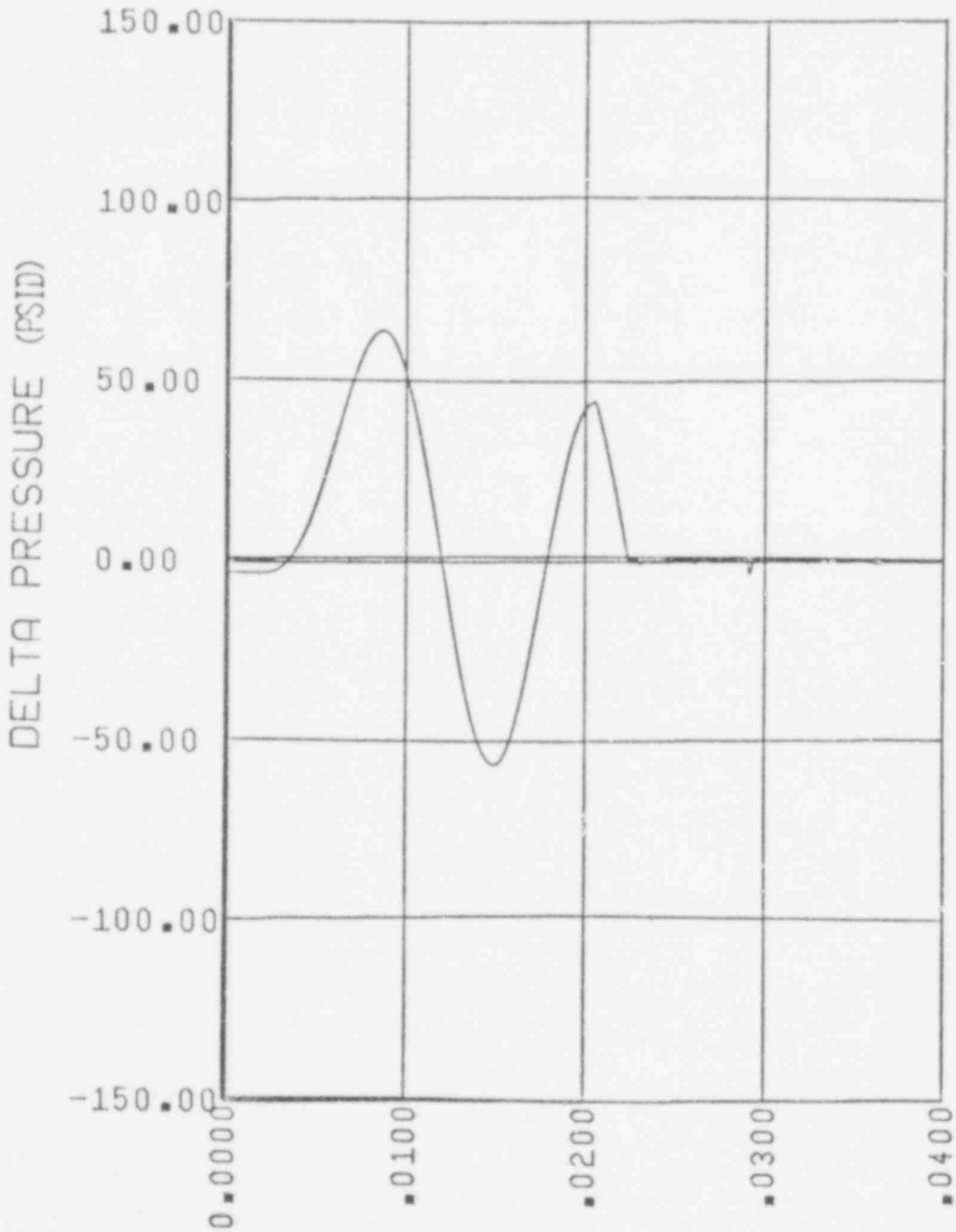

FIGURE 3.2-19
CEFLASH-4B PREDICTION
CSE TEST P-75
PRESSURE IN CASE INSTRUMENT RING
(NODE 23)

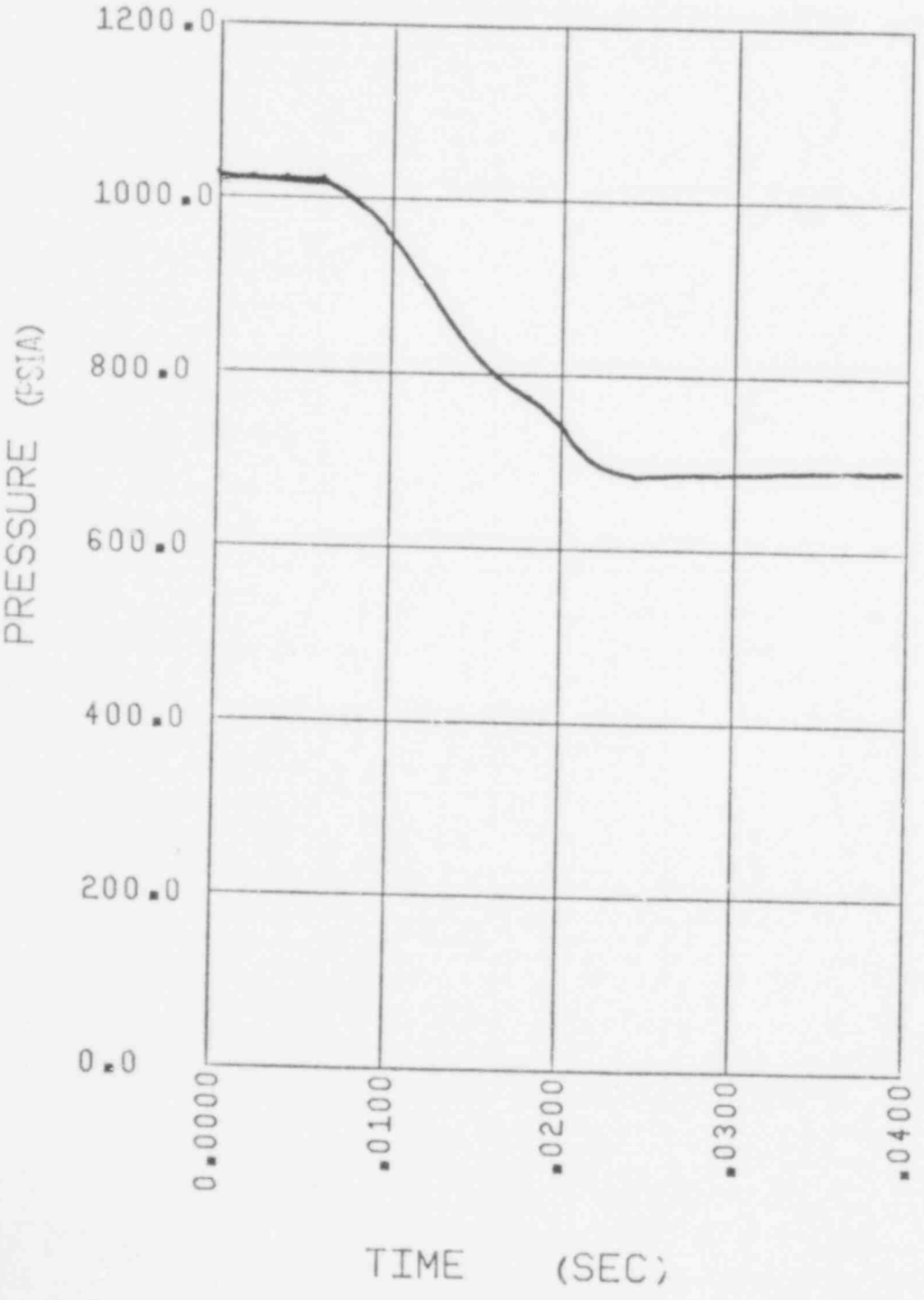

FIGURE 3.2-20
CEFLASH-4B PREDICTION
CSE TEST B-75
PRESSURE BELOW CORE PLATE
(NODE 39)

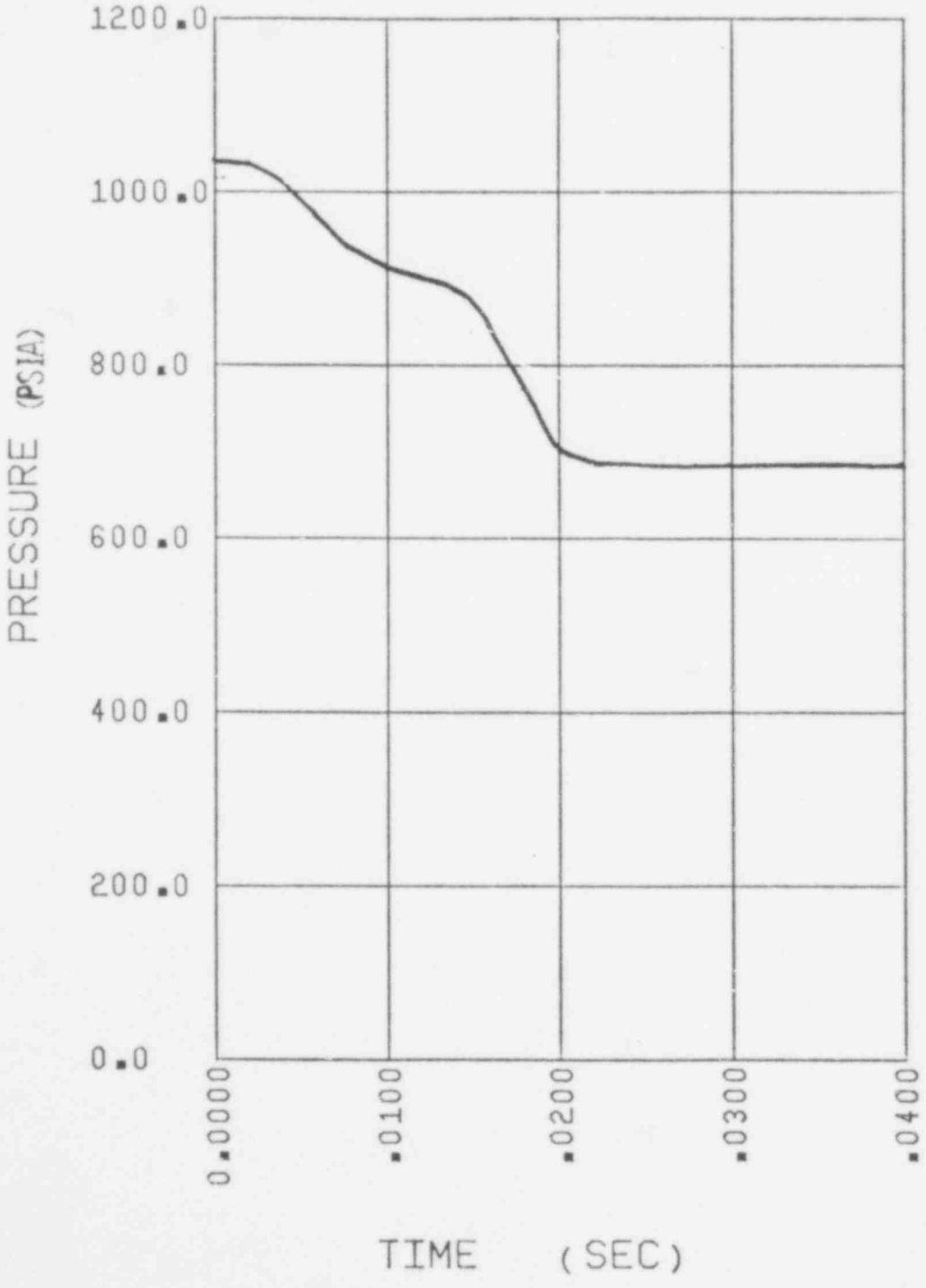

FIGURE 3.2-21

CEFLASH-4B PREDICTION
CSL TEST B-75
PRESSURE IN DOWNCOMER ANNULUS
(NODE 02)

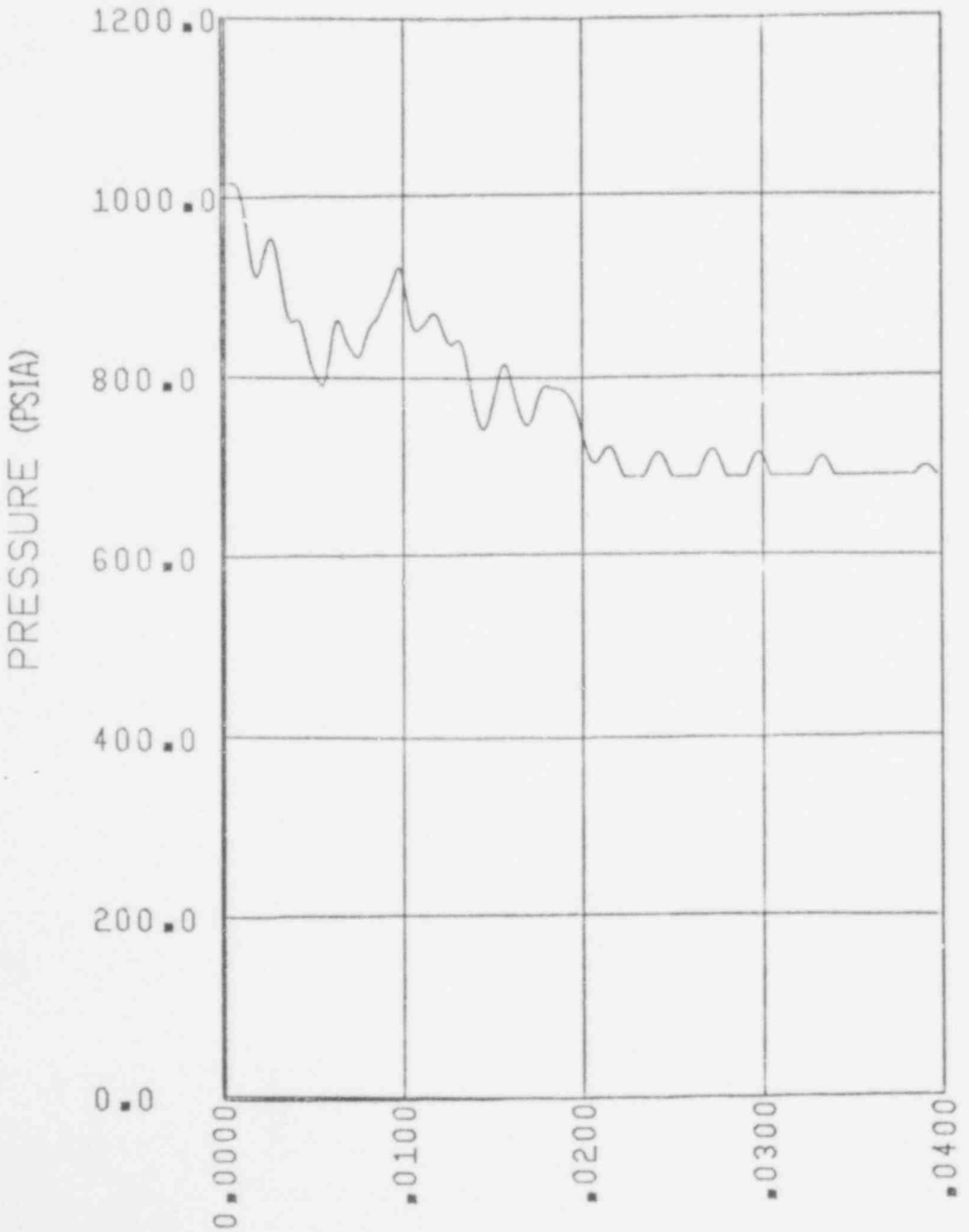

597 110

FIGURE 3.2-22

CEFLASH-4B PREDICTION
CSE TEST B-75
PRESSURE IN DOWNCOMER ANNULUS
(NODE 68)

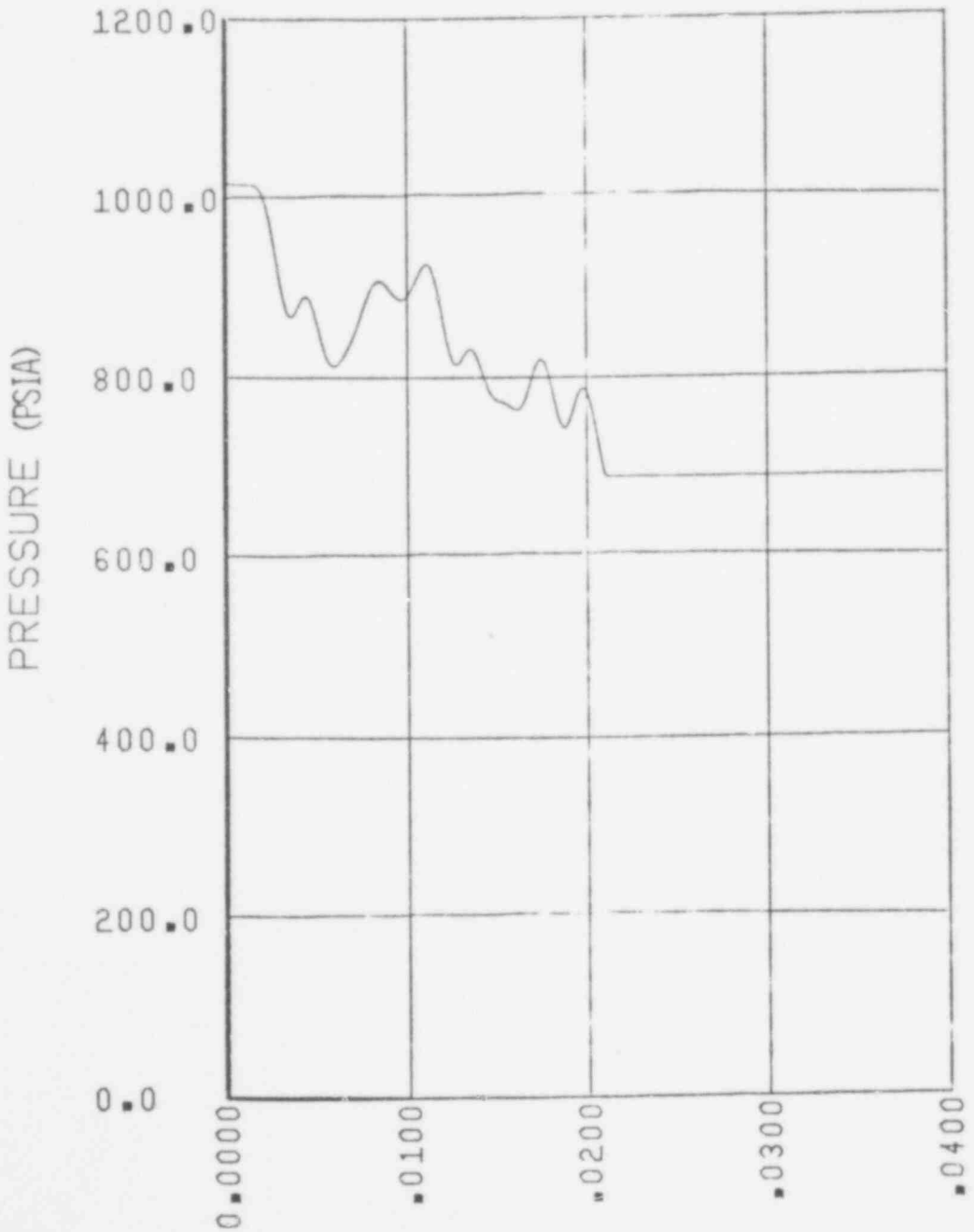

597 111

CEFLASH-4B PREDICTION
CSE TEST B-75
PRESSURE IN CORE REGION
(NODE 26)

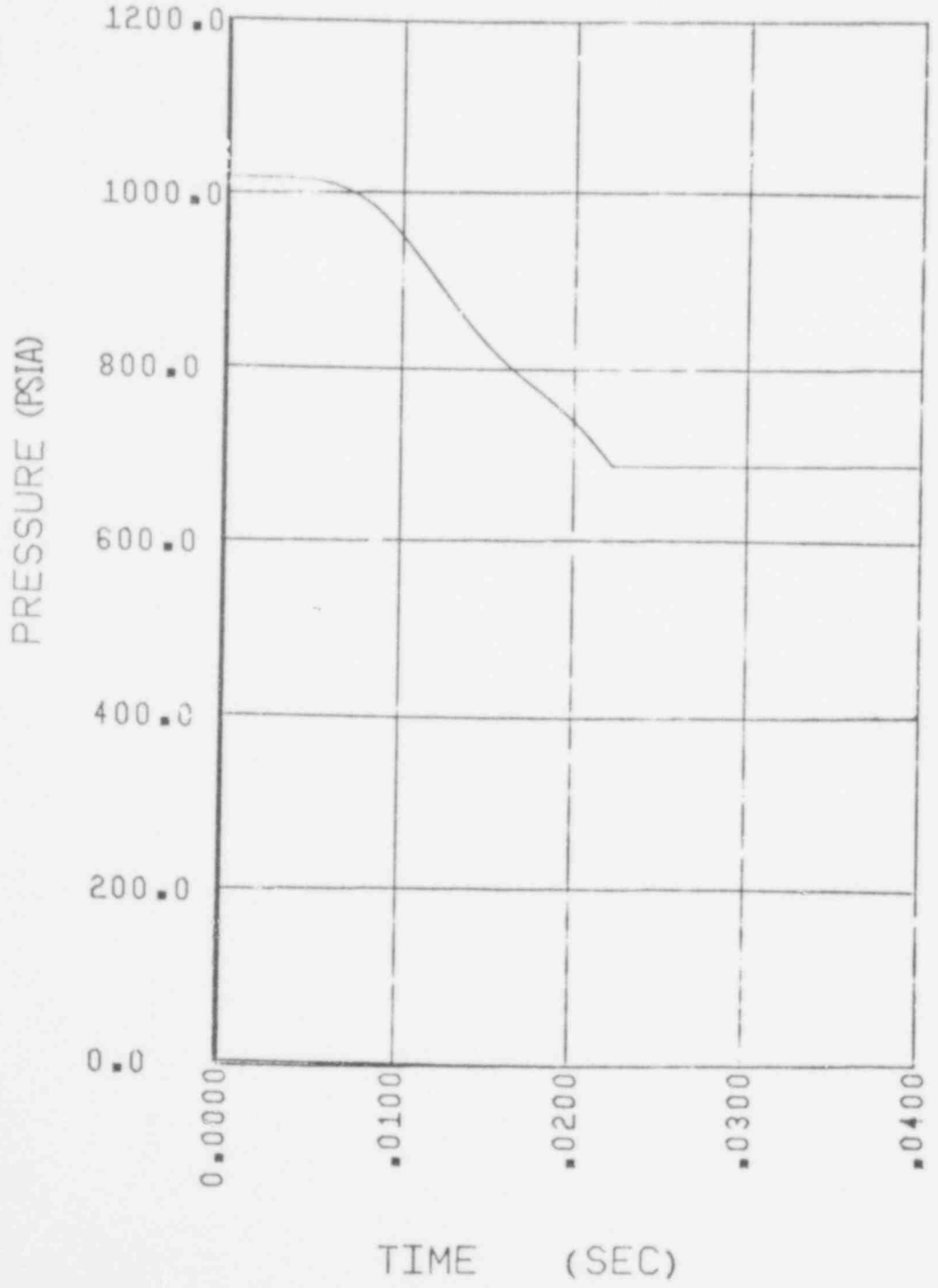

FIGURE 3.2-24
CEFLASH-4B PREDICTION
CSE TEST B-75
PRESSURE IN UPPER GUIDE STRUCTURE REGION
(NODE 3)

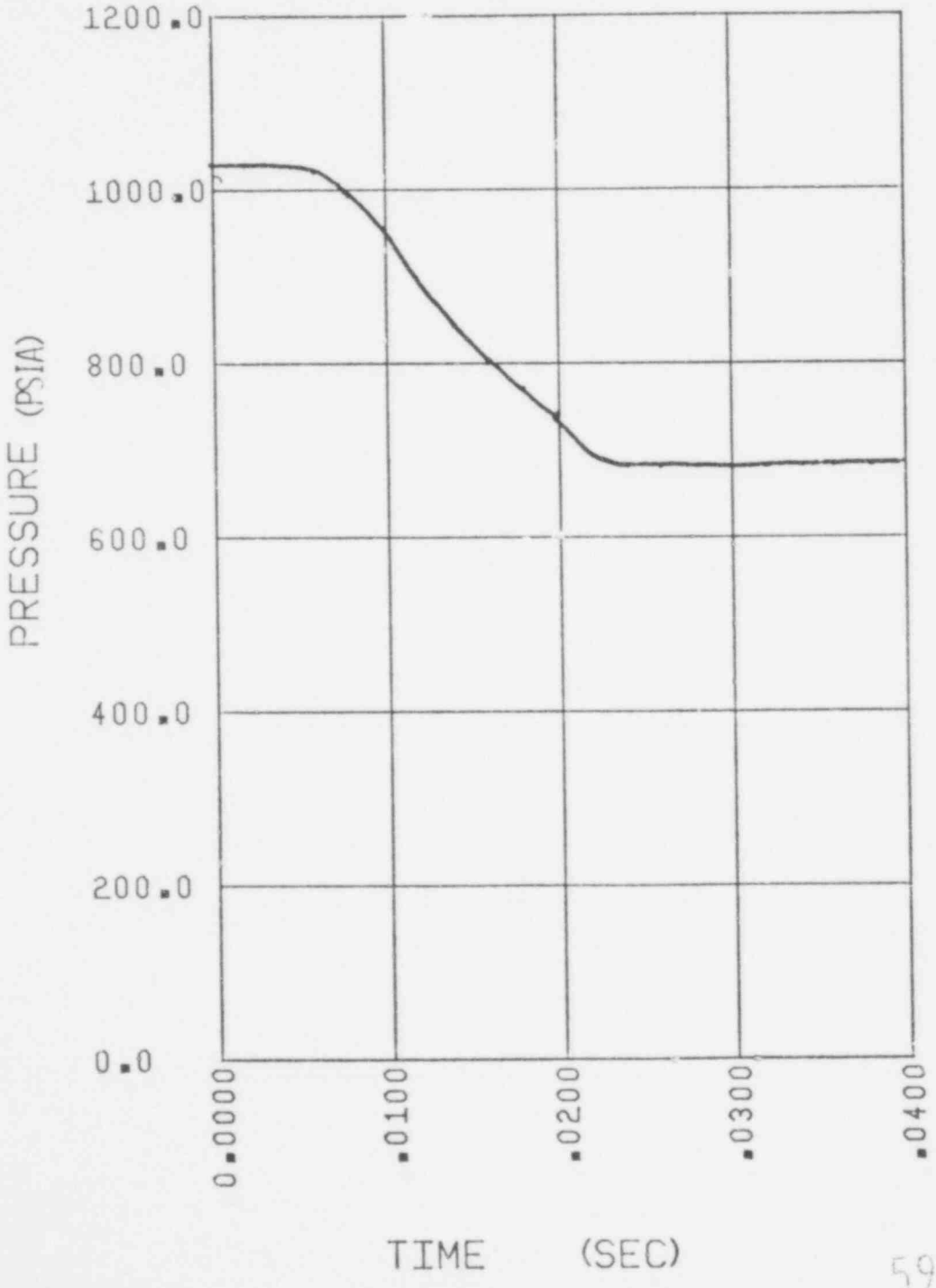

597 113

Figure 3.2-25
CEFLASH-4B PREDICTED BREAK FLOW RATE
CSE TEST B-75
(FLOWPATH 38)

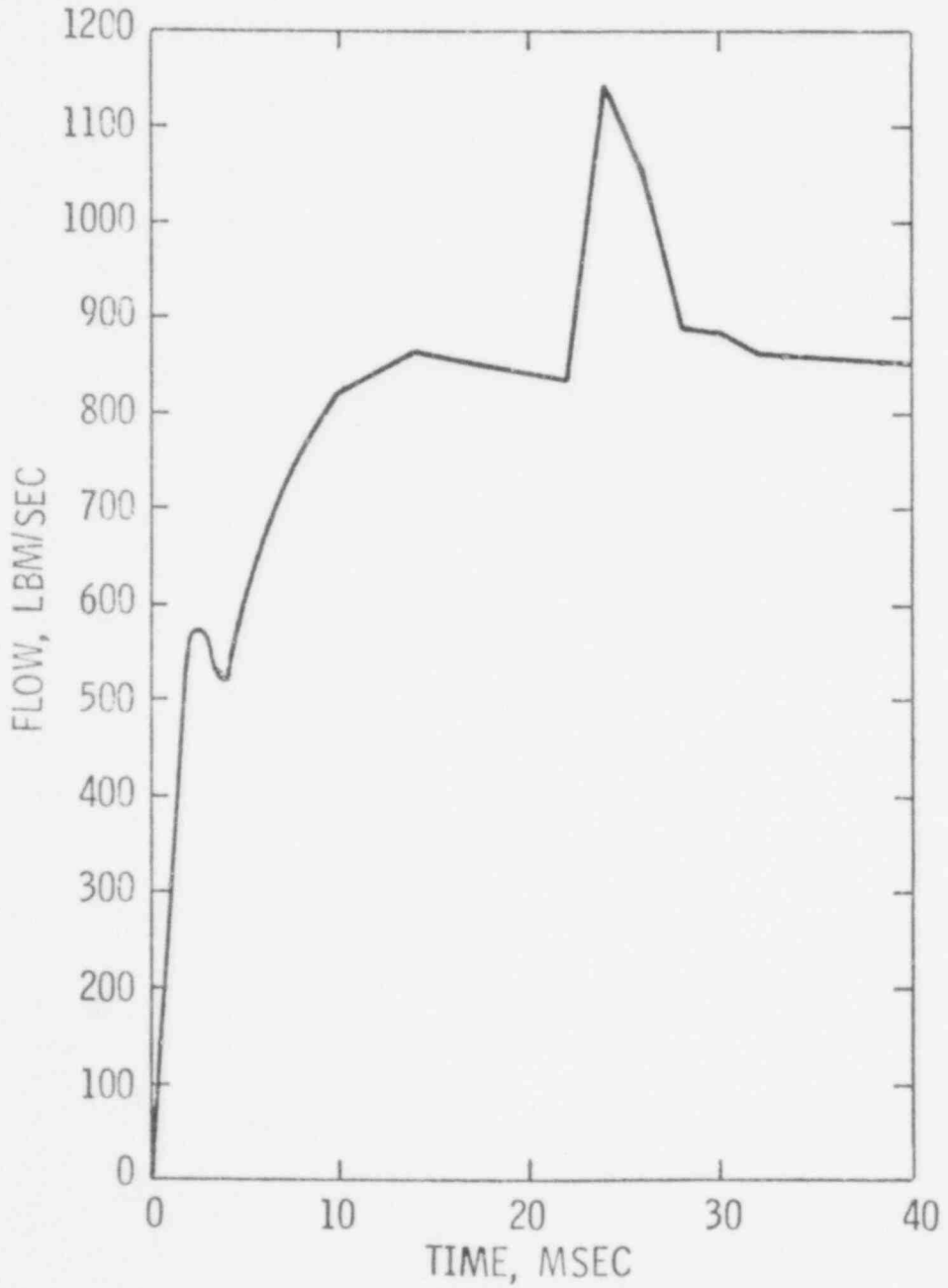

597 114

FIGURE 3.2-26

COMPARISON OF CEFLASH-4B CSE PREDICTIONS
(PRESSURE AT NODE 16)

--- CSE MODEL WITH NO DIRECT PATH BETWEEN NODE 5 AND NODE 25 (SEE FIGURE 3.2-1)

— CSE MODEL WITH A DIRECT PATH BETWEEN NODE 5 AND NODE 25 (SEE FIGURE 3.3 OF REFERENCE 3.2-2)

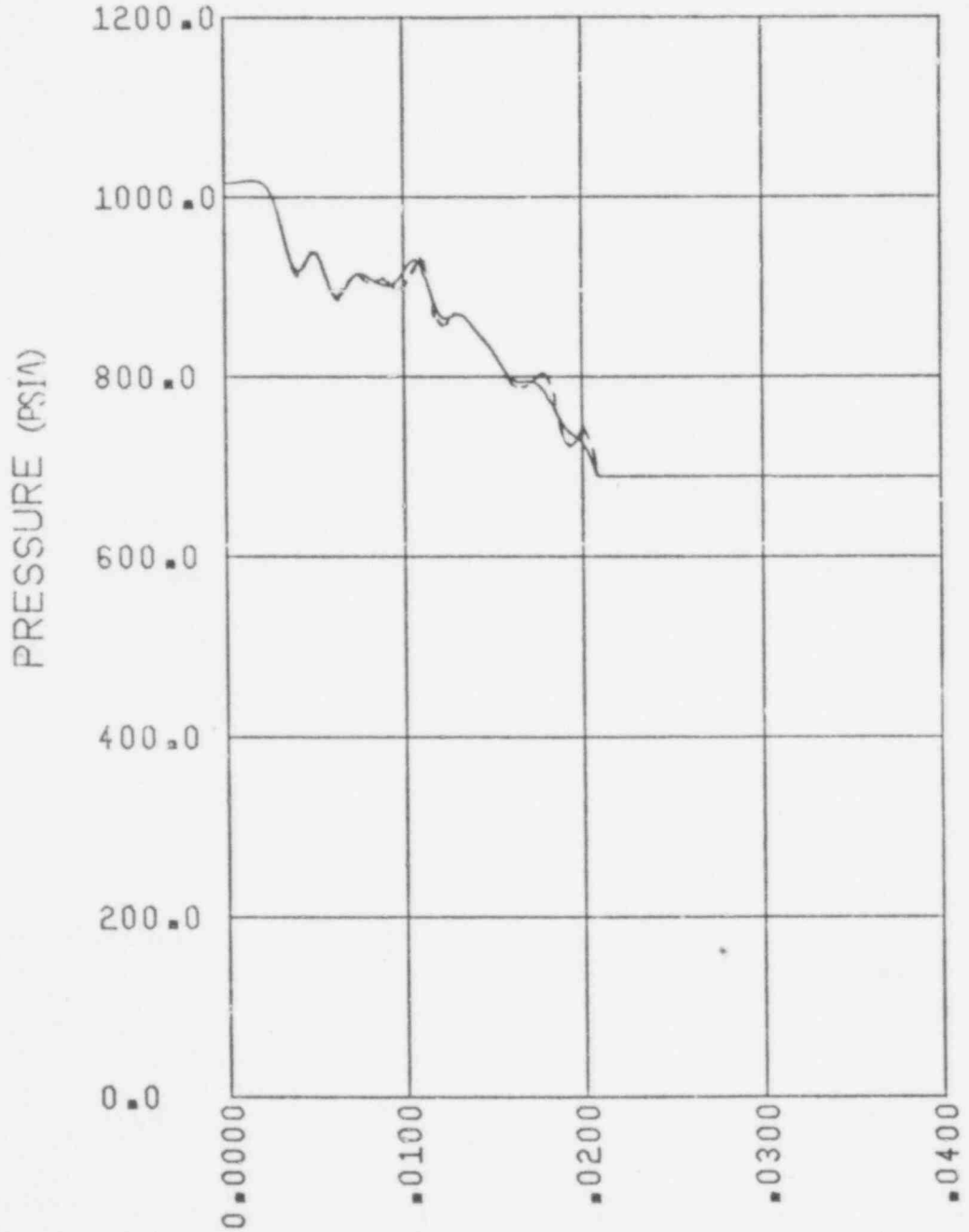

597 115